GEOLOGICAL SURVEY OF CANADA
BULLETIN 566

MARINE GEOLOGY OF HUDSON STRAIT AND UNGAVA BAY, EASTERN ARCTIC CANADA: LATE QUATERNARY SEDIMENTS, DEPOSITIONAL ENVIRONMENTS, AND LATE GLACIAL–DEGLACIAL HISTORY DERIVED FROM MARINE AND TERRESTRIAL STUDIES

Edited by
B. MacLean

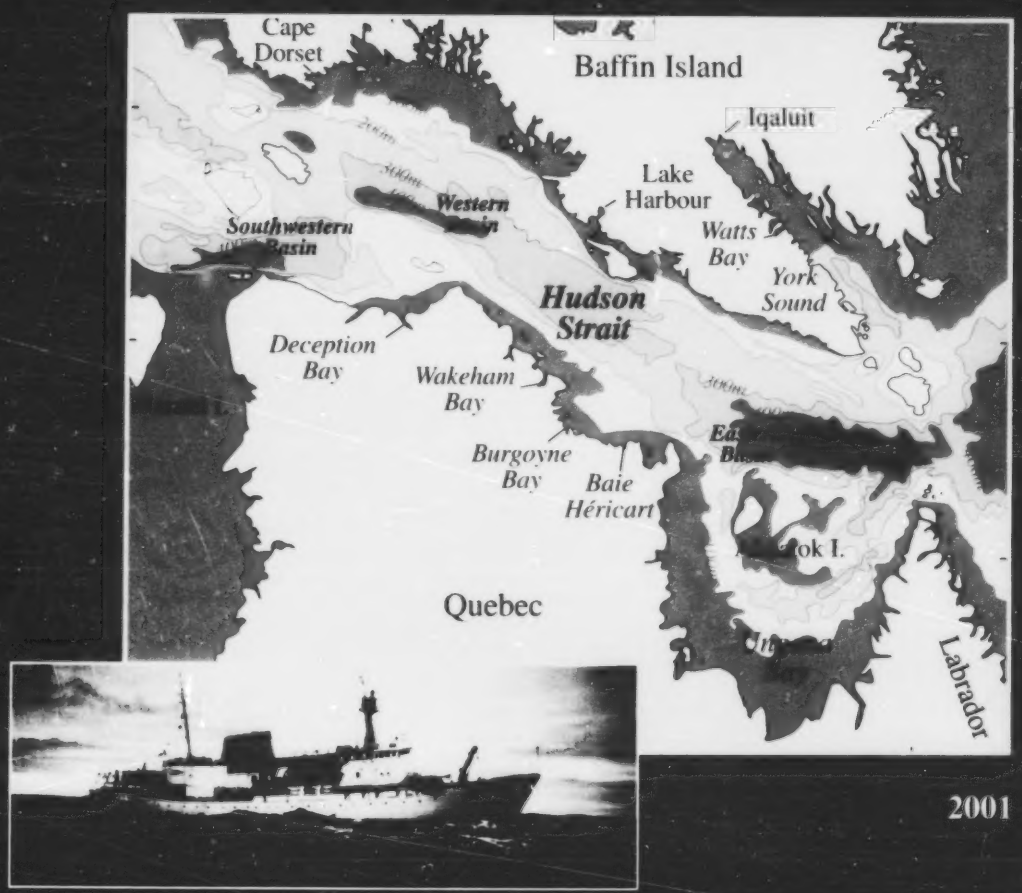

2001

Natural Resources Canada
Ressources naturelles Canada

Canada

101-04626/

GEOLOGICAL SURVEY OF CANADA
BULLETIN 566

MARINE GEOLOGY OF HUDSON STRAIT AND UNGAVA BAY, EASTERN ARCTIC CANADA: LATE QUATERNARY SEDIMENTS, DEPOSITIONAL ENVIRONMENTS, AND LATE GLACIAL–DEGLACIAL HISTORY DERIVED FROM MARINE AND TERRESTRIAL STUDIES

Edited by
B. MacLean

2001

©Her Majesty the Queen in Right of Canada, 2001
Catalogue No. M42-566E
ISBN 0-660-18478-8

Available in Canada from
Geological Survey of Canada offices:

601 Booth Street
Ottawa, Ontario K1A 0E8

3303-33rd Street N.W.
Calgary, Alberta T2L 2A7

101-605 Robson Street
Vancouver, B.C. V6B 5J3

A deposit copy of this publication is also available for reference
in selected public libraries across Canada

Price subject to change without notice

Cover illustration

Index map of the Hudson Strait–Ungava Bay region showing generalized bathymetry. Inset photograph is of *CSS Hudson*, from which the marine studies discussed in this bulletin were conducted. Photograph of *CSS Hudson* by Bedford Institute of Oceanography, Photography.

Critical reviewers

H. Josenhans
J. Shaw

Editor's address

B. MacLean
GSC Atlantic
1 Challenger Drive
P.O. Box 1006
Dartmouth, Nova Scotia B2Y 4A2

Original manuscript submitted: 1999-06
Final version approved for publication: 2001-01

FOREWORD

Part of the Geological Survey of Canada's work in the field of marine geoscience is directed towards research on the surficial deposits of the continental margin. Such investigations provide information on seabed conditions and past and present environments, which aid seabed engineering activities and studies relating to changes in climate and paleoceanograhic conditions through time.

This bulletin presents results of studies of the sediments and late Quaternary history of Hudson Strait and Ungava Bay. These investigations were conducted by Geological Survey of Canada (Atlantic) in collaboration with researchers from other institutions, most notably, University of Colorado, University of Montreal, and University of Louisiana, who have been actively studying the late Quaternary history of adjacent terrestrial and marine areas. Researchers from Centre géoscientifique de Québec and from several other universities also contributed to this study.

This report delineates the principal Quaternary sediment units, their distribution, depositional environments, and late Quaternary chronologies, and provides information on late glacial events, deglaciation of the region, and postglacial environments. A correlation of late glacial and deglacial events in the eastern part of Hudson Strait with the terrestrial record of a late glacial ice advance on southeastern Baffin Island is proposed. Potential ice sources for this late glacial event are examined.

Meltwater and ice-transported sediment derived from Hudson Strait are considered to have been a major source for Heinrich event sediments and associated changes in paleoceanographic conditions recognized in the North Atlantic Ocean. It has also been suggested that surges of late glacial ice across eastern Hudson Strait may represent analogues for behaviour of Antarctic ice in the future in response to global warming and rising sea levels.

As this report illustrates, Hudson Strait represents an extensive natural laboratory for study of a wide variety of Quaternary sedimentary and environmental parameters.

AVANT-PROPOS

L'étude des dépôts superficiels de la marge continentale fait partie du travail de la Commission géologique du Canada dans le domaine des géosciences marines. De telles recherches renseignent sur l'état du fond marin et sur les environnements actuels et passés et soutiennent les travaux d'ingénierie effectués sur le fond marin ainsi que l'étude de l'évolution du climat et des conditions paléocéanographiques.

Le présent bulletin donne les résultats d'études sur les sédiments et le Quaternaire supérieur du détroit d'Hudson et de la baie d'Ungava. Ces études ont été réalisées par la Commission géologique du Canada (Atlantique) en collaboration avec des chercheurs d'autres institutions (notamment la University of Colorado, l'Université de Montréal et la University of Louisiana) qui s'intéressent de près au Quaternaire supérieur de milieux terrestres et marins adjacents à cette région. Des chercheurs du Centre géoscientifique de Québec et de plusieurs autres universités ont également collaboré.

Ce rapport délimite les principales unités sédimentaires du Quaternaire, leur répartition, les milieux sédimentaires et les chronologies du Quaternaire supérieur et renseigne sur les événements tardiglaciaires, la déglaciation de la région et les milieux postglaciaires. Il propose une corrélation des événements tardiglaciaires et de la déglaciation dans la partie orientale du détroit d'Hudson avec les indications relevées d'une avancée tardiglaciaire sur le sud-est de l'île de Baffin. Les sources possibles des glaces de cet événement tardiglaciaire sont également examinées.

On considère que les eaux de fonte et les sédiments transportés par la glace provenant du détroit d'Hudson ont constitué une source importante des sédiments des événements Heinrich et des modifications connexes des conditions paléocéanographiques mises en évidence dans l'Atlantique Nord. Il a aussi été proposé que des crues tardiglaciaires dans la partie orientale du détroit d'Hudson s'apparenteraient au comportement futur de la glace de l'Antarctique en réaction au réchauffement planétaire et à la montée du niveau des océans.

Comme le montre ce rapport, le détroit d'Hudson constitue un vaste laboratoire naturel pour l'étude d'un large éventail de paramètres sédimentaires et environnementaux du Quaternaire.

CONTENTS

Summary/Sommaire 1

Introduction: geographic setting and studies
B. MacLean 5

Glacial-geological record on southern Baffin Island reflecting late glacial ice-sheet dynamics in the eastern Hudson Strait region
W.F. Manley and G.H. Miller 19

Patterns of ice flow and deglaciation chronology for southern coastal margins of Hudson Strait and Ungava Bay
J.T. Gray 31

Late Quaternary stratigraphy of Hatton and Resolution basins, east of Hudson Strait
J.T. Andrews, A.E. Jennings, and B. MacLean 57

Bedrock geology of Hudson Strait and Ungava Bay
B. MacLean 65

Quaternary sediments in Hudson Strait and Ungava Bay
B. MacLean, G. Vilks, I. Hardy, B. Deonarine, A.E. Jennings, and W.F. Manley . . . 71

Foraminiferal biostratigraphy and paleoceanography
A.E. Jennings, G. Vilks, B. Deonarine, A. Silis, and N. Weiner 127

Composition of sediments in Hudson Strait and Ungava Bay
I. Hardy 147

Studies of sediment colour, whole-core magnetic susceptibility, and sediment magnetism of the Hudson Strait–Labrador Shelf region: *CSS Hudson* cruises 90023 and 93034
F.R. Hall, J.T. Andrews, M. Kerwin, and L.M. Smith 161

Ice dynamics modelling of the Hudson Strait region at late glacial time
W.T. Pfeffer 171

Hudson Strait Quaternary sediments and late glacial and deglaciation history: a discussion and summary
B. MacLean, J.T. Andrews, J.T. Gray, F.R. Hall, I. Hardy, A.E. Jennings, W.F. Manley, W.T. Pfeffer, and G. Vilks 181

Author Index 193

IN MEMORIAM
Gus Vilks
1929–1997

SUMMARY

The Quaternary geology of Hudson Strait and Ungava Bay was examined by means of extensive surveys with Huntec™ deep-towed high-resolution seismic-reflection equipment, single-channel seismic-reflection systems, sidescan sonar in shallower areas, and by the collection and study of piston cores and grab samples.

Lower Paleozoic sedimentary rocks, mainly limestone, underlie most of Hudson Strait and form a central platform in Ungava Bay. Precambrian metamorphic and igneous rocks of the adjacent land areas bound these strata near the coasts of Baffin Island, Ungava, and Labrador peninsulas, and form most of the offshore islands. Akpatok Island in Ungava Bay, however, is composed of Paleozoic strata. Calcareous sediments and erratics eroded by glacial ice from the Paleozoic rocks are important indicators of ice-flow patterns and provenance.

Structurally controlled bedrock morphology and regional and local advances and retreats of Laurentide ice have been major factors in the deposition of Quaternary sediments in Hudson Strait and Ungava Bay. Extensive sediment accumulations occur in a large half-graben basin in eastern Hudson Strait and in two structurally similar, but smaller, en échelon basins in the western part of the strait. These are informally termed Eastern, Western, and Southwestern basins. Significant deposits of Quaternary sediments also occur in the south-central part of Hudson Strait, and in parts of Ungava Bay. The survey and sample data distinguish sediment units and facies relationships, and provide information regarding former glacial ice-margin positions and chronologies.

Quaternary sediments comprise five main units. These consist of ice-contact, glaciomarine, and postglacial muddy sediments, postglacial sands and gravels, and locally in eastern Hudson Strait, a unit interpreted to be composed of ice-contact or debris-flow sediments.

Ice-contact sediments are widespread throughout the region. They form the basal Quaternary sequences beneath glaciomarine and postglacial sediments in the basins, and are the main surficial sediment unit in interbasin areas. Very thick multisequence ice-contact deposits occur in four areas. These deposits reach 100 m in thickness in an area southeast of Nottingham Island in the western part of Hudson Strait, 150 m in eastern Ungava Bay, 180 m in Eastern basin, and 360 m at the sill at the eastern entrance to Hudson Strait. Elsewhere ice-contact deposits

SOMMAIRE

La géologie quaternaire du détroit d'Hudson et de la baie d'Ungava a été étudiée en effectuant des relevés détaillés au moyen d'un appareil Huntec de réflexion sismique haute résolution remorqué en profondeur, d'appareils monovoie à haute résolution, et d'un sonar latéral dans les zones peu profondes, ainsi qu'en analysant des échantillons prélevés à l'aide de carottiers à piston et de bennes.

Des roches sédimentaires du Paléozoïque inférieur, surtout du calcaire, se trouvent sous la plus grande partie du fond du détroit d'Hudson et forment une plate-forme centrale dans la baie d'Ungava. Des roches ignées et métamorphiques précambriennes des terres contiguës bordent ces strates près des côtes de l'île de Baffin et des péninsules d'Ungava et du Labrador, et forment la plupart des îles au large. Par contre, l'île Akpatok, située dans la baie d'Ungava, est composée de strates paléozoïques. Les sédiments calcaires et les blocs erratiques érodés des roches paléozoïques par la glace glaciaire constituent d'importants indicateurs du mode d'écoulement et de la provenance des glaces.

La morphologie du substratum rocheux régie par des facteurs structuraux ainsi que les avancées et retraits locaux et régionaux de l'Inlandsis laurentidien ont été des facteurs importants de la sédimentation quaternaire dans le détroit d'Hudson et la baie d'Ungava. On trouve de vastes accumulations de sédiments dans un grand bassin de demi-graben dans la partie orientale du détroit d'Hudson et dans deux bassins en échelons structuralement semblables, mais plus petits, dans la partie occidentale du détroit. On les désigne de façon officieuse bassins Est, Ouest et Sud-ouest. On trouve aussi d'importants dépôts de sédiments quaternaires dans le centre sud du détroit d'Hudson et dans certaines parties de la baie d'Ungava. Les données recueillies permettent de différencier les unités sédimentaires et de déterminer les relations entre les faciès, et nous renseignent sur les positions et chronologies des anciennes marges glaciaires.

Les sédiments quaternaires comportent cinq unités principales, soit des sédiments de contact glaciaire, des sédiments glaciomarins, des sédiments boueux postglaciaires, des sables et graviers postglaciaires et, à certains endroits dans le secteur oriental du détroit d'Hudson, une unité interprétée comme étant composée de sédiments de contact glaciaire ou de coulées de débris.

Les sédiments de contact glaciaire sont largement répandus dans la région. Dans les bassins, ils forment les séquences quaternaires de base sous les sédiments glaciomarins et postglaciaires, et ils constituent les principaux sédiments de surface dans les zones situées entre les bassins. On trouve des dépôts de contact glaciaire à séquences multiples très épais dans quatre régions; leur épaisseur atteint 100 m au dans une zone sud-est de l'île Nottingham dans la partie occidentale du détroit d'Hudson, 150 m dans le secteur oriental de la baie d'Ungava, 180 m dans le bassin Est et 360 m au seuil situé à l'entrée

commonly are in the order of a few metres to 10 m, but thicken locally in morainal deposits. Where sampled at three localities, the ice-contact sediments are diamicts.

Acoustically unstratified sediments interpreted to be ice-contact or debris-flow material occur locally in Eastern basin, where they lie on ice-contact sediments and are overlain by glaciomarine sediments. Overlying sediments rendered them inaccessible for sampling.

Glaciomarine sediments are confined to basin areas, where they overlie ice-contact sediments. They commonly are transitional to ice-contact sediments at former glacial ice-margin settings. The glaciomarine deposits are acoustically stratified clayey and silty sediments that are often rhythmically banded with silty and fine sandy laminations. Deposition occurred in ice-proximal and ice-distal environments. Deposits of glaciomarine sediments mainly range between 5 m and 20 m in thickness, but locally reach 60 m in Eastern basin.

Postglacial muddy sediments are mainly confined to basinal areas, where they overlie glaciomarine sediments. They thinly mantle or infill small depressions on ice-contact deposits locally in some interbasin areas. Thick deposits of postglacial sediments, ranging between 18 m and 30 m, occur in Burgoyne Bay, locally in Eastern basin, in western and southwestern basins, and in southern Ungava Bay. Typically these comprise clayey sediments that have been extensively bioturbated. These thick deposits contain a record of paleoceanographic conditions during the last ca. 8000 years.

Postglacial sediments of variable sandy and gravelly composition form a thin, 10–15 cm veneer on the seabed in areas outside the basins. These result mainly from the winnowing action of bottom currents, but may include material rafted by the seasonal ice cover.

Thick multisequence ice-contact deposits that occur at several localities in Hudson Strait, at the sill at the eastern entrance to the strait, and on the continental shelf are indicative of major glacial ice streams that flowed seaward through Hudson Strait at various times in the past. Sediment and meltwater flux from these events are thought to have been a source of Heinrich events recorded in the Labrador Sea and North Atlantic Ocean sediment sequences. Terrestrial glacial ice-flow data indicate eastward flow of Hudson Strait ice over Nottingham, Salisbury, and Mill islands at the western end of Hudson Strait. Hudson Strait ice impinged on only the tips of coastal promontories on Foxe and Ungava peninsulas, and the boundary between eastward-flowing Hudson Strait ice and coalescing ice from Ungava Peninsula and Baffin Island during the last glaciation of the region mainly lay offshore. Later northward-northeastward ice flow from Ungava Peninsula is evident in western and central areas of Hudson Strait. Marine data indicate this late advance

orientale du détroit d'Hudson. Ailleurs, les dépôts de contact glaciaire font habituellement de quelques mètres à 10 m d'épaisseur, mais par endroits, dans des dépôts morainiques, ils sont plus épais. Les sédiments de contact glaciaire échantillonnés à trois endroits sont diamictiques.

Par endroits dans le bassin Est, on trouve des sédiments acoustiquement non stratifiés que l'on interprète comme étant des dépôts de contact glaciaire ou de coulées de débris qui recouvrent des sédiments de contact glaciaire et qui sont eux-mêmes recouverts par des sédiments glaciomarins. Ces sédiments glaciomarins ont empêché de les échantillonner.

On ne trouve des sédiments glaciomarins que dans des bassins, où ils reposent sur des sédiments de contact glaciaire. Dans les anciens milieux de marge glaciaire, ils passent communément à des sédiments de contact glaciaire. Les dépôts glaciomarins sont des sédiments argileux et silteux acoustiquement stratifiés qui présentent souvent des laminations rythmiques de silt et de sable fin. Ils se sont accumulés dans des milieux glaciaires proximaux et distaux. Leur épaisseur varie principalement entre 5 et 20 m, mais atteint localement 60 m dans le bassin Est.

On trouve des sédiments boueux postglaciaires principalement dans les bassins, où ils reposent sur des sédiments glaciomarins. Par endroits dans certaines zones situées entre les bassins, ils remplissent ou recouvrent d'une mince couche de petites dépressions dans des dépôts de contact glaciaire. On trouve des sédiments postglaciaires, dont l'épaisseur varie entre 18 et 30 m, dans la baie Burgoyne, localement dans le bassin Est, dans des bassins de l'ouest et du sud-ouest et dans le sud de la baie d'Ungava. Il s'agit habituellement de sédiments argileux très bioturbés. Ces dépôts épais renferment des données sur les conditions paléocéanographiques des derniers 8000 ans.

Hors des bassins, des sédiments postglaciaires de composition sableuse et graveleuse variée forment un placage de 10 à 15 cm d'épaisseur sur le fond marin. Ces sédiments sont le produit principalement du lavage par l'action des courants de fond, mais ils peuvent comprendre des matériaux transportés par les glaces saisonnières.

Les dépôts épais de contact glaciaire à séquences multiples que l'on trouve à plusieurs endroits dans le détroit d'Hudson, au seuil situé à l'entrée orientale du détroit et sur la plate-forme continentale, témoignent d'importants courants glaciaires qui s'écoulaient vers l'océan par le détroit d'Hudson à divers moments dans le passé. On croit que les apports de sédiments et d'eaux de fonte liés à ces événements auraient donné lieu aux événements Heinrich enregistrés dans les séquences de sédiments de la mer du Labrador et de l'Atlantique Nord. Des données d'écoulement glaciaire recueillies sur terre révèlent que les glaces du détroit d'Hudson se sont écoulées vers l'est sur les îles Nottingham, Salisbury et Mill, situées à l'extrémité occidentale du détroit d'Hudson. Ces glaces n'ont chevauché que le bout des promontoires côtiers des péninsules Fox et d'Ungava; lors de la dernière glaciation qui a touché la région, la limite entre les glaces du détroit d'Hudson à écoulement vers l'est et les glaces coalescentes de la péninsule d'Ungava et de l'île de Baffin était principalement au large. Des indications d'un écoulement glaciaire subséquent vers le nord-nord-est en

was of limited extent. A radial pattern of ice flow into Ungava Bay is evident from terrestrial data. Akpatok Island shows evidence of a local ice cap and impingement of ice flowing from the west and southwest.

On eastern Meta Incognita Peninsula, ice-flow indicators show ice flow was to the northeast. This northeasterly flowing ice has been interpreted to have impinged on this region on at least three occasions: during the Younger Dryas (H-0) event, ca. 11–10 ka BP; during the Gold Cove advance, 9.9–9.6 ka BP; and during the Noble Inlet advance, 8.9–8.4 ka BP (^{14}C years).

Eastern Basin was occupied during the time of the Noble Inlet advance by an ice sheet that was fully grounded on the basin floor. Grounding (lift-off) lines recorded by sediment transitions and morphologies on the flanks of the basin reflect the progressive thinning of the ice sheet as it waned. This pattern is compatible with the glacial record from Meta Incognita Peninsula during the Noble Inlet advance, as are radiocarbon dates from glaciomarine sediments downslope from the upper grounding line. These correspond to the latter part of the Noble Inlet event. The depth of the upper grounding line on the basin flanks approximates that at the sill at the entrance to Hudson Strait. This, and the absence of glaciomarine sediments higher on the basin flanks, suggest that rapid deglaciation of eastern Hudson Strait occurred when the ice sheet ceased to be pinned at the Hudson Strait sill. An advance of Quebec–Labrador ice centred through Ungava Bay appears to be the most probable source of the ice that occupied Eastern basin and overrode eastern Meta Incognita Peninsula during the Noble Inlet advance, although there are some unresolved concerns with this interpretation. Neither of the other potential sources, Baffin Island ice, nor a Hudson Strait ice stream appear feasible. Glaciological modelling studies have demonstrated that advance of glacial ice across Hudson Strait from Quebec–Labrador is a glaciologically plausible interpretation. Ice of these late across-the-strait glacial advances did not extend far seaward of the sill at the entrance to the strait, unlike earlier major Hudson Strait ice streams, which extended to the outer shelf and shelf break and contributed sediments and meltwater to the Labrador Sea and North Atlantic Ocean.

The change from glaciomarine to postglacial marine conditions occurred ca. 8000–7800 BP in eastern and central Hudson Strait, and possibly slightly later in the west. A later change to cooler, less saline conditions of the present day occurred at ca. 5500 BP.

provenance de la péninsule d'Ungava sont évidentes dans des régions occidentales et centrales du détroit d'Hudson. Des données marines indiquent que cette avancée tardive était peu étendue. Des données terrestres mettent en évidence un écoulement radial des glaces vers la baie d'Ungava. Dans l'île Akpatok, on a trouvé des indications d'une calotte glaciaire locale et du passage de glaces provenant de l'ouest et du sud-ouest.

Sur la partie orientale de la péninsule Meta Incognita, des marques d'écoulement glaciaire révèlent que l'écoulement était vers le nord-est. Les glaces auraient touché la région à au moins trois reprises : pendant l'événement du Dryas récent (H-0; vers 11–10 ka BP); pendant l'avancée de Gold Cove (9,9–9,6 ka BP); et pendant l'avancée de Noble Inlet (8,9–8,4 ka BP) (années ^{14}C).

Lors de l'avancée de Noble Inlet, le bassin Est était occupé par une nappe glaciaire qui était entièrement ancrée au fond du bassin. Les lignes d'ancrage (désancrage) indiquées par les transitions et morphologies des sédiments sur les flancs du bassin témoignent de l'amincissement graduel de la nappe glaciaire. Cette situation est compatible avec les indices de glaciation laissés sur la péninsule Meta Incognita pendant l'avancée de Noble Inlet, tout comme l'est la datation au radiocarbone des sédiments glaciomarins situés en bas de la pente par rapport à la ligne d'ancrage supérieure. Ces sédiments se seraient déposés lors de la dernière partie de l'événement de Noble Inlet. La profondeur de la ligne d'ancrage supérieure sur les flancs du bassin s'approche de celle sur le seuil situé à l'entrée du détroit d'Hudson. Cet état de fait et l'absence de sédiments glaciomarins plus haut sur les flancs du bassin laissent croire que la nappe glaciaire s'est retirée rapidement du secteur oriental du détroit d'Hudson une fois qu'elle s'est désancrée du seuil du détroit. Une avancée des glaces de la région Québec–Labrador centrée sur la baie d'Ungava semble avoir été la source la plus probable des glaces qui ont occupé le bassin Est et ont chevauché la partie orientale de la péninsule Meta Incognita pendant l'avancée de Noble Inlet. Cette interprétation présente quelques problèmes non résolus, mais aucune des autres sources possibles, soit des glaces de l'île de Baffin et un courant glaciaire du détroit d'Hudson, ne semblent plausibles. Des études de modélisation glaciologique ont montré qu'une avancée glaciaire qui aurait traversé le détroit d'Hudson à partir de la région Québec–Labrador constituait une interprétation plausible. Ces avancées glaciaires tardives sur le détroit ne se sont pas étendues loin au large du seuil situé à l'entrée du détroit, contrairement à d'importants courants glaciaires qui s'étaient étendus auparavant sur le détroit d'Hudson jusqu'à la plate-forme continentale externe et l'accore en apportant des sédiments et des eaux de fonte à la mer du Labrador et à l'Atlantique Nord.

Les conditions glaciomarines ont passé à des conditions marines postglaciaires vers 8000–7800 BP dans les parties orientale et centrale du détroit d'Hudson, et peut-être un peu plus tard dans la partie occidentale. Vers 5500 BP, les eaux se sont refroidies et sont devenues moins salines, conditions qui persistent encore de nos jours.

Introduction: geographic setting and studies

Brian MacLean[1]

MacLean, B., 2001: Introduction: geographic setting and studies; in *Marine Geology of Hudson Strait and Ungava Bay, Eastern Arctic Canada: Late Quaternary Sediments, Depositional Environments, and Late Glacial–Deglacial History Derived from Marine and Terrestrial Studies, (ed.) B. MacLean; Geological Survey of Canada, Bulletin 566, p. 5–17.*

Abstract: Hudson Strait is a major waterway that links Hudson Bay and Foxe Basin with the Labrador Sea and North Atlantic Ocean. Ungava Bay forms a large embayment adjoining the eastern part of the strait. In the past, Hudson Strait has been a major discharge route for glacial ice from the northeast sector of the Laurentide Ice Sheet to the North Atlantic Ocean.

Extensive surveys with high-resolution seismic equipment and sampling of seabed sediments, mainly by piston coring techniques, have delineated the principal surficial sediment units, their distribution and depositional environments, and provide information regarding glacial ice margins, glacial-marine interactions, and late glacial-deglacial history, including relationships with events recognized in adjoining terrestrial and marine areas.

This paper reviews the bathymetric and oceanographic settings, seasonal ice conditions, methods of investigation, and the results of previous marine studies. It also acknowledges the significant contributions to this study by many other workers.

Résumé : Le détroit d'Hudson constitue une importante voie d'eau qui relie la baie d'Hudson et le bassin Foxe, d'une part, et la mer du Labrador et l'Atlantique Nord, d'autre part. La baie d'Ungava forme une énorme échancrure contiguë à la partie orientale du détroit. Par le passé, le détroit d'Hudson a formé un important passage par où la glace glaciaire provenant du secteur nord-est de l'Inlandsis laurentidien s'écoulait vers l'Atlantique Nord.

Des relevés détaillés effectués au moyen d'appareils séismographiques à haute résolution et par échantillonnage des sédiments du fond marin (surtout à l'aide de carottiers à piston) ont permis de déterminer les principales unités de sédiments superficiels, leur répartition et les milieux sédimentaires, nous renseignant ainsi sur les marges glaciaires, sur les interactions entre les glaces et la mer et sur l'histoire du tardiglaciaire et de la déglaciation, notamment les relations avec des événements mis en évidence dans les régions terrestres et marines adjacentes.

Le présent article aborde les milieux bathymétrique et océanographique, les conditions de glace saisonnière, les méthodes utilisées et les résultats d'études antérieures, et reconnaît les contributions importantes que de nombreux autres chercheurs ont apportées à cette étude.

[1] Geological Survey of Canada (Atlantic), Bedford Institute of Oceanography, Dartmouth, Nova Scotia B2Y 4A2

INTRODUCTION

Hudson Strait is a major marine waterway, some 800 km in length and 90 km in width, that links the shallow epicontinental seas of Hudson Bay and Foxe Basin with the Labrador Sea and the North Atlantic Ocean. Hudson Strait is bounded to the north by Baffin Island and to the south by Ungava and Labrador peninsulas and by Ungava Bay, which forms a large embayment that adjoins the eastern part of the strait (Fig. 1). This region has been a major discharge route for glacial ice and meltwater from the Laurentide Ice Sheet and probably from preceding (pre-Wisconsinan) ice sheets, to the Labrador Sea and North Atlantic Ocean. Accessible sediment deposits in Hudson Strait and Ungava Bay provide a record of changing conditions extending from late glacial to modern times.

This bulletin comprises a series of individually authored contributions, which outline the principal Quaternary sediment units in Hudson Strait and Ungava Bay, their occurrence, composition, biostratigraphy, depositional environments, chronologies, and magnetic susceptibility characteristics. The late glacial and deglaciation records from adjacent terrestrial and marine areas are discussed, and results of glaciological modelling studies are presented. A summary of the bedrock geology is included. Investigations of the marine areas in Hudson Strait and Ungava Bay were mainly by means of high-resolution seismic-reflection surveys, and analyses of sediment cores and other samples, obtained during five geological cruises between 1985 and 1993, together with information from earlier and coincident investigations in some eastern and western areas by Grant and Manchester (1970), Josenhans et al. (1986), Josenhans and Zevenhuizen (1990), and by

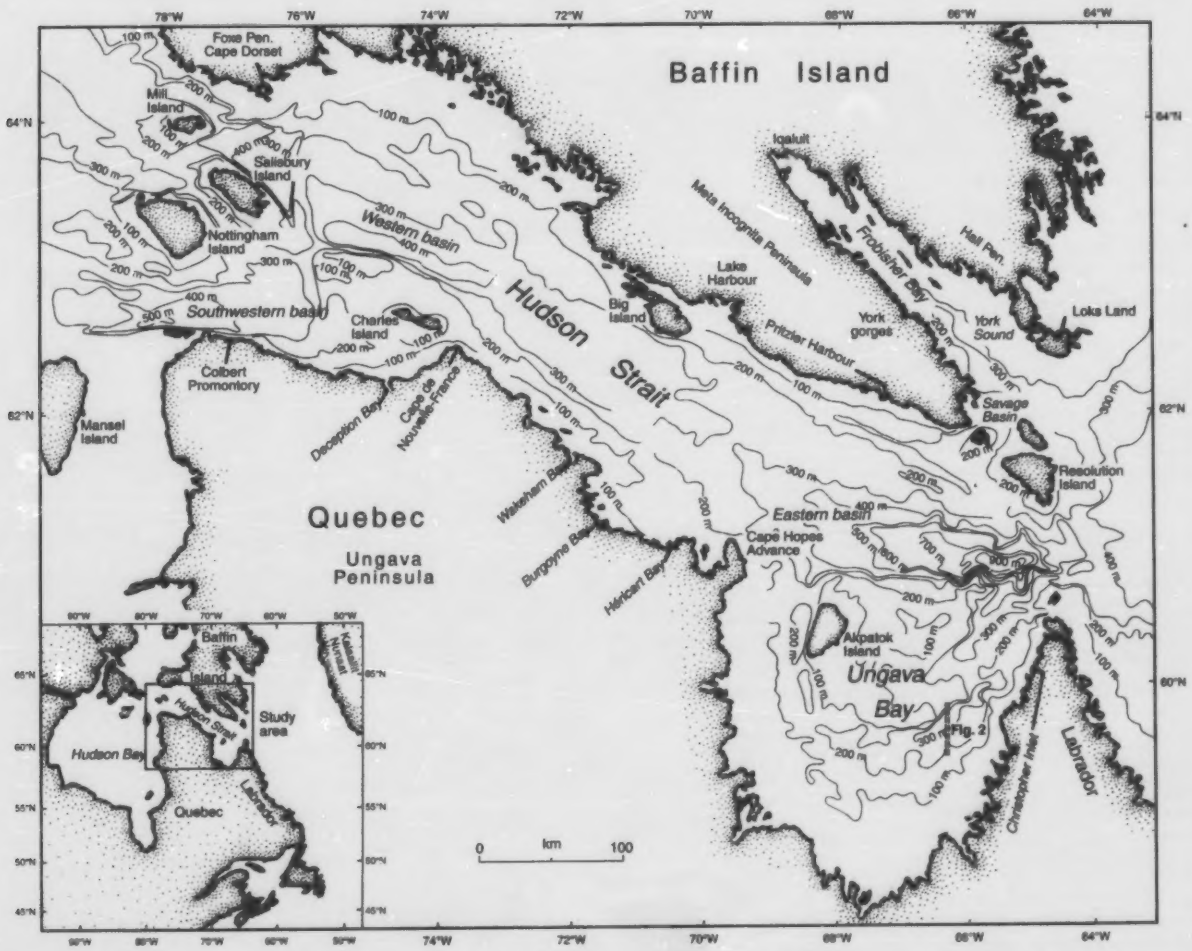

Figure 1. Generalized bathymetry of Hudson Strait and Ungava Bay, showing locations of areas informally referred to as Eastern basin, Western basin, and Southwestern basin in this report. Areas outlined indicate deep basin floor and lower basin flank areas. Location of Figure 2 in southeastern Ungava Bay is indicated.

C.L. Amos (unpub. data, 1979) and K. Asprey (unpub. data, 1980). The results provide information regarding ice-margin geometries, glacial-marine interactions, sedimentation patterns, and paleoceanographic conditions during the transition from late glacial to postglacial conditions. The record from the marine areas is examined relative to late glacial and deglacial events recognized from terrestrial investigations on southern Baffin Island, Ungava and Labrador peninsulas, Akpatok Island, and other offshore islands by researchers from various institutions, together with the sediment record on the continental shelf. Late glacial events described here may in part constitute analogues of earlier glacial conditions, and may also be analogues for future behaviour of the Antarctic Ice Sheet associated with global warming as suggested by Andrews and Tedesco (1992).

Hudson Strait was a major channel for drawdown of Laurentide ice from Hudson Bay and adjacent Quebec and Baffin Island land masses and for discharge of glacial ice and meltwater onto the continental shelf and into the North Atlantic Ocean (*see* e.g. Dyke and Prest, 1987; Hughes, 1987; Andrews, 1989; Andrews et al., 1995b). The glacial ice and meltwater flux from Hudson Strait are thought to have exerted important influences on sedimentary and paleoceanographic processes (e.g. Heinrich events) in the Labrador Sea and North Atlantic Ocean (*see* e.g. Heinrich, 1988; Andrews and Tedesco, 1992; Bond et al., 1992; Broeker et al., 1992; Hillaire-Marcel et al., 1994; Dowdeswell et al., 1995; Andrews, 1998). Marine waters adjacent to and within Hudson Strait were source areas for precipitation on the high plateaus of Quebec–Labrador and Baffin Island (together with adjacent areas of the District of Keewatin and Ontario), areas which were considered by Dyke et al. (1989) to have played a vital part in the initiation of the Laurentide Ice Sheet and its predecessors.

Similar factors may have been important forces in subsequent regional and local ice-sheet expansions and contractions. Among these were relatively short-lived glacial ice advances interpreted to have crossed eastern Hudson Strait from Quebec–Labrador on at least three occasions, and to have variably overridden parts of southeastern Baffin Island and adjacent inner areas of the continental shelf between 11–10 ka BP, 9.9–9.6 ka BP, and 8.9–8.4 ka BP (radiocarbon years). The oldest of these events, recognized as H-0 or DC-0 in the Labrador Sea and North Atlantic Ocean, was interpreted by Andrews et al. (1995a) to have originated from an ice centre over Quebec–Labrador together with ice from another source or sources farther north. Miller and Kaufman (1990) suggested that reduced sea surface and air temperatures resulting from discharge of ice into the North Atlantic Ocean from Hudson Strait combined with increased St. Lawrence River discharge may have caused the Younger Dryas event. The two later glacial advances (Gold Cove and Noble Inlet), interpreted from terrestrial ice-flow indicators (glacial striae, carbonate-rich drift, erratics, and associated deltaic deposits) on Baffin Island, have been extensively discussed by Stravers (1986), Miller et al. (1988), Miller and Kaufman (1990), Stravers et al. (1992), Kaufman et al. (1993a), Manley (1995), and Manley and Miller (2001). These studies interpreted the Gold Cove advance, the second of these events, to have extended northward along Hall Peninsula nearly to Brevoort Island, whereas the subsequent Noble Inlet advance did not reach beyond Meta Incognita Peninsula and adjacent islands. The more limited extent of the Noble Inlet advance is supported by morainal deposits in Savage basin (Stravers and Powell, 1997). Studies of the marine record in Eastern basin (Jennings et al., 1996a, 1998; *see also* MacLean et al., 2001a, b), indicate the presence of a grounded and gradually thinning ice sheet that is consistent with the timing and behaviour of the Noble Inlet advance.

Differing views have been expressed regarding ice sources and configurations for some of these late ice advances on Meta Incognita Peninsula: *see* discussion by England and Smith (1993), who proposed alternate interpretations relating to the Gold Cove and Noble Inlet events, including a local ice source on Meta Incognita Peninsula, and response by Kaufman et al. (1993b). Concerns relating to the latest of these postulated ice advances (Noble Inlet) have been expressed by Lauriol and Gray (1997) on the basis of isotopic ^{18}O composition and ages of mollusc shells, which they considered to be indicative of uninterrupted circulation of marine waters in Hudson Strait at the time of the Noble Inlet advance; and by Gray (2001) based on the above, constraints indicated by the distribution of carbonate drift and erratics (and their absence) on parts of eastern Meta Incognita Peninsula and adjacent islands, and the late glacial record from Akpatok Island.

Westward along Hudson Strait, the terrestrial record shows mainly ice flow towards Hudson Strait from Baffin Island (Blake, 1966; Clarke, 1985; Manley, 1995; Hodgson, 1997; Manley and Miller, 2001) and from Ungava Peninsula (Gray and Lauriol, 1985; Lauriol and Gray, 1987; Bruneau and Gray, 1991, 1997; Gray et al., 1993; Daigneault, 1996; Gray, 2001), except where easterly flowing Hudson Strait ice impinged on tips of coastal promontories. Ice converged into Ungava Bay in the south and west (Gray and Lauriol, 1985; Lauriol and Gray, 1987; Allard et al., 1989) and from parts of northern Labrador peninsula (Gray et al., 1996; Gray, 2001). Ice flow was easterly on Nottingham, Salisbury, and Mill islands at the western end of the strait (Laymon, 1988, 1992).

As a major route for discharge of Laurentide ice and meltwater from the continental interior, Hudson Strait at times would have been very strongly affected by events in Hudson Bay to the west. *See* Hillaire-Marcel (1976), Andrews et al. (1983), Dyke and Prest (1987), Andrews (1989), Dredge and Cowan (1989), Dyke and Dredge (1989), Vincent (1989), Piper et al. (1990), and Clark et al. (1993) for reviews of the glacial and deglaciation history; and Josenhans and Zevenhuizen (1990) and Bilodeau et al. (1990) for results of marine studies in Hudson Bay. Rapid deglaciation of Hudson Bay occurred between about 8400 BP and 8000 BP (Dyke and Prest, 1987) with drainage of glacial Lake Ojibway and entry of the Tyrrell Sea at ca. 8100–8000 BP (Hillaire-Marcel, 1976; Vincent, 1989).

BATHYMETRY AND PHYSIOGRAPHIC SETTING

The generalized bathymetry derived from Chart 5450 (Canadian Hydrographic Service, 1970) is illustrated in Figure 1. The bathymetry of Hudson Strait reflects large-scale control imparted by the underlying bedrock structures, together with the effects of erosion, and the deposition of Quaternary sediments. In a few localities, the sediments reach more than 100 m in thickness. Water depths in excess of 300 m are nearly continuous along Hudson Strait, and greatest depths occur in three half-graben basins: informally designated Eastern, Western, and Southwestern basins in this report.

Eastern basin, which lies in the eastern part of the strait north of Ungava Bay, is the deepest and morphologically most pronounced of the basins. It has an elongated, narrow, deep floor with water depths that reach in excess of 900 m in the eastern part of the basin. Water depths shallow progressively toward the north and west. A fault scarp that constitutes the southern margin of Eastern basin forms an abrupt demarcation between Hudson Strait and Ungava Bay. A narrow sill at a depth of about 385–400 m at the eastern entrance to Hudson Strait separates Eastern basin from the continental shelf.

Western basin lies north of Charles Island in the western part of the strait. It is an elongated basin oriented west-northwest–east-southeast, approximately parallel to the axis of Hudson Strait in that area. Maximum water depths exceed 400 m. As in Eastern basin, water depths in Western and Southwestern basins progressively shallow northward.

Southwestern basin lies southwest of Charles Island and extends westward between Nottingham Island and the western part of Ungava Peninsula. Maximum water depths locally exceed 500 m.

A relatively shallow platform, here informally termed the 'Charles Island platform', with depths mainly in the 90–170 m range separates Western and Southwestern basins. It is almost continuous with a similar but smaller platform area extending southeastward from Salisbury Island (Fig. 1).

Maximum water depths along the central region of Hudson Strait are typically in the 300 m range except locally in the area immediately west of Eastern basin where they are slightly shallower. Depths of 100 m or more extend to within a few kilometres of both the north and south coasts of the strait in many localities.

Bathymetric data are sparse or lacking in several coastal areas, most notably in the region lying east of Cape Dorset in the northwestern part of Hudson Strait, and in parts of western and southern Ungava Bay.

In Ungava Bay a large relatively smooth-topped shallow platform forms the central part of the bay. Akpatok Island, with elevations to 285 m, lies on the platform adjacent to its western margin (Fig. 1). Depths over the platform mainly range between 50 m in the southwest and 150 m in the east and north. Shallowest depths occur over the southwestern part of the platform and adjacent to Akpatok Island. Vertical and steeply stepped walls up to 250 m in height (Grant and Manchester, 1970) illustrated in Figure 2 separate the platform from a marginal channel that surrounds the central platform on the west, south, and east. Maximum depths in the marginal channel range from 250 m in the southwest to 365 m in the east. In contrast to many other coastal areas of Hudson Strait and Ungava Bay, where water depths in the order of 100 m or more occur relatively close to the present coast, a wide zone containing depths shallower than 100 m borders coastal areas of western and southern Ungava Bay (Fig. 1). Where data are available, bathymetry of the shoreward 15–20 km of this zone is very irregular, commonly with depths less than 20 m.

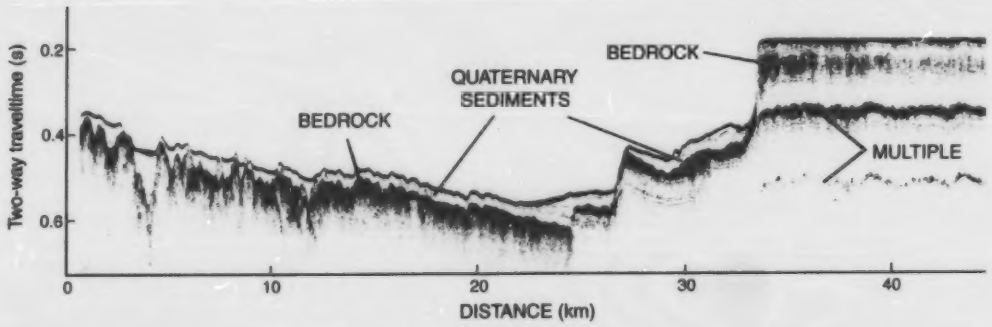

Figure 2. *Single-channel seismic-reflection profile illustrating precipitous morphology at the margin of the central platform in southeastern Ungava Bay. Thick deposits of Quaternary sediments in the marginal channel contrast with very thin deposits on the platform. The boundary between Precambrian rocks and the Paleozoic strata that form the platform occurs approximately 18 km along section (see Fig. 1 for location).*

Relative sea-level elevations at the time of deglaciation stood higher than present due to isostatic depression of the crust by ice loading. Marine limit elevations, ranging between 123 m and 175 m, occur in southern Ungava Bay and westward along the coast of Ungava Peninsula, whereas those along the southern coast of Baffin Island range from less than 30 m in the east to 195 m in the west (Gray et al., 1993).

OCEANOGRAPHY

The major characteristics of the water mass in Hudson Strait and to a lesser extent in Ungava Bay were discussed by Drinkwater (1986), from which the following brief summary is derived. Additional salient features were summarized by Vilks et al. (1989). Figure 3 shows the surface circulation pattern. The region is influenced by water inputs from three main sources and by strong tidal currents. Low-salinity waters from Hudson Bay and Foxe Basin, which includes net flow from the Arctic Archipelago through Fury and Hecla Strait, enter the western end of Hudson Strait and flow eastward along the south side of the strait. High-salinity ocean waters of the Baffin Land Current and Labrador Sea enter the eastern end of Hudson Strait and extend westward along the north side of the strait. Some of these waters flow southward across the strait over Eastern basin and in the area east of Big Island and merge with the eastbound flow along the south side. Surface temperatures and salinities during the ice-free period show a marked across-channel gradient all along Hudson Strait with temperatures being higher and salinities lower to the south. Water entering eastern Hudson Strait includes a strong inflow at depth and intense vertical mixing occurs. This creates a nearly homogeneous water mass in the upper 200 m or more that is characterized by relatively low temperature and high salinity. Temperatures of the underlying waters in the eastern part of Hudson Strait increase with depth below 200 m. In the western part of the strait depths below 200 m consist almost entirely of polar water. Circulation in Ungava Bay is mainly counter-clockwise. Limited oceanographic data indicate lower salinities there than in southern Hudson Strait due to large volumes of fresh water delivered by rivers that drain into Ungava Bay. Only the northeast section of the bay comes under the influence of warmer, more saline waters from the Labrador Sea.

The Hudson Strait–Ungava Bay region is macrotidal. Tides are greatest in the eastern part of the strait and in Ungava Bay where they reach 12.4 m, and diminish westward to 4.7 m at Nottingham Island (Pilot of Arctic Canada, 1959). The main tidal current in Hudson Strait is strong, reaching rates of several knots in some areas (Pilot of Arctic Canada, 1959; Chart 5450, Canadian Hydrographic Service, 1970).

SEA ICE

Sea ice covers Hudson Strait and Ungava Bay for about eight months of the year. This originates from three main sources: winter ice that forms in the region; ice from Foxe Basin and

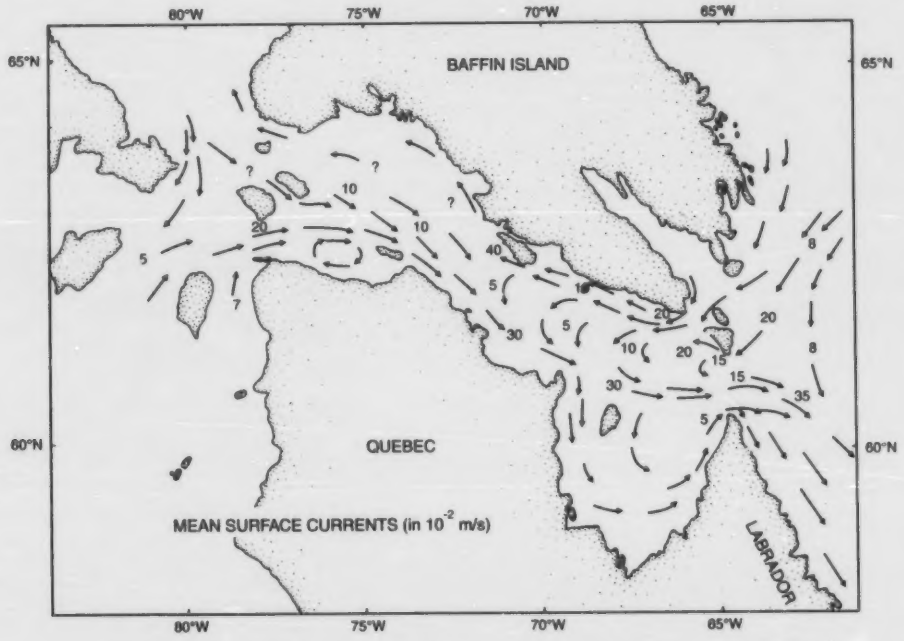

Figure 3. *Surface currents in Hudson Strait and Ungava Bay (after Drinkwater (1986) and Vilks et al. (1989, Fig. 3)). Reprinted with permission from Géographie physique et Quaternaire.*

Hudson Bay that moves eastward into Hudson Strait; and ice from Baffin Bay, Davis Strait, and from offshore eastern Baffin Island that is carried into Hudson Strait by the westbound current. Icebergs enter Hudson Strait from the east and are carried northwestward along the south coast of Baffin Island. Most icebergs cross Hudson Strait east of Big Island and exit the strait in the eastbound current on the south side, but some continue westward as far as Nottingham Island (Pilot of Arctic Canada, 1959; Drinkwater, 1986). Some icebergs also are carried into and around Ungava Bay, mainly in a counter-clockwise direction.

METHODS (MARINE PROGRAMS)

Results for the marine areas of Hudson Strait and Ungava Bay presented in this report come primarily from studies of the seabed geology carried out from *CSS Hudson* during cruises 85027, 90023, and 93034, together with data obtained on an opportunity basis on cruises 82034, 86027, and 92028. These investigations utilized a variety of marine geological and geophysical profiling systems to delineate and sample the seabed and sub-bottom geology. Cruise tracks and core and sample locations are indicated on Figures 4 and 5.

The main survey systems included a Huntec™ deep-towed high-resolution seismic-reflection system fitted with internal and towed hydrophones, and a single-channel seismic-reflection system using a 655 cm^3 compressed air source and (Bolt Technology™ and Haliburton Geophysical™ air and sleeve guns) Nova Scotia Research Foundation™ LT-18 hydrophone. Seismic reflection data were also acquired using 7.6 and 30 m Seismic Engineering™ hydrophone arrays. Towing speed generally was between 5 and 6 knots. A hull-mounted 3.5 kHz 16 transducer array provided sub-bottom profile data where high-speed steaming was required, on station, and at a few other times when the

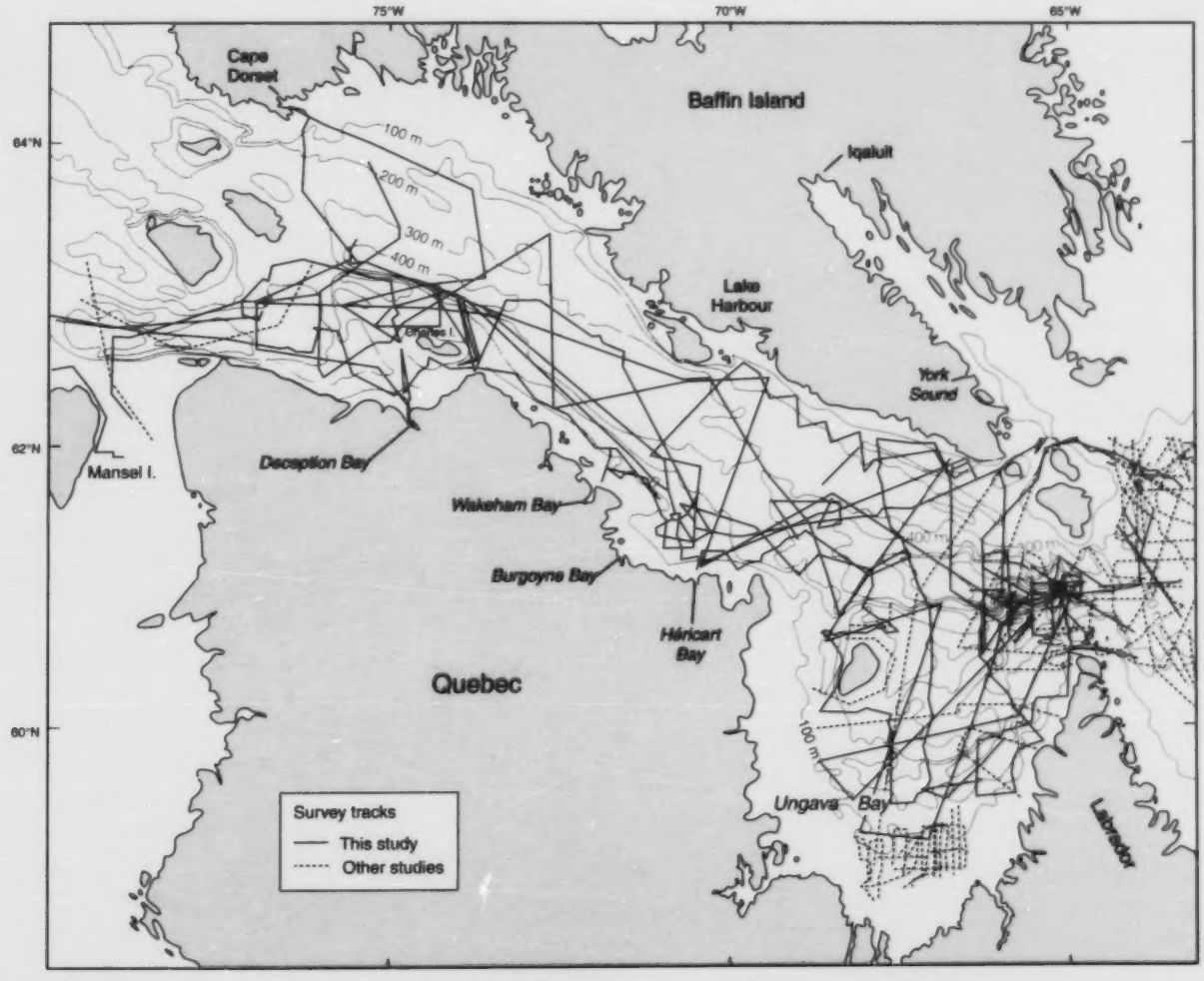

Figure 4. Map showing survey tracks.

Huntec™ system was being serviced. Simultaneous acquisition of data with these systems provided information on both the bedrock and overlying unconsolidated Quaternary sediments. Sidescan sonar data on seafloor features were obtained by means of the Bedford Institute of Oceanography Side Scan Sonar System at 72.5 kHz which provided data along a 1.5 km swath (750 m to either side of the ship's track) in areas where water depths were less than 200 m (the approximate effective limit of the system), and where constraints imposed by the number and configuration of towed systems, currents, and sea conditions permitted. Magnetometer data provided additional bedrock data on cruises 85027, 90023, and 93034. This information was used in support of the seismic data in differentiation of the boundaries between Paleozoic and Precambrian rocks.

Sampling of Quaternary sediment sequences on cruises 85027, 92028, and 93034 mainly was by means of Benthos™ piston corers (6.7 cm I.D.) fitted with a 1364 kg head, which provided very good penetration and core recovery up to 15 m subseafloor depth. Cores recovered on cruise 90023 were by means of the AGC Large Diameter Corer (9.9 cm I.D.). Box-core samples of the top 0.5 m of seafloor sediments were obtained at practically all of the piston core stations. Benthos™ and Leheigh gravity corers used as trigger weight corers also were used alone at a few stations. Attempts to sample ice-contact and other areas of 'hard' sediment in interbasin areas mainly utilized a modified 0.5 m^3 IKU™ clam-shell sampler, and to a lesser extent a large van Veen sampler. Samples of sediments collected in the clam-shell samplers were sluiced and lithologies of the coarse fraction of those samples and of clasts in cores were studied by Klassen (*in* MacLean et al., 1986), Dorion (1991; A. Dorion, unpub. report, 1991) and by Daigneault (1994a, b). Other studies included in situ measurements of sediment temperature and pore pressure at selected core localities by Taylor and Allen (1991), and of the "marine macrobenthos" by Aitken (1991).

Sediment cores were split, photographed, described, and subsampled at sea. Magnetic susceptibility measurements were made by researchers from the Institute of Arctic and Alpine Research, University of Colorado on all the cores prior to splitting. The archive halves of the cores were X-rayed at GSC (Atlantic) following each cruise. Studies of foraminiferal assemblages in the cores mainly were

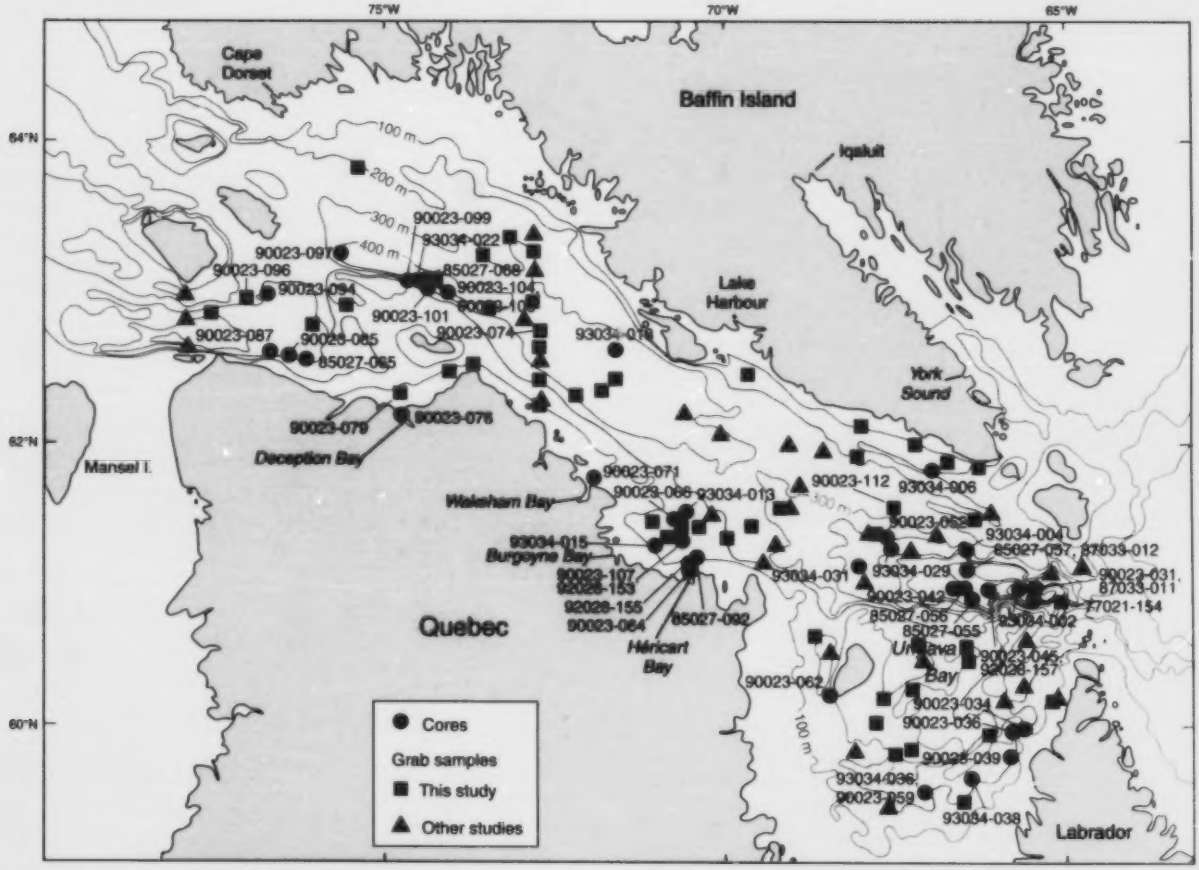

Figure 5. *Map showing locations where samples of Quaternary sediments were obtained during this study.*

undertaken by GSC (Atlantic), but faunal studies of cores from the eastern part of Eastern basin were carried out by the Institute of Arctic and Alpine Research together with textural or other analyses on selected cores. Dating of samples was undertaken mainly by GSC (Atlantic) and by the Institute of Arctic and Alpine Research, University of Colorado.

The precision of available navigational positioning systems improved steadily during the time span of this study, primarily due to the development of the Global Positioning System (GPS) and its availability for civilian use. Positioning during cruises 82034 and 85027 mainly was by BIONAV, an integrated system utilizing Satellite Navigation and Loran-C, supplemented by radar fixing where possible, and providing an accuracy to within approximately 300 m to more than 500 m. Global Positioning System positioning was available for approximately 10 hours per day during cruise 86027 and 20 hours per day during cruise 90023 with positioning accuracy ranging between about 25 m and 150 m. Differential GPS systems used on cruise 93034 provided positioning accuracies of 5–15 m. The greater positioning precision, together with station-approach and on-station data from the hull-mounted 3.5 kHz profiling system, facilitated correlations of core and acoustic profile data. *See* MacLean et al. (1986, 1991, 1994b) for field data relating to cruises 85027, 90023, and 93034.

PREVIOUS MARINE GEOSCIENCE STUDIES RELATING TO HUDSON STRAIT AND UNGAVA BAY

From geophysical surveys in the mid- and late 1960s, Grant and Manchester (1970) outlined the extent of Paleozoic strata in Ungava Bay and the structural and bedrock setting at the eastern end of Hudson Strait. Those earlier studies also provided initial information on the unconsolidated Quaternary sediments overlying the bedrock, and examined the erosional record as indicated by seabed morphology and bedrock components. Thick accumulations of sediments interpreted to be glacial deposits were noted along the east side of Ungava Bay; thick sediments were also noted in the deep eastern part of Hudson Strait. Grant and Manchester (1970) suggested that the morphology of the seabed in the marginal channel in eastern Ungava Bay may result from erosion by an ice stream flowing northeasterly toward Gray Strait (between Button–Lawson islands and Killiniq Island at the northern tip of Labrador) where Løken (1967) had inferred northeasterly glacial ice flow. Fillon and Harmes (1982) obtained a sediment core (77021-154) and high-resolution seismic data in the eastern part of Eastern basin. Although the core apparently was collected from a turbidite sequence, dates of 8730 ± 250 BP and 9100 ± 480 BP obtained on shells from that core provide chronological data regarding marine conditions. Other relevant marine field investigations in Hudson Strait prior to the start of this study in 1985 included: collection of sediment samples by Department of Fisheries and Oceans in connection with shrimp studies, and by P. Jones and K.F. Drinkwater (unpub. report, 1982) in conjunction with chemical, physical, and biological oceanographic studies of Hudson Strait; studies of tidal currents by Drinkwater (1983, 1986); and collection of shallow borehole samples of bedrock and seismic data in the region northeast of Cape Hopes Advance (MacLean and Williams, 1983). Surveys conducted by C.L. Amos and K. Asprey in southern Ungava Bay provided information concerning sediment distribution and thickness.

Information derived from sediment cores and seismic data obtained during the current study has been published in various formats as this project proceeded. These included reconnaissance data on bedrock units and structure, and preliminary information on the surficial sediments of Hudson Strait, from seismic profiles, shallow boreholes, and piston cores (MacLean et al., 1986). These initial results were followed by interpretations of Late Quaternary paleoceanography, biostratigraphy, and depositional environments from foraminifers and textural information from sediment cores in conjunction with data from high-resolution seismic profiles by Vilks et al. (1989), MacLean et al. (1992), Silis (1993), and Jennings et al. (1995, 1998, 2001). A preliminary map compilation showing distribution of the principal surficial sediment units (*in* Piper et al. (1990) was combined with additional data on sediment thicknesses, chronologies, depositional environments, and glacial history from further field studies (profile and core data) by MacLean et al. (1993, 1994a, 1995, 1996) and MacLean (1998). Studies of lithologies of the coarse fraction in samples of seabed sediments obtained by IKU™ and vanVeen clam-shell samplers and of clasts in cores, where accessible, from Hudson Strait and Ungava Bay provided information regarding distribution and dispersal patterns of indicator rock lithologies (Klassen *in* MacLean et al., 1986; A. Doiron, unpub. report, 1991; Daigneault, 1994b). Studies of whole-core magnetic susceptibility and rock and sediment magnetism in sediment cores from various parts of Hudson Strait by Andrews et al. (1991a), Kerwin (1994), and Hall et al. (2001) showed variations related to changes in sediment character, with implications regarding general provenance and ice-flow directions. Magnetic susceptibility data and correlations from additional sediment cores were presented by Manley et al. (1993) and Manley and Kerwin (1994). Core-to-core correlations and interpretations of the late glacial history of the Hudson Strait–Ungava Bay region from 10 500 BP to 8000 BP based on whole-core magnetic susceptibility, biostratigraphic, chronological, and seismic data from the marine studies, together with information from terrestrial investigations, were presented by Andrews et al. (1995b). Thick morainal bank deposits (up to 110 m) that occur across Savage basin (between Meta Incognita Peninsula and Edgell Island) have been interpreted to have accumulated near the terminus of the Noble Inlet advance (Stravers and Powell, 1997). The alignment of that feature conforms well with terrestrial data from Meta Incognita Peninsula pertaining to that advance. Lauriol and Gray (1997) reported on isotopic studies of marine molluscs from Holocene and modern deposits in eastern Hudson Strait and from raised marine sediment deposits on Ungava Peninsula, and their significance relative to paleoceanographic conditions during the time of the Noble Inlet glacial ice advance. Jennings et al. (1998) provided a further interpretation of the late glacial record from Eastern basin, examined evidence for

and against advance of Noble Inlet ice across Hudson Strait, and presented a depositional model for retreat from the Noble Inlet maximum in Eastern basin.

In Hudson Bay, which adjoins Hudson Strait on the west, marine investigations of Quaternary sediments included sedimentological and foraminiferal studies by Leslie (1963, 1964, 1965) and of heavy minerals by Henderson (1983, 1985, 1989). Regional studies of the late glacial and deglaciation record by Josenhans and Zevenhuizen (1990) from high-resolution seismic reflection surveys, sidescan sonar surveys, and sediment core data revealed glaciogenic features, and high-energy bedforms associated with rapid deglaciation of Hudson Bay, possibly the sudden drainage of glacial Lake Ojibway as postulated by Dyke and Prest (1987). Microfaunal and palynological studies of sediment cores by Bilodeau et al. (1990) found evidence of glaciolacustine and glaciomarine environments associated with glacial Lake Ojibway, and the Tyrrell Sea, respectively, and changes in paleoceanographic characteristics during postglacial time. Further studies of the marine geology of eastern (Petite rivière de la Baleine–Grande rivière de la Baleine region) and southeastern Hudson Bay were undertaken by C.L. Amos, B. Ardiles. K. Bentham, C. Davis, I. Hardy, W. LeBlanc, L. Johnson, L. Lockhart, B. MacLean, Y. Michaud, R. Murphy, A. Bornetson, M.H. Ruz, R. Sparkes, T. Sutherland, and J. Zevenhuizen (unpub. report, 1992), and by Zevenhuizen (1996), respectively.

Results of regional studies of the Quaternary geology of the continental shelf offshore southeast Baffin Island and offshore Labrador, which adjoin Hudson Strait to the east, were reported by Praeg et al. (1986), Josenhans et al. (1986), and Josenhans and Zevenhuizen (1989). Other investigations of the continental shelf in the vicinity of Hudson Strait included studies of the sedimentological, chronological, and late glacial-deglaciation records from Resolution and Hatton basins (Evans, 1990; Andrews et al., 1991b, 1994a, b, 2001), and sediment sources, supply, and mechanisms for sediment transport into the Labrador Sea and into the North Atlantic Ocean (Andrews et al, 1994b; Hillaire-Marcel et al., 1994; Andrews, 2000). Jennings et al. (1996b) examined the evidence for erosion of bedrock on the shelf relative to the depositional record in the Labrador Sea sediment succession.

The glacial-deglacial history of the Hudson Strait region included complex events and interactions that involved both terrestrial and marine areas within the region. In addition to the marine studies in Hudson Strait and Ungava Bay indicated above, readers are referred to the papers of this bulletin by Gray (2001), Manley and Miller (2001), and Andrews et al. (2001) that outline findings of the terrestrial studies and studies from the adjacent continental shelf.

As noted earlier in this paper, Hudson Strait was an important contributor of glacial ice, meltwater, and sediment to the continental shelf, Labrador Sea, and North Atlantic Ocean. Selected studies cited below illustrate the extensive literature relating to this subject.

Alley and MacAyeal (1994) examined probable behaviour of Hudson Bay and Hudson Strait ice streams and processes for entrainment of ice-rafted sediments. These modelling studies suggested long periods of gradual ice growth that alternated with short periods of rapid ice discharge, which would be capable of delivering large volumes of sediments, the magnitude and timing of which could satisfy constraints of the North Atlantic Ocean sediment record. Glaciological modelling studies by Pfeffer et al. (1997) examined ice-sheet behavior and constraints relating to the advance of glacial ice across Hudson Strait during the Younger Dryas, and Clark et al. (1996) reconstructed ice-flow patterns from studies of glacial bedforms in northern Quebec. High limestone concentrations in glaciomarine sediments overlying the upper till (dated ca. 8 ka BP) on the Labrador Shelf were considered by Josenhans et al. (1986) to have been derived from erosion of Paleozoic limestone during a late glacial expansion of ice in Hudson Strait and Ungava Bay, and transport of sediments southward along the shelf by the Canadian Current. Hillaire-Marcel et al. (1994) proposed that turbidity currents triggered by surges of the ice margin off Hudson Strait and ice rafting both played a role in the widespread distribution of carbonate and ice-rafted sediments in the Labrador Sea and North Atlantic Ocean. They also suggested that the normal water-current patterns in the Labrador Sea were suspended or greatly reduced during these major glacially driven events. Carbonate-rich sediments in the Labrador Sea that correlate with Heinrich events 1 and 2 in the North Atlantic Ocean were postulated by Andrews and Tedesco (1992) and Andrews et al. (1994b) to have been derived from Hudson Strait ice streams and associated major meltwater events (Andrews et al., 1994a). Studies of the distribution and thickness of Heinrich event layers 1 and 2 by Dowdeswell et al. (1995) showed greatest thicknesses are in the northern Labrador Sea seaward of Hudson Strait–southern Baffin Island, and decrease eastward in the North Atlantic Ocean. Jennings et al. (1996b) examined the evidence for shelf erosion and the seaward extent of ice streams from Hudson Strait and Cumberland Sound during the period H-3 or H-4 to H-0.

A review of data and concepts concerning abrupt changes in late Quaternary marine environments in the North Atlantic Ocean signified by Heinrich events was presented by Andrews (1998). In this, Andrews focused on glaciological factors, sediment sources, and delivery mechanisms, and pointed up gaps in present understanding of the processes involved in these abrupt changes in the marine environments. He presented a model for the triggering of Heinrich events that included such factors as global changes in mass balance, changes in relative sea level at glacial ice margins associated with glacial isostasy, and the basal thermal regime of tide-water ice streams.

ACKNOWLEDGMENTS

The results presented in this Bulletin represent the combined efforts of many individuals and groups without whose excellent and dedicated efforts and support this work could not have been accomplished. Special thanks are due the contributors to this report, not only for their written contributions, but also for their excellent support and collaboration throughout

this study. We wish to extend our sincere thanks to captains F.W. Mauger, L. Strum, F.H. Berchem, and J. Lewis; the crews of *CSS Hudson*; scientific and technical staff from Geological Survey of Canada (Atlantic), who supported these cruises so ably; A. Doiron and R.A. Daigneault of GSC (Quebec) and R. Klassen of GSC (Ottawa) for studies of clast lithologies; A. Taylor, and V. Allen of GSC (Ottawa); W. Briggs, M. Kerwin, W. Manley, and N. Weiner of Institute of Arctic and Alpine Research, University of Colorado; D. Bruneau, T. Brynczka, and E. Thibault of University of Montreal; J. Stravers, R. Powell, M. Escamilla, and J. Miner of Northern Illinois University; A. Aitken of University of Saskatchewan; M. Retelle of Bates College; W. Mode of University of Wisconsin; and H. Boudreau, Canadian Hydrographic Service for their enthusiastic support and helpful discussions at sea. Institute of Arctic and Alpine Research, University of Colorado undertook a large part of the chronological dating associated with this study. That important contribution is gratefully acknowledged. In addition, we wish to extend thanks to Department of Fisheries and Oceans, St. John's, Newfoundland for provision of sediment samples and sample data; to S. Merchant for curation services; to G. Grant, K. Hale and R. Sutherland at GSC (Atlantic); to E. Inglis (ESS Info) for editorial services; to Digital Design Unit (ESS Info) for production; to Cartographic Services Section (ESS Info) for figure preparation; to J. Ceman for studies of foraminiferal assemblages in specific cores and for preparation of diagrams; and to G.H. Miller and H. Josenhans for helpful discussions. Special thanks also go to H. Josenhans, A.C. Grant, and C.F.M. Lewis for provision of additional seismic data pertaining to the continental shelf and Hudson Strait sill; to H. Josenhans for data in southwestern Hudson Strait; and to C.L. Amos for data pertaining to southern Ungava Bay. Studies relating to this project conducted by researchers from the Institute of Arctic and Alpine Research, University of Colorado were supported by various grants from the National Science Foundation, Office of Polar Programs, and Earth Sciences Program. The authors of this report greatly appreciate the helpful comments offered by Doug Hodgson, Heiner Josenhans, and John Shaw who critically read the entire report.

REFERENCES

Aitken, A.
1991: Marine macrobenthos sampled in Frobisher Bay, Hudson Strait and Ungava Bay onboard *CSS Hudson* cruise 90023; *in* MacLean, B., Vilks, G., Aitken, A., Boudreau, H., Briggs, W., Bruneau, D., Doiron, A., Durham, D., Hardy, I., Mode, W., Powell, R., Retelle, M., Stravers, J., Taylor, A., and Allen, V., Cruise Report *CSS Hudson* Cruise 90023, Marine Geological Investigations in Hudson Strait, Ungava Bay, and Frobisher Bay; Geological Survey of Canada, Open File 2372, p. 70–72.

Allard, M., Fournier, A., Gahé, E., and Seguin, M.K.
1989: Le Quaternaire de la côte sud-est de la Baie d'Ungava, Québec nordique; Géographie physique et Quaternaire, v. 43, p. 325–336.

Alley, R.B. and MacAyeal, D.R.
1994: Ice-rafted debris associated with binge/purge oscillations of the Laurentide Ice Sheet; Paleoceanography, v. 9, no. 4, p. 503–511.

Andrews, J.T.
1989: Quaternary geology of the northeastern Canadian Shield: *in* Chapter 3 of Quaternary Geology of Canada and Greenland, (ed.) R.J. Fulton; Geological Survey of Canada, Geology of Canada, no. 1, p. 276–317 (*also* Geological Society of America, The Geology of North America, v. K-1).
1998: Abrupt changes (Heinrich events) in late Quaternary North Atlantic marine environments: a history and review of data and concepts; Journal of Quaternary Science, v. 13, p. 3–16.
2000: Explained and unexplained spatial and temporal variability in rates of marine sediment accumulation along the northeast margin of the Laurentide Ice Sheet ≤ 14 Ka; Journal of Sedimentary Research, v. 70, no. 4, p. 782–787.

Andrews, J.T. and Tedesco, K.
1992: Detrital carbonate-rich sediments, northwestern Labrador Sea: implications for ice-sheet dynamics and iceberg rafting (Heinrich) events in the North Atlantic; Geology, v. 20, p. 1087–1090.

Andrews, J.T., Briggs, W.M., and Weiner, N.
1991a: Rock and paleo-magnetic studies of cored sediments from Hudson Strait and Ungava Bay; *in* Current Research, Part E; Geological Survey of Canada, Paper 91-1E, p. 317–320.

Andrews, J.T., Erlenkeuser, H., Evans, L.W., Briggs, W.M., and Jull, A.J.T.
1991b: Meltwater and deglaciation, SE Baffin Shelf (NE margin of Laurentide Ice Sheet) between 13.5 and 7 Ka: from O and C stable isotope data; Paleoceanography, v. 6, no. 5, p. 621–637.

Andrews, J.T., Erlenkeuser, H., Tedesco, K., Aksu, A.E., and Jull, A.J.T.
1994a: Late Quaternary (Stage 2 and 3) meltwater and Heinrich events, Northwest Labrador Sea; Quaternary Research, v. 41, p. 26–34.

Andrews, J.T., Jennings, A.E., Kerwin, M., Manley, W., Miller, G.H., Bond, G., and MacLean, B.
1995a: A Heinrich-like event, H-0 (DC-0): source(s) for detrital carbonate in the North Atlantic during the Younger Dryas chronozone; Paleoceanography, v. 10, no. 5, p. 943–952.

Andrews, J.T., Jennings, A.E., and MacLean, B.
2001: Late Quaternary stratigraphy of Hatton and Resolution basins east of Hudson Strait; *in* Marine Geology of Hudson Strait and Ungava Bay, Eastern Arctic Canada: Late Quaternary Sediments, Depositional Environments, and Late Glacial–Deglacial History Derived from Marine and Terrestrial Studies, (ed.) B. MacLean; Geological Survey of Canada, Bulletin 566.

Andrews, J.T., MacLean, B., Kerwin, M., Manley, W., Jennings, A.E., and Hall, F.
1995b: Final stages in the collapse of the Laurentide Ice Sheet, Hudson Strait, Canada, NWT: ^{14}C AMS dates, seismic stratigraphy, and magnetic susceptibility logs; Quaternary Science Reviews, v. 14, p. 983–1004.

Andrews, J.T., Shilts, W.W., and Miller, G.H.
1983: Multiple deglaciations of the Hudson Bay Lowlands, Canada, since deposition of the Missinaibi (last interglacial?) Formation; Quaternary Research, v. 19, p. 18–37.

Andrews, J.T., Tedesco, K., Briggs, W.M., and Evans, L.W.
1994b: Sediments, sedimentation rates, and environments, southeast Baffin Shelf and northwest Labrador Sea, 8-26 ka; Canadian Journal of Earth Sciences, v. 31, p. 90–103.

Bilodeau, G., DeVernal, A., Hillaire-Marcel, C., and Josenhans, H.
1990: Postglacial paleoceanography of Hudson Bay: stratigraphic, microfaunal, and palynological evidence; Canadian Journal of Earth Sciences, v. 27, p. 946–963.

Blake, W., Jr.
1966: End moraines and deglaciation chronology in northern Canada with special reference to southern Baffin Island; Geological Survey of Canada, Paper 66-26, 31 p.

Bond, G., Heinrich, H., Broecker, W.S., Labeyrie, L., McManus, J., Andrews, J.T., Huon, S., Jantschik, R., Clasen, S., Simet, C., Tedesco, K., Klas, M., Bonani, G., and Ivy, S.
1992: Evidence for massive discharges of icebergs into the glacial Northern Atlantic; Nature, v. 360, p. 245–249.

Broecker, W.S., Bond, G., McManus, J., Klas, M., and Clark, E.
1992: Origin of the North Atlantic's Heinrich events; Climate Dynamics, v. 6, p. 265–273.

Bruneau, D. and Gray, J.T.
1991: Géologie des formations en surface, région de Salluit et du cap de Nouvelle-Franc, Québec; Commission géologique du Canada, carte 11-1990, échelle 1/250 000.
1997: Ecoulements glaciers et déglaciation hative (ca 11 ka BP?) du nord-est de la péninsule d'Ungava, Québec, Canada; Canadian Journal of Earth Sciences, v. 34, p. 1089–1100.

Canadian Hydrographic Service
1970: Chart 5450, Hudson Strait; Department of Energy, Mines and Resources, Ottawa, Ontario, scale 1:1 000 000.

Clark, C.D., Knight, J.K., and Gray, J.T.
1996: Reconstructing ice dynamic scenarios for the Ungava sector of the Laurentide Ice Sheet; *in* 26th Arctic Workshop, Institute of Arctic and Alpine Research, University of Colorado, Boulder, Colorado, March 1996, Program with Abstracts, p. 18.

Clark, P.U.
1985: A note on the glacial geology and postglacial emergence of the Lake Harbour region, Baffin Island, N.W.T.; Canadian Journal of Earth Sciences, v. 22, p. 1864–1871.

Clark, P.U., Clague, J.J., Curry, B.B., Dreimanis, A., Hicock, S.R., Miller, G.H., Berger, G.W., Eyles, N., Lamothe, M., Miller, B.B., Mott, R.J., Oldale, R.N., Stea, R.R., Szabo, J.P., Thorleifson, L.H., and Vincent, J-S.
1993: Initiation and development of the Laurentide and Cordilleran ice sheets following the last interglaciation; Quaternary Science Reviews, v. 12, p. 79–114.

Daigneault, R.A.
1994a: Résultats préléminaires sur la composition lithologique de la fraction grossière des sédiments quaternaires du détroit d'Hudson et de la baie d'Ungava: Territoire du Nord-Ouest; *in* MacLean, B., Loncarevic, B.D., Hardy, I., Brown, R.G.B., Daigneault, R.A., Day, M., Kerwin, M.W., and Manley, W.F., Cruise Report *CSS Hudson* Cruise 93034 in Hudson Strait-Ungava Bay, Canadian Eastern Arctic; Geological Survey of Canada, Open File 2818, Appendix D, p. 1–3.
1994b: CSS Hudson, croisière 93-034: composition lithologique de la fraction grossière des sédiments quaternaires du détroit d'Hudson et de la baie d'Ungava, Territories du Nord- Ouest; Commission géologique du Canada, Dossier public 2414, 47 p.
1996: Géologie des formation en surface, région de Salluit et des lacs Nuvilik, Québec-Territories du Nord-Ouest; Commission géologique du Canada, carte 1862A, échelle 1/250 000.

Doiron A.
1991: Studies of clast lithology and provenance (in Hudson Strait and Ungava Bay); *in* MacLean, B., Vilks, G., Aitken, A., Boudreau, H., Briggs, W., Bruneau, A. Doiron, D., Durham, D., Hardy, I., Mode, W., Powell, R., Retelle, M., Stravers, J., Taylor, A., and Allen, V., Cruise Report *CSS Hudson* Cruise 90023, Marine Geological Investigations in Hudson Strait, Ungava Bay, and Frobisher Bay; Geological Survey of Canada, Open File 2372, p. 69.

Dowdeswell, J.A., Maslin, M.A., Andrews, J.T., and McCave, I.N.
1995: Iceberg production, debris rafting, and the extent and thickness of Heinrich layers (H-1, H-2) in North Atlantic sediments; Geology, v. 23, p. 301–304.

Dredge, L.A. and Cowan, W.R.
1989: Quaternary geology of the southwestern Canadian Shield; *in* Chapter 3 of Quaternary Geology of Canada and Greenland, (ed.) R.J. Fulton; Geological Survey of Canada, Geology of Canada, no. 1 (*also* Geological Society of America, The Geology of North America, v. K-1) p. 214–249.

Drinkwater, K.F.
1983: Moored current meter data from Hudson Strait, 1982; Canada Fisheries and Aquatic Sciences, Data Report 381, 46 p.
1986: Physical oceanography of Hudson Strait and Ungava Bay; *in* Canadian Inland Seas, (ed.) I.P. Martini; Oceanographic Series, no. 44, Elsevier, Amsterdam, Netherlands, p. 237–264.

Dyke, A.S. and Dredge, L.A.
1989: Quaternary geology of the northwestern Canadian Shield; *in* Chapter 3 of Quaternary Geology of Canada, Geology of Canada, no. 1 (*also* Geological Society of America, The Geology of North America, v. K-1), p. 189–214.

Dyke, A.S. and Prest, V.K.
1987: Late Wisconsinan and Holocene history of the Laurentide Ice Sheet; Géographie physique et Quaternaire, v. XLI, no. 2, p. 237–263.

Dyke, A.S., Vincent, J-S., Andrews, J.T., Dredge, L.A., and Cowan, W.R.
1989: The Laurentide Ice Sheet and an introduction to Quaternary geology of the Canadian Shield; *in* Chapter 3 of Quaternary Geology of Canada and Greenland, (ed.) R.J. Fulton; Geological Survey of Canada, Geology of Canada, no. 1, p. 178–189 (*also* Geological Society of America, The Geology of North America, v. K-1).

England, J. and Smith, I.R.
1993: Late glacial ice margins and deglacial chronology for southeastern Baffin Island and Hudson Strait, eastern Canadian Arctic: discussion; Canadian Journal of Earth Sciences, v. 30, p. 1749–1752.

Evans, L.W.
1990: Late Quaternary stratigraphy of the Hatton and Resolution basins, Southeast Baffin Island Shelf, N.W.T., Canada; M.Sc. thesis, University of Colorado, Boulder, Colorado, 189 p.

Fillon, R.H. and Harmes, R.A.
1982: Northern Labrador Shelf glacial chronology and depositional environments; Canadian Journal of Earth Sciences, v. 19, p. 162–192.

Grant, A.C. and Manchester, K.S.
1970: Geophysical investigations in the Ungava Bay-Hudson Strait region of northern Canada; Canadian Journal of Earth Sciences, v. 7, p. 1062–1076.

Gray, J.T.
2001: Patterns of ice flow and deglaciation chronology for southern coastal margins of Hudson Strait and Ungava Bay; *in* Marine Geology of Hudson Strait and Ungava Bay, Eastern Arctic Canada: Late Quaternary Sediments, Depositional Environments, and Late Glacial–Deglacial History Derived from Marine and Terrestrial Studies, (ed.) B. MacLean; Geological Survey of Canada, Bulletin 566.

Gray, J.T. and Lauriol, B.
1985: Dynamics of the late Wisconsin ice sheet in the Ungava Peninsula, interpreted from geomorphical evidence; Arctic and Alpine Research, v. 17, p. 279–310.

Gray, J.T., Decker, V., Guidon, L., Guenette, C., and Clark, C.
1996: Late glacial ice flow patterns in the northwest Torngat Mountains: evidence for an important local dispersal centre; *in* 26th Arctic Workshop, Institute of Arctic and Alpine Research, University of Colorado, March 14–16, 1996, Program with Abstracts, p. 43–44b.

Gray, J.T., Lauriol, B., Bruneau, D., and Ricard, J.
1993: Postglacial emergence of Ungava Peninsula and its relationship to glacial history; Canadian Journal of Earth Sciences, v. 30, p. 1676–1696.

Hall, F.R., Andrews, J.T., Kerwin, M., and Smith, L.M.
2001: Studies of sediment colour, whole-core magnetic susceptibility, and sediment magnetism of the Hudson Strait–Labrador Shelf region: *CSS Hudson* cruises 90023 and 93034; *in* Marine Geology of Hudson Strait and Ungava Bay, Eastern Arctic Canada: Late Quaternary Sediments, Depositional Environments, and Late Glacial–Deglacial History Derived from Marine and Terrestrial Studies, (ed.) B. MacLean; Geological Survey of Canada, Bulletin 566.

Heinrich, H.
1988: Origin and consequences of cyclic ice rafting in the Northeast Atlantic Ocean during the past 130,000 years; Quaternary Research, v. 29, p. 143–152.

Henderson, P.J.
1983: A study of the heavy mineral distribution in the bottom sediments in Hudson Bay; *in* Current Research, Part A; Geological Survey of Canada, Paper 83-1A, p. 347–351.
1985: Dispersal patterns of specific heavy mineral species and granule composition in Hudson Bay bottom sediments; *in* Workshop, Arctic Land-Sea Interaction, Dartmouth, Nova Scotia, November 6–8, 1985, Abstracts, p. 194–195.
1989: Data report: description and composition of cores and grab samples, Hudson 87-028, Hudson Bay; Geological Survey of Canada, Open File 2081, 157 p.

Hillaire-Marcel, C.
1976: La déglaciation et le relèvement isostatique sur la cê est de la baie d'Hudson; Cahiers de géographie de Québec, v. 20, p. 185–220.

Hillaire-Marcel, C., DeVernal, A., Bilodeau, G., and Wu, G.
1994: Isotope stratigraphy, sedimentation rates, deep circulation, and carbonate events in the Labrador Sea during the last - 200 ka; Canadian Journal of Earth Sciences, v. 31, p. 63–89.

Hodgson, D.A.
1997: Last glacial ice flows over western Meta Incognita Peninsula, southern Baffin Island, Northwest Territories; *in* Current Research 1997-C; Geological Survey of Canada, p. 179–184.

Hughes, T.
1987: Ice dynamics and deglaciation models when ice sheets collapsed; *in* North America and Adjacent Oceans During the Last Glaciation, (ed.) W.F. Ruddiman and H.E.J. Wright; Geological Society of America, p. 183–220.

Jennings, A.E., Andrews, J.T., Weiner, N.J., Manley, W.F., MacLean, B., and Barber, D.C.
1995: Strategies and progress in unravelling the chronology of Hudson Strait deglaciation; *in* The 25th Arctic Workshop, Centre d'Etudes Nordiques, Université Laval, Quebec, March 1995, p. 90.

Jennings, A.E., MacLean, B., Manley, W.F., and Andrews, J.T.
1996a: Reconciling terrestrial and marine evidence for the last ice advance across Eastern Hudson Strait; *in* Geological Society of America, Annual Meeting, Denver, Colorado, October 28–31, 1996, Abstracts with Program, p. A-434.

Jennings, A.E., Manley, W.F., MacLean, B., and Andrews, J.T.
1998: Marine evidence for the last glacial advance across Eastern Hudson Strait, Eastern Canadian Arctic; Journal of Quaternary Science, v. 13, p. 501–514.

Jennings, A.E., Tedesco, K.A., Andrews, J.T., and Kirby, M.E.
1996b: Shelf erosion and glacial ice proximity in the Labrador Sea during and after Heinrich events (H-3 or 4 to H-0) as shown by foraminifera; *in* Late Quaternary Paleoceanography of the North Atlantic Margins, (ed.) J.T. Andrews, W.E.N. Austin, H. Bergsten, and A.E. Jennings; Geological Society of London, Special Publication 111, p. 29–49.

Jennings, A.E., Vilks, G., Deonarine, B., Silis, A., and Weiner, N.
2001: Foraminiferal biostratigraphy and paleoceanography; *in* Marine Geology of Hudson Strait and Ungava Bay, Eastern Arctic Canada: Late Quaternary Sediments, Depositional Environments, and Late Glacial–Deglacial History Derived from Marine and Terrestrial Studies, (ed.) B. MacLean; Geological Survey of Canada, Bulletin 566.

Josenhans, H. and Zevenhuizen, J.
1989: Quaternary Geology of Labrador Sea, Surficial Geology and Physical Properties, Map II; *in* Geological Survey of Canada, Frontier Geoscience Program Basin Atlas Series, Labrador Sea (co-ord) J.S. Bell; Energy, Mines and Resources Canada, Ottawa, Ontario.
1990: Dynamics of the Laurentide Ice Sheet in Hudson Bay, Canada; Marine Geology, v. 92, p. 1–26.

Josenhans, H.W., Zevenhuizen, J., and Klassen, R.A.
1986: The Quaternary geology of the Labrador Shelf; Canadian Journal of Earth Sciences, v. 23, p. 1190–1213.

Kaufman, D.S., Miller, G.H., Stravers, J.A., and Andrews, J.T.
1993a: Abrupt early Holocene (9.9-9.6 ka) ice stream advance at the mouth of Hudson Strait, Arctic Canada; Geology, v. 21, p. 1063–1066.

Kaufman, D.S., Miller, G.H., Stravers, J.D., Manley, W.F., and Duvall, M.L.
1993b: Late glacial ice margins and deglaciation chronology for southeastern Baffin Island and Hudson Strait, eastern Canadian Arctic; reply; Canadian Journal of Earth Sciences, v. 30, p. 1753–1758.

Kerwin, M.W.
1994: Final stages in the collapse of the Laurentide Ice Sheet: a rock magnetic and sedimentological study from Hudson Strait, Canada; M.Sc. thesis, University of Colorado, Boulder, Colorado, 189 p.

Lauriol, B. and Gray, J.T.
1987: The decay and disappearance of the Late Wisconsinan ice sheet in Ungava Bay, northern Québec, Canada; Arctic and Alpine Research, v. 19, p. 109–126.
1997: La composition isotopique des mollusques marins et sa relation à la déglaciation de la péninsule d'Ungava, Canada; Géographie physique et Quaternaire, v. 51, p. 185–199.

Laymon, C.A.
1988: Glacial geology of western Hudson Strait, Canada, with reference to Laurentide Ice Sheet dynamics; Ph.D. thesis, University of Colorado, Boulder, Colorado, 345 p.
sique et Quaternaire, v. 51, p. 185–199.

Laymon, C.A. (cont.)
1992: Glacial geology of western Hudson Strait, Canada, with reference to Laurentide Ice Sheet dynamics; Geological Society of America, Bulletin, v. 104, p. 1169–1177.

Leslie, R.J.
1963: Foraminiferal study of a cross-section of Hudson Bay, Canada; Geological Survey of Canada, Paper 63-16, 28 p.
1964: Sedimentology of Hudson Bay, District of Keewatin; Geological Survey of Canada, Paper 63-48, 31 p.
1965: Ecology and paleoecology of Hudson Bay foraminifera; Bedford Institute of Oceanography, Report 65-6, Dartmouth, Nova Scotia, 191 p.

Løken, O.H.
1967: Notes on the bathymetry of Gray Strait, northern Labrador, Canada; Geographical Bulletin 9, p. 57–61.

MacLean, B.
1998: Quaternary sediments and bedrock in Ungava Bay, N.W.T., Canada; *in* 28th Arctic Workshop, Institute of Arctic and Alpine Research, University of Colorado, Boulder, Colorado, March 12–14, 1998, Program and Abstracts, p. 103–105.

MacLean, B. and Williams, G.L.
1983: Geological investigations of Baffin Island Shelf in 1982; *in* Current Research, Part B; Geological Survey of Canada, Paper 83-1B, p. 309–315.

MacLean, B., Andrews, J.T., Gray, J.T., Hall, F.R., Hardy, I., Jennings, A.E., Manley, W.F., Pfeffer, W.T., and Vilks, G.
2001a: Hudson Strait Quaternary sediments and late glacial and deglaciation history: a discussion and summary; *in* Marine Geology of Hudson Strait and Ungava Bay, Eastern Arctic Canada: Late Quaternary Sediments, Depositional Environments, and Late Glacial–Deglacial History Derived from Marine and Terrestrial Studies, (ed.) B. MacLean; Geological Survey of Canada, Bulletin 566.

MacLean, B., Andrews, J.T., Jennings, A.E., Manley, W.F., Hardy, I., Vilks, G., and Deonarine, B.
1996: Late Quaternary sediments in eastern Hudson Strait: relations with late glacial advances on southeastern Baffin Island; *in* 26th Arctic Workshop, Institute of Arctic and Alpine Research, University of Colorado, Boulder, Colorado, March 14–16, 1996, Program with Abstracts, p. 86–88.

MacLean, B., Hardy, I., Jennings, A.E., Manley, W.F., and Kerwin, M.W.
1994a: Late glacial ice in Eastern Hudson Strait: new offshore evidence; *in* 24th Arctic Workshop, Institute of Arctic and Alpine Research, University of Colorado, Boulder, Colorado, March 17–19, 1994, Abstracts, p. 132–134.

MacLean, B., Loncarevic, B.D., Hardy, I., Brown, R.G.B., Daignesult, R.A., Day, M., Kerwin, M.W., and Manley, W.F.
1994b: Cruise Report *CSS Hudson* Cruise 93034 in Hudson Strait-Ungava Bay, Canadian Eastern Arctic; Geological Survey of Canada, Open File 2818, 131 p.

MacLean, B., Vilks, G., Aitken, A., Boudreau, H., Briggs, W., Bruneau, A., Doiron, D., Durham, D., Hardy, I., Mode, W., Powell, R., Retelle, M., Stravers, J., Taylor, A., and Allen, V.
1991: Cruise Report *CSS Hudson* Cruise 90023, marine geological investigations in Hudson Strait, Ungava Bay, and Frobisher Bay; Geological Survey of Canada, Open File 2372, 152 p.

MacLean, B., Vilks, G., and Deonarine, B.
1992: Depositional environments and history of late Quaternary sediments in Hudson Strait and Ungava Bay: further evidence from seismic and biostratigraphic data; Géographie physique et Quaternaire, v. 46, p. 311–329.
1993: The history of depositional environments for Late Quaternary sediments in Hudson Strait and Ungava Bay; *in* 23rd Arctic Workshop, Byrd Polar Research Center, Ohio State University, April 1–3, 1993, Abstracts, p. 54–55.

MacLean, B., Vilks, G., Deonarine, B., Hardy, I., and Ceman, J.
1995: Quaternary sediments in Hudson Strait and Ungava Bay; *in* The 25th Arctic Workshop, Centre d'Etudes Nordiques, Université Laval, Quebec, March 16–18, 1995, p. 116–118.

MacLean, B., Vilks, G., Hardy, I., Deonarine, B., Jennings, A.E., and Manley, W.F.
2001b: Quaternary sediments in Hudson Strait and Ungava Bay; *in* Marine Geology of Hudson Strait and Ungava Bay, Eastern Arctic Canada: Late Quaternary Sediments, Depositional Environments, and Late Glacial–Deglacial History Derived from Marine and Terrestrial Studies, (ed.) B. MacLean; Geological Survey of Canada, Bulletin 566.

MacLean, B., Williams, G.L., Sanford, B.V., Klassen, R.A., Blakeney, C., and Jennings, A.
1986: A reconnaissance study of bedrock and surficial geology of Hudson Strait, N.W.T.; *in* Current Research, Part B; Geological Survey of Canada, Paper 86-1B, p. 617–635.

Manley, W.F.
1995: Late-glacial record of ice-sheet/ocean interactions, Hudson Strait and southern Baffin Island, Eastern Canadian Arctic; Ph.D. thesis, University of Colorado, Boulder, Colorado, 262 p.

Manley, W.F. and Kerwin, M.W.
1994: *CSS Hudson* cruise 93034 magnetic susceptibility measurements; *in* MacLean, B., Loncarevic, B.D., Hardy, I., Brown, R.G.B., Daigneault, R.A., Day, M., Kerwin, M.W., and Manley, W.F., Cruise Report CSS Hudson Cruise 93034 in Hudson Strait-Ungava Bay, Canadian Eastern Arctic; Geological Survey of Canada, Open File 2818, Appendix C, p. 1–14.

Manley, W.F. and Miller, G.H.
2001: Glacial–geological record on southern Baffin Island reflecting late glacial ice-sheet dynamics in the eastern Hudson Strait region; *in* Marine Geology of Hudson Strait and Ungava Bay, Eastern Arctic Canada: Late Quaternary Sediments, Depositional Environments, and Late Glacial–Deglacial History Derived from Marine and Terrestrial Studies, (ed.) B. MacLean; Geological Survey of Canada, Bulletin 566.

Manley, W.F., MacLean, B., Kerwin, M.W., and Andrews, J.T.
1993: Magnetic susceptibility as a Quaternary correlation tool: examples from Hudson Strait sediment cores, eastern Canadian Arctic; *in* Current Research, Part D; Geological Survey of Canada, Paper 93-1D, p. 137–145.

Miller, G.H. and Kaufman, D.S.
1990: Rapid fluctuations of the Laurentide ice sheet at the mouth of Hudson Strait: new evidence for ocean/icesheet interactions as a control on the Younger Dryas; Paleoceanography, v. 5, no. 6, p. 907–919.

Miller, G.H., Hearty, P.J., and Stravers, J.A.
1988: Ice-sheet dynamics and glacial history of southeasternmost Baffin Island and outermost Hudson Strait; Quaternary Research, v. 30, p. 116–136.

Pfeffer, W.T., Dyurgerov, M., Kaplan, M., Dwyer, J., Sassolas, C., Jennings, A., Raup, B., and Manley, W.
1997: Numerical modelling of late glacial Laurentide advance of ice across Hudson Strait: insights into terrestrial and marine geology, mass balance, and calving flux; Paleoceanography, v. 12, p. 97–110.

Pilot of Arctic Canada
1959: Pilot of Arctic Canada Volume II; Issued by Canadian Hydrographic Service, Department of Mines and Technical Surveys, Queen's Printer, Ottawa, 434 p.

Piper, D.J.W., Mudie, P.J., Fader, G.B., Josenhans, H.W., MacLean, B., and Vilks, G.
1990: Quaternary geology; Chapter 10 *in* Geology of the Continental Margin of Eastern Canada, (ed.) M.J. Keen and G.L. Williams; Geological Survey of Canada, Geology of Canada, no. 2, p. 475–607 (*also* Geological Society of America, The Geology of North America, v. I-1).

Praeg, D.B., MacLean, B., Hardy, I.A., and Mudie, P.J.
1986: Quaternary geology of the southeast Baffin Island continental shelf; Geological Survey of Canada, Paper 85-14, 38 p.

Silis, A.B.
1993: Late Quaternary foraminiferal biostratigraphy of Hudson Strait; Geological Survey of Canada, Open File 3340, 127 p.

Stravers, J.A.
1986: Glacial geology of outer Meta Incognita Peninsula, southern Baffin Island, Arctic Canada; Ph.D. thesis, University of Colorado, Boulder, Colorado, 231 p.

Stravers, J.A. and Powell, R.D.
1997: Glacial debris flow deposits on the Baffin Island shelf: seismic facies architecture of till-tongue-like deposits; Marine Geology, v. 143, p. 151–168.

Stravers, J.A., Miller, G.H., and Kaufman, D.S.
1992: Late glacial ice margins and deglacial chronology for southeastern Baffin Island and Hudson Strait, eastern Canadian Arctic; Canadian Journal of Earth Sciences, v. 29, p. 1000–1017.

Taylor, A. and Allen, V.
1991: Geothermal and sediment physical properties program; *in* MacLean, B., Vilks, G., Aitken, A., Boudreau, H., Briggs, W., Bruneau, A. Doiron, D., Durham, D., Hardy, I., Mode, W, Powell, R., Retelle, M., Stravers, J., Taylor, A., and Allen, V., Cruise Report CSS Hudson Cruise 90023, Marine Geological Investigations in Hudson Strait, Ungava Bay, and Frobisher Bay; Geological Survey of Canada, Open File 2372, p. 32–65.

Vilks, G., MacLean, B., Deonarine, B., Currie, C.G., and Moran, K.
1989: Late Quaternary paleoceanography and sedimentary environments in Hudson Strait; Géographie physique et Quaternaire, v. 43, no. 2, p. 161–178.

Vincent, J-S.
1989: Quaternary geology of the southeastern Canadian Shield; *in* Chapter 3 of Quaternary Geology of Canada and Greenland, (ed.) R.J. Fulton; Geological Survey of Canada, Geology of Canada, no. 1, p. 249–275 (*also* Geological Society of America, The Geology of North America, v. K-1).

Zevenhuizen, J.
1996: Late Quaternary and surficial marine geology of southeastern Hudson Bay; M.Sc. thesis, Dalhousie University, Halifax, Nova Scotia, 215 p.

Glacial-geological record on southern Baffin Island reflecting late glacial ice-sheet dynamics in the eastern Hudson Strait region

William F. Manley[1] and Gifford H. Miller[2]

Manley, W.F. and Miller, G.H., 2001: Glacial-geological record on southern Baffin Island reflecting late glacial ice-sheet dynamics in the eastern Hudson Strait region; in *Marine Geology of Hudson Strait and Ungava Bay, Eastern Arctic Canada: Late Quaternary Sediments, Depositional Environments, and Late Glacial–Deglacial History Derived from Marine and Terrestrial Studies, (ed.) B. MacLean; Geological Survey of Canada, Bulletin 566, p. 19–30.*

Abstract: Field observations, sediment analyses, and radiocarbon dating completed over the last decade have led to new ice-sheet reconstructions for southern Baffin Island and eastern Hudson Strait. Past ice-flow patterns are apparent from sediment provenance indicators and striated bedrock surfaces. The timing of events is constrained by over 150 ^{14}C determinations on molluscs from ice-contact, deglacial, and postglacial deposits. Together, the data indicate that glacier ice from the Labrador Dome of the Laurentide Ice Sheet pulsed northward across Hudson Strait at least twice during the waning stages of the late Wisconsin glaciation. Evidence and reconstructed ice dynamics are summarized here for the Gold Cove advance (ca. 9900–9600 ^{14}C years BP) and the Noble Inlet advance (ca. 8900–8400 ^{14}C years BP). Two stratigraphic sections – from the York delta and Noble Inlet – best constrain the origin, extent, and timing of the Noble Inlet advance, and are described in detail. The evidence for northward to northeastward flow on eastern Meta Incognita Peninsula contrasts with the glacial-terrestrial record farther west (near Lake Harbour), where striations and provenance indicators document southward flow into Hudson Strait prior to coastal deglaciation at about 8200 ^{14}C years BP. In sum, the available data attest to spatially complex, abrupt ice-sheet dynamics.

Résumé : Des observations de terrain, des analyses de sédiments et la datation au radiocarbone effectuées depuis une décennie ont permis de nouvelles reconstitutions des nappes glaciaires qui ont couvert la partie méridionale de l'île de Baffin et la partie orientale du détroit d'Hudson. Les indicateurs de la provenance des sédiments et les surfaces striées du socle rocheux révèlent les anciens modes d'écoulement des glaces. Plus de 150 datations au ^{14}C de mollusques prélevés dans des sédiments de contact glaciaire, des sédiments mis en place lors de la déglaciation et des sédiments postglaciaires circonscrivent la chronologie des événements. L'ensemble des données indique que de la glace glaciaire provenant du dôme du Labrador, qui faisait partie de l'Inlandsis laurentidien, s'est écoulée vers le nord et a traversé le détroit d'Hudson au moins deux fois pendant les derniers stages de la Glaciation du Wisconsin supérieur. Le présent article résume les données sur l'avancée glaciaire de Gold Cove (vers 9900–9600 ans ^{14}C BP) et celle de Noble Inlet (vers 8900–8400 ans ^{14}C BP) ainsi que la reconstitution de la dynamique de ces glaces. Deux coupes stratigraphiques (provenant du delta de la rivière York et de l'inlet Noble) qui circonscrivent au mieux l'origine, l'étendue et la chronologie de l'avancée de Noble Inlet sont décrites en détail. Les indices d'un écoulement de direction nord à nord-est dans la partie orientale de la péninsule Meta Incognita contrastent avec les données de glaciation recueillies sur terre plus loin à l'ouest (près de la baie Lake Harbour), où des stries et des indicateurs de provenance montrent qu'un écoulement vers le sud dans le détroit d'Hudson s'est produit avant la déglaciation des côtes vers 8200 ans ^{14}C BP. En somme, les données disponibles témoignent de la présence de nappes glaciaires géographiquement complexes et très dynamiques.

[1] Institute of Arctic and Alpine Research and Center for Geochronologic Research, University of Colorado, Boulder, Colorado, U.S.A. 80309-0450

[2] Institute of Arctic and Alpine Research, Center for Geochronologic Research, and Department of Geological Sciences, University of Colorado, Boulder, Colorado, U.S.A. 80309-0450

INTRODUCTION

Glacial-geological study of southern Baffin Island (Fig. 1, 2) began nearly a century ago. Bell (1901) documented striations on Meta Incognita Peninsula and concluded that an ice sheet on the peninsula moved southward, merging with an ice stream occupying Hudson Strait that emptied eastward into the Labrador Sea. Little more was known, however, until the study of Blake (1966), who obtained the first radiocarbon dates from the region, mapped a variety of ice-flow indicators, and described patterns of sediment lithology tied to glacial provenance. Blake (1966) inferred that an outlet glacier in the strait impinged on the northern shore of the strait before 8 ka BP (dates in ^{14}C years BP in this paper unless otherwise stated). This reconstruction was supported by later reconnaissance study in the vicinity of Lake Harbour by Clark (1985).

Glacial-geological evidence north of Meta Incognita Peninsula led Blake (1966) and Miller (1980) to believe that Frobisher Bay had been filled by southeastward-flowing ice about 10 ka BP and again, partially, about 8 ka BP. Several theses provide additional details on the glacial history of Frobisher Bay and southeastern Meta Incognita Peninsula (Muller, 1980; Colvill, 1982; Lind, 1983; Squires, 1984; Stravers, 1986).

Beginning in the late 1980s, however, field-based research led to new data and paradigms (Miller et al., 1988; Miller and Kaufman, 1990; Stravers et al., 1992; Kaufman et al., 1993a, b; Manley, 1995, 1996). First, ice-flow patterns were mapped in detail by actively searching for striated bedrock surfaces preserved under thin mantles of overlying sediment, rather than relying entirely on weathered, subaerially

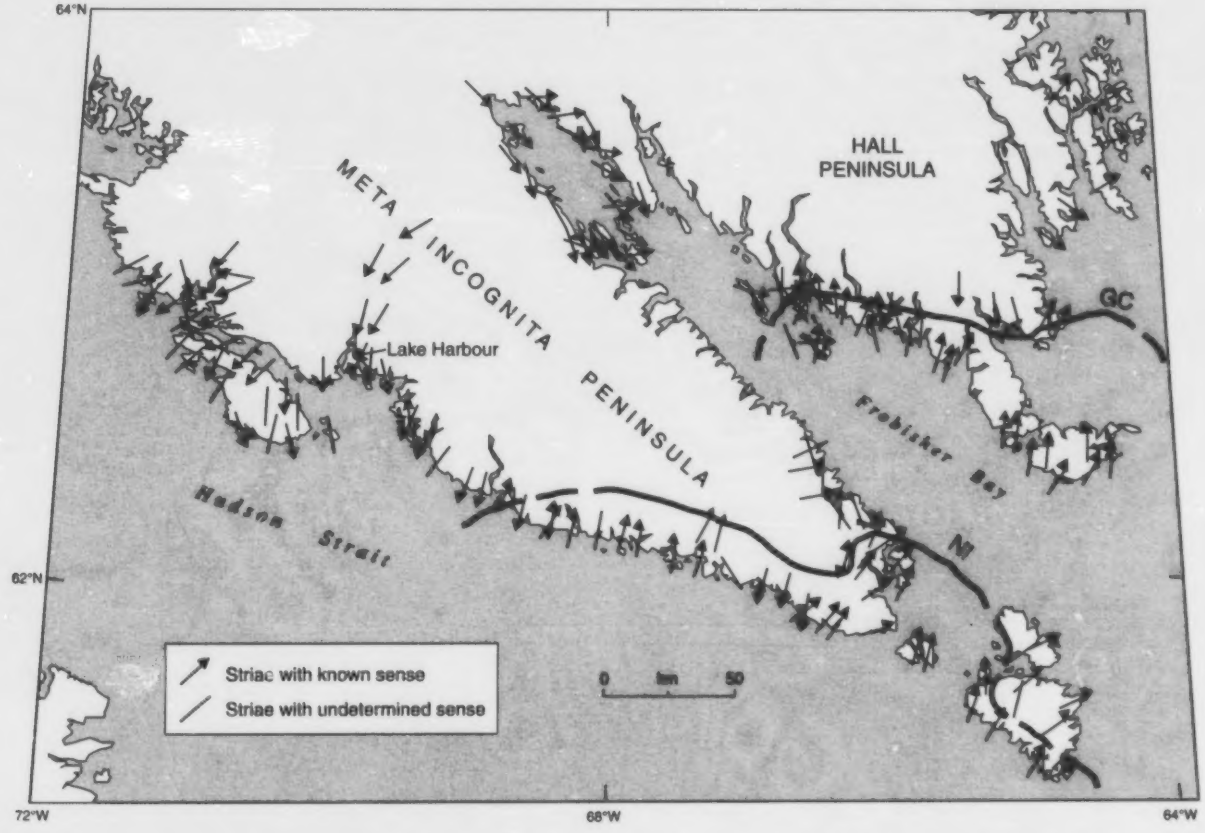

Figure 1. *Past ice-flow patterns reconstructed from striation measurements, southern Baffin Island. Each arrow or line segment represents an average of observations at one to several sites. Striations were measured above the marine limit on summits or rolling uplands, where ice flow would not have been channelled by local topography. A variety of flow directions are preserved, including (late glacial) southward flow into Hudson Strait near western Meta Incognita Peninsula (Manley, 1996), both southeastward and eastward flow in inner and central Frobisher Bay (Duvall, 1993; Manley and Moore, 1995), and the dominant northward to northeastward flow pattern preserved across much of the study area (Miller et al., 1988; Miller and Kaufman, 1990; Stravers et al., 1992; Kaufman et al., 1993a; Manley, 1995). Inferred limits of the Gold Cove (GC) and Noble Inlet (NI) advances are shown with grey lines* (modified from *references cited above).*

exposed bedrock. Often the unidirectional sense of flow could be determined by examination of small stoss-and-lee features exposed in shallow striation pits. Other flow indicators — mapped in greater resolution — include limestone erratics in till, scoured from the Paleozoic bedrock and marine sediment of Hudson Strait and Frobisher Bay, and glacially transported molluscs, scoured from previously deposited marine or glaciomarine sediment. More than 300 sediment samples were analyzed for per cent carbonate and other parameters related to provenance. The elevation of the deglacial marine limit was measured at closely spaced sites. Finally, the research benefited from the advent of Accelerator Mass Spectrometry (AMS) radiocarbon dating. Molluscs reworked into till above the marine limit were dated individually to identify the youngest specimens within mixed-age assemblages, which provide close maximum ages for glacier advance. Coupled with dates on molluscs from ice-contact, deglacial, and postglacial deposits, the history of glacial dynamics in the region is constrained by more than 150 radiocarbon determinations (cf. Manley and Jennings, 1996).

This paper presents a review of the terrestrial glacial-geological evidence on southeastern Baffin Island, a summary of the inferred major glacial events, and detail on two important stratigraphic sections. The direction of past glacier movement has been mapped from striations at more than 155 sites (Fig. 1). The presence or absence of foreign erratics was observed at more than 101 sites on eastern Meta Incognita Peninsula (Fig. 3). Additional evidence for sediment provenance comes from analysis of carbonate content in 74 samples (Fig. 4). Radiocarbon ages constraining the timing of the younger glacial advance are given in Table 1. Other dates from the region are reported in Miller et al. (1988), Kaufman et al. (1993a), Manley (1995, 1996), and Manley and Jennings (1996).

GOLD COVE ADVANCE

Much of our efforts in the last seven years have been directed toward a detailed reconstruction of the more extensive northward pulse, the Gold Cove advance (Miller and Kaufman,

Figure 2. *Eastern Meta Incognita Peninsula. Black dots show radiocarbon-dated localities. Numbered localities are keyed to radiocarbon ages constraining the timing of the Noble Inlet advance, listed in Table 1. Other, unlabelled sites correspond with radiocarbon dates additionally presented in Manley (1995). The York delta (site 37) is shown as an irregular black polygon near the head of York Sound. Associated gorges and meltwater spillways to the south and west are shown by irregular black lines. The stratigraphic section illustrated in Figure 8 is from site 20, near the head of Noble Inlet.*

1990; Stravers et al., 1992; Duvall, 1993; Kaufman et al., 1993a, b; Pfeffer et al., 1997). Geochemical analyses of till samples, observations of erratic limestone clasts, and measurements of striations from over 55 sites (Fig. 1) allow us to outline the following history. From a dome over Labrador, Ungava Bay, and central Quebec, an ice margin advanced across the deep Eastern basin of Hudson Strait, traversed Meta Incognita Peninsula and Frobisher Bay, and established an ice margin on eastern Hall Peninsula 400 km from its source. More than 60 radiocarbon dates on marine molluscs, including 27 AMS ^{14}C dates on single specimens, constrain the maximum extension of the advance to 9900–9600 BP (Fig. 5). The chronology shows that the advance crossed more than 150 km of open water within about 200 radiocarbon years; then retreated more than 350 km within another two centuries. At the mouth of Hudson Strait, the discharge of ice calving into the Labrador Sea would have been 300–2400 km^3/year (Miller and Kaufman, 1990). The Gold Cove advance may have been the culmination of a major glacial oscillation that began with iceberg discharge at the mouth of the strait during DC-0 (correlative with Heinrich Event 0, as recorded in the Resolution Basin and elsewhere; Andrews et al. (1995a); Pfeffer et al. (1997)).

NOBLE INLET ADVANCE

Recently our attention has been focused on the youngest Labradorean pulse to reach southeastern Baffin Island, the Noble Inlet advance (Miller et al., 1988; Stravers et al., 1992; Kaufman et al., 1993b; Manley and Miller, 1994; Manley, 1995; cf. England and Smith, 1993; Gray et al., 1995; Gray, 2001). Striations at 53 sites record northward to northeastward flow onto Meta Incognita Peninsula, across its tip into southern Frobisher Bay, and onto or across Resolution Island (Fig. 1). Geochemical analyses and foreign erratics in till along this 240 km wide swath also document a southerly source (Fig. 3, 4; Manley, 1995). Glacier ice at least 350 m thick dammed an ice-contact lake that drained through gorges cut across the peninsula to form the York delta, a massive glaciomarine and glaciofluvial deposit in outer Frobisher Bay (Fig. 2; *see* below). Radiocarbon dates concentrated near the tip of the peninsula and from the York delta define advance and retreat (Fig. 6; Table 1). These include nine ^{14}C determinations on molluscs from till or glacially overridden sediments that predate glacier advance across each site, fourteen dates for the York delta and ice-contact or ice-marginal deltas deposited during the advance, and nine dates from postglacial

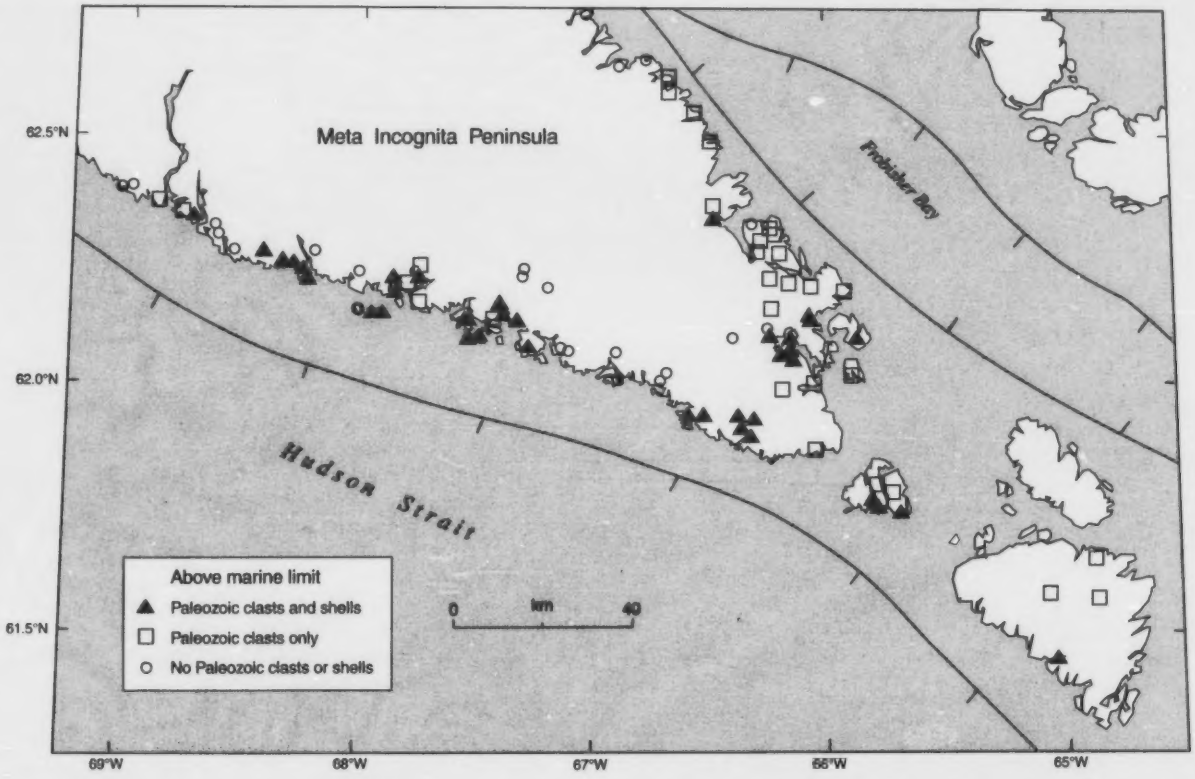

Figure 3. *Sediment provenance indicators above the marine limit, including clasts of Paleozoic limestone and dolostone or fragments of marine molluscs reworked into drift (till) above the marine limit (Manley, 1995). These occurrences are evidence for a northward component of glacier movement across marine or glaciomarine sediment in Hudson Strait. Hachured lines indicate extent of Paleozoic carbonate bedrock in Hudson Strait and Frobisher Bay. Other areas are floored by Precambrian granitic gneiss.*

Table 1. Radiocarbon dates from southeastern Baffin Island constraining the age of the Noble Inlet advance.

Site[1]	Laboratory number	Reported radiocarbon age (^{14}C years BP)[2]	Corrected radiocarbon age (^{14}C years BP)[3]	Elevation (m aht)[4]	Marine limit (m aht)[4]	Material[5]	Reference[6]
From till and glaciofluvial sediment above the marine limit, predating Noble Inlet advance							
21	GX-8943	9385 ± 280	8935 ± 280	60–70	42	Mm	6, 7
26	AA-2223	9090 ± 90	8640 ± 90	65	43	Ms	8
20	AA-14024	9065 ± 80	8615 ± 80	72	42	Ms	9, 10
26	AA-14029	8950 ± 65	8500 ± 65	65	43	Ms	9, 10
From till below the marine limit, predating Noble Inlet advance							
25	AA-2350	9500 ± 90	9050 ± 90	15	44	Ms	8
From overridden glaciomarine sediment, predating Noble Inlet advance							
20	AA-14025	9370 ± 80	8920 ± 80	-2	42	Ms	9, 10
22	AA-14026	9090 ± 95	8640 ± 95	-2	42	Msp	9, 10
22	GSC-3951	8640 ± 100	8600 ± 50	-2	42	Mmp	6, 7
On reworked, abraded shell fragment from ice-contact delta, predating Noble Inlet advance							
24	AA-17257	9650 ± 70	9200 ± 70	38	43	Ms	9, 10
From the York delta, dating Noble Inlet advance							
35	GSC-1903	9010 ± 380	8970 ± 190	<60	86	Ms	3
37	GSC-463	8840 ± 160	8800 ± 80	20	80	Mm	1, 2
37	SI-4368	8820 ± 110	8780 ± 110	7	80	Mm	4, 5
37	GSC-2991	8790 ± 380	8750 ± 190	55	80	Mm	4, 5
37	GSC-463-2	8710 ± 180	8670 ± 90	20	80	Mm	1, 2
37	SI-5173	8660 ± 175	8620 ± 175	25	80	Mm	5
From ice-contact or ice-marginal glaciomarine sediment, dating Noble Inlet advance							
19	GX-9766	9310 ± 220	8860 ± 220	10	30	Mmp	6, 7
20	GSC-4607	8810 ± 90	8770 ± 45	6–20	42	Mm	7
19	GX-8194	9190 ± 195	8740 ± 195	10	30	Mmp	6, 7
20	AA-17255	9130 ± 65	8680 ± 65	16	42	Ms	9, 10
27	GSC-3468	8660 ± 110	8620 ± 55	3–10	50	Mm	6, 7
19	GSC-3648	8600 ± 110	8560 ± 55	10	30	Mmp	6, 7
20	GSC-3469	8580 ± 150	8540 ± 75	16	42	Mmp	6, 7
18	AA-14028	8905 ± 65	8455 ± 65	19	27	Ms	9, 10
From deglacial galciomarine sediment, postdating Noble Inlet advance							
4	AA-10645	8760 ± 65	8310 ± 65	19	65	Ms	9, 10
9	AA-10648	8525 ± 60	8075 ± 60	11	48	Ms	9, 10
11	AA-2349	8500 ± 90	8050 ± 90	-2.5	38	Ms	8
11	AA-6299	8365 ± 75	7915 ± 75	-1.5	38	Mm	8
4	GSC-5526	7690 ± 90	7650 ± 45	12	65	Mm	9, 10
7	AA-10649	8045 ± 60	7595 ± 60	16	56	Ms	9, 10
9	AA-2625	7765 ± 105	7315 ± 105	11	45	Ms	8
From postglacial marine sediment, postdating Noble Inlet advance							
23	GX-13022	8780 ± 230	8330 ± 230	10	50	Mmp	6, 9
20	GSC-3404	8240 ± 90	8200 ± 45	2	42	Mmp	6, 7

[1] Site numbers are keyed to Figure 2. *See* Manley (1995) for additional sites and radiocarbon dates.
[2] Radiocarbon dates were reported as follows: AA and GX dates are ^{13}C-corrected, normalized to $\delta^{13}C_{=-25‰}$, with error terms of ±1σ, as per convention of Stuiver and Pollach (1977); GSC dates are ^{13}C corrected, normalized to $\delta^{13}C_{=0‰}$, with error terms of ±2σ; SI dates are not ^{13}C corrected, with error terms of ±1σ.
[3] Radiocarbon ages were recalculated to a common format as follows: ^{13}C corrected (with measured or assumed δ^{13}C value), normalized to $\delta^{13}C_{=-25‰}$, and corrected for an assumed marine reservoir effect of 450 years, with error terms of ±1 σ.
[4] Elevation of dated sample and nearby marine limit are reported in metres above mean high tide.
[5] Materials used for dating: M, marine mollusc; s, single individual; m, multiple individuals; p, exclusively or mostly paired valves.
[6] Original references and additional sources for stratigraphic context: 1, Blake (1966); 2, Lowdon et al. (1967); 3, Lowdon and Blake (1973); 4, Muller (1980); 5, Andrews and Short (1983); 6, Miller et al. (1988); 7, Andrews et al. (1989); 8, Kaufman and Williams (1992); 9, Manley and Jennings (1996); 10, this study. All dates were previously presented in Manley (1995).

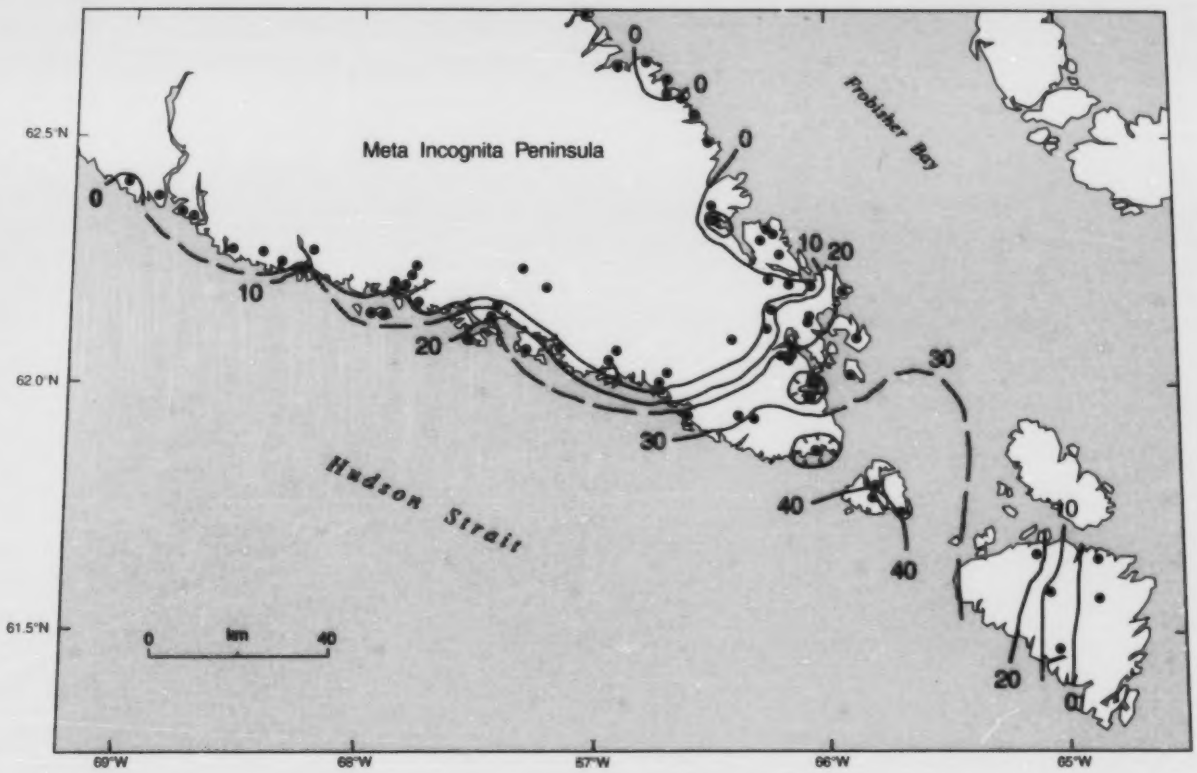

Figure 4. *Contour map of per cent carbonate in the matrix (<2 mm) of drift above the marine limit. Small dots show sampling sites. Data are* from *Stravers (1986), Miller et al. (1988), and Manley (1995).*

Figure 5.

Time-distance diagram with radiocarbon dates used to constrain the position and timing of the Gold Cove advance. Twelve AMS ^{14}C dates from Hall Peninsula, ranging 10.8–9.8 ka BP, are on single fragments of marine molluscs reworked into till above the marine limit. These dates and others (black circles and squares) constrain a period of open-water conditions in outer Frobisher Bay, followed shortly thereafter by advance onto Hall Peninsula. Geochemical analyses of the associated till, and striations on bedrock under the till, indicate a southerly provenance. Radiocarbon dates from postglacial deltas (open circles) indicate ice-marginal retreat off Hall Peninsula beginning 9.6 ka BP. The transect shown here extends northeastward from the southeastern tip of Meta Incognita Peninsula across Frobisher Bay onto and across Loks Land. Vertical lines are ±1 sigma errors. Modified from *Kaufman et al. (1993a).*

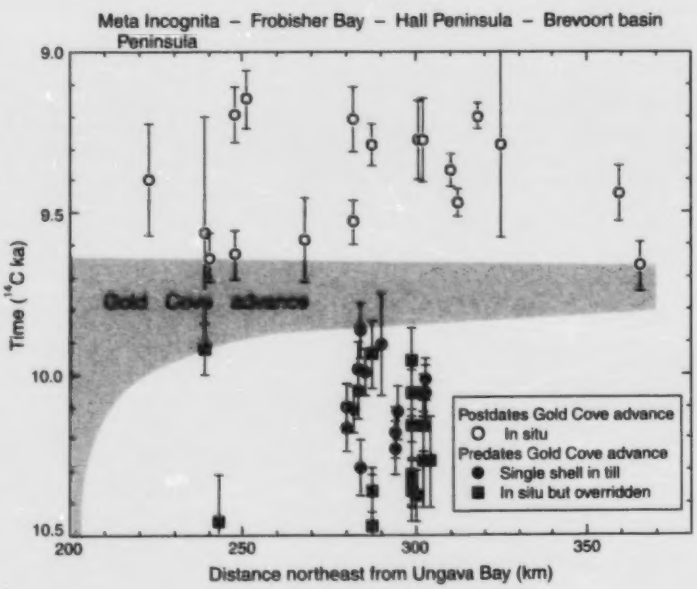

deposits that constrain the opening of outermost Meta Incognita Peninsula to the waters of Hudson Strait. The advance appears to have been abrupt, may have been double-pulsed, and occurred during fluctuations in atmospheric radiocarbon that affect the accuracy of the dating method (cf. Pearson et al., 1993).

Thus, the evidence on southeastern Baffin Island points toward a major northward advance of the Labrador Dome approximately 8.9–8.4 ka BP (ca. 10 000–9450 calendar years BP). A simple ice-flow model quantifies rates of iceberg calving into the Labrador Sea of 64–560 km^3/year (Manley, 1995). The maximum extent of the advance appears to coincide with a 110 m thick, ice-contact morainal bank that lies between Noble Inlet and the northern tip of Edgell Island (Fig. 2; Stravers and Powell, 1997). At this site, a southwest-facing ice-proximal morainal slope and subaqueous debris-flow transport to the northeast are further evidence for Noble Inlet ice flow perpendicular to Hudson Strait. The timing, extent, and flow direction of the advance are consistent with recent assessments of ice-grounding and the marine-geological record in the Eastern basin of the strait (Jennings et al., 1998; MacLean et al., 2001).

Evidence indicates that the Noble Inlet advance originated from the Labrador Dome (cf. Miller et al., 1988; Stravers et al., 1992; Kaufman et al., 1993b; Manley, 1995), rather than representing divergence or deflection of flow near the terminus of a southeast-moving Hudson Strait ice stream (cf. Dyke and Prest, 1987; England and Smith, 1993; Gray, 2001). First, onshore striation evidence for southeastward flow is limited to a single observation on Big Island (southwest of Lake Harbour, Fig. 1). Also, carbonate-rich drift in the Lake Harbour region is found only below the marine limit, is glaciomarine sediment, and is not till deposited by southeast-flowing ice (cf. Fig. 3, 4; Manley, 1996). Second, the pattern of ice flow recorded by striations within the maximum, ^{14}C dated extent of the Noble Inlet advance are not consistent with divergent flow near the mouth of a southeast-flowing ice stream (which would involve northward flow close to the mouth, shifting to northeastward and eastward flow along the lateral ice-stream margin). Instead, the flow patterns fan from northeastward near Resolution Island and Noble Inlet to northward farther west, with basal ice movement uphill and away from any calving margin. Also, the northeastward to northward flow encompasses 240 km of coastline, and is not limited to the tip of Meta Incognita

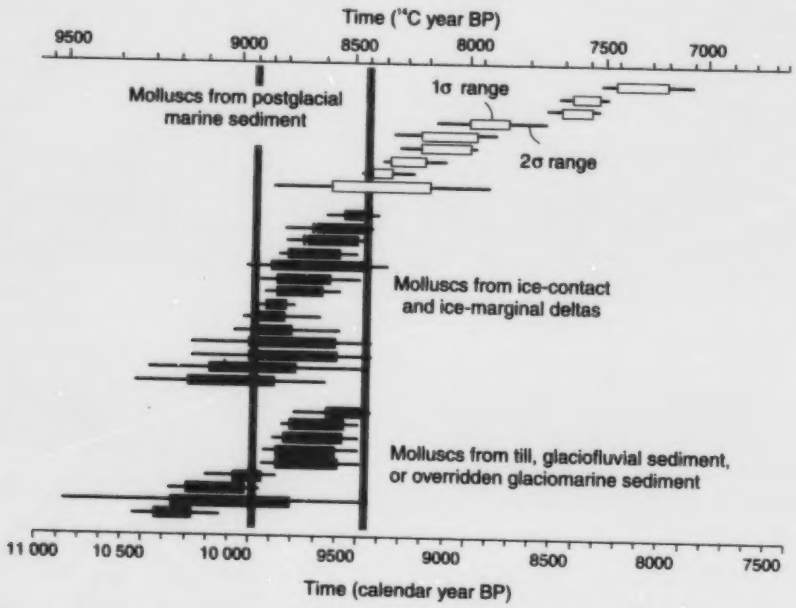

Figure 6. *Radiocarbon dates constraining onset and retreat of the Noble Inlet advance (Manley, 1995). Dates are clustered into three groups that predate, coincide with, or postdate glacier advance across each dated site, based on independent geomorphic and stratigraphic criteria. For example, molluscs from till, outwash, and glaciomarine sediment overlain by till should predate glacier advance (see Table 1). Within each group, the dates are arranged vertically by decreasing age, and have been calibrated to calendar years (bottom axis), with corresponding ages in radiocarbon years before present (^{14}C BP) shown on the upper axis. In agreement with ice-contact deltas and kame terraces observed within its maximum extent, the advance may have oscillated slightly during retreat, and/or may have been time-transgressive in both advance and retreat. The dates constrain the Noble Inlet advance to approximately 8900–8400 BP (ca. 10 000–9450 calendar years BP).*

Peninsula. Finally, by definition the striation patterns and movement of ice necessitate an ice-surface slope that grades upward to the south and southwest, toward the source of the ice.

We believe that the timing, extent, and ice-surface reconstruction for the Noble Inlet advance are consistent with glacial-geological evidence from the south shores of the strait, including deglaciation of Akpatok Island by ca. 8.1 ka BP (Gray, 2001). The complexity in former ice-flow patterns in and near Ungava Bay (with dominant northward and northeastward flow and subsidiary eastward and northwestward flow) can be explained by rapid deglacial drawdown and southward migration of a calving embayment into eastern Ungava Bay following the Noble Inlet advance. Finally, the provenance data reported by Gray (2001) are consistent with northward to northeastward flow from Ungava Bay during one or more advances during the late Wisconsin glaciation. We stress that multiple-age assemblages of molluscs, due to glacial reworking of older sediment into both till and glaciomarine sediment, are commonplace in the region, and interpretation of radiocarbon dates requires careful consideration of single-specimen ^{14}C determinations, as well as absolute dating errors of about 100 years or more due to uncertainties in marine reservoir correction and other factors.

Correlation of the Noble Inlet advance with depositional events in the Eastern basin of Hudson Strait (Jennings et al., 1996, 1998; MacLean et al., 2001) hinges on radiocarbon chronologies. For this reason, detail is provided here on two stratigraphic sections tied to maximum and late phases of the Noble Inlet advance.

The first section is a wave-cut exposure into the distal edge of the York delta (Fig. 7; Blake, 1966; Muller, 1980; Miller and Stravers, 1987; Stravers et al., 1992). At the base of the section lies a diamicton, interpreted as till, which is overlain by several metres of prodelta glaciomarine sediment. This horizon is overlain by progradational deltaic foreset beds, in turn overlain by topset gravels of a sandur that extends upward and southward to the apex of the delta at the mouth of the York gorges. Four dates on molluscs were obtained from the section (Lowdon et al., 1967; Muller, 1980; Andrews and Short, 1983; all dates corrected for ^{13}C fractionation and marine reservoir effect; *see* Manley (1995)). A fifth date was obtained on molluscs from glaciomarine sediment draping a nearby, low hill (8750 ± 190 BP; GSC-2991; Muller, 1980). A sixth date is on molluscs from a distal, subsidiary arm of the delta that reached western Jackman Sound (8970 ± 190 BP; GSC-1903; Lowdon and Blake, 1973).

Together the dates average 8770 ± 120 BP (mean ± s.d.), reflecting the timing of meltwater and sediment diversion through the York gorges to the York delta from an ice-dammed lake south of the drainage divide of the peninsula. Lake levels at 300–360 m elevation, coincident with the lowest reaches of the gorges, are recorded by beach ridges and small deltas north of Pritzler Harbour (Blake, 1966; Stravers et al., 1992). A smaller gorge leading to one of the lacustrine deltas requires that ice dammed a separate valley farther west (Manley, 1995). Formation of the proglacial lakes requires that an ice mass reached a surface elevation of at least 360 m across an east-west span of at least 35 km on Meta Incognita Peninsula (as much as 170 km across southern Meta Incognita Peninsula based on meltwater spillways 200–520 m above sea level and other geomorphic evidence presented by Kleman and Jansson (1996)). Striations and provenance indicators just south of the position of the ice dam indicate that ice moved north-northeastward (Miller et al., 1988; Manley, 1995). Ice-surface elevations therefore climbed to the south-southwest, and may have reached 400–500 m or more where Noble Inlet ice crossed Eastern basin. This configuration most likely existed during the maximum phase of the advance.

The second section lies at the head of Noble Inlet, where a large ice-contact delta is dissected and infilled by a small marine delta (Fig. 8; the "Noble Inlet cut & fill delta" described by Miller and Stravers (1987), Miller et al. (1988), and Manley (1995)). A date of 8920 ± 80 BP is on molluscs from distal glaciomarine sediment overlain by till, and a date of 8615 ± 80 BP is on a single, abraded shell fragment reworked into till and deposited above the marine limit. The stratigraphic context of these molluscs indicate that they predate one or more glacier advances across the site. Three dates on molluscs from proximal glaciomarine sediment quantify the establishment of an ice margin at the southwestern edge of the delta. They average 8665 ± 60 BP. Finally, a date of 8200 ± 45 BP exists for shells collected from an inset, sandy postglacial delta, providing a minimum age for local deglaciation. Striated limestone clasts, calcareous matrix,

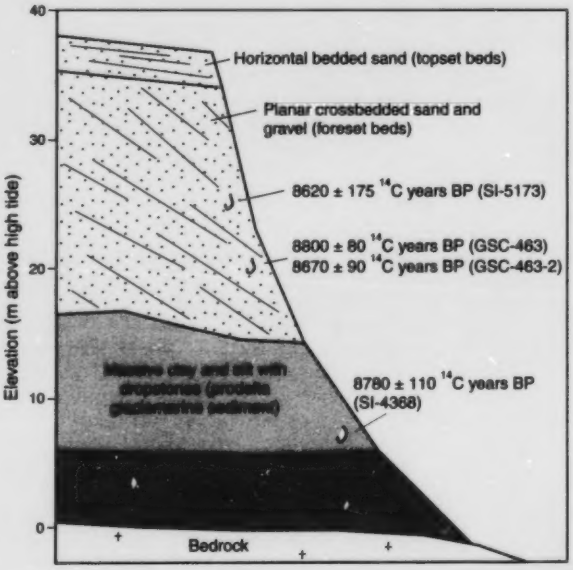

Figure 7. *Schematic stratigraphic section of the distal, wave-cut edge of the York delta, showing stratigraphic units and associated radiocarbon dates. Also shown are small symbols depicting molluscs (see Fig. 8). See Figure 2 for location and Table 1 for additional radiocarbon information.* Modified from *Miller and Stravers (1987) and Manley (1995).*

and northward to northeastward striations document a Labradorean provenance for the ice that deposited the glaciomarine sediment and till.

The ice margin associated with the ice-contact delta appears to have been a recessional one, related to a stillstand and minor readvance during overall retreat. The delta lies 10–25 km upflow of the maximum extent of the Noble Inlet advance, and was associated with relatively thin ice channelled into the valley at the head of Noble Inlet (Miller et al., 1988; Manley, 1995). Available radiocarbon dates suggest deposition of the ice-contact delta approximately one century after formation of the York delta. The date of 8615 ± 80 BP for the glacially transported fragment is evidence for a minor readvance of a few kilometres, immediately before deposition of the ice-contact delta. These observations are consistent with evidence from nearby ice-contact and ice-marginal deltas, which describe minor oscillation of an ice margin during overall retreat, ca. 8600–8500 BP, with ice-surface elevations of about 60–300 m at the coast. Final, coastal deglaciation occurred ca. 8400–8300 BP.

Thus, the maximum phase of the Noble Inlet advance appears to have occurred ca. 8770 BP, based on the chronology of deposition of the York delta. Minor readvances during overall retreat occurred ca. 8600–8500 BP, before deglaciation of the southeast Baffin Island coast ca. 8400–8300 BP.

SOUTHWARD FLOW NEAR LAKE HARBOUR

In contrast, the terrestrial glacial-geological record farther west records flow from an ice cap on Meta Incognita Peninsula (Fig. 1; Manley, 1996). Striations at 60 sites along 200 km of coastline document southward to southwestward flow from the western highlands of the peninsula. Noncalcareous till and a paucity of limestone erratics are consistent with deposition from ice that scoured Precambrian rocks of the peninsula. Available radiocarbon dates indicate that the southward flow occurred before 8200 BP, apparently coeval with northward flow of the Noble Inlet advance. An offshore moraine, 50 km southeast of Lake Harbour, might mark the maximum extent of southward flow into the strait (MacLean et al., 1986; Manley, 1995). Coastal deglaciation occurred at about 8200 BP.

A single striation site southwest of Lake Harbour documents the impingement of a Hudson Strait ice stream onto southern Baffin Island. Uncommon limestone erratics in the region might be related to this event, which occurred centuries or millennia before the southward flow (Manley, 1996). Surprisingly little evidence exists onland to support reconstruction of an ice stream parallel to the axis of Hudson Strait.

Glaciomarine sediment is common in the Lake Harbour region below the marine limit (Manley, 1996). Ten radiocarbon dates describe its deposition spanning ca. 8100–7700 BP. Limestone erratics and calcareous matrix in the drift attest to a calving margin at this time in Hudson Bay, Foxe Basin, or potentially from a retreating Labradorean margin in Ungava Bay.

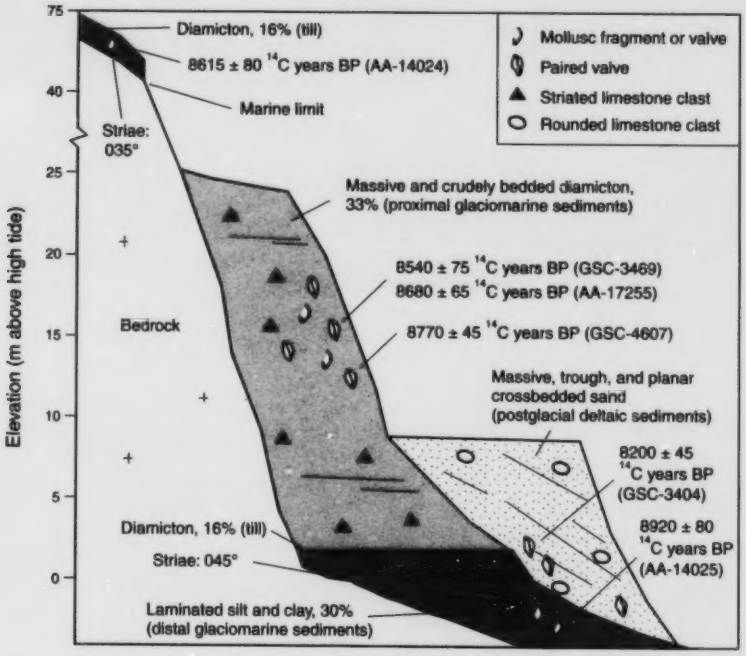

Figure 8.

Schematic stratigraphic section of the "Noble Inlet cut & fill delta", showing stratigraphic units, associated radiocarbon dates, and striation measurements. Till forms a thin veneer capping a hill above the massive ice-contact delta, which is infilled by a small postglacial delta. Percentages, where given, indicate the per cent carbonate in the matrix of sediment samples. See *Figure 2 for location and Table 1 for additional radiocarbon information, and Manley (1995) for a more detailed description.* Modified from *Miller and Stravers (1987) and Manley (1995).*

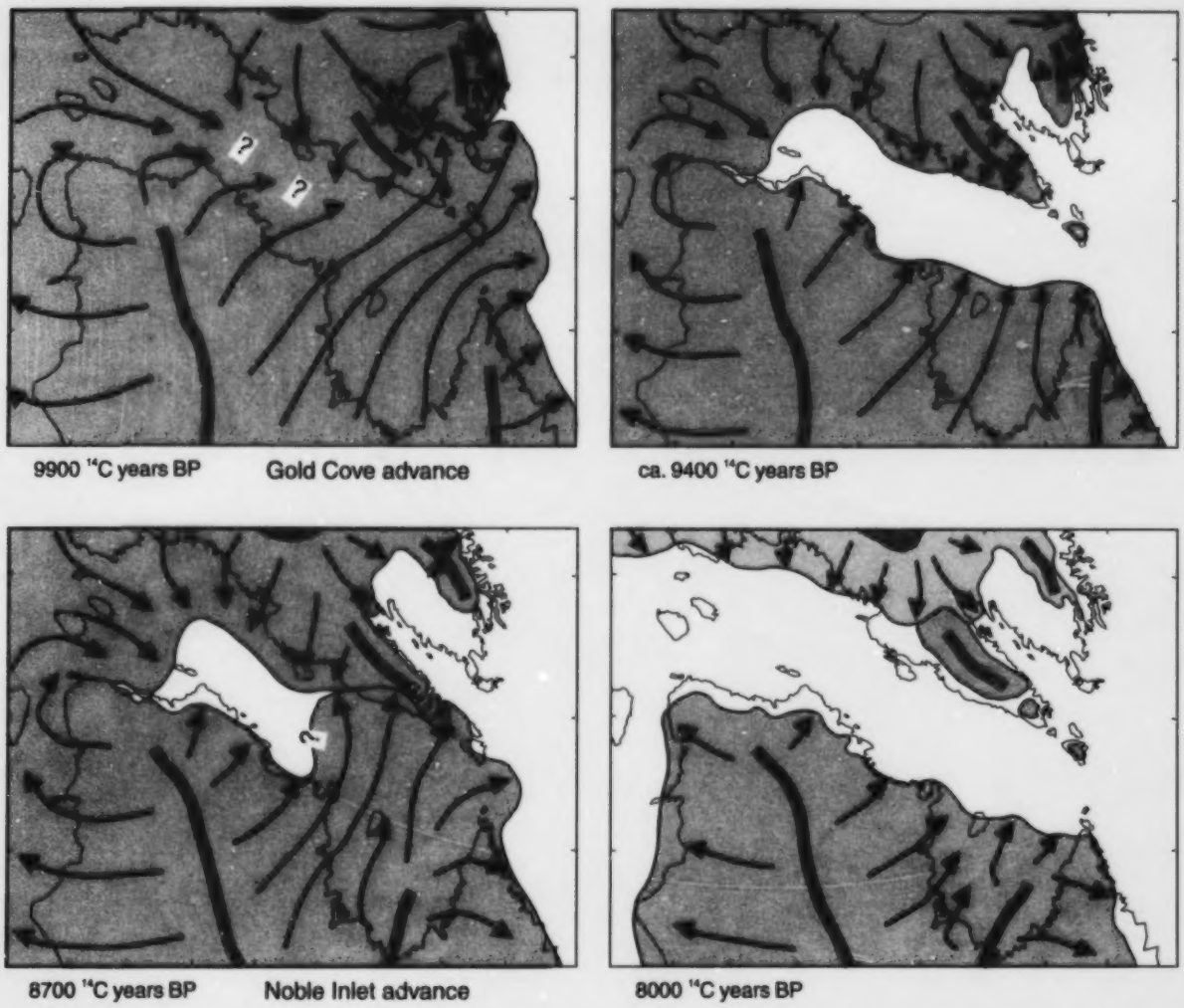

Figure 9. *Summary of inferred glacial events in the Hudson Strait region, based on ice-flow directions (striation and provenance data), radiocarbon dates, and location of moraines and other ice-marginal features* (modified from *Stravers et al., 1992; Kaufman et al., 1993a; Andrews et al. 1995b, Fig. 4; Manley, 1995). Reproduced with permission from Elsevier Science.*

IMPLICATIONS FOR EVENTS IN HUDSON STRAIT

Together the glacial-geological data on southern Baffin Island provide an empirical model for complex ice-sheet behaviour in eastern Hudson Strait (Fig. 9). Foremost among the conclusions are 1) the Labrador Dome played a dominant role in the glacial history of eastern Hudson Strait during the last glacial-interglacial transition (specifically 10 000–7500 BP), with minor glacial input from an ice cap on western Meta Incognita Peninsula, and little evidence for a late glacial Hudson Strait ice stream impinging on Baffin Island; 2) the Gold Cove and Noble Inlet events were abrupt, requiring only a few centuries to cross Hudson Strait and/or Frobisher Bay, with only a few centuries more for ice-marginal retreat; 3) Frobisher Bay and Hudson Strait were at least partially ice-free prior to each advance, based on the ages of individual molluscs reworked into till; and 4) final deglaciation of the northern fringe of Hudson Strait occurred ca. 8400–8200 BP. In sum, the onshore record establishes a framework for comparison with paleoceanographic events and depositional environments as recorded in sediments in the Eastern basin, elsewhere in Hudson Strait, and in Ungava Bay.

ACKNOWLEDGMENTS

Our greatest thanks go to Brian MacLean, who has inspired us and many others to conduct research in the Hudson Strait region. We also thank Darrell Kaufman (Northern Arizona University), Anne Jennings, and John Andrews (University of Colorado) for numerous discussions. The manuscript benefited from comments by the critical reviewers D.A. Hodgson, H. Josenhans, and J. Shaw. The research was made possible through NSF grant EAR-9005179.

REFERENCES

Andrews, J.T. and Short, S.K.
1983: Radiocarbon Date List V: Baffin Island, N.W.T., Canada, and Radiocarbon Date List II: Labrador and Northern Quebec, Canada; Institute of Arctic and Alpine Research, Occasional Paper 40, 71 p.

Andrews, J.T., Bond, G., Jennings, A.E., Kerwin, M., Kirby, M., MacLean, B., Manley, W., and Miller, G.H.
1995a: A Heinrich-like event, H-0 (DC-0): source(s) for detrital carbonate in the North Atlantic during the Younger Dryas chronozone; Paleoceanography, v. 10, p. 943–952.

Andrews, J.T., Laymon, C.A. and Griggs, W.M.
1989: Radiocarbon Date List III: Labrador and Northern Quebec, Canada, and Radiocarbon Date List VI: Baffin Island, N.W.T., Canada; Institute of Arctic and Alpine Research, Occasional Paper 46, University of Colorado, Boulder, Colorado, 85 p.

Andrews, J.T., MacLean, B., Kerwin, M., Manley, W., Jennings, A.E., and Hall, F.
1995b: Final stages in the collapse of the Laurentide Ice Sheet, Hudson Strait, Canada, NWT: 14C AMS dates, seismic stratigraphy, and magnetic susceptibility logs; Quaternary Science Reviews, v. 14, p. 983–1004.

Bell, R.
1901: Report of an exploration on the northern side of Hudson Strait; Geological Survey of Canada, Annual Report, Volume XI, Part M, 38 p.

Blake, W., Jr.
1966: End moraines and deglaciation chronology in northern Canada with special reference to southern Baffin Island; Geological Survey of Canada, Paper 66-26, 31 p.

Clark, P.
1985: A note on the glacial geology and postglacial emergence of the Lake Harbour region, Baffin Island, N.W.T.; Canadian Journal of Earth Sciences, v. 22, p. 1864–1871.

Colvill, A.
1982: Glacial landforms at the head of Frobisher Bay, Baffin Island, Canada; M.Sc. thesis, University of Colorado, Boulder, Colorado, 202 p.

Duvall, M.L.
1993: Late Foxe glacial geology of the mid-bay area of Frobisher Bay, southeast Baffin Island, Northwest Territories; M.Sc. thesis, University of Colorado, Boulder, Colorado, 103 p.

Dyke, A.S. and Prest, V.K.
1987: Late Wisconsinan and Holocene history of the Laurentide Ice Sheet; Géographie physique et Quaternaire, v. XLI, no. 2, p. 237–263.

England, J. and Smith, I.R.
1993: Late glacial ice margins and deglacial chronology for southeastern Baffin Island and Hudson Strait, eastern Canadian Arctic: Discussion; Canadian Journal of Earth Sciences, v. 30, p. 1749–1752.

Gray, J.T.
2001: Patterns of ice flow and deglaciation chronology for southern coastal margins of Hudson Strait and Ungava Bay; *in* Marine Geology of Hudson Strait and Ungava Bay, Eastern Arctic Canada: Late Quaternary Sediments, Depositional Environments, and Late Glacial–Deglacial History Derived from Marine and Terrestrial Studies, (ed.) B. MacLean; Geological Survey of Canada, Bulletin 566.

Gray, J., Brynczka, T., Manley, W., and Miller, G.
1995: Recent observations on glacial flow patterns and postglacial isostatic uplift variations on Resolution and Edgell Islands; *in* 25th Arctic Workshop, Centre d'Études Nordiques, Université Laval, Québec, Quebec, p. 68–70.

Jennings, A.E., MacLean, B., Manley, W.F., and Andrews, J.T.
1996: Reconciling terrestrial and marine evidence for the last ice advance across eastern Hudson Strait; Geological Society of America, Abstracts with Programs, v. 28, no. 7, p. A434.

Jennings, A.E., Manley, W.F., MacLean, B., and Andrews, J.T.
1998: Marine evidence for the last glacial advance across Eastern Hudson Strait, Eastern Canadian Arctic; Journal of Quaternary Science, v. 13, p. 501–514.

Kaufman, D.L. and Williams, K.M.
1992: Radiocarbon Date List VII: Baffin Island, N.W.T., Canada; Institute of Arctic and Alpine Research, Occasional Paper 48, University of Colorado, Boulder, Colorado, 82 p.

Kaufman, D.S., Miller, G.H., Stravers, J.A., and Andrews, J.T.
1993a: An abrupt early Holocene (9.9–9.6 kyr BP) ice stream advance at the mouth of Hudson Strait, Arctic Canada; Geology, v. 21, p. 1063–1066.

Kaufman, D.S., Miller, G.H., Stravers, J.D., Manley, W.F., and Duvall, M.L.
1993b: Late glacial ice margins and deglacial chronology for southeastern Baffin Island and Hudson Strait, eastern Canadian Arctic: Reply; Canadian Journal of Earth Sciences, v. 30, p. 1753–1758.

Kleman, J. and Jansson, K.
1996: Glacial landforms of southern Baffin Island; Department of Physical Geography, Stockholm University, Stockholm, Sweden, scale 1:600 000.

Lind, E.K.
1983: Environmental conditions and history of the Holocene deglaciation for the Cape Rammelsberg area, southern Baffin Island, N.W.T., Canada; M.Sc. thesis, University of Colorado, Boulder, Colorado, 219 p.

Lowdon, J.A. and Blake, W., Jr.
1973: Geological Survey of Canada, Radiocarbon Dates XIII; Geological Survey of Canada, Paper 73-7, 61 p.

Lowdon, J.A., Fyles, J.G., and Blake, W., Jr.
1967: Geological Survey of Canada Radiocarbon Dates VI; Geological Survey of Canada, Paper 67-2B, 42 p.

MacLean, B., Andrews, J.T., Gray, J.T., Hall, F.R., Hardy, I., Jennings, A.E., Manley, W.F., Pfeffer, W.T., and Vilks, G.
2001: Hudson Strait Quaternary sediments and late glacial and deglaciation history: a discussion and summary; *in* Marine Geology of Hudson Strait and Ungava Bay, Eastern Arctic Canada: Late Quaternary Sediments, Depositional Environments, and Late Glacial–Deglacial History Derived from Marine and Terrestrial Studies, (ed.) B. MacLean; Geological Survey of Canada, Bulletin 566.

MacLean, B., Williams, G.L., Sanford, B.V., Klassen, R.A., Blakeney, C., and Jennings, A.E.
1986: A reconnaissance study of the bedrock and surficial geology of Hudson Strait, N.W.T.; *in* Current Research, Part B; Geological Survey of Canada, Paper 86-1B, p. 617–635.

Manley, W.F.
1995: Late-glacial record of ice-sheet/ocean interactions, Hudson Strait and southern Baffin Island, eastern Canadian Arctic; Ph.D. thesis, University of Colorado, Boulder, Colorado, 266 p.
1996: Late-glacial flow patterns, deglaciation, and postglacial emergence of south-central Baffin Island and the north-central coast of Hudson Strait, eastern Canadian Arctic; Canadian Journal of Earth Sciences, v. 33, p. 1499–1510.

Manley, W.F. and Jennings, A.E.
1996: Radiocarbon Date List VIII: Eastern Canadian Arctic, Labrador, Northern Quebec, East Greenland Shelf, Iceland Shelf, and Antarctica; Institute of Arctic and Alpine Research, Occasional Paper 50, 163 p.

Manley, W.F. and Miller, G.H.
1994: Reassessment of the Noble Inlet advance: an early Holocene surge(?) across Hudson Strait onto Baffin Island, eastern Canadian Arctic; Geological Society of America, Abstracts with Programs, v. 26, no. 7, p. A-127.

Manley, W.F. and Moore, J.J.
1995: Early Holocene glacial interactions in inner Frobisher Bay, southern Baffin Island, Nunavut; *in* 25th Arctic Workshop, Centre d'Études Nordiques, Université Laval, Québec, Quebec, p. 123–125.

Miller, G.H.
1980: Late Foxe glaciation of southern Baffin Island, Northwest Territories, Canada; Geological Society of America, Bulletin, v. 91, p. 399–405.

Miller, G.H. and Kaufman, D.S.
1990: Rapid fluctuations of the Laurentide ice sheet at the mouth of Hudson Strait: new evidence for ocean/ice-sheet interactions as a control on the Younger Dryas; Paleoceanography, v. 5, p. 907–919.

Miller, G.H. and Stravers, J.A.
1987: Glacial geology and Holocene events, outer Frobisher Bay; *in* Cumberland Sound and Frobisher Bay, Southeastern Baffin Island, N.W.T., (ed.) J.T. Andrews, R. Gilbert, J.D. Jacobs, G.H. Miller, W.N. Mode, and J.D. Stravers; XIIth INQUA Congress, Field Excursion Guide Book C-2, p. 63–84.

Miller, G.H., Hearty, J., and Stravers, J.A.
1988: Ice-sheet dynamics and glacial history of southeasternmost Baffin Island and outermost Hudson Strait; Quaternary Research, v. 30, p. 116–136.

Muller, D.S.
1980: Glacial geology and Quaternary history of southeast Meta Incognita Peninsula, Baffin Island, Canada; M.Sc. thesis, University of Colorado, Boulder, Colorado, 211 p.

Pearson, G.W., Becker, B., and Qua, F.
1993: High-precision 14C measurement of German and Irish oaks to show the natural 14C variations from 7890 to 5000 BC; Radiocarbon, v. 35, p. 93–104.

Pfeffer, W.T., Dyurgerov, M., Kaplan, M., Dwyer, J., Sassolas, C., Jennings, A., Raup, B., and Manley, W.
1997: Numerical modeling of late glacial Laurentide advance of ice across Hudson Strait: insights into terrestrial and marine geology, mass balance, and calving flux; Paleoceanography, v. 12, p. 97–110.

Squires, C.
1984: The Late Foxe deglaciation of the Burton Bay area, southeastern Baffin Island, N.W.T.; M.A. thesis, University of Windsor, Windsor, Ontario, 186 p.

Stravers, J.A.
1986: Glacial geology of outer Meta Incognita Peninsula, southern Baffin Island, Arctic Canada; Ph.D. thesis, University of Colorado, Boulder, Colorado, 231 p.

Stravers, J.A. and Powell, R.D.
1997: Glacial debris flow deposits on the Baffin Island shelf: seismic facies architecture of till-tongue-like deposits; Marine Geology, v. 143, p. 151–168.

Stravers, J.A., Miller, G.H., and Kaufman, D.S.
1992: Late glacial ice margins and deglacial chronology for southeastern Baffin Island and Hudson Strait, eastern Canadian Arctic; Canadian Journal of Earth Sciences, v. 29, p. 1000–1017.

Stuiver, M. and Polach, H.A.
1977: Reporting of ^{14}C data; Radiocarbon, v. 19, p. 355–363.

Patterns of ice flow and deglaciation chronology for southern coastal margins of Hudson Strait and Ungava Bay

James T. Gray[1]

Gray, J.T., 2001: Patterns of ice flow and deglaciation chronology for southern coastal margins of Hudson Strait and Ungava Bay; in *Marine Geology of Hudson Strait and Ungava Bay, Eastern Arctic Canada: Late Quaternary Sediments, Depositional Environments, and Late Glacial–Deglacial History Derived from Marine and Terrestrial Studies, (ed.) B. MacLean; Geological Survey of Canada, Bulletin 566, p. 31–55.*

Abstract: Erosional features, erratic occurrences, and carbonate drift distribution on the southern margins of Hudson Strait revealed divergent flow from northern Ungava Peninsula into west-central Hudson Strait, and convergent flow from southern Ungava Peninsula, central Quebec–Labrador, and Torngat Mountains dispersal centres into Ungava Bay. Convergence of ice flows from Hudson Strait and Ungava Bay is suggested by easterly flow overriding the northern Labrador peninsula. In west-central Hudson Strait, only islands and promontories were affected by a Hudson Strait ice stream, that later gave way to northeasterly flow off Ungava Peninsula. Ice retreat in the Torngat Mountains of northern Labrador was succeeded by invasion of easterly flowing and coalescent Ungava Bay and Hudson Strait ice, resulting in the north-trending Sheppard Lake moraines, and glacially dammed lakes farther south. Carbon 14 mollusc dates from Deception Bay indicate an ephemeral opening of Hudson Strait prior to 10 ka BP, but general deglaciation of east-central Hudson Strait occurred at ca. 9 ka BP, with Ungava Bay finally free from ice after 7 ka BP. Late easterly flows across Akpatok Island and ^{14}C ages cannot be easily reconciled with late glacial resurgence of ice northward from Quebec–Labrador across an ice-free Hudson Strait to Noble Inlet on south Baffin Island.

Résumé : Des structures d'érosion, la présence de blocs erratiques et la répartition des sédiments glaciaires carbonatés sur les marges méridionales du détroit d'Hudson témoignent d'un écoulement divergent depuis le nord de la péninsule d'Ungava vers le centre ouest du détroit d'Hudson, et d'un écoulement convergent à partir de centres de dispersion dans le sud de la péninsule d'Ungava, la région Québec central–Labrador et les monts Torngat vers la baie d'Ungava. L'écoulement glaciaire vers l'est dans la partie septentrionale de la péninsule du Labrador porte à croire qu'il y a eu convergence des glaces provenant du détroit d'Hudson et de la baie d'Ungava. Dans le centre ouest du détroit d'Hudson, seuls les îles et les promontoires ont été chevauchés par un courant glaciaire en provenance du détroit d'Hudson qui par la suite a laissé place à un écoulement nord-est au large de la péninsule d'Ungava. Suivant le retrait des glaces dans les monts Torngat, dans le nord du Labrador, les glaces coalescentes de la baie d'Ungava et du détroit d'Hudson ont avancé vers l'est et ont produit les moraines de Sheppard Lake de direction nord et des lacs de barrage glaciaire plus loin au sud. Selon des âges ^{14}C obtenus sur des mollusques provenant de la baie Deception, il y a eu déglaciation d'un chenal dans le détroit d'Hudson avant 10 ka BP, alors que la déglaciation générale du centre est de la baie d'Hudson remonte à environ 9 ka BP et la baie d'Ungava était libre de glace après 7 ka BP. Il est difficile de faire accorder les écoulements tardifs vers l'est sur l'île d'Akpatok et les âges ^{14}C avec la réapparition tardive des glaces provenant de la région Québec–Labrador qui ont traversé le détroit d'Hudson libre de glace vers le nord jusqu'à l'inlet Noble dans le sud de l'île de Baffin.

[1] Département de géographie, Université de Montréal, Montréal, Quebec H3C 3J7

INTRODUCTION

Dominant source areas for ice sheets reaching eastern Hudson Strait were Quebec–Labrador peninsula, the ice stream flowing into and down Hudson Strait from Hudson Bay–Foxe Basin and Keewatin dispersal centres, and the Meta Incognita Peninsula on southernmost Baffin Island. Since Manley and Miller (2001) have already discussed the ice-flow record for the Baffin Island coastal margins of Hudson Strait, the focus in the first part of this paper will be on the presentation of ice-flow patterns for the south coast of Hudson Strait, including offshore islands, notably Akpatok Island, and for the coastal margins of Ungava Bay (Fig. 1), derived from erosional and depositional evidence including glacial erratic dispersal. A special section is devoted to discussion of the significance of the dispersal patterns of distinctive New Quebec geosyncline iron-formation and Paleozoic carbonate erratics to downstrait and cross-strait ice flow in the eastern Hudson Strait sector.

The second part of the paper deals with the deglaciation chronology in Hudson Strait and Ungava Bay, derived mainly from marine shell dates from the southern coastal fringe and the offshore islands, and also from seafloor cores. This latter aspect prompts a discussion on the question of the Noble Inlet readvance — the second of two late glacial advances from southern Ungava Bay across an ice-free Hudson Strait onto southern Baffin Island, initially proposed by Miller et al. (1988), elaborated on by Stravers et al. (1992), Kaufman et al. (1993a, b), Manley (1995), Andrews et al. (1995), and Jennings et al. (1998), but subjected to some criticism by England and Smith (1993), Gray et al. (1997), Lauriol and Gray (1997), and Bruneau and Gray (1997).

ICE-FLOW PATTERNS

Evidence for ice-flow direction is predominantly erosional: derived from striae pits, roches moutonnées, and crag-and-tail, drumlinoid, and fluting features, but depositional evidence in the form of certain erratic lithologies, and in the form of morphological features — terminal, lateral, and ablation moraines, eskers, and glacially dammed lake shorelines — also proved useful. With regard to the erosional evidence, the following rationale suggests that striae indicate

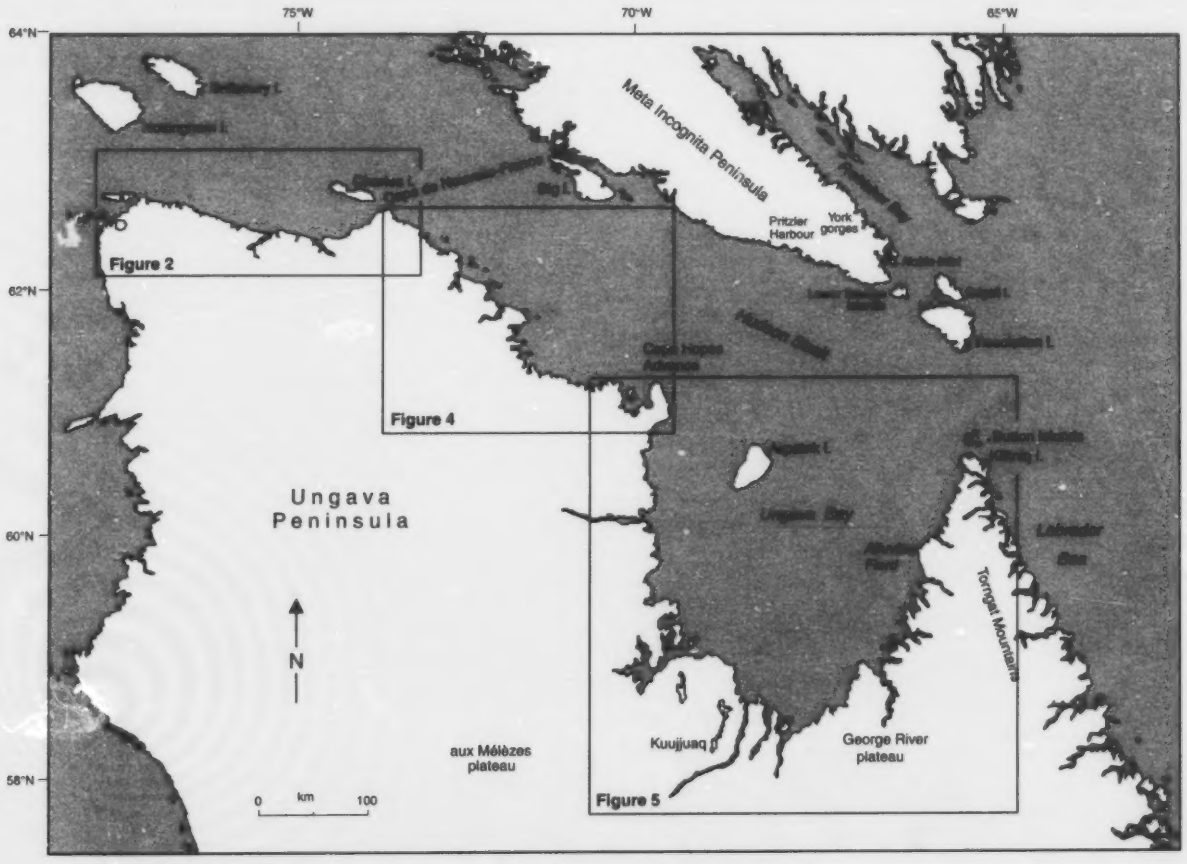

Figure 1. Location of study areas.

ice flows occurring entirely within the Late Wisconsin. Striae could generally be found when pits were dug in a protective till cover. Where occasionally observed on exposed bedrock, the proximity of a sediment cover suggested recent exhumation. Their absence from most exposed bedrock outcrops can be attributed to surface weathering processes in operation during the postglacial interval and, in the case of many wave-washed surfaces, over an even shorter post-coastal emergence interval. If the short postglacial interval of ca. 8 ka BP is sufficient to eliminate such features, then the only possibility for survival through a much longer mid-Wisconsinan interstadial would be beneath a protective sediment cover; however, no evidence has been found for multiple-age tills with intervening pedogenesis or nonglacial sediments, with the notable exception of a localized occurrence, preserved in a deep gorge on Akpatok Island (Thibault et al., 1995). It is therefore reasonable to conclude that the passage of the ice sheets during the last glacial period remoulded the surface. Multiple striae directions at individual sites therefore reflect the temporally changing importance of different ice dispersal centres during the last glacial period.

Concerning the depositional evidence of ice flows, useful erratic clast lithologies were reddish-purple Fenimore Formation iron-rich argillite, Chioak Formation conglomerate and sandstone, and Abner Formation dolomite, all associated with the New Quebec geosyncline (Avramtchev, 1985; Goulet, 1995) and limestone from within the Paleozoic basin (MacLean, 2001). The dispersal of erratics from outcrops of these formations is unquestionably of some use, in that it permits the extent of influence from different flow sources to be determined. It does not permit sequential ordering of individual flow events, however. More useful in this regard is the spatial configuration of the glacial landforms mentioned above, which in specific areas allow both ice-flow directions and the order of events to be established.

Northernmost Ungava Bay and Charles Island

Figure 2 is a compilation of all erosional evidence for glacial flows between Ivujivik and Cape de Nouvelle-France, and for offshore Charles Island, based on evidence presented in Daigneault (1990, 1996), Laymon (1992), and Bruneau and Gray (1997). On the margins of the Ungava Peninsula north of the Cape Smith Proterozoic belt, ice flows were radial into Hudson Strait. For the Salluit Fiord and Deception Bay sector, however, ice flows to the north into the western Hudson Strait basin show topographically controlled deflection into these inlets.

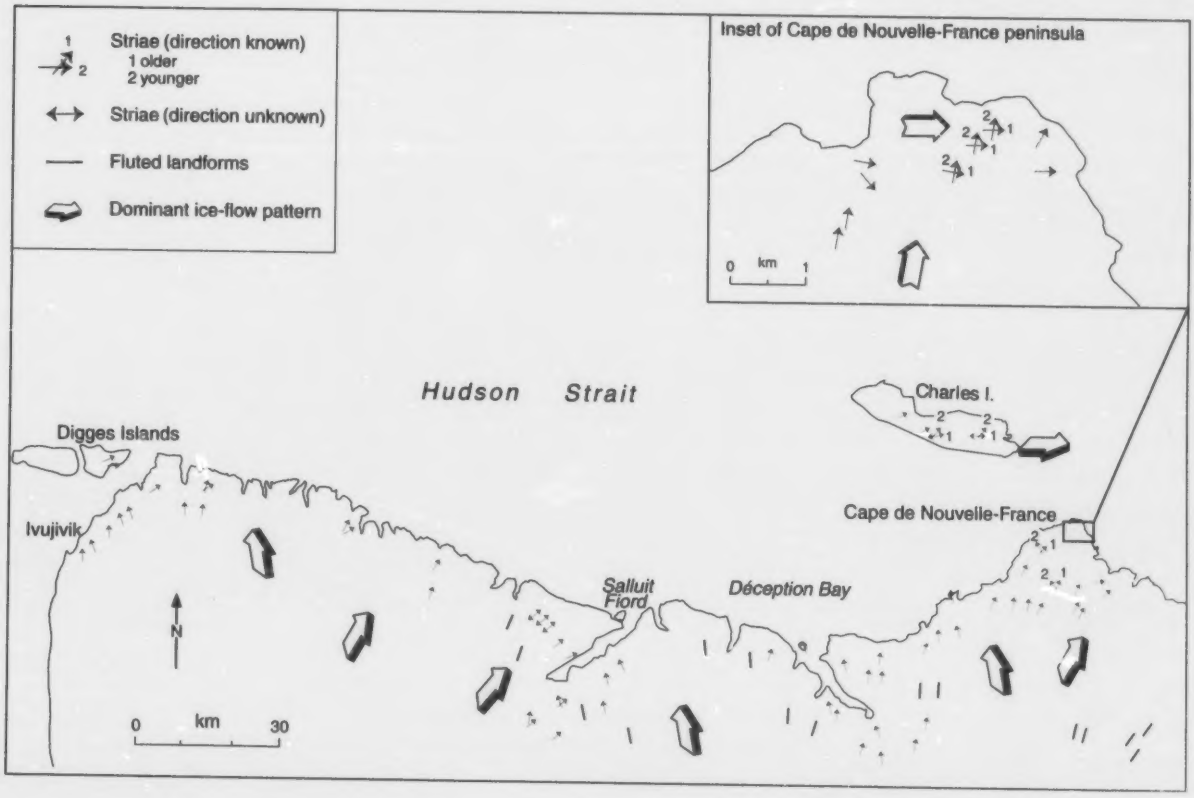

Figure 2. *Ice-flow indicators along north coast of Ungava Peninsula. Based on data in Daigneault (1990, 1996), Bruneau and Gray (1991, 1997), and Laymon (1992).*

On Charles Island two directions of ice flow were noted. The dominant flow easterly as evidenced by striae and grooves, noted at recently exposed sites between sea level and the till-covered summits at 170 m a.s.l. on the north side of the island. In a narrow belt of high ground situated at 135–155 m, 0.5–1 m deep sculptured channels (p-forms), trending west to east indicate subglacial meltwater flow. On low-lying northwest Charles Island, a series of similarly oriented wave-modified eskers is also associated with subglacial evacuation of meltwater. Although criteria for differentiating between eastward or westward flow were lacking, the reasonable inference can be made that these features indicate the evacuation of Laurentide ice and subglacial meltwater in a downstrait direction. Such a flow can be regarded as a continuation of the west-to-east flow noted by Laymon (1992) for Nottingham, Salisbury, and Mill islands at the western end of the strait. An offshore corollary for such meltwater flows is shown by 20–50 m deep channels on the seismostratigraphic record at a location 70 km north of Charles Island (MacLean et al., 2001, Fig. 15).

A secondary flow to the north-northeast and northeast has been identified by Daigneault (1993, 1996) and Bruneau and Gray (1997) at five sites near the ridge crest of the island. On the basis of striae etched onto the ice-proximal surfaces of west-east oriented grooves, it appears that this flow postdated the main flow to the east; however, other erosional and depositional forms indicative of northeast to north-northeast flow are lacking, especially at low altitudes. It appears likely to have been associated with a short-lived surge of ice into Hudson Strait from a dispersal centre on the northwest Ungava plateau, after initial westwards retreat of the main ice front in Hudson Strait (Bruneau and Gray, 1997). Corroboration for this event is found in the marine seismostratigraphic record north of Charles Island (MacLean et al., 2001, Fig. 21) that shows evidence for overriding of stratified glaciomarine sediments by nonstratified ice-contact sediments. The nonstratified sediments are overlain by a thin veneer of postglacial sediments, suggesting that this readvance must have occurred immediately prior to final disintegration of the ice sheet in western Hudson Strait. The grounded limit of this northeast advance may not have extended farther than the southern slope of the western marine basin, as suggested by a lateral transition in the marine record from nonstratified ice-contact sediments to stratified glaciomarine sediments (MacLean et al., 2001, Fig. 19).

On the mainland, in the vicinity of Cape de Nouvelle-France, at the northeast tip of the Ungava Peninsula, a similar dual ice-flow pattern was repeated (inset *in* Fig. 2). At six sites with intersecting striae, the earlier ice flows show considerable variability in flow direction from northeast to east-southeast. This variability is a function of distance inland from the tip of the peninsula. Ice flowing northeast off the Ungava plateau must have been rapidly deflected towards the east by the eastward-flowing Hudson Strait ice stream, as is the case for the Digges Islands at the northwest extremity of Ungava Peninsula (Laymon, 1992). That this earlier flow was also the dominant glacial flow is revealed by grooves, roches moutonnées, and deep crescentic gouges observed at the studied outcrops.

The latest, and less dominant ice flow at three sites at Cape de Nouvelle-France is to the north-northeast; however, at three sites situated 10–15 km southwest of the cape, the youngest flow was to the northwest. Also at two sites, situated 10 km southeast of the cape, the only ice-flow directions were

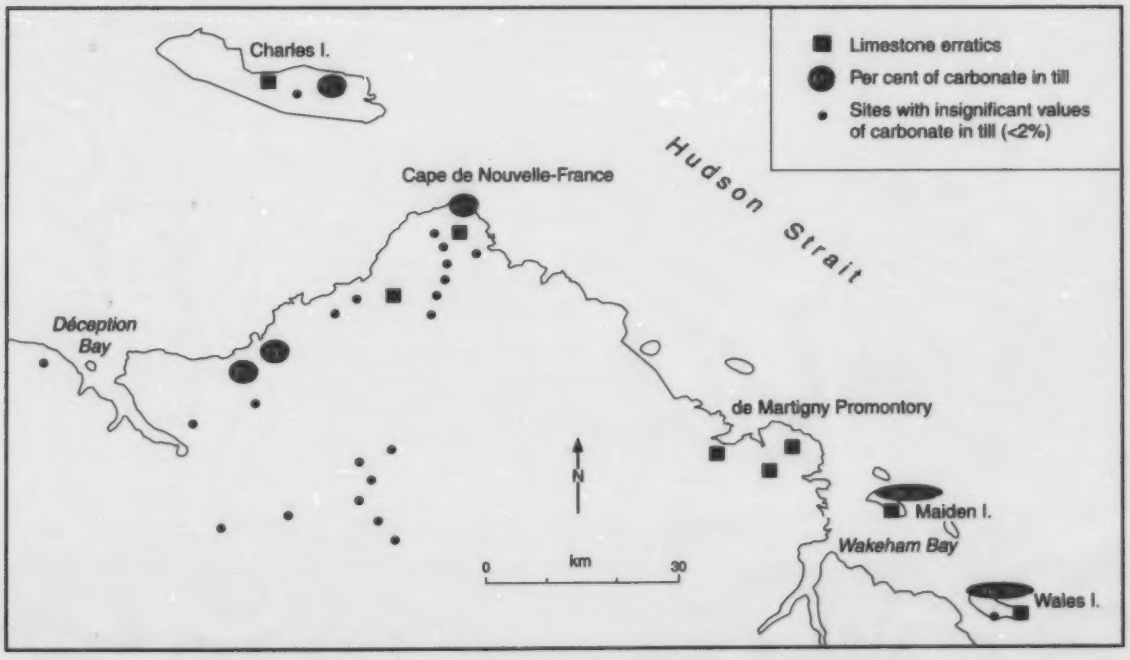

Figure 3. *Distribution of Paleozoic limestone erratics and carbonate content in drift above the postglacial marine limit on northeast Ungava Peninsula. Based on data by Bruneau and Gray (1997).*

to the east. These directions are perpendicular to the local coastline and suggest a fanning out of ice flows from a residual ice cap situated on the Ungava plateau to the south, into an ice-free Hudson Strait. This evidence of a later ice flow from Ungava Peninsula into an ice-free Hudson Strait corroborates the previously discussed evidence of flow of northwest Ungava Peninsula ice to the north-northeast and northeast across Charles Island.

Depositional evidence, based on the distribution of limestone erratics and Chittick carbonate analyses for sites above the postglacial marine limit, support the erosional evidence, indicating almost no onlap of a Hudson Strait ice stream along the coast (Fig. 3). Limestone erratics were found in sparse numbers at only four sites on the northernmost Ungava Peninsula coast — one on Charles Island and three at Cape de Nouvelle-France. Total carbonate content in till, above locally well defined wave-washing limits revealed significant values of more than 1% at only two sites at Cape de Nouvelle-France, and at two sites in a coastal moraine between Deception Bay and Cape de Nouvelle-France. Elsewhere along the coast, Paleozoic limestone fragments were noted in deposits below local marine wave-washing limits. Those found in subaqueous deposits at the head of fiords such as Salluit Fiord and Deception Bay, are most probably related to grounded icebergs calved off from the Hudson Strait ice stream, during its final retreat phase.

Northeast coast of Ungava Peninsula: Cape de Nouvelle-France–Cape Hopes Advance

East of Cape de Nouvelle-France (Fig. 4), observed striae and ancillary erosional evidence, and data published by Low (1899), Daigneault (1996), and Bruneau and Gray (1997) reveal no evidence of onlap by the Hudson Strait ice stream

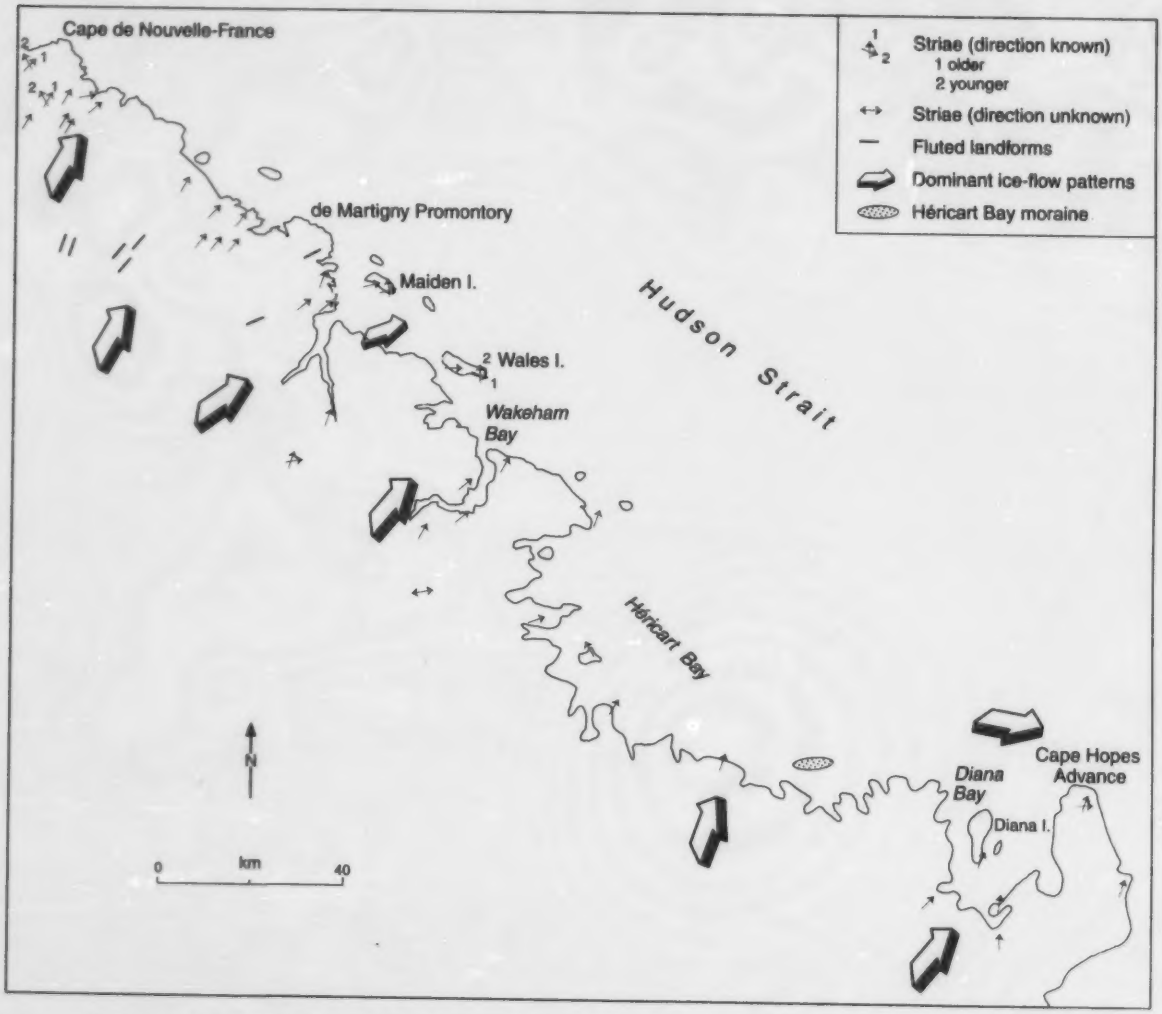

Figure 4. Ice-flow indicators along northeast Ungava Peninsula coast. Based on data in Low (1899), Gangloff et al. (1976), Bruneau and Gray (1991, 1997), and Daigneault (1996).

along the generally high, rugged, and fiord-indented coast, with the exception of the low-lying peninsula culminating at Cape Hopes Advance. In general, ice flow was perpendicular to the coastline. Between Cape de Nouvelle-France and Wakeham Bay including the offshore Wales and Maiden islands, abundant evidence was found for offshore ice flow to the northeast or east from an ice cap formed on the nearby 600 m a.s.l. Ungava plateau. A secondary, older flow to the north, at one site on Wales Island may be associated with initial invasion of the island by a thick ice tongue flowing out of the Wakeham Bay fiord.

Occasional limestone erratics above the marine limit in the De Martigny Promontory sector and on Wales and Maiden islands, and high values for total carbonate content (Fig. 3) seemed initially to conflict with the striae evidence, suggesting some overriding by the Hudson Strait ice stream; however, intensive study of both Wales and Maiden islands clearly indicates that locally high carbonate values and the presence of limestone fragments are found in a narrow altitudinal range, associated with old, glacially overridden, marine shell-bearing terraces, about 50 m above the well defined postglacial marine-washing limits. Clearly the Ungava Peninsula ice sheet coalesced with the Hudson Strait ice stream well offshore during the last glaciation. Seismostratigraphic data presented by MacLean et al. (1986, 1992, 2001) show evidence of a limited late glacial readvance of relatively thin Ungava ice into an ice-free Hudson Strait to a position about 20–30 km offshore. Most interesting is a 70 m thick submarine moraine ridge, 20 km offshore in Héricart Bay (Fig. 4; MacLean et al., 1996; MacLean et al., 2001, Fig. 12).

From Wakeham Bay to Diana Bay along a fiord-indented coast, striae observations by Low (1899) revealed a transition to northerly flows off the Ungava plateau into Hudson Strait. Directional changes, corresponding to general changes in coastline configuration, suggest that local topographic control was exerted on a relatively thin ice sheet. Only at Cape Hopes Advance did the Hudson Strait ice stream again touch the Ungava Peninsula coast, where west-east oriented striae and grooves were observed at three sites. On the southernmost outcrop, crossing striae were noted, the dominant direction being from south-southwest to north-northeast, and the secondary orientation west-east. Drumlinoid features noted by Gray and Lauriol (1985) also show a south-southwest–north-northeast trend, and it is suggested that a flow to the north-northeast, off the northeastern tip of Ungava Peninsula into Hudson Strait, succeeded the west-east downstrait flow. A little farther south, on Diana Island and at the head of Diana Bay, no trace of the Hudson Strait ice stream could be found, the striae patterns indicating ice flow off the Ungava Peninsula to the north-northeast and northeast (Gangloff et al., 1976).

Ungava Bay coast

Striae and fluting patterns mapped by Gangloff et al. (1976), Hardy (1976), Lauriol (1982), Gray and Lauriol (1985), Allard et al. (1989), Klassen et al. (1991), and Gray et al. (1996) are shown in Figure 5. For the west coast of Ungava Bay, north of Kangirsuk (at Payne Bay), there is a general trend of ice flow to the northeast. Farther south, between Kangirsuk and aux Feuilles Bay, ice flows are also dominantly to the northeast. This trend is also noted for the area around the confluence of the aux Mélèzes River and Caniapiscau River. For the lower Koksoak and à la Baleine river valleys the dominant flow pattern, revealed by glacially moulded features, shifts around towards the north. Thus a radial pattern of ice flow into Ungava Bay is suggested by the dominant ice-flow features; however, individual sites with different directions from the main regional trends, or displaying crossing striae, indicate multiple directions of ice flow. At widely separated localities, along the west coast of Ungava Bay, evidence of a secondary flow to the east has been noted by Gangloff et al. (1976), Lauriol (1982), and by Clark et al. (2000); points A–D in Fig. 5). Since the west-to-east-trending striae are not reproduced in the drumlinoid forms, it can be concluded that they represent an earlier flow pattern, prior to the establishment of the dominant northeast flow into Ungava Bay.

A critical outcrop, displaying two flow directions is located on the west bank of the Koksoak River at Kuujjuaq (point E *in* Fig. 5). Previous interpretations from this site have led to contradictory conclusions concerning the relative age of ice flows to the north and to the northeast (Gangloff et al., 1976; Lauriol, 1982; Gray and Lauriol, 1985). A recent detailed analysis of the striae patterns at this site clearly indicates that a dominant flow to the north, represented both by striae and by whaleback forms and grooves in the vicinity, was overprinted by a more recent ice flow to the northeast. Other observations by Low (1898), Gangloff et al. (1976), and by the present author between Kuujjuaq and the Koksoak estuary, provide supportive evidence for these two ice flows. This change in flow direction from north to northeast, is difficult to interpret in relation to the dynamics of the Late Wisconsinan Quebec–Labrador ice sheet. It probably represents the increased dominance of a late surviving ice dispersal centre on the southern part of the aux Mélèzes plateau southwest of Ungava Bay, after thinning and marginal retreat southwards of the main Quebec–Labrador ice dome (Lauriol and Gray, 1987).

Along the southeastern and eastern Ungava Bay coast between Kuujjuaq and the northern tip of Labrador, there is a tripartite division of dominant ice flows (Fig. 5). Dominant ice flow was 1) to the north and north-northeast between Kuujjuaq and the George River estuary, 2) to the northwest on the east coast between Kangiqsualujjuaq (on the George River) and Alluviaq Fiord, and 3) to the east-northeast and east-southeast on the northernmost part of the Labrador peninsula and on Killiniq Island and Button Islands.

For the southernmost sector, the source of the ice flow is to the south on the central Quebec–Labrador plateau. More specifically, Allard et al. (1989) found evidence from the overall drumlinoid and striae patterns, and from specific cases of crossing drumlin ridges and intersecting striae, that an earlier ice lobe flowed north-northwest but curved around progressively to the north as it crossed the coastline, and that a later shift in ice-dispersal patterns caused the flow direction to be displaced 20–30° towards the east (i.e. from north to north-northeast). Such a change could reflect the initial importance of north-northwest ice flows into southeast Ungava Bay from an ice dome situated in the southern

Torngat Mountains and on the George River plateau, during initial build-up of the Quebec–Labrador ice sheet, with a transition to northerly flow, as a dispersal centre in south-central Quebec became dominant. Striated facets on recently emerged bedrock surfaces on the westernmost of the Saglaersoak Islands in southernmost Ungava Bay revealed a northerly flow of ice, followed by a northwesterly flow. Previous observations on the easternmost of these islands by Klassen et al. (1992) suggest, however, a reverse order of glacial flows. One critical outcrop, 12 km south of Kangiqsualujjuaq (locality F *in* Fig. 5), revealed fortuitous survival, through burial by 8 m of sediments, of well preserved striae,

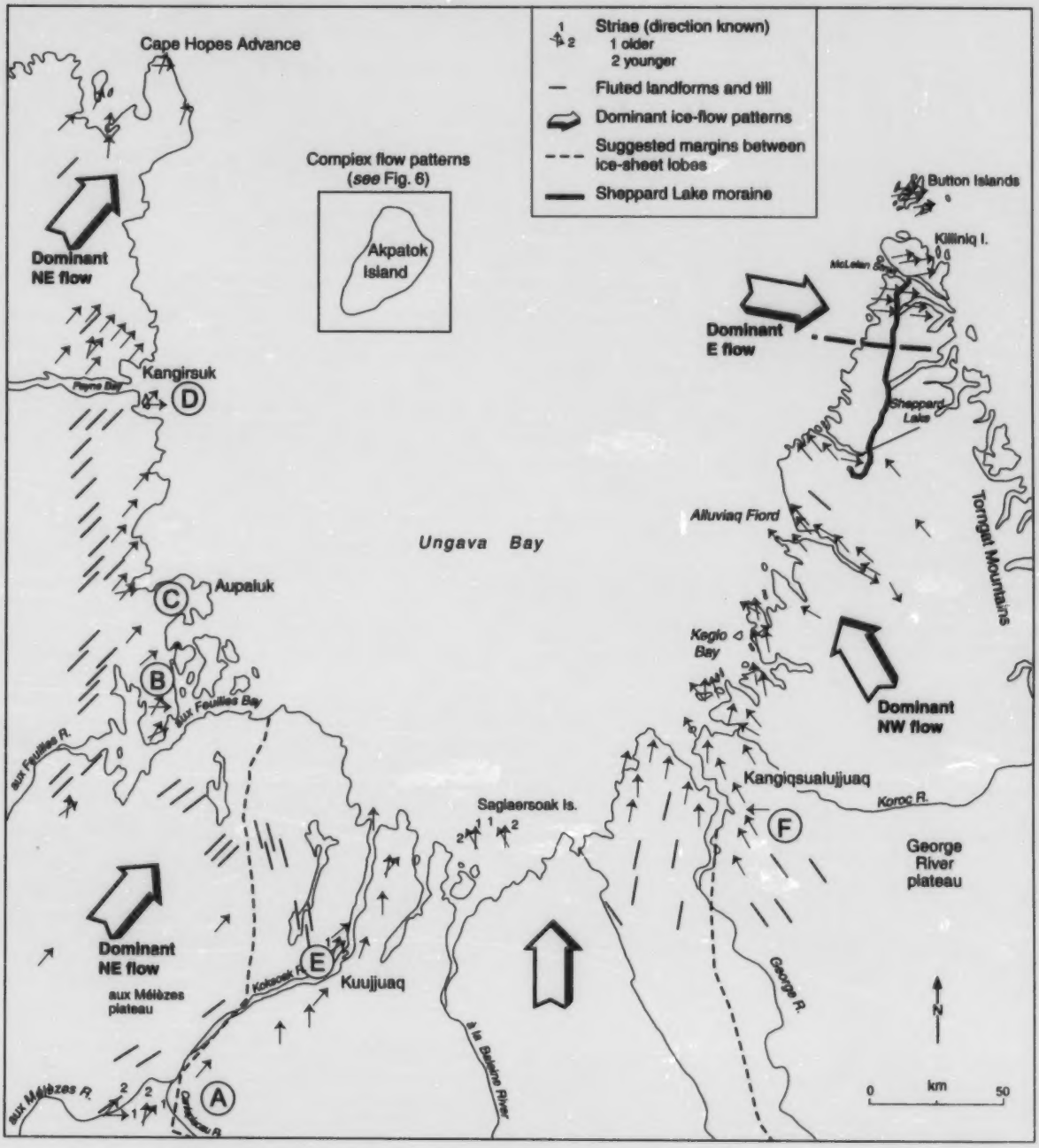

Figure 5. *Ice-flow indicators in the Ungava Bay region. Based on data in Løken (O.H. Løken, unpub. report, 1964), Gangloff et al. (1976), Hardy (1976), Gray and Lauriol (1985), Allard et al. (1989), Klassen et al. (1992), Gray et al. (1996), Brisebois (1998), and Clark et al. (2000).*

crescentic fractures, and gouges, indicative of an ancient flow to the west, originating in the Torngat Mountains to the east (Allard et al., 1989). The exposure above the outcrop displayed a basal unit of glaciotectonically deformed and oxidized sands and gravels, of fluvioglacial or fluvial origin, overlain by an upper till unit, suggesting the possibility that this westerly flow predates the Late Wisconsinan glacial advance.

Although the dominant ice flow between Alluviaq Fiord and the Koroc River estuary was to the northwest, striae with crescentic gouges and roches moutonnées at two low-altitude sites in the lower Alluviaq River valley indicate penetration in a southeast direction into the Torngat Mountains of an ice tongue from Ungava Bay. Roche moutonnée evidence up to an elevation of 350 m a.s.l. on the Quebec–Labrador watershed tends to support the view initially expressed by Ives (1957) that Ungava Bay ice crossed the interfluve and attained the Labrador coast; however, at elevations of 250–300 m on the north side of Alluviaq Fiord, three glacially eroded surfaces clearly showed a single direction of ice flow to the northwest towards Ungava Bay. Crag-and-tail features on the 300 m a.s.l. plateau on the north side of Alluviaq Fiord, also indicate outflow from the Torngat Mountains to Ungava Bay. No sites showing the dual flows were observed, and therefore it is rather difficult to categorize their order of occurrence.

Figure 3 in MacLean et al. (2001) reveals thick ice-contact deposits in the deep marginal channel, situated at the eastern margin of the Ungava Bay platform, all the way from McLelan Strait, south of Killiniq Island, to the limit of mapping northwest of Alluviaq Fiord. At one locality these deposits attain a thickness of 150 m and show multiple sedimentary facies (MacLean et al., 1995; MacLean et al., 2001, Fig. 9). These deposits may have resulted from dumping of debris by northwest-flowing ice, coalescing or abutting against an ice mass occupying the Ungava Bay platform.

Farther north, striae and crag-and-tail and fluted till features indicate eastward ice flow, fanning around from east-northeast across the Button and Killiniq islands to east-southeast across the northern tip of the Labrador peninsula, where summits exceeding 500 m a.s.l. were completely overrun by the ice sheet. This ice sheet represented the confluence of both a Hudson Strait ice stream and Ungava Bay ice with all its feeder lobes from the Quebec–Labrador peninsula, including the southern Torngat Mountains region. A linearly contiguous end moraine, outwash plain, and outwash delta complex, mapped and described by Løken (1962; O.H. Løken, unpub. report, 1964) as the Sheppard moraines, runs north-northeast–south-southwest along the peninsula for a distance of 100 km between Killiniq Island and Sheppard Lake, and represents the latest recognizable eastern margin of the continental ice sheet in northern Labrador (Fig. 5).

Akpatok Island

Akpatok Island is situated at a critical location, where ice flows to the north and northeast from Ungava Peninsula and Quebec–Labrador and to the east-southeast down Hudson Strait could have potentially converged. Figure 6 summarizes information from striae pits and fluting forms, and also shows a north-trending moraine-ridge complex and an east-trending curvilinear dark band interpreted as a former englacial moraine (Løken, 1978; Gray et al., 1990, 1994; Brynczka, 1996). Along with erratic provenance patterns (Fig. 7), these features permit a general reconstruction of events associated with the last glaciation, which demonstrate that the island had both developed its own ice cap, and been invaded by continental ice from the west and from the south.

The early development of an ice cap of local provenance, prior to invasion by continental ice, is suggested by the basal unit of grey calcareous till over most of the island, by the relative absence of crystalline erratics, and by the divergent pattern towards the northeast and southeast of striae and bedrock fluting in the northeast sector of the island. This ice sheet may eventually have extended to the northeast as a grounded mass on the very shallow (<100 m deep) Ungava marine platform, that was probably emergent at the Last Glacial Maximum. On the west side of the island, four sites suggest ice flow off the island to the west and northwest, which could be related to the inception of the island ice cap. At a third site on the plateau 10 km northeast of Gregson Creek, recently exposed from beneath a 15 m thick till cover (point A *in* Fig. 6), two orientations were observed, the earlier one west-east with an undetermined sense of flow, and the later one showing flow to the west-northwest associated with a local ice cap.

With the progressive development of the continent-based Laurentide Ice Sheet, individual lobes moving respectively north from central Quebec–Labrador, northeast and east-northeast from Ungava Peninsula, and east-southeast down Hudson Strait, must have surrounded and invaded Akpatok Island. A moraine ridge and meltwater complex, 2–5 km wide, and up to 30 m high, running south-southwest from Hell Point to south of Langley Creek is characterized by a ridge on the west side, composed mostly of calcareous till, which appears to have been scraped from presently thinly till-mantled bedrock to the west. The crest of this ridge has been locally overridden and fluted by west-east ice flow. To the east, there is a broad zone of hummocky moraines, with an abundance of crystalline erratics, and a north-trending zone of ice-contact meltwater deposits. The relatively acidic matrix permitted the ready identification of this zone on the basis of a continuous vegetation cover showing dark grey in Figure 6.

This complex represents an important marginal position of an ice lobe, originating on the Ungava Peninsula, and invading the island from the west-northwest. The north-south oriented ice contact meltwater features may have developed in an interlobate position between the invading lobe from the west and the existing Akpatok ice cap. Since ice-flow indicators show a northeast trend on the Ungava Peninsula mainland (Fig. 5) but a shift to the east-southeast across western Akpatok Island (Fig. 6), it appears likely that the Ungava Peninsula lobe was also constrained by a Hudson Strait ice stream to the north, and became deflected towards the east-southeast as it invaded Akpatok Island, 100 km east of the mainland.

Additional evidence, indicating extension of the Ungava Peninsula lobe across the island, is provided by a curvilinear dark band, trending variably eastward across the southern

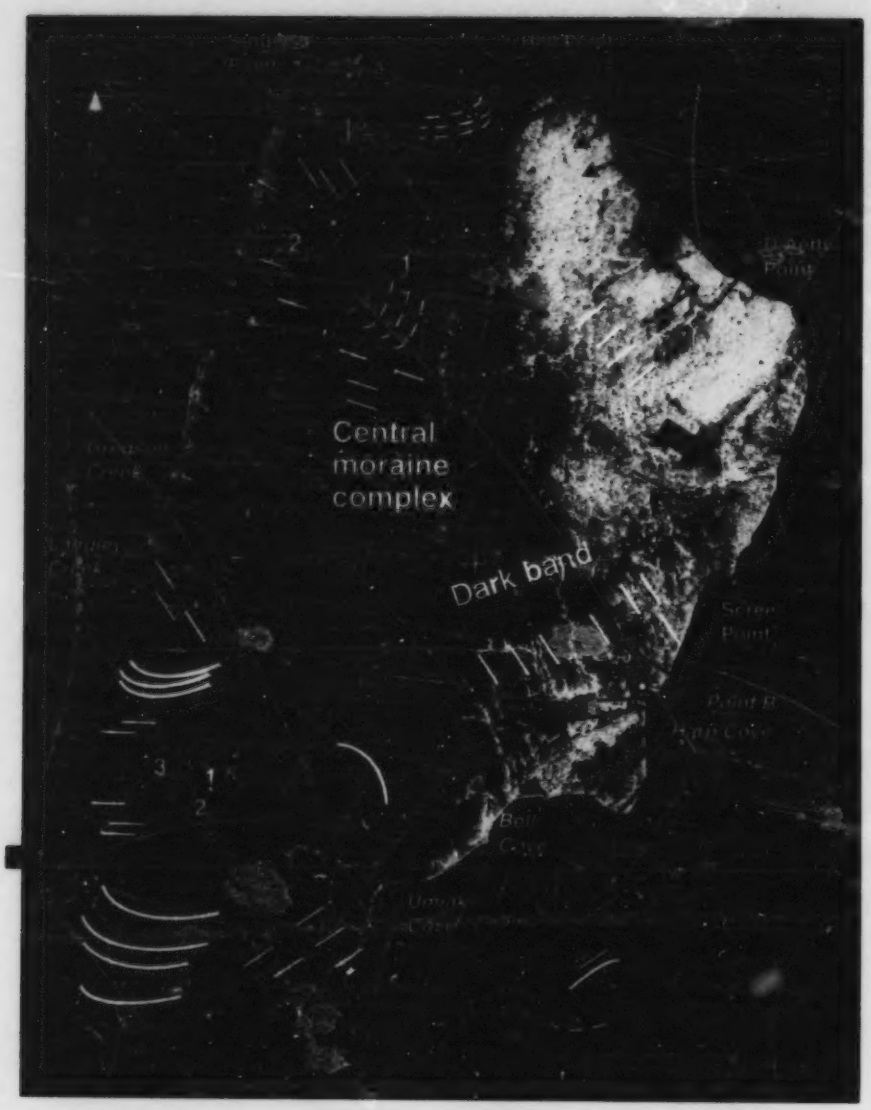

Figure 6. *Glacial landforms on LANDSAT thematic mapper image of Akpatok Island. Based on data in Gray et al. (1994) and Giugni et al. (1996).*

part of the island (Fig. 6). The dark colour results from a dense and moist vegetation carpet developed on a 0.5–2 m thick mantle of till, composed exclusively of crystalline clasts, of Canadian Shield origin, and with negligible carbonate content in the matrix. During melt out from an englacial moraine, the debris became draped in the form of a ribbon over all local relief, and also over the most southerly ridge of the north-trending moraine complex, described above. This, and the occasional presence of undeformed kames on the dark band, demonstrate that eastward flow of Ungava Peninsula ice across southern Akpatok Island, remained dominant up to the time of final deglaciation.

The curvilinear pattern of the dark band in plan view, indicates that the original englacial moraine was deformed prior to melt out. This deformation most likely occurred as a result of contact of the eastward-moving Ungava Peninsula ice lobe, with a second ice lobe impacting the Akpatok Island coast from the south. The parallelism between the form of the dark band and other, less visible, greyish bands and that of the southern cliff coastline of Akpatok Island is not fortuitous. If the ice lobes were of only moderate thickness, an ice lobe of southern provenance, abutting against the 200 m high cliffs, would have constrained the margin of both the western and southern lobes to follow the coastline. A striated surface with well preserved miniature bidirectional rat-tails, on the plateau above Harp Cove, provides additional evidence concerning

these conflicting ice flows (point B *in* Fig. 6). Here, a south-southeast to north-northwest ice flow was succeeded over a short time interval, probably without deglaciation of the surface, by west-to-east flow.

Figure 7 shows the distribution over Akpatok Island of identifiable erratics from the New Quebec geosyncline. These include ironstones from the Sokoman Formation and Baby Formation, dolomite from the associated Abner Formation, and conglomerate and sandstone from the Chioak Formation (Goulet, 1995; Giugni et al., 1996). Provenance arcs constructed on the basis of the extreme geographical limits of source outcrops suggest a wide range of possible ice flows which could bring these erratics onto the island. What is most interesting is that, although the glacial geomorphological features suggest the dominance of easterly flow across the island (Fig. 6), earlier ice flows from the southwest must have permitted erratics from the Chioak and Abner formations to be carried onto the island.

After liberation of the island by the western ice lobe, a slight readvance of Akpatok Island ice, or marginal overriding of the island by ice moving north-northeast from southwest Ungava Bay is indicated by striae found beneath a 1 m

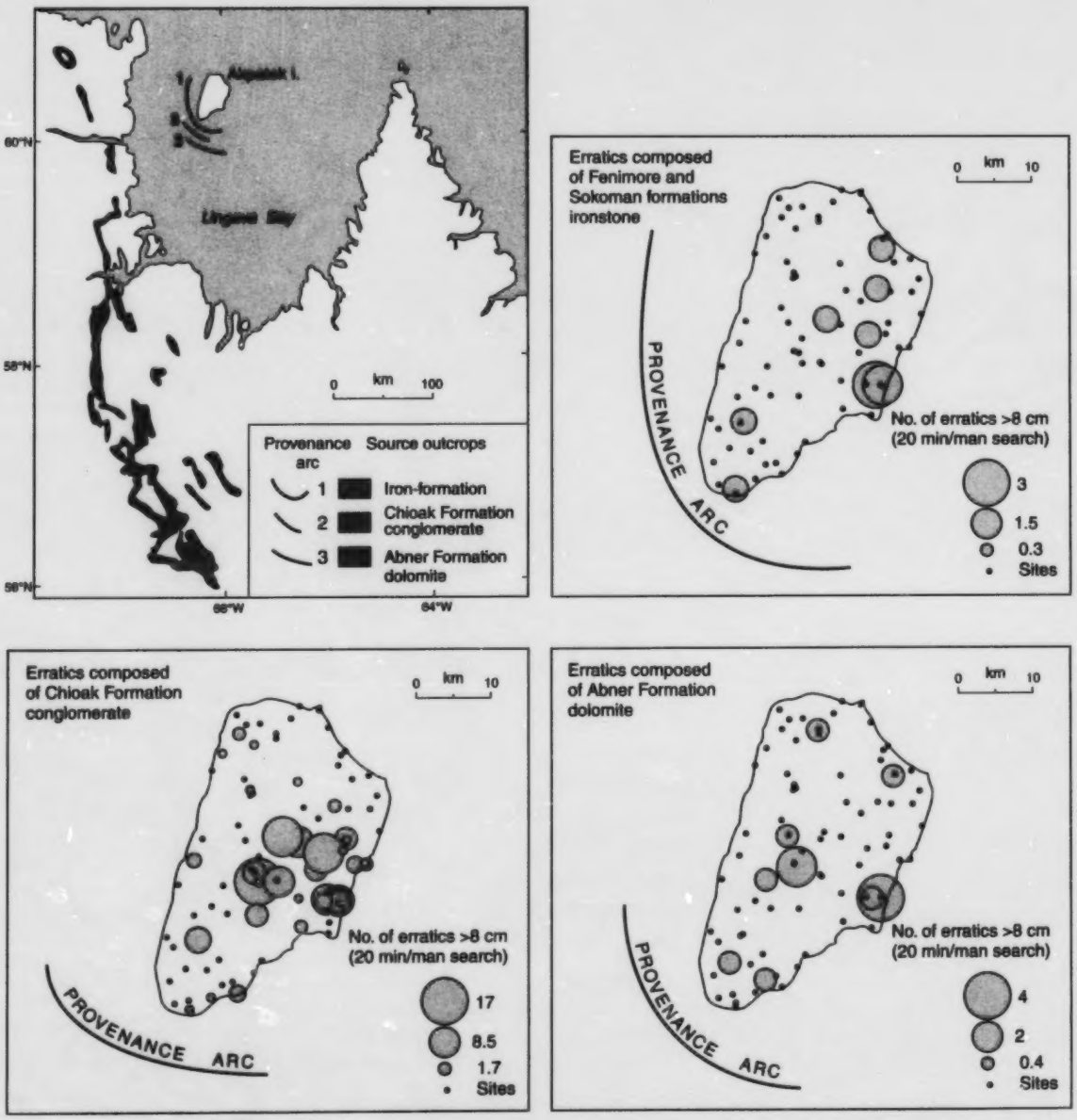

Figure 7. *Dispersion of New Quebec geosyncline erratics on Akpatok Island. Based on data* in *Gray et al. (1990) and Giugni et al. (1996).*

thick layer of reworked marine silt at the northwest tip of Akpatok Island. There is absolutely no morphological evidence, however, to suggest that the island was significantly affected by the late glacial ice surges of Quebec–Labrador ice to the north or northeast across Hudson Strait, postulated by Miller et al. (1988), Miller and Kaufman (1990), Stravers et al. (1992), Kaufman et al. (1993a), and Manley and Miller (2001) as originating in southern Ungava Bay. If such surges occurred, the southern ice lobe of Quebec–Labrador origin must have 1) been too thin to override the island, or 2) passed eastward of the island which at that time was probably still covered by the Ungava Peninsula ice lobe from the west.

NEW QUEBEC GEOSYNCLINE ERRATICS AND CARBONATE DRIFT DISPERSAL AROUND THE PERIPHERY OF EASTERN HUDSON STRAIT

New Quebec geosyncline erratics

The distribution of New Quebec geosyncline ironstone, conglomerate, and sandstone erratics on the floor of Ungava Bay and Hudson Strait, and on adjacent terrestrial surfaces, is shown in Figure 8. Due to the small size of the available sample population from box cores and clam-shell or other grab sampler devices, in comparison with the terrestrial sites, ironstone

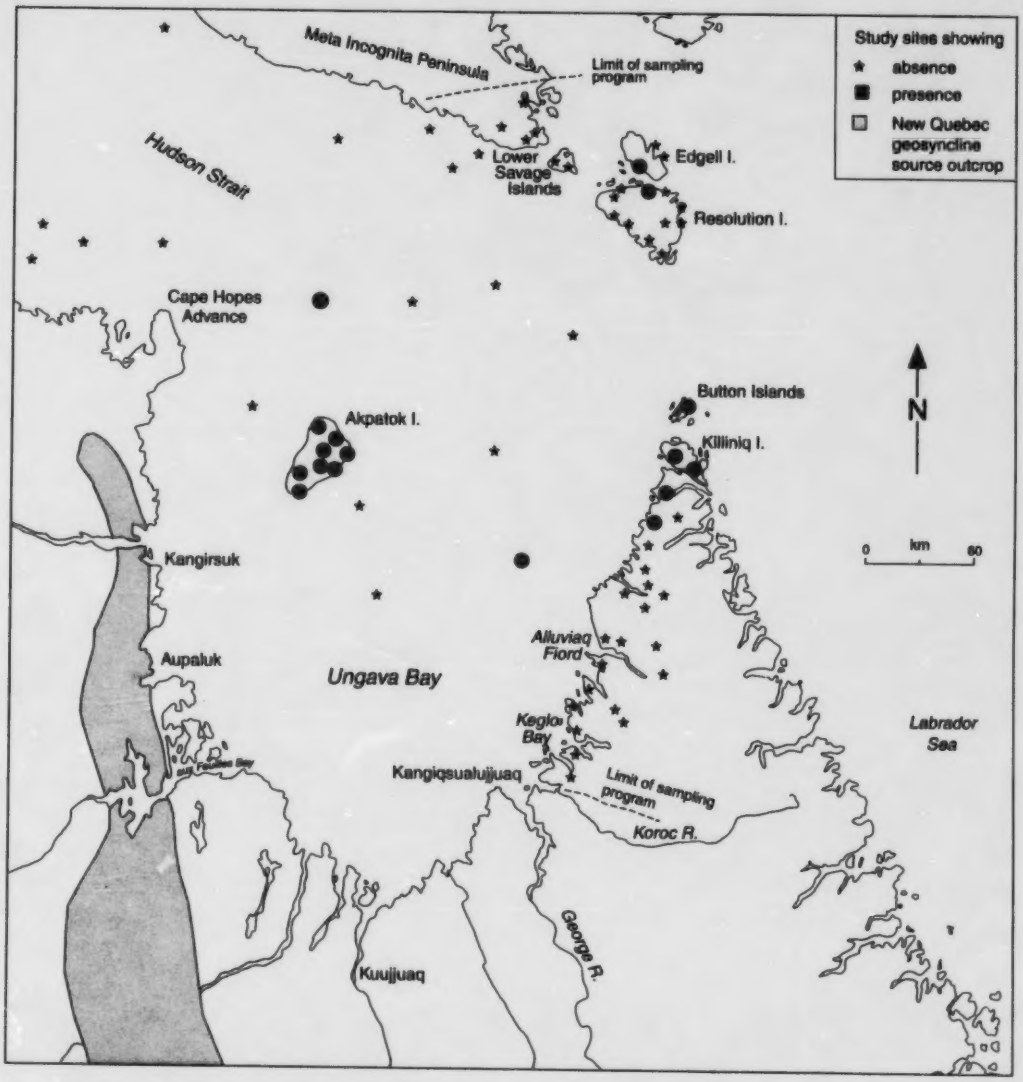

Figure 8. *Presence or absence of ironstone, conglomerate, and sandstone erratics in relation to the probable source in the New Quebec geosyncline. Based on data* in *Gray et al. (1994, 1995, 1997) and Daigneault (1994).*

erratics were noted at only two marine sites. The data from terrestrial sites to the northeast of the source outcrops is more informative. Not surprisingly, Akpatok Island revealed the greatest density of sites with such erratics; however, they were also found at five sites in northernmost Labrador more than 250 km distant, and at two sites on northern Resolution and southern Edgell islands. There has therefore been transport in a northeast direction to such outlying locations by Quebec–Labrador ice at some stage during a glacial cycle.

Such erratics have not been observed by any researchers on Meta Incognita Peninsula, however, nor in the southern part of the Labrador peninsula. Without any ironstone erratic evidence at the tip of the Meta Incognita Peninsula, it is difficult to envisage an exclusively Ungava Bay source for north-northeast late glacial ice resurgences into southern Frobisher Bay, as suggested by Miller et al. (1988), Stravers et al. (1992), and Manley and Miller (2001). Without a single distinctive erratic from the New Quebec geosyncline, it is equally difficult to envisage the eastward flow of a thick continental ice sheet from the west across southern Ungava Bay, through or over the main sector of the Torngat Mountains in Labrador, as suggested by Ives (1957, 1958) and Clark (1988, 1991).

Carbonate drift derived from Paleozoic bedrock in Hudson Strait and Ungava Bay

The distribution of carbonate drift, above the postglacial marine limit to the east and northeast of the large Paleozoic bedrock areas in Hudson Strait and Ungava Bay, in association with ice-flow directions (Fig. 9) may be used to assess 1) the peripheral zones attained by ice sheets moving down Hudson Strait and/or across Ungava Bay; and 2) by corollary, the highland zones which may have excluded these continental ice sheets, and been occupied by a complex of autonomous ice caps or mountain glaciers.

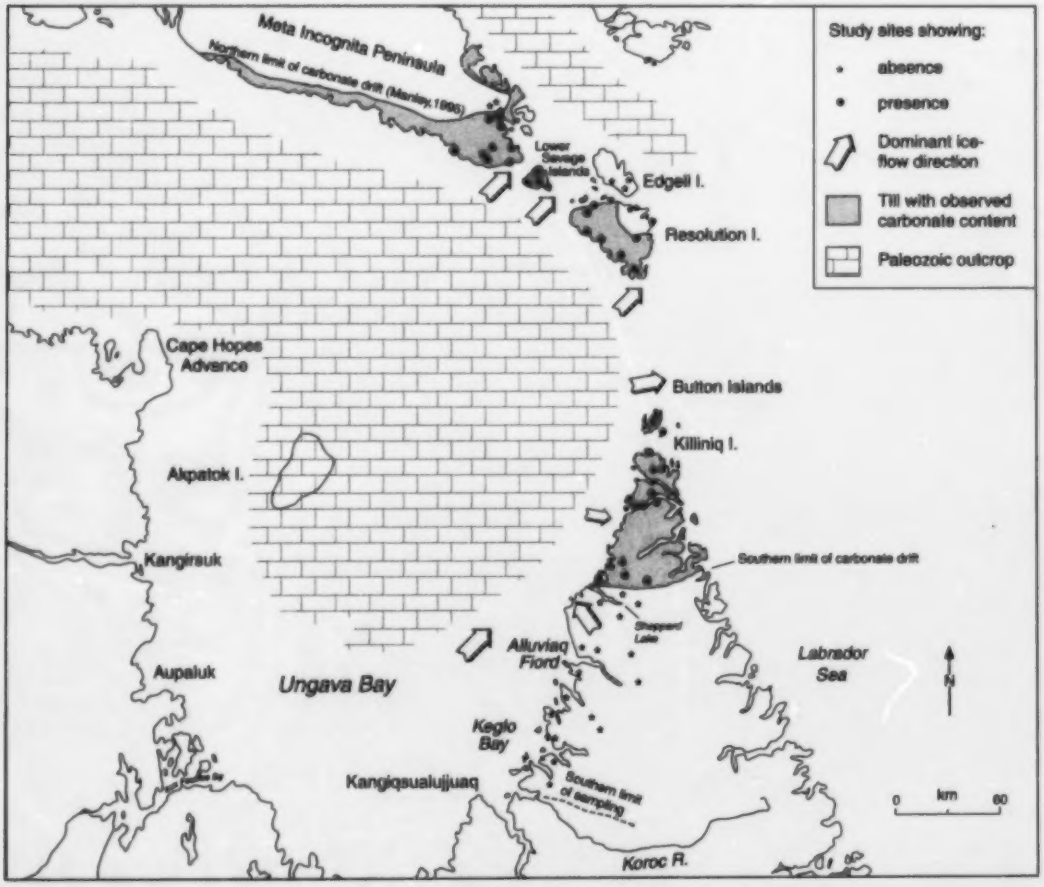

Figure 9. *Significant (>1%) carbonate drift content around the eastern periphery of Hudson Strait. Data* from *Stravers et al. (1992), Gray et al. (1995, 1997), and Manley (1995).*

In the northern Labrador peninsula significant values of carbonate drift, shown in detail in Figure 10, have been found only north of Sheppard Lake. As previously discussed, the dominant erosional ice-flow patterns between Sheppard Lake and the George River estuary were to the northwest from the Torngat Mountains. Even after late glacial retreat of the Torngat Mountains ice, the flow of the ice sheet emanating from the George River plateau and sweeping around in an arc from the north to the north-northeast (Allard et al., 1989) would not have scoured the Paleozoic platform. This accounts for the total absence of carbonate drift between Keglo Bay, and Alluviaq Fiord, despite the fact that an Ungava Bay ice mass dammed glacial lakes upstream from these estuaries, and may even have penetrated inland along the floor of the Alluviaq River valley.

North of Sheppard Lake, the carbonate content in till was also associated with the occasional presence of limestone erratics. Carbonate content in till at summit sites on the Button Islands attains values of up to 85% (Fig. 10; Gray et al., 1996). On Killiniq Island and on the mainland, carbonate content varied more commonly between 0 and 10%, carbonate drift being noted on the highest summits at elevations of up to 550 m. The previously discussed evidence of the striae and

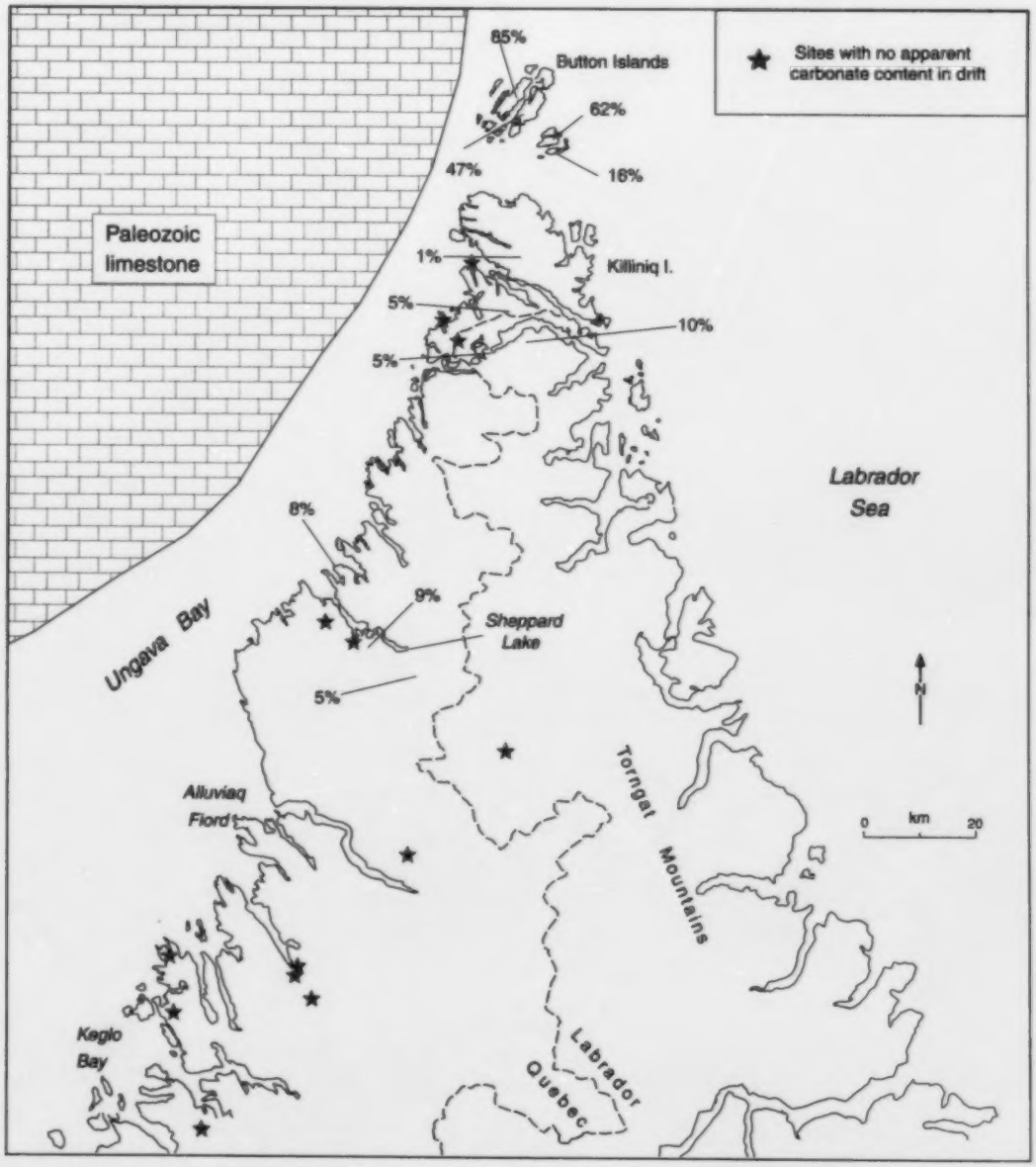

Figure 10. *Distribution of carbonate in till in northern Labrador.*

fluted till showing latest ice flows to the east-southeast, east and east-northeast, combined with this northerly increase in carbonate content of the till, is indicative of a major west-east ice stream down Hudson Strait. Contemporaneous flow of Quebec–Labrador ice across Ungava Bay must have been diverted to the east by a Hudson Strait ice stream. Although the barrier of Resolution Island undoubtedly could have contributed to easterly funnelling of Ungava Bay ice through the entrance of Hudson Strait, there is no topographic or bathymetric feature which would cause east-southeast flow across the northern Labrador peninsula, up to 60 km south of the strait entrance.

On Resolution Island carbonate-rich drift was found almost exclusively along the southwest coast of the island, and was associated with coastal till terraces. Carbonate drift was not observed on northeast Resolution Island, nor on Edgell Island. This fact is rather puzzling, in view of the consistently southwest-to-northeast and south-to-north ice flows across both islands, and the occasional limestone erratics noted at sites on the north and east coasts of Resolution Island (Gray et al., 1995). The latter evidence clearly indicates that ice in eastern Hudson Strait overtopped Resolution and Edgell islands at some stage during the last glaciation, attaining a minimum elevation of 400 m.

Farther west, carbonate drift was noted at the highest elevations of 200 m on the Lower Savage Islands (Fig. 9), and glacial striae and p-forms indicate overriding by ice from eastern Hudson Strait (Gray et al., 1997). A carbonate drift limit of about 400 m in elevation on southeast Meta Incognita Peninsula, along with striae indicating flow to the northeast, and major meltwater flows draining through the York canyons to Frobisher Bay enabled Miller et al. (1988), Stravers et al. (1992), and Manley (1995) to demonstrate that the tip of the peninsula had been overrun by ice flowing from Hudson Strait onshore.

SYNTHESIS OF ICE FLOWS IN HUDSON STRAIT AND UNGAVA BAY SECTOR

Figure 11 brings together all the ice-flow data discussed in this paper, and also additional data from the tip of Meta Incognita Peninsula and Lower Savage, Resolution, and Edgell islands (Miller et al., 1988; Stravers et al., 1992; Gray et al., 1995; Manley, 1995), in an attempt to present a composite view of the dominant ice flows affecting Hudson Strait and Ungava Bay during the last glaciation. These flows cannot be tied to specific time intervals, and are most probably regionally diachronous; however, it is possible to draw general conclusions from the data.

In the first place, the flow patterns confirm the existence of long-postulated, major dispersal centres in the Ungava Peninsula, in central Quebec–Labrador, and on Meta Incognita Peninsula. They also indicate an ice-dispersal centre along the north-south axis of the central Torngat Mountains. On the Labrador peninsula south of Sheppard Lake, the absence of Paleozoic limestone and New Quebec geosyncline iron-formation erratics, and of carbonate content in the till matrix, not only on the high summits, but also at valley floor and coastal plateau sites, is remarkable. The sedimentological data clearly supports the erosional evidence, suggesting that for most of the last glaciation, dominant ice flow to the northwest from the Torngat Mountains excluded ice flow from the main Quebec–Labrador ice sheet into the region. This evidence is in contradiction to views expressed by Ives (1957, 1958) and more recently by Clark (1988, 1991), who have argued for dominant eastward flow of continental ice through the Torngat Mountains, downplaying the autonomous role of this mountain barrier in the evolution of the continental ice sheet.

Secondly, the northernmost tip of the Labrador peninsula was overrun by Ungava Bay ice deflected to the east by an important ice stream flowing southeast down Hudson Strait. The evidence from offshore islands (in particular, Digges, Salisbury, Nottingham, Charles, Big, and Akpatok islands) and mainland promontories (Cape de Nouvelle-France and Cape Hopes Advance) indicates deviation of contributory ice flows from the Ungava Peninsula towards the east by this ice stream.

Thirdly, on Akpatok Island, a large end-moraine complex with a south-southwest trend, marks an important eastern margin of a northern Ungava ice lobe, which may have abutted against a locally developed ice cap. Till flutes and striae indicate subsequent overriding of this margin by eastward-flowing ice. A curvilinear englacial moraine traversing the island was formed by the interaction of converging ice lobes from both southern and western sources, and is indicative of the last overriding of the island by continental ice.

Finally, there is evidence of north-northeast and northeast ice flows on the northeast margin of Hudson Strait, from the tip of Meta Incognita Peninsula to Resolution Island. Late glacial resurgences of Ungava Bay ice to the north-northeast across an ice-free eastern Hudson Strait, after earlier ice retreat, were proposed by Miller et al. (1988), Stravers et al. (1992), Kaufman et al. (1993a), and Manley and Miller (2001) to explain the ice-flow data, and also other chronostratigraphic evidence from sites near the mouth of Frobisher Bay; however, it is difficult to reconcile this hypothesis with the important easterly flows of continental ice across Akpatok Island, and the northern tip of Labrador, and the total lack of evidence for northerly flow, in these sectors. In order to deal more fully with this question the deglaciation chronology for the sector must first be discussed.

DEGLACIATION CHRONOLOGY IN HUDSON STRAIT AND UNGAVA BAY

Tables 1 and 2 list details of 82 late glacial or early postglacial radiocarbon dates obtained by several researchers for each sector along the southern coastline of Hudson Strait, for Ungava Bay, and for the northern Labrador peninsula (Fig. 12, 13). These dates were obtained mainly from marine molluscs, but occasionally from basal gyttja of both terrestrial and marine origin. The mollusc dates are from the basal units of marine and terrestrial stratigraphic sequences, or

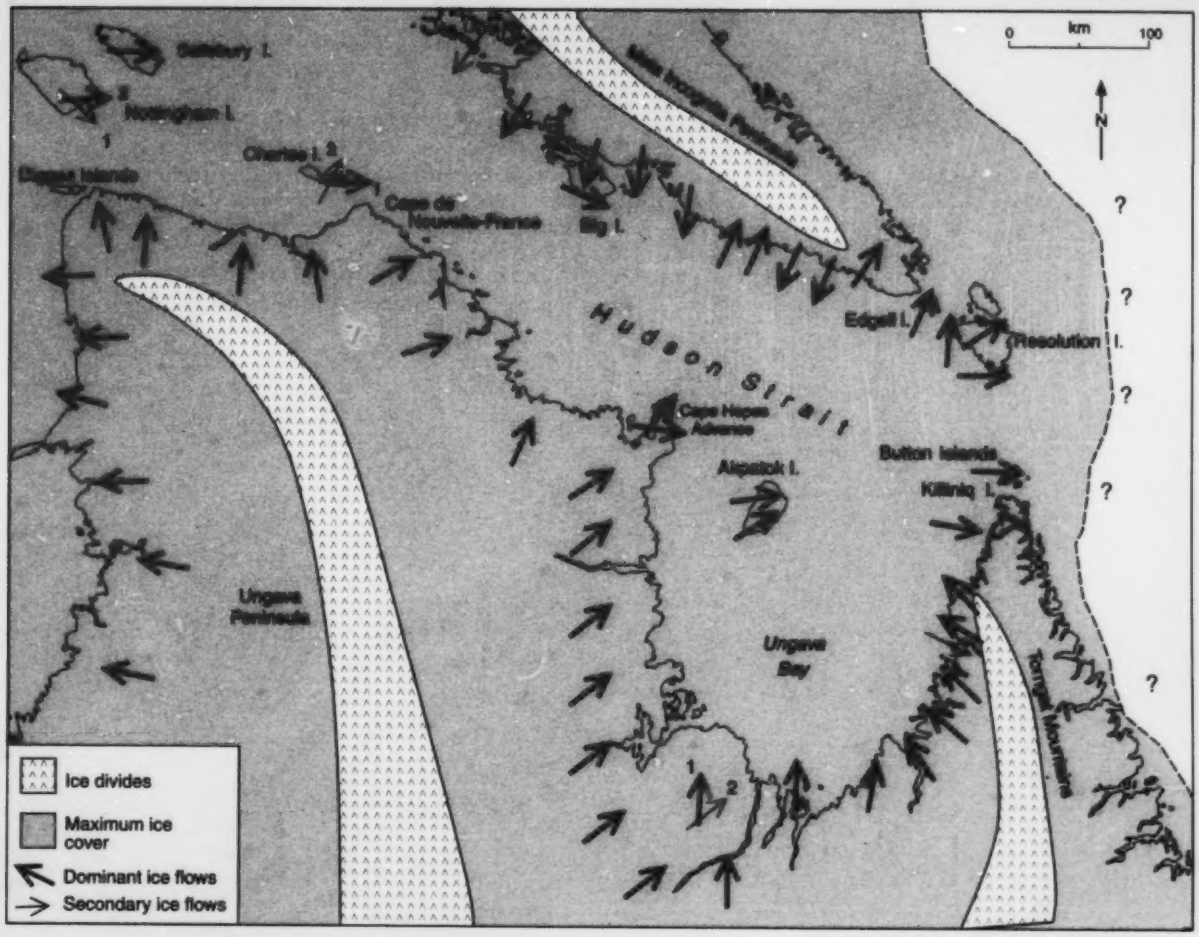

Figure 11. *Synthesis of dominant Late Wisconsinan ice flows in Ungava Bay and Hudson Strait. Compiled from data in this paper for the southern coastal margins, and from data in Miller et al. (1988), Laymon (1988), Stravers et al. (1992), Manley (1995, 1996), and Gray et al. (1995) for the northern coastal margins.*

from littoral or sublittoral sites close to the postglacial upper marine limit. In a few instances, marine molluscs were clearly not in situ, but represent reasonable minimum dates for establishment of postglacial marine conditions. Foraminifera dates from the base of the marine cores were not included, but their significance and associated problems are discussed by Jennings et al. (1998; 2001). Most of the dates replicate those published in Gray et al. (1993) and in Lauriol and Gray (1997), and they provide a background for the following discussion concerning 1) a possible early opening of Hudson Strait between 11 ka BP and 10 ka BP, 2) the delimitation of ice margins in the Hudson Strait–Ungava Bay sector between 9.5 ka BP and 6 ka BP and, 3) the controversial question of the occurrence and the provenance of a major resurgence of Laurentide ice across or down Hudson Strait between 9 ka BP and 8 ka BP (the Noble Inlet advance described by Miller et al. (1988) and Stravers et al. (1992)).

The question of an early opening of Hudson Strait between 11 ka BP and 10 ka BP

Two critical terrestrial sites along Hudson Strait suggest the possibility of a marine incursion along Hudson Strait as early as 11–10 ka BP, i.e. during a late glacial phase when the Laurentide ice cover still remained intact over Foxe Basin, Hudson Bay, and the surrounding lands. These sites are located in the lower Deception River valley in northern Ungava Peninsula, and at the northwest tip of Akpatok Island (Fig. 12). Table 1 lists a series of 17 conventional and AMS dates obtained on multiple shell samples from several laboratories, and on single valves at the AMS facility at University of Arizona, courtesy of Gifford Miller of the Institute of Arctic and Alpine Research (Lauriol and Gray, 1987; Kaufman et al., 1992; Gray et al., 1993; Manley and Jennings, 1996; Lauriol and Gray, 1997; Bruneau and Gray, 1997). The

two oldest mollusc dates from a silty clay bed at the base of a 60 m thick subaqueous fan (Fig. 12a) suggest a possible initial opening of western Hudson Strait between 11 ka BP and 10.5 ka BP, a scenario which is also supported by a date of 10 450 ± 250 BP (I-488) obtained by Matthews (1967) for *Hiatella arctica* on a marine terrace at the head of Deception Bay. This could well correspond with the marine interval recognized by Miller and Kaufman (1990) and Kaufman et al. (1993a) in eastern Hudson Strait, prior to the Gold Cove readvance. This terrestrial evidence is also given substantial support by the evidence from marine cores in the Wakeham Bay–Héricart Bay sector of central Hudson Strait, where,

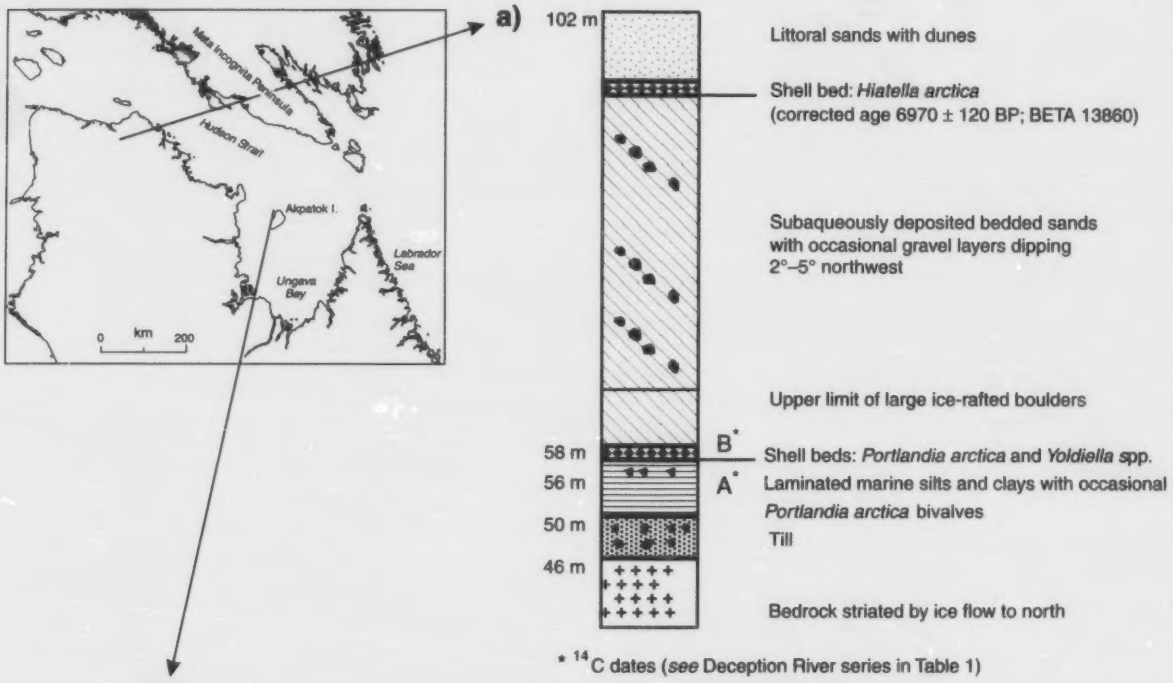

Figure 12. *Marine shell dates indicative of early postglacial opening of central Hudson Strait. Photograph by J. Gray. GSC 2001-006*

based on tentative extrapolation of sedimentation rates between dated horizons, MacLean et al. (1992) and MacLean and Vilks (1992) suggested that glaciomarine conditions may have been present in south-central Hudson Strait as early as 11.9–10 ka BP; however, all the other basal dates from the Deception River series, fall within a much younger and still unacceptably wide range — between 9.6 ka BP and 8.3 ka BP. The biggest problem is the 2.5 ka range of dates for marine shells in the same 12 cm thick, fine sand horizon (zone B *in* Table 1).

Two possibilities can be advanced for the moment, for the age discrepancies in zones A and B (Table 1, Fig. 12a). For the lowest zone A, comprising isolated, in situ, delicate bivalves of *Portlandia arctica*, there is a possibility, suggested to the author by Claude Hillaire-Marcel, of Geotop Laboratory at University of Quebec at Montreal, of variable uptake of dissolved inorganic carbon by the molluscs, in their endobenthic phase, from the surrounding sediments. The important problem, with regard to this hypothesis, is that the carbonate content of the silty clays surrounding the shell beds in zone A (Table 1, Fig. 12a) is very low (about 1%). This does not of course preclude the uptake of inorganic carbon, precipitated earlier in the marine phase, and subsequently dissolved and transported upwards through the marine sediments by pore waters. For the upper zone B, comprising three thin beds of highly concentrated bivalves of *Portlandia arctica* and *Yoldiella fraterna*, there is a possibility of a mixed age population due

Table 1. Reservoir-corrected marine shell ^{14}C dates, Deception Bay and northwest Akpatok Island.

1. Deception River series (latitude 62°07.2'N; longitude 74°16.3'W) (Fig. 12a)					
Sample no.	**Species**	**^{14}C date[1]**	**Lab. no.**	**Nature of date**	**Reference**
A) Dispersed bivalve mollusc horizon in silty clays, 56 m a.h.w.m. below transition to bedded sands					
RD 3-1A	*Portlandia arctica*	9390 ± 220 BP	Beta-11121	AMS: multivalve	Gray et al. (1993)
RD 3-92-1LP	*Portlandia arctica*	9435 ±170 BP	A-17262	AMS: 1 periostracum	Manley and Jennings (1996) Lauriol and Gray (1997)
RD 3-92-1LB	*Portlandia arctica*	8595 ± 80 BP	AA-17261	AMS: 1 valve	Lauriol and Gray (1997)
RD 3-92-1LA	*Portlandia arctica*	8335 ± 80 BP	AA-17260	AMS: 1 valve	Lauriol and Gray (1997)
RD 3-92-1L	*Portlandia arctica*	8265 ± 65 BP	AA-14686	AMS: 1 valve	Lauriol and Gray (1997)
B) 3 rich biocoenosis, in 12 cm thick basal sands, 0.4 m above transition from silty clays, at 58 m a.h.w.m.					
RD 3-1B	*Yoldiella fraterna,*	9610 ±140 BP	Beta 13861	Conventional	Gray et al. (1993)
RD 3-1B	*Yoldiella fraterna, Portlandia arctica*	9535 ± 90 BP	Beta 29085	Conventional	Gray et al. (1993)
RD 3-1B	*Portlandia arctica*	9000 ± 60 BP	TO 1397	AMS: multivalve	Gray et al. (1993)
RD 3-1B	*Yoldiella fraterna, Portlandia arctica*	8510 ±115 BP	GSC 4335	Conventional	Gray et al. (1993)
RD 3-92-2B	*Portlandia arctica*	10 960 ± 130 BP	AA 17263	AMS: 1 valve	Manley and Jennings (1996) Lauriol and Gray (1997)
RD 3-1B	*Portlandia arctica*	10 675 ± 100 BP	AA 7562	AMS: 1 valve	Manley and Jennings (1996) Lauriol and Gray (1997)
RD 3-1B	*Portlandia arctica*	8875 ±100 BP	AA 8393	AMS: 1 valve	Manley and Jennings (1996) Lauriol and Gray (1997)
RD 3-1B	*Portlandia arctica*	8545 ±120 BP	AA 8395	AMS: 1 valve	Manley and Jennings (1996) Lauriol and Gray (1997)
RD 3-1B	*Portlandia arctica*	8425 ±110 BP	AA 8394	AMS: 1 valve	Manley and Jennings (1996) Lauriol and Gray (1997)
2. Deception Bay series (latitude 62°07'N; longitude 74°39'W). Shells from frost boils on terrace at 86 m a.h.w.m.					
Sample no.	**Species**	**^{14}C date[1]**	**Lab. no.**	**Nature of date**	**Reference**
I 488	*Hiatella arctica*	10 450 ± 250 BP	I 488	Conventional	Matthews (1967)
3. Akpatok I. (latitude 60°34.4'N; longitude 68°10.1'W). In diamicton at marine limit, 76 m a.h.w.m. (Fig. 12b)					
Sample No.	**Species**	**^{14}C date[1]**	**Lab. no.**	**Nature of date**	**Reference**
AKP-720	Marine shell fragments	11 970 ± 90 BP	TO 1736	AMS: multivalve	Gray et al. (1993)
AKP-92-72B	*Portlandia arctica*	8 560 ± 70 BP	TO 3764	AMS: 2 valves	Gray et al. (1993)

[1] All dates are quoted in ^{14}C years BP with 1δ. Conventional dates were obtained for large samples by either liquid scintillation or gas proportional counting apparatus, and have not been specifically corrected for an ocean reservoir effect, which increases the sample age by a mean value of 450 years (Mangerud and Gulliksen, 1975) nor for ^{13}C isotope fractionation, which reduces it by a mean value of 410 years. The laboratory quoted ages may thus be considered as reasonably compensated for both effects. AMS dates from the University of Arizona (AA) incorporate corrections for both effects, in being normalized to $\delta\,^{13}C = -25‰$, and being subjected to a subtraction of 450 years from the uncorrected laboratory age. AMS dates quoted by Toronto Isotrace (TO) and Beta Analytic Inc. (Beta) were normalized to $\delta\,^{13}C = 0‰$, equivalent to a reservoir correction of only 410 years.

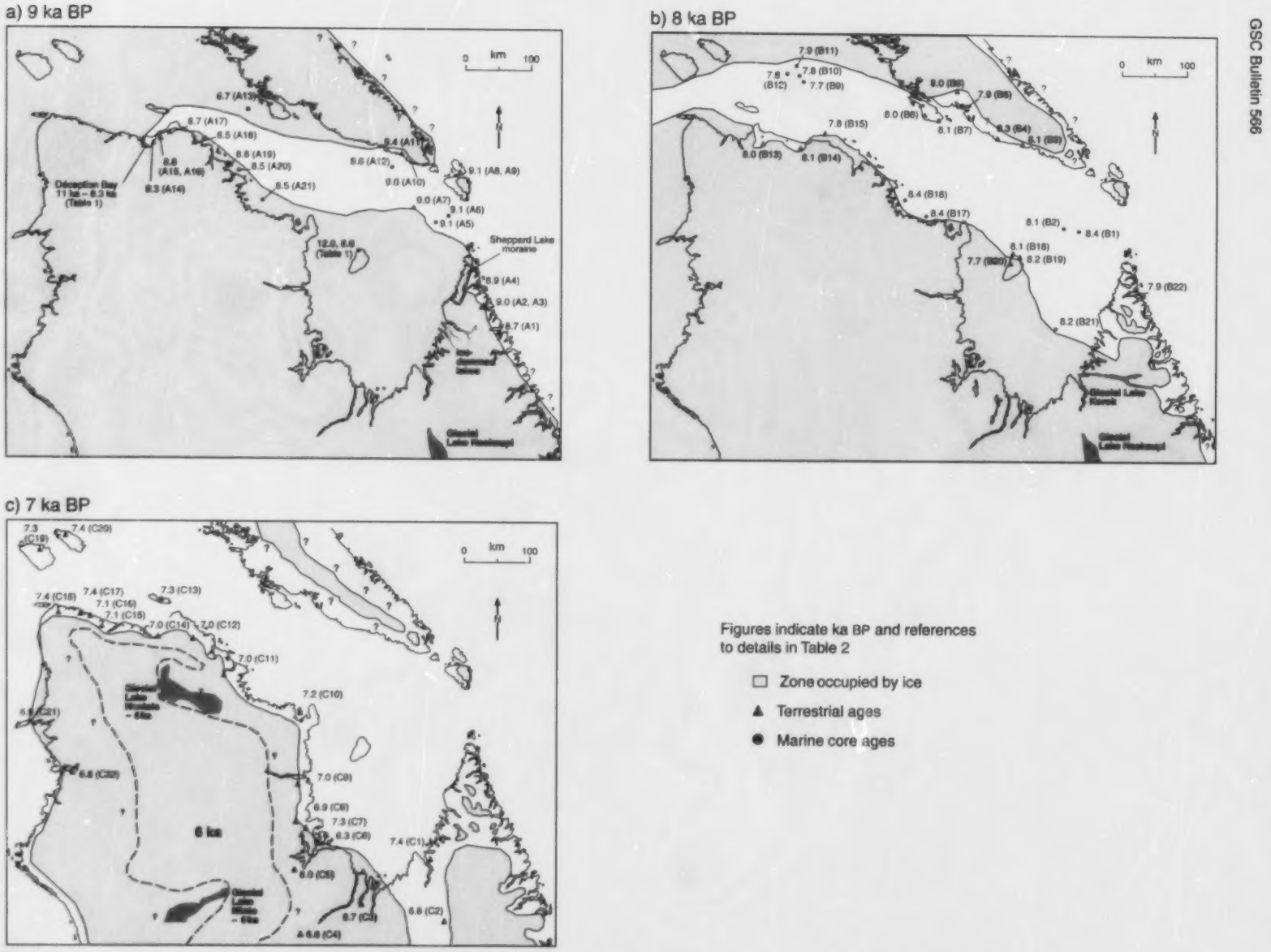
a) 9 ka BP
b) 8 ka BP
c) 7 ka BP
0 km 100
Figures indicate ka BP and references to details in Table 2
Zone occupied by ice
Terrestrial ages
Marine core ages
Sheppard Lake moraine
6 ka

Figure 13. *Proposed margins of Laurentide Ice Sheet in Ungava Bay–Hudson Strait sector between 9 ka BP and 7 ka BP.*

to seasonal flushing of individual molluscs from the upper layers of nearby silty clays, followed by their redeposition in the basal sand layers of the section.

Although these uncertainties remain to be resolved, the oldest single valve dates do suggest an opening of Hudson Strait as early as 11–10.5 ka BP. The group of seven single valve dates in the range 9.4–8.3 ka BP, at the base of the thick deposit of subaqueous sands, indicate either the prolonged existence of this marine phase, or else a subsequent closing by ice of western Hudson Strait until about 9.4 ka BP. The latter hypothesis is preferred, on the basis of other dates, between 9.3 ka BP and 8.7 ka BP, obtained for the coastal zone between Deception Bay and Cape de Nouvelle-France (Table 2, Fig. 13a). It is also in concordance with the chronology for closing of eastern Hudson Strait during the Gold Cove resurgence (Miller and Kaufman, 1990; Stravers et al., 1992; Kaufman et al., 1993a).

Farther east, at the northwest tip of Akpatok Island (Fig. 12b), a date for multiple, small shell fragments incorporated subsequent to their biocoenosis in a thin diamicton, just above the upper limit of postglacial storm beaches, suggested a possible opening of eastern Hudson Strait as early as 12 ka BP (Table 1), but a mixed age population of pre- and post-Late Wisconsinan molluscs seems much more likely. A date of 8.6 ka BP obtained for two identifiable, but unfortunately unpaired *Portlandia arctica* valves from the same section, provides an alternative, much younger age for initial deglaciation of the site, prior to a subsequent readvance to the north and north-northeast indicated by striae beneath the 1 m thick diamicton in which the shells have been incorporated.

Ice margins in the Hudson Strait–Ungava Bay sector between 9.5 ka BP and 6 ka BP

Figure 13 portrays the successively shrinking northeast margin of the Laurentide Ice Sheet in the Hudson Strait–Ungava Bay sector, based on pertinent ^{14}C dates between 9 ka BP and 6 ka BP (Table 2). Starting with the situation at 9 ka BP (Fig. 13a), dates from the head of three fiords along the east coast of the Labrador peninsula (Løken, 1962; Clark and Josenhans, 1986; Clark, 1990) indicate that ice margins had already withdrawn inland to the west. The north-trending Sheppard moraines, with accompanying proglacial outwash and deltaic deposits, and west-east-oriented fluting patterns in till, mark a readvance of the eastern margin of the ice sheet shortly after initial retreat from the coast.

Withdrawal inland of the outlet tongues from the Torngat Mountains ice cap, while ice still filled southeast Ungava Bay, led to the development of glacially dammed lakes, with conspicuous shoreline terraces up to about 200 m a.s.l. in the valleys draining the west flank of the Labrador peninsula, from Alluviaq Fiord southward (Gray et al., 1996). Two sequences of steep-sided transversal till ridges, preserved in small valleys to the north and south of Alluviaq Fiord, are interpreted as De Geer moraines. They appear to have been formed, as sublacustrine features at the retreating eastern margin of the Ungava Bay ice barrier, in the manner described by Holdsworth (1973), immediately prior to deglaciation of eastern Ungava Bay. The total absence of New Quebec geosyncline ironstone, conglomerate, sandstone, and limestone erratics and of carbonate content in the till matrix, for coastal and inland sites, at all altitudes, south of Sheppard Lake (Fig. 8, 9, 10) suggest that the most probable source of the ice at the eastern edge of this barrier was the George River plateau, southeast of Ungava Bay, well to the east of the New Quebec geosyncline and also well to the south of Paleozoic bedrock in Ungava Bay.

Farther north, on southern Edgell Island, two single valve dates from marine silts, situated immediately below the postglacial marine limit (Gray et al., 1995) indicate that the Laurentide ice margin must have withdrawn to the west or southwest shortly prior to 9.1 ka BP. Basal shell dates from marine cores in eastern Hudson Strait (Fillon and Harmes, 1982; Manley and Jennings, 1996) suggest minimal ages for

Table 2. ^{14}C ages delimiting ice margins in Ungava Bay and Hudson Strait (9.5–6.0 ka BP).

9.5–8.5 ka BP (Fig. 13a)						
Location	Site no.	Species dated	^{14}C Age[1]	Lab No.	Type of date	Reference
A1		Marine shells	8700 ± 470 BP	GX 9293[2]	Conventional	Clark and Josenhans (1986)
A2		Marine shells	8960 ± 110 BP	Beta 33216	Unspecified	Clark (1990)
A3		Marine shells	9000 ± 200 BP	L-642	Conventional	Løken (1962)
A4		Marine shells	8930 ±120 BP	Beta 33217	Unspecified	Clark (1990)
A5	93034-002	*Nuculana pernula*	9055 ± 80 BP	AA 13172	AMS : 1 valve	Manley and Jennings (1996)
A6	77021-154	*Nuculana pernula*	9120 ± 240 BP	GSC 2946	Conventional	Fillon and Harmes (1982)
A7	93034-004	*Nuculana* sp.	8980 ± 50 BP	CAMS 25764	AMS: paired valve	Manley and Jennings (1996)
A8	EI 94-1E	*Mya truncata*	9150 ±140 BP	AA 16404	AMS: 1 valve	Manley and Jennings (1996)
A9	EI 94-1E	*Mya truncata*	9030 ± 80 BP	AA 16405	AMS: 1 valve	Manley and Jennings (1996)
A10	M 86-B544	Marine shells	9010 ± 95 BP	AA 6301	AMS: fragments	Kaufman and Williams (1992)
A11	B5-12-65	*Hemithyris psittacea*	9380 ± 395 BP	GSC 2026	Conventional	Lowdon et al. (1977)
A12	GRL 1071-5	*Portlandia arctica*	8575 ± 90 BP	AA 13173	AMS: paired valve	Manley and Jennings (1996)
A13	93034-008	*Portlandia arctica*	8675 ± 65 BP	AA 13175	AMS: fragments	Manley and Jennings (1996)
A14	JR13	*Portlandia arctica*	9290 ±180 BP	Beta 19853	AMS: fragments	Manley and Jennings (1996)
A15	CB9	*Portlandia arctica*	8800 ± 70 BP	TO 1274[3]	AMS: fragments	Manley and Jennings (1996)
A16	CB9	*Portlandia arctica*	8765 ± 80 BP	AA 7561[3]	AMS: fragments	Gray et al. (1993)
A17	M 41	*Yoldiella fraterna*	8690 ± 70 BP	TO 1275	AMS: multivalve	Gray et al. (1993)
A18	LT2	*Yoldiella fraterna*, *Portlandia arctica*	8470 ± 70 BP	TO 1738	AMS: multivalve	Gray et al. (1993)
A19	Wales 92-124-125	Aquatic moss: *Hygrohypnum alpestris*	8820 ± 60 BP	AA	AMS: 8.3 mg	This study
A20	3023-071	*Portandia arctica*	8520 ± 80 BP	TO 2466	AMS: 1 valve	McLean et al. (1992)
A21	93034-013	*Portandia arctica*	8465 ± 65 BP	AA 13174	AMS: 1 valve	Manley and Jennings (1996)

Table 2. (cont.)

8.5–7.5 ka BP (Fig. 13b)						
Location	Site no.	Species dated	^{14}C Age	Lab no.	Type of date	Reference
B1	90023-045	*Portlandia arctica*	8355 ± 60 BP	AA 12884	AM: paired valve	Manley and Jennings (1996)
B2	85027-057	*Portlandia arctica*	8060 ± 70 BP	TO 750	AMS: 1 valve	Manley and Jennings (1996)
B3	WM 92-51	*Portlandia arctica*	8075 ± 60 BP	AA 10648	AMS: 1 fragment	Manley and Jennings (1996)
B4	WM92-37A	*Portlandia arctica*	8310 ± 65 BP	AA 10645	AMS: 1 valve	Manley and Jennings (1996)
B5	WM91-08B	*Mya truncata*	7910 ± 60 BP	AA7893	AMS: 1 valve	Manley and Jennings (1996)
B6	WM92-23	*Hiatella arctica*	7995 ± 55 BP	AA 10251	AMS: 1 valve	Manley and Jennings (1996)
B7	WM93-49A	*Portlandia arctica*	8105 ± 95 BP	AA 12609	AMS: 1 valve	Manley and Jennings (1996)
B8	Site 4	Marine shells	7980 ± 110 BP	GSC 425	Conventional	Blake (1966)
B9	90023-104	*Portlandia* sp.	7720 ± 60 BP	AA 12889	AMS: multivalve	Manley and Jennings (1996)
B10	90023-101	*Portlandia* sp.	7810 ± 60 BP	AA 12888	AMS: paired valve	Manley and Jennings (1996)
B11	85027-068	*Portlandia arctica*	7860 ± 70 BP	TO 751	AMS: multivalve	Manley and Jennings (1996)
B12	90023-099	*Yoldiella* sp.	7820 ± 70 BP	AA 12887	AMS: paired valve	Manley and Jennings (1996)
B13		Marine shells	7970 ±125 BP	GSC 672	Conventional	Matthews (1967)
B14	RD7C	*Mya truncata*	8050 ±130 BP	Beta 19020	Conventional	Gray et al. (1993)
B15	MB-9	*Balanus hameri*	7830 ±100 BP	Beta 19011	Conventional	Gray et al. (1993)
B16	90023-086	*Portlandia arctica*	8420 ± 80 BP	TO 2472	AMS: paired valve	MacLean et al. (1992)
B17	90023-107	Marine shells	8390 ± 70 BP	TO 2472	Multivalve	MacLean et al. (1992)
B18	AKP92-72C	*Macoma calcarea*	8110 ± 70 BP	AA 14687	AMS: 1 valve	Lauriol and Gray (1997)
B19	AKP 89-85	*Macoma calcarea*	8170 ± 80 BP	TO 1737	AMS: multivalve	Gray et al. (1993)
B20	AKP90-27B	*Mya truncata*	7690 ± 70 BP	TO 2440	AMS: multivalve	Gray et al. (1993)
B21	93034-38	*Yoldiella fraterna*	8220 ± 60 BP	CAMS 18690	AMS: 1 valve	Manley and Jennings (1996)

7.5–6.0 ka BP (Fig. 13c)						
Location	Site no.	Species dated	^{14}C Age	Lab. no.	Type of date	Reference
C1		Marine shells	7380 ± 90 BP	UL 358	Conventional	Allard et al. (1989)
C1[3]		Marine shells	7310 ± 100 BP	UL 259	Conventional	Allard et al. (1989)
C2		Basal gyttja	6815 ± 125 BP	SI 1959	Conventional	Short (1981)
C3		Marine shells	6720 ± 100 BP	MBN 198	Conventional	Gangloff and Pissart (1963)
C4	KAN 94-2A	*Hiatella arctica*	6640 ± 60 BP	TO 5677	AMS: 1 valve	This study
C5	LAU-24	Basal gyttja	5980 ± 205 BP	GX 5091[2]	Conventional	Lauriol (1982)
C6	NA-I	*Mya truncata*	6300 ± 75 BP	DIC 1277	Conventional	Lauriol and Gray (1987)
C7	F1	Marine organics	7350 ± 320 BP	GX 5093[2]	Conventional	Gray et al. (1980)
C8	A10	*Mytilus edulis*	6920 ± 205 BP	GX 5308[2]	Conventional	Gray et al. (1980)
C9		*Mya truncata* sp.	6990 ± 150 BP	I 9632	Conventional	Gray et al. (1980)
C10		*Hiatella arctica*	7220 ± 115 BP	I 9246	Conventional	Gray et al. (1980)
C11	WB-4	*Mya, Macoma* sp.	7000 ± 110 BP	GSC 5202	Conventional	Gray et al. (1980)
C12	DH-3	*Macoma calcarea*	6740 ± 100 BP	Beta 11100	Conventional	Gray et al. (1980)
C13	LT-14	*Mya, Macoma* sp.	7020 ± 90 BP	Beta 34762	Conventional	Gray et al. (1980)
C14	CHA-16	*Hiatella arctica, Mya* sp.	7320 ± 50 BP	GSC 4745	Conventional	Gray et al. (1980)
C15	RD3-1C	*Hiatella arctica*	6980 ± 110 BP	Beta 13850	Conventional	Gray et al. (1980)
C16		Marine shells	7050 ± 150 BP	L 702A	Conventional	Matthews (1966)
C17		Marine shells	7160 ± 195 BP	I 726	Conventional	Matthews (1966)
C18		Marine shells	7350 ± 150 BP	L 702B	Conventional	Matthews (1966)
C19		Marine shells	7350 ± 150 BP	GSC 327	Conventional	Matthews (1966)
C20		Marine shells	7350 ± 45 BP	GSC 4038	Conventional	Laymon (1988)
C21		Marine shells	7400 ± 290 BP	GX 9996[2]	Conventional	Gray et al. (1993)
C22		*Hiatella arctica, Mytilus edulis*	6850 ± 110 BP	GSC 4332	Conventional	Gray et al. (1993)
C23		*Serripes groenlandicus*	6810 ± 250 BP	UQ 834	Conventional	Gray et al. (1993)

[1] All dates are quoted in ^{14}C years BP with 1δ. Conventional dates were obtained for large samples by either liquid scintillation or gas proportional counting apparatus, and have not been specifically corrected for an ocean reservoir effect, which increases the sample age by a mean value of 450 years (Mangerud and Gulliksen, 1975) nor for ^{13}C isotope fractionation, which reduces it by a mean value of 410 years. The laboratory quoted ages may thus be considered as reasonably compensated for both effects. AMS dates from the University of Arizona (AA) incorporate corrections for both effects, in being normalized to $\delta^{13}C = -25‰$, and being subjected to a subtraction of 450 years from the uncorrected laboratory age. AMS dates quoted by Toronto Isotrace (TO) and Beta Analytic Inc (Beta) were normalised to $\delta^{13}C = 0‰$, equivalent to a reservoir correction of only 410 years.
[2] These dates from Geochron were subject to a 450 year reservoir correction
[3] Repeat date from same horizon

westward calving of the ice front of ca. 9 ka BP. Support for the concept of extremely rapid westward calving of ice in Hudson Strait is lent by marine shell dates in the interval 9.4–8.7 ka BP from terrestrial sites in two spatially distinct sectors: 1) on the southwest coast of the Meta Incognita Peninsula, in the vicinity of Pritzler Harbour (Lowdon et al., 1977; Kaufman and Williams, 1992), and 2) at the northern extremity of Ungava Peninsula (Gray et al., 1993; Lauriol and Gray, 1997; Bruneau and Gray, 1997). The latter includes the controversial sequence of dates at the Deception River section discussed earlier (*see* Table 1), and also marine mollusc dates obtained from three sites on thick glaciomarine deposits along a well defined margin of the Ungava Peninsula ice sheet in the vicinity of Cape de Nouvelle-France. An age of 8.8 ka BP for semiaquatic fresh-water moss macrofossils at the base of a gyttja core on Wales Island (locality A19 *in* Table 2) also indicates that the ice margin must have previously withdrawn onto the mainland in the vicinity of Wakeham Bay.

At 8 ka BP the retreating ice front had liberated northeast Ungava Bay, including the northern extremity of Akpatok Island (Gray et al., 1993; Manley and Jennings, 1996; Lauriol and Gray, 1997), and the southwest coast of Meta Incognita Peninsula (Manley and Jennings, 1996; Manley and Miller, 2001). In western Hudson Strait, Salluit Fiord had become ice-free (Matthews, 1967) and a marine channel had opened into Hudson Bay, leading to the Tyrrell Sea incursion (Dredge and Cowan, 1989); however, the ice sheet still remained pinned on Nottingham and Salisbury islands, judging from the absence of dates older than 7.4 ka BP in this sector (Laymon, 1992). Dates from sites near the marine limit inland

from the north coast of Ungava Peninsula suggest that the ice front remained in a fairly stable position on the edge of the Ungava plateau between 9 ka BP and 8 ka BP. This phase of stability was probably associated with a zone of thick ice-proximal glaciomarine deposits, which extends discontinuously along the northeast tip of Ungava Peninsula from Deception Bay to De Martigny Promontory (Gray et al., 1993; Bruneau and Gray, 1997).

Dates from westernmost Hudson Strait (Matthews, 1967; Laymon, 1992) suggest that Hudson Strait had become entirely ice-free about 7 ka BP. Most of Ungava Bay had now been deglaciated, but an Ungava Peninsula ice sheet still occupied its southwest extremity (Lauriol and Gray, 1987; Allard et al., 1989; Gray et al., 1993). Separation of the eastern margin of this ice sheet from a residual ice sheet occupying the southern Torngat Mountains and the George River plateau (Fig. 13c) permitted the drainage of large glacially dammed lakes Naskaupi and MacLean (Ives, 1960) into Ungava Bay. A basal gyttja date of 6.8 ka BP (locality C2 *in* Table 2) in the drained lake basin (Short, 1981) indicates that this separation of ice sheets probably occurred about 7 ka BP. A small ice cap may have persisted on eastern Resolution Island and valley glaciers probably continued to occupy the Torngat Mountains. Possibly, a significant ice sheet, much larger than the present small Terra Nivea and Grinnell ice caps, still existed on Meta Incognita Peninsula at this stage.

Final disappearance of major residual masses of the Laurentide Ice Sheet on Ungava Peninsula did not occur until after 6 ka BP. Basal gyttja and peat bog dates obtained by Richard (1981) and by Lauriol and Gray (1983, 1987), suggested that ice remained on the southern aux Mélèzes plateau until as late as 5 ka BP. Residual ice masses were responsible for blocking drainage of major valleys into Ungava Bay, leading to the development of a series of linear glacial lakes (Lauriol and Gray, 1983, 1987; Gray et al., 1993) during this final phase of glaciation. One or several spillways from the most northerly of these lakes, glacial Lake Nantais (Fig. 13c), into the Whitley Bay–Burgoyne Bay sector of Hudson Strait may have been responsible for the abnormally thick section of postglacial muds indicated by the seismostratigraphic section at marine core site 93034-015 (MacLean et al., 2001, Fig. 25).

The question of a Noble Inlet advance across Hudson Strait between 9 ka BP and 8 ka BP

A late resurgence of north- or north-northeast-moving Quebec–Labrador ice across Hudson Strait, known as the Noble Inlet advance, has been postulated by Miller et al. (1988), Stravers et al. (1992), Manley (1995), and Manley and Miller (2001) to have overridden the tip of Meta Incognita Peninsula, up to an elevation of about 350 m a.s.l. Initially the interval attributed by Stravers et al. (1992) to this event on the basis of many dates for glaciomarine distal and proximal deposits was 8.7–7.9 ka BP; however, further dates have led Manley (1995) and Manley and Miller (2001) to suggest a much narrower time frame between 8.9 ka BP and 8.4 ka BP. Two important anomalies concerning the Noble Inlet advance are worthy of discussion. The first concerns the marine environment of Hudson Strait during the time period attributed to the event, and the second, the proposed source of the ice stream south of Ungava Bay.

Concerning the marine environment of Hudson Strait, it would be expected that such an advance would lead to grounding of the ice on the floor of eastern Hudson Strait, between 8.9 ka BP and 8.4 ka BP. The marine seismostratigraphic and microfaunal data by Jennings et al. (1998, 2001) and MacLean et al. (2001, Fig. 34, 35) certainly confirm that the ice sheet must have been grounded on the 385–400 m deep sill separating Hudson Strait from the Labrador Sea. This should have blocked the circulation of high-salinity currents into central and western Hudson Strait, leading to drastically reduced salinity, especially in the context of the influx of large quantities of meltwater from the marine and terrestrial ice margins along the strait; however, 16 mollusc samples, 8 of them single valves have furnished ages throughout the interval 8.9–8.4 ka BP (Table 1, 2). The dominant species is *Portlandia arctica*, which according to Bilodeau (unpub. report, 1986) requires relatively high salinities, in excess of 29‰, for optimal development. Although it is true that the water behind an ice barrier could remain stratified with dense, saline waters at the bottom, until eventual reopening of Hudson Strait, nine of the dated mollusc samples, including four single valves were from the surficial water layer within 50 m of the marine limit, suggesting that salinity levels were maintained by continuing circulation of ocean currents into Hudson Strait throughout the interval attributed to the Noble Inlet advance.

Although limited in number, the stable oxygen isotope ratios obtained from mollusc samples at sites dated between 9 ka BP and 8 ka BP, are similar to values postdating 6 ka BP and present-day values (Lauriol and Gray, 1997, Fig. 5) for the common species *Mya truncata, Hiatella arctica,* and *Macoma calcarea*, suggesting similar high-salinity conditions, to those prevailing since the disappearance of the continental-scale ice sheets. The evidence therefore suggests, as in the case of the ^{14}C dates, uninterrupted circulation of high-salinity ocean currents into Hudson Strait between 9 ka BP and 8 ka BP. A significant lowering and greater regional variability of the δ PDB ^{18}O values for the succeeding 8–6 ka BP interval was attributed by Lauriol and Gray (1997) to the meltwater flux into Hudson Strait and Ungava Bay, associated with the main phase of ice disintegration.

Akpatok Island is the most critically located of the islands which should theoretically have been in the path of the Noble Inlet readvance of Quebec–Labrador ice onto Meta Incognita Peninsula. In order to have attained a minimal height of 350 m on the peninsula, according to the limestone drift limits and the elevations of glaciolacustrine terraces leading to the York canyons described by Miller et al. (1988), Manley (1995), and Manley and Miller (2001), such an ice stream should have been at least several hundreds of metres thicker, as it crossed Akpatok Island 200 km farther south. An ice-sheet simulation model developed by Pfeffer et al. (1997) and Pfeffer (2001) gave derived ice elevation profiles of about 800 m, for a fast-moving ice stream in the vicinity of Akpatok Island at the Noble Inlet maximum. Such an ice stream should

have left distinct traces in the form of northward-trending striae and fluting forms in till, as the last significant glacial landforms on the island; however, as described earlier in this paper, the striae and fluting patterns, and the dark band englacial moraine are unequivocal evidence for a last major occupation of the island by coalescent flows from the west and the southwest. Fragmentary evidence of earlier flow of ice to the north or northeast from southern Ungava Bay across the island is present in the form of occasional Chioak and Abner formation erratics in the interior of the island.

On the eastern periphery of the proposed trajectory for the Noble Inlet advance, the tip of the Labrador peninsula, Killiniq Island, and the Button Islands show no trace of ice flows to the north-northeast. It is conceivable that if such a readvance occurred, the ice may have fanned out to the east near the mouth of Hudson Strait, thereby explaining the flow directions to the east-northeast and east-southeast noted for this sector; however, the north-northeast–south-southwest configuration of the Sheppard moraines, their relatively low maximum elevations of 350 m, the lack of a significant downward gradient to the north along their length, the presence of a high-carbonate drift signal in the northern part, and its absence in the southern part, are all features that may be more easily explained by a fanning out to the east of relatively thin Ungava Bay ice, rather than by north-northeast flow of a thick, rapidly flowing ice sheet across eastern Hudson Strait. The absence of erratics from the New Quebec geosyncline iron-formation on either the Lower Savage Islands or the Meta Incognita Peninsula, but their presence in equally distal locations at the northern tip of Labrador and on Resolution and Edgell islands also suggests that the continental ice sheet crossing Meta Incognita Peninsula did not have a provenance in southern Ungava Bay.

For these reasons, the present author remains reluctant to accept the concept of a Noble Inlet readvance of ice from southern Ungava Bay across Hudson Strait subsequent to 9 ka BP, although the evidence for the construction of the York delta within the interval ca. 9.0–8.6 ka BP by meltwater flowing eastward to Frobisher Bay through the York canyons from a proglacially dammed lake on the Hudson Strait flank of the watershed (Manley and Miller, 2001) is difficult to explain without invoking a contemporaneous ice mass impinging on the north shore of Hudson Strait. It is preferable to leave the question there for the moment, with the statement that there remain problems concerning both the source area and timing of the proposed ice surge.

CONCLUSIONS

The following series of general conclusions can be drawn from the evidence presented on ice flows and deglaciation chronology along the southern coastline and on the offshore islands of Hudson Strait and Ungava Bay.

1) The great ice stream discharging Laurentide ice to the east and east-southeast down Hudson Strait to the Labrador Sea, was the dominant flow a short distance offshore, during the Late Wisconsin; however, this ice stream only impinged on the coast itself at a few promontories, Cape de Nouvelle-France, Cape Hopes Advance, and most evidently at the mouth of Hudson Strait itself, on the northern tip of the Labrador peninsula.

2) Striae and rare fluting patterns for the north and northeast sectors of Ungava Peninsula generally show divergent flow perpendicular to the coastline of the peninsula, which continued offshore into Hudson Strait after retreat westwards of the Hudson Strait ice stream.

3) Around the southwest, south, and southeast shores of Ungava Bay and on Akpatok Island, however, a clearly convergent pattern of ice flow is shown, not only by striae patterns, but also by abundant bedrock flutings and drumlinized till.

4) The importance of the Torngat Mountains as an autonomous centre of outflow of ice is demonstrated by the dominant flow to the northwest into Ungava Bay.

5) The northern part of the Labrador peninsula and the Button Islands and Killiniq Island were overrun to more than 600 m a.s.l. by ice flow to the east-southeast, east, and east-northeast. This resulted from the coalescence of the Hudson Strait ice stream with one or more ice lobes exiting Ungava Bay, into the Labrador Sea.

6) The possibility that much of Hudson Strait became deglaciated prior to 10 ka BP is suggested by two single-valve mollusc dates from the Deception River site in the western basin, and by a date from northwest Akpatok Island; however, the evidence remains controversial, since other single-valve dates from the Deception River site are grouped in the 9.4–8.3 ka BP range.

7) Basal radiocarbon dates on molluscs and organic material, in terrestrial exposures and marine cores, and on molluscs from terraces near local postglacial marine limits allowed the reconstruction of the margins of the ice sheet for the period 9–7 ka BP (with extrapolation inland to 6 ka BP).

8) Finally the ice-flow evidence along the southern periphery of eastern Hudson Strait, as well as ^{14}C ages and δ PDB ^{18}O values from marine molluscs, do not support the concept of a brief surge of ice northward out of Ungava Bay, across a generally ice-free eastern Hudson Strait, up to 350 m a.s.l. on Meta Incognita Peninsula, during the Noble Inlet event, recognized there as occurring between 8.9 ka BP and 8.4 ka BP. Given possible errors in radiocarbon dates — the statistical error, the imprecision of reservoir corrections, the possibility of mixed age populations, and the possible differential uptake of inorganic carbon by infaunal molluscs, it is hardly surprising that the chronology of such an ephemeral advance of the ice is problematic. Given also that ice flowlines cannot easily be extrapolated in Hudson Strait and Ungava Bay from the ice-proximal zones on the west and south margins, to the ice-distal zones on the north and east margins, and due to the diachronous nature of the evidence, it may be some time before the detailed pattern of late glacial ice surges is interpreted correctly.

ACKNOWLEDGMENTS

Vincent Decker prepared the illustrations for this paper. The field assistance provided by numerous other graduate and undergraduate students over many summers is gratefully acknowledged. In particular, I would like to thank my co-authors on previous papers: B. Lauriol, B Hétu, C.D. Clark, L. Giugni, P. Gangloff, C. Hillaire-Marcel, B. de Boutray, D. Bruneau, and J. Richard. The Canadian Coastguard provided excellent shipboard and helicopter logistics for the fieldwork over many summers between 1990 and 2000. This was invaluable in view of the difficult access to many of the Hudson Strait locations. The Northern Scientific Training Grants Program of the Ministry of Indian Affairs and Northern Development and the Natural Sciences and Engineering Research Council of Canada provided financial support for the field research. Several radiocarbon dates were provided by the Geological Survey of Canada with the help of R. McNeely. Other dates were provided by G. Miller of the Geochronology Laboratory, Institute of Arctic and Alpine Research, University of Colorado with the assistance of W. Manley and D. Kaufman. The contribution of the critical readers of the manuscript — D. Hodgson, H. Josenhans, and J. Shaw — were much appreciated. Finally, a debt of thanks is due to B. MacLean for this excellent co-ordination of the Hudson Strait research and for many fruitful discussions on this contribution.

REFERENCES

Allard, M., Fournier, A., Gahe, E., and Séguin, M.K.
1989: Le quaternaire de la côte sud-est de la Baie d'Ungava, Québec nordique; Géographie et physique Quaternaire, v. 43, p. 325–336.

Andrews, J.T., MacLean, B., Kerwin, M., Manley, W., Jennings, A.E., and Hall, F.
1995: Final stages in the collapse of the Laurentide ice sheet, Hudson Strait, Canada, NWT: 14C AMS dates, seismic stratigraphy, and magnetic susceptibility logs; Quaternary Science Reviews, v. 14, p. 983–1004.

Avramtchev, L.
1985: Carte géologique du Québec, Carte No 2000 du DV 84-2; Ministère de l'Energie et des Ressources, Gouvernement du Québec, échelle 1/1 500 000.

Blake, W., Jr.
1966: End moraines and deglaciation chronology in northern Canada with special reference to Southern Baffin Island; Geological Survey of Canada, Paper 66-26, 31 p.

Bruneau, D. and Gray, J.T.
1991: Géologie des formations en surface, région de Salluit et du cap de Nouvelle-France area; Commission géologique du Canada, carte préliminaire public 11-1990, échelle 1/ 500 000.
1997: Écoulements glaciaires et déglaciation hâtive (ca 11 ka BP?) du nord-est de la péninsule d'Ungava, Québec, Canada; Canadian Journal of Earth Sciences, v. 34, p. 1089–1100.

Brynczka, T.
1996: Utilisation du sonar et des stries dans le cadre d'études sur la glaciation du Wisconsinien Supérieur dans la baie d'Ungava et le détroit d'Hudson; Mémoire de maîtrise, Département de Géographie, Université de Montréal, Montréal, Quebec, 138 p.

Clark, C.D., Knight, J.K., and Gray, J.T.
2000: Geomorphological reconstruction of the Labrador Sector of the Laurentide Ice Sheet; Quaternary Science Reviews, v. 19, p. 1343–1366.

Clark, P.U.
1988: Glacial geology of the Torngat Mountains, Labrador; Canadian Journal of Earth Sciences, v. 25, p. 1184–1198.
1990: Reconnaissance study of the glacial geology of northernmost Labrador; *in* Program and Abstracts, 19th Arctic Workshop, Institute of Arctic and Alpine Research, University of Colorado, Boulder, Colorado, p. 19.
1991: Landscapes of glacial erosion, Torngat Mountains, Northern Labrador-Ungava; The Canadian Geographer, v. 35, no. 2, p. 208–213.

Clark, P. and Josenhans, H.W.
1986: Late Quaternary land-sea correlations, northern Labrador and Labrador Shelf; *in* Current Research, Part B; Geological Survey of Canada, Paper 86-1B, p. 171–178.

Daigneault, R-A.
1990: Résultats préliminaires sur les directions d'écoulement glaciaire dans la région de Salluit et des lacs Nuvilik, Nouveau-Québec; dans Recherches en cours, Partie C; Commission géologique du Canada, Étude 90-1C, p. 25–29.
1993: Quaternary geology; *in* Geology of the Eastern Cape Smith Belt: Parts of the Kangiqsujuaq, cratère du Nouveau-québec and lacs Nuvilik map area, Quebecs, (ed.) M.R. St-Onge and S.B. Lucas; Geological Survey of Canada, Memoir 438, p. 96–99.
1994: CSS Hudson, croisière 93-034: Composition lihologique de la fraction grossière des sédiments quaternaires du détroit d'Hudson et de la Baie d'Ungava, Territoires du Nord-Ouest; Commission géologique du Canada, Dossier public 2414, 37 p.
1996: Géologie des formations en surface, région de Salluit et des lacs Nuvilik, Québec - Territoires du Nord-Ouest; Commission géologique du Canada, Carte 1862A, échelle, 1/ 500 000.

Dredge, L.A. and Cowan, W.R.
1989: Quaternary geology of the southwestern Canadian Shield; *in* Chapter 3 of Quaternary Geology of Canada and Greenland, (ed.) R.J. Fulton; Geological Survey of Canada, Geology of Canada, no. ? p. 214–249 (*also* Geological Society of America, The Geology of North America, v. K-1).

England, J. and Smith, I.R.
1993: Late glacial ice margins and deglacial chronology for southeastern Baffin Island and Hudson Strait, eastern Canadian Arctic; Discussion; Canadian Journal of Earth Sciences, v. 30, p. 1749–1752.

Fillon, R.H. and Harmes, R.A.
1982: Northern Labrador shelf chronology and depositional environments; Canadian Journal of Earth Sciences, v. 19, p. 162–192.

Gangloff, P. and Pissart, A.
1983: Évolution géomorphologique et palses minérales près de Kuujjuaq (Fort Chimo), Québec; Bulletin de la Société géographique de Liège, vol. 19, p. 119–132.

Gangloff, P., Gray, J.T., and Hillaire-Marcel, C.
1976: Reconnaissance géomorphologique sur la côte ouest de la baie d'Ungava; Revue de Géographie de Montréal, vol. 30, n° 4, p. 339–348.

Giugni, L., Thibault, E., and Gray, J.T.
1996: Erratic deposits as a tool for interpretation of ice flow patterns affecting Akpatok Island, Ungava Bay; *in* Program and Abstracts, 26th Arctic Workshop, Institute of Arctic and Alpine Research, University of Colorado, Boulder, Colorado, p. 36–39.

Goulet, N.
1995: Étude structurale, stratigraphique et géochronologique de la partie nord de la Fosse du Labrador; Rapport MB 95-36, Ministère des Ressources Naturelles, Gouvernement du Québec, 35 p.

Gray, J.T. and Lauriol, B.
1985: Dynamics of the Late Wisconsin ice sheet in the Ungava Peninsula interpreted from geomorphological evidence; Arctic and Alpine Research, v. 17, p. 289–310.

Gray, J.T., Brynczka, T., Giugni, L., and Thibault, E.
1994: Multiple flow patterns of the Laurentide ice sheet on Akpatok Island, Ungava Bay, Arctic Canada; *in* Program and Abstracts, 24th Arctic Workshop, Institute of Arctic and Alpine Research, University of Colorado, Boulder, Colorado, p. 27–30.

Gray, J.T., Brynczka, T., Manley, W., and Miller, G.
1995: Recent observations on glacial flow patterns and postglacial uplift variations on Resolution and Edgell Islands; *in* Program and Abstracts, 25th Arctic Workshop, Centre d'Études Nordiques, Université Laval, Ste-Foy, Quebec, p. 68–70.

Gray, J.T., Clark, C., Lauriol, B., and Decker, V.
1997: A critical appraisal of the Noble Inlet advance: an alternative scenario for events in eastern Hudson Strait between 9000 and 8000 ^{14}C yrs BP; *in* Program and Abstracts, 27th Arctic Workshop, Department of Geography, University of Ottawa, Ottawa, Ontario, p. 90–93.

Gray, J.T., de Boutray, B., Hillaire-Marcel, C., and Lauriol, B.
1980: Postglacial emergence of the west coast of Ungava Bay; Arctic and Alpine Research, v. 12, p. 19–30.

Gray, J.T., Decker, V., Guindon, L., Guenette, C., and Clark, C.
1996: Late glacial ice flow patterns in the northwest Torngat Mountains: evidence for an important local dispersal centre; *in* Program and Abstracts 26th Arctic Workshop, Institute of Arctic and Alpine Research, University of Colorado, Boulder, Colorado, p. 43–44.

Gray, J.T., Lauriol, B., Bruneau, D., and Ricard, J.
1993: Postglacial emergence of Ungava Peninsula, and its relationship to glacial history; Canadian Journal of Earth Sciences, v. 30, p. 1676–1696.

Gray, J.T., Lauriol, B., and Sloan, V.
1990: Geomorphological evidence for the partial overriding of Akpatok Island, Ungava Bay, by two lobes of Laurentide ice; *in* Program and Abstracts, 19th Arctic Workshop, Institute of Arctic and Alpine Research, University of Colorado, Boulder, Colorado, p. 27–30.

Hardy, R.
1976: Région des lacs Roberts - des Chefs; Ministère d'Energie et des Ressources, Québec, Rapport Général 171, 99 p.

Holdsworth, G.
1973: Ice deformation and moraine formation at the margin of an ice cap adjacent to a proglacial lake; *in* Research in Polar and Alpine Geomorphology, 3rd Guelph Symposium on Geomorphology, (ed.) B.D. Fahey and R.D. Thompson; Geo Abstracts, Norwich, p. 187–199.

Ives, J.D.
1957: Glaciation of the Torngat Mountains, Northern Labrador; Arctic, v. 10, no. 2, p. 67–87.
1958: Glacial geomorphology of the Torngat Mountains, Northern Labrador; Geographical Bulletin, v. 12, p. 47–75.
1960: Former ice dammed lakes and the deglaciation of the middle reaches of the George River, Labrador-Ungava; Geographical Bulletin, v. 14, p. 44–70.

Jennings, A.E., Manley, W.F., MacLean, B., and Andrews, J.T.
1998: Marine evidence for the last glacial advance across eastern Hudson Strait, eastern Canadian Arctic; Journal of Quaternary Science, v. 13, no. 6, p. 501–514.

Jennings, A.E., Vilks, G., Deonarine, B., Sills, A., and Weiner, N.
2001: Foraminiferal biostratigraphy and paleoceanography; *in* Marine Geology of Hudson Strait and Ungava Bay, Eastern Arctic Canada: Late Quaternary Sediments, Depositional Environments, and Late Glacial–Deglacial History Derived from Marine and Terrestrial Studies, (ed.) B. MacLean; Geological Survey of Canada, Bulletin 566.

Kaufman, D. and Williams, K.M.
1992: Radiocarbon Date List VII: Baffin Island, N.W.T., Canada; Institute of Arctic and Alpine Research, University of Colorado, Occasional Paper 48, 82 p.

Kaufman, D., Miller, G.H., Gray, J.T., Stravers, J.A., Lauriol, B., Bruneau, D., and Jull, T.
1992: Chronology and configuration of late-glacial (12-8 ka) fluctuations of the Labrador Dome at the mouth of Hudson Strait; *in* Program and Abstracts, 22nd Arctic Workshop, Institute of Arctic and Alpine Research, University of Colorado, Boulder, Colorado, p. 78–80.

Kaufman, D., Miller, G.H., Stravers, J.A., and Andrews, J.T.
1993a: An abrupt early-Holocene (9.9-9.6) kyr BP ice stream advance at the mouth of Hudson Strait, Arctic Canada; Geology, v. 21, p. 1063–1066.

Kaufman, D., Miller, G.H., Stravers, J.A., Manley, W.F., and Duvall, M.L.
1993b: Late glacial ice margins and deglacial chronology for southeastern Baffin Island and Hudson Strait, eastern Canadian Arctic: Reply; Canadian Journal of Earth Sciences, v. 30, p. 1753–1758.

Klassen, R.A., Paradis, S., Bolduc, A.M., and Thomas, R.D.
1992: Glacial landforms and deposits, Labrador, Newfoundland and Eastern Québec; Geological Survey of Canada, Map 1814A, scale 1:1 000 000.

Lauriol, B.
1982: Géomorphologie quaternaire du sud de l'Ungava; Paleo-Québec, vol. 15, 174 p.

Lauriol, B. and Gray, J.T.
1983: Un lac glaciaire dans la région du Lac Minto, Nouveau-Québec; Canadian Journal of Earth Sciences, v. 20, p. 1488–1492.
1987: The decay and disappearance of the Late Wisconsinan ice sheet in the Ungava Peninsula, northern Québec, Canada; Arctic and Alpine Research, v. 19, p. 109–126.
1997: La composition isotopique des mollusques marins et sa relation à la déglaciation de la péninsule d'Ungava; Géographie physique et Quaternaire, vol. 51, n° 2, p. 185–199.

Laymon, C.A.
1988: Glacial geology of western Hudson Strait, Canada, with reference to Laurentide Ice Sheet dynamics; Ph.D. thesis, University of Colorado, Boulder, Colorado, 345 p.
1992: Glacial geology of western Hudson Strait, Canada, with reference to Laurentide Ice Sheet dynamics; Geological Society of America, Bulletin, v. 104, p. 1169–1177.

Løken, O.H.
1962: The late-glacial and postglacial emergence and the deglaciation of northernmost Labrador; Geographical Bulletin, v. 17, p. 23–56.
1978: Postglacial tilting of Akpatok Island, Northwest Territories; Canadian Journal of Earth Sciences, v. 15, p. 1547–1553.

Low, A.P.
1898: Report on a traverse of the northern part of the Labrador Peninsula from Richmond Gulf to Ungava Bay; Geological Survey of Canada, Annual Report, Part L, v. 9, 43 p.
1899: Report on an exploration of part of the south shore of Hudson Strait and Ungava Bay; Geological Survey of Canada, Annual Report, v. 11, 55 p.

Lowdon, J.A., Robertson, I.M., and Blake, W.
1977: Geological Survey of Canada Radiocarbon Date List XVII; Geological Survey of Canada, Paper 77-7, 25 p.

MacLean, B.
2001: Bedrock geology of Hudson Strait and Ungava Bay; *in* Marine Geology of Hudson Strait and Ungava Bay, Eastern Arctic Canada: Late Quaternary Sediments, Depositional Environments, and Late Glacial–Deglacial History Derived from Marine and Terrestrial Studies, (ed.) B. MacLean; Geological Survey of Canada, Bulletin 566.

MacLean, B. and Vilks, G.
1992: New seismo-, bio-, and chronostratigraphic data on Quaternary sediments in Hudson Strait and Ungava Bay; *in* Program and Abstracts, 22nd Arctic Workshop, Institute of Arctic and Alpine Research, University of Colorado, Boulder, Colorado, p. 95–97.

MacLean, B., Andrews, J.T., Jennings, A., Manley, W., Hardy, I., Vilks, G., and Deonarine, B.
1996: Late Quaternary sediments in eastern Hudson Strait: relations with late glacial ice advances on southeastern Baffin Island; *in* Program and Abstracts, 26th Arctic Workshop, Institute of Arctic and Alpine Research, University of Colorado, Boulder, Colorado, p. 86–88.

MacLean, B., Vilks, G., and Deonarine, B.
1992: Depositional environments and history of late Quaternary sediments in Hudson Strait and Ungava Bay: further evidence from seismic and biostratigraphic data; Géographie physique et Quaternaire, v. 46, no. 3, p. 311–330.

MacLean, B., Vilks, G., Deonarine, B., Hardy, I., and Ceman, J.
1995: Quaternary sediments in Hudson Strait and Ungava Bay; *in* Program and Abstracts, 25th Arctic Workshop, Centre d'Études Nordiques, Université Laval, Ste-Foy, Quebec, p. 116–118.

MacLean, B., Vilks, G., Hardy, I., Deonarine, B., Jennings, A.E., and Manley, W.F.
2001: Quaternary sediments in Hudson Strait and Ungava Bay; *in* Marine Geology of Hudson Strait and Ungava Bay, Eastern Arctic Canada: Late Quaternary Sediments, Depositional Environments, and Late Glacial–Deglacial History Derived from Marine and Terrestrial Studies, (ed.) B. MacLean; Geological Survey of Canada, Bulletin 566.

MacLean, B., Williams, G.L., Sanford, B.V., Klassen, R.A., Blakeney, C., and Jennings, A.
1986: A reconnaissance study of the bedrock and surficial geology of Hudson Strait, N.W.T.; *in* Current Research, Part B; Geological Survey of Canada, Paper 86-1B, p. 617–635.

Mangerud, J. and Gulliksen, S.
1975: Apparent radiocarbon ages of recent marine shells from Norway, Spitsbergen and Arctic Canada; Quaternary Research, v. 5, p. 263–273.

Manley, W.F.
1995: Late glacial record of ice sheet/ocean interactions, Hudson Strait and southern Baffin Island, eastern Canadian Arctic; Ph.D. thesis, University of Colorado, Boulder, Colorado, 262 p.
1996: Late-glacial flow patterns, deglaciation and postglacial emergence of south-central Baffin Island and the north-central coast of Hudson Strait, eastern Canadian Arctic; Canadian Journal of Earth Sciences, v. 33, p. 1499–1510.

Manley, W.F. and Jennings, A.
1996: Radiocarbon date list VIII: eastern Canadian Arctic, Labrador, northern Québec, East Greenland Shelf, Iceland Shelf, and Antarctica; Institute of Arctic and Alpine Research, University of Colorado, Occasional Paper 50, 163 p.

Manley, W.F. and Miller, G.H.
2001: Glacial–geological record on southern Baffin Island reflecting late glacial ice-sheet dynamics in the eastern Hudson Strait region; *in* Marine Geology of Hudson Strait and Ungava Bay, Eastern Arctic Canada: Late Quaternary Sediments, Depositional Environments, and Late Glacial–Deglacial History Derived from Marine and Terrestrial Studies, (ed.) B. MacLean; Geological Survey of Canada, Bulletin 566.

Matthews, B.
1966: Radiocarbon dated postglacial land uplift in northern Ungava, Canada; Nature, v. 211, p. 1164–1166.
1967: Late Quaternary land emergence in northern Ungava, Québec; Arctic, v. 20, p. 176–202.

Miller, G.H. and Kaufman, D.S.
1990: Rapid fluctuations of the Laurentide ice sheet at the mouth of Hudson Strait: new evidence for ocean/ice sheet interactions as a control on the Younger Dryas; Paleoceanography, v. 5, p. 907–919.

Miller, G.H., Hearty, J., and Stravers, J.A.
1988: Ice-sheet dynamics and glacial history of southeasternmost Baffin Island and outermost Hudson Strait; Quaternary Research, v. 30, p. 907–919.

Pfeffer, W.T.
2001: Ice dynamics modelling of the Hudson Strait region at late glacial time; *in* Marine Geology of Hudson Strait and Ungava Bay, Eastern Arctic Canada: Late Quaternary Sediments, Depositional Environments, and Late Glacial–Deglacial History Derived from Marine and Terrestrial Studies, (ed.) B. MacLean; Geological Survey of Canada, Bulletin 566.

Pfeffer, W.T., Dyurgerov, M., Kaplan, M., Dwyer, J., Sassolas, C., Jennings, A., Raup, B., and Manley, W.
1997: Numerical modelling of late glacial Laurentide advance of ice across Hudson Strait: insights into terrestrial and marine geology, mass balance and calving flux; Paleoceanography, v. 12, p. 97–110.

Richard, P.J.H.
1981: Paléophytogéographie postglaciaire en Ungava par l'analyse pollinique; Paléo-Québec, vol. 13, 153 p.

Short, S.K.
1981: Radiocarbon list I. Labrador and northern Québec, Canada; Institute of Arctic and Alpine Research, University of Colorado, Boulder, Colorado, Occasional Paper 36, 33 p.

Stravers, J.A., Miller, G.H., and Kaufman, D.S.
1992: Late glacial ice margins and deglacial chronology for southeastern Baffin Island and Hudson Strait, eastern Canadian Arctic; Canadian Journal of Earth Sciences, v. 29, p. 1000–1017.

Thibault, E., Auclair, M., Gray, J.T., and Lamothe, M.
1995: Application of optically stimulated luminescence (OSL) to the chronostratigraphy of marine and glacigenic sediments on Akpatok Island, Ungava Bay; *in* Program and Abstracts, 25th Arctic Workshop, Centre d'Études Nordiques, Université Laval, Ste-Foy, Quebec, p. 188–189.

Late Quaternary stratigraphy of Hatton and Resolution basins, east of Hudson Strait

John T. Andrews[1], Anne E. Jennings[1], and Brian MacLean[2]

Andrews, J.T., Jennings, A.E., and MacLean, B., 2001: Late Quaternary stratigraphy of Hatton and Resolution basins, east of Hudson Strait; in *Marine Geology of Hudson Strait and Ungava Bay, Eastern Arctic Canada: Late Quaternary Sediments, Depositional Environments, and Late Glacial–Deglacial History Derived from Marine and Terrestrial Studies, (ed.) B. MacLean; Geological Survey of Canada, Bulletin 566, p. 57–64.*

Abstract: Resolution and Hatton basins lie on the continental shelf northeast of Resolution Island, and east of the sill at the entrance to Hudson Strait, respectively. The basins are bordered shoreward and in part underlain by thick multiple ice-contact sequences deposited in the lee of higher standing Precambrian rocks northeast of Resolution Island and of the sill at the entrance to Hudson Strait west of Hatton basin. Glaciomarine sediments overlie ice-contact sediments in the basins and intertongue with, or appear laterally transitional to, the uppermost of the multiple ice-contact sequences. Sediments in both basins were deposited from ice originating in Hudson Strait.

Cores in glaciomarine sediments in Resolution basin yielded basal dates greater than 20 ka BP, and higher in the section indicate a subtle change in sediment character coincident with dates that just slightly postdate Heinrich event H-1 (ca. 14.5 ka BP), and possibly may relate to that event. Deglaciation occurred 13–12 ka BP and was followed between 11 ka BP and 10 ka BP by a major ice advance from south to north across outer Hudson Strait and the inner shelf.

In Hatton basin cores show a relatively similar chronological pattern with a 13 ka BP date near the shelf break and farther west dates of 11.3 ka BP, younging upsection to 9–8 ka BP.

Résumé : Les bassins Resolution et Hatton se trouvent respectivement sur la plate-forme continentale au nord-est de l'île Resolution et à l'est du seuil situé à l'entrée du détroit d'Hudson. Ils sont bordés du côté de la côte par d'épaisses séquences multiples de sédiments de contact glaciaire déposées en aval de roches précambriennes plus élevées au nord-est de l'île Resolution et du seuil à l'entrée du détroit d'Hudson, à l'ouest du bassin Hatton, et se composent en partie de ces sédiments. Des sédiments glaciomarins recouvrent des sédiments de contact glaciaire dans les bassins et s'entremêlent avec la séquence terminale de sédiments de contact glaciaire ou semblent passer latéralement à celle-ci. Les sédiments dans les deux bassins ont été déposés à partir de glaces provenant du détroit d'Hudson.

Des carottes de sédiments glaciomarins prélevées dans le bassin Resolution ont donné des âges de base de plus de 20 ka BP; plus haut dans la coupe, on a observé un changement subtil de la nature des sédiments qui coïncide avec des dates légèrement postérieures à l'événement Heinrich H-1 (environ 14,5 ka BP) et qui pourrait être lié à cet événement. La déglaciation a eu lieu à 13–12 ka BP et a été suivie, entre 11 et 10 ka BP, d'une importante avancée glaciaire qui a progressé du sud au nord sur la zone externe du détroit d'Hudson et la plate-forme interne.

Les carottes du bassin Hatton présentent une chronologie comparable, avec un âge de 13 ka BP près de l'accore et des âges de 11,3 ka BP plus à l'ouest qui passent à 9–8 ka BP plus haut dans la coupe.

[1] Institute of Arctic and Alpine Research and Department of Geological Sciences, Box 450, University of Colorado, Boulder, Colorado, U.S.A. 80309

[2] Geological Survey of Canada (Atlantic), Bedford Institute of Oceanography, P.O. Box 1006, Dartmouth, Nova Scotia

INTRODUCTION

Hatton basin is the name applied to the large basin which lies seaward of the Hudson Strait sill (Fig. 1). Resolution basin is a much smaller feature on the northwest flank of Hatton basin. The purpose of this paper is to briefly describe the uppermost stratigraphy and chronology of sediments within these two basins in order to provide a context for the subsequent deposition within Hudson Strait. The major focus is on the chronology of the uppermost (cored) sediments, i.e. the nature and age of the sediments from the surface to a depth of about 12 m below sea level.

The Quaternary and basement stratigraphy of the area has been outlined in two publications (Josenhans et al., 1986; Praeg et al., 1986), and more generally in Osterman et al. (1985), Andrews et al. (1991a, b), and Piper et al. (1990). Cores have been taken from the area on several cruises; those with substantial ^{14}C chronologies and associated paleoenvironmental parameters are listed in Table 1 (Fig. 1). Studies by Evans (1990) and Kerwin (1994) concentrated respectively wholly or in part on this region.

The region of the shelf east of the Hudson Strait sill is a critical area within the context of rapid ice-sheet surges and/or collapse during North Atlantic Ocean Heinrich events. These are seen in deep-sea sediments from the Labrador Sea eastward toward the northeast North Atlantic Ocean off Spain–Portugal and Ireland (Heinrich, 1988; Andrews and Tedesco, 1992; Bond et al., 1992; Broecker et al., 1992; Bond and Lotti, 1995). Although there are debates on mechanisms (Alley and MacAyeal, 1994), provenance (Bond and Lotti, 1995), and sources (Robinson et al., 1995; Gwiazda et al., 1996; Revel et al., 1996), there is little doubt that a large fraction of the ice discharge involved in these events occurred

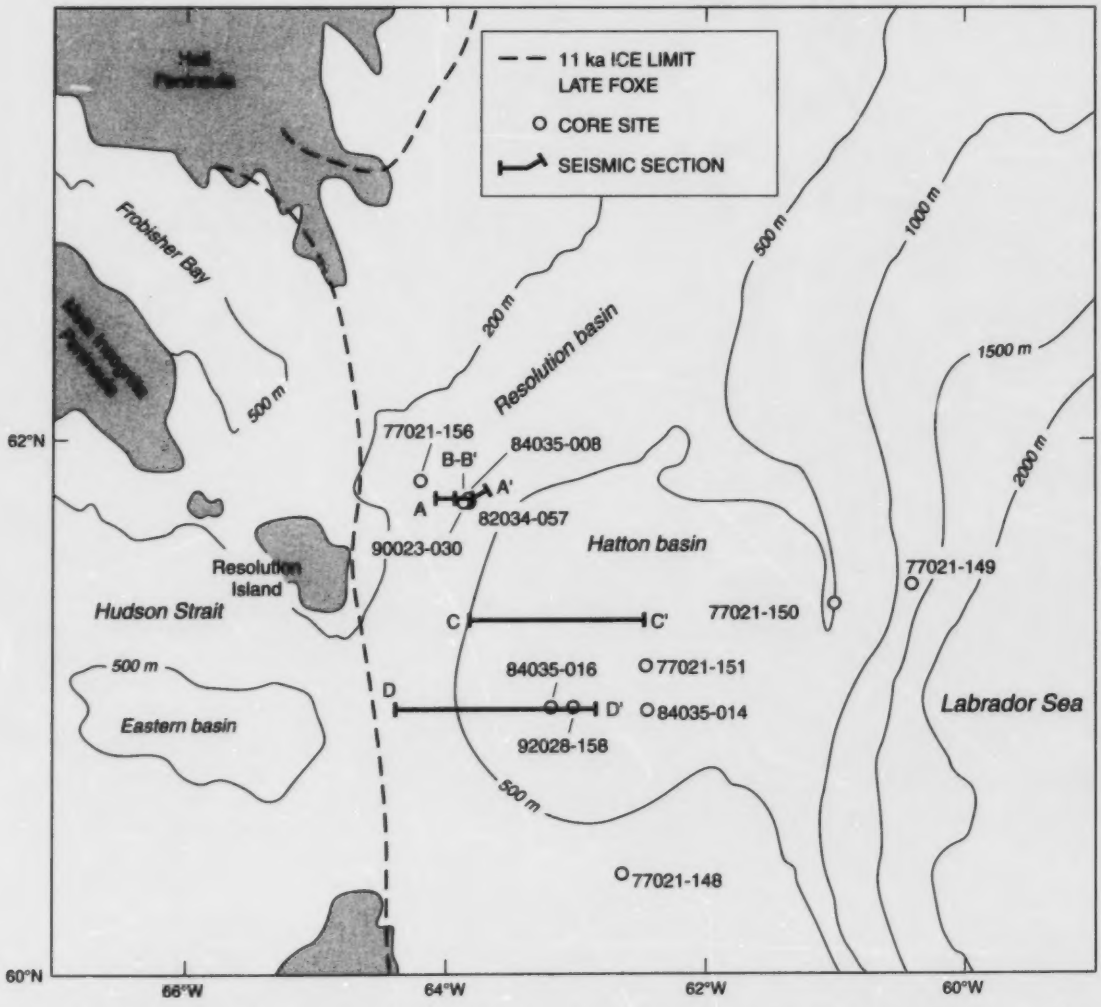

Figure 1. *Locations of Resolution and Hatton basins, cores cited in Table 1, and seismic sections illustrated in Figures 2–5 (modified from Andrews et al., 1991a, Fig. 2).*

Table 1. Cores studied in the area of Hatton and Resolution basins with basal radiocarbon dates (*see* Andrews et al., 1994).

Core ID	Latitude, longitude	Water depth (m)	Basal dates		Core top dates	
			Core depth (cm)	Date	Core depth (cm)	Date
Resolution basin						
77021-156 twc	61°51.05'N, 64°12.03'W	497			7.5 cm	1920 ± 70 BP
77021-156 pc				>26 550	0–2 cm	8935 ± 140 BP
90023-030 twc	61°47.31' N, 63°49.56'W	572			5–7 cm	9905 ± 205 BP
90023-030 LCF			776 cm	12 475 ± 130 BP	8–10 cm	9995 ± 100 BP
82034-057pc	61°46.8'N, 63°49.7'W	549	405 cm	14 915 ± 250 BP	3.5 cm	7850 ± 65 BP
			322 cm	13 175 ± 150 BP		
			325 cm	14 005 ± 110 BP		
			415 cm	25 170 ± 420 BP		
84035-008 pc	61°47.2'N, 63°49.9'W	580	805 cm	12 290 ± 100 BP	0–5 cm	8975 ± 150 BP
			822 cm	>30 000		
Hatton basin						
77021-150 pc	61°23'N, 61°0.8'W	543	101 cm	13 000 ± 220 BP	0 cm	6975 ± 60 BP
77021-151 pc	61°15'N, 62°47.17'W	603	543 cm	11 375 ± 125 BP	5–7 cm	7940 ± 80 BP
			543 cm	11 275 ± 125 BP		
84035-016 pc	60°59.8'N, 63°11.4'W	603			14 cm	8002 ± 70 BP
84035-014 pc	60°59.2'N, 62°27.3'W	605	516 cm	10 340 ± 70 BP		
92028-158 pc	61°00'N, 62°55.57'W	622	930 cm	9620 ± 95 BP	0 cm	3660 ± 80 BP

twc = trigger core
pc = piston core
LCF = long core facility

from Hudson Strait and that the ice must have tracked across Hatton basin. Radiocarbon dating indicates the following ^{14}C ages for the latest Heinrich events; their estimated durations would be ±1 ka BP(Dowdeswell et al., 1995). Radiocarbon age estimates for Heinrich events are H-0: 9–11 ka BP (coeval with the Younger Dryas chronozone); H-1: ca. 14.5 ka BP; H-2: ca. 20.5 ka BP; H-3: ca. 27 ka BP; and H-4: ca. 35 ka BP.

The following sections outline the stratigraphic and chronological settings in Resolution and Hatton basins. Both basins provide evidence relating to glacial ice advances from Hudson Strait onto the continental shelf.

STRATIGRAPHIC SETTINGS

Resolution basin

Seismic-reflection data indicate that Resolution basin lies in the outer part of a broad bedrock depression that is coincident with the contact between Tertiary sedimentary rocks and Precambrian metamorphic and igneous rocks. The contact between these rock units occurs near the western margin of the depression (Fig. 2). An angular unconformity developed across the bedrock forms a well defined demarcation with the overlying Quaternary sediments. Acoustically unstratified, multiple-sequence ice-contact deposits comprising four members, totalling 160 m in thickness, adjoin the basin to the southwest i.e. towards Resolution Island (Fig. 2) (Praeg et al., 1986). These have been deposited in the lee of the higher standing Precambrian rocks (large-scale crag-and-tail deposits) in a configuration similar to that at the west side of Hatton basin where thick ice-contact deposits abut the sill at the entrance to Hudson Strait. The more extensive lower ice-contact members form the basal Quaternary deposits beneath acoustically stratified glaciomarine sediments that subsequently were deposited in Resolution basin (Fig. 2, 3). The upper sediments total 10–11 m in thickness (Fig. 3). The upper half of the glaciomarine sequence is characterized on high-resolution seismic-reflection profiles by finer, more closely spaced acoustic reflectors than those in the lower part of the section. A tongue of the uppermost ice-contact member interfingers midway in the glaciomarine sequence in the southwestern part of the basin (Fig. 3). Glaciomarine sediments overlying the tongue are transitional upslope to ice-contact sediments. These features mark the seaward limit of grounded glacial ice at that time (Praeg et al., 1986). Where

penetrated by core 82034-057 (Fig. 3) the glaciomarine sediments in the basin are mainly well to poorly stratified sandy silt and clay with variable numbers of dropstones. Detrital carbonate content is variable with the greatest abundance in units with most abundant dropstones (Evans, 1990). Low-abundance, low-diversity foraminiferal assemblages occur in the bottom metre of the core and in two intervals higher in the core (1.3–2 m and 0.2–0.8 m). These suggest periods of ice-proximal conditions separated by periods when glacial ice was more distal (Praeg et al., 1986). Fluctuations between ice-proximal and ice-distal or seasonally open-water conditions were also recognized by Evans (1990) in core 84035-008 (Fig. 1), which lies approximately 0.7 km north of locality 057, however, she considered the record there in general to have been more proximal. On the northern and seaward flanks of Resolution basin the acoustically stratified glaciomarine sediments above 500–550 m present water depth have been extensively reworked through scouring of the seabed by grounding icebergs, and the acoustic continuity of the beds has been destroyed. This process has extensively modified glaciomarine sediments in many areas of the southeast Baffin Shelf (Praeg et al., 1986), and transformed them into an iceberg turbate as defined by Vorren et al. (1983). High-resolution seismic-reflection and sample data indicate that postglacial muddy sediments are absent in most areas of Resolution basin, their occurrence being limited to a small, thin, localized deposit. A thin, sandy surface veneer was present in core 82034-057 (Praeg et al., 1986).

Hatton basin

The geological setting at Hatton basin resembles that at Resolution basin in a number of respects. It is situated in a broad depression on the inner part of the shelf, the inner margin of which is coincident with the contact between Tertiary sedimentary rocks that underlie the shelf and Precambrian metamorphic or igneous rocks that compose the adjacent land masses and the sill at the entrance to Hudson Strait. At the western margin of the depression, a succession of stacked, acoustically massive, ice-contact sequences totalling 360 m in thickness have been deposited adjacent to the sill at the entrance to Hudson Strait (MacLean et al., 1990). Five or possibly six ice-contact members are represented (Fig. 4). Single-channel seismic-reflection data along a transect due east from the mouth of Hudson Strait along 61°N latitude indicate

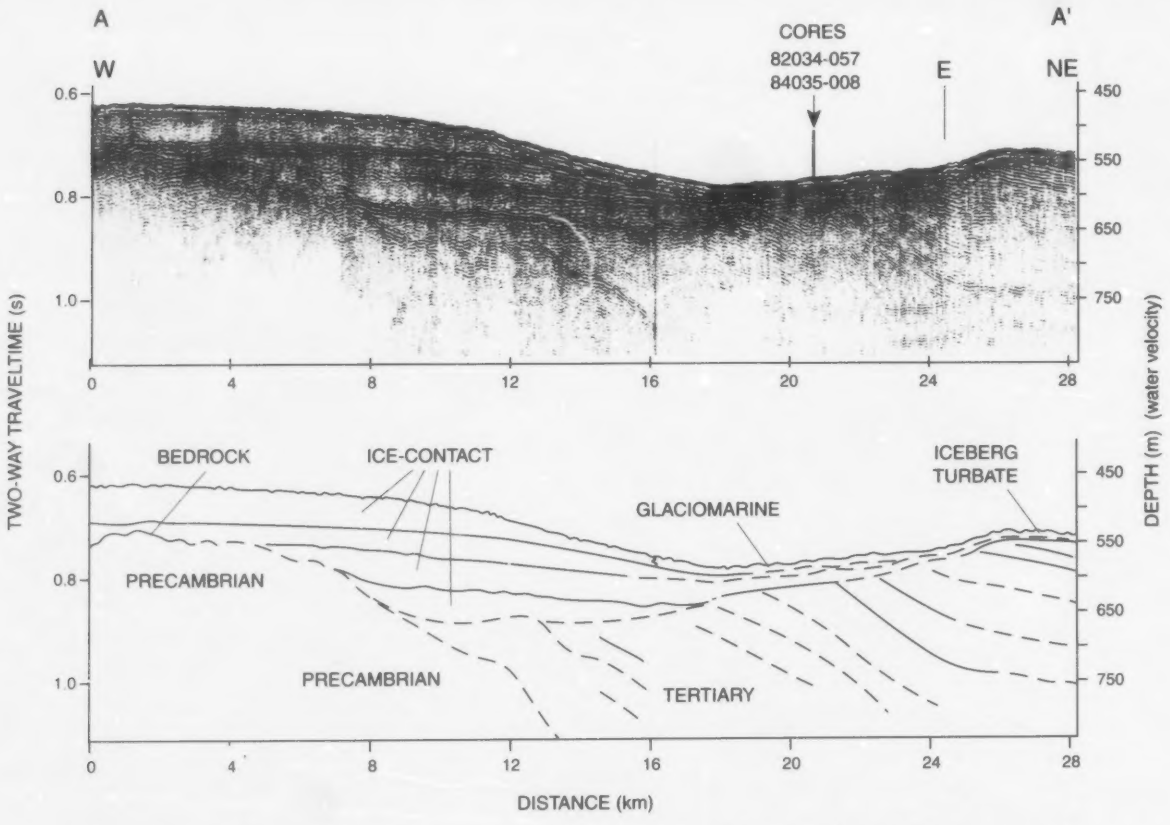

Figure 2. *Single-channel seismic-reflection profile A-A′ across Resolution basin illustrating multiple ice-contact sequences and glaciomarine sediments (see Fig. 1 for location) (modified from Praeg et al., 1986, Fig. 11).*

that one or more of the lower ice-contact units from the deposit at the sill underlie Hatton basin (Fig. 4). Stratigraphic relations in the basin are best illustrated by seismic-reflection data along a transect across the northern part of the basin along 61°20′N latitude (Fig. 5). There, a massive sequence of acoustically unstratified sediments that thickens westwards to a maximum of 70 m forms the lower part of the Quaternary succession. Some weak acoustic stratification may occur locally, but the unit is considered to be primarily an ice-contact deposit. The unit terminates to the east against the

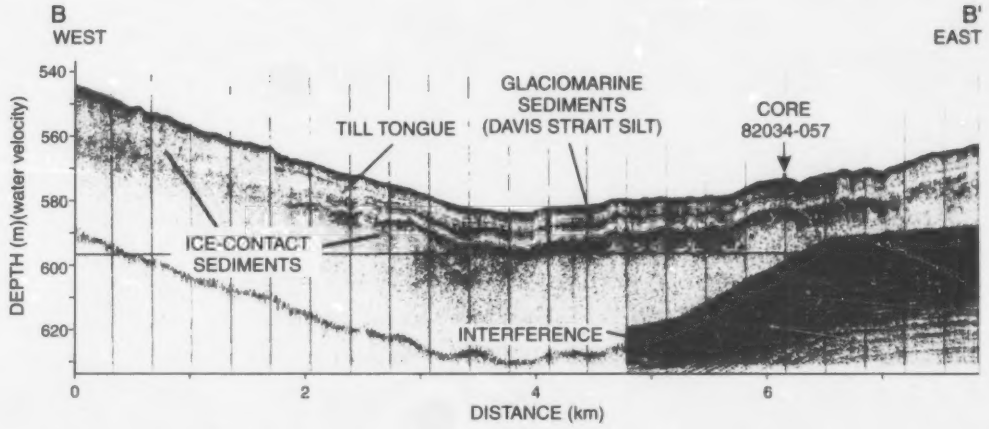

Figure 3. *Huntec™ high-resolution seismic-reflection profile B-B′ showing glaciomarine and ice-contact sediment relationships in Resolution basin and the location of cores 82034-057 and 84035-008 (after Praeg et al., 1986, Fig. 12) (see Fig. 1 for profile location).*

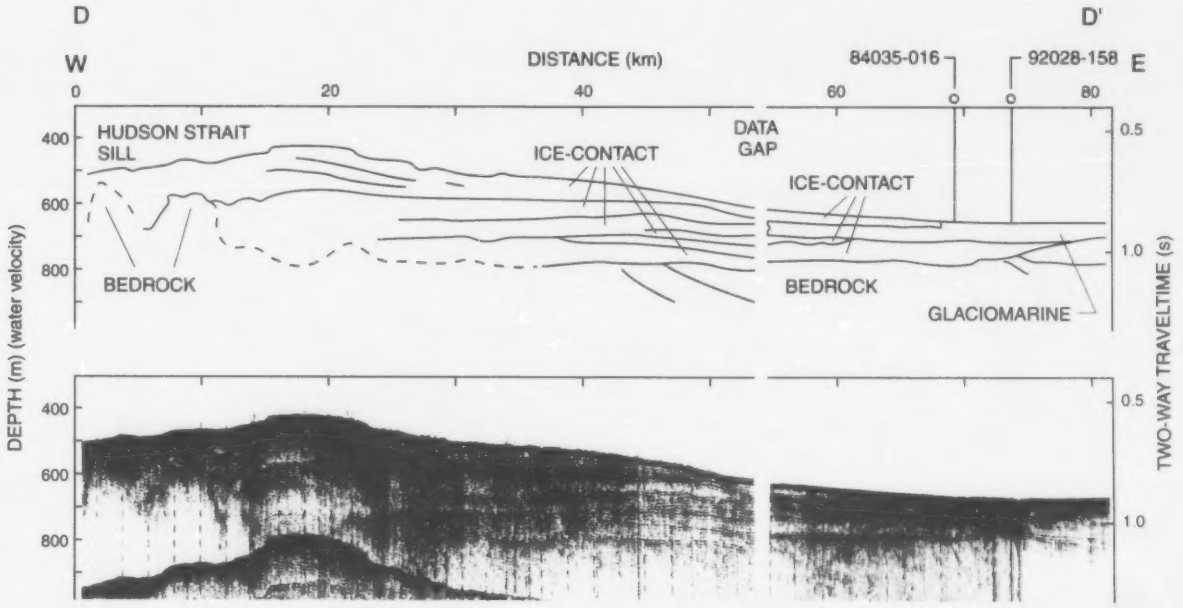

Figure 4. *Single-channel seismic-reflection profile D-D′ illustrating multiple ice-contact sequences adjacent to the sill at the entrance to Hudson Strait. These form the western margin of Hatton basin. Locations of cores 84035-016 and 92028-158 are indicated (see Fig. 1 for profile location). (Modified from MacLean (1997) Figure 2 in Kluwer Academic Publishers:- Glaciated Continental Margins: An Atlas of Acoustic Images, p. 89, published by Chapman & Hall, 1997. Reproduced with kind permission from Kluwer Academic Publishers.)*

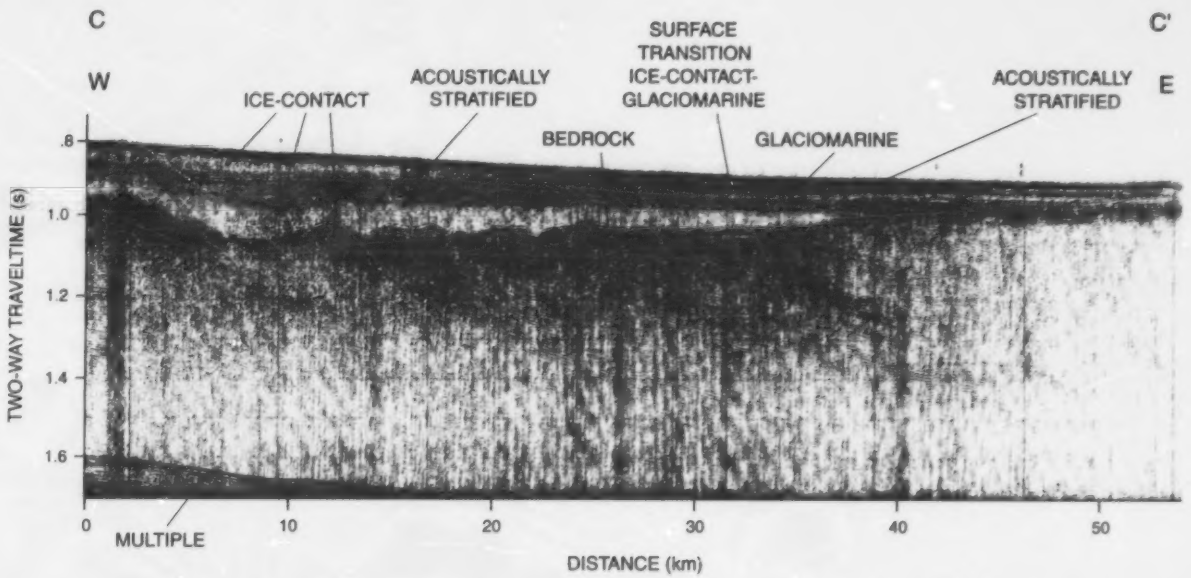

Figure 5. *Single-channel seismic-reflection profile transect C-C′ west-east across the northern part of Hatton basin showing glaciomarine and ice-contact sequences beneath the basin (see Fig. 1 for location).*

bedrock rise at the eastern side of the basin, and to the west on the northern transect against bedrock and earlier ice-contact deposits 45 km east of Resolution Island. These beds are overlain by a 50 m thick unit of mainly acoustically stratified sediments. Sediments of this unit appear to interfinger or intertongue with ice-contact sediments shoreward and with thick deposits of ice-contact sediments on the shelf to seaward. Single-channel and high-resolution seismic-reflection data indicate that acoustically unstratified sediments of the upper ice-contact deposits at the Hudson Strait sill form a seaward-thinning wedge of sediments that overlies the acoustically stratified unit eastward to about 63°15′W longitude where they are transitional to glaciomarine sediments (Josenhans et al., 1986; Evans, 1990; Andrews et al., 1994). This marks the maximum seaward extent of late glacial ice advances grounded on the Hudson Strait sill. The uppermost glaciomarine sediments appear to be in the order of 20 m in thickness. They overlie the thick, acoustically stratified unit and may represent a continuation of those sequences. These beds also appear to be transitional to ice-contact sediments at the seaward margin of Hatton basin. Where cored, the glaciomarine sediments comprise variably silty, clayey, and sandy material with dropstones. Carbonate content seldom is less than 30% and is consistently higher than in Resolution basin. Foraminiferal assemblages indicate fluctuations between ice-proximal and ice-distal environments (Evans, 1990). High-resolution seismic-reflection data show no indications of postglacial sediments and core data suggests deposition of such sediments was sparse (Evans, 1990; Andrews et al., 1994).

Radiocarbon chronology

Samples of Foraminifera and Mollusca from sediments east of the Hudson Strait sill have been radiocarbon dated over the last decade or more. Most of these are reported in detail in the Institute of Arctic and Alpine Research Radiocarbon Date Lists (Andrews et al., 1989; Kaufman and Williams, 1992; Manley and Jennings, 1996). The vast majority are AMS dates on small (1–10 mg) samples. The dates are corrected by 450 years for the ocean reservoir effect, however, in reality we do not know how this parameter might have varied during deglaciation. The correction might be as much as 800 years (Bard et al., 1994), but this would not make a fundamental difference to our notion of the chronology of events.

Table 1 shows dates on core tops, or the nearest date to the surface, and basal dates. Furthermore, additional information is provided on some cores, such as the dates from both the piston and trigger cores if these were available. In Resolution basin, three of the cores have Marine Isotope Stage (MIS) 2 or 3 radiocarbon ages at their base, i.e. dates greater than 20 ka BP. In core 82034-057 a subtle but noticeable change in the sediment occurs at 320–325 cm with a date below the contact of 14 005 ± 110 BP and immediately above, the reported date is 13 175 ± 150 BP. The lower date is a few hundred years younger than Heinrich event 1 (H-1) off Hudson Strait in the Labrador Sea (ca. 14 500 BP) (Andrews et al., 1994; Hillaire-Marcel et al., 1994; Jennings et al., 1996), but dating uncertainties do not preclude the hypothesis that this represented the erosion of shelf sediments by an ice advance associated with event H-1. In the cores that do not bottom in sediments with associated ^{14}C dates of 20 ka BP or more, the ages we have obtained indicate that this area was deglaciated

by 13–12 ka BP (Table 1). Dates from core tops invariably reflect sediment starvation once the main ice sheet had retreated well within Hudson Strait. Thus dates at or close to the retrieved core tops have ages that range from ca. 9900 BP to 7850 BP. It is probable that a few centimetres to a few tens of centimetres of sediment may have been lost during the piston coring operation (but note agreement between "tw" and "pc" in the "giant" coring site of 90023-030), but even so, it is certain that during the last 8000 ^{14}C years the net sediment accumulation in Resolution basin has been extremely low (Andrews et al., 1991a).

Cores from Hatton basin (Table 1) have a somewhat similar pattern of radiocarbon dates. For example, the basal date from the short 77021-150 core, situated toward the shelf-break is 13 000 ± 220 BP. Moving toward the west, hence toward the sill, two dates from basal sediments in cire 77021-151 predate H-0 dates of 11 375 BP and 11 275 BP. Above the 50 cm or so, basal sediment AMS dates of 9–8 ka BP occur (Andrews et al., 1990). This might suggest that this site was covered by glacial ice during the first northward advance of ice across Hudson Strait from Labrador around 11 ka BP (Andrews et al., 1995), that is during the Younger Dryas–Heinrich H-0 event; however, the work of Jennings et al. (1995) has indicated that interpretation of AMS radiocarbon dates from ice-proximal glacial marine settings is complicated. Reworking is always a potential problem and thus dates should be considered as 'less than or equal to' in terms of their final depositional chronology. Core top and/or near surface dates from Hatton basin (Table 1) range from ca. 3660 BP to ca. 6975 BP, suggesting marginally higher net sediment accumulation here than in Resolution basin during the postglacial, i.e. less than 8 ka BP.

One intriguing question in the Hatton basin stratigraphy and chronology is why there are not apparently thick sequences of sediments associated with the final retreat of the ice sheet along Hudson Strait and into Hudson Bay around 8000 ^{14}C years ago (Andrews and Falconer, 1969; Dyke and Prest, 1987). Farther south along the Labrador Shelf (Hall et al., 1999), in Karlsfni Trough, and even farther south in Cartwright Saddle, there are 1–4 m of carbonate-rich sediments that are associated with this final event in Hudson Strait–Hudson Bay; however, the depositional record in Hatton basin over the same period is relatively short, and apparently the sediment plumes did not make their way northward to Resolution basin as there the records show virtually no net sediment deposition younger than 10 ka BP (Table 1).

ACKNOWLEDGMENTS

We wish to extend sincere thanks to captains, crews, and scientific staff of the *CSS Hudson* for their excellent work and co-operation in carrying out these studies. We wish also to acknowledge the contribution of R.H. Fillon, the collector of the 1977 cores used in this study and the assistance provided by Iris Hardy and curation staff at GSC Atlantic. Special thanks are extended to D.A. Hodgson, H. Josenhans, and J. Shaw for helpful comments and review of this paper. The research of Andrews and Jennings was supported by the Office of Polar Programs at the United States National Science Foundation.

REFERENCES

Alley, R.B. and MacAyeal, D.R.
1994: Ice-rafted debris associated with binge-purge oscillations of the Laurentide Ice Sheet: Paleoceanography, v. 9, p. 503–511.

Andrews, J.T. and Falconer, G.
1969: Late glacial and postglacial history and emergence of the Ottawa Islands, Hudson Bay, N.W.T.: evidence on the deglaciation of Hudson Bay; Canadian Journal Earth Sciences, v. 6, p. 1263–1276.

Andrews, J.T. and Tedesco, K.
1992: Detrital carbonate-rich sediments, northwestern Labrador Sea: implications for ice-sheet dynamics and iceberg rafting (Heinrich) events in the North Atlantic; Geology, v. 20, p. 1087–1090.

Andrews, J.T., Bond, G., Jennings, A.E., Kerwin, M., Kirby, M., MacLean, B., Manley, W., and Miller, G.H.
1995: A Heinrich like-event, H-0 (DC-0) : source(s) for detrital carbonate in the North Atlantic during the Younger Dryas chronozone; Paleoceanography, v. 10, p. 943–952.

Andrews, J.T., Erlenkeuser, H., Evans, L.W., Briggs, W.M., and Jull, A.J.T.
1991a: Meltwater and deglaciation, SE Baffin Shelf (NE margin Laurentide Ice Sheet) between 13.5 and 7 ka: from O and C stable isotope data; Paleoceanography, v. 6, no. 5, p. 621–637.

Andrews, J.T., Evans, L.W., Williams, K.M., Briggs, W.M., Erlenkeuser, H., Hardy, I., and Jull, A.J.T.
1990: Cryosphere/ocean interactions at the margin of the Laurentide Ice Sheet during the Younger Dryas Chron: SE Baffin Shelf, Northwest Territories; Paleoceanography, v. 5, p. 921–935.

Andrews, J.T., Jennings, A.E., MacLean, B., Mudie, P., Praeg, D., and Vilks, G.
1991b: The surficial geology of Canadian eastern Arctic and Polar continental shelves; Continental Shelf Research, v. 11, p. 791–819.

Andrews, J.T., Laymon, C.A., and Briggs, W.M.
1989: Radiocarbon Date List VI, Baffin Island and III Labrador-Ungava; Institute of Arctic and Alpine Research, University of Colorado, Occasional Paper No. 46, p. 85.

Andrews, J.T., Tedesco, K., Briggs, W.M., and Evans, L.W.
1994: Sediments, sedimentation rates, and environments, SE Baffin Shelf and NW Labrador Sea 8 to 26 KA; Canadian Journal of Earth Sciences, v. 31, p. 90–103.

Bard, E., Arnold, M., Mangerud, J., Paterne, M., Labeyrie, L., Duprat, J., Melieres, M.-A., Sonstegaard, E., and Duplessy, J.-C.
1994: The North Atlantic atmosphere-sea surface 14C gradient during the Younger Dryas climatic event; Earth and Planetary Science Letters, v. 126, p. 275–287.

Bond, G., Heinrich, H., Broecker, W.S., Labeyrie, L., McManus, J., Andrews, J.T., Huon, S., Jantschik, R., Clasen, S., Simet, C., Tedesco, K., Klas, M., Bonani, G., and Ivy, S.
1992: Evidence for massive discharges of icebergs into the glacial Northern Atlantic; Nature, v. 360, p. 245–249.

Bond, G.C. and Lotti, R.
1995: Iceberg discharges into the North Atlantic on millennial time scales during the last glaciation; Science, v. 267, p. 1005–1009.

Broecker, W.S., Bond, G., McManus, J., Klas, M., and Clark, E.
1992: Origin of the Northern Atlantic's Heinrich events; Climatic Dynamics, v. 6, p. 265–273.

Dowdeswell, J.A., Maslin, M.A., Andrews, J.T., and McCave, I.N.
1995: Iceberg production, debris rafting, and the extent and thickness of Heinrich layers (H-1, H-2) in North Atlantic sediments; Geology, v. 3, p. 301–304.

Dyke, A.S. and Prest, V.K.
1987: Late Wisconsinan and Holocene history of the Laurentide Ice Sheet; Geographie physique et Quaternaire, v. 41, p. 237–263.

Evans, L.W.
1990: Late Quaternary stratigraphy of the Hatton and Resolution Basins, southeast Baffin Island Shelf, N.W.T., Canada; M.Sc. thesis, University of Colorado, Boulder, Colorado, 189 p.

Gwiazda, R.H., Hemming, S.R., and Broecker, W.S.
1996: Tracking the sources of icebergs with lead isotopes: the provenance of ice-rafted debris in Heinrich layer 2; Paleoceanography, v. 11, no. 1, p. 77–93.

Hall, F.R., Andrews, J.T., Jennings, A.E., Vilks, G., and Moran, K.
1999: Late Quaternary sediments and chronology of the NE Labrador Shelf (Karlsefni Trough, Saglek Bank): links to glacial history; Geological Society of America, Bulletin, v. 111, p. 1700–1713.

Heinrich, H.
1988: Origin and consequences of cyclic ice rafting in the Northeast Atlantic Ocean during the past 130,000 years; Quaternary Research, v. 29, p. 143–152.

Hillaire-Marcel, C., de Vernal, A., Bilodeau, G., and Wu, G.
1994: Isotope stratigraphy, sedimentation rates, deep circulation, and carbonate events in the Labrador Sea during the last ~200 kyr; Canadian Journal of Earth Sciences, v. 31, p. 63–89.

Jennings, A.E., Andrews, J.T., Weiner, N.J., Manley, W.F., MacLean, B., and Barber, D.C.
1995: Strategies and progress in unravelling the chronology of Hudson Strait deglaciation; *in* 25th Arctic Workshop, University of Laval, Quebec, Quebec, Abstracts Volume, p. 90.

Jennings, A.E., Tedesco, K.A., Andrews, J.T., and Kirby, M.E.
1996: Shelf erosion and glacial ice proximity in the Labrador Sea during and after Heinrich events (H-3 or 4 to H-0) as shown by formanifera; *in* Late Quaternary Palaeoceanography of the North Atlantic Margins, (ed.) J.T. Andrews, W.E.N. Austin, H. Bergsten, and A.E. Jennings; Geological Society, Special Publications, p. 29–49.

Josenhans, H.W., Zevenhuizen, J., and Klassen, R.A.
1986: The Quaternary geology of the Labrador Shelf; Canadian Journal of Earth Sciences, v. 23, p. 1190–1214.

Kaufman, D.S. and Williams, K.M.
1992: Radiocarbon Date List VII: Baffin Island, N.W.T., Canada; Institute of Arctic and Alpine Research, University of Colorado, Boulder, Colorado, Occasional Paper 48, 82 p.

Kerwin, M.W.
1994: Final stages in the collapse of the Laurentide Ice Sheet: a rock magnetic and sedimentological study from Hudson Strait, Canada; M.Sc. thesis, University of Colorado, Boulder, Colorado, 189 p.

MacLean, B.
1997: Thick multiple ice-contact deposits adjoining the sill at the entrance to Hudson Strait, Canada; *in* Glaciated Continental Margins: an Atlas of Acoustic Images; (ed.) T.A. Davies, T. Bell, A.K. Cooper, H. Josenhans, L. Polyak, A. Solheim, M.S. Stoker, and J.A. Stravers; Chapman & Hall, London, United Kingdom, p. 88–89.

MacLean, B., Praeg, D.B., Josenhans, H.W., and Klassen, R.
1990: Hudson Strait and Ungava Bay; *in* Quaternary Geology, Chapter 10, Piper, D.J.W., Mudie, P.J., Fader, G.B., Josenhans, H.W., MacLean, B., and Vilks, G. *in* - Geology of the Continental Margin of Eastern Canada, (ed.) M.J. Keen and G.L. Williams; Geological Survey of Canada, Geology of Canada, no. 2, p. 545–549 (*also* Geological Society of America, The Geology of North America, v. I).

Manley, W.F. and Jennings, A.E.
1996: Radiocarbon Date List VIII: Eastern Canadian Arctic, Labrador, Northern Quebec, East Greenland Shelf, Iceland Shelf, and Antarctica; Institute of Arctic and Alpine Research, University of Colorado, Boulder, Colorado, Occasional Paper No. 50, 163 p.

Osterman, L.E., Miller, G.H., and Stravers, J.A.
1985: Late and mid-Foxe Glaciation of southern Baffin Island; *in* Quaternary Environments: Eastern Canadian Arctic, Baffin Bay, and Western Greenland, (ed.) J.T. Andrews; Allen and Unwin, London, United Kingdom, p. 520–545.

Piper, D.J.W., Mudie, P.J., Fader, G.B., Josenhans, H.W., MacLean, B., and Vilks, G.
1990: Quaternary Geology; *in* Geology of the Continental Margin of Eastern Canada, (ed.) M.J. Keen and G.L. Williams; Geological Society of America, Boulder, Colorado, p. 475–607.

Praeg, D.B., MacLean, B., Hardy, I.A., and Mudie, P.J.
1986: Quaternary geology of the southeast Baffin Island continental shelf; Geological Survey of Canada, Paper 85-14, 38 p.

Revel, M., Sinko, J.A., Grousset, F.E., and Biscaye, P.E.
1996: Sr and Nd isotopes as tracers of North Atlantic lithic particles: paleoclimatic implications; Paleoceaonography, v. 11, p. 95–113.

Robinson, S.G., Maslin, M.A., and McCave, N.
1995: Magnetic susceptibility variations in upper Pleistocene deep-sea sediments of the N.E. Atlantic: implications for ice rafting and palaeocirculation at the last Glacial Maximum; Paleoceanography, v. 10, p. 221–250.

Vorren, T.O., Hald, M., Edwardsen, M., and Lind-hansen, O-W.
1983: Glaciogenic sediments and sedimentary environments on continental shelves; general principles with a case study from the Norwegian Shelf; *in* Glacial Deposits in North-west Europe, (ed.) J. Ehlers; A.A. Balkema, Rotterdam, Netherlands, p. 61–73.

Bedrock geology of Hudson Strait and Ungava Bay

Brian MacLean[1]

MacLean, B., 2001: Bedrock geology of Hudson Strait and Ungava Bay; in *Marine Geology of Hudson Strait and Ungava Bay, Eastern Arctic Canada: Late Quaternary Sediments, Depositional Environments, and Late Glacial–Deglacial History Derived from Marine and Terrestrial Studies, (ed.) B. MacLean; Geological Survey of Canada, Bulletin 566, p. 65–69.*

Abstract: This paper summarizes information regarding the bedrock geology underlying Hudson Strait and Ungava Bay interpreted from seismic reflection data together with shallow borehole information, published data from adjoining terrestrial areas, and from an exploratory well on Akpatok Island.

Hudson Strait is underlain primarily by Lower Paleozoic sedimentary rocks (mainly calcareous carbonate rocks) that contact Precambrian metamorphic rocks of the adjacent land masses not far from the coasts of Baffin Island and Ungava and Labrador peninsulas. These sedimentary rocks also form the central platform in Ungava Bay. Younger strata, possibly of Mesozoic age occur locally in Eastern basin and their presence has also been postulated in parts of western and southwestern Hudson Strait.

Three half-graben structures, downfaulted against older rocks at their southern margins, form prominent structural features in the floor of Hudson Strait. Phanerozoic (mainly Lower Paleozoic) sedimentary rocks thicken southward in these structures reaching 2000 m or more in Eastern basin. These basins have been sites for deposition of Quaternary sediments that locally reach more than 100 m in thickness.

Calcareous sediments and erratics derived from glacial erosion of the Paleozoic strata are important markers in interpreting ice-flow patterns in the region and sediment dispersal seaward.

Résumé : Le présent article résume la géologie du substratum rocheux du détroit d'Hudson et de la baie d'Ungava telle qu'interprétée à partir de données de réflexion sismique, de données provenant de forages peu profonds et d'un puits d'exploration foré dans l'île Akpatok, et de données publiées recueillies dans des régions terrestres adjacentes. Le détroit d'Hudson comporte principalement des roches sédimentaires du Paléozoïque inférieur (surtout des roches carbonatées calcaires) qui font contact avec des roches métamorphiques précambriennes des terres adjacentes près des côtes de l'île de Bafffin et des péninsules d'Ungava et du Labrador. Ces roches sédimentaires composent également la plate-forme centrale de la baie d'Ungava. Par endroits dans le bassin Est, on trouve des strates plus jeunes, remontant peut-être au Mésozoïque; on suppose qu'elles seraient aussi présentes dans certaines parties occidentales et centrales du détroit d'Hudson.

Trois demi-grabens, affaissés contre des roches plus anciennes à leurs marges méridionales, constituent d'importantes structures sur le fond du détroit d'Hudson. Dans ces structures, des roches sédimentaires phanérozoïques (surtout du Paléozoïque inférieur) s'épaississent vers le sud, atteignant 2000 m ou plus dans le bassin Est. Des sédiments quaternaires, d'une épaisseur dépassant 100 m par endroits, se sont également accumulés dans ces bassins.

Des sédiments calcaires et des blocs erratiques provenant de l'érosion glaciaire des strates paléozoïques constituent des repères importants pour l'interprétation des modes d'écoulement glaciaire dans la région et de la dispersion de sédiments vers le large.

[1] Geological Survey of Canada (Atlantic), Bedford Institute of Oceanography, Dartmouth, Nova Scotia B2Y 4A2

BEDROCK UNITS

Data from shallow borehole samples and regional seismic surveys indicate that Hudson Strait is mainly underlain by Lower Paleozoic sedimentary rocks (Fig. 1). These strata also form the large central platform in Ungava Bay of which Akpatok Island is an emergent part. The bedrock geology has been reported on by Grant and Manchester (1970), Workum et al. (1976), Sanford et al. (1979), MacLean and Williams (1983), MacLean et al. (1986), Miller and Williams (1988), and MacLean (1998), and illustrated by Wheeler et al. (1996) and Sanford and Grant (1999). Precambrian metamorphic and igneous rocks of the adjacent land areas of Baffin Island, Ungava and Labrador peninsulas, and offshore islands (*see* Wheeler et al., 1996) form the bedrock in the zones bordering the coasts and underlie the Paleozoic rocks farther offshore (Fig. 1). The Paleozoic strata commonly form cuesta ridges (Fig. 2) near the contact with Precambrian rocks on the northern margins of Eastern and Western basins, from which point they thicken southward in each of the structural basins (MacLean et al., 1986).

The Paleozoic rocks are mainly carbonate considered to be of Late Ordovician age (Caradoc–Ashgill) (Miller and Williams, 1988), but Silurian strata possibly are represented in the eastern part of the strait and also in the region west and southwest of Charles Island. Distribution of the bedrock units was outlined by MacLean et al. (1986) and tentative correlations were suggested with stratigraphic units recognized by Heywood and Sanford (1976) on Southampton, Coats, and Mansell islands in northern Hudson Bay, and by Workum et al. (1976) in the Premium Homestead Akpatok L-26 well on Akpatok Island.

Eroded remnants of younger, apparently lithologically different strata, possibly of Mesozoic age, occur within Eastern basin (Fig. 1, 3) (Grant and Manchester, 1970; MacLean et al., 1986; Wheeler et al., 1996; Sanford and Grant, 1999). These beds appear in part to have been downdropped relative to adjacent Ordovician and Silurian beds. A small borehole sample of faunally barren sandstone was recovered from these strata. Mesozoic (?Cretaceous) strata have also been interpreted to occur in Western and Southwestern basins (Wheeler et al., 1996; Sanford and Grant, 1999).

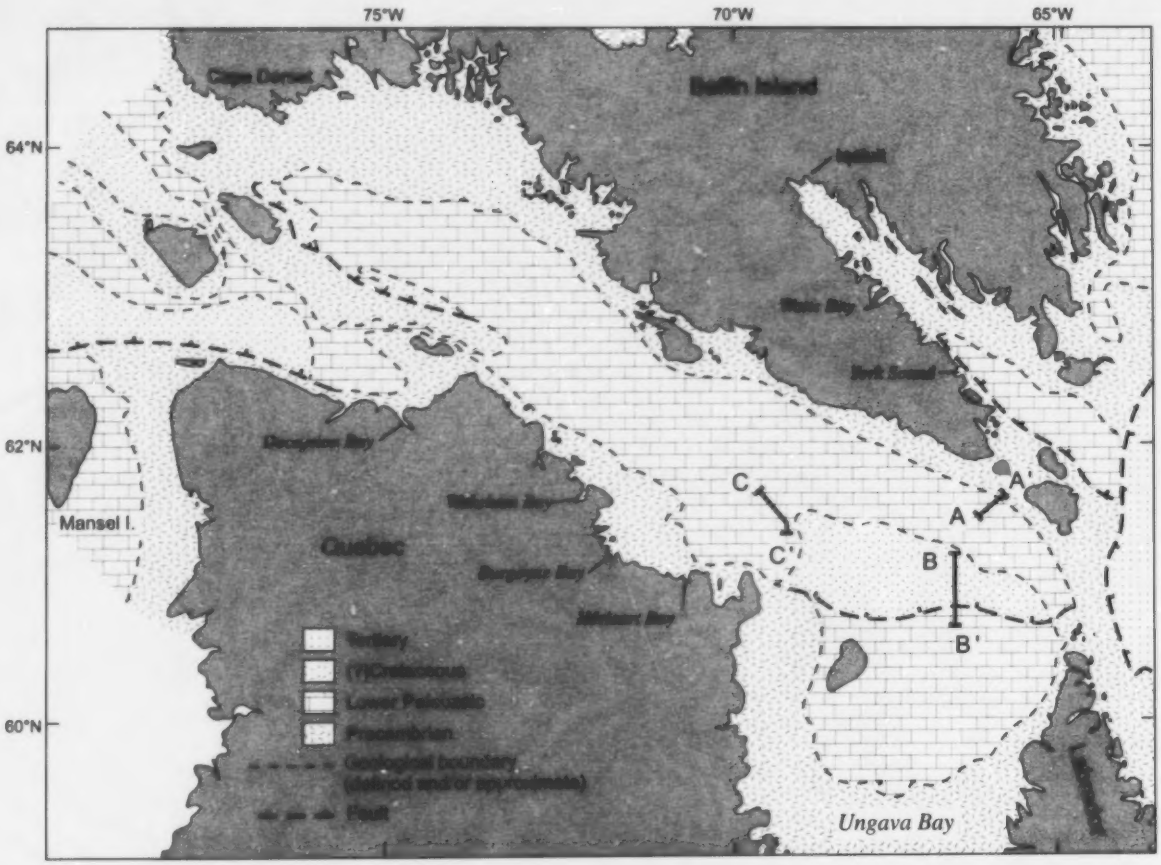

Figure 1. *Geological map showing the distribution of Precambrian (mainly metamorphic and igneous rocks), Paleozoic (mainly carbonate rocks), and inferred Cretaceous bedrock in Hudson Strait and Ungava Bay interpreted from geophysical data, borehole samples, and information from adjacent terrestrial areas* (modified from *MacLean et al., 1986 and Wheeler et al., 1996).*

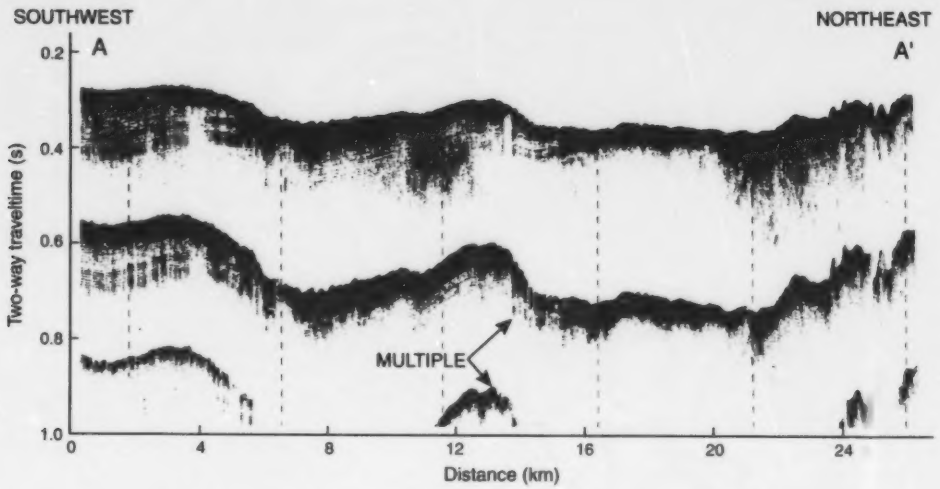

Figure 2. *Seismic reflection profile A-A' showing onlap of eroded Lower Paleozoic strata on Precambrian rocks, and associated cuesta ridges at the northern margin of Eastern basin. The zero edge of the Paleozoic rocks occurs about 21 km along section (see Fig. 1 for location) (after MacLean et al., 1986, Fig. 64.7).*

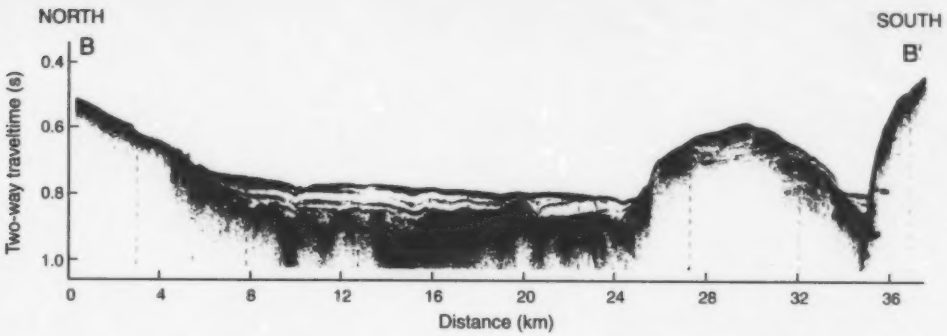

Figure 3. *Seismic reflection profile B-B' oriented north–south across Eastern basin showing stratigraphic and structural relations of strata in the basin floor. Downdropped strata (22–34.5 km along section) inferred to be of probable Mesozoic (?Cretaceous) age adjoin the fault scarp at the southern margin of the basin, 34.5 km along section. Paleozoic strata of the Ungava platform lie south of the fault (see Fig. 1 for location) (after MacLean et al., 1986, Fig. 64.5).*

The distinctive character of sediments derived from glacial erosion of the Paleozoic carbonate rocks is an important marker in interpreting former ice-flow patterns in the region, and disperal of sediments from Hudson Strait and Ungava Bay to the Labrador Sea, North Atlantic Ocean, and the Labrador Shelf.

STRUCTURAL FEATURES

Three half-graben structures form prominent bathymetric basins (Eastern, Western, and Southwestern basins) in the floor of Hudson Strait (MacLean, 2001, Fig. 1). In each instance strata within these basins have been downfaulted against older rocks at the southern margins of the structures. These basins have been loci for deposition of Quaternary sediments.

The central region of Hudson Strait is gently synclinal in aspect with stratigraphically equivalent strata forming the bedrock surface where sampled on both north and south sides of the strait.

The following outlines the structural settings of the three basins in Hudson Strait and of Ungava Bay.

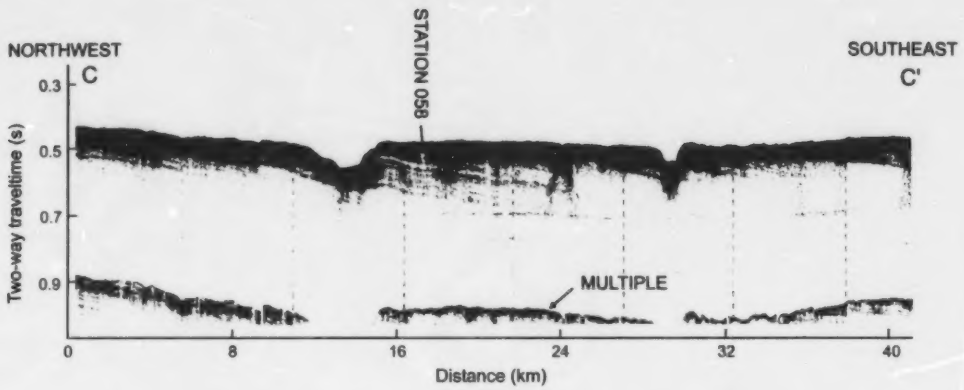

Figure 4. *Seismic reflection profile C-C' illustrating a succession of Paleozoic strata thickening southward in eastern Hudson Strait. These beds have been extensively bevelled by erosion. Two former erosional channels (possibly of subglacial origin) cut the bedrock. The location of a borehole sample site on these strata is indicated (see Fig. 1 for location) (after MacLean et al., 1986, Fig. 64.9).*

EASTERN BASIN

The largest of the half grabens lies north of Ungava Bay in the eastern part of Hudson Strait (Fig. 1; MacLean, 2001, Fig. 1). It is informally termed Eastern basin in this report. It is separated from the continental shelf by a sill at a depth of 385–400 m at the eastern entrance to the strait. A fault scarp forms the southern margin of the half-graben structure approximately coincident with the northern margin of Ungava Bay. Water depths in Eastern basin reach in excess of 900 m.

Phanerozoic strata (mainly Lower Paleozoic) underlying Eastern basin thicken southward (Fig. 2, 3, 4) and reach in the order of 2000 m or more in thickness (Grant and Manchester, 1970; MacLean et al., 1986). As indicated earlier, strata tentatively inferred to be Mesozoic occur locally near the southern margin of Eastern basin (Fig. 1, 3)

WESTERN AND SOUTHWESTERN BASINS

Western and Southwestern basins, in the western portion of Hudson Strait (Fig. 1; MacLean, 2001, Fig. 1) are en échelon half-graben features.

Western basin lies north of Charles Island. It is an elongated feature approximately parallel to the axis of the strait and contains water depths in excess of 400 m. It is bounded to the south by Precambrian and Paleozoic rocks that compose the "Charles Island platform" of which Charles Island is a part. Water depths gradually shallow northward in both Western and Southwestern basins.

Southwestern basin lies to the southwest and west of Charles Island. Water depths locally exceed 500 m in the southwestern part of the basin. Silurian strata may be included in the stratigraphic sequences that underlie that basin (MacLean et al., 1986).

Wheeler et al. (1996) inferred the occurrence of Mesozoic rocks locally in Western and Southwestern basins, and the extension of these strata into northeastern Hudson Bay and adjacent to Southampton Island.

UNGAVA BAY

In Ungava Bay relationships observed on seismic profiles at the southern and eastern margins of the central platform indicate that rocks interpreted to be an extension of the Precambrian igneous and metamorphic rocks of Labrador and Ungava peninsulas are overlain by the mainly flat-lying Paleozoic strata that compose the prominent platform (MacLean, 2001, Fig. 2). No indication of faulting was observed on the seismic data at the boundary between these units. The absence of major faulting between these units is also indicated by the depth (335 m below sea level) at which Precambrian rocks were encountered beneath the Paleozoic strata of the platform in the Premium Homestead Akpatok L-26 well drilled on Akpatok Island (Workum et al., 1976).

ACKNOWLEDGMENTS

Special thanks are extended to D.A. Hodgson, H. Josenhans, and J. Shaw for undertaking review of this paper and for their helpful comments and to B.V. Sanford and G.L. Williams for valuable input and discussions.

REFERENCES

Grant, A.C. and Manchester, K.S.
1970: Geophysical investigations in the Ungava Bay–Hudson Strait region of northern Canada; Canadian Journal of Earth Sciences, v. 7, p. 1062–1076.

Heywood, W.W. and Sanford, B.V.
1976: Geology of Southampton, Coats, and Mansell Islands, District of Keewatin, Northwest Territories; Geological Survey of Canada, Memoir 382, 35 p.

MacLean, B.
1998: Quaternary sediments and bedrock in Ungava Bay, N.W.T., Canada; *in* 28th Arctic Workshop, Institute of Arctic and Alpine Research, University of Colorado, Boulder, Colorado, March 12–14, 1998, Program and Abstracts, p. 103–105.
2001: Introduction: geographic setting and studies; *in* Marine Geology of Hudson Strait and Ungava Bay, Eastern Arctic Canada: Late Quaternary Sediments, Depositional Environments, and Late Glacial–Deglacial History Derived from Marine and Terrestrial Studies, (ed.) B. MacLean; Geological Survey of Canada, Bulletin 566.

MacLean, B. and Williams, G.L.
1983: Geological investigations of Baffin Island Shelf in 1982; *in* Current Research, Part B; Geological Survey of Canada, Paper 83-1B, p. 309–315.

MacLean, B., Williams, G.L., Sanford, B.V., Klassen, R.A., Blakeney, C., and Jennings, A.
1986: A reconnaissance study of bedrock and surficial geology of Hudson Strait, N.W.T.; *in* Current Research, Part B; Geological Survey of Canada, Paper 86-1B, p. 617–635.

Miller, A.M. and Williams, G.L.
1988: The essential role of palynology for bedrock mapping in Hudson Strait; Palynology, v. 12, p. 224.

Sanford, B.V. and Grant, A.C.
1999: Paleozoic and Mesozoic geology of the Hudson and Southeast Arctic Platforms; Geological Survey of Canada, Open File 3595, scale 1:2 500 000.

Sanford, B.V., Grant, A.C., Wade, J.A., and Barss, M.S.
1979: Geology of Eastern Canada and adjacent areas; Geological Survey of Canada, Map 1401A, scale 1:2 000 000.

Wheeler, J.O., Hoffman, P.F., Card, K.D., Davidson, A., Sanford, B.V., Okulitch, A.V., and Roest, W.R. (comp.)
1996: Geological Map of Canada, Geological Survey of Canada, Map 1860A, scale 1:5 000 000.

Workum, R.H., Bolton, T.E., and Barnes, C.R.
1976: Ordovician geology of Akpatok Island, Ungava Bay, District of Franklin; Canadian Journal of Earth Sciences, v. 13, p. 157–178.

Quaternary sediments in Hudson Strait and Ungava Bay

B. MacLean[1], G. Vilks[2], I. Hardy[1], B. Deonarine[1], A.E. Jennings[3], and W.F. Manley[3]

MacLean, B., Vilks, G., Hardy, I., Deonarine, B., Jennings, A.E., and Manley, W.F., 2001: Quaternary sediments in Hudson Strait and Ungava Bay; in Marine Geology of Hudson Strait and Ungava Bay, Eastern Arctic Canada: Late Quaternary Sediments, Depositional Environments, and Late Glacial–Deglacial History Derived from Marine and Terrestrial Studies, (ed.) B. MacLean; Geological Survey of Canada, Bulletin 566, p. 71–125.

Abstract: Quaternary sediments comprise five main units based on their acoustic character on high-resolution seismic profiles and sample data. These comprise ice-contact sediments, glaciomarine sequences, postglacial muds, postglacial sands and gravels, and locally in Eastern basin an acoustically unstratified unit of undetermined ice-contact or debris-flow origin.

Sediment deposits, with the exception of some of the ice-contact sequences, are thickest and most complete in the basinal areas in Hudson Strait and Ungava Bay. These deposits are the main source of information regarding changing conditions, depositional and paleoceanographic environments, and chronologies in the marine areas of this region from late glacial time, through deglaciation, to more modern time. Information obtained relating to ice-margin positions, glacial-marine interactions, environments, and radiocarbon dates from fauna in cores provide a basis for correlations with the record of events in adjacent terrestrial and marine areas.

In this paper the sediments, stratigraphic relationships, and late glacial-deglacial settings in each of the main basins and other relevant localities are illustrated and described, and associated chronological data are presented.

Résumé : D'après les profils sismiques à haute résolution et les données obtenues sur des échantillons, les sédiments quaternaires comportent cinq unités principales, soit des sédiments de contact glaciaire, des séquences glaciomarines, des boues postglaciaires, des sables et graviers postglaciaires et, par endroits dans le bassin Est, une unité acoustiquement non stratifiée d'origine indéterminée, soit de contact glaciaire ou de coulée de débris.

À l'exception de certaines des séquences de contact glaciaire, les sédiments les plus épais et les plus complets se trouvent dans les bassins du détroit d'Hudson et de la baie d'Ungava. Ces dépôts constituent la principale source d'information sur l'évolution des conditions, les milieux sédimentaires et paléocéanographiques et les chronologies dans les secteurs marins de la région au tardiglaciaire, pendant la déglaciation et jusqu'à aujourd'hui. Les données recueillies sur les positions des marges glaciaires, les interactions entre les glaces et la mer, les milieux et la datation au radiocarbone de restes animaux prélevés dans des carottes, constituent un fondement pour les corrélations avec les événements survenus dans les régions terrestres et marines adjacentes.

Cet article illustre et décrit les sédiments, les relations stratigraphiques et les milieux des phases tardiglaciaire et déglaciaire dans chacun des principaux bassins et dans d'autres endroits pertinents, et présente des données chronologiques connexes.

[1] Geological Survey of Canada (Atlantic), Dartmouth, Nova Scotia B2Y 4A2
[2] Geological Survey of Canada (Atlantic), Dartmouth, Nova Scotia B2Y 4A2 (deceased)
[3] Institute of Arctic and Alpine Research, University of Colorado, Boulder, Colorado, U.S.A. 80309

SEDIMENT UNITS

Five sediment units have been recognized in Hudson Strait and Ungava Bay on the basis of acoustic data from regional surveys with shallow and high-resolution seismic systems, together with visual, textural, X-radiographic, and paleontological data from sediment cores and grab samples. The units comprise ice-contact sediments, ice-contact or debris-flow sediments, glaciomarine sediments, postglacial muds, and locally, postglacial sands and gravels. The distribution of these units at the seabed is indicated on the surficial geological map (Fig. 1, in pocket). Thick sediment accumulations occur in the three main basins, in the south-central region of the strait, in the marginal channel surrounding the central platform in Ungava Bay, and locally in multisequence ice-contact deposits elsewhere. Total Quaternary sediment thicknesses are indicated on Figure 2 (in pocket). Figures 3, 4, 5 (in pocket) show thickness data for ice-contact, glaciomarine, and postglacial muddy sediments, respectively.

The acoustic character of the sediment units recognized in Hudson Strait and Ungava Bay (outlined previously by Vilks et al. (1989) and MacLean et al. (1992, 1995)) is similar to that of sediments deposited in comparable environments in other offshore areas of eastern and northern Canada (*see* e.g. Josenhans et al., 1986; King and Fader, 1986; Praeg et al., 1986; MacLean et al., 1989; Syvitski, 1991), and in other northern latitude areas (e.g. Dowdeswell and Scourse, 1990; Vorren et al., 1990; Davies et al., 1997).

Ice-contact sediments (unit 1)

Sediments of this unit are acoustically unstratified deposits that typically overlie bedrock, or lie on previously deposited glacial sediments, and form constructional features. Where sampled in Hudson Strait by cores and in an IKU™ clam-shell sample, sediments of unit 1 are matrix-supported, clast-rich diamicts (Hardy, 2001) that are faunally barren. Diamict sediments possibly representative of ice-contact deposits were also recovered at two other IKU™ stations. The acoustic character, stratigraphic and facies relations, morphology, and diamictic texture of these sediments are similar to ice-contact sediments (glacial drift) identified in other offshore areas (e.g. King, 1970; Fader et al., 1982; Vorren et al., 1984; Josenhans et al., 1986; King and Fader, 1986; Praeg et al., 1986; MacLean et al., 1989). Substantial discussion exists in the literature, as exemplified by the papers cited below, concerning origins, transport, and depositional mechanisms interpreted for deposits of acoustically unstratified sediments (*see* e.g. Vorren et al., 1983, 1990; King et al., 1987, 1991; Powell and Molnia, 1989; Alley et al., 1989; Boulton, 1990; Dowdeswell and Scourse, 1990; Stoker, 1990; Syvitski, 1991; King, 1993).

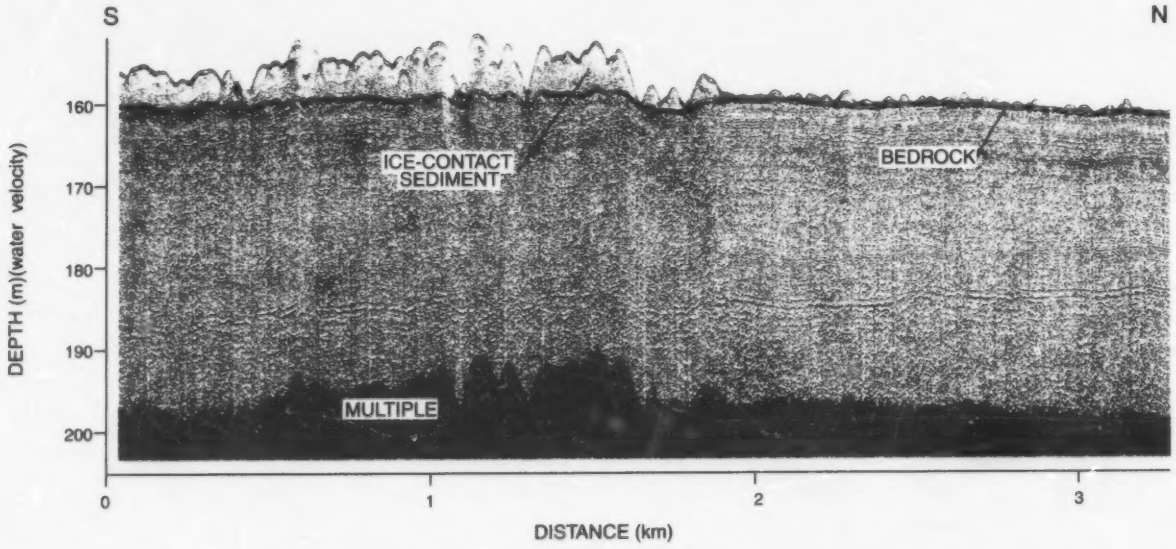

Figure 6. *Huntec™ high-resolution seismic-reflection profile illustrating the acoustically unstratified character of ice-contact deposits and variations in thickness. The abrupt change in sediment thickness at this locality is thought to mark the offshore (northern) limit of a late glacial ice advance in the Héricart Bay region of south-central Hudson Strait.* (See *Fig. 1 for location of section.*)

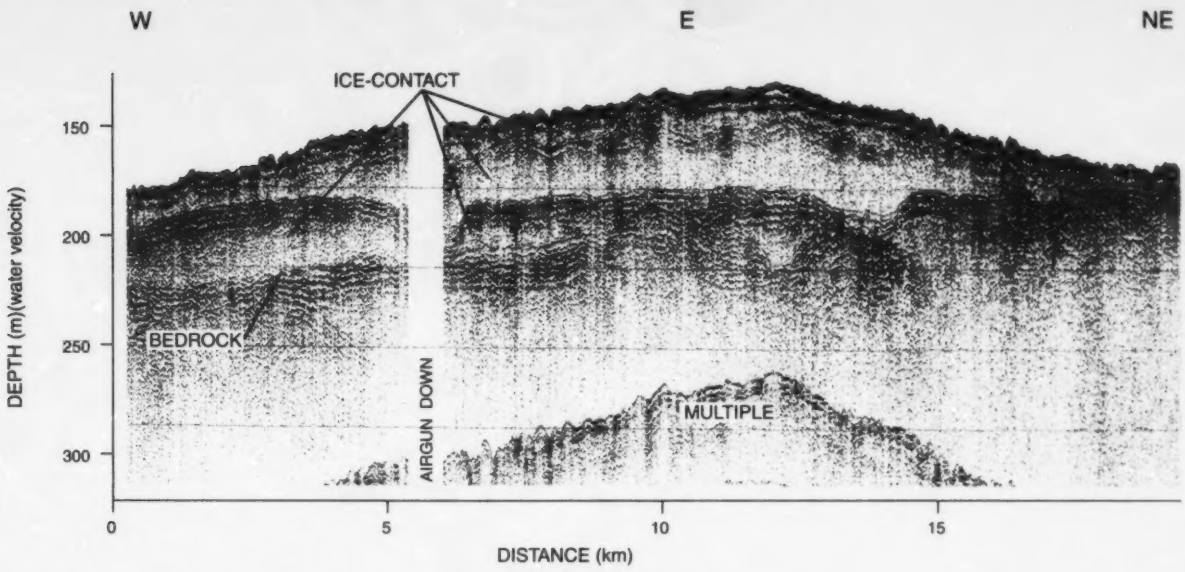

Figure 7. *Huntec™ high-resolution seismic-reflection profile illustrating three or more sequences of ice-contact deposits in the region offshore Salluit in western Hudson Strait.* (See *Fig. 1 for location of section.*)

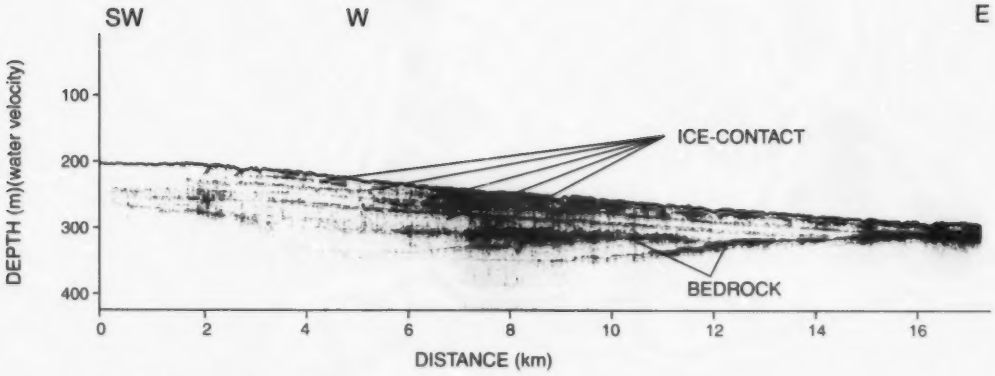

Figure 8. *Single-channel seismic-reflection profile showing multiple ice-contact sequences totalling more than 100 m in thickness southeast of Nottingham Island in western Hudson Strait. The deposit thins both eastward and southward. These sediments are the product of successive ice advances in this area.* (See *Fig. 1 for location of section.*)

In the Hudson Strait region sediments included in unit 1 are considered on the basis of their acoustical, textural, faunal (barren), stratigraphic relationships, and morphology to have been deposited primarily in ice-contact subglacial or ice-margin environments. This unit locally may include previously deposited glaciomarine or marine sediments whose distinctive acoustic character has been lost due to loading and remolding by subsequent glacial ice advances. Iceberg turbate (Vorren et al., 1983) and debris-flow material locally may be represented.

Distribution, thickness, and stratigraphic relations

Ice-contact sediments are widely distributed throughout the region. They form the basal sequences beneath overlying glaciomarine and postglacial sediments in the basins and are the main surficial sediment unit in interbasin areas, on upslope parts of basin flanks, and on the central platform in Ungava Bay. Figure 1 shows areas where ice-contact sediments are exposed at the seabed.

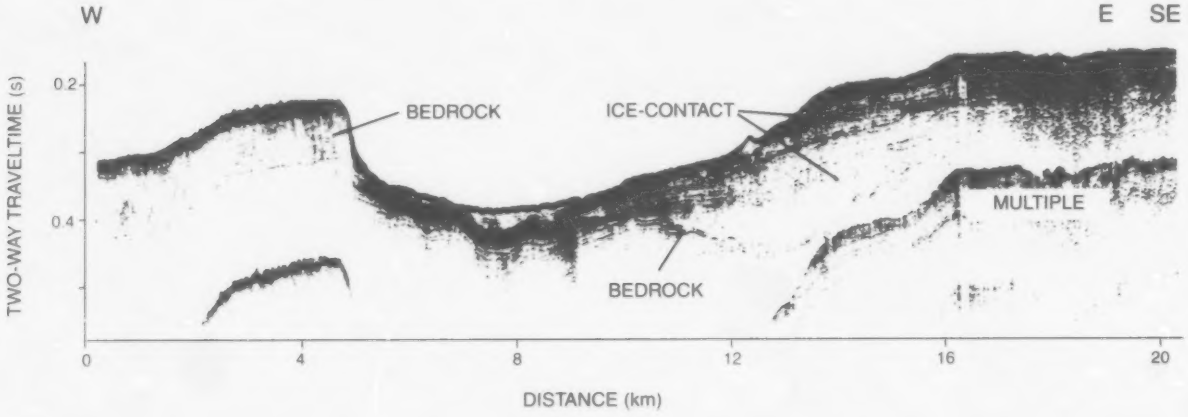

Figure 9. *Single-channel seismic-reflection profile illustrating multisequence ice-contact sediments up to 150 m in thickness adjacent to the east coast of Ungava Bay.* (Modified from *MacLean et al., 1991, Fig. 4.*) (See *Fig. 1 for location of section.*)

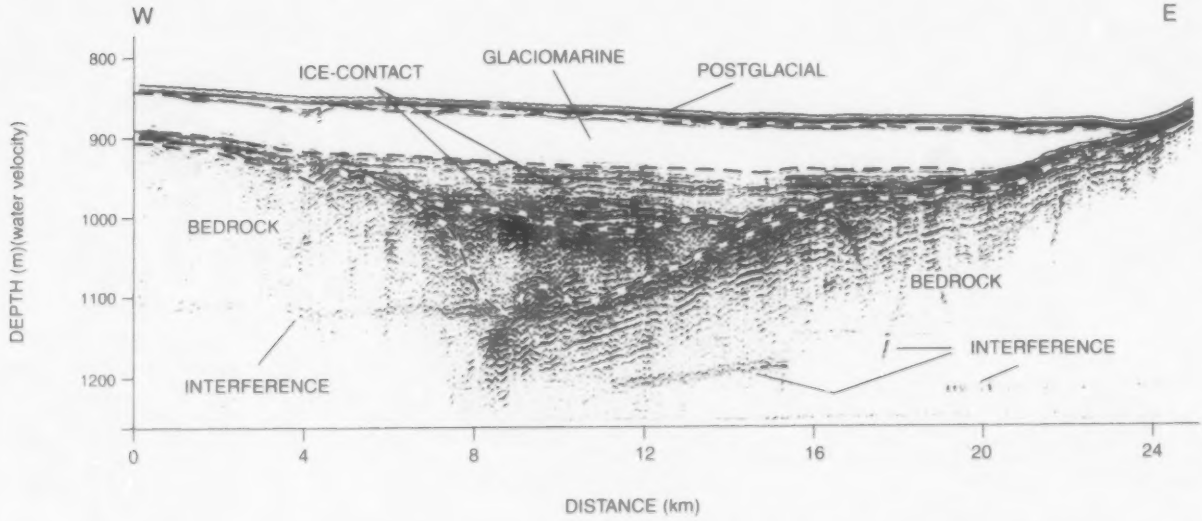

Figure 10. *Single-channel seismic-reflection profile showing ice-contact sediments up to 180 m in thickness filling a depression eroded in the bedrock beneath Eastern basin.* (See *Fig. 1 for location of section.*)

Ice-contact deposits are of variable thickness, in general ranging from a few metres or less to 10 m or more (Fig. 3, 6). Seismic data indicate the presence of two or more superimposed ice-contact sequences in a number of areas (e.g. Fig. 7). The greatest thicknesses of ice-contact sediments occur in multisequence deposits in four areas (Fig. 3): 100 m in the area southeast of Nottingham Island in the western part of Hudson Strait (Fig. 8); 150 m in eastern Ungava Bay (Fig. 9); 180 m in Eastern basin (Fig. 10); and 360 m on the continental shelf adjacent to the sill at the entrance to Hudson Strait (Fig. 11). These deposits, each of which contain five or more ice-contact sediment members, are the product of repeated glacial ice advances and retreats.

Locally, ice-contact sediments form constructional features that are interpreted to be moraines as exemplified in Figures 12, 13, and 14. Deposition of these features appears to have been associated with ice-margin locations, grounding lines, and probable temporary stillstand positions during ice-sheet retreat. Ice-contact sediments also fill or partly fill depressions and channels cut into the bedrock (Fig. 15, 16, 17), some of which may represent subglacial valleys.

In the region between Big Island and Wakeham Bay in the central part of Hudson Strait, and in a few other small isolated localities indicated by the striped pattern areas on Figure 1, surficial sediments are very thin (less than approximately 1 m) and in many places indistinguishable on acoustic profiles from the underlying bedrock. Where sediments in small mounds or filling small depressions are of sufficient thickness to be resolved by the high-resolution seismic systems, they generally resemble ice-contact sediments. Within the striped pattern areas on Figure 1, it is probable that ice-contact sediments are discontinuous, and the seabed may include areas where bedrock is exposed, or only thinly mantled by ice-contact sediments or by a veneer of sand or gravel.

In the floors of the basins and on the lower basin flanks, ice-contact sediments commonly are overlain by glaciomarine sediments. They are transitional to glaciomarine sediments in many former ice-margin or grounding-line localities (e.g. Fig. 18, 19, 20). Locally in the south-central part of Hudson Strait and in Western basin ice-contact sediments deposited by later glacial advances lie on previously deposited glaciomarine or marine sediments (Fig. 12, 21).

Where ice-contact sediments are exposed at the seabed in current-swept areas outside the basins, the surface of these sediments has been modified by winnowing and by iceberg scouring. Locally ice-contact sediments are thinly and discontinuously mantled by postglacial muddy sediments.

Ice-contact and debris-flow sediments (unit 2)

This unit consists of sediments that are relatively acoustically transparent, which overlie more acoustically dense ice-contact sediments, and are in turn overlain by glaciomarine sediments in Eastern basin (Fig. 22). Sediments that bear some resemblance acoustically and stratigraphically to this unit also occur in Western basin. Unit 2 in Eastern basin contains two partially superimposed sequences with a thin interval of acoustically stratified sediments between

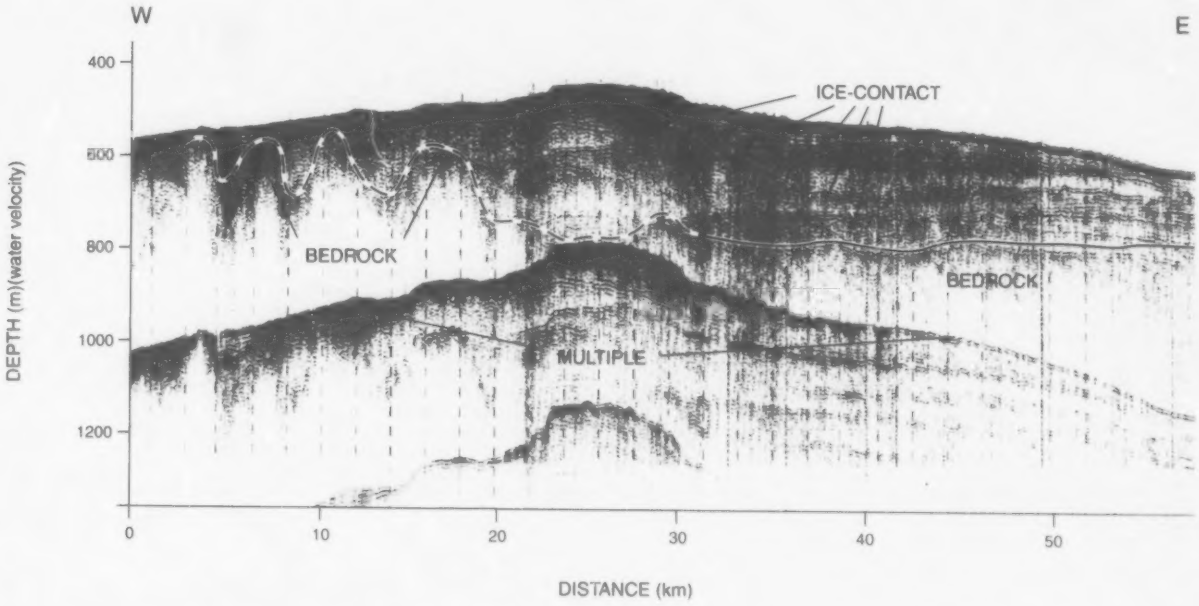

Figure 11. *Single-channel seismic-reflection profile showing multiple ice-contact sequences totalling 360 m in thickness deposited on the continental shelf at the Atlantic Ocean side of the sill at the eastern entrance to Hudson Strait.* (Modified from *MacLean, 1997a, Fig. 2; profile courtesy of H. Josenhans.*) (See *Fig. 1 for location of section.*)

them (Fig. 22). Unit 2 sediments appear to be continuous laterally with acoustically denser ice-contact sediments towards the margins of the deep basin. Vilks et al. (1989), while favouring a glacial origin, indicated that the sediments of unit 2 possibly could represent marine sediments remolded by light glacial ice loading or by debris-flow activity.

Glaciomarine sediments (unit 3)

Sediments of unit 3 are distinctive, acoustically strongly stratified sequences that immediately overlie ice-contact sediments. They directly overlie bedrock in a few localities. Typically these sediments have a draped depositional style that mimics the irregular underlying surface (Fig. 22). They are transitional laterally to ice-contact sediments in many former ice-margin settings. These relationships will be discussed in more detail in the description of the geology of the basins. High-resolution seismic-reflection profiles commonly show variations in the intensity of individual reflectors or groups of reflectors within this unit (e.g. Fig. 18, 20, 22) that are considered to relate to factors such as changes in texture, composition, and physical properties associated with the distance from the ice margin, and transport and depositional processes. For further discussion of these processes *see* Powell (1984), King and Fader (1986), Powell and Molnia (1989); *see also Glaciomarine Environments: Processes and Sediments* (Dowdeswell and Scourse, 1990) and *The Seabed of The Canadian Shelf* (Amos and Collins, 1991).

X-radiographic and visual examination of cores from 26 localities in Hudson Strait and Ungava Bay indicate sediments of this unit typically are laminated silts and clays, often with rhythmically banded intervals containing thin silt and fine to very fine sand laminae (rhythmites) (Hardy, 2001). Variably sandy and gravelly intervals occur in several localities, as do scattered individual grains or clasts. Foraminiferal assemblages indicate that deposition of unit 3 sediments occurred in glaciomarine ice-proximal and ice-distal environments (Vilks et al., 1989; MacLean et al., 1992; Jennings et al., 2001). Commonly these assemblages indicate an upsection change from ice-proximal to ice-distal conditions. Occurrences of mollusc shells in cored samples of these sediments are relatively rare.

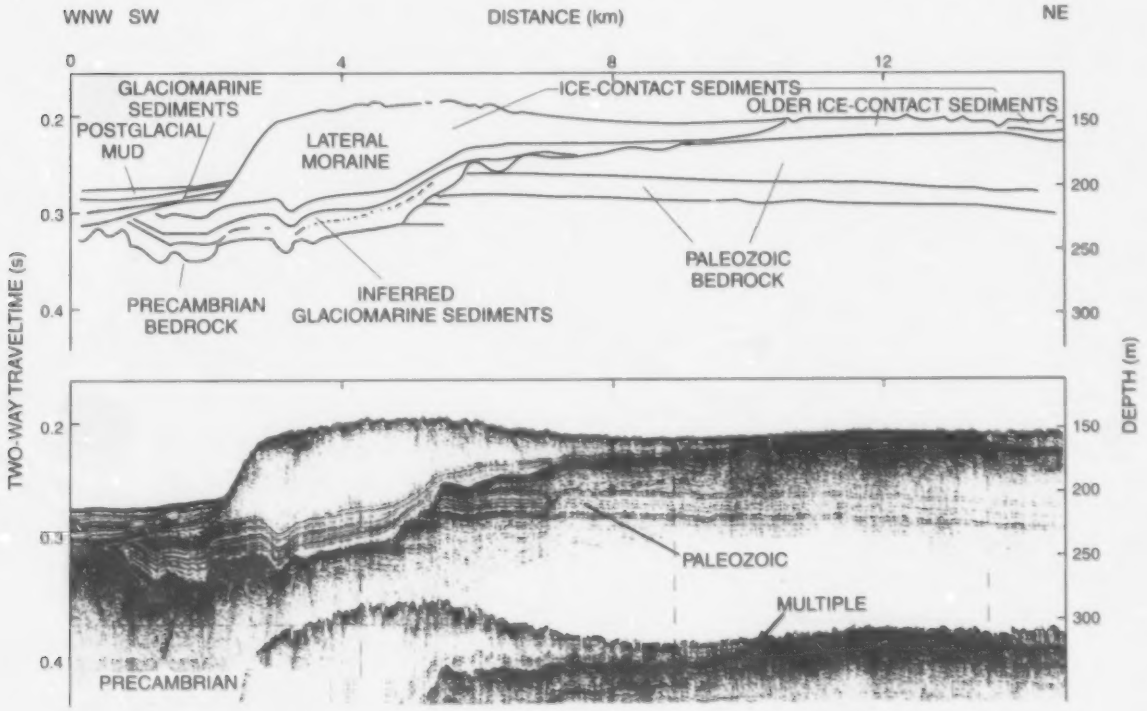

Figure 12. *Single-channel seismic-reflection profile showing a moraine up to 70 m thick lying on acoustically stratified sediments (inferred to be glaciomarine) 20 km offshore from Héricart Bay in south-central Hudson Strait. Shoreward (southwest) of the moraine the acoustically stratified sediments were erosionally truncated by glacial ice. They are unconformably overlain by younger glaciomarine and postglacial sediments. The boundary between the underlying Precambrian and Paleozoic rocks occurs approximately 3.5 km along the section.* (Modified from *MacLean 1997b, Fig. 3* in *Kluwer Academic Publishers: Glaciated Continental Margins: An Atlas of Acoustic Images, p. 87, published by Chapman & Hall, 1997. Reproduced with kind permission from Kluwer Academic Publishers.)* (See *Fig. 1 for location of section.)*

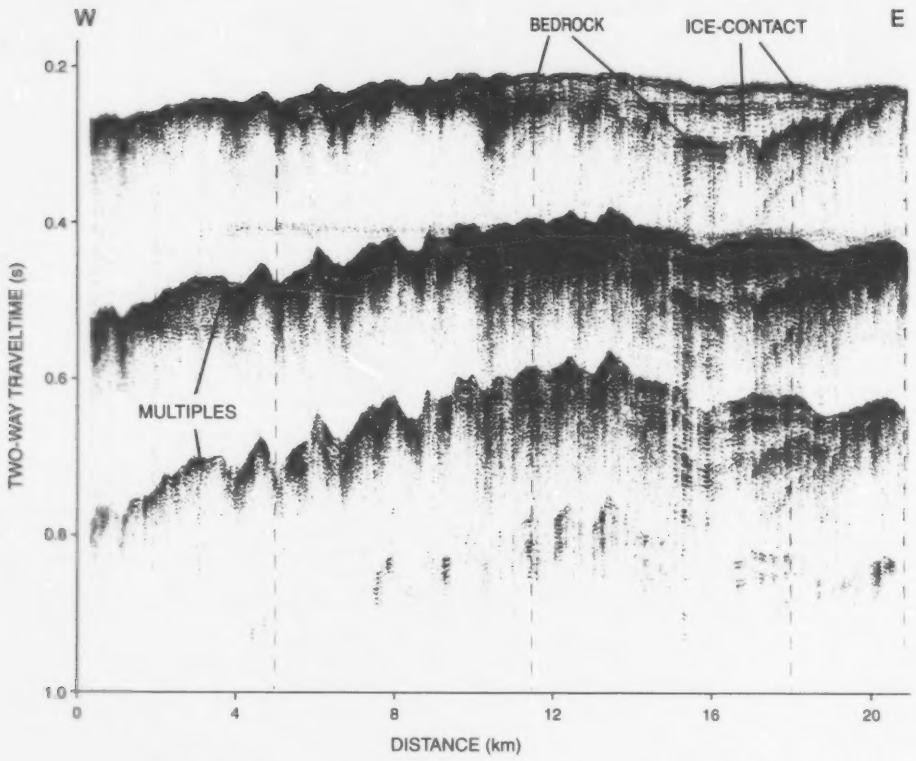

Figure 13. *Single-channel seismic-reflection profile showing multiple ice-contact deposits that form a moraine southeast of Big Island on the north side of Hudson Strait.* (Modified from *MacLean et al., 1986, Fig. 64.16.*) (See *Fig. 1 for location of section.*)

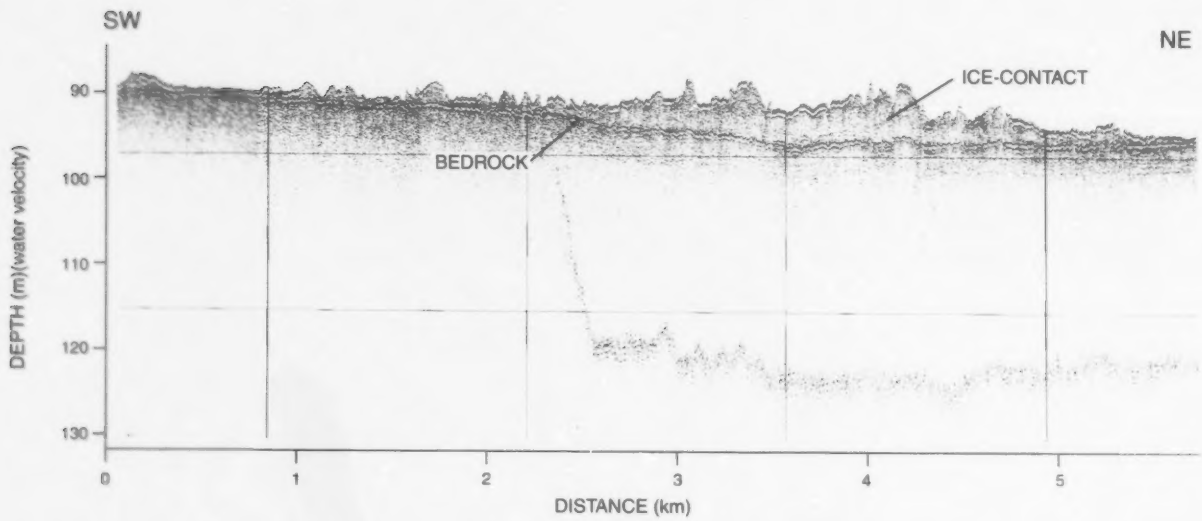

Figure 14. *Huntec^{TM} high-resolution seismic-reflection profile showing a moraine developed southeast of Akpatok Island on the southern part of the central platform in Ungava Bay.* (See *Fig. 1 for location of section.*)

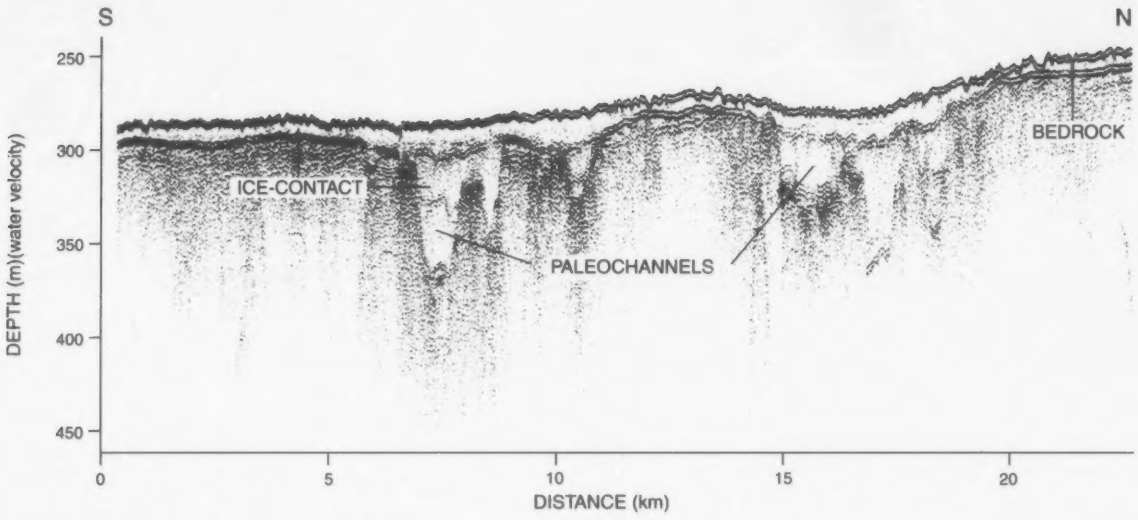

Figure 15. *Single-channel seismic-reflection profile showing acoustically stratified sediments filling probable subglacial meltwater channels on the northern flank of Western basin, 70 km north of Charles Island. (See Fig. 1 for location of section.)*

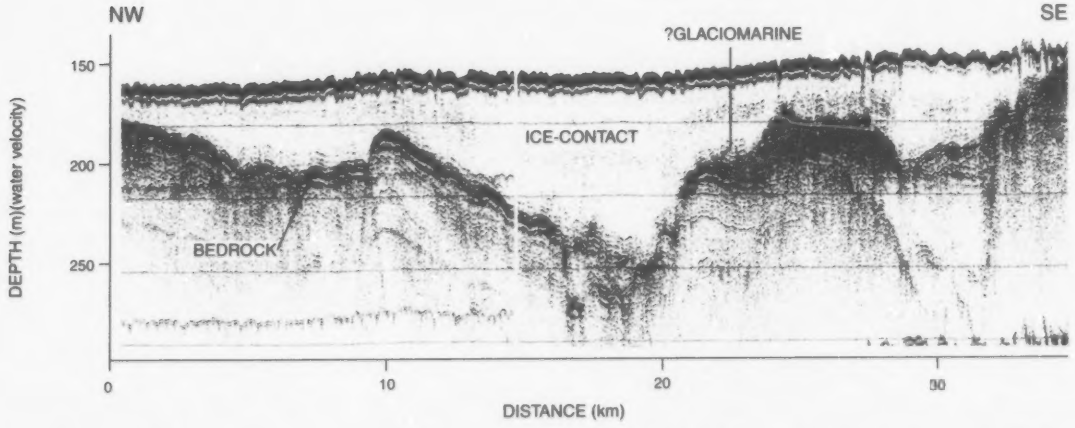

Figure 16. *Single-channel seismic-reflection profile showing a thick deposit of acoustically unstratified sediments inferred to be ice-contact sediments that fills a large depression some 7 km east of Charles Island. Bedrock attitudes suggest the depression largely is a structurally controlled feature; however, the sub-bottom channel-like feature 30 km along section may be of erosional origin. (See Fig. 1 for location of section.)*

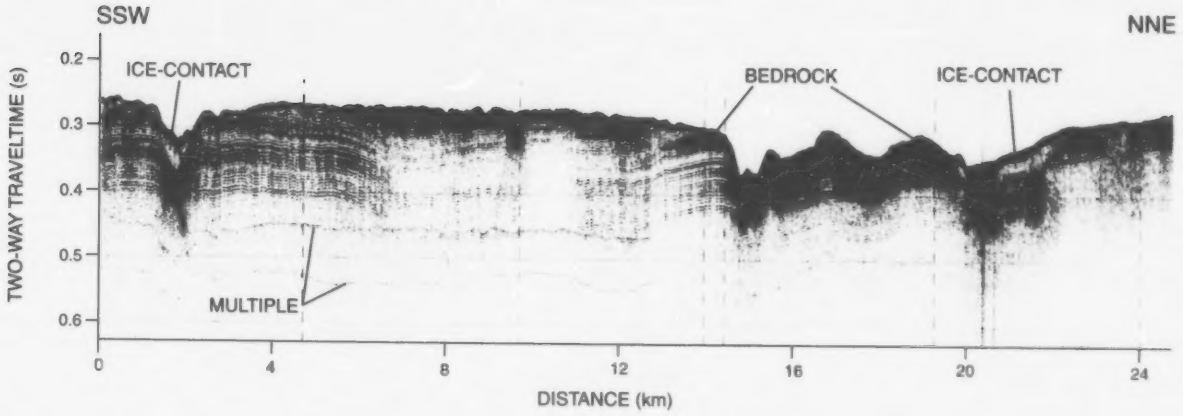

Figure 17. *Single-channel seismic-reflection profile showing partly filled valleys cut into the bedrock north of Cape Hopes Advance near the western margin of Eastern basin. These features, like those in Figure 15 may have been eroded by subglacial meltwater.* (See *Fig. 1 for location of section.*)

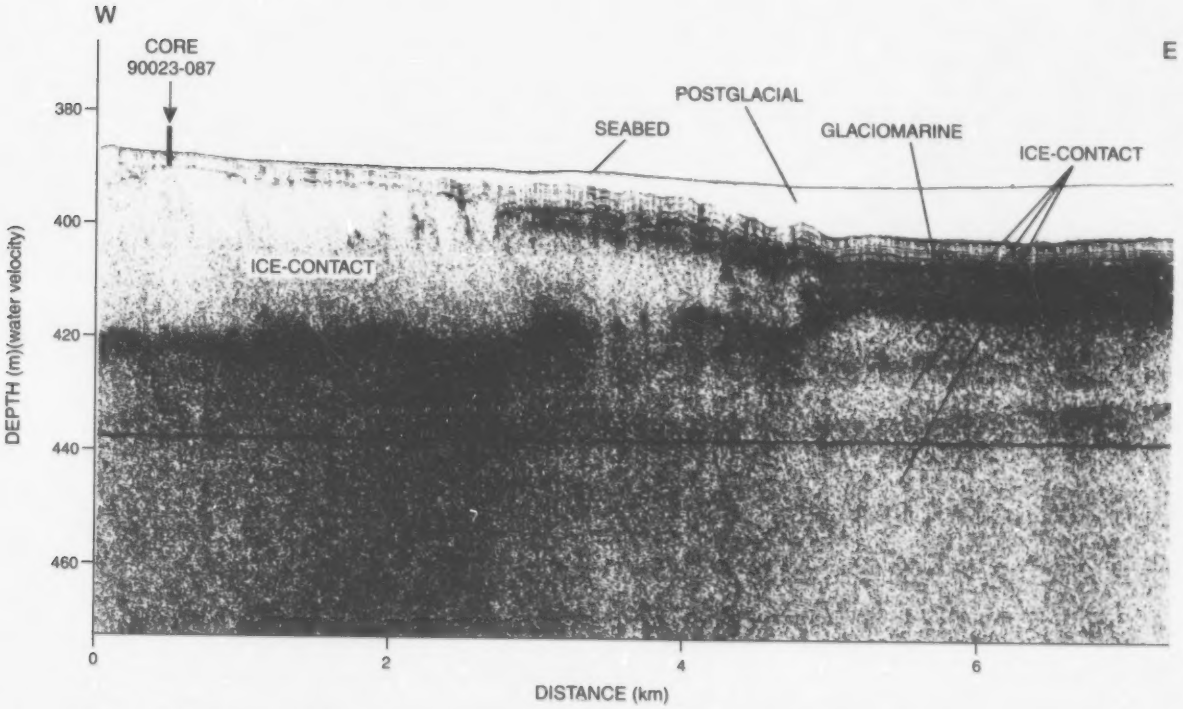

Figure 18. *Huntec™ high-resolution seismic-reflection profile showing the intertonguing of glaciomarine and ice-contact sediments at a former glacial-ice-margin position 18 km northeast of Colbert Promontory in southwestern Hudson Strait. Core 90023-085 sampled the glaciomarine and overlying postglacial sediments at a site 11 km east of the transition. Extrapolated position of core 90023-087 is indicated.* (Modified from *MacLean et al., 1991, Fig. 12, and MacLean et al., 1992, Fig. 16.) Reproduced with permission from Géographie physique et Quaternaire.* (See *Fig. 1 for location of section.*)

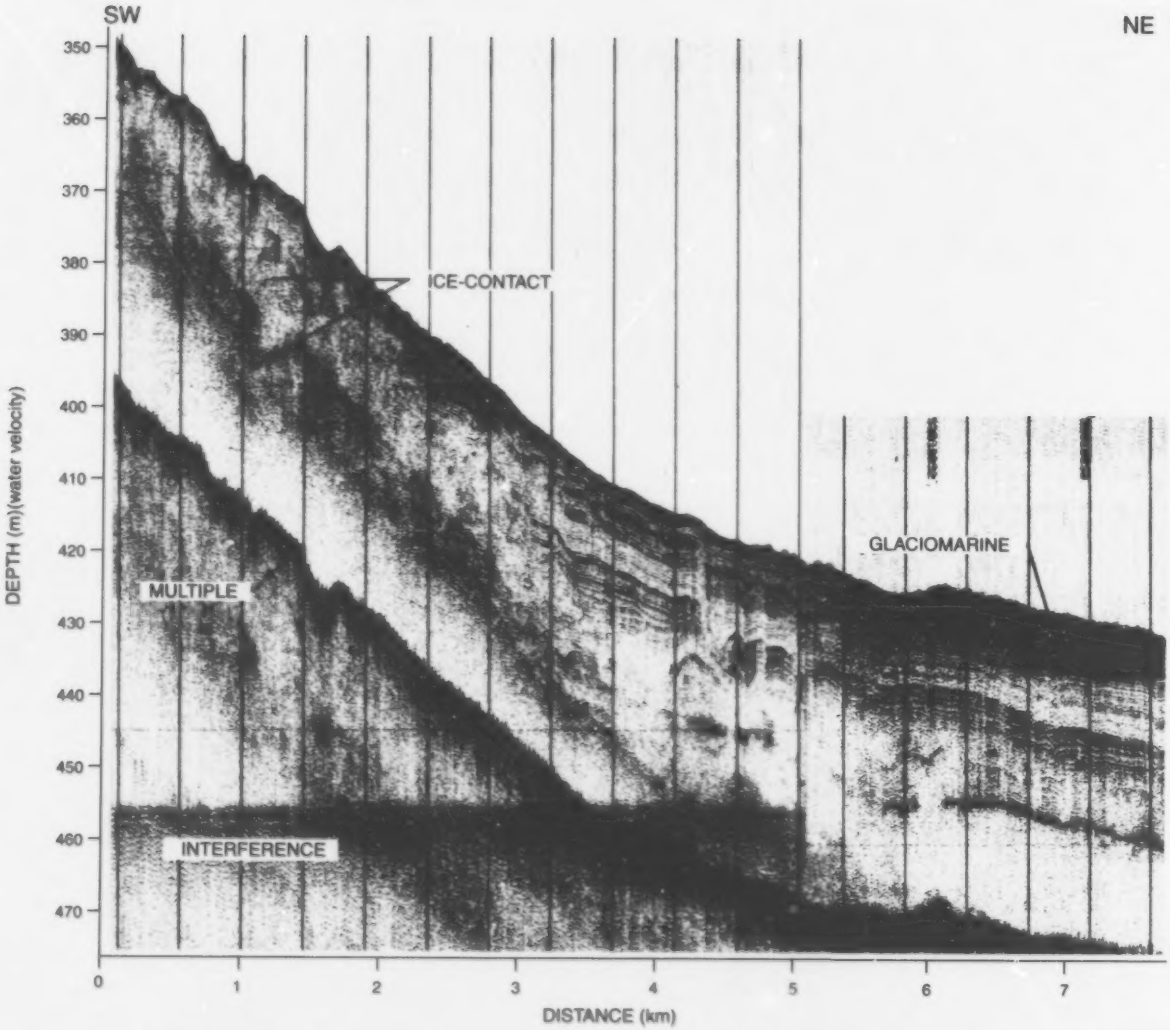

Figure 19. *Huntec™ high-resolution seismic-reflection profile showing lateral transition of glaciomarine sediments to ice-contact sediments (approximately 3 km along section) at the southern margin of Western basin north of Charles Island.* (See *Fig. 1 for location of section.*)

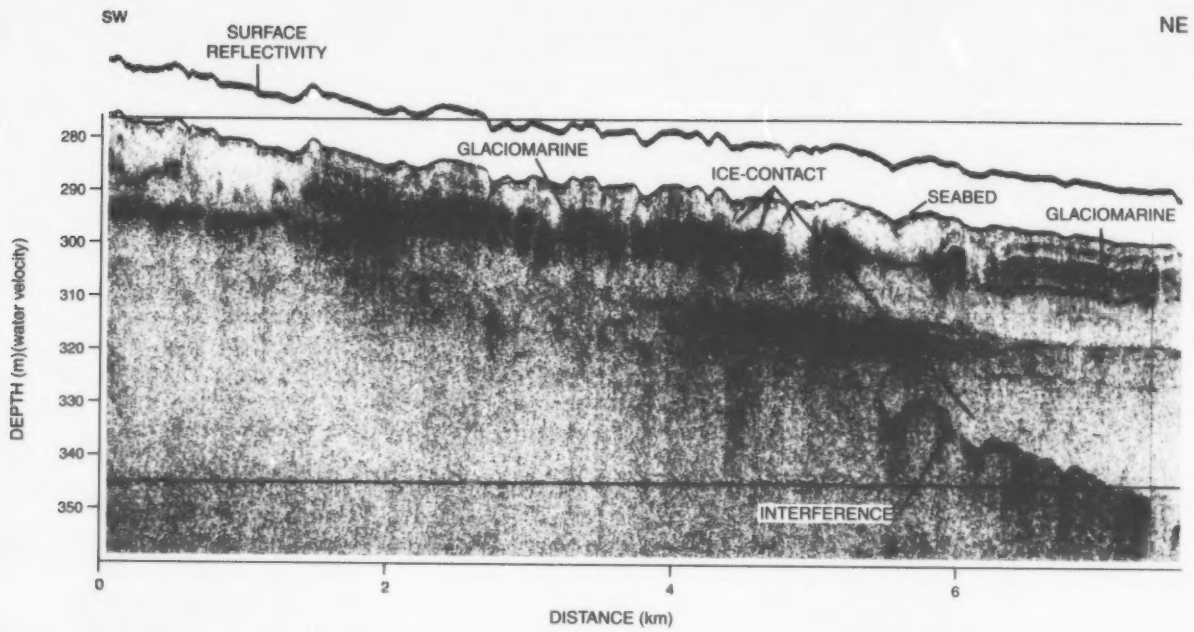

Figure 20. *Huntec™ high-resolution seismic-reflection profile southeast of Nottingham Island in western Hudson Strait showing lateral transition of glaciomarine to ice-contact sediments at 1.4 km along section, and further sporadic transitions to about 6 km along section. (See Fig. 1 for location of section.)*

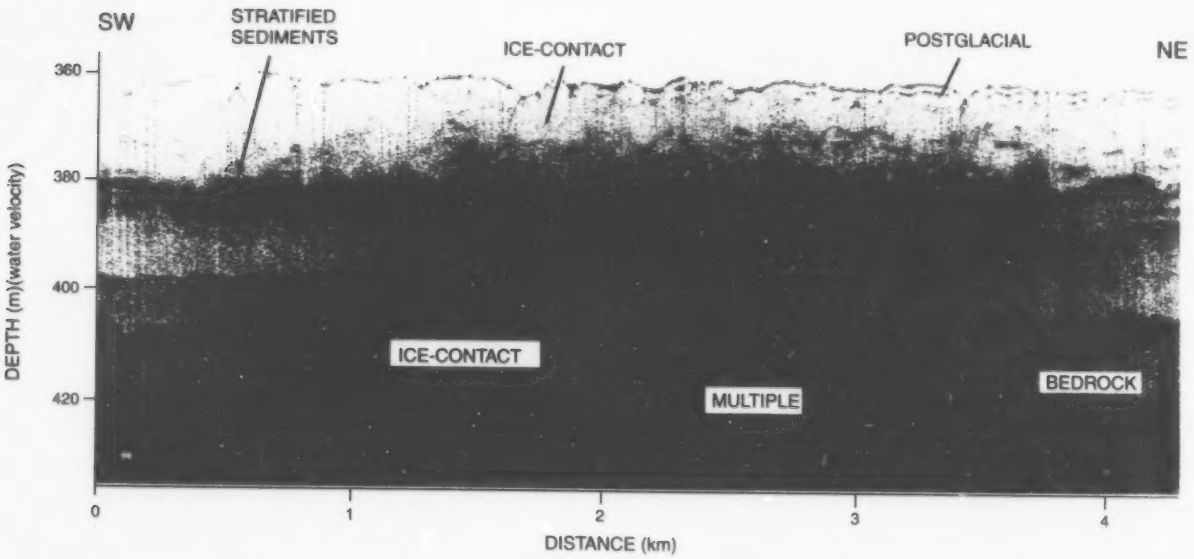

Figure 21. *Huntec™ high-resolution seismic-reflection profile showing glacially overridden acoustically stratified sediments considered to represent previously deposited glaciomarine sediments that are locally preserved in the region north and northeast of Charles Island. (See Fig. 1 for location of section.)*

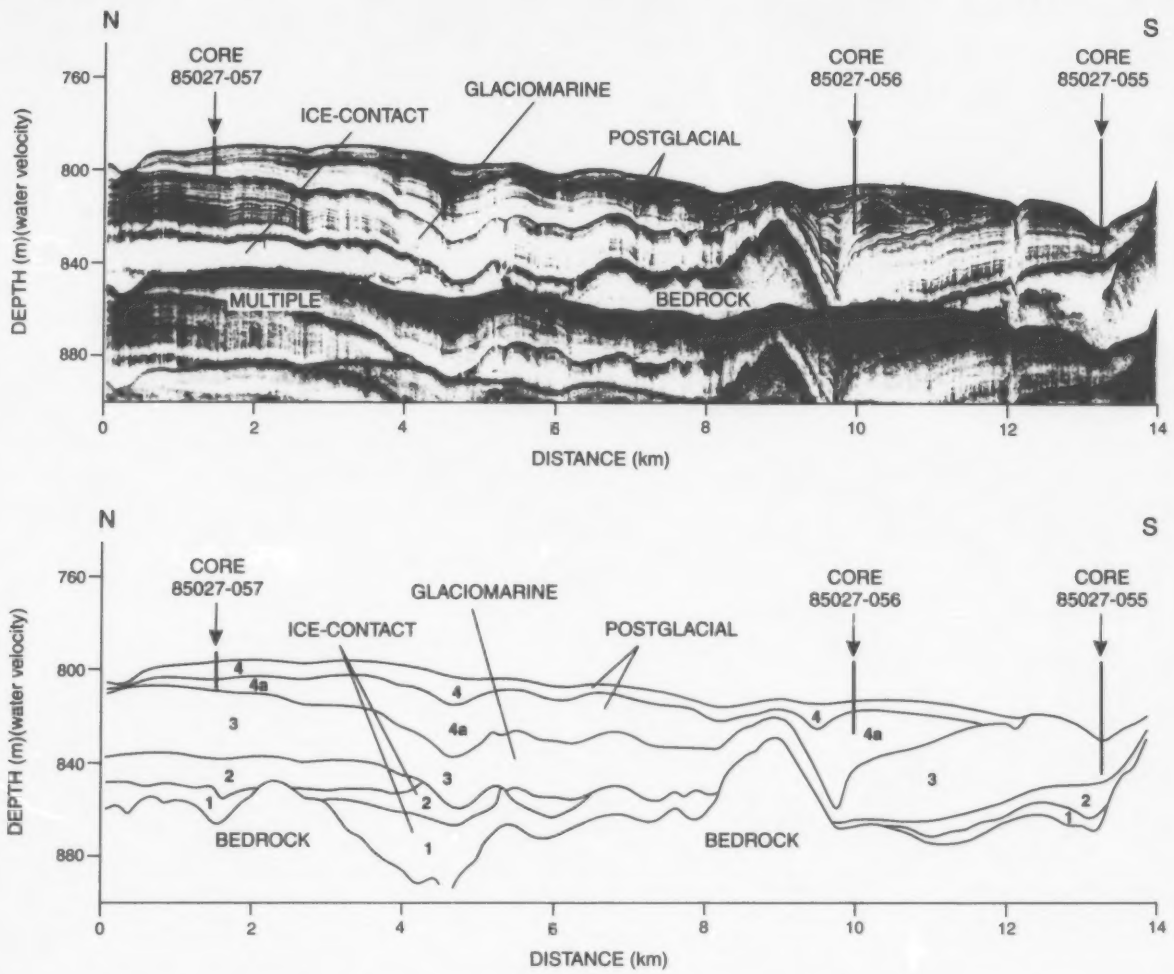

Figure 22. *Huntec™ high-resolution seismic-reflection profile north-south across Eastern basin illustrating ice-contact, glaciomarine, and postglacial sediment units and core localities in the basin floor along that transect. Core sites 87033-012 and 87033-013 lie near those of 85027-057 and 85027-055, respectively. Acoustically stratified glaciomarine sediments (unit 3) mimic the shape of the surface upon which they were deposited. Underlying acoustically unstratified, relatively transparent sediments (unit 2) at this locality were considered by Vilks et al. (1989) to represent glacial, debris-flow, or remolded sediments. Early postglacial sediments (unit 4a), 9–10 km along section, display thinning and thickening related to an increased current regime.* (Modified from *Vilks et al., 1989, Fig. 6.) Reproduced with permission from Géographie physique et Quaternaire.* (See *Fig. 1 for location of section.)*

Distribution and thickness

Unit 3 glaciomarine sediments are confined almost entirely to Eastern, Western, and Southwestern basins, the south-central region of Hudson Strait, and to parts of the marginal channel in Ungava Bay (Fig. 1, 4). Localized deposits occur southwest of Big Island and in a few other small, isolated localities. Glaciomarine sediments reach a thickness of 60 m locally in Eastern basin, but mainly range between 5 m and 20 m in other occurrences (Fig. 4; MacLean et al., 1995). In many of these areas they are overlain by postglacial sediments.

Overriding of glaciomarine sediments by late, local ice advances is evident in a few localities, notably in the Héricart Bay–Wakeham Bay region of south-central Hudson Strait (Fig. 23, 24) and north and northeast of Charles Island (Fig. 21). Incorporation of some reworked material from previously deposited glaciomarine and marine sediments within glaciomarine sediments in the Héricart Bay region and in Eastern and Western basins is indicated by foraminiferal assemblages, anomalously old age dates, and stratigraphic reversals of dates (Manley, 1995; Jennings et al., 1998, 2001).

Postglacial muds (unit 4)

Postglacial muddy sediments are acoustically weakly stratified to transparent. These sediments, like those of unit 3, occur mainly in basinal and other deep-water areas (Fig. 1). Deposits of postglacial sediments attain thicknesses of 30 m or more locally in the Burgoyne Bay region of south-central Hudson Strait and locally in Eastern basin, 18 m in parts of Western basin, and in excess of 20 m in southern Ungava Bay (Fig. 5, 22, 25, 26, 27). Elsewhere in the Hudson Strait–Ungava Bay region the sediments of unit 4 occur as relatively thin deposits only a few metres or less in thickness overlying glaciomarine sequences, or locally thinly mantling

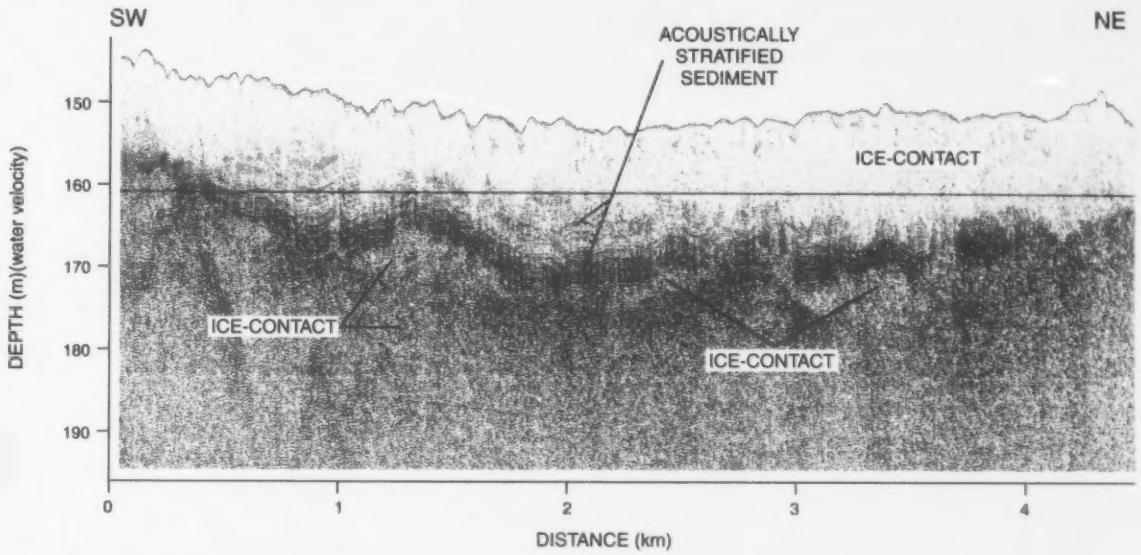

Figure 23. *Huntec™ high-resolution seismic-reflection profile showing acoustically stratified sediments inferred to be glaciomarine in origin overlain by ice-contact sediments in the Burgoyne Bay–Whitley Bay area of south-central Hudson Strait. The upper part of the glaciomarine beds displays extensive erosion by the subsequent glacial ice advance. (See Fig. 1 for location of section.)*

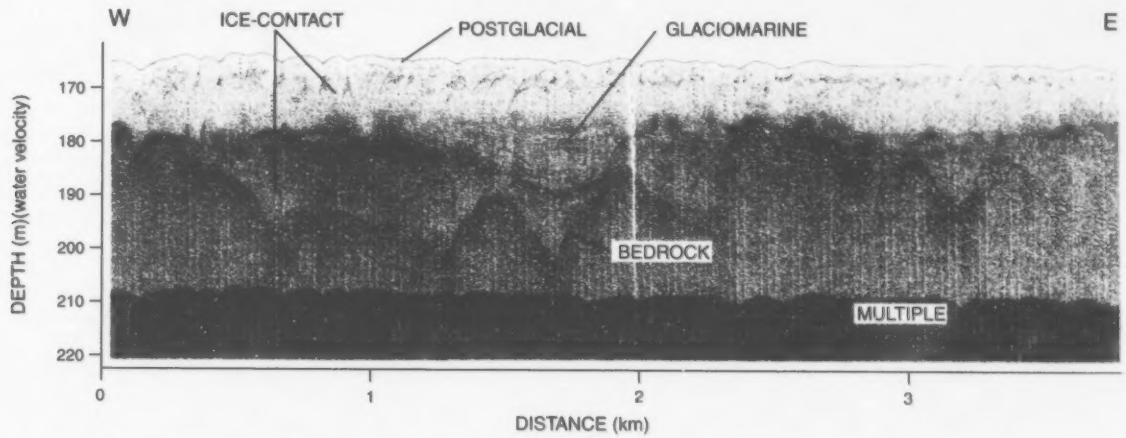

Figure 24. *Huntec™ high-resolution seismic-reflection profile illustrating erosional remnants of glacially overridden glaciomarine sediments that are preserved in several localities in the Héricart Bay region. Foraminifers contained in sediments eroded from such deposits are a likely source of 'old' age dates and stratigraphic inversions of dates obtained from cores in more recent glaciomarine sediments in the Héricart Bay region. (See Fig. 1 for location of section.)*

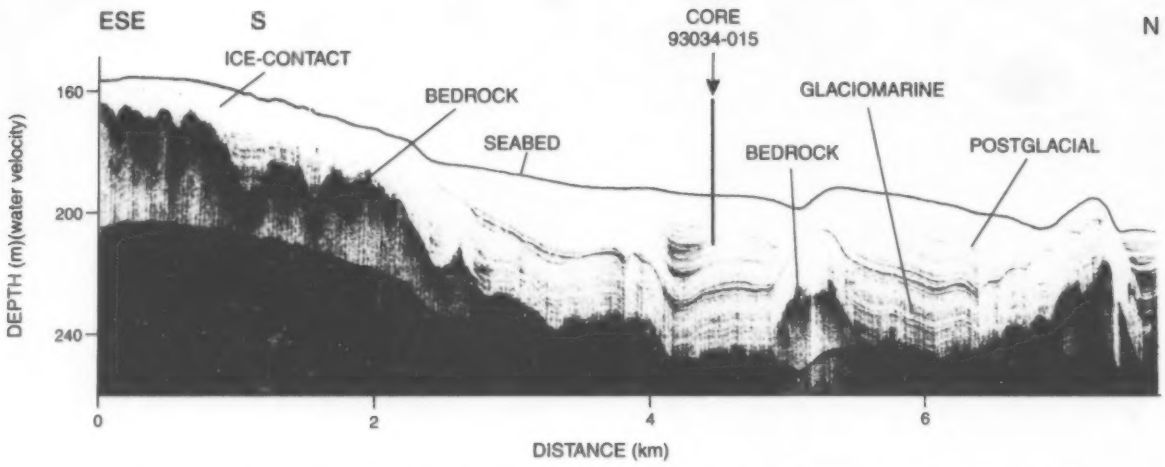

Figure 25. *Huntec™ high-resolution seismic-reflection profile illustrating glaciomarine and postglacial sediments in the Burgoyne Bay region of south-central Hudson Strait. Postglacial sediments up to 30 m thick overlie and onlap the glaciomarine beds. Core 93034-015 provides an expanded sediment record of the last 3300 years in this area. The extrapolated position of core 93034-015 is indicated.* (Modified from *MacLean et al., 1991, Fig. 10, and MacLean et al., 1992, Fig. 13.) Reproduced with permission from Géographie physique et Quaternaire.* (See *Fig. 1 for location of section.)*

and infilling depressions on the surface of ice-contact deposits. Where cored, unit 4 deposits typically comprise extensively bioturbated clayey sediments that locally contain mollusc shells and shell fragments. A few ice-rafted, pebble- or boulder-sized clasts occur (Hardy, 2001). Thick deposits of postglacial muddy sediments record marine paleoceanographic conditions that have existed since the retreat of glacial ice from the region.

Postglacial sands and gravels (unit 5)

A thin (<10–15 cm) layer consisting primarily of variably gravelly and sandy sediments, produced by the winnowing action of strong tidal currents and by ice rafting, mantles the main surficial sediment units and forms the immediate seabed in many areas that lie outside the basins. This veneer is indistinguishable acoustically from the underlying main sediment units, and they are not differentiated on the surficial sediment distribution map (Fig. 1) except locally in the vicinity of Resolution Island and Button Islands where they were mapped by Praeg et al. (1986) and by Josenhans et al. (1989).

REGIONAL GEOLOGICAL SETTINGS IN MARINE AREAS OF HUDSON STRAIT AND UNGAVA BAY

This section discusses the Quaternary sediment settings in Eastern, Western, and Southwestern basins, the central region of Hudson Strait, and in Ungava Bay. These are the prime marine localities in this region for information regarding paleoenvironments, sediment ages, and the late glacial, deglaciation, and postglacial history.

Eastern Hudson Strait

High-resolution seismic-reflection profiles and information from 11 piston core localities (MacLean, 2001, Fig. 4, 5) form a broad database that outlines the sedimentary and biostratigraphic framework, depositional environments, facies relationships, and chronologies of sediments in the eastern part of Hudson Strait. Figures 1–5 show the distribution and thickness of the main sediment units. The greatest accumulation of sediments in the Hudson Strait region lies in the deep floor of Eastern basin where thicknesses commonly are in the order of 70–100 m or more and locally reach 260 m (Fig. 3, 10). Deposits are much thinner on the basin flanks.

Eastern basin floor

Sediment units and relationships in a north to south direction across the basin floor are illustrated in Figure 22, and Figures 10, 28, 29, 30, 31 show deposits and relationships along parts of the basin floor in a west to east direction. These are shown diagrammatically in Figures 32 and 33. Acoustically unstratified sediments, considered to be ice-contact deposits, form the basal Quaternary sediments (Fig. 10, 22, 30). Locally they reach 180 m in thickness. These are interpreted to be mainly successive ice-contact deposits (Fig. 10, 30). These sediments, deeply buried in the basin floor, are beyond the reach of our conventional sampling systems, but where sampled on the basin flank, ice-contact sediments are clast-rich matrix-supported diamictons (Hardy, 2001).

Basal ice-contact sediments in the floor of the western part of Eastern basin are separated from overlying glaciomarine sequences by acoustically unstratified relatively transparent sediments up to about 15 m in thickness

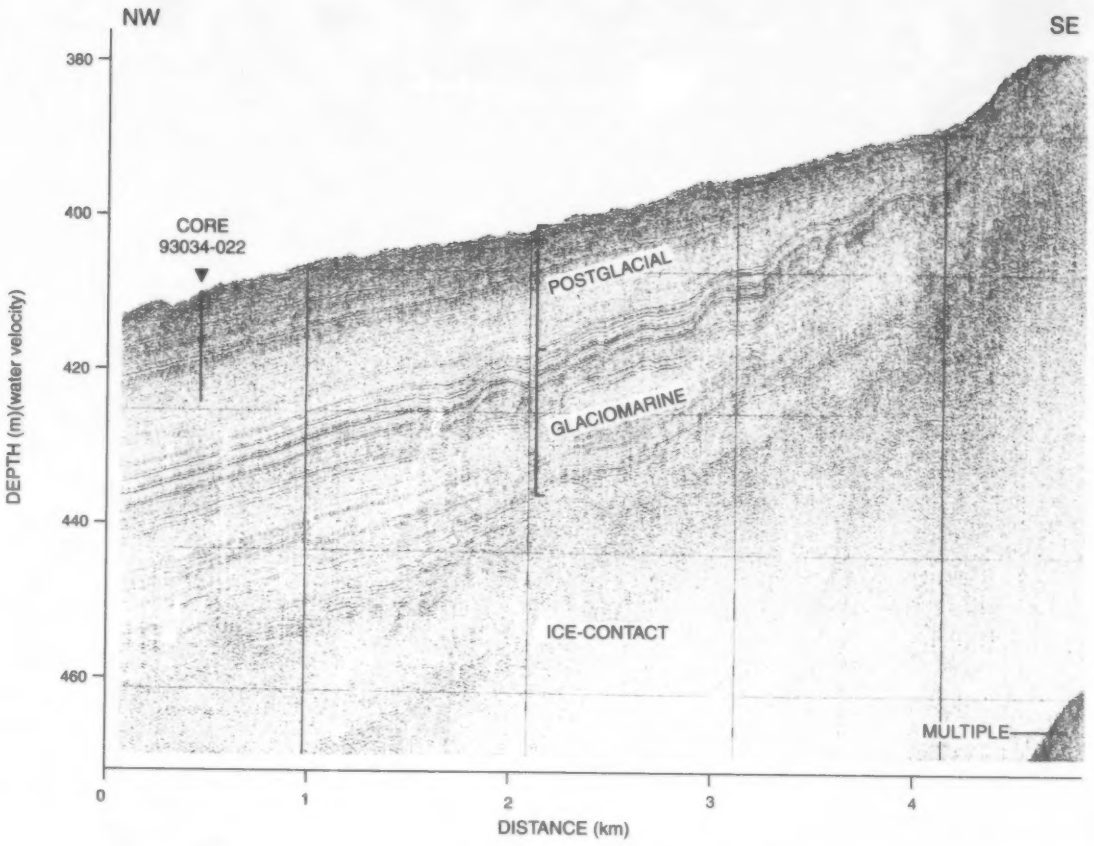

Figure 26. *Huntec™ high-resolution seismic-reflection profile illustrating a thick deposit of postglacial sediments that locally overlies glaciomarine sediments in Western basin. The transect illustrates sediment relationships adjacent to the southern margin of the basin north of Charles Island. Foraminifers from core 93034-022 interval 1238–1240 cm yielded a radiocarbon date of 5090 ± 60 BP (Table 2, uncorrected for reservoir effect).* (See *Fig. 1 for location of section.*)

(Fig. 22). Two superimposed sequences of these sediments locally are separated by a thin interval (approximately 2 m) of acoustically stratified sediment. Similar deposits may occur elsewhere in Eastern basin, but if so, they acoustically are not as distinct. Depositional mechanisms associated with these sediments are undefined. Vilks et al. (1989) and MacLean et al. (1992) favoured a glacial origin for this material on the basis of its stratigraphic and lateral facies relationships, but noted that debris-flow or glacially remolded sediments could be represented. Where the two sequences are superimposed (Fig. 22), the lobe-like aspect of the upper sequence and the stratified sediments separating it from the lower sequence suggest sediment emplacement rather than remolding of previously deposited sediments.

These lower sequences are overlain by glaciomarine sediments that form an acoustically distinct unit (Fig. 22) that locally attains a thickness of 60 m or more in the deepest part of the basin (Fig. 4, 29). Correlations along high-resolution seismic profiles suggest stratigraphic equivalents of the glaciomarine sequences cored and dated ca. 8.6–8.5 ka BP (all marine age dates reported in this paper are in ^{14}C radiocarbon years. A 450 year reservoir correction has been applied) on the northern and western flanks of the basin lie deep (30 m) within that thick sequence (Jennings et al., 1998) (Fig. 32, 33). Glaciomarine sediments locally intertongue with acoustically unstratified sediments in the basin-floor sequences (Fig. 29) and are transitional to ice-contact sediments adjacent to former ice-sheet grounding positions on the basin flanks.

The glaciomarine sediments include intervals that are rhythmically banded with thin silt and fine sand laminae (Hardy, 2001). These resemble deposits termed cyclopsams and cyclopels (Powell and Molnia, 1989). Magnetic susceptibility values show a pronounced correlation with these and other sedimentological changes in these sediments that relate

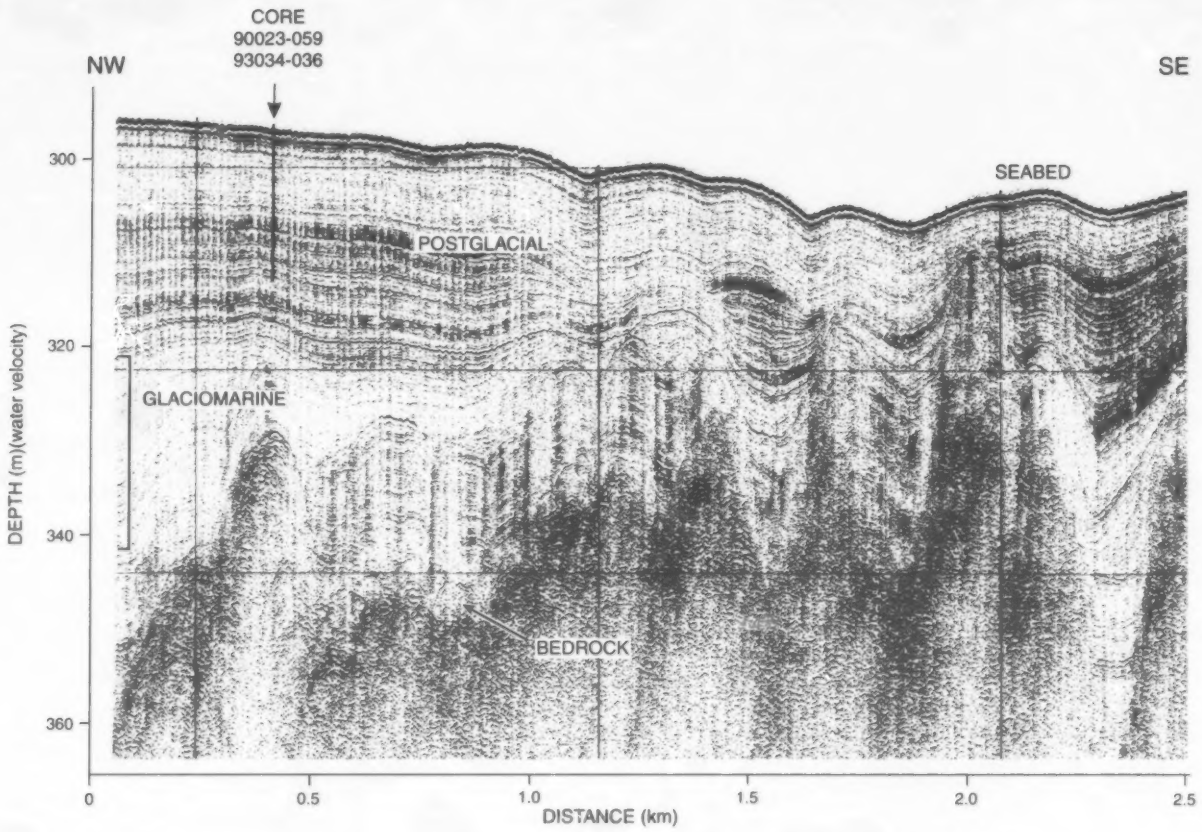

Figure 27. *Huntec™ high-resolution seismic-reflection profile illustrating thick deposits of postglacial sediments that occur in southeastern Ungava Bay. They unconformably overlie acoustically stratified sediments that are inferred to be glaciomarine. Radiocarbon dates obtained from core 93034-036 are listed in Table 2. (See Fig. 1 for location of section.)*

to variations in sediment supply, source, and texture (Manley and Kerwin *in* MacLean et al., 1994b; Kerwin, 1994; Andrews et al., 1995; Jennings et al., 1995; Hall et al., 2001).

Foraminiferal assemblages in the glaciomarine sediments indicate that deposition occurred in ice-proximal and ice-distal environments (Vilks et al., 1989). These are discussed by Jennings et al. (2001). Some anomalous foraminiferal species, radiocarbon dates, date inversions, and the presence of clay clasts indicate that reworked material is contained within the ice-proximal glaciomarine sediments (Jennings et al., 1998, 2001; Hardy, 2001). Kerwin (1994) noted an upward reduction in magnetic minerals and an increased calcium carbonate content in core 90023-045 (Fig. 28) as conditions changed from ice proximal to ice distal ca. 8400 BP. This indicates a relative reduction in the amount of material derived from Precambrian sources versus that from Paleozoic source areas. The change from glaciomarine to postglacial conditions in Eastern basin occurred ca. 8000–7900 BP.

Postglacial sediments overlie glaciomarine sediments in the floor of Eastern basin (Fig. 1). These commonly are relatively thin deposits only a few metres thick, but locally they attain 30 m (Fig. 5, 22, 28). The postglacial sediments in Eastern basin have been divided by Vilks et al. (1989) and Jennings et al. (2001) into early and late postglacial on the basis of changes in foraminiferal assemblages associated with changes in paleoceanographic conditions. During early postglacial time warmer and more saline waters were present in Eastern basin in greater proportions than at present. Variations in paleoceanographic conditions were accompanied by changes in depositional style. Local thickening and thinning of early postglacial sediments (Fig. 22) reflect the interaction of stronger bottom currents with seabed morphology.

The floor of Eastern basin locally has received inputs of remobilized glaciomarine and postglacial sediments from the basin flanks through debris-flow action.

Eastern basin flanks

The half-graben structural control imparts long northern and northwestern flanks to Eastern basin. These progressively shallow to the north and northwest (Fig. 33; MacLean, 2001, Fig. 1). They contrast with a shorter and steeper eastern margin adjoining the sill at the entrance to Hudson Strait, and the abrupt fault scarp that forms the southern margin of the basin. Ice-contact sediments form the basal Quaternary sediments on the basin flanks. Samples of diamict sediments recovered in cores 93034-029 and 93034-031 (*see* Fig. 35, 36; Hardy, 2001; MacLean, 2001, Fig. 5) are considered to be from this unit. In a few instances older ice-contact sediments contained in bedrock depressions underlie the areally extensive later deposits. Ice-contact sediments commonly are less than 10 m in thickness, but locally increase by up to several metres at former ice-sheet grounding-line (lift off)–still-stand positions on the basin flanks (Fig. 34), and in what may be morainal features in the area northeast and east of Cape Hopes Advance (Fig. 3).

Glaciomarine sediments overlie ice-contact sediments on the lower northern and northwestern flanks of Eastern basin (Fig. 1, 4). Core samples of these sequences were obtained at six localities (Fig. 22, 35, 36, 37, 38, 39, Table 1; MacLean, 2001, Fig. 5). These sediments laterally are transitional upslope to ice-contact sediments as exemplified in Figures 33, 34, and 35. These transitions mark ice-sheet grounding-line (lift off) positions (MacLean et al., 1994a, 1996; Jennings et al., 1998). These have been observed on six survey tracks that transect the northern and northwestern flanks of the basin over a distance of 110 km (MacLean, 2001, Fig. 4). Two main stages of glaciomarine to ice-contact transition have been recognized on the northern flank of Eastern basin. The lower transition occurs at present-day water depths between about 422 m and 442 m, and the upper transition between depths of approximately 345 m and 404 m. These are illustrated in Figures 34 and 35. There the lower half of the glaciomarine sequence is laterally transitional to ice-contact sediments at a present-day water depth of about 442 m, and approximately 4 km upslope, the upper half of the glaciomarine sequence similarly is transitional to ice-contact sediments. Thickening of the ice-contact deposits adjacent to

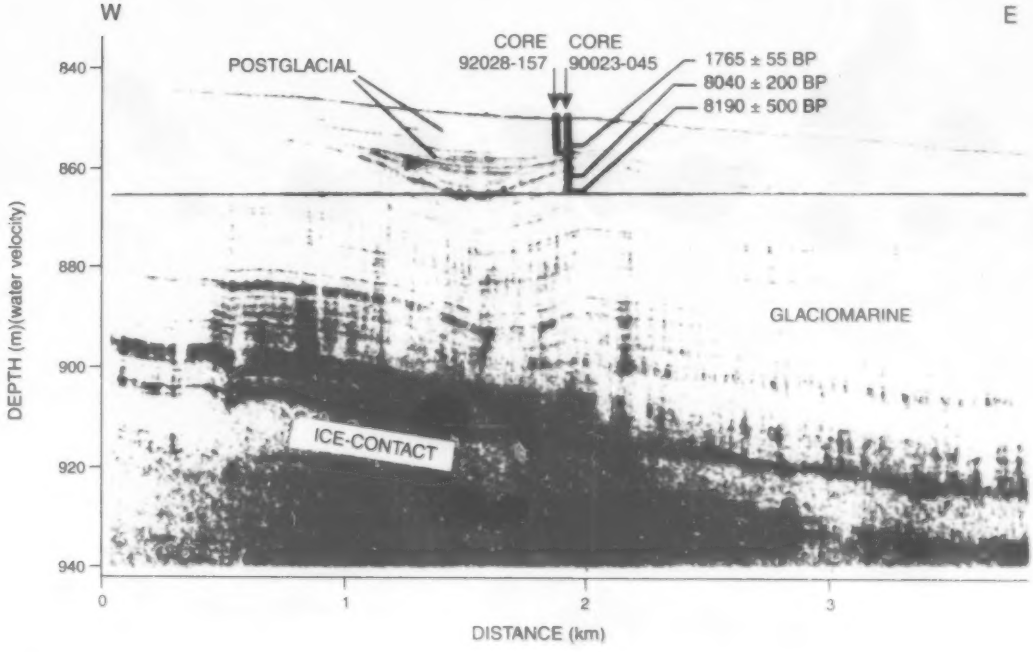

Figure 28. *Huntec™ high-resolution seismic-reflection profile illustrating ice-contact, glaciomarine, and postglacial sediments at the core 90023-045/92028-157 locality in the deep floor of Eastern basin. Selected chronological data bracket the change from glaciomarine to postglacial conditions.* (Modified from *Andrews et al., 1995, Fig. 6A.) Quaternary Science Reviews, v. 14, p. 983–1004, © 1996. Reprinted with permission from Elsevier Science.)* (See *Fig. 1 for location of section.)*

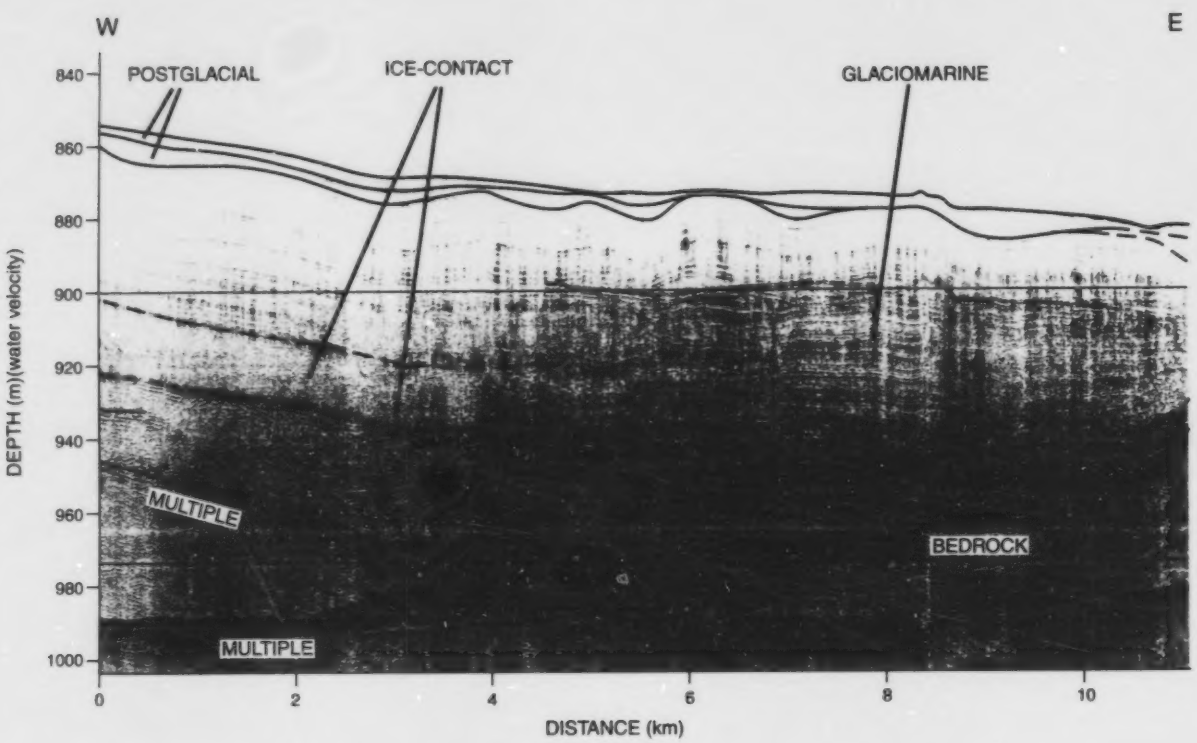

Figure 29. *Huntec™ high-resolution seismic-reflection profile oriented west to east, midway along Eastern basin showing a 100 m thick sequence containing intertonguing glaciomarine and acoustically unstratified sediments that are interpreted to be ice-contact deposits. Seismic correlations suggest that beds near the base of the acoustically stratified sequence at the western end of the section are approximate stratigraphic equivalents of the 8540 BP interval in core 90023-042 (Fig. 31; Table 2).* (See *Fig. 1 for location of section.*)

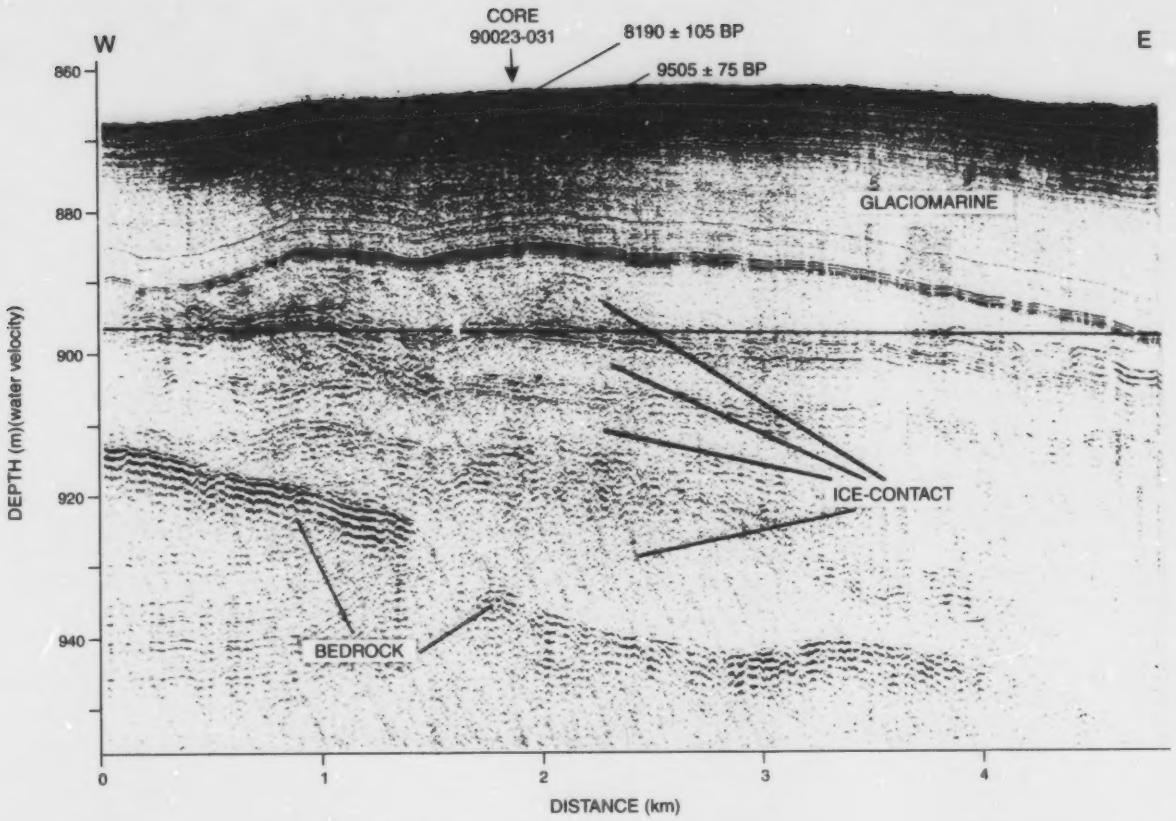

Figure 30. *Huntec™ high-resolution seismic-reflection profile illustrating successive ice-contact deposits and overlying glaciomarine sediments in the deep easternmost part of Eastern basin. Postglacial sediments are thin to absent in this part of the basin. The extrapolated core 90023-031 locality is indicated.* (See *Fig. 1 for location of section.*)

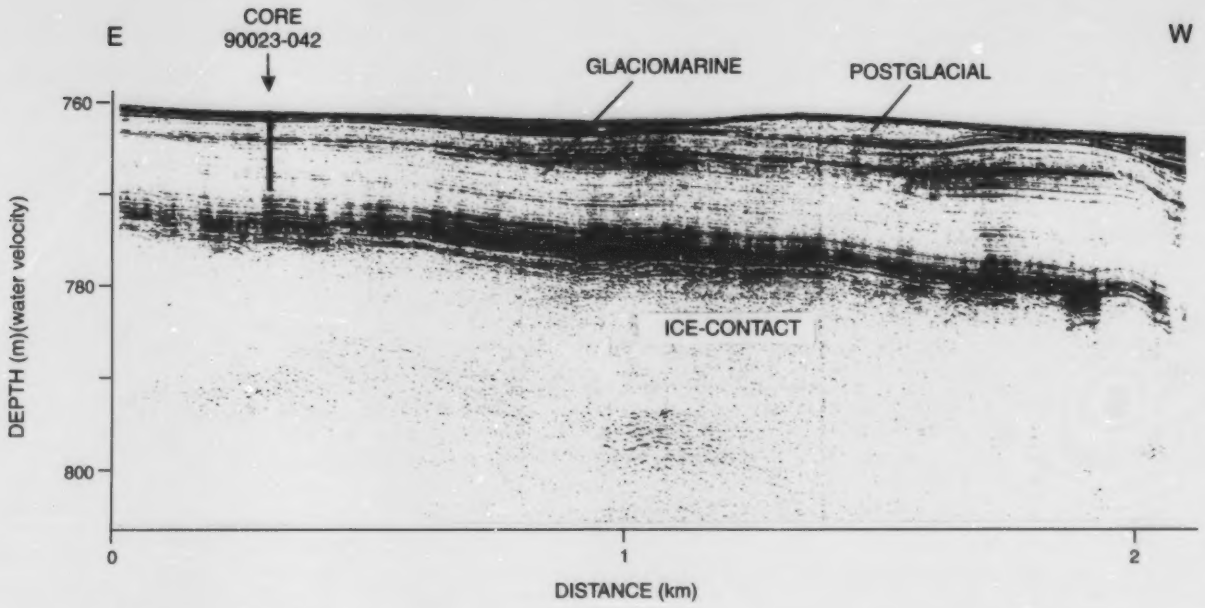

Figure 31. *Huntec™ high-resolution seismic-reflection profile showing sequences cored at the core 90023-042 locality in the western part of the floor of Eastern basin.* (Modified from *Andrews et al., 1995, Fig. 6B.) Quaternary Science Reviews, v. 14, p. 983–1004. © 1996. Reprinted with permission from Elsevier Science.* (See *Fig. 1 for location of section.)*

the transition areas suggests these mark brief stillstand lift-off positions as the ice sheet thinned and waned. There are also indications locally of transitions at slightly greater depths.

On the more gently sloping northwest flank a succession of four small, relatively evenly spaced lift-off features occurs between present depths of 454 m and 416 m followed by a fifth farther upslope at 370 m, and by the upper grounding line at about 347 m. These features mark the progressive upslope retreat of the ice-sheet grounding line on that flank. Seismic profile data suggest a former grounding-line (lift-off) position may also occur at the top of a small scarp at the base of the northwestern flank (474 m) and toward the base of northern flank transects. Acoustic resolution in those areas, however, is impaired by abrupt changes in bathymetric elevations.

Former grounding-line locations have also been observed on seismic profiles at depths ranging between 350 m and 409 m on four transects across the southern margin of Eastern basin. Seismic resolution on the southern margin in general is poorer than on the north flank due to the steep bathymetry.

In the deep eastern part of the basin, acoustically strongly stratified glaciomarine sediments that overlie ice-contact sediments at the 93034-002 core locality low on the northern flank (Fig. 37; MacLean, 2001, Fig. 5) tongue with and grade laterally into unstratified sediments 3.7 km upslope to the north at a depth of 703 m. Relationships suggest that this may be a deeper grounding-line position.

Biostratigraphy and textural composition of the sediments on the floor and flanks of Eastern basin are discussed by Jennings et al. (2001) and by Hardy (2001).

Reservoir corrected radiocarbon ages ranging between 9505 BP and 7945 BP have been obtained on shells and foraminifers in nine cores from glaciomarine sediments in the floor of Eastern basin and downslope from the grounding line on its northern flank (Table 2), together with a date of 9100 ± 480 BP obtained by Fillon and Harmes (1982) from core 77021-154. Foraminifers in two cores (93034-029 and 93034-004) (Fig. 35, 39) from the lower part of the glaciomarine sediments on the flank yielded radiocarbon ages of 10 050 BP and 10 620 BP, and a 9820 BP age (stratigraphically inverted) was obtained from the upper part of the section farther east at the 93034-002 locality (Fig. 37, Table 2). These three dates, and a stratigraphically inverted date of 11 665 ± 260 BP in core 90023-045 (Fig. 28) from sediments in the basin floor appear to be anomalously 'old', and are thought to indicate the presence of reworked material in the dated samples (Jennings et al., 1998, 2001).

Glaciomarine sediments have not been recognized on high-resolution seismic-reflection profiles above the upper grounding line, except locally in a small valley 22 km from the coast of Baffin Island (Fig. 40; MacLean, 2001, Fig. 4) where they were deposited during later stages of ice retreat. A paired *Portlandia arctica* valve in core 93034-006 from that

locality yielded a radiocarbon date of 8575 ± 90 BP (Table 2). If glaciomarine sediments were deposited elsewhere above the grounding line, they have been remolded.

Postglacial sediments on the lower part of the basin flanks generally are in the order of 1–2 m or less. They are not recognizable acoustically above the upper grounding line on the northern flank of Eastern basin except in a few, small, isolated occurrences in seabed depressions or valleys (Fig. 1); however, an IKU™ clam-shell sample of very cohesive postglacial clayey sediments that in part are silty and sandy, underlying a thin sandy and gravelly veneer, from a locality 16 km north of the grounding line (core 90023-112) (MacLean, 2001, Fig. 5) suggests that thin deposits of postglacial sediments variably mantle and partly infill small depressions on the surface of the ice-contact deposits on the northern flank of Eastern basin. Foraminifers from those sediments at the core 90023-112 locality yielded a reservoir-corrected radiocarbon age of 7660 ± 360 BP (Table 2). The thinness of such deposits generally renders them acoustically indistinguishable from underlying sediment units, and they are not differentiated on Figure 1.

Parallel–subparallel ice-keel scour marks that trend east-southeast, approximately parallel to the axis of Hudson Strait, occur in several shallow-water localities (≥100 m) adjacent to eastern Meta Incognita Peninsula where terrestrial ice-flow directions are to the northeast and north-northeast. The parallel and consistent orientation of these features suggests they were not created by groundings of individual small bergs, the random scours and impacts of which are also seen in this area; however, orientation of the parallel features approximates that of westbound currents along that section of coast. The origin of these features is unresolved.

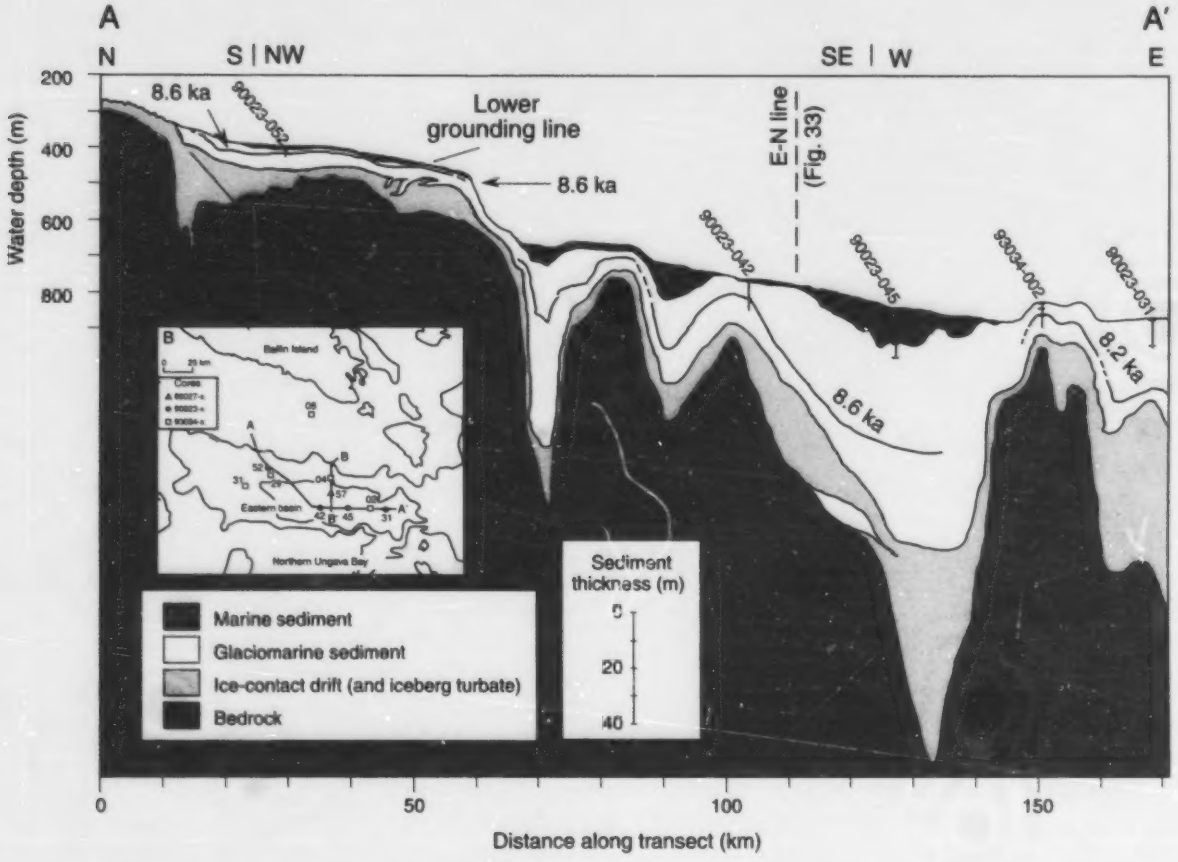

Figure 32. *Diagrammatic cross-section showing the sedimentary section, core localities, and dated intervals along a northwest-east transect along Eastern basin.* (Modified from *Jennings et al., 1998, Fig. 9.*) *Copyright John Wiley & Sons Limited. Reproduced with permission.*

Western and southwestern basins

As in Eastern basin, the southward-deepening, half-graben, structurally controlled morphology of both Western and Southwestern basins has been an important factor in the manner of sediment deposition in those areas of Hudson Strait.

Data from high-resolution and single-channel seismic-reflection profiles and from five piston cores in Western basin and four in Southwestern basin provide information regarding the Quaternary sediments in these basins. Distribution and thickness of the main Quaternary sediment units are indicated in Figures 1, 2, 3, 4, 5.

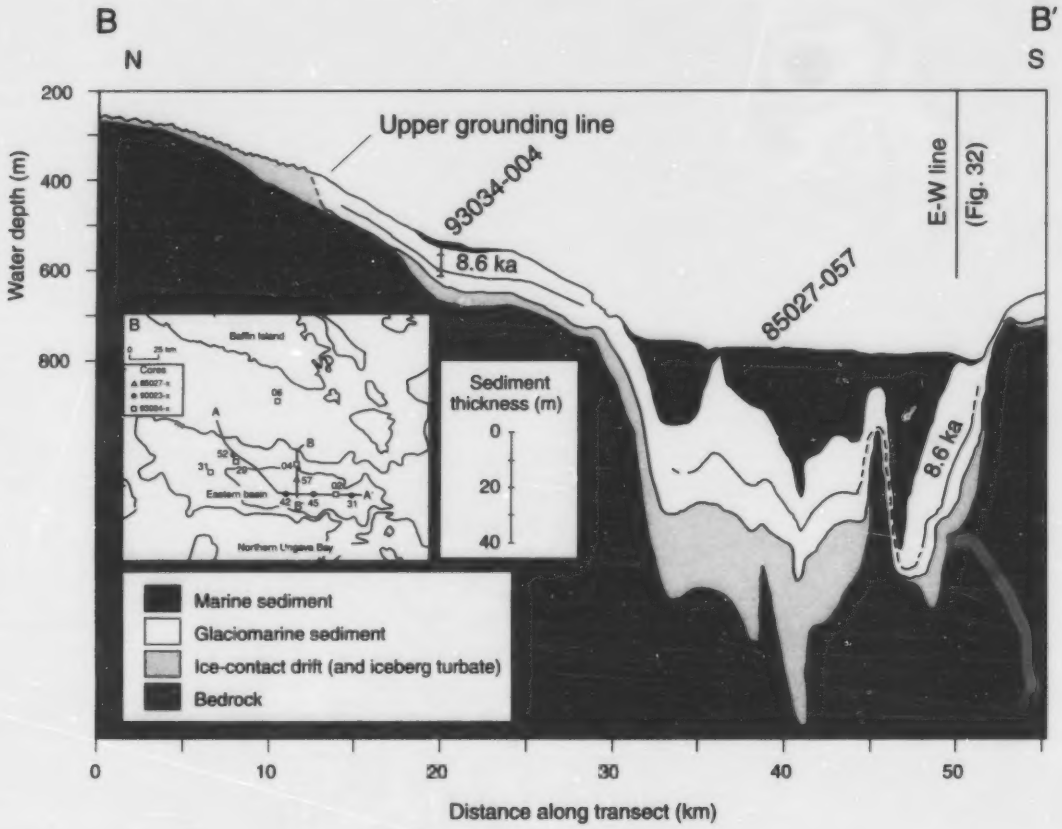

Figure 33. *Diagrammatic cross-section showing sedimentary relationships along a north to south transect across the western part of Eastern basin.* (After *Jennings et al., 1998, Fig. 10.*) *Copyright John Wiley & Sons Limited. Reproduced with permission.*

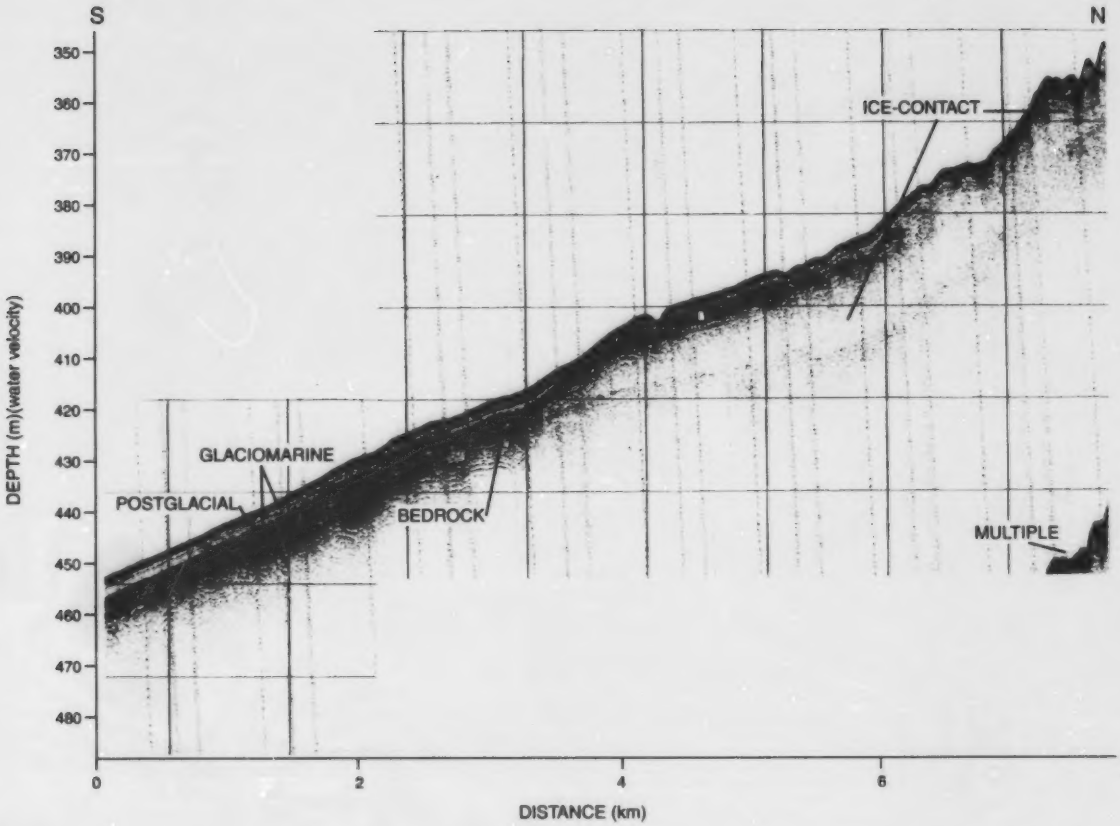

Figure 34. *Huntec™ high-resolution seismic-reflection profile illustrating glaciomarine–ice-contact facies transitions at former ice-sheet grounding (lift off) positions on the northern flank of Eastern basin. The lower and upper halves of the glaciomarine sequences present on the left, upslope are transitional laterally to ice-contact sediments at approximately 3.5 km and 6.5 km along section, respectively.* (See *Fig. 1 for location of section.)*

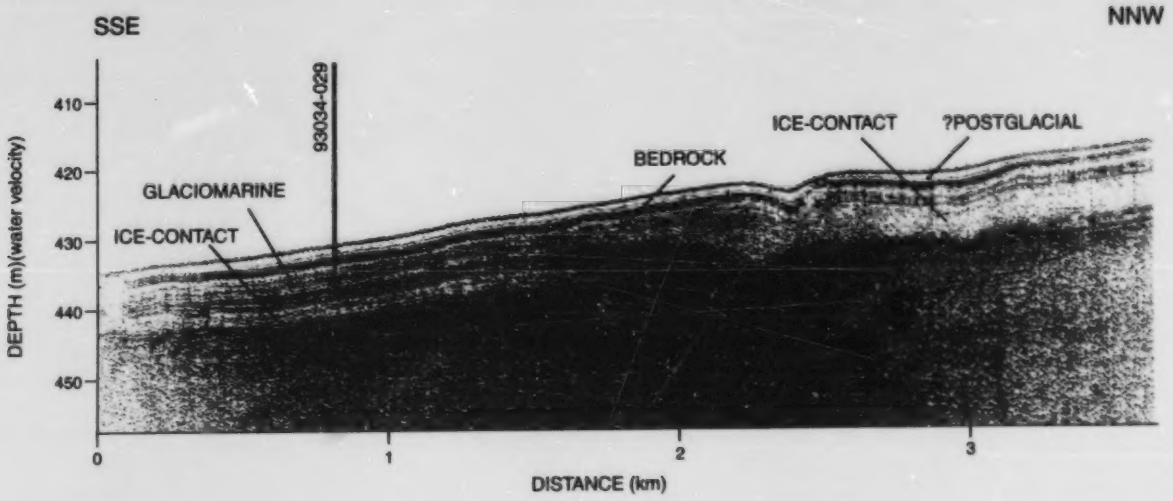

Figure 35. *Huntec™ high-resolution seismic-reflection profile showing the lateral transition of the lower part of the acoustically stratified glaciomarine sequence to ice-contact sediments at the lower grounding line (lift-off position) 1.7 km along section, a short distance upslope from the site of core 93034-029 on the northern flank of Eastern basin. (See Fig. 1 for location of section.)*

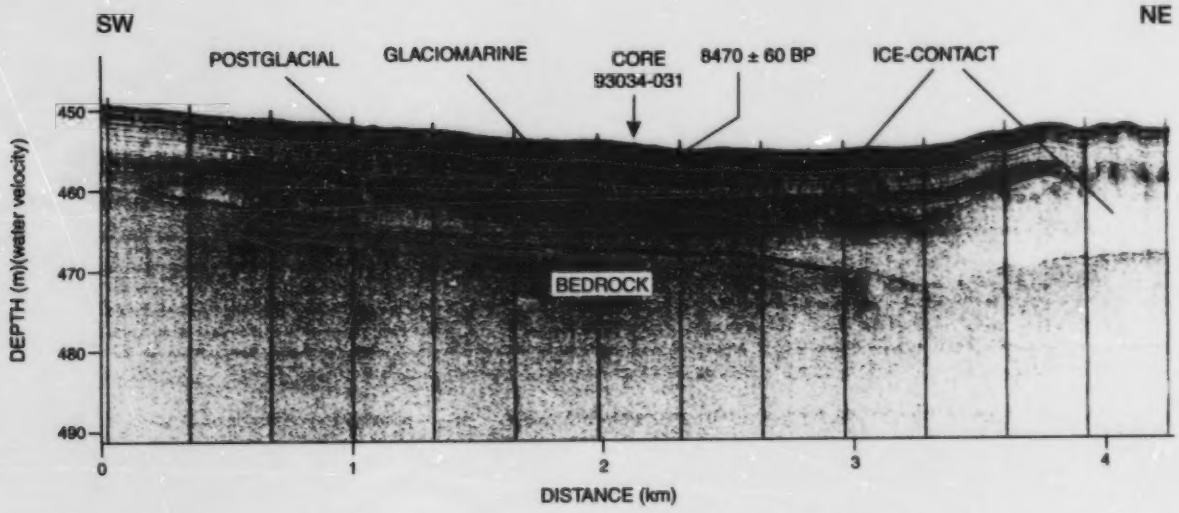

Figure 36. *Huntec™ high-resolution seismic-reflection profile showing the sediment section and chronological data at the core 93034-031 locality on the lower part of the western flank of Eastern basin. Ice-contact diamicts are overlain by glaciomarine ice-proximal and ice-distal sediments that in turn are overlain by a thin cover of postglacial sediments. (See Fig. 1 for location of section.)*

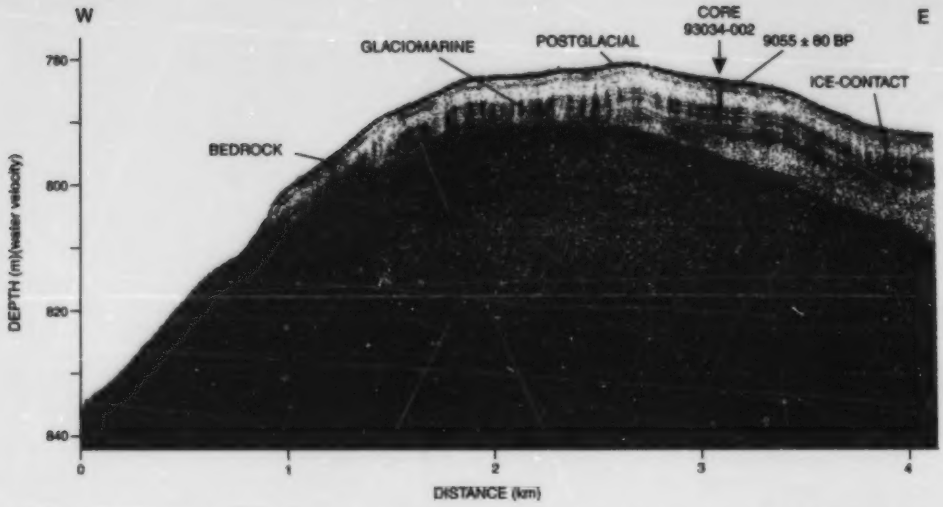

Figure 37. *Huntec™ high-resolution seismic-reflection profile showing sediment units in the vicinity of core 93034-002 on a protrusion of the northern flank midway along Eastern basin. The core site lies in similar sediments a short distance upslope of the area indicated on this west-east transect. Ice-contact sediments are absent over much of the western flank of this morphological feature and thicken eastward in its lee. Debris-flow activity has removed the upper part of the sediment section on the west flank. (See Fig. 1 for location of section.)*

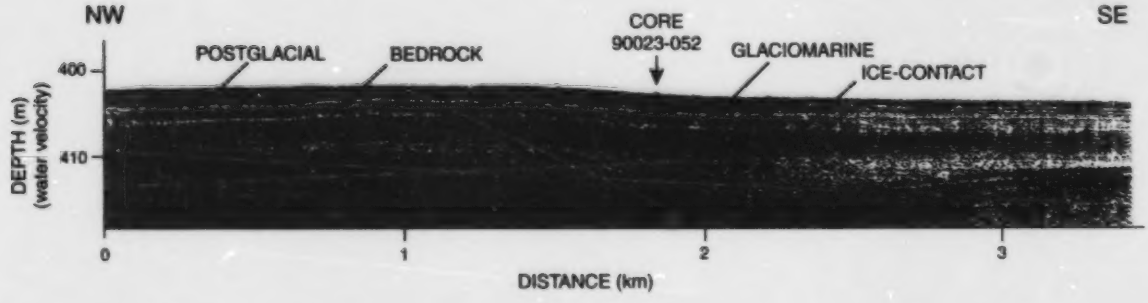

Figure 38. *Huntec™ high-resolution seismic-reflection profile illustrating glaciomarine and ice-contact sediments at the core 90023-052 locality on the northern flank of Eastern basin. The glaciomarine sediments are laterally transitional to ice-contact sediments 15 km to the northwest. (See Fig. 1 for location of section.)*

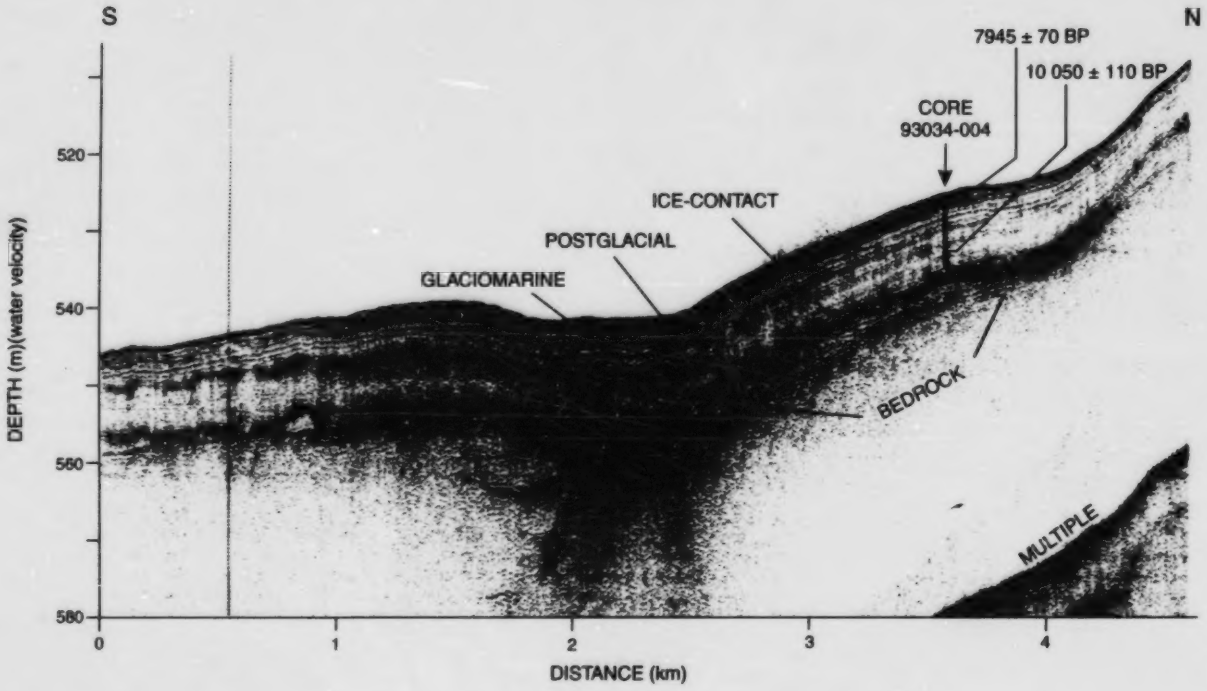

Figure 39. *Huntec™ high-resolution seismic-reflection profile showing the core 93034-004 locality downslope from the ice-sheet grounding line (lift-off position) on the northern flank of Eastern basin. Ice-contact sediments up to approximately 3 m thick underlie the glaciomarine sequences. Postglacial sediments are less than 1 m thick. Selected radiocarbon dates are indicated.* (See *Fig. 1 for location of section.*)

Western basin

Seismic-reflection profile sections illustrate the sedimentary setting: Figure 41, oriented west to east along part of the axis of the basin, shows sediment sequences totalling some 120 m in thickness; Figure 42, a southwest to northeast transect across the basin north of Charles Island, shows the thickest deposits in that area occur in an asymmetrical 12 km wide zone on and adjoining the southern flank of the basin; and Figure 43, a southwest to northeast transect across the southern margin of the basin between Charles and Salisbury islands, shows the complex nature of bedrock and Quaternary geology in that area. Sediments generally in the order of 8–12 m in thickness, but locally thickening to 30 m where they infill depressions, extend northward for 65 km on the northern flank of the basin (Fig. 2). Farther north they become thin and discontinuous.

Acoustically mainly unstratified sediments with a dark tone on seismograms form a massive deposit up to 90 m in thickness that lies on a well defined bedrock surface along part of the southern floor of Western basin (Fig. 41) and on its southern flank adjoining the Charles Island platform (Fig. 42). Acoustically, these resemble an ice-contact deposit. The spatial geometry (Fig. 42) suggests that this material may be the product of deposition by ice flowing northward from the Charles Island platform, or an erosional remnant of an earlier deposit. Stratified sediments underlie these sediments near their western limit (Fig. 41).

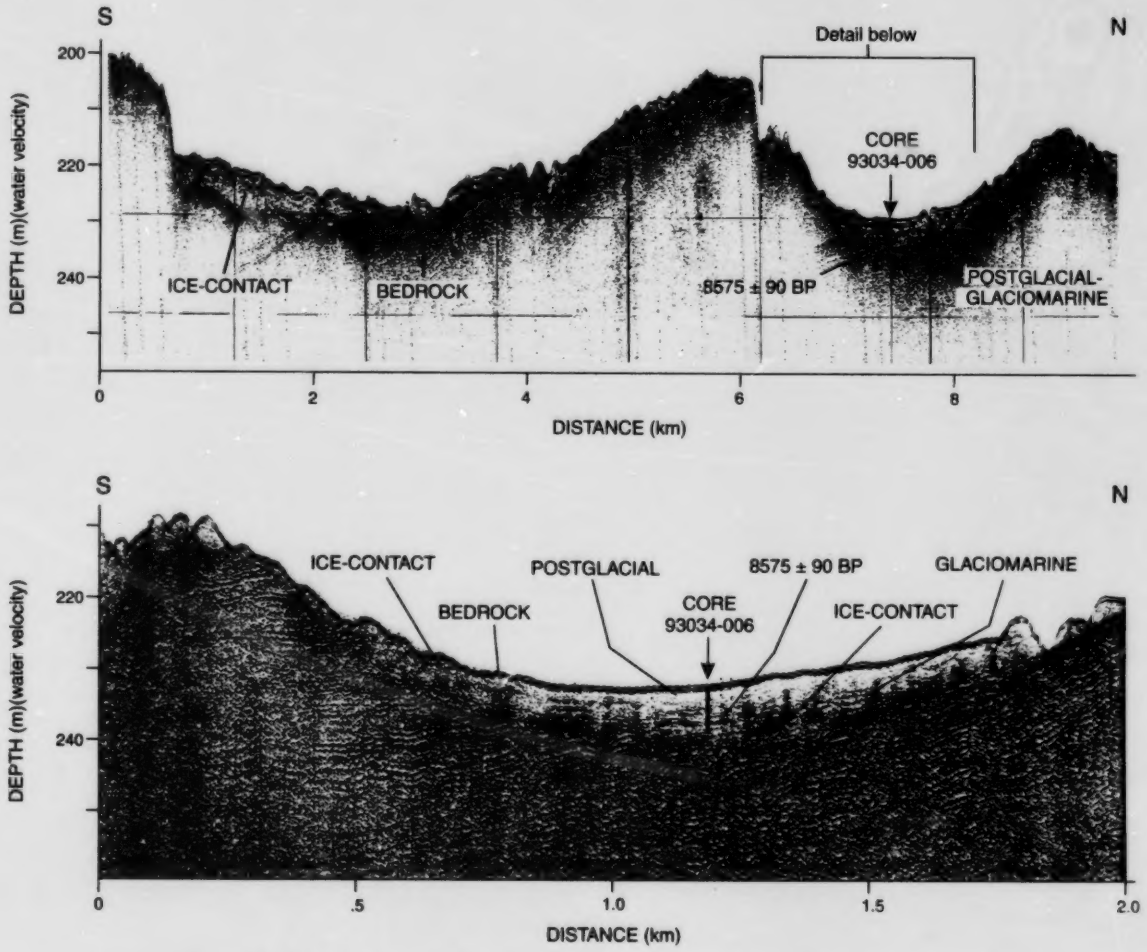

Figure 40. *Huntec™ high-resolution seismic-reflection profiles showing in the upper diagram, sedimentary sequences that occur locally in small valleys between cuesta ridges formed by Paleozoic rocks in the core 93034-006 region 22 km from the coast of Baffin Island. The lower profile shows the sediment section at the core 93034-006 site in more detail. Sedimentary and spatial relationships and chronological data suggest that deposition of the glaciomarine sediments in this area occurred when the ice sheet (Noble Inlet) was briefly pinned on the adjoining cuesta ridges late in its retreat.* (See *Fig. 1 for location of section.*)

Overlying the massive acoustically unstratified deposit (and bedrock where the lower unit is absent) are acoustically unstratified, relatively more transparent, ice-contact sediments that attain a thickness of 50 m near the western limit of the basin (beyond the western margin of Fig. 41).

These in turn are overlain by acoustically well stratified glaciomarine sediments up to 34 m in thickness (Fig. 4, 43, 44). Core samples from five localities indicate these mainly are laminated silty and clayey sediments containing some grains and clasts (Hardy, 2001). Deposition was in ice-proximal and ice-distal environments (Vilks et al., 1989; MacLean et al., 1992; Jennings et al., 2001). The basal part of the glaciomarine sequence in the eastern part of the basin appears to have been remolded by glacial ice-loading and/or debris-flow activity. North of Charles Island glaciomarine sequences locally contain cut-and-fill features that presumably are associated with debris-flow events. Glaciomarine sediments are transitional laterally to ice-contact sediments in basin-margin settings as illustrated by Figure 19.

In areas north and northeast of Charles Island, acoustically stratified sediments inferred to be glaciomarine are locally overlain by up to 20 m of ice-contact sediments deposited by later glacial ice advances (Fig. 21). The advancing ice eroded and deformed the uppermost beds of the acoustically stratified sediments to varying degrees.

Table 1. Core locations, water depths, and core recoveries.

Core number and type	Latitude	Longitude	Water depth (m)	Core length (cm)	Region
77021-154[1]	60°53.70'N	65°26.60'W	933	779	East basin
85027-055[1]	60°56.72'N	66°25.84'W	805	1062	East basin
85027-056[1]	60°58.11'N	66°29.73'W	777	1181	East basin
85027-057[1]	61°04.26'N	66°25.60'W	790	1190	East basin
85027-065[1]	62°35.92'N	76°07.02'W	333	300	Southwest basin
85027-068[1]	63°04.50'N	74°18.55'W	435	1060	West basin
85027-092[1]	61°12.50'N	70°26.99'W	171	249	Central Hudson Strait
85027-096[1]	61°20.72'N	67°44.70'W	392	717	East basin
85027-097[1]	61°20.69'N	67°44.43'W	392	162	East basin
87033-011[2]	60°55.93'N	65°24.68'W	896	1244	East basin
87033-012[2]	61°03.45'N	66°26.04'W	772	1519	East basin
87033-013[2]	60°57.49'N	66°26.75'W	786	1460	East basin
90023-031[3]	60°57.10'N	65°26.70'W	872	727	East basin
90023-034[3]	59°59.41'N	65°44.03'W	336	352	East Ungava Bay
90023-036[3]	59°57.81'N	65°53.89'W	332	931	East Ungava Bay
90023-039[3]	59°47.06'N	65°55.82'W	387	956	East Ungava Bay
90023-042[3]	60°57.01'N	66°36.95'W	761	881	East basin
90023-045[3]	60°56.80'N	66°06.28'W	845	1179	East basin
90023-052[3]	61°19.48'N	67°36.21'W	402	275	East basin
90023-059[3]	59°32.01'N	67°13.26'W	290	787	South Ungava Bay
90023-062[3]	60°15.76'N	68°32.98'W	234	256	West Ungava Bay
90023-064[3]	61°07.50'N	70°34.60'W	196	987	Central Hudson Strait
90023-066[3]	61°27.82'N	70°51.00'W	193	749	Central Hudson Strait
90023-071[3]	61°46.72'N	71°56.65'W	110	616	Central Hudson Strait
90023-076[3]	62°09.70'N	74°42.28'W	67	587	Deception Bay
90023-085[3]	62°36.95'N	76°22.53'W	380	548	Southwest basin
90023-087[3]	62°38.89'N	76°39.77'W	390	370	Southwest basin
90023-094[3]	63°00.97'N	76°38.60'W	320	499	Southwest basin
90023-097[3]	63°14.96'N	75°32.68'W	427	662	West basin
90023-099[3]	63°03.97'N	74°33.96'W	386	479	West basin
90023-101[3]	63°02.99'N	74°18.24'W	389	776	West basin
90023-104[3]	62°59.58'N	74°00.04'W	410	582	West basin
90023-106[3]	62°59.38'N	73°59.90'W	412	497	West basin
90023-107[3]	61°20.67'N	70°37.77'W	182	720	Central Hudson Strait
92028-153[1]	61°20.64'N	70°37.73'W	184	758	Central Hudson Strait
92028-155[1]	61°09.50'N	70°34.20'W	196	1072	Central Hudson Strait
92028-157[4]	60°56.86'N	66°07.86'W	860	561	East basin
92028-158[1]	61°00.00'N	62°55.57'W	622	1121	Hatton Basin
93034-002[1]	60°56.78'N	65°41.98'W	822	702	East basin
93034-004[1]	61°13.45'N	66°25.93'W	526	793	East basin
93034-006[1]	61°46.45'N	66°51.74'W	223	486	East Hudson Strait
93034-013[1]	61°30.01'N	70°43.41'W	201	868	Central Hudson Strait
93034-015[1]	61°17.96'N	71°03.79'W	200	1467	Central Hudson Strait
93034-018[1]	62°37.29'N	71°35.68'W	338	861	Central Hudson Strait
93034-022[1]	63°04.35'N	74°29.82'W	410	1252	West basin
93034-029[1]	61°15.04'N	67°32.95'W	430	742	East basin
93034-031[1]	61°08.25'N	66°01.73'W	454	1016	East basin
93034-036[1]	59°32.03'N	67°13.20'W	297	1456	South Ungava Bay
93034-038[1]	59°38.17'N	66°13.07'W	376	1170	East Ungava Bay

[1] Benthos™ piston corer (6.8 cm I.D), fitted with 1364 kg head
[2] Long Coring Facility
[3] AGC large-diameter corer (10 cm I.D.)
[4] Benthos™ gravity corer (6.8 cm I.D.), fitted with 1364 kg head

Table 2. Radiocarbon dates.

Core or IKU station	Core interval (cm)	Laboratory number	Reported age (^{14}C years BP)	Corrected age[1] (^{14}C years BP)	Material[2]	Weight (mg)	Published references
Eastern Hudson Strait							
77021-154	101	AA-3103		8280 ± 80	S	n.d.	Andrews et al., 1995
	102–110	GSC-2698	8730 ± 250	8690 ± 250	S	n.d.	Fillon and Harmes, 1982
	200–300	GSC-2946	9100 ± 480	9060 ± 480	S	n.d.	Fillon and Harmes, 1982
	575–557	AA-5117	9000 ± 170	8550 ± 170	S	2.7	Kaufman and Williams, 1992
85027-057	242–246	TO-1870	5930 ± 70	5480 ± 70	Fm	19	MacLean et al., 1992
	742–747	TO-1871	8470 ± 90	8020 ± 90	Fm	10	Vilks *in* Manley and Jennings, 1996
	782–788	TO-748	7880 ± 70	7840 ± 70	Ss[3]	51	Vilks et al., 1989
	814–822	TO-749	7730 ± 70	7690 ± 70	Sp[3]	260	Vilks et al., 1989
	862–870	TO-750	8060 ± 70	8020 ± 70	Ss[3]	41	Vilks et al., 1989
	1072–1078	TO-1860	8360 ± 70	7910 ± 70	Sv	n.d.	Vilks *in* Manley and Jennings, 1996
87033-012	1454–1456	AA-11590	8460 ± 95	8010 ± 95	F	2	Andrews et al., 1995
90023-031	3	AA-11420		8190 ± 105	Fm	n.d.	Andrews et al., 1995
	5–7	AA-14210	8640 ± 105	8190 ± 105	Fm	4	Kerwin, 1994
	700–725	AA-11448	9955 ± 75	9505 ± 75	Fm	4	Kerwin, 1994
90023-042	517–525	AA-10253	9040 ± 85	8590 ± 85	Fs	3.8	Andrews et al., 1995
90023-045	2–4	AA-8961	2215 ± 55	1765 ± 55	Fs	4	Andrews in Manley and Jennings, 1996
	90	AA-13228	7835 ± 90	7385 ± 90	Fp	5.8	Kerwin, 1994
	198–200	AA-8962	7675 ± 115	7225 ± 115	Fs	7.9	Manley et al., 1993
	398–399	AA-8963	7600 ± 60	7115 ± 60	Fm	5.4	Manley et al., 1993
	480–483	AA-17379	7785 ± 140	7335 ± 140	Fs	3.5	Andrews et al., 1995
	480–483	AA-17380	8155 ± 130	7705 ± 130	Fs	2.1	Andrews et al., 1995
	630–633	AA-11880	12 115 ± 260	11 665 ± 260	Fm	3.0	Kerwin, 1994
	695–705	AA-8964	9730 ± 70	9280 ± 70	Fm	4.0	Manley et al., 1993
	777–779	AA-11879	8490 ± 200	8040 ± 200	Sp[3]	3.0	Kerwin, 1994
	1165–1175	AA-12884	8805 ± 60	8355 ± 60	Sp[3]	34	Kerwin, 1994
	1165–1175	CAMS-17146	8640 ± 500	8190 ± 500	Fs	1	Andrews et al., 1995
90023-052	175–178	AA-10254	9075 ± 75	8625 ± 75	Fs	5.8	Andrews et al., 1995
90023-112	IKU	T0-3668	8110 ± 360	7660 ± 360	Fs	7.0	MacLean *in* Manley and Jennings, 1996
93034-002	3–5	CAMS-25670	3970 ± 60	3520 ± 60	F	5.8	Jennings *in* Manley and Jennings, 1996
	144	AA-13172	9505 ± 80	9055 ± 80	Ss[3]	17.9	MacLean et al., 1996
	135–145	AA-17391	10 270 ± 285	9820 ± 285	Fs	1.9	Jennings *in* Manley and Jennings, 1996
	344–360	CAMS-25758	8640 ± 70	8190 ± 70	F, S, O	2.5	Jennings *in* Manley and Jennings, 1996
93034-004	top	CAMS-25759	820 ± 80	370 ± 80	F	2.3	Jennings *in* Manley and Jennings, 1996
	20	CAMS-25762	8030 ± 60	7580 ± 60	Fs	6.4	Jennings *in* Manley and Jennings, 1996
	79	AA-13055	8395 ± 70	7945 ± 70	Sp[5]	27.8	Manley and Jennings, 1996
	260–262.5	CAMS-25764	9430 ± 50	8980 ± 50	Sp	7.1	Jennings *in* Manley and Jennings, 1996
	600–620	CAMS-25761	9060 ± 60	8610 ± 60	Fm	5.3	Jennings *in* Manley and Jennings, 1996
	738–762	CAMS-17401	10 500 ± 110	10 050 ± 110	Fm	1	Jennings *in* Manley and Jennings, 1996
93034-006	380	AA-13173	9025 ± 90	8575 ± 90	Sp[3]	7.1	MacLean et al., 1996
93034-029	280–285	CAMS-18689	11 070 ± 60	10 620 ± 60	Fm, Sf	1.9	MacLean *in* Manley and Jennings, 1996
93034-031	397–400	CAMS-18688	8920 ± 60	8470 ± 60	Fs	3.5	MacLean *in* Manley and Jennings, 1996

Table 2. (cont.)

Core or IKU station	Core interval (cm)	Laboratory number	Reported age (^{14}C years BP)	Corrected age[1] (^{14}C years BP)	Material[2]	Weight (mg)	Published references
Central Hudson Strait							
85027-092	224–228	CAMS-29558	8450 ± 50	8000 ± 50	Fm	3.4	B. MacLean (unpub. data, 1996)
90023-064	195	TO-2459	6760 ± 70	6310 ± 70	S	479	Manley et al., 1993
	225	TO-2460	6880 ± 70	6430 ± 70	Sf[4]	297	Manley et al., 1993
	250	TO-2462	7060 ± 70	6610 ± 70	Ss[5]	339	Manley et al., 1993
	460–462	TO-3263	8160 ± 150	7710 ± 150	Fm	3.7	Manley et al., 1993
90023-066	21–23	TO-3264	6960 ± 110	6510 ± 110	Fm	7.6	Manley and Jennings, 1996
	230	TO-2461	8350 ± 80	7900 ± 80	Ss[3]	93	MacLean et al., 1992
	728	TO-2463	8850 ± 90	8400 ± 90	3Sp[3]	224	MacLean et al., 1992
	743	TO-2464	8830 ± 80	8380 ± 80	Sp[3]	80	Maclean et al., 1992
90023-071	360–362	TO-2465	8570 ± 230	8120 ± 230	Ss[3]	14	MacLean et al., 1992
	408	TO-2466	8930 ± 80	8480 ± 80	Sv[3]	448	MacLean et al., 1992
	561–565	AA-10650	11 095 ± 110	10 645 ± 110	Fm	3.5	Manley and Jennings, 1996
90023-107	32–38	AA-11440	12 035 ± 80	11 585 ± 80	Fm	3.4	Manley, 1995
	80–82	TO-2471	8450 ± 70	8000 ± 70	Sv[3]	66	MacLean et al., 1992
	150–153	AA-11441	9515 ± 70	9065 ± 70	Fm	6.5	Manley, 1995
	208–212	AA-11442	9245 ± 85	8795 ± 85	Fm	6.3	Manley, 1995
	236	TO-2472	8800 ± 70	8350 ± 70	Sf	124	MacLean et al., 1992
	261–263	AA-11443	9750 ± 70	9300 ± 70	Fm	3.3	Manley, 1995
	310–319	AA-11444	9410 ± 70	8960 ± 70	Fm	3.3	Manley, 1995
	406–412	AA-11445	10 170 ± 70	9720 ± 70	Fm	3.4	Manley, 1995
	497–499	TO-3274	9400 ± 190	8950 ± 190	Fm	5.8	Manley, 1995
	533–539	AA-10255	10 780 ± 140	10 330 ± 140	Fm	3.2	Manley, 1995
92028-153T	0–5	TO-3664	970 ± 70	520 ± 70	Fs	13.1	Manley, 1995
92028-155	920–925	AA-10256	11 170 ± 100	10 720 ± 100	Fm	2.9	Manley, 1995
93034-013	238	AA-13174	8915 ± 65	8465 ± 65	Sp[3]	15.1	Manley, 1995
	456–459	CAMS-19996	14 370 ± 180	13 920 ± 180	SFM	1.6	Manley, 1995
	658–669	CAMS-19255	33 320 ± 1810	32 870 ± 1810	SFM	2.0	Manley, 1995
93034-015	106	BETA-72892	1180 ± 50		Sp[6]	281	Schafer *in* Manley and Jennings, 1996
	305	BETA-72891	1700 ± 60		Sp[5]	750	Schafer *in* Manley and Jennings, 1996
	560	BETA-72890	2060 ± 40		Sp[5]	2070	Schafer *in* Manley and Jennings, 1996
	1300	BETA-78140	3340 ± 60		Sp	n.d.	Schafer *in* Manley and Jennings, 1996
93034-018	108	AA-13175	9125 ± 65	8675 ± 65	Sf[3]	11.8	Manley and Jennings, 1996
	396–399	CAMS-22023	8990 ± 80	8540 ± 80	Fm, O	1.8	MacLean *in* Manley and Jennings, 1996
	848–851	CAMS-22022	27 670 ± 440	27 220 ± 440	Fm, Sf	2	MacLean *in* Manley and Jennings, 1996
Western Hudson Strait							
85027-065	294–299	TO-293	6280 ± 50	6240 ± 50	S[4]	610	Vilks et al., 1989
85027-068	989–996	TO-751	7903 ± 70	7863 ± 70	Sf[3]	64	Vilks et al., 1989
90023-074	IKU	TO-3667	1300 ± 60	850 ± 60	Fs	18	MacLean *in* Manley and Jennings, 1996
90023-079	IKU	AA-10651	7840 ± 70	7390 ± 70	Fm	7.2	Manley and Jennings, 1996
90023-085	98–100	TO-3265	8170 ± 140	7720 ± 140	Fm	13.6	MacLean and Vilks *in* Manley and Jennings, 1996
90023-096	IKU	TO-3666	7940 ± 90	7490 ± 90	Fs	9.0	MacLean *in* Manley and Jennings, 1996
90023-097	340–342	TO-3266	7940 ± 920	7490 ± 920	Fm	8.2	MacLean *in* Manley and Jennings, 1996
90023-099	0–5	AA-12886	2180 ± 50	1730 ± 50	Fs	6	Kerwin, 1994
	150	TO-2470	8550 ± 160	8100 ± 160	Sf	30	Vilks *in* MacLean et al., 1992

Table 2. (cont.)

Core or IKU station	Core interval (cm)	Laboratory number	Reported age (^{14}C years BP)	Corrected age[1] (^{14}C years BP)	Material[2]	Weight (mg)	Published references
	316–320	TO-3269	7230 ± 830	6780 ± 830	Fm	4.7	Vilks *in* Manley and Jennings, 1996
	320–325	AA-12887	8270 ± 70	7820 ± 70	Sp[8]	4.3	Kerwin, 1994
90023-101	2–5	AA-10655	2655 ± 45	2205 ± 45	Fm	7.1	Kerwin, 1994
	158–160	TO-3270	8038 ± 510	7930 ± 510	Fm	5.8	Kerwin, 1994
	318–322	TO-3270	8740 ± 280	8290 ± 280	F	4.0	Kerwin, 1994
	360–362	TO-3272	8510 ± 110	8060 ± 110	F	4.8	Andrews et al., 1995
	366	AA-12888	8260 ± 60	7810 ± 60	Sp[3]	258	Kerwin, 1994
	558–560	TO-3273	8490 ± 270	8040 ± 270	F	4.0	Kerwin, 1994
	743–745	AA-10656	8920 ± 65	8470 ± 65	Fm	1.4	Kerwin, 1994
90023-104	90–95	AA-12889	8170 ± 60	7720 ± 60	S	14.8	Andrews et al., 1995
	320–325	AA-12890	8465 ± 90	8015 ± 90	Fm	1.6	Andrews et al., 1995
93034-022	710	Beta-78138	4070 ± 50		Sp	n.d.	Schafer *in* Manley and Jennings, 1996
	1238–1240	CAMS-18687	5090 ± 60		Fm	3.8	Schafer *in* Manley and Jennings, 1996
Ungava Bay							
90023-034	70–75	CAMS-10359	8240 ± 150	7790 ± 150	Fm	1.0	Andrews et al., 1995
90023-036	241	TO-2456	6630 ± 70	6180 ± 70	S	306	Andrews et al., 1995
	372	TO-2457	6850 ± 70	6400 ± 70	S[5]	363	Andrews et al., 1995
	828–829	TO-2458	7260 ± 70	6810 ± 70	Sf[6]	304	Andrews et al., 1995
93034-036	20	Beta-75312	890 ± 80		Ss	n.d.	Schafer *in* Manley and Jennings, 1996
	167–170	Beta-75311	1380 ± 60		Sp	n.d.	Schafer *in* Manley and Jennings, 1996
	1164	Beta-78141	2850 ± 90		S	n.d.	Schafer *in* Manley and Jennings, 1996
	1378	Beta-78139	3140 ± 60		Sg	n.d.	Schafer *in* Manley and Jennings, 1996
93034-038	940	CAMS-18690	8670 ± 60	8220 ± 60	S	19	MacLean *in* Manley and Jennings, 1996

[1] Radiocarbon dates have been normalized to -25%, and a correction applied for a marine reservoir effect of 450 ^{14}C years. 'Old' age dates and dates out of stratigraphic order are considered to result from the presence of reworked material.

[2] F, benthic foraminifers (Fs, single species; Fm, mixed species); Fp, planktonic foraminifers; O, ostracodes; S, shell; Sf, shell fragments; Sg, gastrapod; Ss, single valve; Sp, paired valves; Sv, valves; SFM, shells and foraminifers

[3] *Portlandia arctica*
[4] *Clinocardium ciliatum*
[5] *Macoma calcarea*
[6] *Nucula ternuis*
[7] *Nuculana pernula*
[8] *Yoldiella* sp.

n.d. = no data

The AMS radiocarbon dates (Table 2) obtained on foraminifers and on shell valves and fragments in cores from glaciomaine sediments in Western basin show age inversions and apparent poor chronological fits between cores that we infer reflect the presence of reworked material; however, of the dates obtained on foraminifers from core 90023-101 (Andrews et al., 1995; Manley and Jennings, 1996; MacLean, 2001, Fig. 5), two are relatively consistent stratigraphically: 8470 ± 65 BP from 743–745 cm, approximately 1.8 m below the glaciomarine ice-proximal–ice-distal boundary; and 8060 ± 110 BP from 360–362 cm, about the middle of the ice-distal sediments. Paired *Portlandia* sp. valves from 366 cm, approximately the same downcore depth as the latter, yielded a slightly younger, but relatively compatible date of 7810 ± 60 BP. Foraminifers from 158–160 cm just below the boundary between ice-distal and postglacial sediments in core 90023-101 yielded a date of 7930 ± 510 BP, but the broad potential error range renders it indefinite. In core

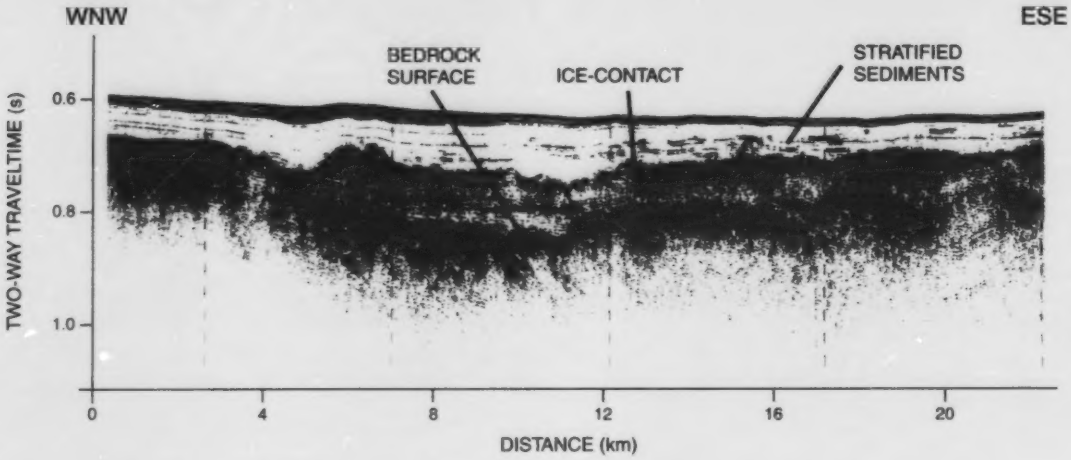

Figure 41. *Single-channel seismic-reflection profile oriented west to east along part of Western basin showing the main sediment units. Ice-contact deposits comprising two or more members locally totalling 90 m or more in thickness are overlain by acoustically stratified sediments. Stratification occurs locally within the lower unit approximately 8 km along section.* (Modified from *MacLean et al., 1986, Fig. 64.15.*) (See *Fig. 1 for location of section.*)

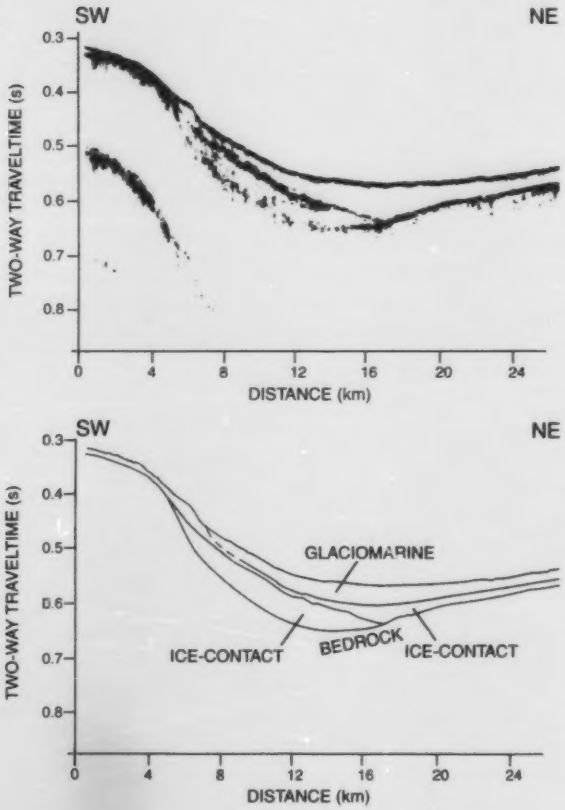

Figure 42.

Single-channel seismic-reflection profile showing sediment unit configuration along a transect across Western basin obliquely from southwest to northeast in the region north of Charles Island. Sediments that form the lower part of the ice-contact deposits are confined to the area on and adjoining the southern flank of the basin. (Modified from *Vilks et al., 1989, Fig. 10.*) *Reproduced with permission from Géographie physique et Quaternaire.* (See *Fig. 1 for location of section.*)

85027-068 (Fig. 44), 3 km to the north, fragments of a *Portlandia arctica* specimen apparently broken during splitting of the core, from 5.2 m below the top of sediments considered by Vilks et al. (1989) to be ice proximal, yielded an AMS radiocarbon date of 7863 ± 70 BP (Vilks et al., 1989). (Dates to which a 410 year reservoir correction was applied in some earlier publications have been adjusted to a 450 year correction in this report.) This date appears to be rather young for such an environment relative to the regional deglaciation database.

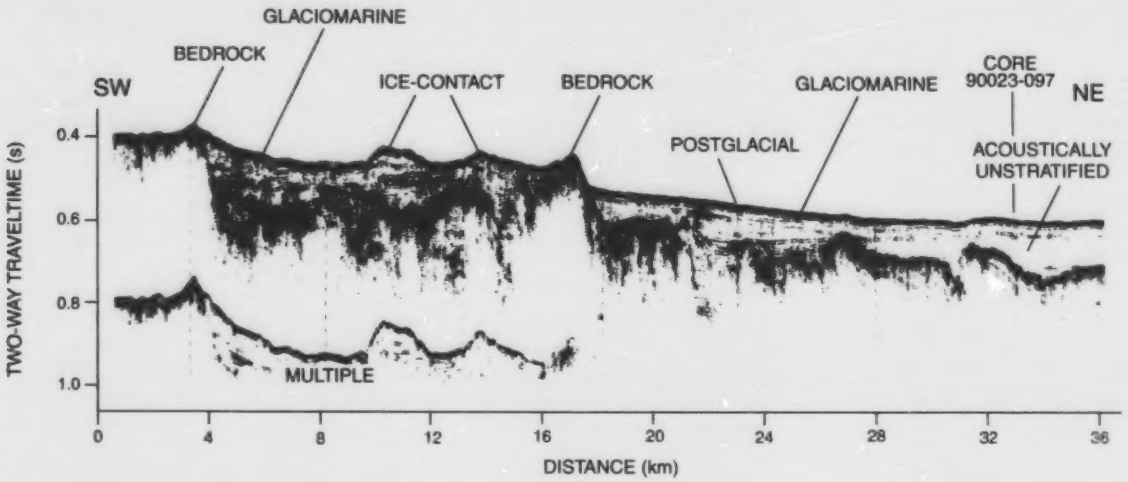

Figure 43. *Single-channel seismic-reflection profile showing very irregular sub-bottom morphology and Quaternary sediment deposits along a southwest to northeast transect across the western part of Western basin.* (Modified from *MacLean et al., 1986, Fig. 64.7.*) (See *Fig. 1 for location of section.*)

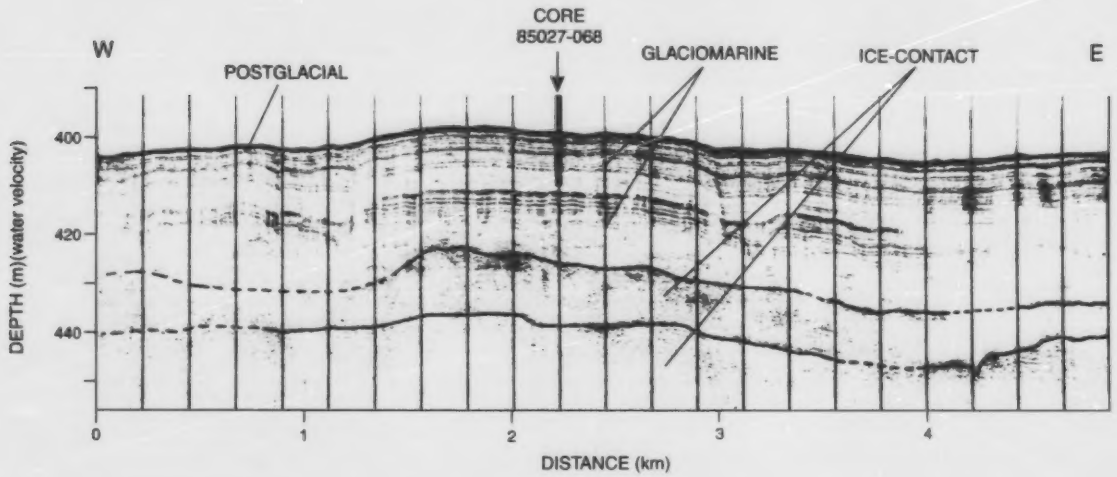

Figure 44. *Huntec™ high-resolution seismic-reflection profile along the axis of Western basin showing sediments in the vicinity of the extrapolated core 85027-068 locality. Eighteen metres of glaciomarine sediments are underlain by thick deposits of ice-contact sediments that comprise several members. One to two metres of postglacial sediments overlie the glaciomarine sequences.* (Modified from *Vilks et al., 1989, Fig. 8.*) *Reproduced with permission from Géographie physique et Quaternaire.* (See *Fig. 1 for location of section.*)

Locations of the main occurrences of postglacial sediments are indicated on Figure 1. Locally these deposits reach 18 m in thickness north of Charles Island in the central area of the basin (Fig. 5, 26). These are one of the thicker deposits of postglacial sediments in Hudson Strait. Acoustically, these beds range from weakly stratified to relatively transparent. They progressively thin toward the southern margin of the basin, and pinch out to the east and west along the basin axis. Core 93034-022 sampled the upper 12.5 m of these sediments. They primarily are grey and olive-grey bioturbated clayey sediments. Foraminiferal assemblages (J.A. Ceman, unpub. report, 1995) and AMS radiocarbon dates (uncorrected for reservoir effect) of 5090 ± 60 BP from near the bottom of the core and 4070 ± 50 BP from 710 cm (Schafer *in* Manley and Jennings, 1996; Table 2) confirm these as postglacial sediments. Extrapolated positions on seismic profiles suggest that core 90023-099 some 3.7 km to the west, which MacLean et al. (1992) had considered primarily of glaciomarine origin on the basis of preliminary faunal and chronological data, may have sampled these same sequences. Reservoir-corrected radiocarbon dates of 7820 ± 70 BP on paired *Yoldiella* sp. valves from the 320–325 cm interval, approximately at the ice-proximal–ice-distal boundary identified by Silis (1993), and 1730 ± 50 BP on foraminifers from 0–5 cm are the most reliable dates from core 90023-099 (Table 2).

Small pockets or thin veneers of postglacial sediments locally mantle older sediments and bedrock on the northern flank of Western basin and at other localities within and beyond the basin margins.

Southwestern basin

Ice-contact sediments are the dominant Quaternary sediment in terms of areal distribution. Thicknesses are variable, ranging from less than 1 m in the northeastern part of the basin adjacent to Charles Island to 30–50 m or more locally in southeastern and southwestern areas, and to more than 100 m in the west (Fig. 3). Thick deposits (up to 110 m) of acoustically dense material occur in a broad bedrock depression 15 km north of Colbert Promontory. It is not known whether or not this material is of glacial origin.

Acoustically rather similar sediments occur locally 30 km to the northeast where they form an elevated deposit 40 m thick. Morphology of the feature resembles a moraine, but it may be an erosional remnant. Attempts to sample this deposit with a large IKU™ clam-shell sampler were unsuccessful. The older sediments north and northwest of Colbert Promontory are overlain by ice-contact sediments that thicken westward where they reach in excess of 100 m. The upper part of that sequence terminates in a tonguing relationship with glaciomarine sediments northeast of Colbert Promontory (Fig. 18).

Acoustically stratified sediments deposited in glaciomarine ice-proximal and ice-distal environments are confined to the western half of the basin (Fig. 1) where they overlie and in places are transitional to ice-contact sediments (Fig. 18, 20). They generally range in thickness from 2 m or less to 15 m (Fig. 4). They are mainly laminated silty and clayey sediments containing scattered rock and clay clasts. But in the northwestern part of the basin the sediments sampled by core 90023-094, which are transitional to ice-contact sediments 18 km to the southwest, are in general siltier and sandier and contain many more clasts than those sampled farther south in the basin.

A very stiff grey clay, overlain by a few centimetres of coarse sediments, sampled at IKU™ station 90023-096, 38 km southeast of Nottingham Island, contains a foraminiferal assemblage typical of glaciomarine ice-proximal conditions. These microfossils yielded a reservoir corrected age of 7490 ± 90 BP (Table 2). The site (MacLean, 2001, Fig. 5) (approximately 1 km southwest of the area shown in Fig. 20) lies near the transition from thick glaciomarine sediments to ice-contact sediments southeast of Nottingham Island and south of Salisbury Island. These data suggest that this locality marks the approximate glacial ice limit southeast of Nottingham Island at ca. 7500 BP. This fits relatively well with Laymon's (1991) findings that residual ice remained on Nottingham Island until at least 7200 BP, and with a date of 7400 ± 290 BP on shells from a frost boil on Salisbury Island (Laymon, 1988) that provides a minimum age for deglaciation in that area.

A radiocarbon date of 7390 ± 70 BP (Table 2) was obtained 13 km north of Deception Bay in Southwestern basin (IKU station 90023-079) on foraminifers in a stiff clayey sediment, resembling that from station 90023-096. This sediment lies on ice-contact sediments, and is overlain by a thin gravel veneer. The foraminiferal assemblage is more typical of postglacial sediments, and suggests that deposition at that locality was removed from strong glacial influences; however, geotechnical measurements indicate that the stiff clayey sediments are overconsolidated and have undergone some loading (K. Moran, pers. comm., 1991).

Acoustically weakly stratified to transparent postglacial sediments extensively overlie glaciomarine sediments in the southwestern part of the basin (Fig. 1, 18). Where these deposits are well developed, acoustic stratification is weakest in the upper one-half to one-third of the postglacial sequence. The basal 1–2 m of the postglacial section locally contain brief, smoothly bounded discontinuities that have been infilled and covered by later sedimentation. Both upper and lower sequences thin and pinch out laterally. Where sampled at the core 90023-085 locality (MacLean, 2001, Fig. 5), these are mainly clayey and silty sediments, in part mottled and burrowed. Postglacial sediment thicknesses range from about 2 m to 9 m (Fig. 5).

Radiocarbon ^{14}C AMS ages obtained on postglacial sediments in Southwestern basin (Table 2) comprise: 7720 ± 140 BP on foraminifers in postglacial sediments 20 cm above the postglacial-glaciomarine faunal boundary in core 90023-085 (interval 98–100 cm); and 6240 ± 50 BP on a single valve of *Cliocardium ciliatum* from sediments in core 85027-065

(interval 294–299 cm). The latter core, originally considered to reflect distal ice retreat (Vilks et al., 1989) is now interpreted to be entirely in postglacial sediments on the basis of data from core 90023-085 (Jennings et al., 2001). Technical problems affected core recovery at both of these localities.

South-central Hudson Strait

The Héricart Bay–Wakeham Bay region bordering Ungava Peninsula in the south-central part of Hudson Strait (MacLean, 2001, Fig. 1) holds sediment deposits that are important sources of data relating to the late Quaternary history of the region. High-resolution and single-channel seismic-reflection profiles and eight piston cores provide information regarding depositional environments, late glacial ice extent, deglaciation, postglacial paleoceanographic conditions, and chronologies. Figures 1, 3, 4, and 5 outline the distribution and thickness of the principal sediment units.

High-resolution seismic profiles show that ice-contact sediments and overlying acoustically stratified sediments (glaciomarine and possibly marine) have been overridden by late glacial ice in several areas (Fig. 23, 24). Similarly, a 70 m thick morainal deposit 20 km north of Héricart Bay lies on acoustically stratified sediments (Fig. 12). Glacial ice that constructed this feature occupied the area shoreward of the moraine and eroded the beds previously deposited in that area (Fig. 12). Younger glaciomarine and postglacial sediments overlie the truncated beds and onlap the proximal side of the moraine. The pebble fraction in grab samples of surface sediments atop the moraine consisted predominantly (80%) of crystalline lithology, in contrast to samples from other localities in the strait where sedimentary rock fragments typically constituted 50% or more of the pebble fraction. The high crystalline composition of the rock fragments at the moraine suggest a northern Quebec origin for the ice that deposited that feature (R.A. Klassen *in* MacLean et al., 1986). The spatial geometry of the feature also points to that conclusion.

Figures 45 and 46 illustrate overriding and interfingering relations associated with deposition of ice-contact and glaciomarine sediments at and adjacent to the margin of a late glacial ice advance in the vicinity of cores 90023-107 and 92028-153 20 km north-northwest of the moraine, and in the core 90023-066 area, 18 km farther to the northwest (Table 1; MacLean, 2001, Fig. 5). At both localities, beds in the lower part of the glaciomarine sequence adjacent to the core sites have been overridden and variably remolded by the advancing ice that extended to within 1–2 km of the core locations. The upper part of the glaciomarine sequence was deposited contemporaneously with the ice-contact sediments of the advance. These relationships are best illustrated by Figure 46.

Sediments in the 90023-107 area (Fig. 1, 45) lie in what may have been an embayment or window in the grounded ice margin. Abrupt thinning of ice-contact sediments 8 km to the north (Fig. 6) appears to mark the limit of the late ice advance in that direction.

The section at the 90023-107 and 92028-153 localities (Fig. 45) contains 16 m of acoustically stratified glaciomarine sediments that lie on Paleozoic bedrock and thin deposits of ice-contact sediments. Up to approximately 3 m of postglacial sediments overlie the glaciomarine sediments (MacLean et al., 1992; Manley et al., 1993; Manley, 1995). Core 90023-107 sampled the upper 6.8 m of the glaciomarine section and 20 cm of the postglacial section. Core 92028-153 recovered a slightly thicker postglacial section and bottomed in the ice distal part of the glaciomarine sequence (Silis, 1993). Magnetic susceptibility profiles provide a good correlation between cores 90023-107 and 92028-153 (Manley et al., 1993; Manley, 1995).

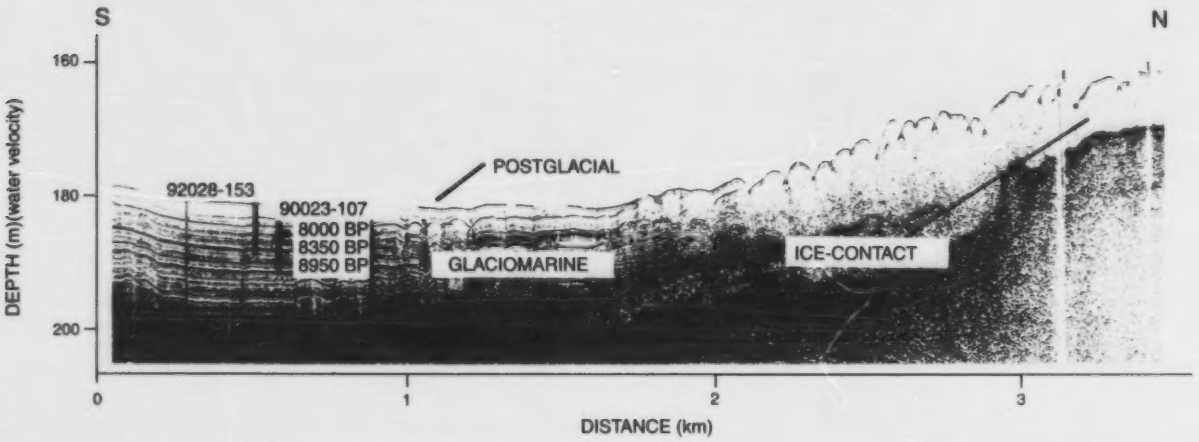

Figure 45. *Huntec™ high-resolution seismic-reflection profile illustrating glaciomarine sediments and lateral relationships with ice-contact sediments in the vicinity of the 90023-107 core site and extrapolated 92028-153 site north of Héricart Bay in south-central Hudson Strait. Chronological data shown are considered the most reliable of dates obtained from core 90023-107 (Table 2).* (Modified from *MacLean et al., 1991, Fig. 9, and MacLean et al., 1992, Fig. 10.) Reproduced with permission from Géographie physique et Quaternaire.* (See *Fig. 1 for location of section.)*

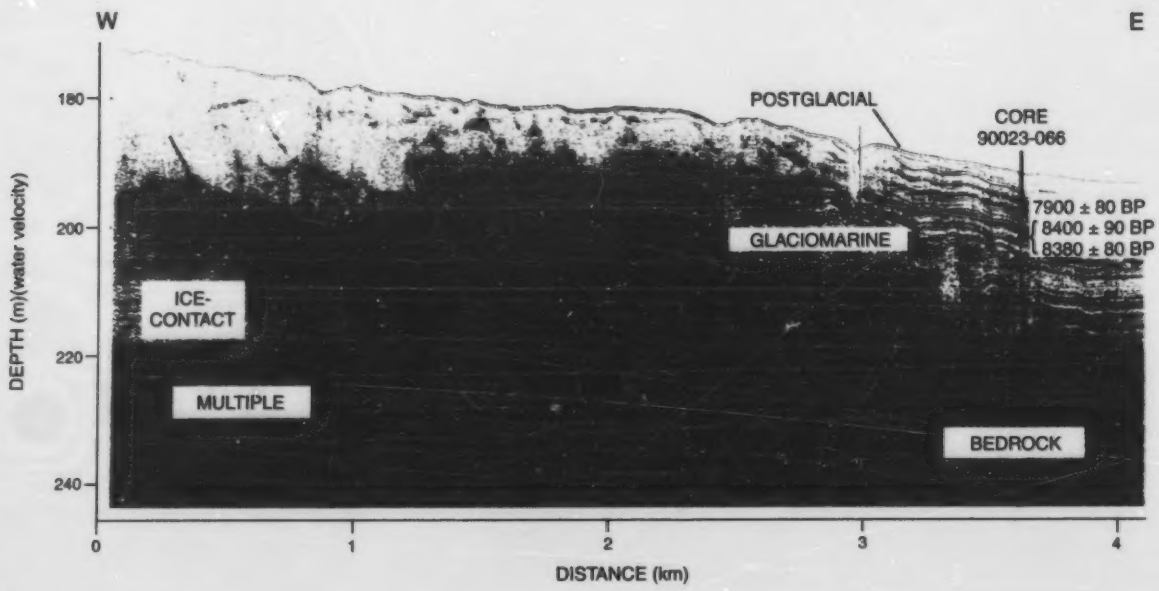

Figure 46. *Huntec™ high-resolution seismic-reflection profile displaying glaciomarine–ice-contact stratigraphic and facies relationships associated with a late glacial ice advance that overrode the earlier sediments to within less than 1 km of the core 90023-066 site in the Héricart Bay area. The glacial ice in this area was only lightly bearing on the previously deposited sediments. Selected radiocarbon dates are indicated.* (Modified from *MacLean et al., 1992, Fig. 11.*) *Reproduced with permission from Géographie physique et Quaternaire.* (See *Fig. 1 for location of section.*)

Core 90023-066 (Fig. 46) and core 93034-013 (Fig. 47) 8 km to the northeast, in the northern part of the Héricart Bay area, together provide the deepest sampling of the glaciomarine section in this region. The glaciomarine section at the core 90023-066 locality is 24 m in thickness (Fig. 46). The core sampled the upper 7.09 m of this succession together with 0.4 m of overlying postglacial sediments. The glaciomarine section is continuous between the 90023-066 and 93034-013 localities, but is reduced in thickness to 16 m in the latter area. Some condensation occurs within the section, but the thinner section at 93034-013 mainly is because the sediments that form the uppermost 5–6 m of the glaciomarine section at the 90023-066 locality are absent at the 93034-013 site. The beds sampled at the bottom of 90023-066 stratigraphically are approximately equivalent to those at the 2.2 m interval of 93034-013, which sampled an additional 6.7 m of the underlying beds. Radiocarbon dates on mollusc valves in glaciomarine sediments in core 90023-066 range from 7900 ± 80 BP (single valve) at a downcore depth of 230 cm to 8400 ± 90 and 8380 ± 80 BP (respectively on one single, and three intact specimens of *Portlandia arctica*) from depths of 728 cm and 743 cm, respectively. The latter dates correlate well stratigraphically with a date of 8465 ± 65 BP on paired *Portlandia arctica* valves from 238 cm depth in core 93034-013 (Table 2).

Foraminiferal assemblages suggest that the basal 5 m of core 93034-013 were deposited in more ice-proximal glaciomarine conditions than the overlying sediments where ice-distal conditions prevailed at that locality and during deposition of the bottom 2.5 m of core 90023-066. Upsection in core 90023-066 (upper 5 m) assemblages record the approaching proximity of the late ice advance (Silis, 1993; Jennings et al., 2001).

Further evidence of partial overriding of acoustically stratified sediments by a late ice advance is to be found in the Burgoyne Bay region 20 km to the southwest (Fig. 25; MacLean et al., 1992; MacLean, 2001, Fig. 1). Seaward of the late ice-contact deposits the sediment sequence contains some 25–30 m of acoustically stratified sediments, interpreted to be glaciomarine beds, overlain by equally thick deposits of postglacial sediments.

The westernmost core in this area of Hudson Strait, core 90023-071, from a locality 9 km off Wakeham Bay and 68 km northwest of the 90023-066 locality (MacLean, 2001, Fig. 5), also was sited near a former glacial ice-margin position (Fig. 48). Twenty-four metres of acoustically stratified glaciomarine sediments lie on ice-contact sediments and are overlain by 2–3 m of acoustically transparent postglacial sediments (MacLean et al., 1992). The core sampled the upper 5.76 m of the glaciomarine section plus 40 cm of overlying postglacial sediments. Foraminiferal assemblages (Silis, 1993) and X-radiographic and visual log data suggest that the glaciomarine ice-proximal–ice-distal boundary occurs near

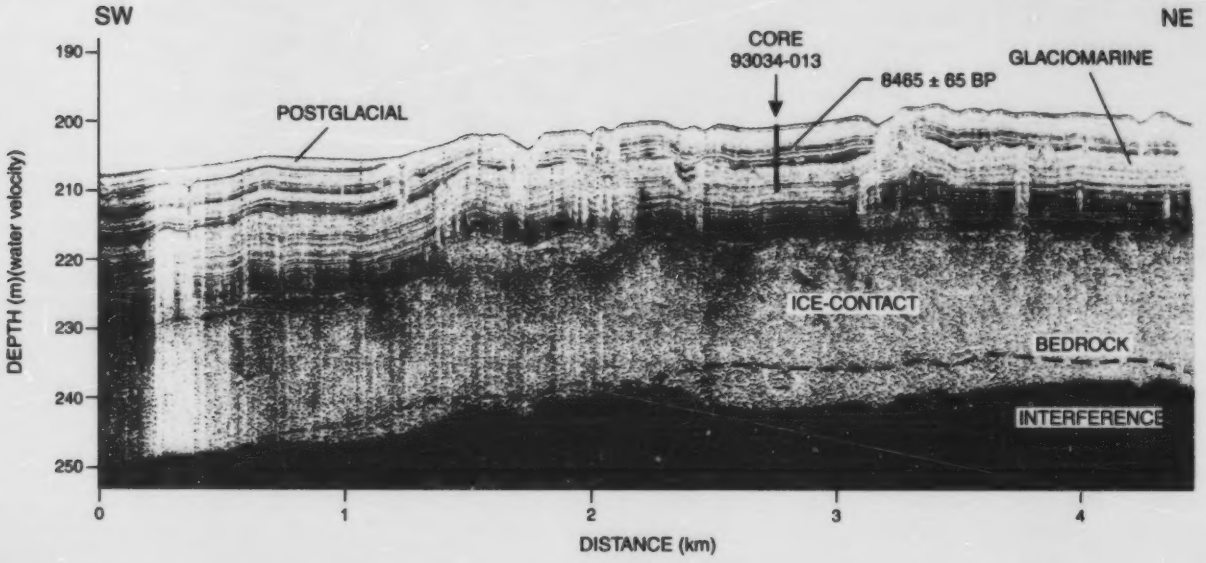

Figure 47. *Huntec™ high-resolution seismic-reflection profile showing the glaciomarine sediment section and underlying ice-contact sediments at the core 93034-013 locality in south-central Hudson Strait. The 2.5 m interval in core 93034-013 is stratigraphically equivalent to sediments at the bottom of core 90023-066. Stratigraphic position of the 8465 ± 65 BP dated interval is indicated. Identification of the bedrock surface is from single-channel seismic-reflection data. (See Fig. 1 for location of section.)*

the base of the core. This conforms with lateral glaciomarine–ice-contact facies relationships and vertical changes in the character of the acoustic reflectors (Fig. 48).

The suite of glaciomarine sediments and setting at each of the core localities in this area are essentially similar to, and for the most part, time equivalents of one another. Radiocarbon dates obtained from paired mollusc valves are considered to be reliable; however, age dates obtained on foraminifers have been problematic as exemplified by those from core 90023-107 (Table 2). Inconsistencies in benthonic foraminiferal assemblages, and age-date inversions indicate inclusion of reworked material in the glaciomarine section (Manley, 1995; Jennings et al., 2001). This reflects the proximity of an advancing glacial ice margin and of overridden glaciomarine or marine sediments near many of the core localities. Radiocarbon dates of 8380 ± 80 BP and 8465 ± 65 BP on paired mollusc valves from cores 90023-066 and 93034-013, respectively, cited earlier are considered to be reliable. Dates of 8120 ± 230 BP and 8480 ± 80 BP on mollusc valves from depths of 360–362 cm and 408 cm, respectively in core 90023-071 off Wakeham Bay (Table 2) are in good agreement with comparable dates from 90023-066 and 93034-013. Of the dates from core 90023-107 (Table 2), the 8000 ± 70 BP and 8350 ± 70 BP dates, respectively, on two *Portlandia arctica* valves and fragments, and mollusc fragments, appear to be the most accurate. Extrapolation of sedimentation rates between those dated intervals and the 8950 ± 190 BP interval suggests that it too may be correct (Manley, 1995).

Foraminifers from downcore intervals in core 93034-013 yielded dates of 13 920 ± 180 BP and 32 870 ± 1810 BP (Table 2). As noted by Manley (1995) the 32 870 BP date in particular, whether in situ or not, indicates that pre-late Wisconsinan sediments are present in south-central Hudson Strait. Similarly, a date of 25 210 ± 390 BP from marine shells on Maiden Island, 37 km northwest of the 90023-071 core locality (Bruneau and Gray, 1991), and dates in the 41 000–23 000 BP range from mollusc fragments reworked into till on Meta Incognita Peninsula, are indicative of pre-late Wisconsinan marine conditions in Hudson Strait (Blake, 1966; Manley, 1995).

The region offshore Héricart Bay possibly was peripheral to the western margin of the Noble Inlet ice (Manley, 1995). The core dates and seismostratigraphic relations indicate that a small further glacial advance began before 8500 BP and endured until deglaciation of the region ca. 8000–7800 BP. Preservation of overridden acoustically stratified glaciomarine sediments beneath acoustically relatively transparent ice-contact sediments at several localities suggests that the late glacial ice advance in the Héricart Bay region was only lightly bearing on the seabed (almost buoyant) and therefore relatively thin (MacLean et al., 1992; Manley, 1995).

Deposits of postglacial sediments up to 30 m thick occur in Burgoyne Bay (Fig. 25). This is one of the thickest occurrences of postglacial marine sediments in Hudson Strait. Where sampled by core 93034-015 the postglacial sediments are mainly dark grey to black bioturbated muds (Hardy, 2001;

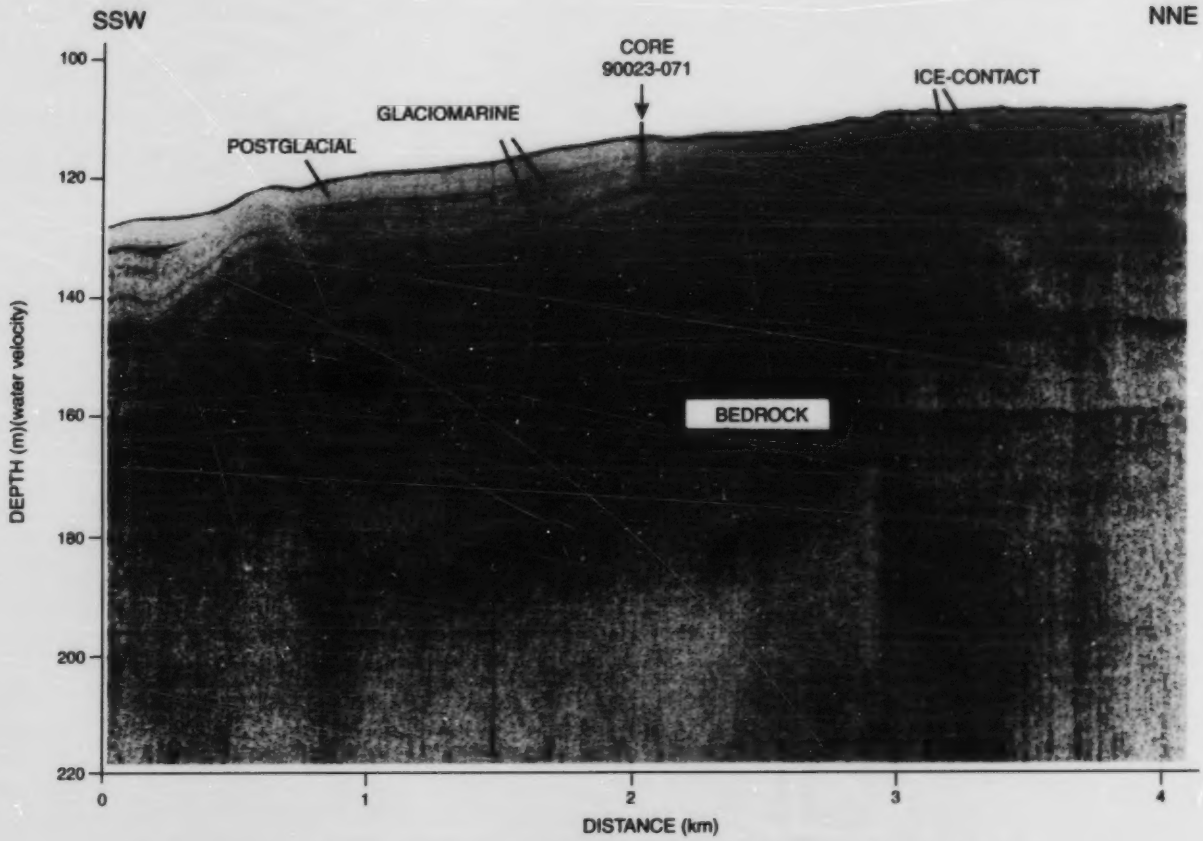

Figure 48. *Huntec™ high-resolution seismic-reflection profile illustrating sediment sequences and relationships in the vicinity of the extrapolated core 90023-071 locality offshore Wakeham Bay in south-central Hudson Strait. Glaciomarine sediments laterally are transitional to ice-contact sediments 3 km along section. Seventeen metres of stratified sediments underlie the interval that was cored. (*Modified from *MacLean et al., 1992, Fig. 15.) Reproduced with permission from Géographie physique et Quaternaire. (*See *Fig. 1 for location of section.)*

J.A. Ceman, unpub. report, 1994). Large deltaic deposits nearby on Ungava Peninsula (R.A. Daigneault, pers. comm., 1993) suggest a fluvial source for the extensive postglacial deposits in Burgoyne Bay, possibly related to drainage of glacial Lake Nantais (Gray, 2001). The AMS radiocarbon dates (uncorrected for reservoir effect) on molluscs in core 93034-015 ranged from 1180 ± 50 BP at a downcore depth of 106 cm to 3340 ± 60 BP at a depth of 1300 cm (Table 2; C. Schafer *in* Manley and Jennings, 1996).

North-central Hudson Strait

Glaciomarine sediments occur in a relatively small, isolated deposit 37 km southwest of Big Island (Fig. 1, 4, 49; MacLean, 2001, Fig. 1). Water depths are in the order of 345–350 m. Core 93034-018 sampled the upper 8.6 m of sediments. They comprise mainly clayey sediments with numerous fine silty and sandy laminae, and rhythmite sequences that are more prevalent lower in the section. These sediments are characterized on Huntec™ high-resolution profiles at the core site by relatively closely spaced parallel acoustic reflections. Laterally, they thin and become more irregular. Underlying beds display a coarser acoustic pattern with numerous discontinuities and deformations that become more pronounced toward the margins of the deposit. Approximately 2 m of postglacial sediments cover the underlying sediments at the core 93034-018 locality.

Foraminifers and a mollusc fragment from a downcore depth of 848–851 cm in core 93034-018, which approximates the top of the lower unit, yielded a radiocarbon date of 27 220 ± 440 BP (Table 2). Whether that is representative of those beds or results from inclusion of reworked material in the sediments is not known.

Radiocarbon dates of 8540 ± 80 BP on foraminifers and ostracodes from a depth of 396–399 cm and 8675 ± 65 BP on mollusc fragments from 108 cm downcore in core 93034-018

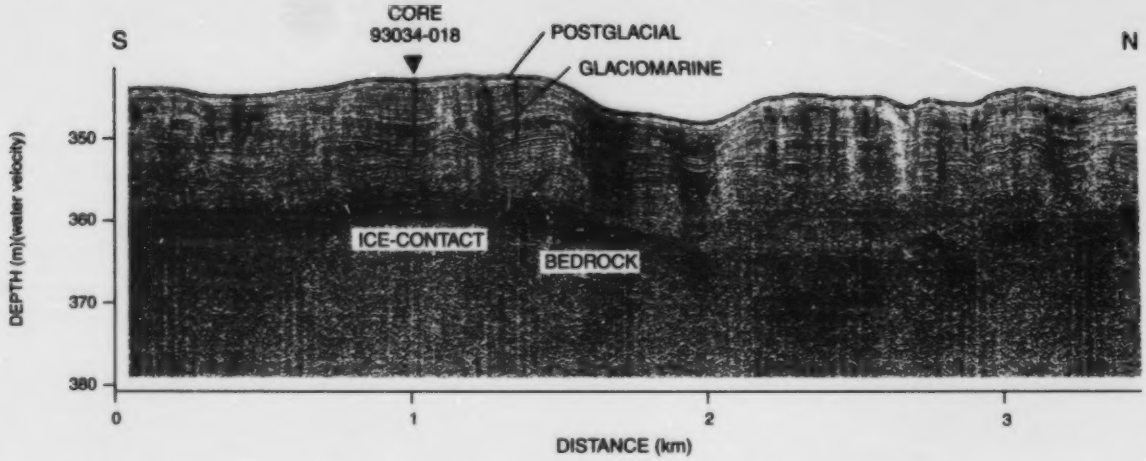

Figure 49. *Huntec™ high-resolution seismic-reflection profile showing the sedimentary setting at the core 93034-018 locality southwest of Big Island in north-central Hudson Strait.* (See *Fig. 1 for location of section.*)

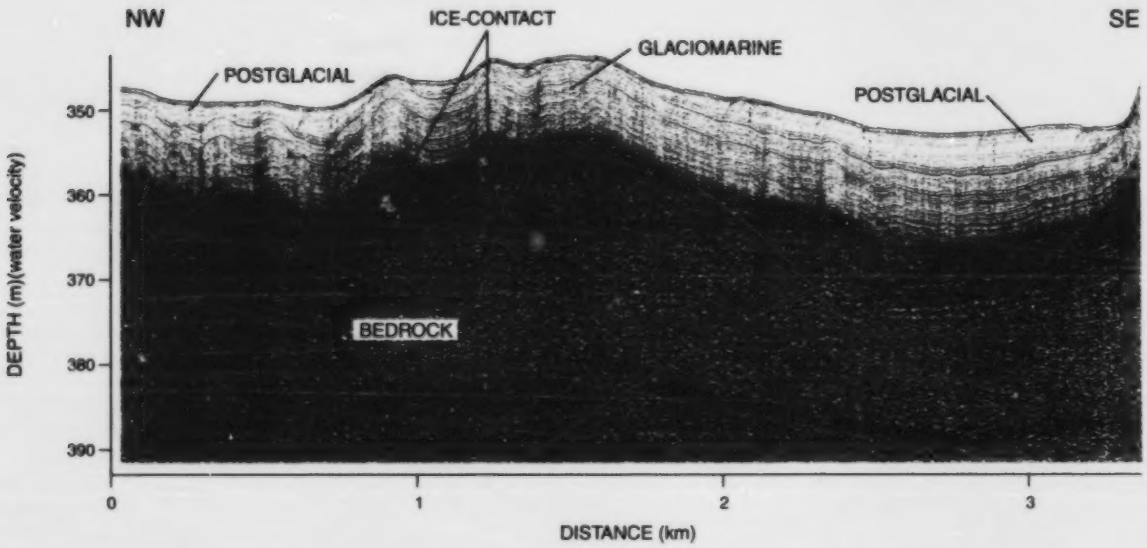

Figure 50. *Huntec™ high-resolution seismic-reflection profile illustrating sediments in the marginal channel in eastern Ungava Bay. Acoustically dense ice-contact deposits are overlain by acoustically stratified glaciomarine sediments in a draped depositional style. Postglacial sediments partly fill depressions on the surface of the glaciomarine sediments.* (See *Fig. 1 for location of section.*)

(Table 2) are stratigraphically inverted. This locality lies near the 8.5 ka southern limit of Baffin Island ice postulated by Stravers (1986).

Ungava Bay

Data from high-resolution and single-channel seismic-reflection profiles, four piston cores, and grab samples (MacLean, 2001, Fig. 4, 5) provide information on the main sediment units represented. These data extend and complement knowledge of the late Quaternary history of the Ungava Bay region derived from studies of the geological record on Akpatok Island and onshore areas around Ungava Bay primarily by J.T. Gray, B. Lauriol, M. Allard, O.H. Løken, C. Clark, and their colleagues (*see* Gray, 2001).

Deposition of Quaternary sediments in Ungava Bay has been strongly influenced by several factors. These include the pronounced seabed morphology comprising the shallow central platform and the bordering marginal channel (MacLean, 2001, Fig. 1); the complex glacial history, which also has been influenced by the morphology; the large drainage basin emptying into southern Ungava Bay; and bottom currents. The distribution of sediment units and the thickness of those deposits (Fig. 1, 2, 3, 4, 5) reflect the action and interaction of these various factors.

Marginal channel, east and southeast of the platform

Acoustically unstratified ice-contact sediments of unit 1 form the basal Quaternary deposits. The thickest occurrences of ice-contact sediments are adjacent to the coast along the east side of the bay. Multiple ice-contact sequences there locally total 150 m in thickness (Fig. 3, 9). Their location and configuration suggest deposition by glacial ice flowing into eastern Ungava Bay from the Labrador peninsula (MacLean et al., 1995). This is compatible with evidence for northwesterly flow of Torngat ice in the region south of Sheppard Lake on Labrador peninsula found by Gray et al. (1996). Ice-contact sediments elsewhere in the marginal channel in the eastern part of Ungava Bay mainly are in the order of 5–15 m in thickness. Sediments of this unit form the seabed throughout much of the eastern Ungava Bay area. They are overlain by acoustically stratified glaciomarine sediments that occur in a narrow belt along part of the western side of the eastern channel (Fig. 1, 50). The glaciomarine sediments at the southern end of that occurrence are truncated by a very smooth erosional surface (Fig. 51).

Glaciomarine sediments overlie ice-contact deposits in the southern part of the channel east and southeast of the platform (Fig. 1, 4). They were cored at three localities (Fig. 52, 53, 54; MacLean, 2001, Fig. 5). Cores 90023-034 and 90023-039 penetrated thin layers of postglacial sediments (approximately 1 m and 2 m thick, respectively) into underlying silty and clayey sediments that are variably laminated and in part bioturbated. Foraminiferal assemblages in core 90023-034 indicate a depositional environment under the influence of both glaciomarine and marine conditions (Silis, 1993; Jennings et al., 2001). An AMS radiocarbon age of 7790 ± 150 BP (Table 2) from a downcore depth of 70–75 cm approximately dates the end of glaciomarine conditions (Andrews et al., 1995). Ice-proximal conditions prevailed during deposition of strongly laminated and in part rhythmically banded sediments that form the lower 3.3 m of core 90023-039. Overlying sediments were deposited in environments similar to those in core 90023-034 (Silis, 1993). Core 93034-038 (Fig. 54; MacLean, 2001, Fig. 5) the longest of these cores, consists mainly of grey silty and clayey sediments that display extensive rhythmic banding and some clasts. Depositional environments were similar to those in cores 90023-034 and 90023-039 (Jennings et al., 2001). Postglacial sediments in core 93034-038 totalled only 50 cm (J.A. Ceman, unpub. report, 1994). Mollusc valves from the 940 cm interval yielded a radiocarbon date of 8220 ± 60 BP (Table 2).

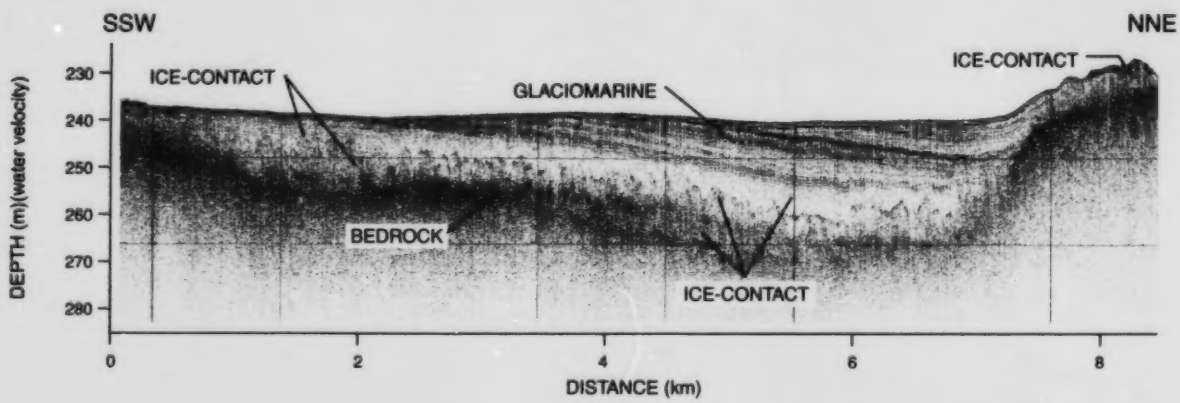

Figure 51. *Huntec™ high-resolution seismic-reflection profile showing a smooth erosional truncation of the glaciomarine sediments near the southern limit of their occurrence in the eastern marginal channel in Ungava Bay. (See Fig. 1 for location of section.)*

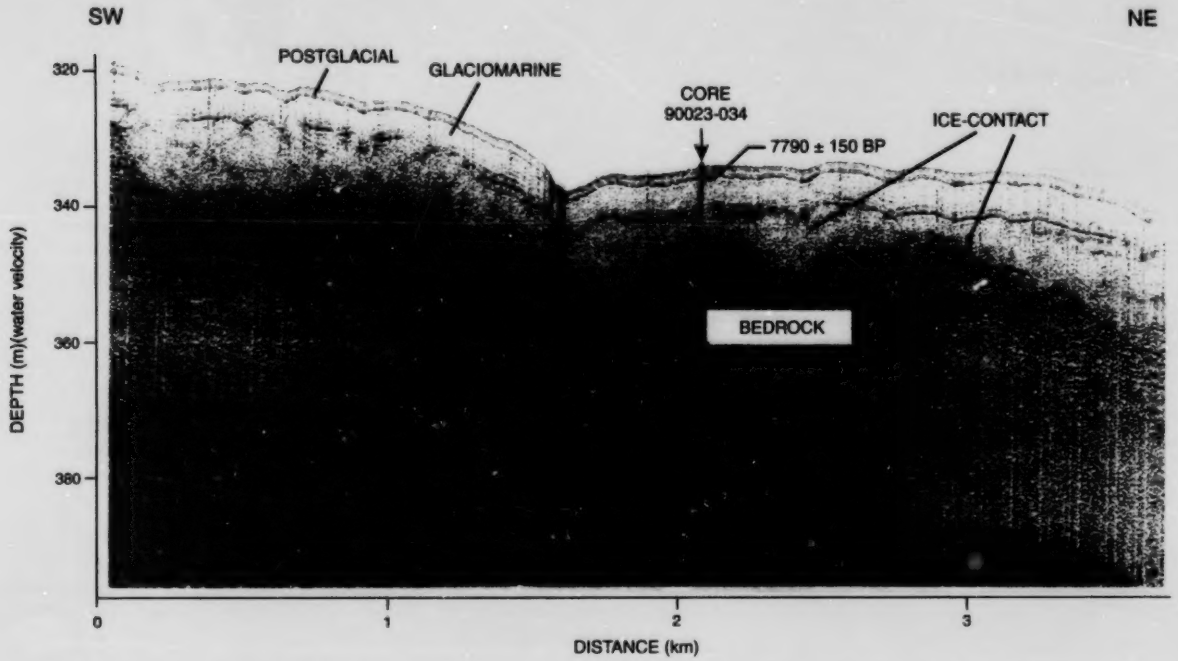

Figure 52. *Huntec™ high-resolution seismic-reflection profile showing sediment units at the core 90023-034 locality in eastern Ungava Bay. Five metres of glaciomarine sediments lie on ice-contact sediments and are overlain by 1–2 m of postglacial sediments.* (See *Fig. 1 for location of section.*)

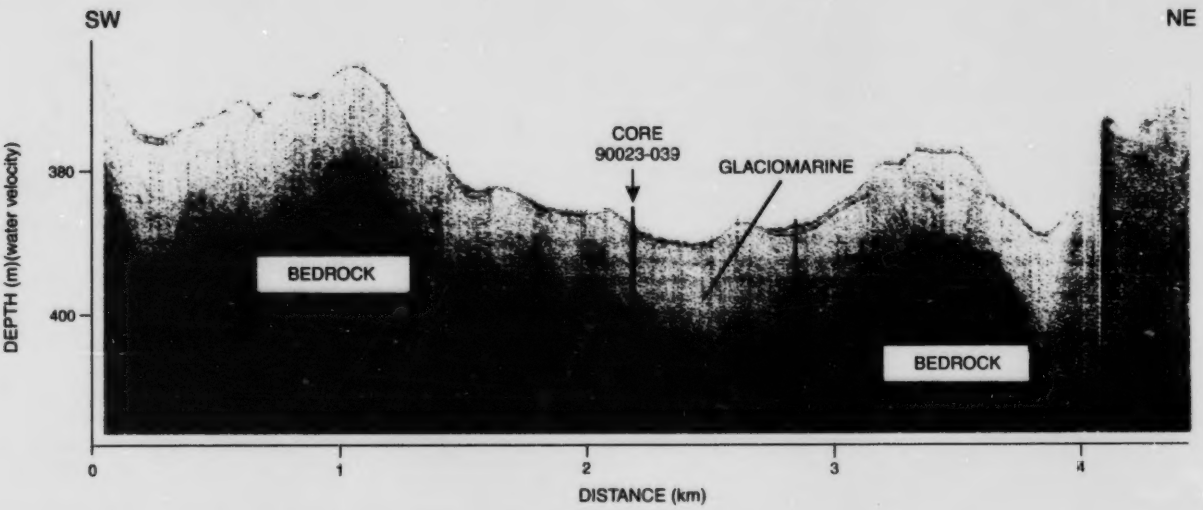

Figure 53. *Huntec™ high-resolution seismic-reflection profile illustrating the acoustic character of sediments at the core 90023-039 locality in eastern Ungava Bay.* (See *Fig. 1 for location of section.*)

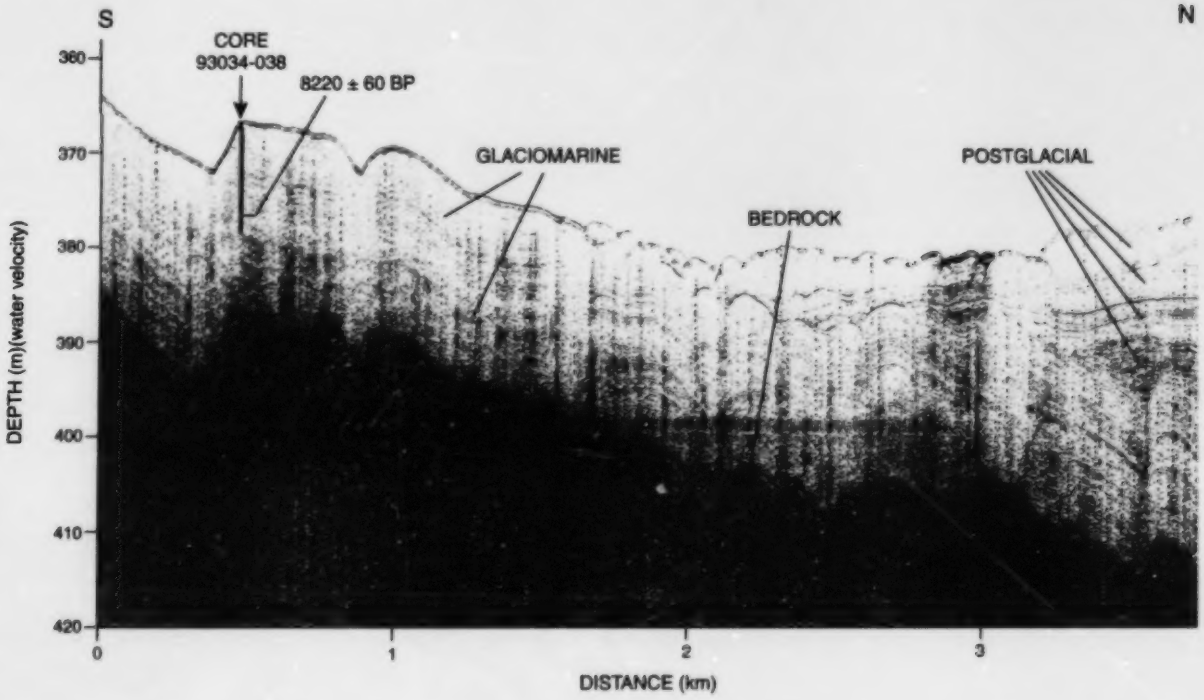

Figure 54. *Huntec™ high-resolution seismic-reflection profile showing sediments at the core 93034-038 locality in southeastern Ungava Bay (see Fig. 57 for a broader perspective of the setting). Glaciomarine sediments appear to lie directly on bedrock and to constitute the entire Quaternary section at this locality except for 0.5 m of postglacial sediments at the seabed (not visible on the acoustic profile). The acoustic stratification and draped depositional style are typical of glaciomarine deposits elsewhere, but resolution of acoustic reflectors associated with these sediments in this region of eastern Ungava Bay is less distinct than in most localities in Hudson Strait. (See Fig. 1 for location of section.)*

Postglacial sediments with progradational internal reflections locally overlie glaciomarine and ice-contact sediments adjacent to the platform in the vicinity of a bathymetric constriction in the marginal channel near 60°N (Fig. 55, 56, 57). The physical setting of these occurrences suggests they resulted from the action of bottom currents around the central platform. Where sampled by core 90023-036 (Fig. 55, 56; MacLean, 2001, Fig. 5) these are mainly laminated silty and clayey sediments containing some thin sand layers, and intervals of alternating black and grey silty clay each some 4–6 cm thick. The AMS radiocarbon ages obtained on mollusc shells in these sediments ranged from 6180 ± 70 BP to 6810 ± 70 BP (Table 2).

Marginal channel, south

The marginal channel south of the central platform contains ice-contact, glaciomarine, and postglacial sediments whose combined thickness in places exceeds 60 m. Figures 58 and 59 illustrate the variable stratigraphy in this area.

Ice-contact sediments are 10–20 m thick in the eastern part of this region, a continuation of the thick sequences along the eastern side of the channel seen farther north. In the southern part of the channel where Quaternary sediments infill and variably cover the very irregular surface on the Precambrian bedrock (Fig. 59), reliable differentiation of sediment units becomes difficult. Acoustically unstratified and stratified sediments are variably superimposed on one another, and lateral changes in extent and acoustic character are frequent (Fig. 59). In places these resemble ice-contact–glaciomarine sediment transitions observed in other localities, and they may be indicative of similar relations in this area; however, a variety of depositional mechanisms and environments may be represented. Glaciomarine sediments locally have been incised by erosional processes (Fig. 60).

Postglacial sediments in the central part of the southern marginal channel reach 30 m or more in thickness (Fig. 27), one of the thickest deposits of postglacial sediments in the Hudson Strait–Ungava Bay region. These sediments were sampled by core 90023-059 in 1990, and again in 1993 at

approximately the same location by core 93034-036 (Table 1) in order to sample deeper in the sediment section. Both cores bottomed in postglacial sediments. These mainly are dark grey to black bioturbated clayey sediments. Foraminiferal assemblages are essentially similar to those recognized in core 90023-059 by Vilks (*in* MacLean et al.,1992) and to those in thick postglacial sequences in the central and western parts of Hudson Strait (J.A. Ceman, unpub. report, 1995; Jennings et al., 2001; C. Schafer, J. Ceman, B. MacLean, F. Cole, G. Vilks, work in progress, 2001). Radiocarbon dates obtained on mollusc and cephalopod shells in core 93034-036 range from 890 ± 80 BP at a downcore depth of 20 cm to 3140 ± 60 BP at a depth of 1378 cm (Table 2; J.A. Ceman, unpub. report, 1995; Schafer *in* Manley and Jennings, 1996). No reservoir correction has been applied to those dates because of uncertainty as to an appropriate correction factor. The thick deposits of postglacial sediments in this area may reflect fluvial input from the large drainage basin that empties into southern Ungava Bay (MacLean et al., 1992). This may affect reservoir retention time.

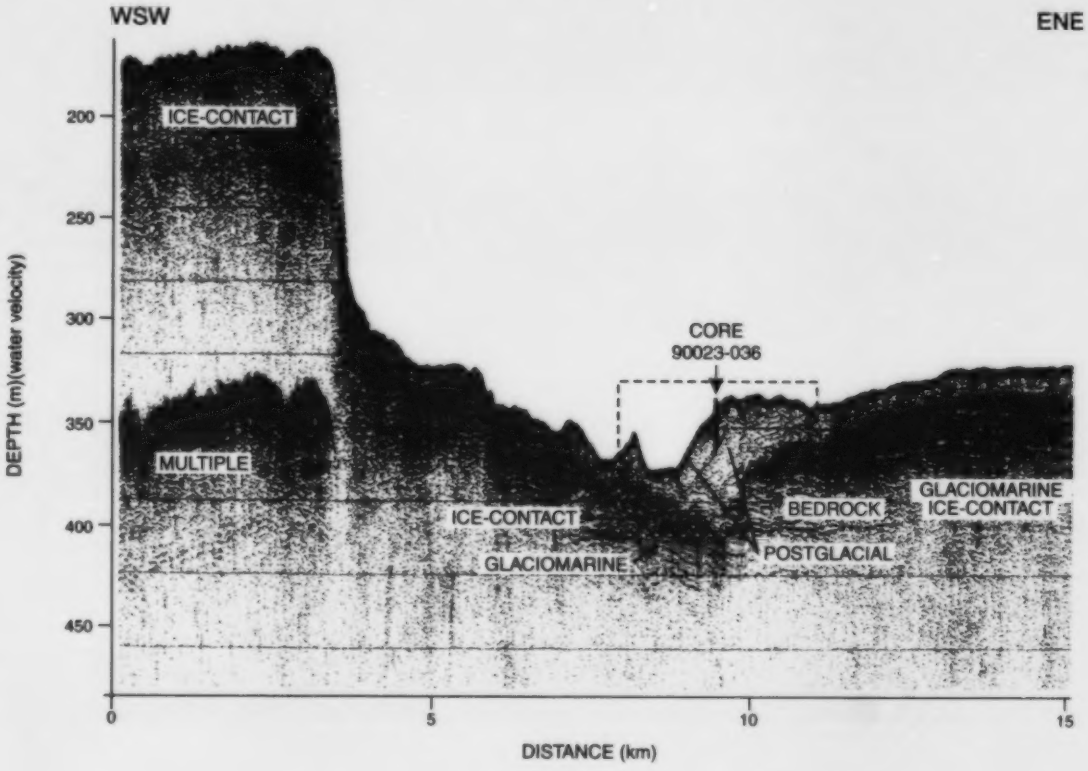

Figure 55. *Single-channel seismic-reflection profile showing morphology and sediment deposits that overlie Paleozoic strata adjacent to the platform in a bathymetrically constricted area in eastern Ungava Bay just south of 60°N latitude. Prograded postglacial sediments 10 km along section are shown in more detail in Figure 56.* (See *Fig. 1 for location of section.*)

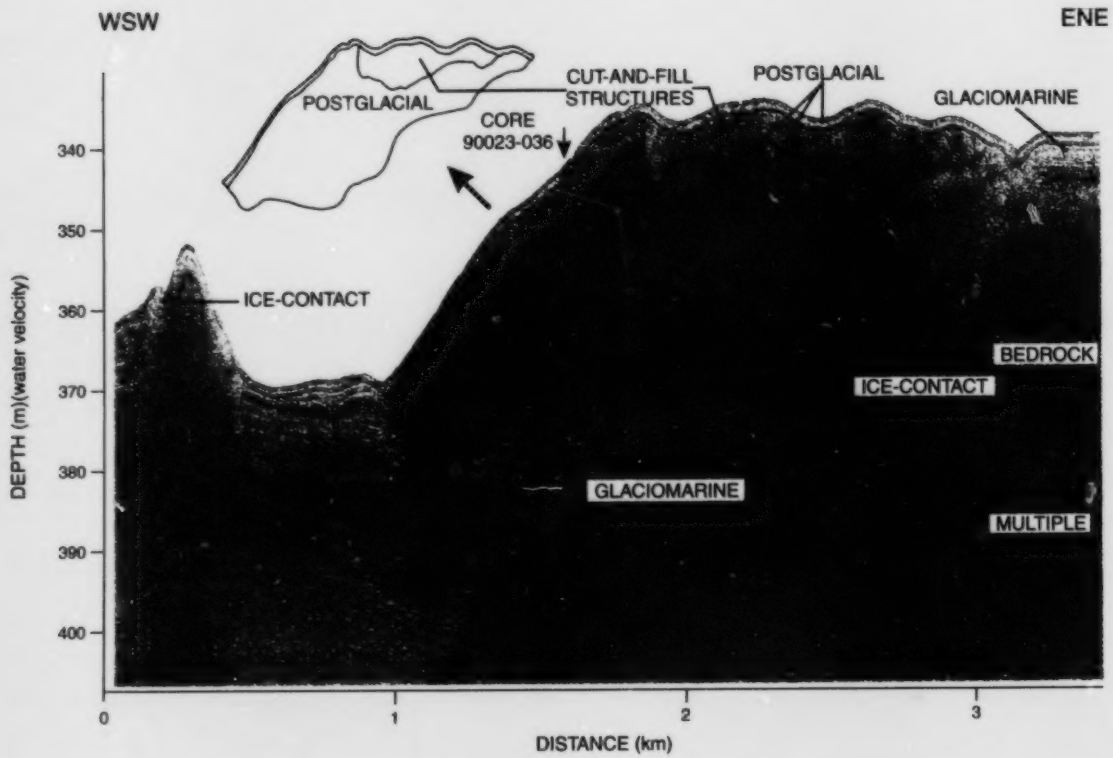

Figure 56. *Huntec™ high-resolution seismic-reflection profile illustrating prograded postglacial sediments that occur in the area indicated on Figure 55. These sediments lie unconformably on glaciomarine and ice-contact sediments. Their origin is attributed to water-current patterns adjacent to the platform margin and bathymetric constrictions in eastern Ungava Bay. The core 90023-036 locality is indicated.* (Modified from *MacLean et al., 1991, Fig. 5; and Andrews et al. 1995, Fig. 6E.) Quaternary Science Reviews, v. 14, p. 983–1004,* © *1996. Reprinted with permission from Elsevier Science.* (See *Fig. 1 for location of section.)*

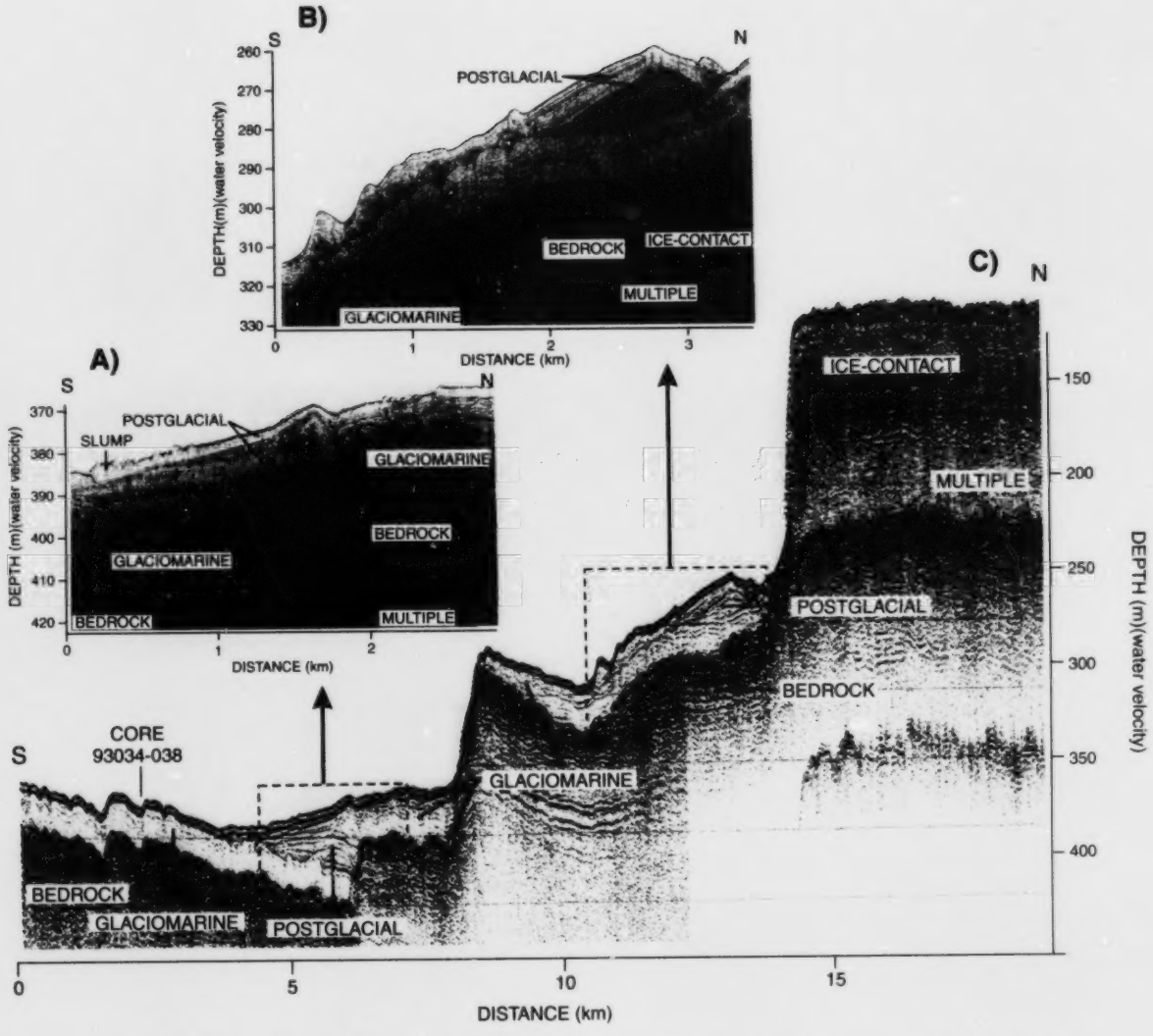

Figure 57. *Single-channel seismic-reflection profile further illustrating the morphological and geological setting adjacent to the central platform in eastern Ungava Bay. Insets show sediment deposits attributed to the action of water currents adjacent to the steep escarpments. Location of core 93034-038 is indicated. The boundary between Precambrian and Paleozoic rocks occurs 6 km along section.* (See *Fig. 1 for location of section.*)

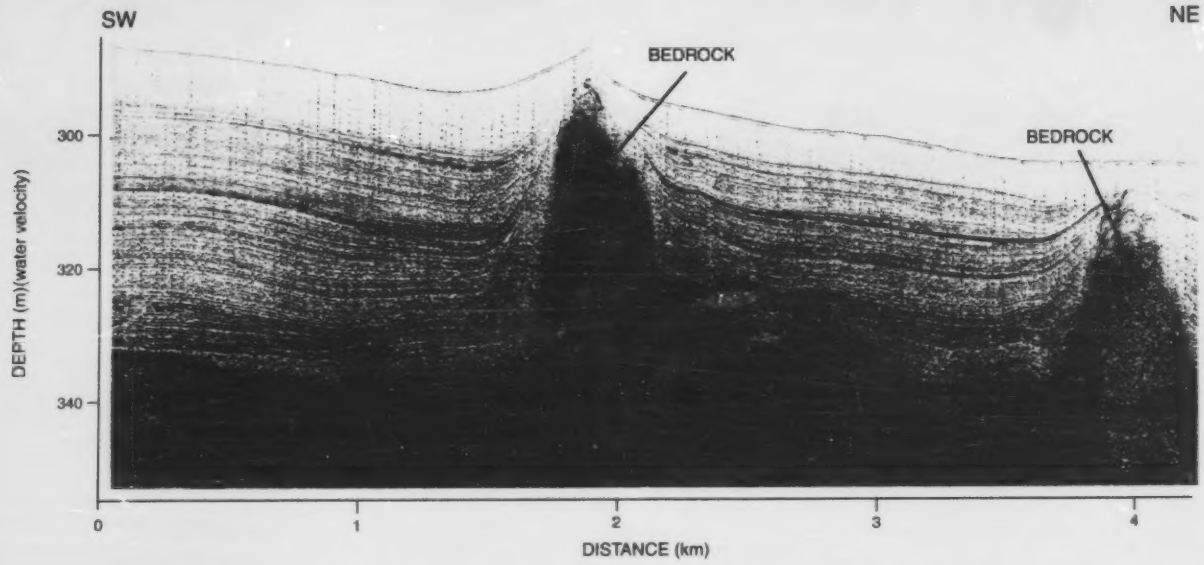

Figure 58. *Huntec™ high-resolution seismic-reflection profile showing thick sediment deposits that infill and overtop the irregular bedrock morphology in southern Ungava Bay (MacLean et al., 1991, Fig. 6). (See Fig. 1 for location of section.)*

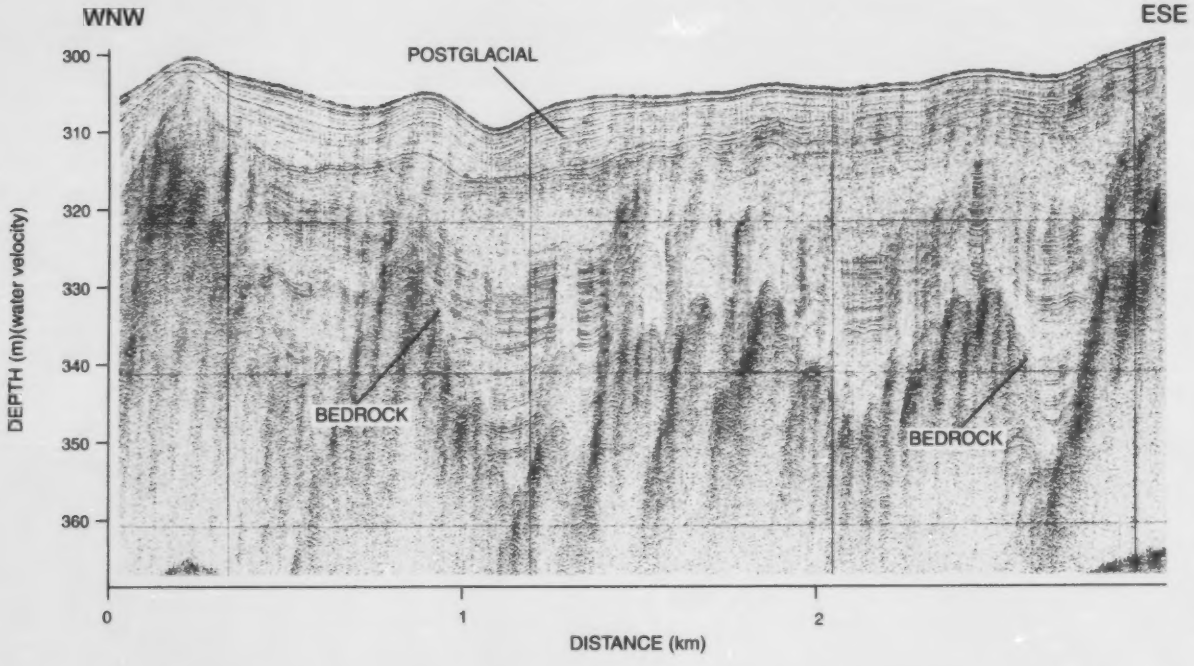

Figure 59. *Huntec™ high-resolution seismic-reflection profile illustrating sediment sequences in the marginal channel south of the platform in Ungava Bay. Acoustically unstratified sediments variably overlie, underlie, and laterally interrupt acoustically stratified sequences. (See Fig. 1 for location of section.)*

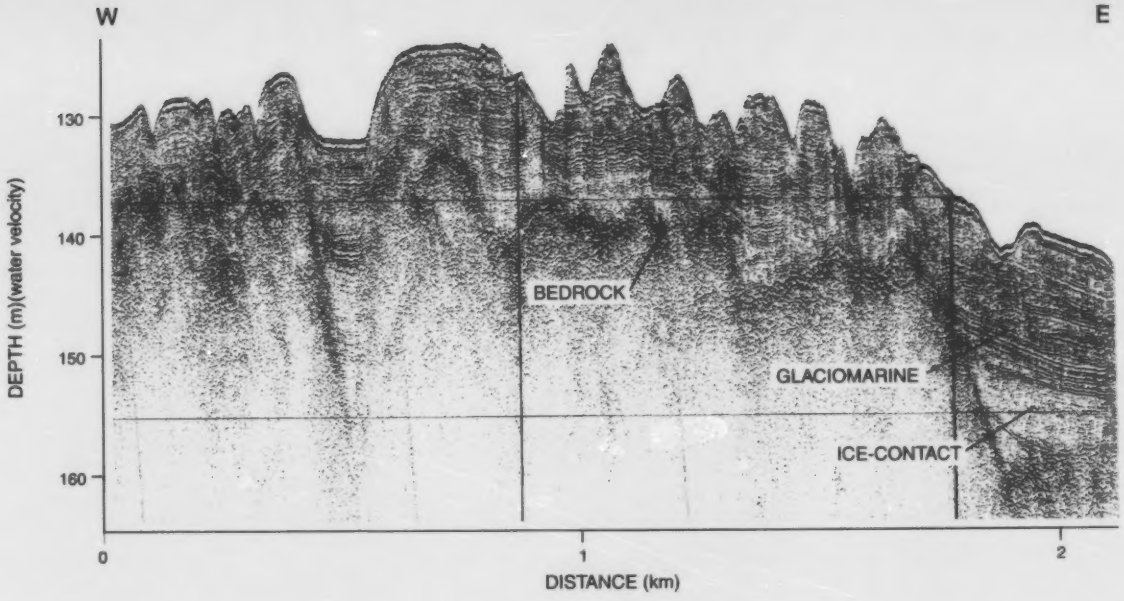

Figure 60. *Huntec™ high-resolution seismic-reflection profile illustrating erosionally incised glaciomarine sediments in 130 m water depth observed locally on the southernmost Huntec™ transect (west-east) in southern Ungava Bay.* (See *Fig. 1 for location of section.*)

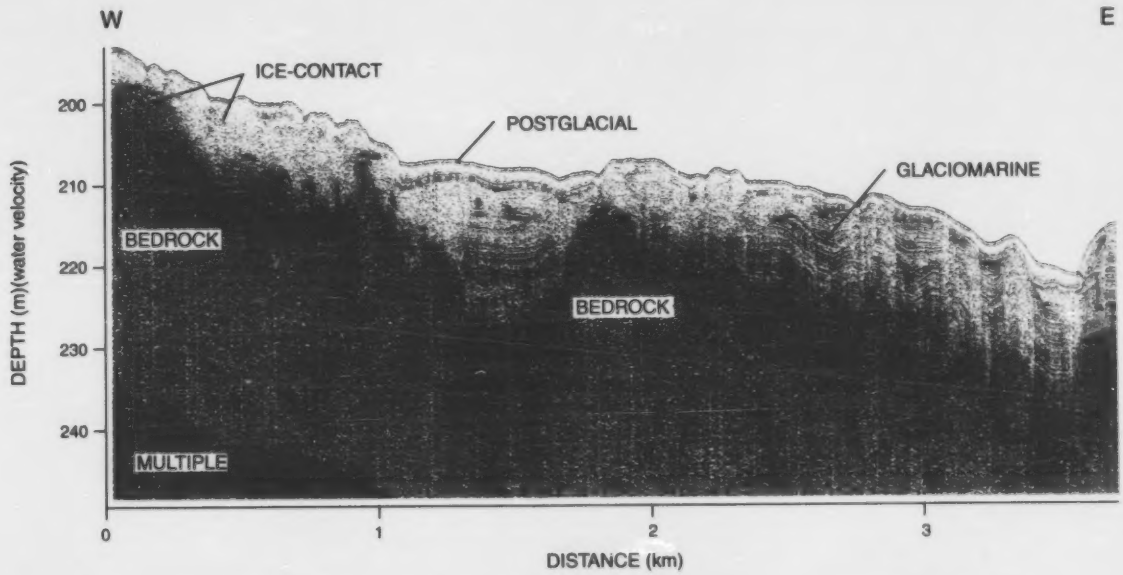

Figure 61. *Huntec™ high-resolution seismic-reflection profile south-southwest of Akpatok Island showing glaciomarine sediments that have been overridden and partly eroded by a subsequent glacial advance. Ice-contact to glaciomarine facies transitions also appear to occur.* (See *Fig. 1 for location of section.*)

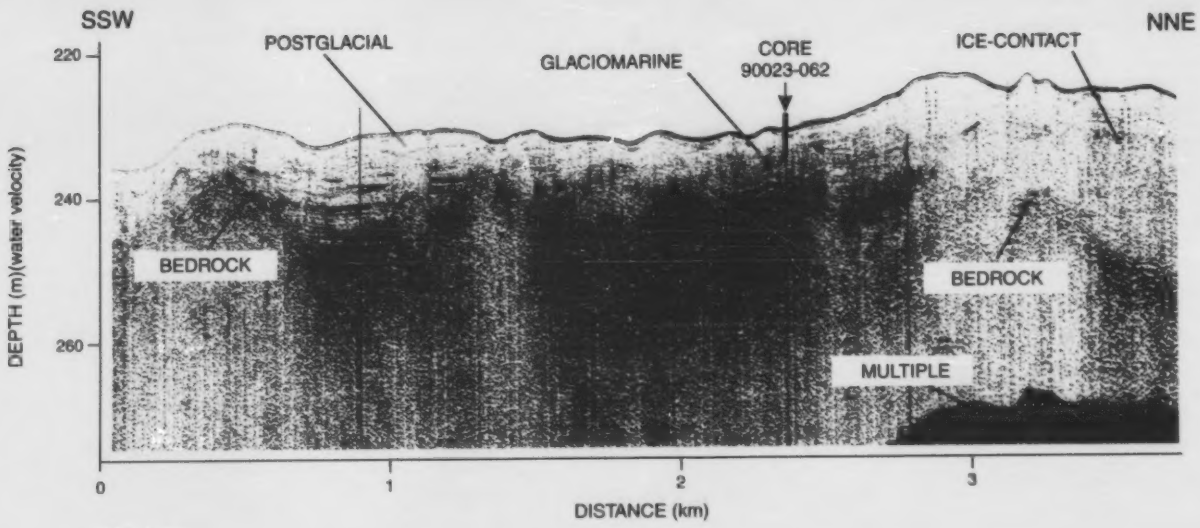

Figure 62. *Huntec™ high-resolution seismic-reflection profile showing the geological setting in the vicinity of the core 90023-062 locality west of Akpatok Island. As in Figure 61 relationships suggest impingement of glacial ice and sediments on glaciomarine sediments, and ice-contact–glaciomarine facies transitions. (See Fig. 1 for location of section.)*

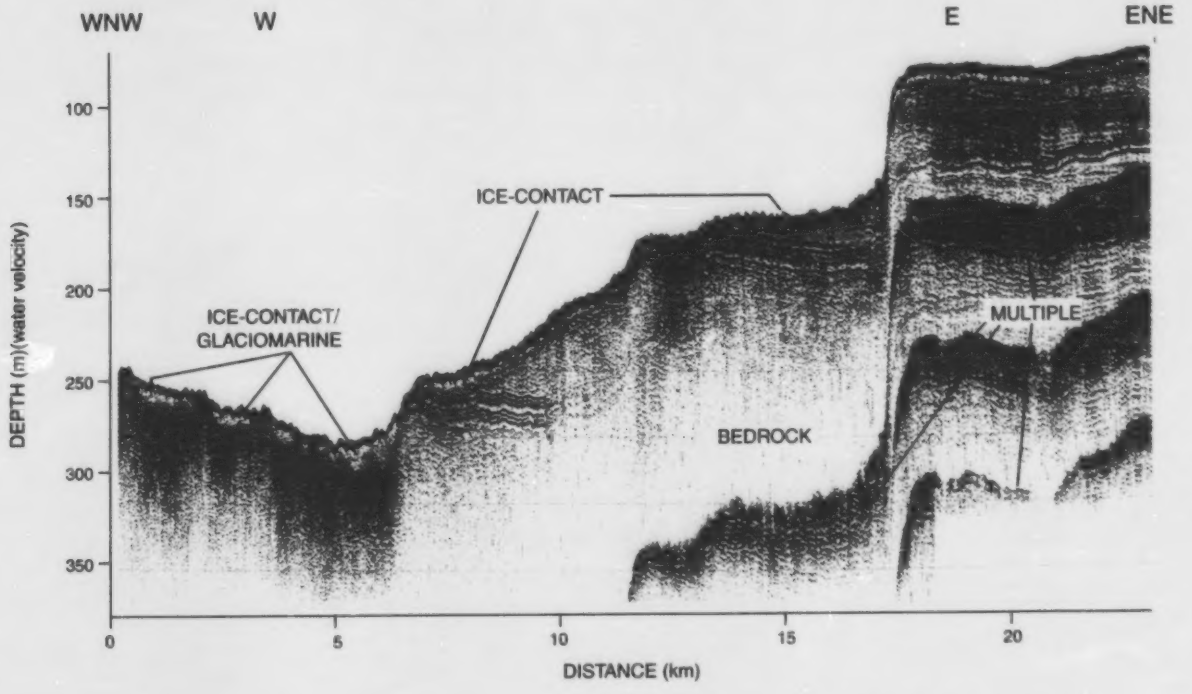

Figure 63. *Single-channel seismic-reflection profile illustrating the morphological and sediment setting at the margin of the central platform northwest of Akpatok Island. Surficial sediments on the platform adjacent to the margin are thin (1–2 m) to absent in this area. The boundary between Precambrian and Paleozoic rocks occurs 6.4 km along section. (See Fig. 1 for location of section.)*

Marginal channel, west

Ice-contact sediments are the principal sediment unit in the marginal channel along the west side of the platform (Fig. 1). Deposits commonly range from 4–12 m in thickness, but locally reach 30–40 m where multiple sequences occur (Fig. 3). Glaciomarine sediments, up to 20 m thick, and postglacial sediments (up to a few metres) are confined to bathymetric deeper areas southwest and west of Akpatok Island (Fig. 1, 4, 5; MacLean, 2001, Fig. 1). Relationships displayed on high-resolution seismic-reflection profiles indicate that glaciomarine sediments in part have been overridden by glacial ice that deposited ice-contact sediments (Fig. 61, 62). The later ice-contact sediments in places are transitional laterally to glaciomarine sediments.

Core locality 90023-062 lies near such a facies transition (Fig. 62). Foraminiferal assemblages indicate that sediments composing the lower 100 cm of the core were deposited in an ice-proximal environment. The overlying 120 cm of sediments contain some marine foraminiferal elements in addition to those that are typically glaciomarine. Postglacial sediments compose the top 20 cm of the core (Silis, 1993). The ice-proximal zone is mainly a clay-rich, grey sediment with some clay clasts, whereas the overlying zone contains a greater amount of sand grains and granules (Silis, 1993). Andrews et al. (1995) suggested that high magnetic susceptibility values for core 90023-062 may indicate that the sediments at this locality mainly were derived from the nearby Precambrian terrain.

West of the deeper water areas of the western channel (MacLean, 2001, Fig. 1) ice-contact sediments infill and cover an irregular morphology on Precambrian rocks. Locally they overlie acoustically stratified sediments in some of the bedrock depressions.

Central platform

High-resolution seismic data indicate that Paleozoic rocks that compose the shallow central platform in Ungava Bay are variably mantled by acoustically unstratified sediments that range in thickness from less than 1 m to about 5 m (Fig. 1, 2, 3). These are interpreted to be mainly ice-contact sediments. Figures 55, 57, and 63 (*see also* MacLean, 2001, Fig. 2) illustrate the platform margin morphologies, sediment deposits on the platform shoulders, and the generally thin sediments that commonly mantle the outer areas of the platform top. Unstratified sediment deposits up to 9 m thick occur near the

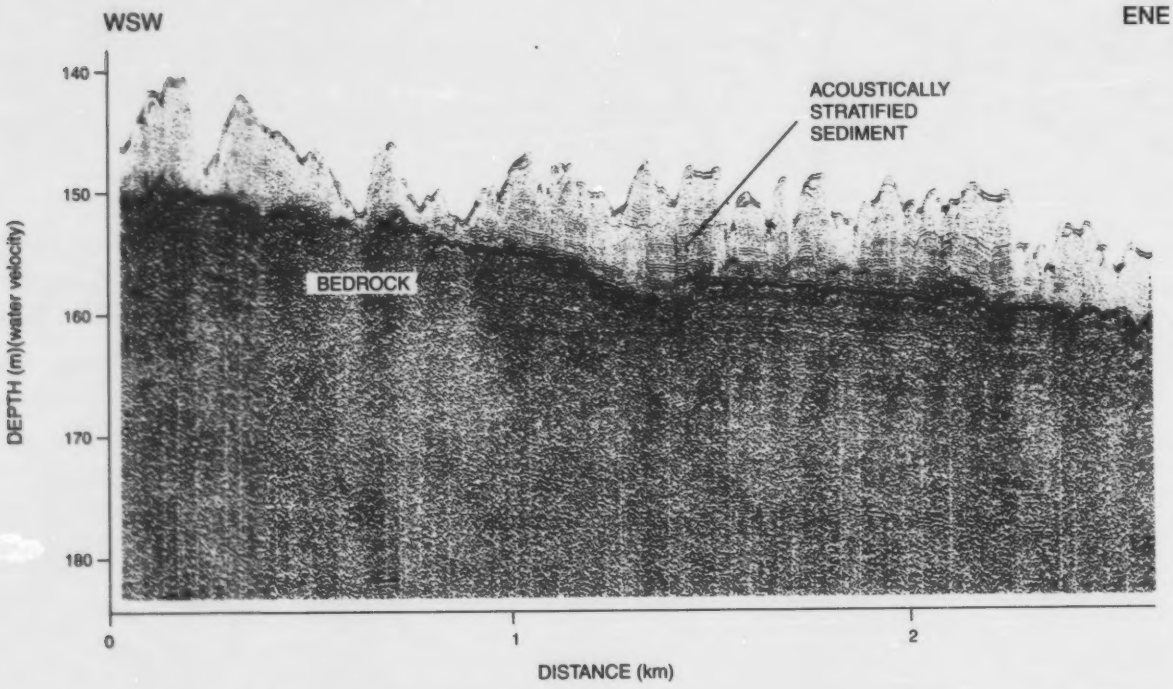

Figure 64. *Huntec™ high-resolution seismic-reflection profile illustrating very irregular surface morphology developed locally on sediments on the shoulder of the central platform in southeastern Ungava Bay. For the most part the sediments are acoustically unstratified, but locally sediments with acoustic stratification typical of glaciomarine sediments occur.* (See *Fig. 1 for location of section.*)

platform margin in the south and southeast. Locally in the southeast these include deeply incised acoustically stratified and unstratified sediments (Fig. 64).

Low ridges of ice-contact sediments have been intersected in a few localities by survey traverses. The most prominent of these are in a region 42 km east and east-southeast of southernmost Akpatok Island. Sediment thicknesses in some of these ridges reach in excess of 10 m (Fig. 65). These features lie in a region where northerly ice flow is inferred from terrestrial data (Gray et al., 1994; Gray, 2001) and they are interpreted to be glacial flutings. In profile they resemble glacial flutings in Lake Ontario delineated by Lewis et al. (1997) by means of high-resolution seismic profiling and swath-mapping systems. Sidescan sonograms acquired simultaneously with the seismic data in this area show shallow, ice-keel scour marks that trend approximately north-south (Fig. 66). The parallel-subparallel orientation and the size and shape of these scour features suggest they are ice-sheet sole marks on the surface of the flutes. Small ridges resembling moraines were encountered at two localities in this general area, one 33 km to the east (Fig. 67), and the other 20 km to the southeast (Fig. 14). Several small ridges or mounds also were intersected in the area between these features, and in the area that lies between them and the platform margin to the southwest. Northeast of these morainal features, small accumulations occur in a few localities, but for the most part sediments across the platform in that direction are very thin and possibly discontinuous to about 60°N, where continuous deposits a few metres in thickness resume in conjunction with increasing water depths. The change occurs at a present-day water depth of approximately 130 m.

Generally thin sediments were encountered northeast of Akpatok Island (Fig. 2). Thicknesses reach a few metres in a few localities, but are mostly in the order of 1–2 m or less, mainly in what appear to be ice-scour berms. Sediment thicknesses increase as water depths increase below 150 m on the northern part of the platform. Due north of Akpatok Island a small morainal ridge occurs in 160 m water depth 3 km south of the northern edge of the platform. To the northeast a moraine or stillstand feature up to 5 m in thickness occurs in 228 m present water depth at a point near where depths begin to increase rapidly northward into Eastern basin of Hudson Strait (Fig. 3). Features that we interpret to be moraines also occur to the north and northwest on the western flank of Eastern basin (Fig. 3).

Modification of seafloor sediments

Seafloor sediments in areas exposed to the action of bottom currents in Hudson Strait and Ungava Bay have undergone modification to varying degrees through winnowing of fines and the development of gravelly and sandy lag deposits. In general these deposits are less than 20 cm in thickness. This primarily has occurred in the shallower regions of the strait outside the basin areas.

Seafloor sediments in many areas on the upper part of the basin flanks and between the basins have been subjected to scour and impact by grounding ice keels. Parallel or subparallel orientation of ice-keel scours in several areas suggests those features are sole marks formed by either glacial ice sheets or large masses of ice. They contrast with the generally more random scour paths and impact features associated with individual bergs, but as indicated by Gray (2001), the data are inconclusive because the orientation of the scours in some areas coincides with the main present-day water-current directions. Although icebergs do now enter Hudson Strait to a limited degree, many of the features observed may be relict.

High-resolution seismic-reflection profiles indicate that large erosional scars locally have been cut into Quaternary sediments on the flanks of Eastern basin. These have been attributed to debris-flow events (MacLean, 1994).

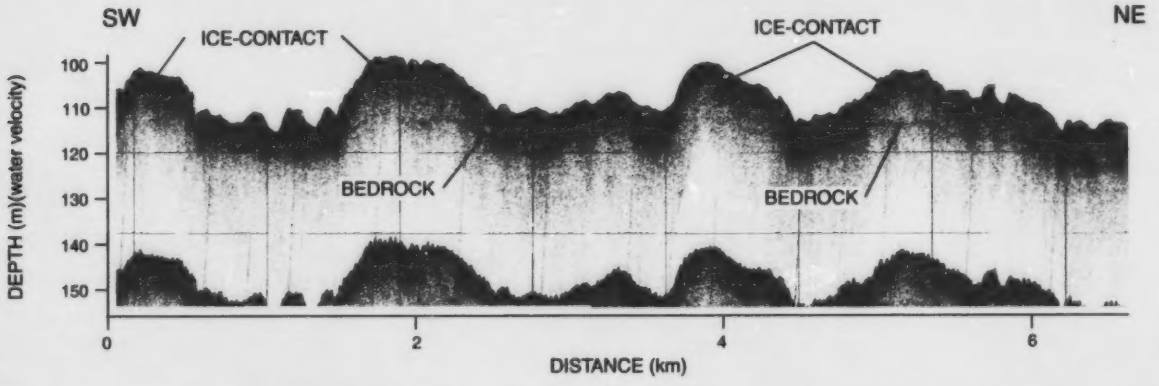

Figure 65. *Huntec™ high-resolution seismic-reflection profile showing ridges of ice-contact sediments interpreted to be glacial flute marks southeast of Akpatok Island on the central Ungava Bay platform. (See Fig. 1 for location of section.)*

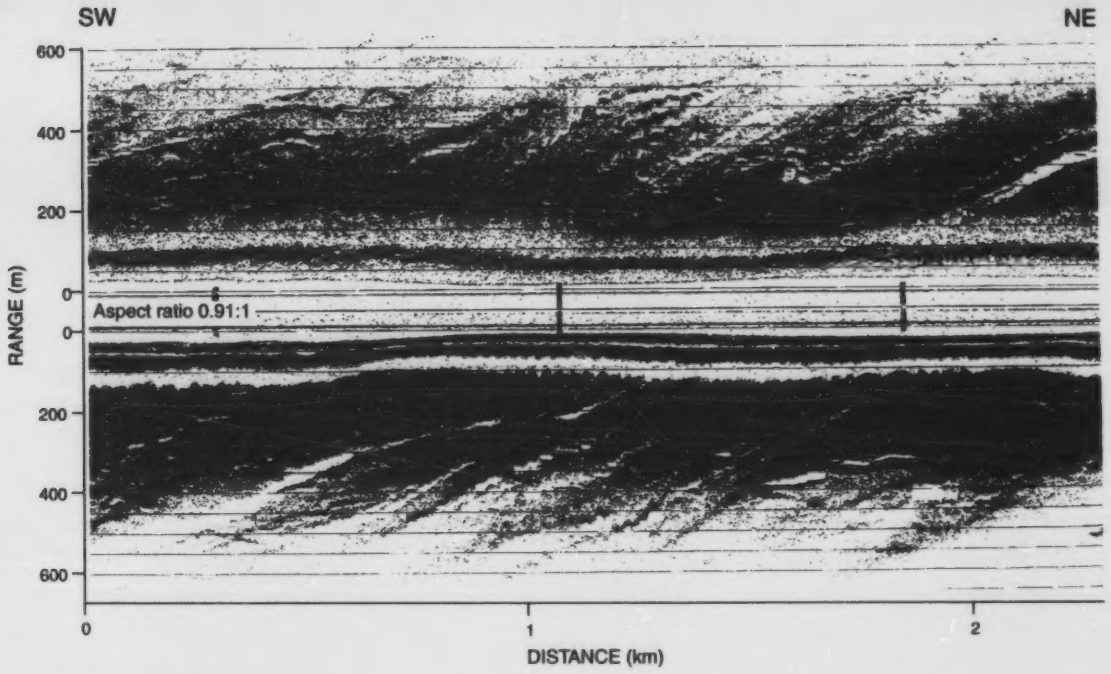

Figure 66. *Sidescan sonogram showing subparallel shallowly incised ice scours trending approximately north-south within the area illustrated in Figure 65. The pronounced subparallel orientation of these features suggests that they are ice-sheet sole marks rather than features formed by individual iceberg groundings.* (See *Fig. 1 for location of section.*)

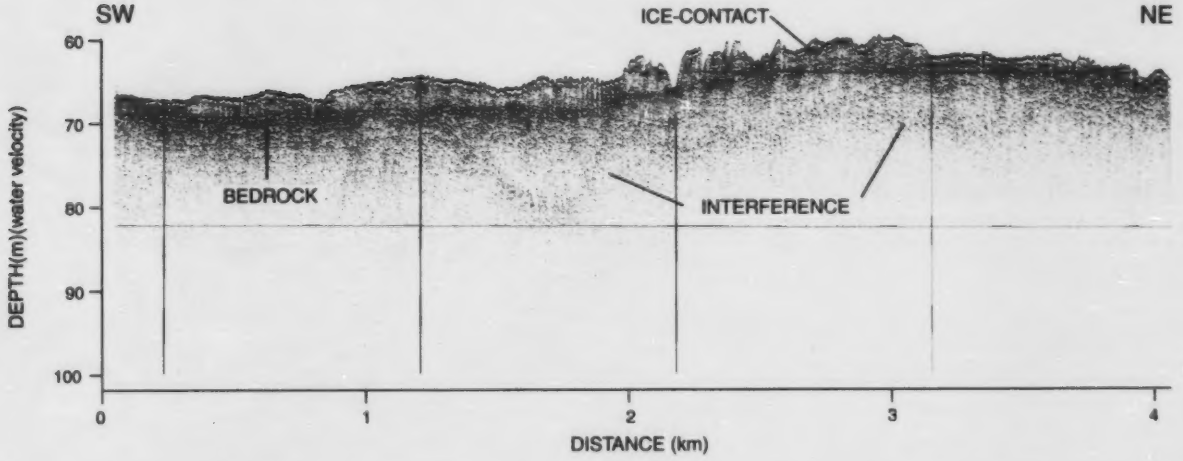

Figure 67. *Huntec™ high-resolution seismic-reflection profile illustrating a small morainal feature on the central Ungava Bay platform 38 km east of Akpatok Island.* (See *Fig. 1 for location of section.*)

Indications of these events have been found in two main areas. The largest lies in 855 m water depth low on the northern flank near the eastern end of the basin. Intersected on an east-west track approximately normal to the downslope direction, the cross-sectional width of the scar is some 12.5 km (Fig. 68). A second area occurs in 660–800 m of water midway along the northern flank of Eastern basin. Two scar localities 18 km apart are 10 km and 2.8 km wide, respectively (Fig. 69). In the larger of these, the 8–10 m thick predominantly glaciomarine sediment sequence appears to have been completely removed down to the ice-contact sediments. Displaced material locally overlies sediments on the adjacent basin floor. Figure 70 illustrates a nearby and possibly related debris-flow scar or zone of sediment failure low on the northern flank of Eastern basin some 6 km north of the core 85027-057 locality. Some of the debris-flow material has been deposited on the basin floor adjacent to the base of the northern flank in that area.

Although there is no direct indication of the age of these events, deposition of the displaced sediment stratigraphically appears to postdate other sediments in the floor of the basin, and no subsequent sedimentation is evident in the scars. This may suggest they are of relatively recent origin, but modern sedimentation rates in general are low in most parts of this region. The number and locations of earthquake epicentres in eastern Hudson Strait (Anglin et al., 1990) suggest a possible relationship with these events, either as cause or effect.

ACKNOWLEDGMENTS

We wish to thank captains F.W. Mauger, L. Strum, F.H. Berchem, and J. Lewis, the crews of *CSS Hudson*, scientific and technical staff from Geological Survey of Canada (Atlantic) and from other institutions for their excellent support and co-operation in conducting these studies. Special thanks are extended to John Andrews for many helpful discussions and his strong tangible and intangible support in so many ways throughout this study. Our sincere thanks also go to G.H. Miller, colleagues of the authors, and participants in Arctic Workshop discussions for helpful advice and comments, and to T.W. Stafford, Jr., Laboratory for Accelerator Radiocarbon Research, Institute of Arctic and Alpine Research, University of Colorado for his very willing and valuable help in the radiocarbon dating of samples. We also wish to extend special thanks to D.A. Hodgson, H. Josenhans, and J. Shaw for helpful comments and for review of this paper.

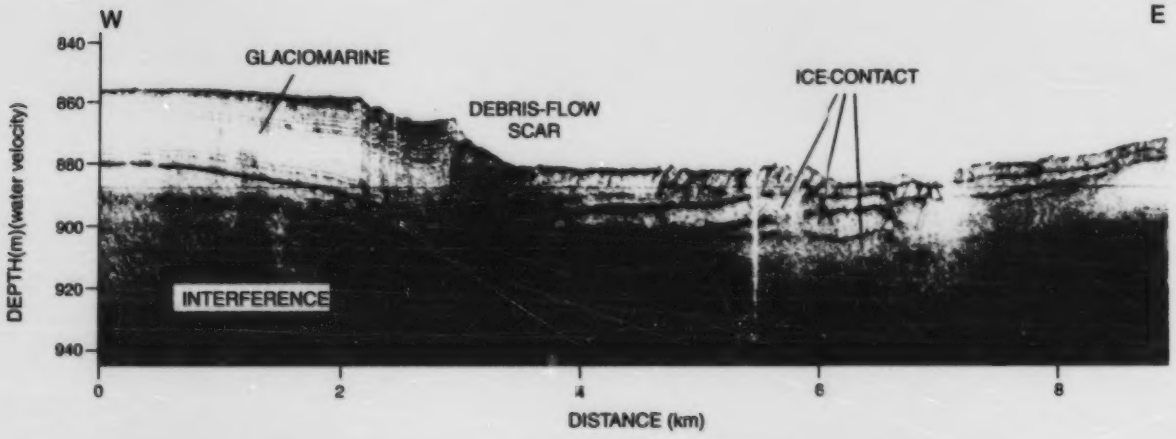

Figure 68. *Huntec™ high-resolution seismic-reflection profile oriented west to east showing a major scar 12.5 km wide, attributed to debris-flow action, cut in glaciomarine sediments on the lower northern flank in the eastern part of Eastern basin.* (See *Fig. 1 for location of section.*)

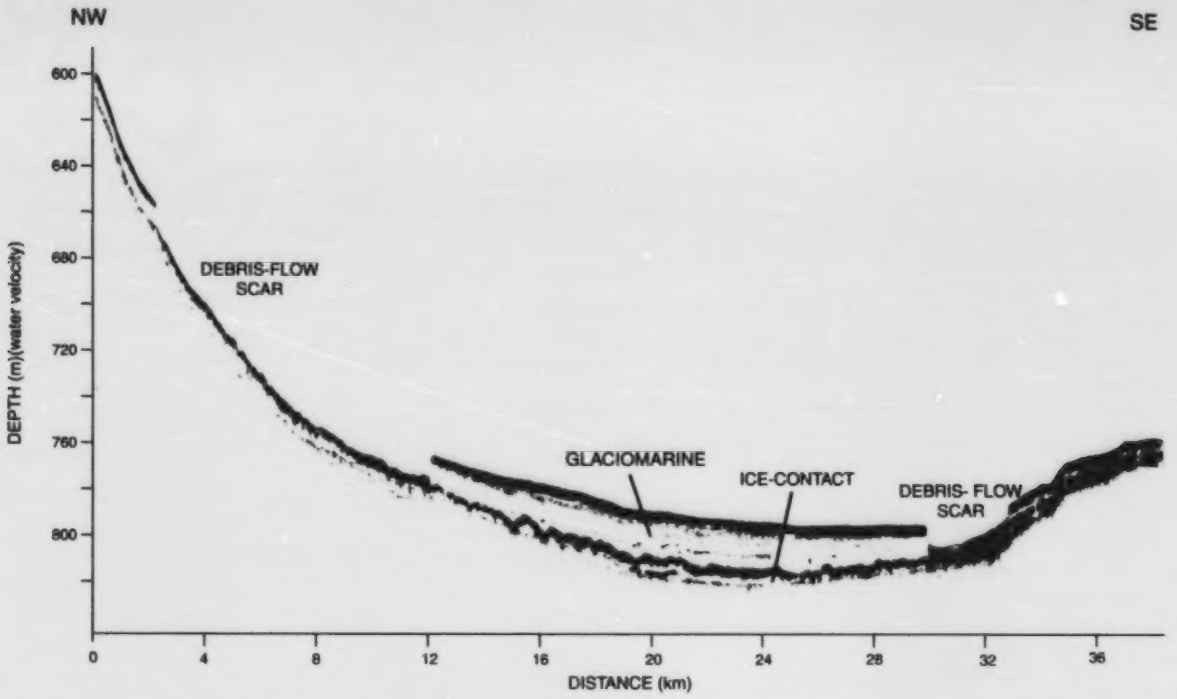

Figure 69. *A 3.5 kHz profile showing two other debris-flow erosional scars on the northern flank of Eastern basin. The locality lies midway along the basin 46 km west-northwest of the feature shown in Figure 68. Complete removal of sediments down to the ice-contact deposits appears to have occurred in the larger of the scars illustrated on this figure.* (See *Fig. 1 for location of section.*)

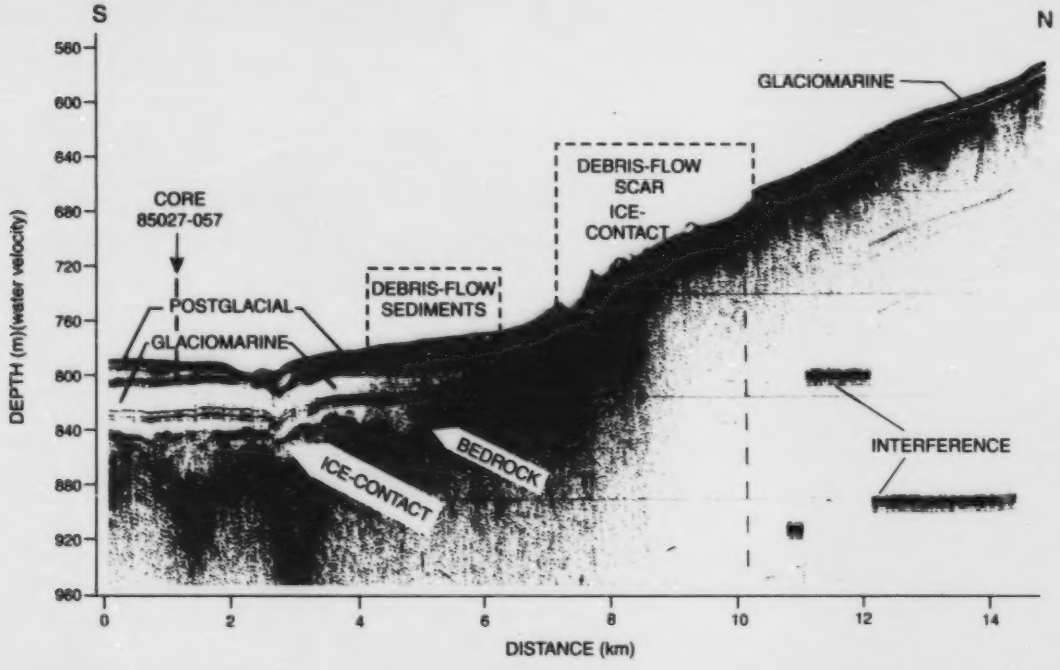

Figure 70. *Single-channel seismic-reflection profile showing a debris-flow scar on a south-north transect across the northern flank of Eastern basin 3 km west-northwest of the westernmost scar in Figure 70. The close spatial proximity of these features suggests they may relate to the same event. Some of the displaced sediment lies on the basin floor adjacent to the base of the slope.* (See *Fig. 1 for location of section.*)

REFERENCES

Alley, R.B., Blankenship, D.D., Rooney, S.T., and Bentley, C.R.
1989: Sedimentation beneath ice shelves - the view from ice stream B; Marine Geology, v. 85, p. 101–120.

Amos, C.L. and Collins, M. (ed.)
1991: The seabed of the Canadian Shelf; Continental Shelf Research, v. 11, no. 8–10, 1311 p.

Andrews, J.T., MacLean, B., Kerwin, M., Manley, W., Jennings, A.E., and Hall, F.
1995: Final stages in the collapse of the Laurentide Ice Sheet, Hudson Strait, Canada, NWT: 14C AMS dates, seismic stratigraphy, and magnetic susceptibility logs; Quaternary Science Reviews, v. 14, p. 983–1004.

Anglin, F.M., Wetmiller, R.J., Horner, R.B., Rogers, G.C., and Drysdale, J.A.
1990: Seismicity Map of Canada; Geological Survey of Canada, Canadian Geophysical Atlas, Map 15, scale 1:10 000 000.

Blake, W., Jr.
1966: End moraines and deglaciation chronology in northern Canada with special reference to southern Baffin Island; Geological Survey of Canada, Paper 66-26, 31 p.

Boulton, G.S.
1990: Sedimentary and sea level changes during glacial cycles and their control on glacimarine facies architecture; *in* Glacimarine Environments: Processes and Sediments, (ed.) J.A. Dowdswell and J.D. Scourse; Geological Society, Special Publication No. 53, p. 15–52.

Bruneau, D. et Gray, J.T.
1991: Géologie des formations en surface, région de Salluit et du cap de Nouvelle-France, Québec; Commission géologique du Canada, carte 11-1990, échelle 1/250 000.

Davies, T.A., Bell, T., Cooper, A., Josenhans, H., Polyak, L., Solheim, A., Stoker, M., and Stravers, J. (ed.)
1997: Glaciated Continental Margins; An Atlas of Acoustic Images; Chapman & Hall, London, United Kingdom, 315 p.

Dowdeswell, J.A. and Scourse, J.D. (ed.)
1990: Glacimarine Environments: Processes and Sediments; Geological Society (London), Special Paper No. 53, 423 p.

Fader, G.B., King, L.H., and Josenhans, H.W.
1982: Surficial geology of the Laurentian Channel and the western Grand Banks of Newfoundland; Canadian Hydrographic Service, Marine Sciences Paper 21; Geological Survey of Canada, Paper 81-22, 37 p.

Fillon, R.H. and Harmes, R.A.
1982: Northern Labrador Shelf glacial chronology and depositional environments; Canadian Journal of Earth Sciences, v. 19, p. 162–192.

Gray, J.T.
2001: Patterns of ice flow and deglaciation chronology for southern coastal margins of Hudson Strait and Ungava Bay; *in* Marine Geology of Hudson Strait and Ungava Bay, Eastern Arctic Canada: Late Quaternary Sediments, Depositional Environments, and Late Glacial–Deglacial History Derived from Marine and Terrestrial Studies, (ed.) B. MacLean; Geological Survey of Canada, Bulletin 566.

Gray, J.T., Brynczka, T., Giugni, L., Thibauld, E., and Lauriol, B.
1994: Multiple flow patterns of the Laurentide ice sheet on Akpatok Island, Ungava Bay, Arctic Canada; *in* 24th Arctic Workshop, Institute of Arctic and Alpine Research, University of Colorado, March 17–19, 1994, Program and Abstracts, p. 160–162.

Gray, J.T., Decker, V., Guindon, L., Guenette, C., and Clark, C.
1996: Late glacial ice flow patterns in the northwest Torngat Mountains: evidence for an important local dispersal centre; in 26th Arctic Workshop, Boulder, Colorado, March 14–16, 1996, Program with Abstracts, p. 43–44b.

Hall, F.R., Andrews, J.T., Kerwin, M., and Smith, L.M.
2001: Studies of sediment colour, whole-core magnetic susceptibility, and sediment magnetism of the Hudson Strait–Labrador Shelf region: *CSS Hudson* cruises 90023 and 93034; *in* Marine Geology of Hudson Strait and Ungava Bay, Eastern Arctic Canada: Late Quaternary Sediments, Depositional Environments, and Late Glacial–Deglacial History Derived from Marine and Terrestrial Studies, (ed.) B. MacLean; Geological Survey of Canada, Bulletin 566.

Hardy, I.
2001: Composition of sediments in Hudson Strait and Ungava Bay; *in* Marine Geology of Hudson Strait and Ungava Bay, Eastern Arctic Canada: Late Quaternary Sediments, Depositional Environments, and Late Glacial–Deglacial History Derived from Marine and Terrestrial Studies, (ed.) B. MacLean; Geological Survey of Canada, Bulletin 566.

Jennings, A.E., Andrews, J.T., Weiner, N.J., Manley, W.F., MacLean, B., and Barber, D.C.
1995: Strategies and progress in unravelling the chronology of Hudson Strait deglaciation; *in* The 25th Arctic Workshop, Centre d'Études Nordiques, Université Laval, Ste. Foy, Quebec, March 1995, p. 90.

Jennings, A.E., Manley, W.F., MacLean, B., and Andrews, J.T.
1998: Marine evidence for the last glacial advance across Eastern Hudson Strait, Eastern Canadian Arctic; Journal of Quaternary Science, v. 13, p. 501–514.

Jennings, A.E., Vilks, G., Deonarine, B., Silis, A., and Weiner, N.
2001: Foraminiferal biostratigraphy and paleoceanography; *in* Marine Geology of Hudson Strait and Ungava Bay, Eastern Arctic Canada: Late Quaternary Sediments, Depositional Environments, and Late Glacial–Deglacial History Derived from Marine and Terrestrial Studies, (ed.) B. MacLean; Geological Survey of Canada, Bulletin 566.

Josenhans, H. and Zevenhuizen, J.
1989: Quaternary Geology I: Quaternary History; *in* Frontier Geoscience Program - East Coast Basin Atlas Series - Labrador Sea, (co-ord.) J.S. Bell; Geological Survey of Canada, Atlas, p. 8.
1990: Dynamics of the Laurentide Ice Sheet in Hudson Bay, Canada; Marine Geology, v. 92, p. 1–26.

Josenhans, H.W., Zevenhuizen, J., and Klassen, R.A.
1986: The Quaternary geology of the Labrador Shelf; Canadian Journal of Earth Sciences, v. 23, p. 1190–1213.

Josenhans, H.W., Zevenhuizen, J., and Marsters, J.
1989: Quaternary Geology II: Surficial Geology and Physical Properties; *in* Frontier Geoscience Program - East Coast Basin Atlas Series - Labrador Sea, (co-ord.) J.S. Bell; Geological Survey of Canada Atlas, p. 10.

Kaufman, D.S. and Williams, K.M. (comp.)
1992: Radiocarbon Date List VII: Baffin Island, N.W.T., Canada; Institute of Arctic and Alpine Research, University of Colorado, Boulder, Colorado, Occasional Paper No. 48, 82 p.

Kerwin, M.W.
1994: Final stages in the collapse of the Laurentide Ice Sheet: a rock magnetic and sedimentological study from Hudson Strait, Canada; M.Sc. thesis, University of Colorado, Boulder, Colorado, 189 p.

King, L.H.
1970: Surficial geology of the Halifax-Sable Island map area; Marine Sciences Branch, Department of Energy, Mines, and Resources, Paper 1, 16 p.
1993: Till in the marine environment; Journal of Quaternary Science, v. 8, p. 347–358.

King, L.H. and Fader, G.B.J.
1986: Wisconsinan glaciation of the Atlantic continental shelf of southeast Canada; Geological Survey of Canada, Bulletin 363, 72 p.

King, L.H., Rokoengen, K., Fader, G.B., and Gunleiksrud, T.
1991: Till-tongue stratigraphy; Geological Society of America, Bulletin, v. 103, p. 637–659.

King, L.H., Rokoengen, K., and Gunleiksrud, T.
1987: Quaternary seismostratigraphy of the Mid-Norwegian Shelf, 65°-67°30′N - A till tongue stratigraphy; The Continental Shelf and Petroleum Technology Research Institute A/S (IKU), Trondheim, Norway, Publication 114, 58 p.

Laymon, C.A.
1988: Glacial geology of western Hudson Strait, Canada, with reference to Laurentide ice sheet dynamics; Ph.D. thesis, University of Colorado, Boulder, Colorado, 345 p.
1991: Marine episodes in Hudson Strait and Hudson Bay, Canada, during the Wisconsin Glaciation; Quaternary Research, v. 35, p. 53–62.

Lewis, C.F.M., Mayer, L., Cameron, G.D., and Todd, B.J.
1997: Drumlins in Lake Ontario; *in* Glaciated Continental Margins: an Atlas of Acoustic Images; (ed.) T.A. Davies, T. Bell, A.K. Cooper, H. Josenhans, L. Polyak, A. Solheim, M.S. Stoker, and J.A. Stravers; Chapman & Hall, London, United Kingdom, p. 48–49.

MacLean, B.
1994: Debris flows and seabed erosion in eastern Hudson Strait; *in* 24th Arctic Workshop, Institute of Arctic and Alpine Research, University of Colorado, Boulder, Colorado, March 17–19, 1994, Abstracts, p. 129–131.
1997a: Thick multiple ice-contact deposits adjoining the sill at the entrance to Hudson Strait, Canada; *in* Glaciated Continental Margins: An Atlas of Acoustic Images, (ed.) T.A. Davies, T. Bell, A.K. Cooper, H. Josenhans, L. Polyak, A. Solheim, M.S. Stoker, and J.A. Stravers; Chapman & Hall, London, United Kingdom, p. 88–89.
1997b: Submarine lateral moraine in the south central region of Hudson Strait, Canada; *in* Glaciated Continental Margins: An Atlas of Acoustic Images, (ed.) T.A. Davies, T. Bell, A.K. Cooper, H. Josenhans, L. Polyak, A. Solheim, M.S. Stoker, and J.A. Stravers; Chapman & Hall, London, United Kingdom, p. 86–87.
2001: Introduction: geographic setting and studies; *in* Marine Geology of Hudson Strait and Ungava Bay, Eastern Arctic Canada: Late Quaternary Sediments, Depositional Environments, and Late Glacial–Deglacial History Derived from Marine and Terrestrial Studies, (ed.) B. MacLean; Geological Survey of Canada, Bulletin 566.

MacLean, B., Andrews, J.T., Jennings, A.E., Manley, W.F., Hardy, I., Vilks, G., and Deonarine, B.
1996: Late Quaternary sediments in eastern Hudson Strait: relations with late glacial advances on southeastern Baffin Island; *in* 26th Arctic Workshop, Institute of Arctic and Alpine Research, University of Colorado, Boulder, Colorado, March 14–16, 1996, Program with Abstracts, p. 86–88.

MacLean, B., Hardy, I., Jennings, A.E., Manley, W.F., and Kerwin, M.W.
1994a: Late glacial ice in Eastern Hudson Strait: new offshore evidence; *in* 24th Arctic Workshop, Institute of Arctic and Alpine Research, University of Colorado, Boulder, Colorado, March 17–19, 1994, Abstracts, p. 132–134.

MacLean, B., Loncarevic, B.D., Hardy, I., Brown, R.G.B., Daigneault, R.A., Day, M., Kerwin, M.W., and Manley, W.F.
1994b: Cruise Report CSS Hudson Cruise 93034 in Hudson Strait-Ungava Bay, Canadian Eastern Arctic; Geological Survey of Canada, Open File 2818, 136 p.

MacLean, B., Sonnichsen, G., Vilks, G., Powell, C., Moran, K., Jennings, A., Hodgson, D., and Deonarine, B.
1989: Marine geological and geotechnical investigations in Wellington, Byam Martin, Austin, and adjacent channels, Canadian Arctic Archipelago; Geological Survey of Canada, Paper 89-11, 69 p.

MacLean, B., Vilks, G., Aitken, A., Briggs, W., Bruneau, D., Doiron, A., Escamilla, M., Hardy, I., Miner, J., Mode, W., Powell, R., Retelle, M., Stravers, J., Taylor, A., and Weiner, N.
1991: Investigations of the Quaternary geology of Hudson Strait and Ungava Bay, Northwest Territories; *in* Current Research, Part E; Geological Survey of Canada, Paper 91-1E, p. 305–315.

MacLean, B., Vilks, G., and Deonarine, B.
1992: Depositional environments and history of late Quaternary sediments in Hudson Strait and Ungava Bay: further evidence from seismic and biostratigraphic data; Géographie physique et Quaternaire, v. 46, p. 311–329.

MacLean, B., Vilks, G., Deonarine, B., Hardy, I., and Ceman, J.
1995: Quaternary sediments in Hudson Strait and Ungava Bay; *in* The 25th Arctic Workshop, Centre d'Études Nordiques, Université Laval, Ste. Foy, Quebec, March 16–18, 1995, p. 116–118.

MacLean, B., Williams, G.L., Sanford, B.V., Klassen, R.A., Blakeney, C., and Jennings, A.
1986: A reconnaissance study of bedrock and surficial geology of Hudson Strait, N.W.T.; *in* Current Research, Part B; Geological Survey of Canada, Paper 86-1B, p. 617–635.

Manley, W.F.
1995: Late-glacial record of ice-sheet/ocean interactions, Hudson Strait and southern Baffin Island, Eastern Canadian Arctic; Ph.D. thesis, University of Colorado, Boulder, Colorado, 252 p.

Manley, W.F. and Jennings, A.E. (comp.)
1996: Radiocarbon Date List VIII: Eastern Canadian Arctic, Labrador, Northern Quebec, East Greenland Shelf, Iceland Shelf, and Antarctica; Institute of Arctic and Alpine Research, University of Colorado, Boulder, Colorado, Occasional Paper, No. 50, 163 p.

Manley, W.F., MacLean, B., Kerwin, M.W., and Andrews, J.T.
1993: Magnetic susceptibility as a Quaternary correlation tool: examples from Hudson Strait sediment cores, eastern Canadian Arctic; *in* Current Research, Part D; Geological Survey of Canada, Paper 93-1D, p. 137–145.

Piper, D.J.W., Mudie, P.J., Fader, G.B., Josenhans H.W., MacLean, B., and Vilks, G.
1990: Quaternary geology; Chapter 10 *in* Geology of the Continental Margin of Eastern Canada, (ed.) M.J. Keen and G.L. Williams; Geological Survey of Canada, Geology of Canada, no. 2, p. 475–607 (*also* Geological Society of America, The Geology of North America, v. I-1).

Powell, R.D.
1984: Glacimarine processes and inductive lithofacies modelling of ice shelf and tidewater glacier sediments based on Quaternary examples; Marine Geology, v. 57, p. 1–52.

Powell, R.D. and Molnia, B.F.
1989: Glacimarine sedimentary processes, facies and morphology of the south-southeast Alaska Shelf and Fiords; Marine Geology, v. 85, p. 359–390.

Praeg, D.B., MacLean, B., Hardy, I.A., and Mudie, P.J.
1986: Quaternary geology of the southeast Baffin Island continental shelf; Geological Survey of Canada, Paper 85-14, 38 p.

Silis, A.B.
1993: Late Quaternary foraminiferal biostratigraphy of Hudson Strait; Geological Survey of Canada, Open File 3340, 127 p.

Stoker, M.S.
1990: Glacially-influenced sedimentation on the Hebridean slope, northwest United Kingdom continental margin; *in* Glacimarine Environments: Processes and Sediments, (ed.) J.A. Dowdeswell and J.D. Scourse; Geological Society, Special Publication No. 53, p. 349–362.

Stravers, J.A.
1986: Glacial geology of outer Meta Incognita Peninsula, southern Baffin Island, Arctic Canada; Ph.D. thesis, University of Colorado, Boulder, Colorado, 251 p.

Syvitski, J.P.M.
1991: Towards an understanding of sediment deposition on glaciated continental shelves; *in* The Seabed of the Canadian Shelf, (ed.) C.L. Amos and M. Collins; Continental Shelf Research, v. 11, no. 8–10, p. 897–937.

Vilks, G., MacLean, B., Deonarine, B., Currie, C.G., and Moran, K.
1989: Late Quaternary paleoceanography and sedimentary environments in Hudson Strait; Géographie physique et Quaternaire, v. 43, no. 2, p. 161–178.

Vorren, T.O., Hald, M., Edvardsen, M., and Lind-Hansen, O-W.
1983: Glacigenic sediments and sedimentary environments on continental shelves: general principles with a case study from the Norwegian Shelf; *in* Glacial Deposits in North-west Europe; A.A. Balkema, Rotterdam, Netherlands, p. 61–73.

Vorren, T.O., Hald, M., and Thomsen, E.
1984: Quaternary sediments and environments on the continental shelf off northern Norway; Marine Geology, v. 57, p. 229–257.

Vorren, T.O., Lebesbye, E., and Larsen, K.B.
1990: Geometry and genesis of the glacigenic sediments in the southern Barents Sea; *in* Glacimarine Environments: Processes and Sediments, (ed.) J.A. Dowedswell and J.D. Scource; Geological Society, Special Publication No. 53, p. 269–288.

Foraminiferal biostratigraphy and paleoceanography

A.E. Jennings[1], G. Vilks[2], B. Deonarine[3], A. Silis[4], and N. Weiner[1]

Jennings, A.E., Vilks, G., Deonarine, B., Silis, A., and Weiner, N., 2001: Foraminiferal biostratigraphy and paleoceanography; in *Marine Geology of Hudson Strait and Ungava Bay, Eastern Arctic Canada: Late Quaternary Sediments, Depositional Environments, and Late Glacial–Deglacial History Derived from Marine and Terrestrial Studies, (ed.) B. MacLean; Geological Survey of Canada, Bulletin 566, p. 127–146.*

Abstract: Foraminifers in the sediment sequences have been a key component in the delineation of the biostratigraphic framework and depositional environments, and in providing insights into the paleoceanographic history. Together with sparse macrofossils they have been used extensively in radiocarbon dating to establish chronologies in Hudson Strait. The biostratigraphic framework developed primarily from benthonic foraminiferal assemblages shows that distinctive faunal zones are associated with glaciomarine proximal and distal environments, and with postglacial marine environments. These include distinct differences in species diversity and population numbers. Planktonic foraminifers generally are absent or very sparse in the glaciomarine sequences. The other principal sediment unit, ice-contact material, is essentially barren of fauna. Dating and interpretative problems arise in some localities due to the presence of reworked material derived from glacial erosion and transport of previously deposited glaciomarine and marine sediments. The foraminiferal biostratigraphy associated with the main sediment units in each of the principal basins and relevant chronologies are outlined.

Résumé : Les foraminifères trouvés dans les séquences sédimentaires se sont avérés essentiels pour circonscrire le cadre biostratigraphique et les milieux sédimentaires ainsi que pour donner un aperçu de l'histoire paléocéanographique. Ils ont été largement utilisés, de même que des macrofossiles dispersés, à des fins de datation au radiocarbone pour établir des chronologies pour le détroit d'Hudson. Le cadre biostratigraphique élaboré principalement à partir d'assemblages de foraminifères benthiques montre que des faunizones distinctes (en termes de diversité spécifique et de tailles des populations) sont associées à des milieux glaciomarins proximaux et distaux ainsi qu'à des milieux postglaciomarins. Les foraminifères planctoniques sont généralement absents ou très rares dans les séquences glaciomarines. L'autre unité sédimentaire principale, soit les sédiments de contact glaciaire, ne contient pratiquement pas de restes animaux. Certains endroits présentent des problèmes de datation et d'interprétation en raison de la présence de matériaux remaniés provenant de l'érosion glaciaire et du transport de sédiments glaciomarins et marins mis en place auparavant. L'article présente la biostratigraphie des foraminifères associée aux principales unités sédimentaires dans chacun des bassins principaux ainsi que les chronologies pertinentes.

[1] Institute of Arctic and Alpine Research, University of Colorado, Boulder, Colorado 80309-0450
[2] Geological Survey of Canada (Atlantic), Bedford Institute of Oceanography, Dartmouth, Nova Scotia (deceased)
[3] Geological Survey of Canada (Atlantic), Bedford Institute of Oceanography, Dartmouth, Nova Scotia B2Y 4A2
[4] Department of Earth Sciences, University of Waterloo, Waterloo, Ontario N2L 3G1

INTRODUCTION

Foraminiferal biostratigraphy in Hudson Strait provides definitive information regarding depositional environments, independent confirmation of environmental reconstructions based on seismic data, and helps to ascertain the placement of cores in the seismic stratigraphy. As the most commonly radiocarbon dated material in the strait, the foraminifers, together with sparse macrofossils, have been key for constructing the chronology of the sediments as well as for providing insight into the paleoenvironmental and paleoceanographic history of the strait and the role of sediment reworking by glacial activity. In this paper we summarize the biostratigraphic zonation presented by Vilks et al. (1989) and later partially revised by Silis (1993) and Ceman (J.A. Ceman, unpub. report, 1994), and present some new insights into the significance and origins of these zonations based on newly acquired radiocarbon dates and foraminiferal analyses of cores collected in 1993 which build on the data from earlier analyses. The radiocarbon dates used in this paper are listed in MacLean et al. (2001, Table 2); all are marine reservoir corrected. Results from each of the five main depositional basins will be discussed separately.

Faunal zones

Vilks et al. (1989) established a foraminiferal zonation based on five cores collected during cruise 85027: three cores from Eastern basin, one core from Western basin, and one core from Southwestern basin. The chronologies, seismic stratigraphy, and physical properties of the cores indicated that some had penetrated late glacial sediments and that the faunal zones were time transgressive from east to west. The major species in the faunal zones are thought to reflect paleoenvironmental influences of glacial ice fluctuations and regional oceanography, especially changes in paleosalinity (Vilks et al., 1989).

Faunal zone A is dominated by *Elphidium excavatum* forma *clavata* and *Cassidulina reniforme*, two species that commonly codominate in late glacial ice-proximal sediments in the North Atlantic Ocean (e.g. Vilks, 1981; Osterman and Andrews, 1983; Jennings, 1993) and in modern surface sediments in proximity to calving glaciers on Svalbard (Nagy, 1965; Elverhøi et al., 1980; Hald et al., 1994). Zone A has a low diversity and abundance of foraminifers with frequent barren intervals and no planktonic foraminifers. It corresponds to seismic unit 3, and is interpreted to represent ice-proximal glaciomarine conditions.

Faunal zone B is identified from the addition of *Fursenkoina fusiformis* to the species in faunal zone A. Knudsen and Seidenkrantz (1994) showed that this species actually belongs to the newly named species *Stainforthia feylingi*, but to avoid confusion, it will be referred to as *Fursenkoina fusiformis* in this paper because that is the name that has been used throughout the biostratigraphic work on sediments in Hudson Strait. Based on the observations in many studies, this species is highly tolerant of transitional, unstable environmental conditions (*see* Vilks et al., (1989) and Knudsen and Seidenkrantz (1994) for discussion), including large salinity variations and low oxygen levels. The faunal diversity of this zone increases relative to zone A, and planktonic tests occur sporadically in some cores (Silis, 1993). Faunal zone B is interpreted to represent ice-distal glaciomarine environments coincident with the upper part of seismic unit 3 (Vilks et al., 1989; MacLean et al., 1992).

Faunal zone C is limited to the deep Eastern basin. It includes the species from zones A and B plus *Cassidulina teretis* (termed '*C. laevigata*' *in* Vilks et al. (1989) and MacLean et al. (1992), but termed '*Cassidulina neoteretis*' by Seidenkrantz (1995)), *Pullenia osloensis* (revised from *P. quinqueloba* by Silis (1993)), and *Astrononion gallowayi*.

Relative abundances, diversity, and planktonic foraminiferal abundances are higher in zone C than in faunal zones A and B (Silis, 1993). Vilks et al. (1989) proposed that zone C represents an increased influence of warmer, more saline Labrador Sea water in eastern Hudson Strait during the early postglacial interval coincident with the lower part of seismic unit 4 in Eastern basin.

Faunal zone D is characterized by the addition of *Nonionellina labradorica*, *Islandiella helenae*, *I. norcrossi*, *Buccella frigida*, among others, and increased abundances of *Astrononion gallowayi*. Abundances of benthonic and planktonic foraminifers rise significantly in this zone. This zone characterizes the modern sediments in the strait, and correlates with seismic unit 4. Vilks et al. (1989) interpreted it to reflect the increasing influence of arctic-subarctic inner shelf waters during the late postglacial period.

Silis (1993) expanded the earlier work on foraminiferal zonations by inclusion of many more cores from each of the five main Hudson Strait basins. She proposed that a new transitional zone, zone T, between zone A and zone D be added to the biostratigraphic zonation of Vilks et al. (1989). Zone T is characterized by introduction of planktonic tests and fluctuations in diversity and abundances of benthonic foraminifers, with mixtures of zone A, zone B, and zone D faunas. Zone T

Figure 1. *Diagram illustrating faunal zones (FZ), seismic units (SU), and chronology (^{14}C dates) for cores with biostratigraphic information presented in figures and for selected other cores discussed in the text. Asterisks beside radiocarbon dates indicate dating reversals or suspect age data. The figures containing biostratigraphic and seismic data on each core are as follows: 93034-031 (Fig. 2; MacLean et al., 2001, Fig. 36); 93034-029 (MacLean et al., 2001, Fig. 35); 93034-002 (MacLean et al., 2001, Fig. 37); 93034-004 (Fig. 3; MacLean et al., 2001, Fig. 39); 85027-057 (Fig. 5; MacLean et al., 2001, Fig. 22); 90023-045 (Fig. 4; MacLean et al., 2001, Fig. 28); 87033-011 (Fig. 6), 90023-031 (MacLean et al., 2001, Fig. 30); 93034-038 (Fig. 8; MacLean et al., 2001, Fig. 54); 90023-034 (Fig. 7; MacLean et al., 2001, Fig. 52); 90023-062 (MacLean et al., 2001, Fig. 62); 93034-013 (Fig. 10; MacLean et al., 2001, Fig. 47); 90023-066 (Fig. 9; MacLean et al., 2001, Fig. 46); 85027-068 (Fig. 11; MacLean et al., 2001, Fig. 44); 90023-101 (Fig. 12); 90023-085 (Fig. 13; MacLean et al., 2001, Fig. 18).* See *MacLean (2001, Fig. 5) for core locations.*

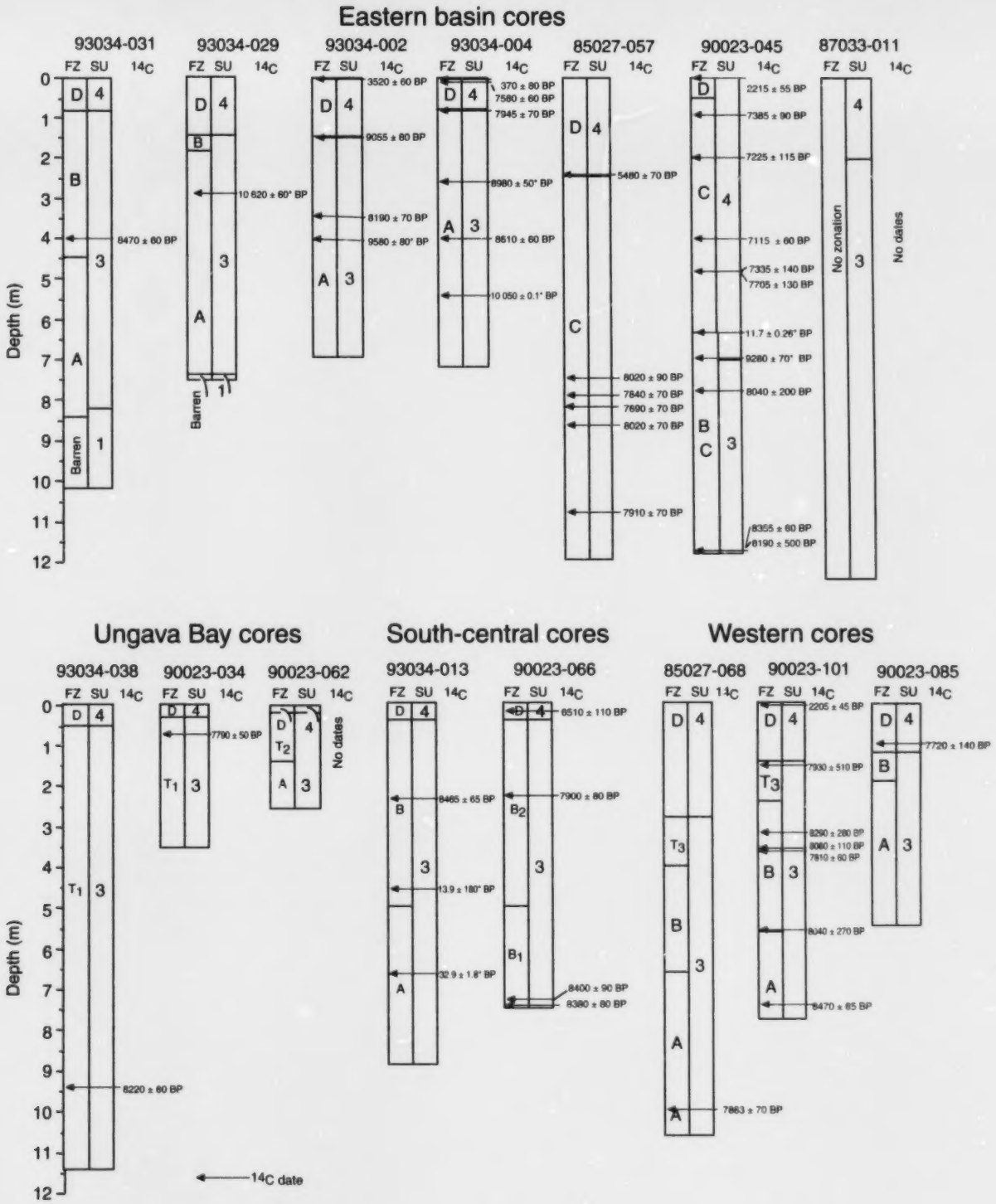
Eastern basin cores
93034-031
93034-029
93034-002
93034-004
85027-057
90023-045
87033-011
FZ SU 14C
Depth (m)
8470 ± 60 BP
10 620 ± 60* BP
3520 ± 60 BP
9055 ± 80 BP
8190 ± 70 BP
9580 ± 80* BP
370 ± 80 BP
7580 ± 60 BP
7945 ± 70 BP
8980 ± 50* BP
8610 ± 60 BP
10 050 ± 0.1* BP
5480 ± 70 BP
8020 ± 90 BP
7840 ± 70 BP
7690 ± 70 BP
8020 ± 70 BP
7910 ± 70 BP
2215 ± 55 BP
7385 ± 90 BP
7225 ± 115 BP
7115 ± 60 BP
7335 ± 140 BP
7705 ± 130 BP
11.7 ± 0.26* BP
9280 ± 70* BP
8040 ± 200 BP
8355 ± 60 BP
8190 ± 500 BP
No zonation
No dates
Barren
Ungava Bay cores
93034-038
90023-034
90023-062
8220 ± 60 BP
7790 ± 50 BP
No dates
South-central cores
93034-013
90023-066
8465 ± 65 BP
13.9 ± 180* BP
32.9 ± 1.8* BP
6510 ± 110 BP
7900 ± 80 BP
8400 ± 90 BP
8380 ± 80 BP
Western cores
85027-068
90023-101
90023-085
7863 ± 70 BP
2205 ± 45 BP
7930 ± 510 BP
8290 ± 280 BP
8060 ± 110 BP
7810 ± 60 BP
8040 ± 270 BP
8470 ± 65 BP
7720 ± 140 BP
14C date

was proposed to represent an unstable marine environment during deglaciation, with elements typical of glaciomarine and postglacial conditions existing simultaneously. In this paper, additional faunal and AMS radiocarbon analyses of Eastern basin cores will be discussed that suggest an alternative explanation for zone T: reworking of previous glaciomarine and marine sediments as a result of a subsequent ice advance.

Eastern basin

Over the course of the five Hudson Strait research cruises, cores were collected that represent the glaciomarine and postglacial deposits, and to a limited degree, underlying ice-contact deposits in Eastern basin. Foraminiferal analyses representing all of these sediment and/or seismic units have been completed (Fig. 1). The comparisons between the seismic facies and biostratigraphic zonations and the paleoenvironmental interpretations are discussed using new data from exemplary cores 93034-031, 93034-029, 93034-002, 93034-004, 90023-042, 90023-045, and 90023-052, and previous data from 85027-055, 85027-056, and 85027-057 (Fig. 1; MacLean, 2001, Fig. 5).

Foraminifers in ice-contact sediments, units 1, 2

Ice-contact sediments (units 1, 2) were recovered in core 93034-031 and at the bottom of core 93034-029 (Fig. 1, 2; MacLean et al., 2001, Fig. 35, 36). These sediments were essentially barren of foraminifers, containing less than one specimen per millilitre.

Foraminifera in proximal glaciomarine sediments, unit 3

Several cores collected sediments of seismic unit 3 (Fig. 1). To obtain the stratigraphically lowest glaciomarine sediments, many of these cores were taken along the basin margins where seismic unit 4 thins to the extent that seismic unit 3

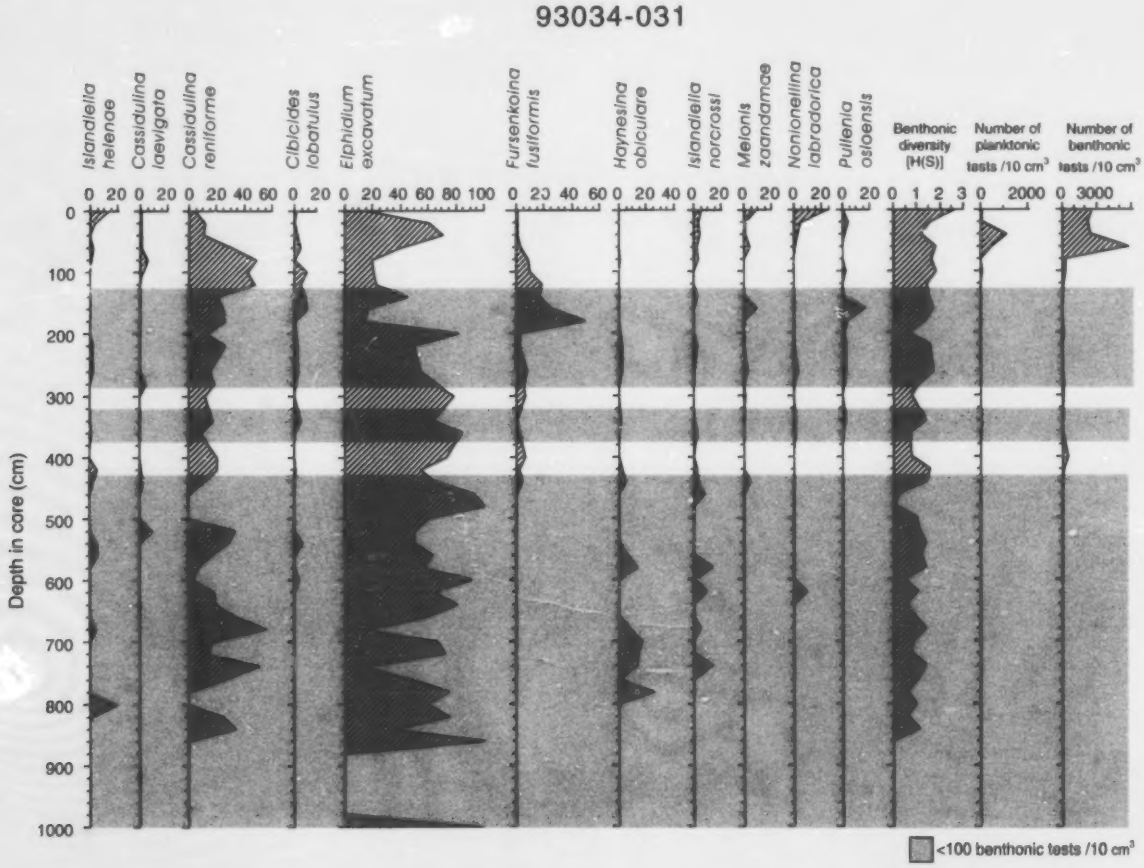

Figure 2. *Abundances (%) of major foraminiferal species in core 93034-031 from Eastern basin. The diamict sediments near the base of the core are faunally barren. The change from glaciomarine to postglacial sediments occurs at a downcore depth of 80 cm* (see also *Fig. 1, MacLean, 2001, Fig. 5; MacLean et al., 2001, Fig. 36; Hardy, 2001, Fig. 2).*

could be penetrated (e.g. MacLean et al., 2001, Fig. 32, 33). Cores 93034-031 (Fig. 2; MacLean et al., 2001, Fig. 36) and 93034-029 (Fig. 1; MacLean et al., 2001, Fig. 35) extend through the most ice-proximal glaciomarine sediments (lowest unit 3) into ice-contact sediments (unit 1/2). Cores 93034-002 (MacLean et al., 2001, Fig. 37) and 93034-004 (Fig. 3; MacLean et al., 2001, Fig. 39) also penetrated through the lowest part of the glaciomarine sediments (the closely spaced basal reflectors) very close to the top of unit 1/2. Cores 90023-042 (MacLean et al., 2001, Fig. 31) and 90023-052 (MacLean et al., 2001, Fig. 38) collected sediments from deep within the glaciomarine unit, but somewhat higher in the section than the above-mentioned cores, above the lowest interval of closely spaced basal reflectors. As these sediments are traced into the thickest part of the unit 3 sequence at the site of core 90023-045 (MacLean et al., 2001, Fig. 32, 28), they are shown to correlate with sediments in the lower half of the section, 25 m below the base of core 90023-045 (MacLean et al., 2001, Fig. 33). The top of the glaciomarine sediments is generally marked by a relative rise in magnetic susceptibility (MS) values that is followed upsection by a distinctive, U-shaped MS low interval that is consistently associated with the basal part of the postglacial sediments of seismic unit 4 (e.g. Fig. 4; Andrews et al., 1995).

In the glaciomarine sediments, unit 3, faunal abundances are very low, generally less than 25 specimens/mL, commonly with fewer than 10 specimens/mL (e.g. Fig. 2). The most dominant species are *Elphidium excavatum* forma *clavata* and *Cassidulina reniforme*, the species definitive of ice-proximal zone A of Vilks et al. (1989). In several of the cores, namely 90023-042, 90023-052, 93034-004, 93034-002, and 93034-031, there are small isolated abundance peaks that are made up solely of these ice-proximal species (e.g. Fig. 2, 3). Radiocarbon dates from these peaks have consistently yielded reservoir-corrected ages between ca. 8.6 ka BP and 8.4 ka BP (Andrews et al., 1995; MacLean et al., 1996; Manley and Jennings, 1996; Jennings et al., 1998).

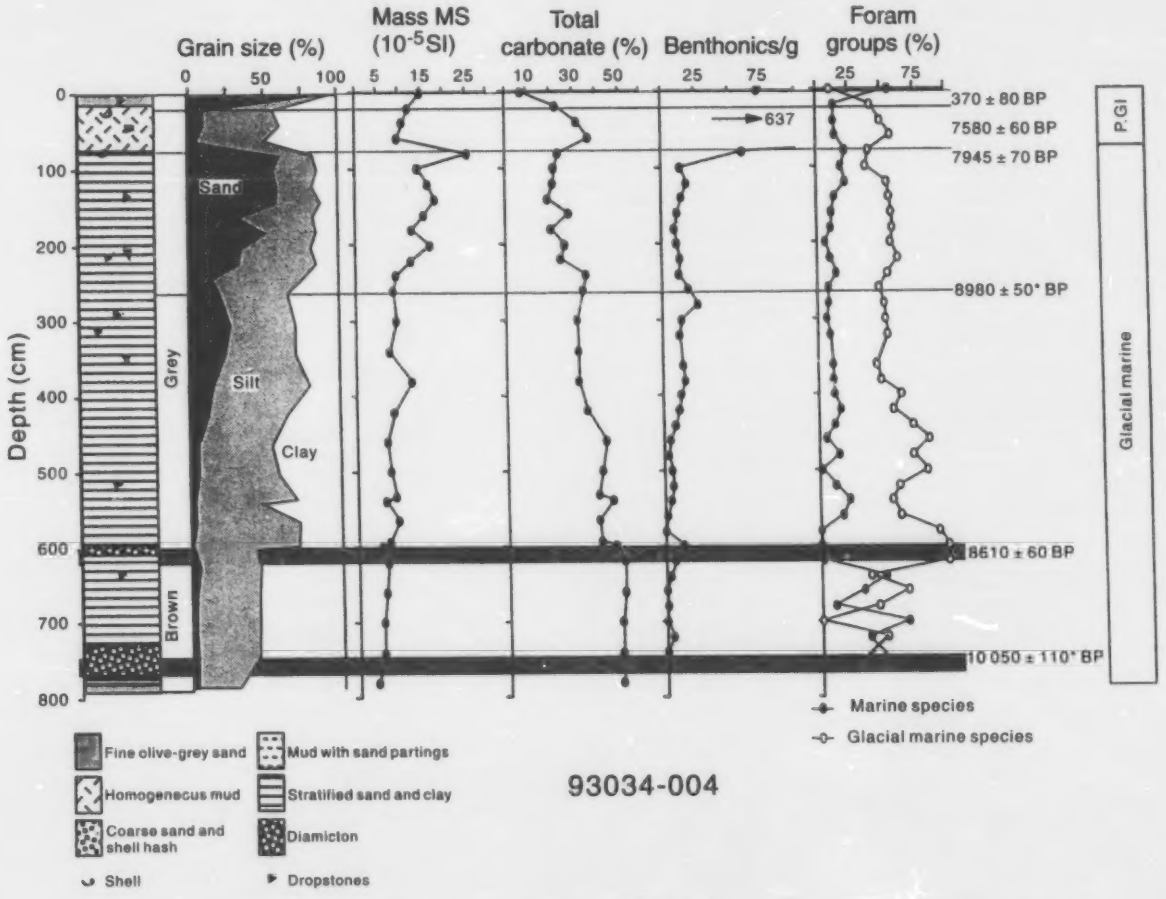

Figure 3. *Grain size, mass magnetic susceptibility, per cent carbonate, benthonic foraminifers, and chronological data from core 93034-004 in Eastern basin. Asterisks by dates indicate dating reversals or suspect age data* (modified from *Jennings et al., 1998, Fig. 5;* see also *Fig. 1; MacLean, 2001, Fig. 5; MacLean et al., 2001, Fig. 39; Hardy, 2001, Fig. 3). P.Gl = Postglacial.*

In addition to the glaciomarine species, however, there are frequent sporadic occurrences of species from virtually all of the other faunal zones, including planktonic foraminifers, *Astrononion gallowayi*, *Melonis zaandamae*, *Islandiella helenae* and *I. norcrossi*, *Cibicides lobatulus*, *Cassidulina teretis*, *Fursenkoina fusiformis*, *Pullenia osloensis*, *Buccella frigida*, *B. arctica* and others (e.g. Fig. 2, and "marine species" in Fig. 3). These species do not make up the abundance peaks. For Eastern basin cores, Silis (1993) assigned the sediments of unit 3 to two faunal zones, unit A and a transitional faunal zone, zone T. She suggested that the juxtaposition of foraminiferal species indicative of widely differing environments could indicate that the paleoceanographic conditions fluctuated during the deposition of the ice-proximal sediments. She proposed a situation somewhat similar to that proposed by Vilks et al. (1989) for faunal zone C, suggesting that more highly saline Labrador Sea water intermittently flooded Eastern basin at the same time that there were still glaciomarine influences on sedimentation and the environment; however, results of radiocarbon dating suggest instead that where multiple species with diverse paleoecological significance occur in low abundance in ice-proximal glaciomarine sediments, these foraminifers are at least partly reworked, and do not represent the environmental conditions at the time of deposition of the glaciomarine sediments. Three radiocarbon dates, one each from the lower parts of cores 93034-002, 93034-004, and 93034-029, in the most ice-proximal sediments were reservoir corrected to between 10.6 ka BP and 9.6 ka BP (Fig. 1; Manley and Jennings, 1996). These dates were obtained from low-abundance zones using all of the well preserved carbonate material present, including juvenile molluscs, ostracodes, and various foraminiferal species (e.g. Fig. 3). These older dates were collected as little as 1.5 m below the younger dates on ice-proximal sedimentation (e.g. Fig. 3). Given the rapid sedimentation rates generally associated with ice-proximal conditions and the paucity of fauna, we suggest that the older dates represent glacial reworking of previously deposited

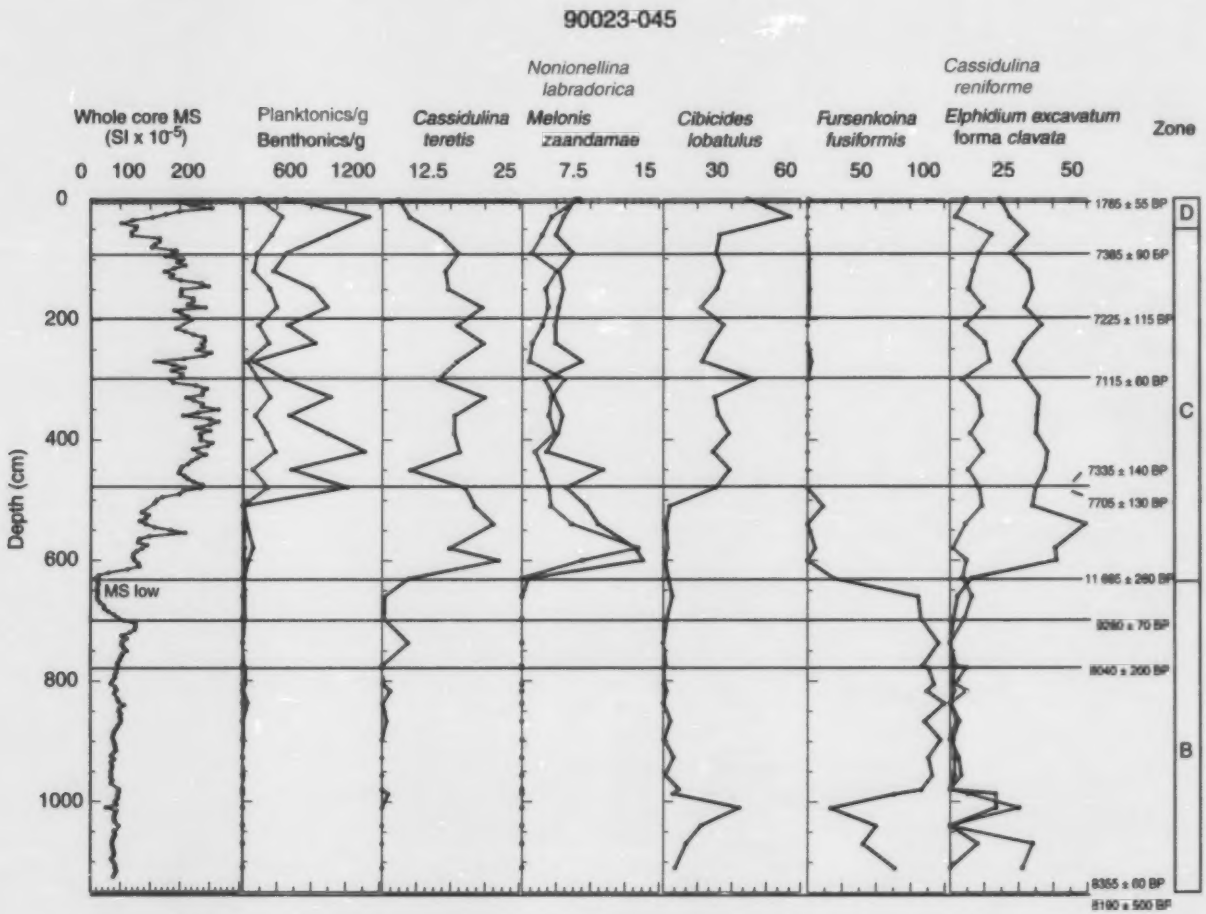

Figure 4. *Abundances (%) of major foraminiferal species in core 90023-045 from Eastern basin and whole-core magnetic susceptibility. Asterisks beside radiocarbon dates indicate dating reversals or suspect age data* (see also *Fig. 1; MacLean, 2001, Fig. 5; MacLean et al., 2001, Fig. 28).*

glaciomarine and marine sediments. In cores 93034-002 and 93034-004, three dates from within and slightly below the MS peak that distinguishes the top of the glaciomarine sediments have been obtained from both single mollusc shells and foraminifers (Fig. 1, 3; Manley and Jennings, 1996). These dates are in the range of 9.9–8.9 ka BP (MacLean et al., 2001, Table 2), consistently too old in comparison to the dates of 8.6–8.4 ka BP that occur lower in the glaciomarine section.

The old dates and stratigraphic reversals suggest that there was considerable reworking (i.e. glacial erosion and redeposition) of previously deposited marine and glaciomarine sediments throughout deposition of the ice-proximal sediments of seismic unit 3. The several dates between 8.6 ka BP and 8.4 ka BP on abundance peaks in ice-proximal species in cores from Eastern basin, suggest that foraminiferal productivity began in Eastern basin during that interval (Jennings et al., 1998). The dating reversals and old ages from both foraminifers and molluscs suggest that the glaciomarine sediments of unit 3 contain both reworked and in situ fauna; however, use of samples from foraminiferal abundance peaks, especially abundance peaks of individual species, and core-to-core seismic correlations of dated intervals have permitted reliable utilization of foraminiferal dates from several Eastern basin cores (e.g. MacLean et al., 2001, Fig. 32, 33). The most conservative interpretation of the overall faunal data in the lower part of the glaciomarine section is that occurrence of anomalous species results from inclusion of reworked material rather than from fluctuating oceanographic conditions and intermittent incursion of Labrador Sea waters into Eastern basin. In the sense of the environmental interpretation, these sediments in Eastern basin likely belong in faunal zone A of Vilks et al. (1989), rather than to a transitional faunal zone T.

Foraminifers in distal glaciomarine sediments, upper unit 3

Faunal zone B occurs only in cores from the thick glaciomarine sediments in the deeper parts of Eastern basin (MacLean et al., 2001, Fig. 22). It was described originally from cores 85027-055 and 85027-057 (Vilks et al., 1989), and has since been recognized as a major component of ice-distal sediments in core 90023-045 (Fig. 1, 4; MacLean et al., 2001, Fig. 28). On seismic profiles these sites contain thick sections of unit 3 (MacLean et al., 2001, Fig. 22, 28, 32, 33). Cores discussed above that sampled faunal zone A tend to have thin glaciomarine sediments and lack the ice-distal facies, such that postglacial sediments overlie the ice-proximal glaciomarine lithofacies and biofacies. At the site of core 90023-045 there are 55 m of glaciomarine sediments of unit 3 (MacLean et al., 2001, Fig. 32). Core 90023-045 ends within faunal zone B. Seismic correlation with core 90023-042 indicates that ice-proximal beds of faunal zone A lie 20–25 m below the base of core 90023-045 when traced from core 90023-042 into the deep basin to the site of core 90023-045 (MacLean et al., 2001, Fig. 32). Two radiocarbon dates were obtained from the base of core 90023-045, one on paired valves of *Portlandia arctica* (8355 ± 60 BP) and the other on *Fursenkoina fusiformis* (8190 ± 500 BP) (Fig. 1, 4; Andrews et al., 1995; Manley and Jennings, 1996; MacLean et al., 2001, Table 2). The dates overlap at one sigma, suggesting that the shell and the foraminifers are coeval, and that the foraminifers in this zone are not reworked from older deposits. Being a larger sample on a single individual, the *Portlandia* date is likely to be more reliable. It indicates that zone B deposition had begun by ca. 8.35 ka BP in Eastern basin. Thus, although there is a thick sediment package represented by the ice-proximal and ice-distal glaciomarine sediments at the site of core 90023-045, this interval likely represents a relatively short time period. Deposition of the glaciomarine ice-proximal sequences is inferred to have commenced coincident with lift off of Noble Inlet ice in the deep basin and to have continued as the ice-sheet grounding line progressively shallowed on the basin flanks.

In Eastern basin core 90023-045, faunal zone B is dominated by *Fursenkoina fusiformis* (Fig. 1, 4). Species that are typical components of zone A occur in very low percentages in this zone, except in the basal metre of the core, where the faunal abundances are less than 10/mL. Above the basal metre, foraminiferal abundances continue to be low, generally less than approximately 40/mL. Planktonic foraminifers (*Neogloboquadrina pachyderma* sinistral) are rare throughout zone B, but gradually rise in abundance upwards in the zone.

According to the biostratigraphic framework published by Vilks et al. (1989) the top of zone B should correspond to the top of the glaciomarine sediments of seismic unit 3. This transition coincides with the base of the MS low interval dated ca. 8 ka BP that occurs in many Eastern basin cores (Andrews et al., 1995) and which occurs at 7 m in core 90023-045 (Fig. 4). A *Portlandia* AMS date of 8040 ± 200 BP that underlies the base of the MS low interval by 78 cm supports the stratigraphic interpretation (Fig. 1, 4); however, faunal zone B appears to persist into the lower MS sediments to about 630 cm, and it is difficult to determine whether zone B truly extends into the base of the postglacial sediments or whether previously deposited sediments of zone B were reworked into the MS low interval. Radiocarbon age reversals at the base and the top of the MS low interval indicate the presence of reworked material within it (Fig. 1, 4). The lower date was obtained on mixed foraminiferal species including *Fursenkoina fusiformis*, but because this species is small and thin walled, and because it was shown to be coeval with the sediments at the base of the zone, it cannot account for all of the reworked material. An even larger stratigraphic reversal occurs at the top of the U-shaped low MS interval at 633 cm. It may be attributed to the anomalously high numbers of the large, dense species *Pyrgo williamsoni* and *Quinqueloculina* sp. that made up a significant portion of the material dated at that level (Manley and Jennings, 1996).

Newly acquired AMS radiocarbon dates on core 85027-057, suggest that this core does not terminate in ice-distal faunal zone B as was originally shown by Vilks et al. (1989) (Fig. 1, 5). The basal date on the core of 7.9 ka BP, and the lack of the low MS interval (Andrews et al., 1995) suggest that this core terminates within the early postglacial sediments of seismic unit 4 and faunal zone C (Fig. 1, 5; MacLean et al., 2001, Fig. 22). The depth at which the MS

low interval occurs in nearby core 87033-012 (Andrews et al., 1995), and a date of 8010 ± 95 BP (Manley and Jennings, 1996) from near the top of the glaciomarine section there support this reinterpretation.

Cores 87033-011 and 90023-031 from the easternmost part of Eastern basin collected what appear to be glaciomarine sediments of unit 3. These sediments have a different acoustic character than glaciomarine sediments elsewhere in the basin in that the acoustic reflections are denser and more closely spaced (Fig. 1; MacLean et al., 2001, Fig. 30). Based upon the MS data, the cores overlap stratigraphically; the low MS interval which marks the glaciomarine-postglacial boundary (Andrews et al., 1995) is present in both cores and is used as a datum. In core 90023-031, the MS low is dated at slightly younger than 8190 ± 105 BP (Kerwin, 1994, 1996), which is consistent with the age of deglaciation determined from other cores. It is difficult to interpret the foraminiferal assemblages in core 87033-011 with no radiocarbon control other than that provided by the MS low interval and correlation with core 90023-031. The MS low interval occurs at 2 m depth, coinciding with the rise in foraminiferal abundance, suggesting that the sediments above 2 m depth are postglacial, and those below are glaciomarine; but the assemblages differ from other foraminiferal assemblages in Eastern basin in terms of the overall high faunal abundance, and the occurrence of planktonic foraminifers, *Cassidulina teretis*, *Cibicides lobatulus*, *Astrononion gallowayi*, and *Pullenia osloensis* throughout the core (Fig. 1, 6). The fauna are suggestive of faunal zone C, but the dating and MS correlation suggest that all of the sediments are glaciomarine rather than postglacial. Further radiocarbon dating would help to determine whether the fauna is partly reworked, explaining the unusual assemblage, or whether it represents a different environment, perhaps reflecting influx of Labrador Sea water, in the easternmost part of Eastern basin during the later part of deglaciation.

Foraminifera in early postglacial sediments, unit 4

Faunal zone C, as originally defined by Vilks et al. (1989) represents the early postglacial time period. In addition to the original Eastern basin cores in which it was described, cores

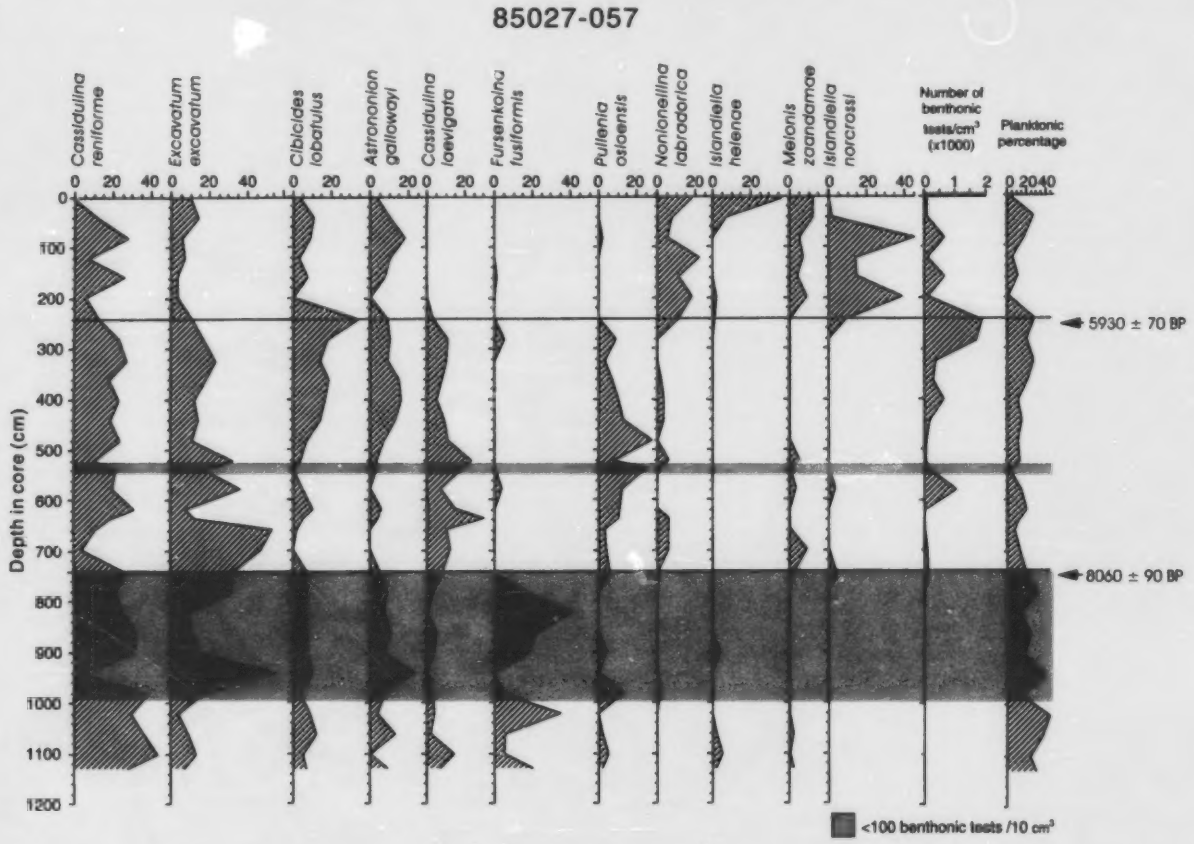

Figure 5. *Abundances (%) of major foraminiferal species in core 85027-057 from Eastern basin and relevant chronological data. The foraminiferal assemblages indicate the sediments in this core were all deposited in a postglacial environment* (see also *Fig. 1; MacLean, 2001, Fig. 5; MacLean et al., 2001, Fig. 22).

85027-056 and 85027-057, it has been recognized in cores 90023-045 and 92028-157, two cores taken very close together in Eastern basin (MacLean et al., 2001, Fig. 28). Silis (1993) suggested that faunal zone C occurs in core 90023-052, but the low faunal abundances (frequently less than 10/mL) do not support this interpretation. In cores 90023-045 and 85027-057 the early part of faunal zone C has low faunal abundances, but is marked by an increase in species diversity and species composition and decreases in percentages of *Fursenkoina fusiformis* (Fig. 4, 5). By 7.7 ka BP the faunal abundances increased abruptly to as high as 2500/mL. Species indicative of postglacial conditions, increased productivity, and the influx of saline Labrador Sea waters into Eastern basin, including *Cassidulina teretis*, *Melonis zaandamae*, and *Nonionellina labradorica* either are introduced or abruptly increase at the zone B/C boundary. Restriction of *Cassidulina teretis* primarily to Eastern basin suggests that the Labrador Sea waters generally could not penetrate farther into the strait than Eastern basin. Independent evidence of increased marine productivity is the large increase in diatom frustules per gram corresponding with the high foraminiferal abundances in the zone (K.M. Williams, unpub. data, *in* Silis (1993)). Increasing percentages of *Cibicides lobatulus* suggest that strong currents were active at

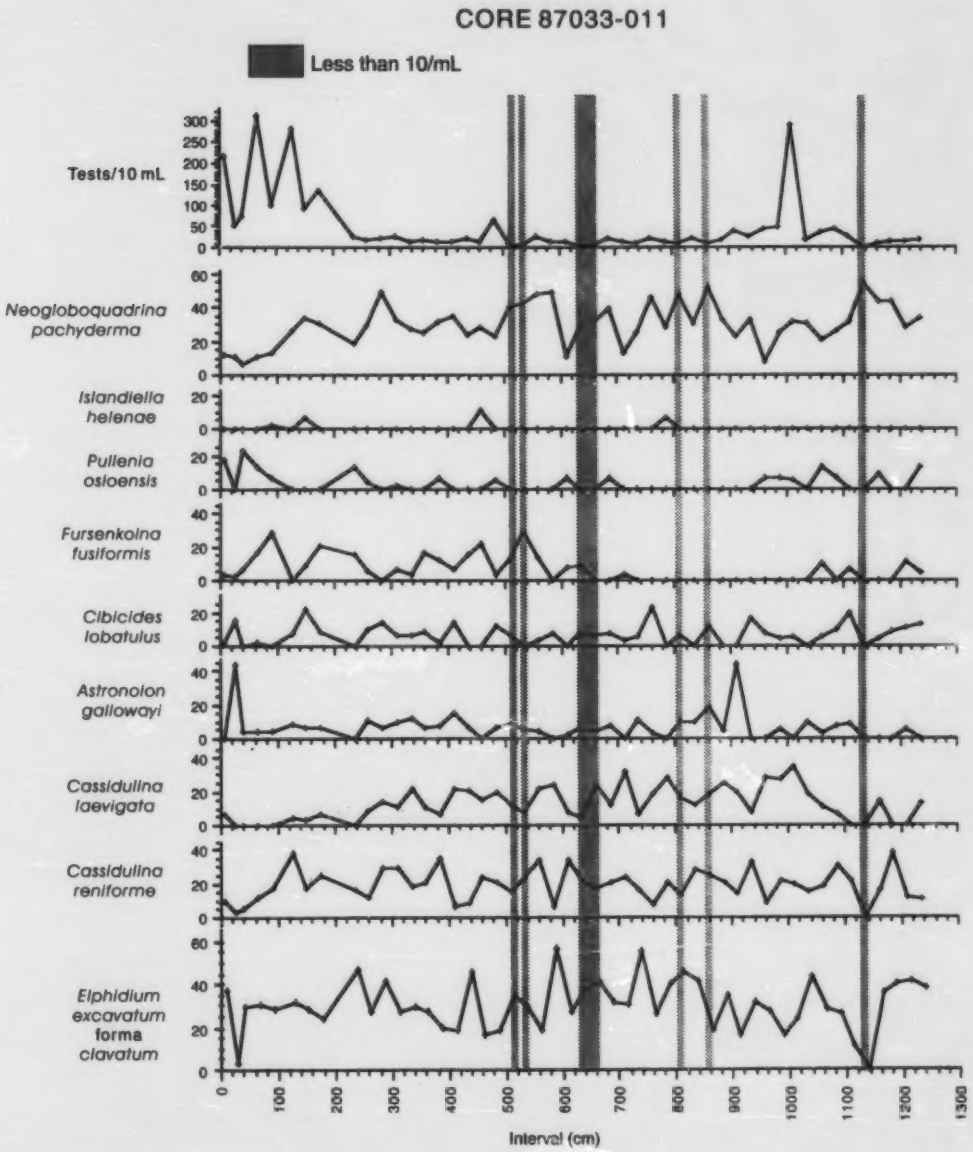

Figure 6. *Abundances (%) of major foraminiferal species in core 87033-011 from easternmost Eastern basin* (see also *Fig. 1; MacLean, 2001, Fig. 5).*

the basin margins during deposition of faunal zone C. Such observations correspond well with the lenticular deposits of seismic unit 4, which have been interpreted to indicate the influence of strong currents (MacLean et al., 1992). The best constraint on the age of the end of faunal zone C is the AMS radiocarbon date of 5480 ± 70 BP on foraminifers in a foraminiferal abundance spike at the top of zone C in core 85027-057 (Fig. 1, 5).

Foraminifera in later postglacial sediments, unit 4

Faunal zone D is present at the top of every Eastern basin core as the surface layer, and is well represented in cores that sample seismic unit 4 (e.g. 85027-057; Fig. 5; MacLean et al., 2001, Fig. 22). The fauna represents the modern foraminiferal fauna in Eastern basin (Fig. 5). It is the zone with the highest diversity in Hudson Strait (Silis, 1993). *Nonionellina labradorica*, *Astrononion gallowayi*, *Buccella arctica*, *Islandiella helenae*, and *I. norcrossi*, though present in zone C, become dominant taxa in zone D. According to the radiocarbon date in core 85027-057, the faunal zone C/D transition occurred ca. 5480 ± 70 BP (Fig. 1). Vilks et al. (1989) and Silis (1993) suggested that zone D represents the increasing influence of arctic-subarctic inner shelf waters in the later postglacial setting.

Ungava Bay

Silis (1993) interpreted the foraminiferal biostratigraphy of Ungava Bay using cores 90023-062 (southwest of Akpatok Island), 90023-034, and 90023-039 (marginal channel) (MacLean, 2001, Fig. 5; MacLean et al., 2001, Fig. 52). She identified faunal zones A and D as well as two distinct transitional zones separating the ice-proximal (A) and postglacial (D) zones (Fig. 1, 7). Zone T_1 in cores 90023-034 and 90023-039 is interpreted to reflect the dual influence of meltwater and high sedimentation rates, and the influx of saline Labrador Sea waters (Fig. 7). In zone T_1 the glaciomarine species typical of zone A, *Elphidium excavatum* forma *clavata* and *Cassidulina reniforme* codominate, but numerous other species characteristic of zones B and D occur sporadically in low percentages. The faunal abundances fluctuate widely from almost barren (<10/mL) to as high as 260/mL. Ceman (J.A. Ceman, unpub. report, 1994) analyzed foraminifers in Ungava Bay core 93034-038 (Fig. 1, 8) which penetrated thick glaciomarine sediments and a thin veneer of postglacial sediments in the marginal channel (MacLean et al., 2001, Fig. 54, 57). He interpreted the assemblages as faunal zone A throughout the glaciomarine sediments in the core indicating ice-proximal glaciomarine conditions; however, these assemblages are very similar to those of zone T_1 of Silis (1993) and more likely reflect the mixed influences of the retreating ice margin in Ungava Bay and the inflow of Labrador Sea water into the marginal channel.

Faunal zone T_2 is limited so far to core 90023-62 (Fig. 1; MacLean et al., 2001, Fig. 62). This zone has up to 150 tests/mL, but in general faunal abundances are low and species percentages do not vary like in zone T_1. As in zone T_1, the typical zone A species are joined in low percentages by species more common of zone D, *Buccella frigida*, *B. arctica*, *Cibicides lobatulus*, *Astrononion gallowayi*, and *Islandiella helenae*. Silis (1993) interpreted this zone to indicate a gradual transition from a glaciomarine to postglacial environment.

All three cores penetrated glaciomarine sediments of seismic unit 3 and retrieved only thin units of seismic unit 4 (Fig. 1). Zone A (or T_1) is present in the bases of cores 93034-038 and 90023-062. A radiocarbon date of 8220 ± 60 BP was obtained in 93034-038 on a mollusc at 9.4 m, about 9 m below the top of the glaciomarine sediments (Fig. 1; MacLean et al., 2001, Fig. 54; Manley and Jennings, 1996). A radiocarbon date of 7790 ± 150 BP was obtained in core 90023-034 on mixed foraminiferal species in a foraminiferal abundance spike in faunal zone T_1 near the top of the glaciomarine sediments (Fig. 1; MacLean et al., 2001, Fig. 52; Manley and Jennings, 1996). These dates suggest that the glacial ice had retreated onto the Ungava platform by 8.2 ka BP if not slightly earlier. The rapid sedimentation rates and ice-distal fauna in parts of Eastern basin at this time are consistent with the ice-proximal and transitional faunas closer to the retreating ice in Ungava Bay. The continued glaciomarine sedimentation, and the characteristics of the transitional faunal assemblage in Ungava Bay reflect the progressive southward retreat of the glacial ice in Ungava Bay and the inflow of Labrador Sea water into the area.

Postglacial sediment deposition in Ungava Bay has been highly variable, ranging from thick deposits that occur in parts of the marginal channel south of the platform to other areas, such as on the platform, where little or no postglacial sediments have been deposited. The thick deposits in the southern part of the marginal channel are the product of a high sedimentation rate marine environment with fluvial input from several large river outlets mixed with an influx of Labrador Sea and Hudson Strait marine waters. Prograded sediments occur locally, adjacent to the platform in the eastern part of the marginal channel. The presence of *Elphidium subarcticum* in the transition zones of the postglacial sediments of the cores Silis (1993) analyzed from that region is consistent with a deltaic environment. Otherwise, the composition of zone D in all of the cores is consistent with zone D fauna at other sites in the strait. Zone D is marked by increasing faunal abundance and diversity and increased percentages of *Nonionellina labradorica*, *Islandiella norcrossi*, *I. helenae*, *Cibicides lobatulus*, *Buccella* spp., *Astrononion gallowayi*, and *Haynesina orbiculare* (Fig. 7, 8).

Foraminifers in core 93034-036 TWC (trigger weight core) were studied by C. Schafer, J. Ceman, B. MacLean, F. Cole, and G. Vilks (unpub. manuscript, 1997) (MacLean, 2001, Fig. 5; MacLean et al., 2001, Fig. 27). Radiocarbon dates on paired molluscs from about 1.7 m in the piston core indicate rapid sedimentation at the site. Assuming a linear sedimentation rate from the average of the two dates at 1.7 m in the piston core to the top of the TWC, C. Schafer and co-workers (C. Schafer, J. Ceman, B. MacLean, F. Cole, and G. Vilks, unpub. data, 1997) calculated an average sedimentation rate of 7.89 year/cm. Calibrating the radiocarbon dates to calendar years, the 1.00 m long TWC extends to

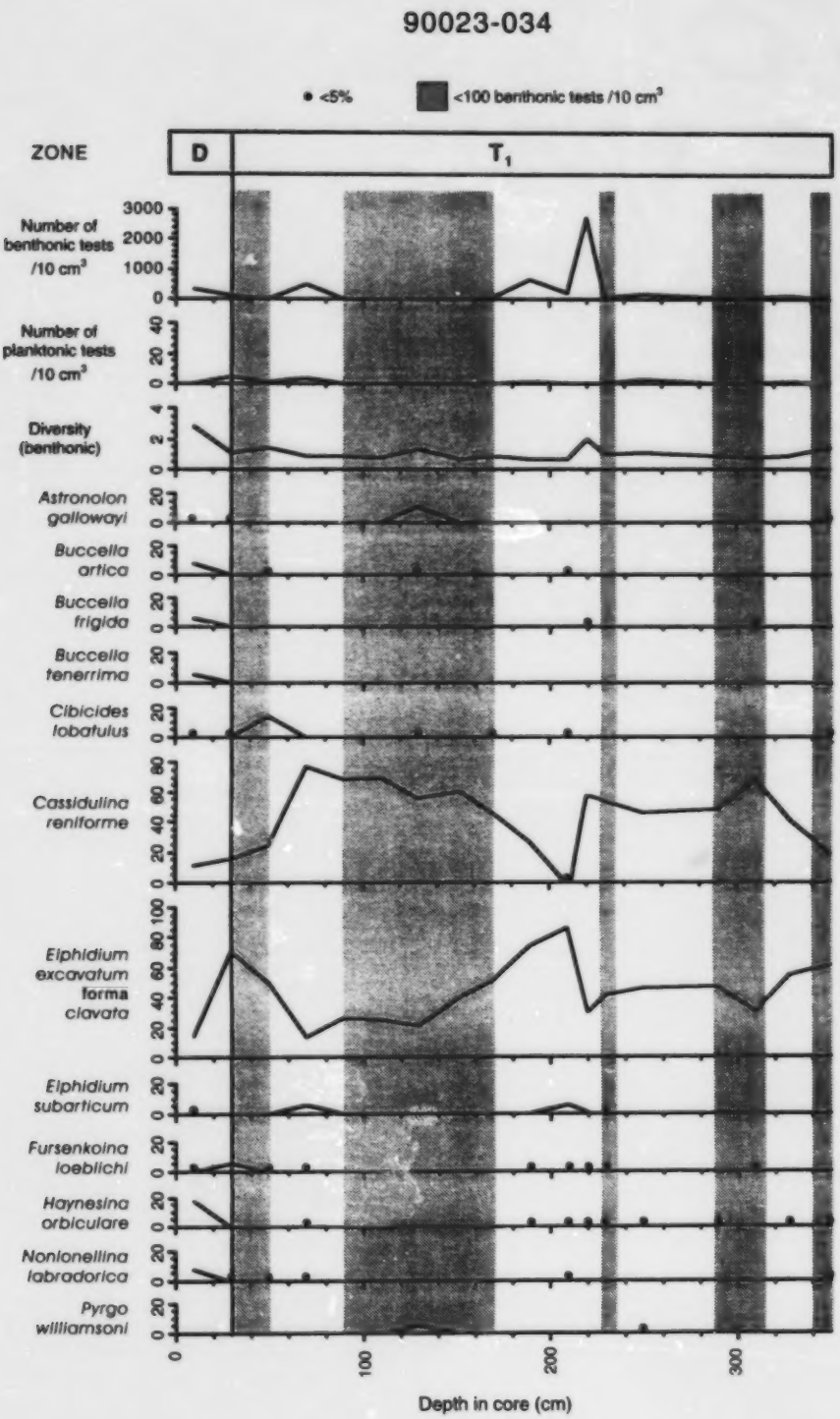

Figure 7. *Abundances (%) of major foraminiferal species in core 90023-034 from eastern Ungava Bay* (from *Silis, 1993*) (see also *Fig. 1; MacLean, 2001, Fig. 5; MacLean et al., 2001, Fig. 52*).

ca. AD 1240, thus encompassing the so-called Little Ice Age interval. Reductions in the percentages of *Elphidium excavatum* and *Fursenkoina fusiformis* during cold intervals in the seventeenth and nineteenth centuries are interpreted to reflect decreased summer stratification and a shift toward more well mixed marine conditions. The modern foraminiferal fauna at the site is dominated by the agglutinated foraminifers *Spiroplectammina biformis* and *Textularia torquata* and the calcareous species *Fursenkoina fusiformis* (=*Stainforthia feylingi*) which reflect the overall dominance of freshwater runoff from the Ungava Bay hinterland.

South-central Hudson Strait

The foraminiferal biostratigraphy of the Wakeham Bay–Héricart Bay area of south-central Hudson Strait has been studied by Vilks (*in* MacLean et al., 1992) and Silis (1993). Seismic profiles show a clear picture of a late glacial ice margin offshore in the area followed by a later readvance of limited extent that overrode and partially reworked previous glaciomarine sediments as it produced a new cycle of ice-contact and glaciomarine sediments (MacLean et al., 2001, Fig. 23; MacLean et al., 1992, 2001). Several cores have been collected in the acoustically stratified glaciomarine sediments transitional to the upper ice-contact deposit; but, determination of the timing of glacial fluctuations has been complicated by the incidence of stratigraphically inverted dates, largely on foraminifers (Manley, 1995). Radiocarbon dates on molluscs generally have yielded younger ages essentially in stratigraphic order, and thus are considered to better constrain the chronology (Manley, 1995).

Two pairs of cores from south-central Hudson Strait (MacLean, 2001, Fig. 5) give a good representation of the biostratigraphy there: cores 90023-107 (MacLean et al., 2001, Fig. 45) and 92023-153; and 90023-066 (Fig. 9; MacLean et al., 2001, Fig. 46) and 93034-013 (Fig. 10;

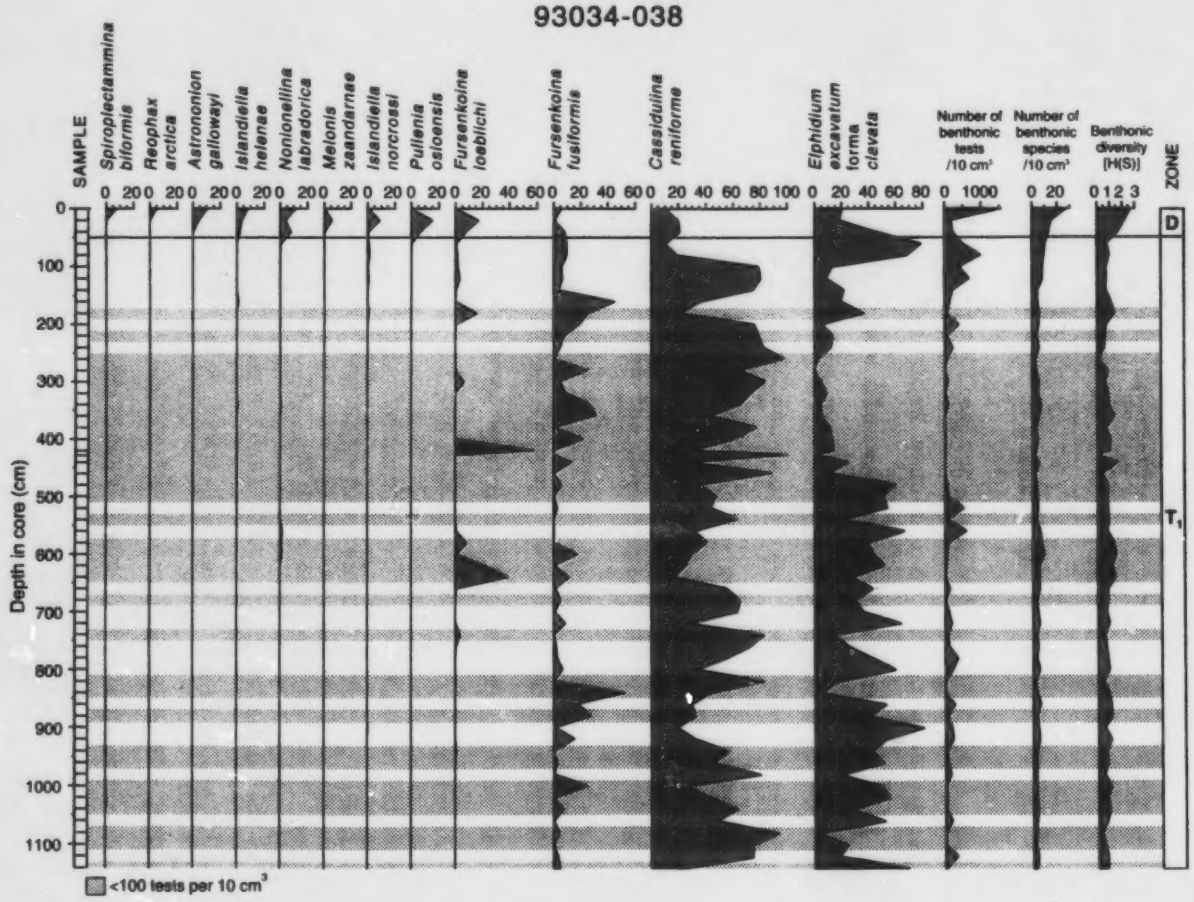

Figure 8. *Abundances (%) of major foraminiferal species in core 93034-038 in southeastern Ungava Bay. The assemblages indicate these sediments are glaciomarine except the top 50 cm which are postglacial (*from *J.A. Ceman, unpub. report, 1994) (*see also *Fig. 1; MacLean, 2001, Fig. 5; MacLean et al., 2001, Fig. 54).*

MacLean et al., 2001, Fig. 47). These cores penetrated glaciomarine sediments of seismic unit 3 with a thin overlying deposit of postglacial seismic unit 4 (Fig. 1; MacLean et al., 1992; Manley, 1995). The seismic stratigraphy suggests that cores 90023-107 and 92028-153 penetrate into the upper part of seismic unit 3 (Manley, 1995). Core 92028-153 contains a more complete record of seismic unit 4, but does not penetrate as far into the glaciomarine sediments of seismic unit 3 as does core 90023-107. Cores 90023-066 and 93034-013 overlap such that the 750 cm level in core 90023-066 corresponds with the 220 cm level in core 93034-013 (i.e. they essentially overlie one another with very little overlap). This correlation is supported by radiocarbon dates on paired mollusc valves in both cores (Fig. 1). Together, these two cores penetrate deeper into unit 3 than does core 90023-107 and may show evidence of the approach of the ice readvance. The discussion of the biostratigraphy therefore concentrates on cores 90023-066 and 93034-013.

The challenge at south-central Hudson Strait sites is to extract the in situ faunal signal from a potential reworked faunal signal that is suggested by inverted radiocarbon dates on foraminifers in some cores and the presence of very old radiocarbon dates in cores 93034-013, 92028-155, 90023-107, and 90023-071 (Fig. 1; Silis, 1993; Manley, 1995; Manley and Jennings, 1996; MacLean et al., 2001, Table 2). High-resolution seismic profiles show that the later glacial ice advances moved across previously deposited glaciomarine sediments nearby. These would have been a source for the reworked material (MacLean et al., 1992, 2001; Manley, 1995).

Silis (1993) suggested that south-central Hudson Strait sites contain a record of a retreating ice margin and a subsequent transition to postglacial marine conditions. She recognized faunal zone A at the base of core 90023-107 in an interval of low abundance (<10/mL) and diversity dominated by *Cassidulina reniforme* and *Elphidium excavatum* forma *clavata*. Upwards in the core the numbers and diversity of the fauna increase. Silis (1993) interpreted this change to record a gradual transition to ice-distal conditions. The fauna include species from the ice-distal zone B, such as *Fursenkoina fusiformis*, as well as those from the postglacial faunal zones, including *Buccella arctica* and *Nonionellina labradorica*.

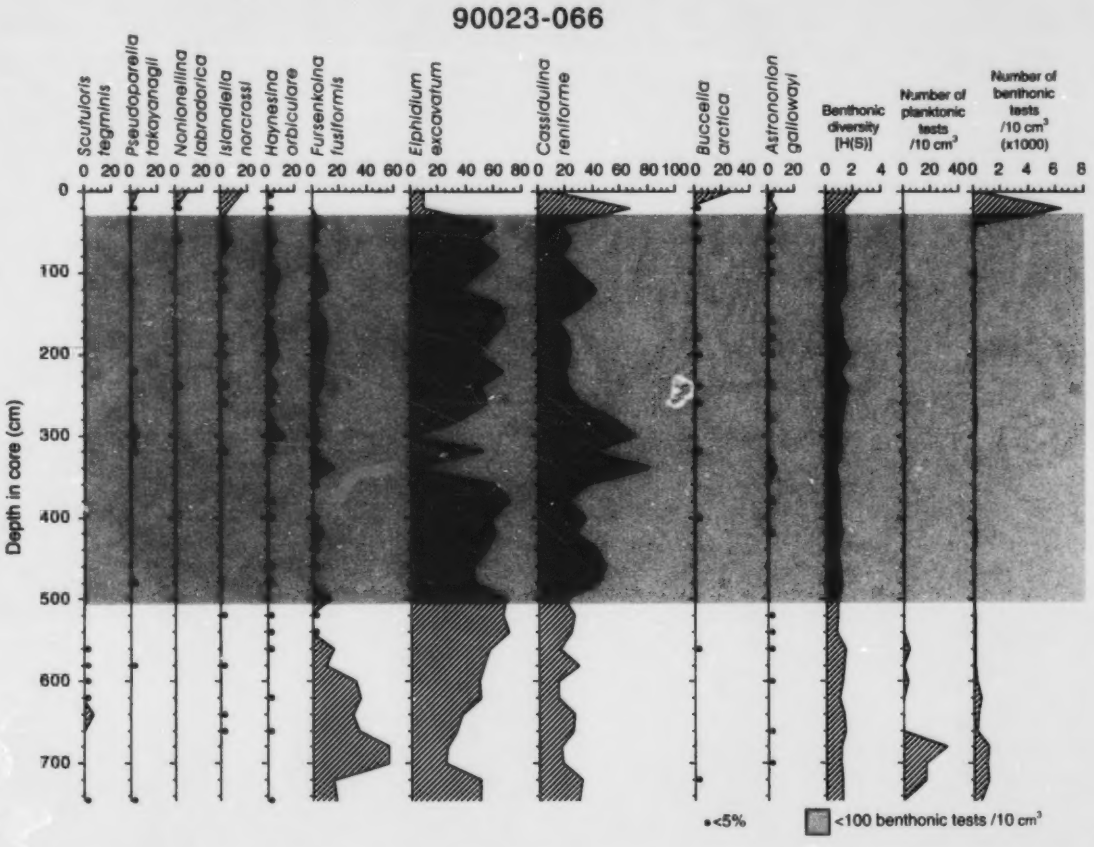

Figure 9. *Abundances (%) of major foraminiferal species in core 90023-066 from central Hudson Strait. The bottom of this core stratigraphically overlaps the top of core 93034-013 by approximately 2.2 m* (see also *Fig. 1; MacLean, 2001, Fig. 5; MacLean et al., 2001, Fig. 46, 47).*

Faunal peaks generally contained such diverse fauna. Several of the faunal peaks were dated and provided inverted radiocarbon dates relative to the mollusc dates (Manley, 1995; Manley and Jennings, 1996). Currently, it is difficult to discriminate between the in situ fauna in these glaciomarine sediments and reworked faunas which the radiocarbon dates show undoubtedly are present. Silis (1993) noted that the faunal changes in the two pairs of cores (90023-107 and 92023-153, 90023-66 and 93034-013) did not provide any basis for correlation, which could reflect the confounding effect of reworked fauna at these sites.

In core 93034-013, low foraminiferal abundances overall, and species of faunal zone A dominate the assemblage from the base of the core to about 5 m suggesting ice-proximal conditions (Fig. 1, 10). As in Eastern basin cores in ice-proximal sediments, the sporadic occurrence in low percentages of species common to ice-distal and postglacial zones indicate reworking of at least part of the fauna from earlier deposits. A date of 32.9 ka BP on mixed foraminifers and a mollusc at 6.6 m confirms that old material was incorporated into the site, but in an unknown quantity (Fig. 1). Above 5 m, benthonic abundances increase and *Fursenkoina fusiformis* becomes a dominant species along with *Cassidulina reniforme* and *Elphidium excavatum* forma *clavata* (Fig. 10). This transition is typical of the change to ice-distal faunal zone B. A radiocarbon date of 13.9 ka BP on foraminifers at 4.5 m suggests reworking, because a shell date of 8.5 ka BP lies only 2 m above it in the same faunal zone, and two shell dates in core 90023-066 in ice-distal faunal zone B also date ca. 8.4 ka BP (Fig. 1, 9). Silis (1993) noted an upward transition in core 90023-066 from a typical ice-distal faunal zone B (B_1) to a zone with lower faunal abundance and decreased percentages of *Fursenkoina fusiformis* (B_2) (Fig. 1, 9). She suggested that this zone reflected the increasing proximity of the later ice readvance. A shell date at 215 cm indicates that

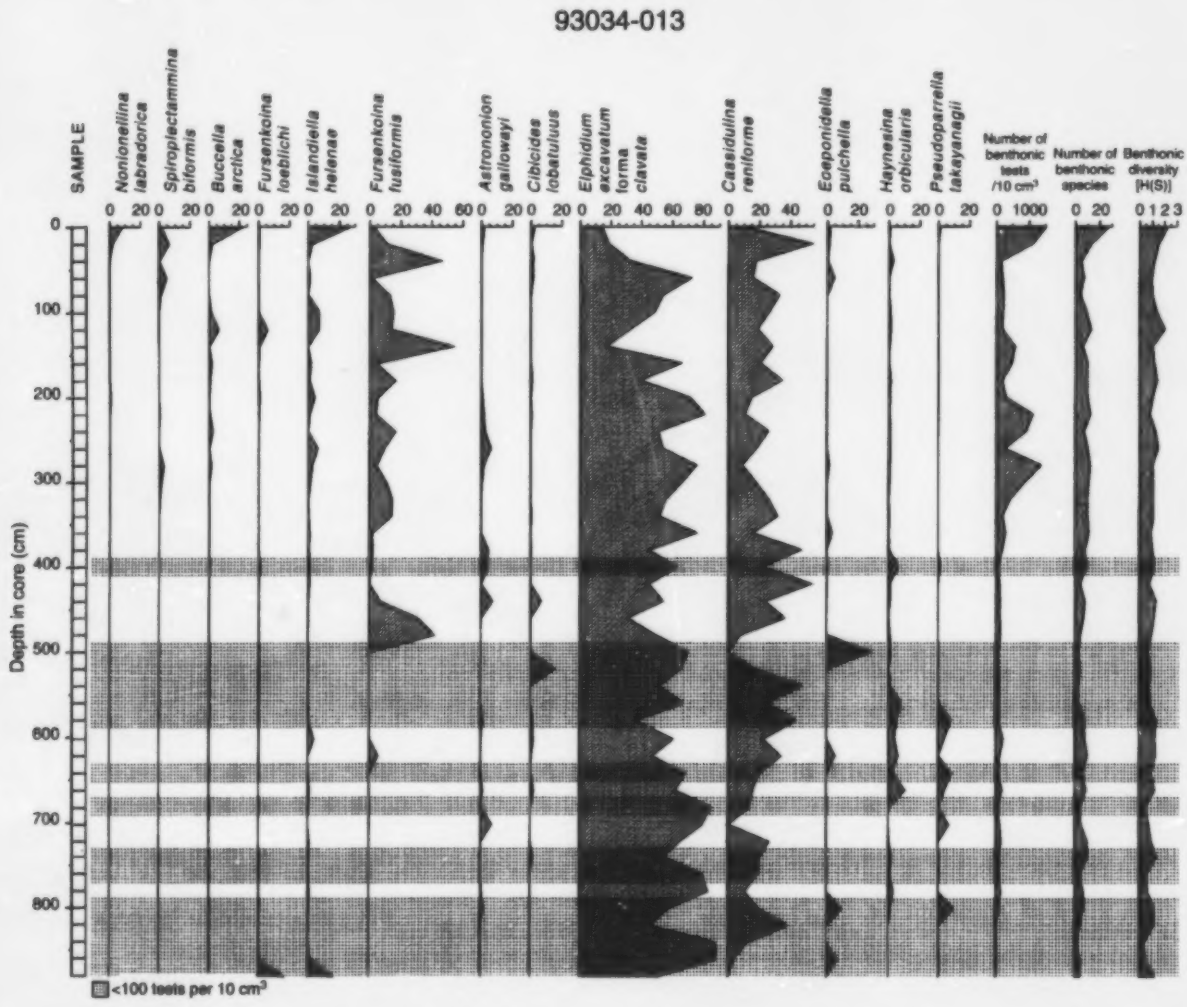

Figure 10. *Abundances (%) of major foraminiferal species in core 93034-013 from central Hudson Strait* (see also *Fig. 1; MacLean, 2001, Fig. 5; MacLean et al., 2001, Fig. 47).*

deposition of these distal glaciomarine sediments was underway at 7.9 ka BP. Postglacial conditions as indicated by the transition to faunal zone D were established by 7.8 ka BP.

Western basin

One core from Western basin, 85027-068, was included in the original biostratigraphy presented by Vilks et al. (1989) (MacLean, 2001, Fig. 5). At this site, the Huntec™ system resolved only seismic unit 3, but faunal data suggest that about 2.5 m of unit 4 overlie the glaciomarine sediments (Fig. 1, 11; MacLean et al., 1992; MacLean et al., 2001, Fig. 44). Consistent with seismic unit 3, core 85027-068 contains faunal zone A, recognized as a low-diversity, low-abundance fauna dominated by the ice-proximal glaciomarine species *Cassidulina reniforme* and *Elphidium excavatum* forma *clavata* (Fig. 1, 11; MacLean et al., 2001, Fig. 44). A radiocarbon date on *Portlandia arctica* indicates that ice-proximal glaciomarine conditions prevailed ca. 7860 ± 70 Bp. Core 85027-068 contains ice-distal faunal zone B, which corresponds with the upper part of seismic unit 3. Faunal zone D in the upper 2.8 m of core 85027-068 indicates that postglacial sediments are present at the site, although they were not resolved definitively in the high-resolution seismic records.

Silis (1993) expanded the faunal analysis of this area by analyzing the biostratigraphy of four additional cores from cruise 90023: 90023-097, 90023-099, 90023-101, and 90023-104; core 90023-099 was also discussed in MacLean et al. (1992). In this paper the data from core 90023-101 are illustrated along with the data from core 85027-068 to represent Western basin biostratigraphy (Fig. 11, 12). In addition to faunal zones A, B, and D, Silis (1993) recognized a transitional zone, faunal zone T_3 between the ice-distal and postglacial zones, B and D in core 90023-101. This zone was identified on the basis of increased abundances of benthonic and planktonic tests relative to zone B, and higher but fluctuating diversities produced by the sporadic influx of *Pullenia osloensis*, *Melonis zaandamae*, *Cassidulina teretis*, and *Nonionellina labradorica*, among others. This zone is interpreted to reflect

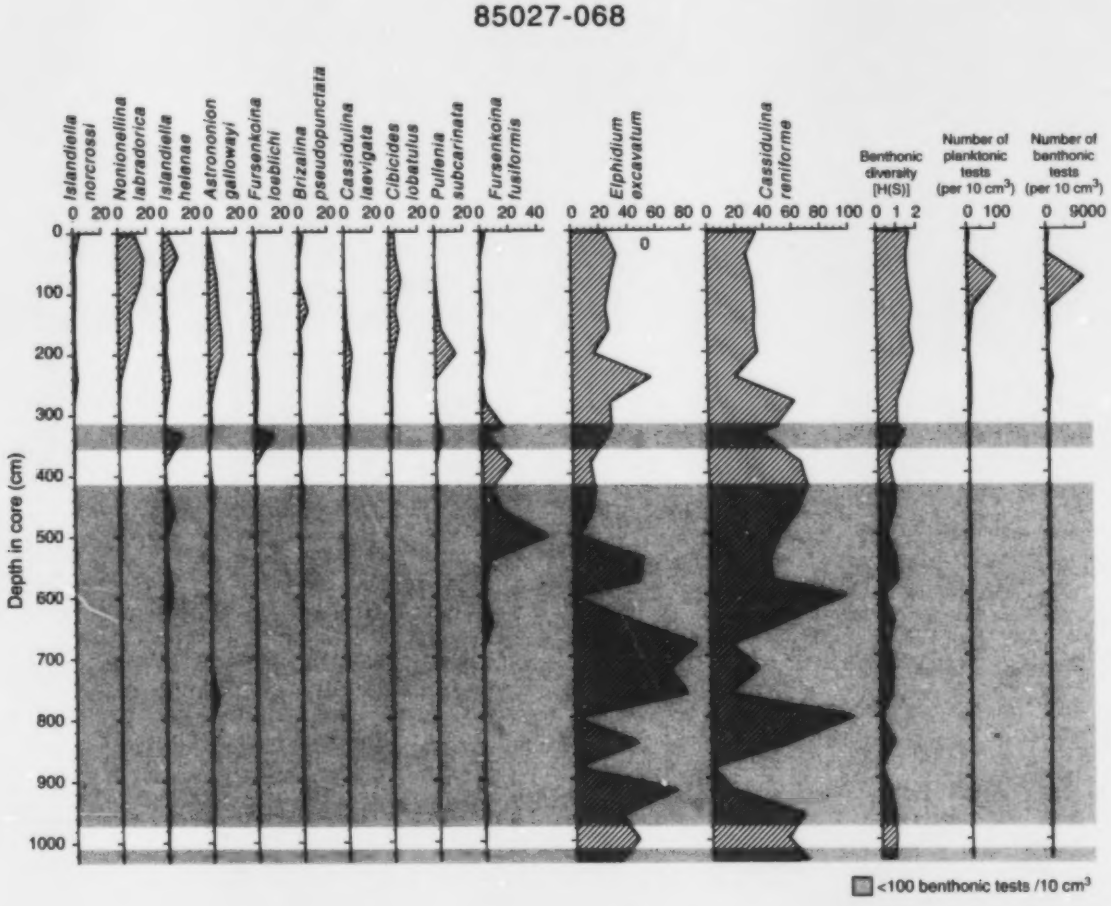

Figure 11. *Abundances (%) of major foraminiferal species in core 85027-068 in Western basin* (see also *Fig. 1; MacLean, 2001, Fig. 5; MacLean et al., 2001, Fig. 44).*

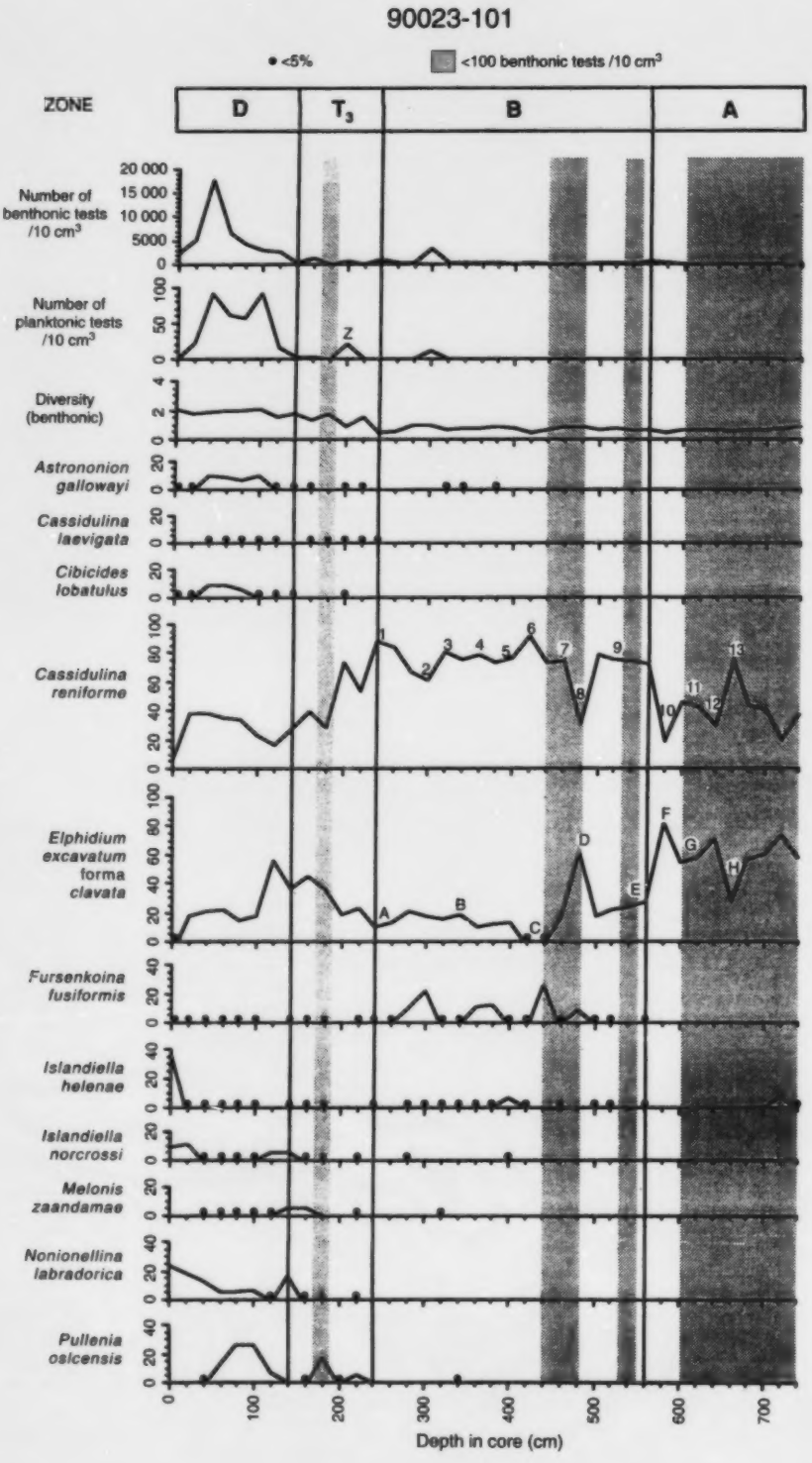

Figure 12.

Abundances (%) of major foraminiferal species in core 90023-101 in Western basin (from *Silis, 1993*) (see also *Fig. 1; MacLean, 2001, Fig. 5*).

fluctuating salinities during the transition to postglacial conditions. It is probably correlative to the top of faunal zone B and sediments of faunal zone C in Eastern basin. The influx of the Labrador Sea and typical arctic shelf fauna supports that correlation and indicates open access to the shelf at the eastern end of the strait. Using Silis' (1993) definition, zone T_3 may be found in core 85027-068 as the upper part of Vilks et al.'s (1989) original zone B. In that case, the zone would include a dark brown (10YR4/3) bed at 300–330 cm which may correlate to the low MS brown bed that occurs at a depth of 2 m in zone T_3 in core 90023-101.

Brown beds throughout the strait frequently exhibit low MS. They occur within the basal beds of the postglacial sediments in Eastern basin (i.e. with basal beds of faunal zone C) and have been proposed as a marker horizon for correlation between Eastern and Western basins (Kerwin, 1994; Andrews et al., 1995). Zone T_3 was identified as the top faunal unit of core 90023-104. A brown bed that occurs at 60 cm in core 90023-104 reinforces the faunal correlations indicated by Silis (1993). Radiocarbon dates from the glaciomarine sediments of these cores are not generally in sequence, but they mainly fall within the range of ca. 8.4–7.8 ka BP, in the time period corresponding to the final deglaciation of Hudson Bay (Hardy, 1977; Andrews et al., 1995).

Faunal diversities and planktonic and benthonic abundances increase in postglacial faunal zone D. Silis (1993) suggested that the decrease in *Fursenkoina fusiformis* and the increase in *Cibicides lobatulus* in this zone, corresponded to the sandier lithofacies. This change may be indicative of the decreased sedimentation rates in most areas during the postglacial, and a relative increase in the affects of currents.

Foraminifers in core 93034-022 TWC (MacLean et al., 2001, Fig. 26) were studied to examine the paleoenvironmental conditions in Western basin during the so-called Little Ice Age (C. Schafer, J. Ceman, B. MacLean, F. Cole, and G. Vilks, unpub. data, 1997). A single radiocarbon date on a paired mollusc at 7.1 m in the piston core indicates rapid sedimentation at the site with an estimated average rate of 5.73 year/cm. The modern fauna at the site are dominated by the arenaceous taxa *Reophax arctica* and *Spiroplectammina biformis*. The calcareous species *Fursenkoina fusiformis* (really *Stainforthia feylingi*) and *Nonionellina labradorica*

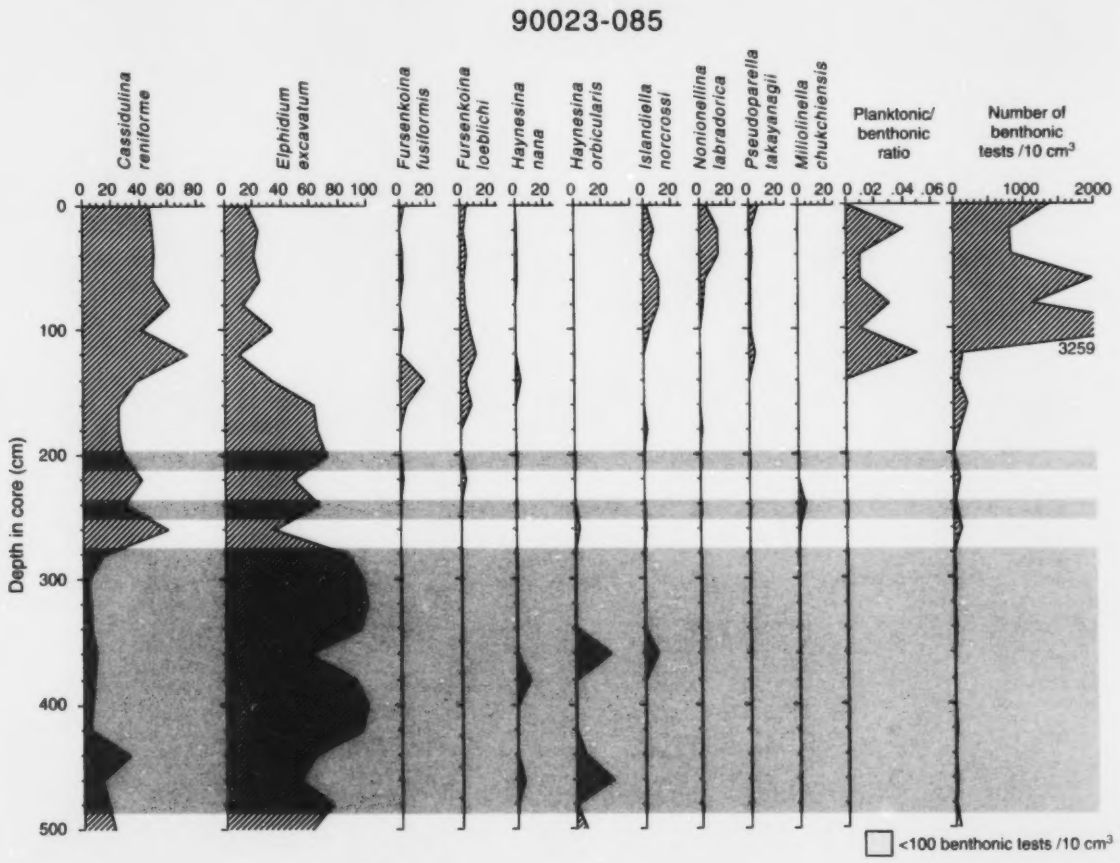

Figure 13. *Abundances (%) of foraminiferal species in core 90023-085 from Southwestern basin (see Fig. 1; MacLean, 2001, Fig. 5; MacLean et al., 2001, Fig. 18).*

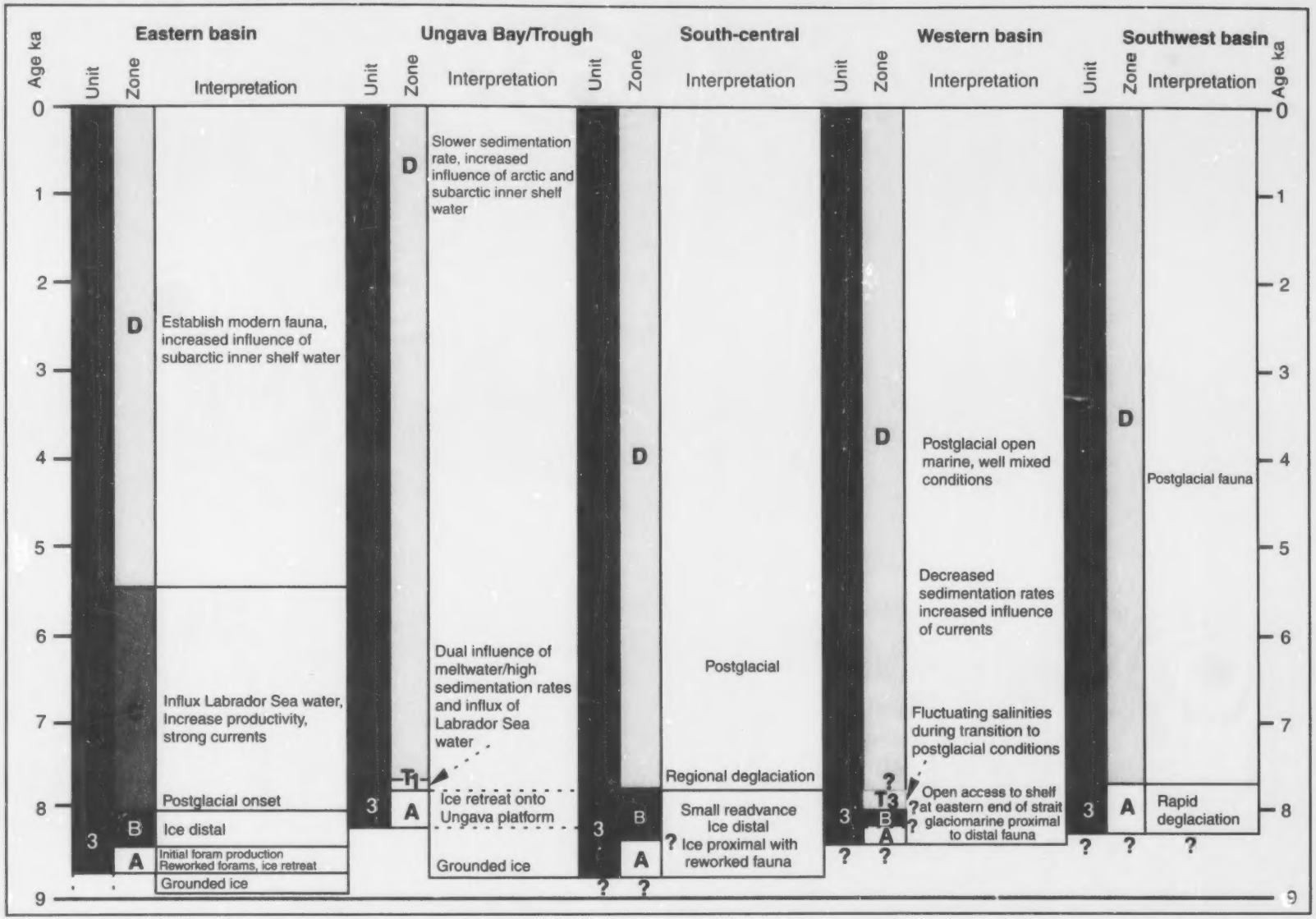

Figure 14. *Summary diagram showing faunal zones, seismic units, and paleoenvironments interpreted for the main Hudson Strait–Ungava Bay basins 9 ka BP to present.*

are also abundant, and along with a consistent presence of planktonic specimens, indicate relatively open marine, well mixed conditions. Cold intervals during the seventeenth and nineteenth centuries are characterized by increased faunal abundances and decreased percentages of calcareous foraminifers. These changes are interpreted to reflect even greater mixing and cooling of bottom-water temperatures at these times.

Southwestern basin

Southwestern basin forms a deep channel that connects Hudson Bay with Hudson Strait. Surface waters that affect the area mainly emanate from Hudson Bay. The biostratigraphy of this area has been studied by Vilks et al. (1989) using core 85027-065, and was later expanded by MacLean et al. (1992) using foraminiferal data from core 90023-085, and by Silis (1993) using three cores: 90023-085, 90023-087, and 90023-094 (MacLean, 2001, Fig. 5). Core 85027-065 was originally considered to have penetrated seismic unit 3 and postglacial sediments of seismic unit 4; however, subsequent seismic profiles and additional cores from the area suggest that core 85027-065 bottomed out above the glaciomarine beds. Data from 90023-085 (MacLean et al., 2001, Fig. 18) which penetrated though the same set of acoustically transparent sediments into the underlying typically well stratified glaciomarine section, supports the placement of core 85027-065 in the postglacial part of the section.

Only three faunal zones were recognized: A, B, and D (Fig. 13). Silis (1993) changed the originally defined A/B boundary in core 90023-085 from 240 cm to 180 cm to correspond to the first occurrence of *Fursenkoina fusiformis* in the core. The three cores analyzed by Silis (1993) contain thick intervals of faunal zone A. This zone was recognized as usual by its low faunal abundance and codominance of *Cassidulina reniforme* and *Elphidium excavatum*; however, in all cores the presence of *Haynesina orbiculare* and *Islandiella norcrossi* was suggested to signify sporadic influxes of low-salinity glacial meltwater (Silis, 1993). Zone B only occurs in core 90023-085 in which it is quite thin; the A/D faunal transition is sharply defined in cores 90023-087 and 90023-094. The poor development of faunal zone B in these cores was interpreted by Silis (1993) to indicate rapid deglaciation.

A radiocarbon date of 7720 ± 140 BP was obtained within faunal zone D, 20 cm above the D/B boundary in core 90023-085. Although the date is on mixed species of benthonic foraminifers, the fact that it is a date on a large abundance spike suggests that it is reliable. This date then provides the best constraint on the onset of postglacial conditions in southwestern Hudson Strait.

SUMMARY

Although many more cores have been studied since the biostratigraphic zonation of Vilks et al. (1989) was presented, the original zonation has proved to be robust. Subsequent foraminiferal research, in conjunction with radiocarbon dating of foraminifers and molluscs, has contributed new insights on reworking of older sediments and the implications of reworking for constructing the chronology of glacial events and paleoceanography. Figure 14 charts the faunal zones, seismic units, and paleoenvironmental interpretations in each of the five main basins of Hudson Strait against radiocarbon years. The foraminiferal zonations reflect the overwhelming environmental changes that occurred between ca. 8.8 ka BP and the present. Deglaciation is reflected by the ice-proximal and ice-distal faunal zones A and B, and by transitional zones peculiar to individual basins. These zones were short-lived, lasting for no more than about 800 years. Final deglaciation was almost instantaneous along the strait, varying by no more than a few hundred years. The foraminiferal zones in the remaining 8000 years of record reflect the influence of the regional oceanography on the shelf and the establishment of the modern tidal and surface ocean current regime in the strait.

ACKNOWLEDGMENTS

Funding for this work was provided by a grant from the United States National Science Foundation (DPP-9224251). We thank D. Hodgson, H. Josenhans, and J. Shaw for reviewing the manuscript.

REFERENCES

Andrews, J.T., MacLean, B., Kerwin, M., Manley, W., Jennings, A.E., and Hall, F.
1995: Final stages in the collapse of the Laurentide ice sheet, Hudson Strait, Canada, NWT: ^{14}C AMS dates, seismic stratigraphy, and magnetic susceptibility logs; Quaternary Science Reviews, v. 14, p. 983–1004.

Elverhøi, A., Liestol, O., and Nagy, J.
1980: Glacial erosion, sedimentation and microfauna in the inner part of Kongsfjorden, Spitsbergen; Saertrykk au Norsk Polarinsstitut, v. 172, p. 33–61.

Hald, M., Steinsung, P.I., Dokken, T., Korsun, S., Polyak, L., and Aspeli, R.
1994: Recent and Late Quaternary distribution of *Elphidium excavatum* f. *Clavatum* in arctic seas; *in* Late Cenozoic Benthic Foraminifera: Taxonomy, Ecology, and Stratigraphy, (ed.) H.P. Sejrup and K.L. Knudsen; Cushman Foundation for Foraminiferal Research, Special Publication no. 32, p. 141–154.

Hardy, L.
1977: La déglaciation et les épisodes lacustr et marin sur le versant Québécois des basses terres de la baie de james; Géographie physique et Quatenaire, vol. 31, p. 261–273.
2001: Composition of sediments in Hudson Strait and Ungava Bay; *in* Marine Geology of Hudson Strait and Ungava Bay, Eastern Arctic Canada: Late Quaternary Sediments, Depositional Environments, and Late Glacial–Deglacial History Derived from Marine and Terrestrial Studies, (ed.) B. MacLean; Geological Survey of Canada, Bulletin 566.

Jennings, A.E.
1993: The Quaternary history of Cumberland Sound, Southeastern Baffin Island: the marine evidence; Géographie physique et Quaternaire, v. 47, p. 21–42.

Jennings, A.E., Manley, W.F., MacLean, B., and Andrews, J.T.
1998: Marine evidence for the last glacial advance across eastern Hudson Strait, eastern Canadian Arctic; Journal of Quaternary Science, v. 13, no. 6, p. 501–514.

Kerwin, M.
1994: Final stages in the collapse of the Laurentide Ice Sheet: a rock magnetic and sedimentological study from Hudson Strait, Canada; M.Sc. thesis, University of Colorado, Boulder, Colorado, 189 p.
1996: A regional stratigraphic isochron (ca. 8000 14C yr B.P.) from the final deglaciation of Hudson Strait; Quaternary Research, v. 46, p. 89–98.

Knudsen, K.L. and Seidenkrantz, M-S.
1994: *Stainforthia feylingi* new species from arctic to subarctic environments, previously recorded as *Stainforthia schreibersiana* (Czjzek); *in* Cenozoic Benthic Foraminifera: Taxonomy, Ecology, and Stratigraphy, (ed.) H.P. Sejrup and K.L. Knudsen; Late Cushman Foundation for Foraminiferal Research, Special Publication no. 32, p. 5–14.

MacLean, B.
2001: Introduction: geographic setting and studies; *in* Marine Geology of Hudson Strait and Ungava Bay, Eastern Arctic Canada: Late Quaternary Sediments, Depositional Environments, and Late Glacial–Deglacial History Derived from Marine and Terrestrial Studies, (ed.) B. MacLean; Geological Survey of Canada, Bulletin 566.

MacLean, B., Andrews, J.T., Jennings, A.E., Manley, W.F., Hardy, I., Vilks, G., and Deonarine, B.
1996: Late Quaternary sediments in eastern Hudson Strait: relations with late glacial advances on southeastern Baffin Island; *in* 26th Arctic Workshop, Boulder, Colorado, March 14–16, 1996; Program with Abstracts, p. 86–88.

MacLean, B., Vilks, G., and Deonarine, B.
1992: Depositional environments and history of late Quaternary sediments in Hudson Strait and Ungava Bay: further evidence from seismic and biostratigraphic data; Géographie physique et Quaternaire, v. 46, p. 311–329.

MacLean, B., Vilks, G., Hardy, I., Deonarine, B., Jennings, A.E., and Manley, W.F.
2001: Quaternary sediments in Hudson Strait and Ungava Bay; *in* Marine Geology of Hudson Strait and Ungava Bay, Eastern Arctic Canada: Late Quaternary Sediments, Depositional Environments, and Late Glacial–Deglacial History Derived from Marine and Terrestrial Studies, (ed.) B. MacLean; Geological Survey of Canada, Bulletin 566.

Manley, W.F.
1995: Late glacial record of ice-sheet/ocean interactions, Hudson Strait and southern Baffin Island, Eastern Canadian Arctic; Ph.D. thesis, University of Colorado, Boulder, Colorado, 252 p.

Manley, W.F. and Jennings, A.E.
1996: Radiocarbon Date List VIII: Eastern Canadian Arctic, Labrador, East Greenland Shelf, Iceland Shelf, and Antarctica; Institute of Arctic and Alpine Research, University of Colorado, Occasional Paper no. 50, 163 p.

Nagy, J.
1965: Quaternary glaciomarine deposits and foraminifera from Edgeoya, Svalbard; Boreas, v. 13, p. 319–332.

Osterman, L. and Andrews, J.T.
1983: Changes in glacial-marine sedimentation in Core HU77-159, Frobisher Bay, Baffin Island, N.W.T.: a record of proximal, distal and ice rafting glacial-marine environments; *in* Glacial-marine Sedimentation, (ed.) B.F. Molnia; Plenum Publishing Corporation, New York, New York, p. 451–493.

Seidenkrantz, M-S.
1995: *Cassidulina teretis* Tappan and *Cassidulina neoteretis* new species (Foraminifera): stratigraphic markers for deep sea and outer shelf areas; Journal of Micropaleontology, v. 14, no. 2, p. 145–157.

Silis, A.B.
1993: Late Quaternary foraminiferal biostratigraphy of Hudson Strait; Geological Survey of Canada, Open File 3340, 127 p.

Vilks, G.
1981: Late glacial-postglacial foraminiferal boundary in sediments; Geoscience Canada, v. 8, p. 48–55.

Vilks, G., MacLean, B., Deonarine, B., Currie, C.G., and Moran, K.
1989: Late Quaternary paleoceanography and sedimentary environments in Hudson Strait; Géographie, physique et Quaternaire, v. 43, p. 161–178.

Composition of sediments in Hudson Strait and Ungava Bay

Iris Hardy[1]

Hardy, I., 2001: Composition of sediments in Hudson Strait and Ungava Bay; in *Marine Geology of Hudson Strait and Ungava Bay, Eastern Arctic Canada: Late Quaternary Sediments, Depositional Environments, and Late Glacial–Deglacial History Derived from Marine and Terrestrial Studies, (ed.) B. MacLean; Geological Survey of Canada, Bulletin 566, p. 147–159.*

Abstract: Information regarding the composition of surficial sediments in Hudson Strait and Ungava Bay comes primarily from Benthos™ piston cores, large diameter and AGC Long Coring Facility cores collected at some fifty localities, together with box cores, and IKU™ clam-shell grab samples from various localities. Many of the coring localities were selected to provide maximum information on the glaciomarine sediments and their chronologies with penetration to the underlying ice-contact sediments where feasible. Cores were also recovered from thick postglacial deposits.

Matrix-supported diamict sediments encountered at and near the base of two cores in Eastern basin are considered to be from ice-contact deposits. These sediments were barren of macrofauna and microfauna. Glaciomarine sediments consist primarily of laminated clayey and silty sediments with some sandy components, occasional dropstones, and coarser intervals. They commonly comprise distinctive rhythmically bedded muddy and sandy sediments (cyclopsams and/or cyclopels). Postglacial muddy sediments typically are dark grey, extensively bioturbated clays. Variably sandy and gravelly sediments form a thin surface veneer in areas exposed to current winnowing.

Résumé : Les données sur la composition des sédiments superficiels du détroit d'Hudson et de la baie d'Ungava proviennent surtout de carottes prélevées à l'aide d'un carottier à piston Benthos[MD], de carottes de grand diamètre et de carottes de la plate-forme de carottage en mer profonde prélevées à une cinquantaine d'endroits, et d'échantillons recueillis à divers endroits au moyen d'un carottier à boîte et d'une benne preneuse IKU[MD]. Bon nombre des lieux de carottage ont été choisis pour obtenir le plus d'information possible sur les sédiments glaciomarins et leurs chronologies et, dans la mesure du possible, le carottage atteignait les sédiments de contact glaciaire sous-jacents. Des carottes ont également été prélevées dans des dépôts postglaciaires épais.

Les sédiments diamictiques à matrice non jointive trouvés à la base ou près de la base de deux carottes provenant du bassin Est sont considérés comme des dépôts de contact glaciaire. Ces sédiments ne contenaient aucun macrofossile ou microfossile animal. Les dépôts glaciomarins comportent principalement des sédiments argileux et silteux laminés, avec quelques composantes sableuses, de rares blocs délestés et des intervalles à granulométrie plus grossière. Ils comprennent souvent des sédiments boueux et sableux à litage rythmique (cyclopsammes ou cyclopèles). Les sédiments boueux postglaciaires sont constitués habituellement d'argiles gris foncé largement bioturbées. Des sédiments de composition sableuse et graveleuse variée forment un placage dans les secteurs soumis au lavage par l'action des courants.

[1] Geological Survey of Canada (Atlantic), Bedford Institute of Oceanography, Dartmouth, Nova Scotia B2Y 4A2

INTRODUCTION

Benthos™ piston and gravity cores, AGC large-diameter cores, and Long Coring Facility cores (*see* 'Methods (marine programs)' section in MacLean (2001)) have been collected at some 50 localities (MacLean et al., 2001, Table 1) in various areas of eastern, central, and western Hudson Strait, and in Ungava Bay (MacLean, 2001, Fig. 5) as a means to ground-truth, high-resolution geophysical surveys conducted during and since the 1980s. Sites cored during cruises 85027, 87033, 90023, 92028, and 93034 delineate the regional Quaternary stratigraphy in Hudson Strait and Ungava Bay, and provide information regarding sediment composition, depositional environments, age, and the regional marine deglaciation history.

Regional seismic and sample data indicate the presence of four main sediment units. Three of these, composed of ice-contact, glaciomarine, and postglacial sediments, respectively, are represented in all the basin areas of Hudson Strait and Ungava Bay. The remaining unit (unit 2) composed of ice-contact or debris-flow sediments occurs as a subsurface deposit in the western part of Eastern basin.

ICE-CONTACT SEDIMENTS (UNIT 1)

Ice-contact sediments form the base of the Quaternary section throughout the region. These acoustically unstratified sediments are regarded as diamictons deposited subglacially or in very close proximity to glacial-ice margins. Two cores, 93034-029 and 93034-031 (MacLean, 2001, Fig. 5), both in Eastern basin, penetrated a short distance into the top of this unit, which at these localities comprises a distinct reddish-brown diamict. Ice-contact sediments were also sampled by an IKU™ clam-shell sampler at station 93034-023, 48 km northwest of Charles Island in the western region of Hudson Strait, where they consist of cohesive grey diamict.

The two cores, 93034-029 and 93034-031 from Eastern basin, illustrate ice-contact sediment composition and boundary relationships with overlying glaciomarine sediments. Core 93034-029 (Fig. 1; MacLean, 2001, Fig. 5; MacLean et al., 2001, Fig. 35) lies a few kilometres downslope from the lower and upper grounding lines on the northern flank of the basin. Diamictons, with a few small interbeds of stratified sediments, constitute the lower 472 cm of this core (Fig. 1). The lowermost 10 cm (732–742 cm) are represented by a distinctive reddish-brown (5YR5/5) diamict at the base of the core. This interval approximates the uppermost part of the ice-contact sediment unit indicated by the seismic profile at this locality (MacLean et al., 2001, Fig. 35); however, some intertonguing of ice-contact–glaciomarine sediments occurs upsection. The overlying 240 cm of sediment (upcore to 492 cm) is a diamict containing numerous till inclusions together with clay and rock clasts within a stiff greyish-brown (2.5Y5/2) to olive-grey (5Y5/2) silt and clay matrix. The brown coloration occurs mainly in the lower 150 cm of this interval (585–735 cm).

These diamict sediments are overlain upcore to 459 cm by rhythmically banded, light olive-grey, silty and clayey sediments that contain small clasts (Fig. 1). They are succeeded by 28 cm of mainly olive-grey, clayey and silty sediments that contain a few clasts of reddish-brown material similar to the sediment encountered at the base of the core. The upper part of this interval is mainly structureless and relatively homogeneous. These sediments are overlain (upcore to 270 cm) by 160 cm of olive-grey clayey-sandy diamict, which also contains reddish-brown clasts. These are succeeded by 30 cm of mainly homogeneous light grey clays, with some thin, silty beds. Rhythmically banded sediments, with clay clasts, overlie these sediments upcore to 210 cm, and they in turn are overlain by 100 cm of structureless olive-grey clay with thin interbeds of gritty sediments that contain dark grey clay clasts, and thin diamict interbeds. Overlying postglacial sediments (identified from foraminiferal assemblages; B. Deonarine, pers. comm. (1994); Jennings et al.(2001)), consist primarily of bioturbated grey clayey sediments with an interval of diamict sediments in the 60–85 cm interval.

The diamicts with interbeds of rhythmically banded sediments that compose core 93034-029 below 270 cm reflect varying sediment inputs and depositional processes related to the ice-sheet grounding lines a short distance upslope. The presence of imported material as evidenced by clay and till clasts, and the diamictic composition of much of this core, is consistent with anomalous foraminiferal assemblages and an anomalously old radiocarbon date of 10 620 ± 60 BP from the 280–285 cm interval (MacLean et al., 2001, Table 2), attributed by Jennings et al.(2001) to the occurrence of reworked material.

Ice-contact diamictons also compose much of the lower 200 cm and more of core 93034-031 located 28 km southwest of the core 93034-029 site (Fig. 2; MacLean, 2001, Fig. 5; MacLean et al., 2001, Fig. 36). These are brown to dark brown (5Y6/2), massive, sandy and silty sediments containing numerous sediment (diamict) clasts and rock clasts. The diamictons in the lower part of the core are overlain by a thin (10 cm) interval of reddish-brown, clayey sediments (5YR5/4), and a lower, till-like unit, containing red sediment clasts at 774–758 cm. Overlying sediments consisting of structureless clays, with interbeds of laminated, brown, silty and clayey sediments, and diamictons that contain sediment clasts (diamict and clay) and rock clasts (crystalline and limestone fragments) extend upcore to about 550 cm. Numerous reddish-brown clasts and grit, similar to those encountered in core 93034-029, occur in the diamict sediments. This red coloration is present in the overlying laminated sediments up to 520 cm. Overlying these beds to 380 cm are structureless clays with occasional thin interbeds of gritty sediments, some of which contain clay clasts and diamictons. Structureless clayey sediments containing a few thin (<2 mm), gritty laminae, and some clay clasts overlie these sediments upcore to 140 cm, where rhythmic banding with silt–fine sand laminae, commences and extends to the top of the glaciomarine sequence at 80 cm. Overlying postglacial sediments consist mainly of clays and silty clays with occasional clasts and a few shell fragments.

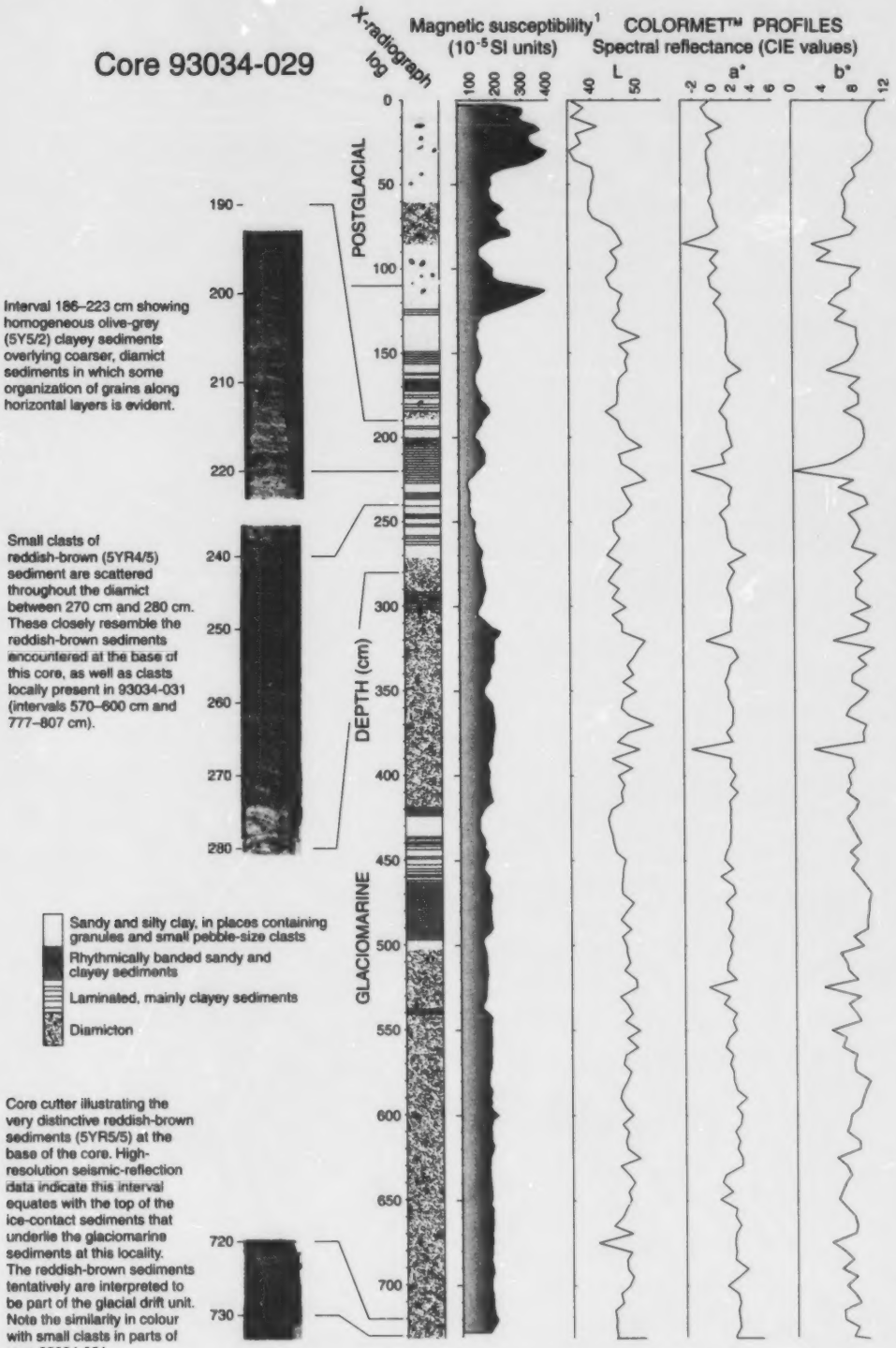
Core 93034-029
X-radiograph log
Magnetic susceptibility[1] (10⁻⁵ SI units)
COLORMET™ PROFILES
Spectral reflectance (CIE values)
L*
a*
b*
POSTGLACIAL
GLACIOMARINE
DEPTH (cm)
Interval 186–223 cm showing homogeneous olive-grey (5Y5/2) clayey sediments overlying coarser, diamict sediments in which some organization of grains along horizontal layers is evident.
Small clasts of reddish-brown (5YR4/5) sediment are scattered throughout the diamict between 270 cm and 280 cm. These closely resemble the reddish-brown sediments encountered at the base of this core, as well as clasts locally present in 93034-031 (intervals 570–600 cm and 777–807 cm).
Core cutter illustrating the very distinctive reddish-brown sediments (5YR5/5) at the base of the core. High-resolution seismic-reflection data indicate this interval equates with the top of the ice-contact sediments that underlie the glaciomarine sediments at this locality. The reddish-brown sediments tentatively are interpreted to be part of the glacial drift unit. Note the similarity in colour with small clasts in parts of core 93034-031.
Sandy and silty clay, in places containing granules and small pebble-size clasts
Rhythmically banded sandy and clayey sediments
Laminated, mainly clayey sediments
Diamicton
The L* values show high variability in the upper 4 m and less variability in the lower half of the core, indicating large changes in lightness and darkness of the sediment in the upper 4 m. The MS values show a similar trend of high variability in the upper 4 m. Colormet™ values for b* shift abruptly toward yellow and values for a* shift toward red (+) at the base of the core (745 cm) corresponding with a visually observed change to 5YR5/5 between 740–742 cm.

[1]Magnetic susceptibility data from W. Manley, Instaar, University of Colorado, U.S.A.

Figure 1. *Core 93034-029 penetrated basal glaciomarine sediments and into underlying ice-contact sediments on the northwestern flank of Eastern basin. Diagram depicts textural, magnetic susceptibility, and colour characteristics of these units and overlying postglacial sediments.*

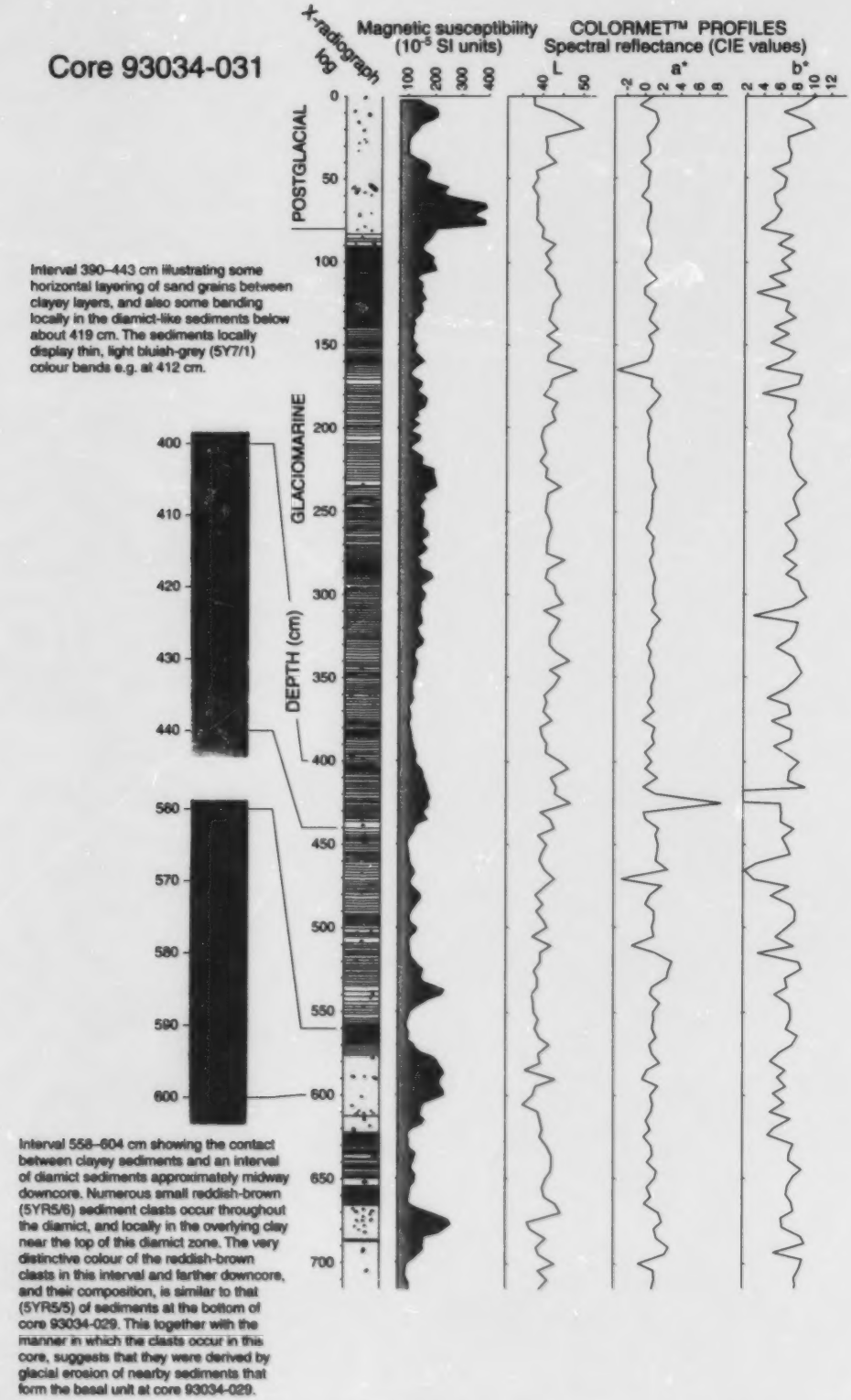
Core 93034-031
X-radiograph log
Magnetic susceptibility (10⁻⁵ SI units)
COLORMET™ PROFILES
Spectral reflectance (CIE values)
L
a*
b*
POSTGLACIAL
GLACIOMARINE
DEPTH (cm)
Interval 390–443 cm illustrating some horizontal layering of sand grains between clayey layers, and also some banding locally in the diamict-like sediments below about 419 cm. The sediments locally display thin, light bluish-grey (5Y7/1) colour bands e.g. at 412 cm.
Interval 558–604 cm showing the contact between clayey sediments and an interval of diamict sediments approximately midway downcore. Numerous small reddish-brown (5YR5/6) sediment clasts occur throughout the diamict, and locally in the overlying clay near the top of this diamict zone. The very distinctive colour of the reddish-brown clasts in this interval and farther downcore, and their composition, is similar to that (5YR5/5) of sediments at the bottom of core 93034-029. This together with the manner in which the clasts occur in this core, suggests that they were derived by glacial erosion of nearby sediments that form the basal unit at core 93034-029.

Figure 2. *Core 93034-031 penetrated postglacial, glaciomarine, and ice-contact sediments on the western flank of Eastern basin. This diagram depicts textural, colour, and magnetic susceptibility characteristics of postglacial, glaciomarine, and ice-contact sediments of core 93034-031.*

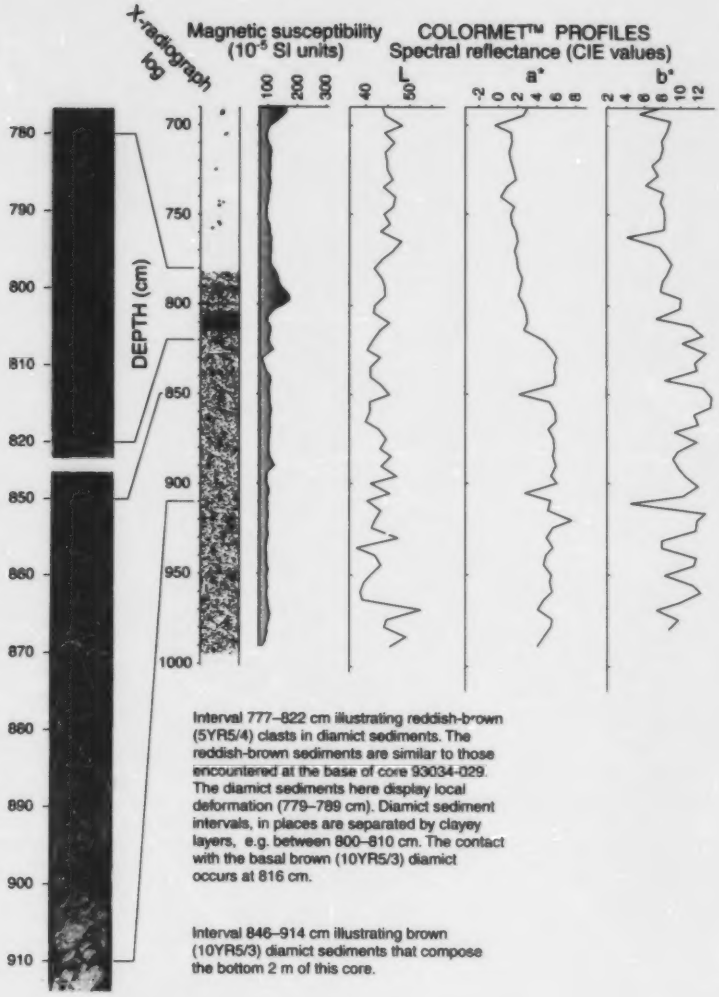

Figure 2. *(cont.)*

The basal ice-contact diamicton is barren of foraminifers upward to 845 cm (Jennings et al., 2001, Fig. 2). As in core 93034-029, the presence of sediment (diamict and clay) clasts and anomalous foraminiferal species in the lower part of the overlying glaciomarine sequence are indicative of reworked sediments. The glaciomarine ice-proximal to ice-distal boundary, occurs at about 440 cm (Jennings et al., 2001, Fig. 1). A radiocarbon date of 8470 ± 60 BP (MacLean et al., 2001, Table 2) was obtained on foraminifers in the 397–400 cm interval, a short distance above this boundary. This date is compatible with approximately equivalent dates from glaciomarine sequences in other Eastern basin cores, 90023-042, 90023-045, 90023-052, 93034-004, and 93034-006 (MacLean et al., 2001, Table 2), and is considered to be reliable.

ICE-CONTACT–DEBRIS-FLOW SEDIMENTS (UNIT 2)

Ice-contact–debris-flow sediments form an acoustically unstratified but relatively acoustically transparent unit, that locally separates underlying, acoustically denser, ice-contact sediments from overlying, glaciomarine sequences in the western part of Eastern basin. The sediments of this unit occur below the reach of available sampling systems, and their textural and biostratigraphic composition have therefore not yet been determined.

GLACIOMARINE SEDIMENTS (UNIT 3)

Glaciomarine sediments overlie ice-contact sediments in basin areas of Hudson Strait, and in parts of the marginal hannel in Ungava Bay. Lateral transitions to ice-contact

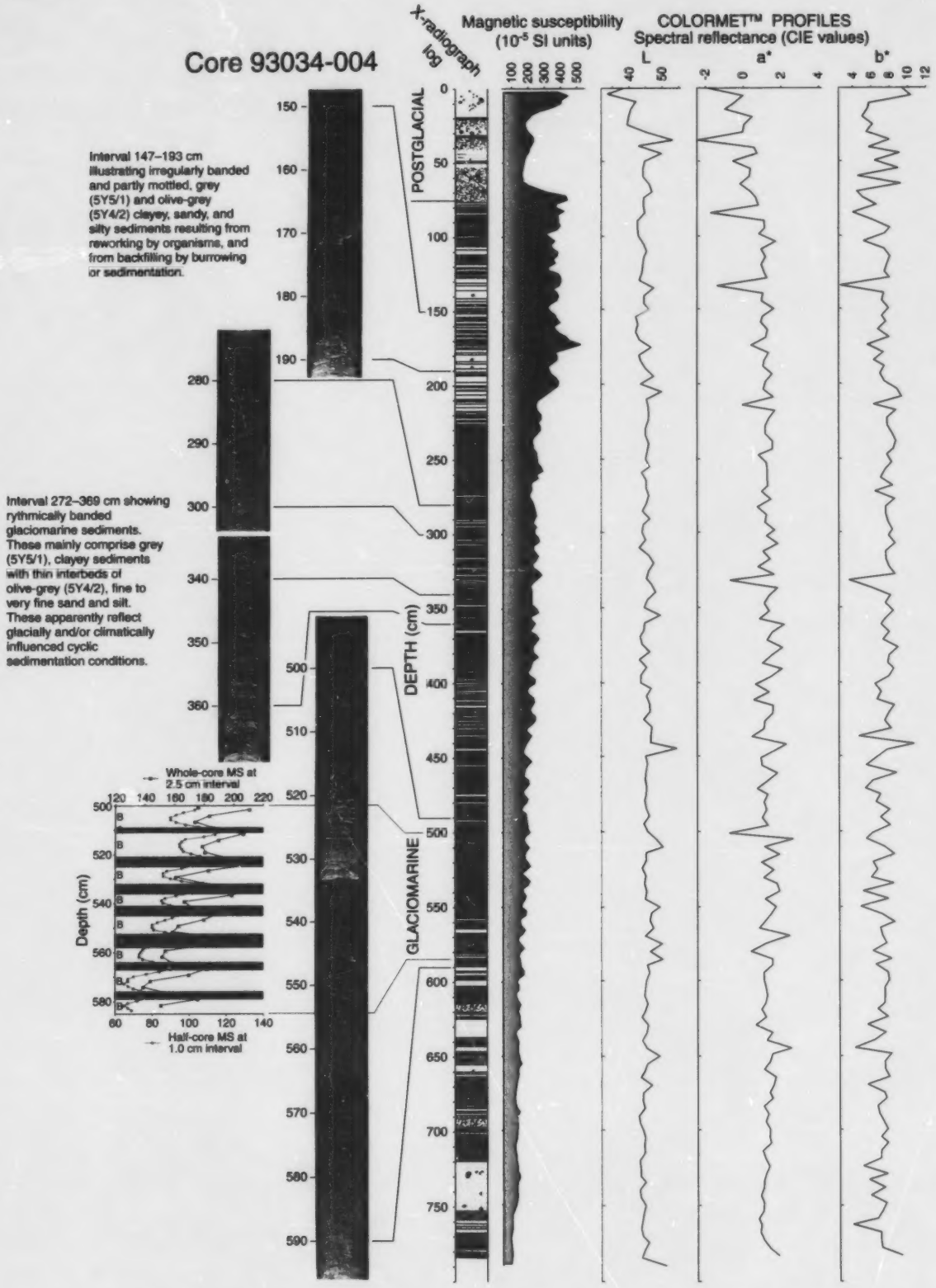
Core 93034-004
X-radiograph log
Magnetic susceptibility (10^{-5} SI units)
COLORMET™ PROFILES
Spectral reflectance (CIE values)
L
a*
b*
Interval 147–193 cm illustrating irregularly banded and partly mottled, grey (5Y5/1) and olive-grey (5Y4/2) clayey, sandy, and silty sediments resulting from reworking by organisms, and from backfilling by burrowing or sedimentation.
Interval 272–369 cm showing rythmically banded glaciomarine sediments. These mainly comprise grey (5Y5/1), clayey sediments with thin interbeds of olive-grey (5Y4/2), fine to very fine sand and silt. These apparently reflect glacially and/or climatically influenced cyclic sedimentation conditions.
Whole-core MS at 2.5 cm interval
Half-core MS at 1.0 cm interval
Depth (cm)
DEPTH (cm)
POSTGLACIAL
GLACIOMARINE

Figure 3. *Textural, colour, and magnetic susceptibility characteristics of glaciomarine and postglacial sediments in core 93034-004 midway along the northern flank of Eastern basin.*

sediments occur adjacent to former glacial margins, and ice-sheet grounding positions. Acoustic profiles and biostratigraphic data (Vilks et al., 1989; MacLean et al., 1992, 2001; Jennings et al., 2001) demonstrate that the Quaternary section penetrated at most core localities is represented by acoustically stratified glaciomarine sediments. At more than 26 core sites, these sediments typically are rhythmically banded and consist of homogeneous grey (5Y6/1), clayey sediments with sandier interlaminations and/or higher concentrations of grit in the matrix, generated perhaps from suspension fallout. At several localities coarse sand- and granule- to larger gravel-sized components occur as scattered grains or clasts throughout the glaciomarine section penetrated, indicating nearby proximity to glacial ice and/or transport by iceberg rafting. Foraminiferal assemblages within these sediments identify ice-proximal to ice-distal environments of deposition (Vilks et al., 1989; Jennings et al., 2001). Macrobenthos such as molluscs are relatively rare. Ice readvance over previously deposited glaciomarine or marine sediments (evident on seismic data in parts of both south-central and western Hudson Strait (MacLean et al., 2001, Fig. 21, 23)) resulted in incorporation of some reworked material in the younger glaciomarine deposits in many areas as indicated by anomalous foraminiferal assemblages (Andrews et al., 1995; Jennings et al., 2001), as well as by sediment clasts and inclusions in cores.

The following briefly describes representative cores of glaciomarine sediments in Eastern basin, central Hudson Strait, and Western and Southwestern basins. Core 93034-004 from a locality 60 km east-southeast of the core 93034-029 site illustrates glaciomarine sequences on the lower northern flank of Eastern basin (Fig. 3; MacLean, 2001, Fig. 5; MacLean et al., 2001, Fig. 39). Visual and X-radiographic analyses show that the lower 195 cm of core 93034-004 consists of variably laminated to structureless greyish-brown (2.5Y5/2), clayey sediments that contain clay clasts, some silt lenses, scattered grains, and a sandy lens towards the base of the core. The overlying section from 600 cm to near 200 cm is composed primarily of clayey sediments rhythmically banded with thin interbeds of olive-grey, fine to very fine sand and silt (Fig. 3). These correspond to well defined rhythmic oscillations in the magnetic susceptibility profile (Fig. 3) (Manley and Kerwin *in* MacLean et. al., 1994). This interval also includes coarse, dark grey (5Y4/2), clayey silt clasts, and occasional pebbles, which reflect the nearby proximity of glacial ice, and sediment input by iceberg rafting. Variably laminated and in part mottled, olive-grey clayey, sandy, and silty sediments, with very fine to fine sand laminae and thin interbeds extend upcore to 75 cm, which is considered to represent the top of the glaciomarine sequence (Jennings et al., 2001). Overlying postglacial sediments in core 93034-004 comprise generally structureless, olive-grey, clayey sediment, with occasional scattered grains and clasts, capped by 14 cm of medium to fine sandy sediment.

Rhythmic banding as illustrated in core 93034-004 is commonly displayed by glaciomarine sediments in the Hudson Strait–Ungava Bay region. Radiocarbon dates (MacLean et al., 2001, Table 2) provide a chronological record for these sediments in core 93034-004. Among these, however, are an 'old' date from the 738–762 cm interval downcore, and an inverted date from the 260–262.5 cm interval, that result from the presence of reworked material as evidenced by occurrences of sediment clasts within the clay matrix.

Cores 90023-066, 90023-107, 92028-153, and 93034-013 (Fig. 4, 5, 6; MacLean, 2001, Fig. 5; MacLean et al., 2001, Fig. 45, 46, 47) provide information on the composition of glaciomarine sediments in the south-central region of Hudson Strait. Of these, cores 90023-066 and 93034-013 together penetrated glaciomarine sediments to a depth of nearly 14 m, and provide the most complete information on the glaciomarine section in that region. Visual and X-radiographic examination show that the basal 78 cm of core 93034-013 (Fig. 4; MacLean et al., 2001, Fig. 47) consists almost entirely of structureless to weakly stratified, olive-grey (5Y4/2), clayey sediment, containing occasional clay clasts. The overlying 26 cm of sediment are more strongly banded, with silty and sandy laminations, thin (1–5 cm thick) interbeds of fine to coarse sand, and scattered small clasts. Similar, but weakly to strongly rhythmically banded sediments, occur upcore to 490 cm where foraminiferal assemblages indicate a change from glaciomarine ice-proximal conditions below, to ice-distal conditions above this depth (Silis, 1993; Jennings et al., 2001). Overlying beds up to 306 cm consist of variably laminated, clayey sediments with some thin, sandy partings and thin interbeds of medium to coarse sand, with occasional shell fragments. These are overlain to 140 cm by olive-grey (5Y4/1) to dark grey (5Y4/2), diamictic sediments, primarily composed of silty clay with numerous rock clasts and some clay clasts. Overlying sediments to the top of the glaciomarine sediments, which occurs at about 40 cm, are composed of dark grey, silty and sandy clay, containing occasional clay clasts. Mottling due to bioturbation occurs within a thin zone of postglacial silty and clayey sediments, that form the upper few centimetres of the core.

Correlations along high-resolution seismic profiles and dates from paired mollusc valves (MacLean et al., 2001, Table 2) demonstrate that the lower beds in core 90023-066 stratigraphically overlap the upper 2.2 m of core 93034-013 (Fig. 4, 5; MacLean et al., 2001, Fig. 46, 47).

The basal 150 cm of sediments (glaciomarine) in core 90023-066 are mainly grey (5Y5/1), silty clay, which contain occasional *Portlandica* sp. shells (paired valves and fragments) (Fig. 5). A distinct trace fossil *planulites* (*see* Hardy, 1991) is well represented throughout this unit. This interval is overlain by 100 cm of massive to weakly stratified clayey silt with some sandy lenses and pods, and occasional clay chips and pebble-sized clasts. Sandy components (pods) become more numerous in the overlying 515–497 cm interval. Above 497 cm, small angular pebble numbers increase (>5% at split coreface), with numerous clay clasts and some sand inclusions concentrated in the 430–400 cm interval. Between 475 cm and 445 cm, a second *planulites* zone was encountered, which demonstrates distinct gradational contact with the sediments above and below this zone. Overlying sediments in the 400–200 cm interval, consist of grey (5Y5/1), clayey silt with fine sand, pebbles, and clay clasts. Occasional

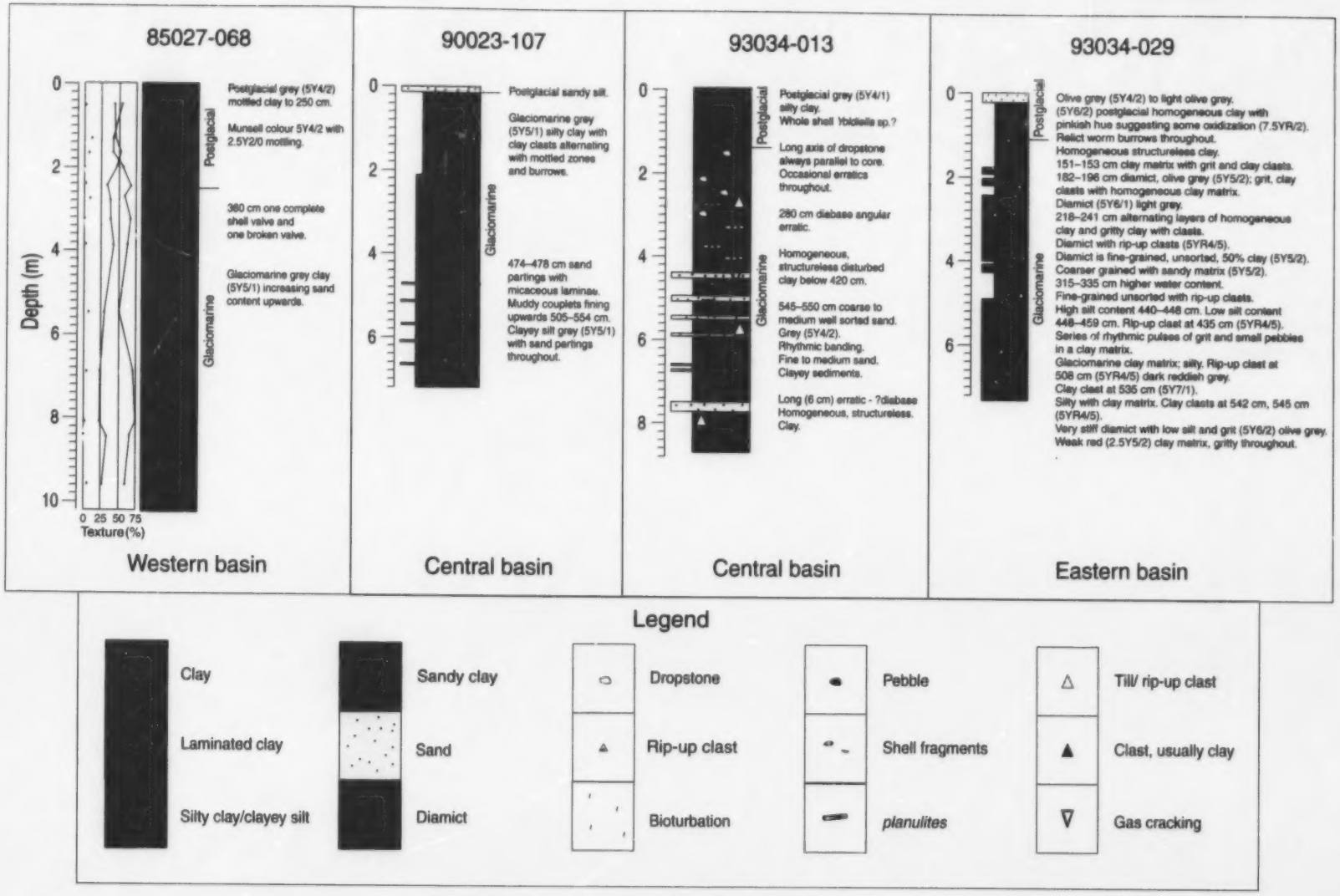
85027-068
Depth (m)
0
2
4
6
8
10
0 25 50 75
Texture (%)
Postglacial
Glaciomarine
Postglacial grey (5Y4/2) mottled clay to 250 cm.
Munsell colour 5Y4/2 with 2.5Y2/0 mottling.
360 cm one complete shell valve and one broken valve.
Glaciomarine grey clay (5Y5/1) increasing sand content upwards.
Western basin
90023-107
Postglacial
Glaciomarine
Postglacial sandy silt.
Glaciomarine grey (5Y5/1) silty clay with clay clasts alternating with mottled zones and burrows.
474–478 cm sand partings with micaceous laminae. Muddy couplets fining upwards 505–554 cm. Clayey silt grey (5Y5/1) with sand partings throughout.
Central basin
93034-013
Postglacial
Glaciomarine
Postglacial grey (5Y4/1) silty clay.
Whole shell Yoldiella sp.?
Long axis of dropstone always parallel to core. Occasional erratics throughout.
280 cm diabase angular erratic.
Homogeneous, structureless disturbed clay below 420 cm.
545–550 cm coarse to medium well sorted sand. Grey (5Y4/2). Rhythmic banding. Fine to medium sand. Clayey sediments.
Long (6 cm) erratic - ?diabase
Homogeneous, structureless. Clay.
Central basin
93034-029
Postglacial
Glaciomarine
Olive grey (5Y4/2) to light olive grey. (5Y6/2) postglacial homogeneous clay with pinkish hue suggesting some oxidization (7.5YR/2). Relict worm burrows throughout. Homogeneous structureless clay. 151–153 cm clay matrix with grit and clay clasts. 182–196 cm diamict, olive grey (5Y5/2); grit, clay clasts with homogeneous clay matrix. Diamict (5Y6/1) light grey. 218–241 cm alternating layers of homogeneous clay and gritty clay with clasts. Diamict with rip-up clasts (5YR4/5). Diamict is fine-grained, unsorted, 50% clay (5Y5/2). Coarser grained with sandy matrix (5Y5/2). 315–335 cm higher water content. Fine-grained unsorted with rip-up clasts. High silt content 440–448 cm. Low silt content 448–459 cm. Rip-up clast at 435 cm (5YR4/5). Series of rhythmic pulses of grit and small pebbles in a clay matrix. Glaciomarine clay matrix; silty. Rip-up clast at 508 cm (5YR4/5) dark reddish grey. Clay clast at 536 cm (5Y7/1). Silty with clay matrix. Clay clasts at 542 cm, 545 cm (5YR4/5). Very stiff diamict with low silt and grit (5Y6/2) olive grey. Weak red (2.5Y5/2) clay matrix, gritty throughout.
Eastern basin
Legend
Clay
Laminated clay
Silty clay/clayey silt
Sandy clay
Sand
Diamict
Dropstone
Rip-up clast
Bioturbation
Pebble
Shell fragments
planulites
Till/ rip-up clast
Clast, usually clay
Gas cracking

Figure 4. *Summary of composition and colour characteristics of sediments in cores 85027-068, 90023-107, 93034-013, and 93034-029.*

thin zones (10–25 cm) of *planulites* and broken *Portlandica* sp. shells are also represented. Sediments upcore to 20 cm, are composed of clayey silt with sandy laminae, pods, and thin interbeds, and some pebbles. A thin reddish-brown (5YR5/4) colour band occurs at 24–25 cm. The uppermost 20 cm consists of olive (5Y4/3), clayey and sandy silt with pebbles, which represent a veneer of postglacial sediments at the top of the core.

Increased content of sand, pebbles, and clay clasts above 500 cm in core 90023-066 (Fig. 5) appear to reflect the closer proximity of the late glacial ice advance (MacLean et al., 2001, Fig. 46), indicated by foraminiferal assemblages (Silis, 1993; Jennings et al., 2001). Old radiocarbon ages (32.9 ka BP and 13.9 ka BP) from foraminifers in the lowermost 4.5 m of core 93034-013 (MacLean et al., 2001, Table 2) may relate to the inclusion of fauna reworked from nearby deposits of

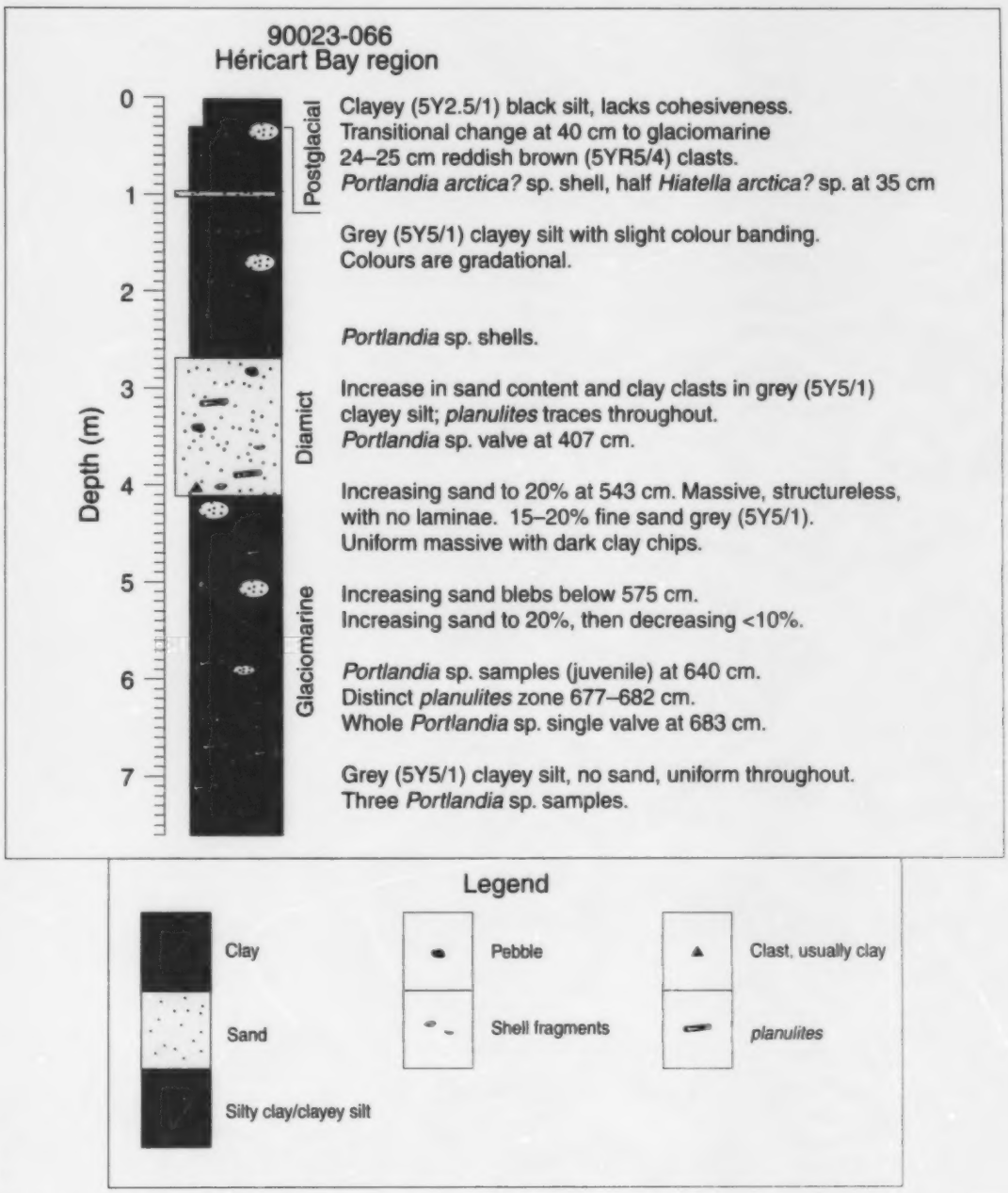
90023-066
Héricart Bay region
Depth (m)
0
1
2
3
4
5
6
7
Postglacial
Diamict
Glaciomarine
Clayey (5Y2.5/1) black silt, lacks cohesiveness.
Transitional change at 40 cm to glaciomarine
24–25 cm reddish brown (5YR5/4) clasts.
Portlandia arctica? sp. shell, half Hiatella arctica? sp. at 35 cm
Grey (5Y5/1) clayey silt with slight colour banding.
Colours are gradational.
Portlandia sp. shells.
Increase in sand content and clay clasts in grey (5Y5/1) clayey silt; planulites traces throughout.
Portlandia sp. valve at 407 cm.
Increasing sand to 20% at 543 cm. Massive, structureless, with no laminae. 15–20% fine sand grey (5Y5/1).
Uniform massive with dark clay chips.
Increasing sand blebs below 575 cm.
Increasing sand to 20%, then decreasing <10%.
Portlandia sp. samples (juvenile) at 640 cm.
Distinct planulites zone 677–682 cm.
Whole Portlandia sp. single valve at 683 cm.
Grey (5Y5/1) clayey silt, no sand, uniform throughout.
Three Portlandia sp. samples.
Legend
Clay
Sand
Silty clay/clayey silt
Pebble
Shell fragments
Clast, usually clay
planulites

Figure 5. *Textural characteristics of glaciomarine and postglacial sediments in core 90023-066 in the Héricart Bay region of south-central Hudson Strait.*

stratified glaciomarine or marine sediments that have been overridden by glacial ice (Miller and Kaufman, 1990; MacLean et al., 2001; Jennings et al., 2001).

In Western basin, core 85027-068 (Fig. 4; MacLean, 2001, Fig. 5; MacLean et al., 2001, Fig. 44) penetrated massive, grey (5Y5/1), glaciomarine mud from 1024 cm to 250 cm. Abundant soft, black clasts (5Y2.5/0), and occasional broken shell fragments occur throughout this interval. Between 887 cm and 800 cm the grey mud is slightly sandier and contains black mottling and laminae. Clasts (dropstones) are observed on X-radiographs and visually upcore to 400 cm where fine sand laminations are encountered. These occur upcore to near 250 cm, the top of the glaciomarine beds. Postglacial sediments in core 85027-068 consist of olive-grey mud (5Y4/2) with occasional mottling, small clasts, and rare shell fragments.

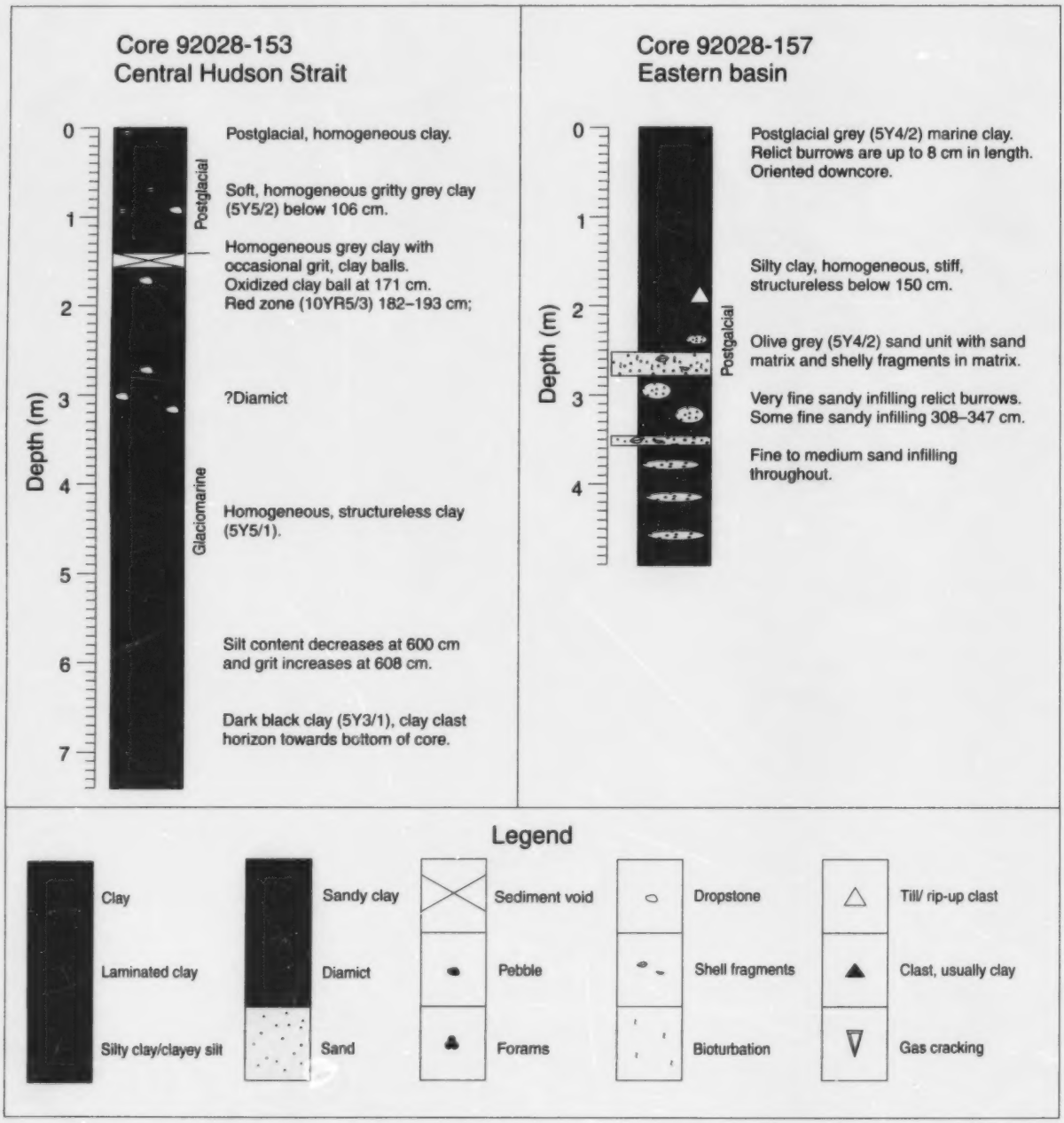

Figure 6. *Textural composition of sediments in cores 92028-153 and 92028-157 in south-central Hudson Strait and Eastern basin.*

Core 90023-085 in Southwestern basin (Fig. 7; MacLean, 2001, Fig. 5; MacLean et al., 2001, Fig. 18) penetrated glaciomarine sediments between 120 cm and the bottom of the core at 550 cm. The lower 28 cm of the core consist of gravels and large, dark grey, clay clasts, which constitute more than 40% of the split core face. These are considered to indicate very close proximity to the ice margin. Overlying these basal beds are variably laminated to massive sediments consisting of grey, silty clay and clayey silt with numerous clay clasts (locally up to approximately 50% by visual inspection of the split core face), and large angular limestone clasts. The exceptionally large number of clay clasts is a very distinctive feature of this core.

Postglacial sediments overlie the glaciomarine beds above 120 cm. These olive-grey (5Y4/3–5Y6/2), silty and clayey sediments contain a few pebbles and clay clasts near the base of that unit (to 90 cm), above which there is an abrupt reduction in clast and pebble content, and the sediments become mottled and burrowed. A thin zone of light brownish-grey sediments (10YR6/2) occurs at 112 cm.

POSTGLACIAL MUDS (UNIT 4)

Deposits of postglacial muddy sediments occur primarily in the basins where they overlie glaciomarine sediments (MacLean et al., 2001, Fig. 1). Typically they are thin, often only 1–2 m thick (MacLean et al., 2001, Fig. 5, 35, 37, 46); however, thicker deposits (up to 30 m) occur locally in Western basin (core 93034-022; MacLean et al., 2001, Fig. 26), in south-central Hudson Strait (core 93034-015; MacLean et al., 2001, Fig. 25), in southern Ungava Bay (core 93034-036; MacLean et al., 2001, Fig. 27), and to a lesser extent in Eastern basin (core 90023-045, core 92028-157; MacLean et al.,

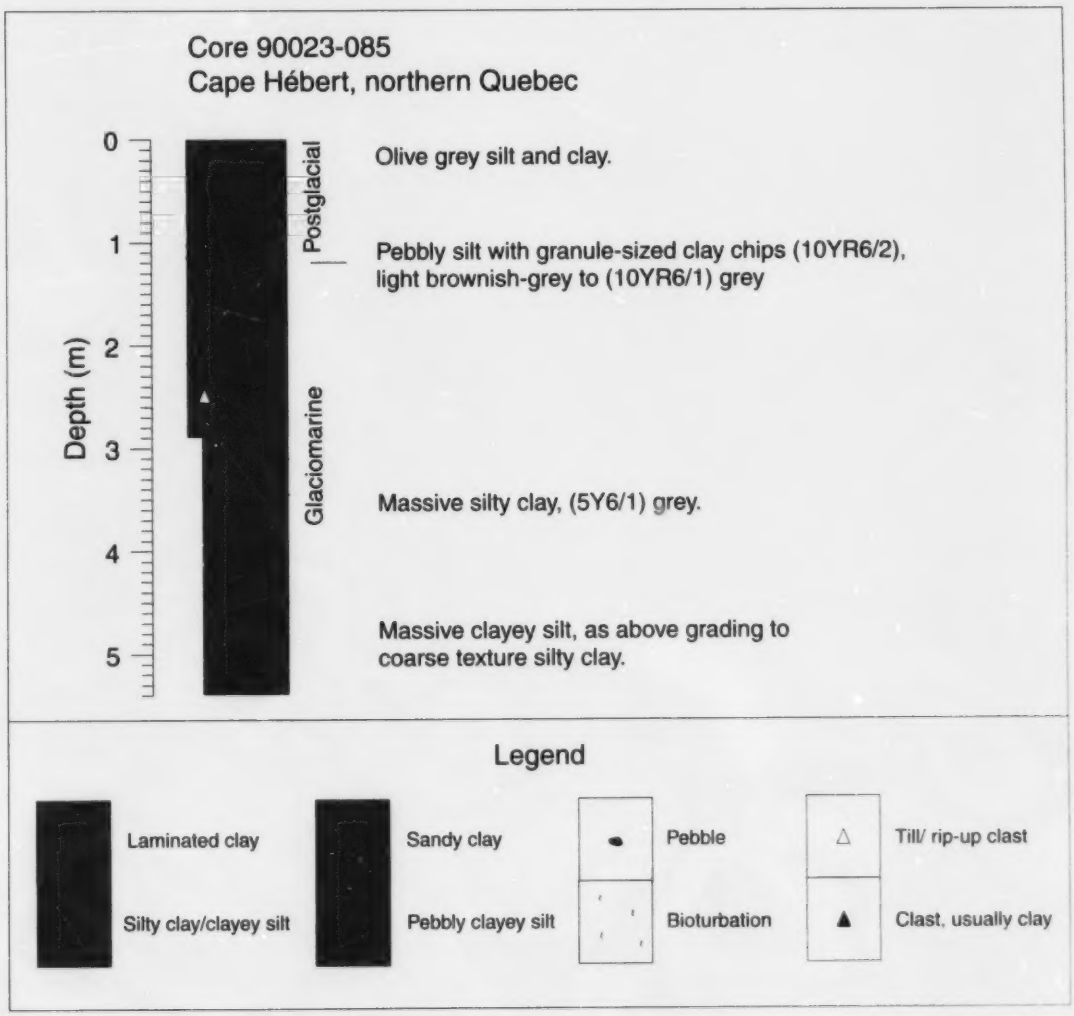

Figure 7. *Postglacial and glaciomarine sediments in core 90023-085 in Southwestern basin.*

2001, Fig. 28) and in Southwestern basin (core 90023-085; MacLean et al., 2001, Fig. 18). These sequences generally consist of olive to dark grey (5Y4/3 to 5Y5/3) varying to black (5Y3/1), bioturbated, clayey sediments that locally contain some mollusc shells or fragments together with some ice-rafted pebbles, which reflect rafting by icebergs or seasonal pack ice. Elsewhere in Hudson Strait and Ungava Bay, postglacial muddy sediments locally infill small depressions on ice-contact deposits. Many areas became sediment-starved following the change from glaciomarine, ice-distal to postglacial, marine conditions ca. 8000–7800 BP. As a result the supply of postglacial sediments has generally been low, except for areas of major fluvial input. In shallow and intermediate depths outside the main basins, modification of seabed sediments by the winnowing action of strong bottom currents has created a coarse sandy and gravelly veneer a few centimetres thick, possibly supplemented by input of some material rafted by the seasonal ice cover.

Cores 90023-045 and 92028-157 from Eastern basin and 93034-022 from Western basin illustrate the typical composition of postglacial muddy sediments in the basins. Cores 90023-045 and 92028-157, collected in more than 845 m water depth, illustrate postglacial sequences in the floor of Eastern basin (Fig. 6, 8; MacLean, 2001, Fig. 5; MacLean et al., 2001, Fig. 28). Core 90023-045 sampled approximately 7 m of postglacial sediments and penetrated 479 cm of underlying glaciomarine sediments (Jennings et al., 2001, Fig. 1). Core 92028-157 (a gravity core) terminated at a depth of 492 cm in postglacial sediments.

Postglacial sediments in these cores mainly consist of variably laminated, olive-grey, clayey silt with interbeds, lenses, and partings of fine to medium sand, occasional coarse sand, and silt, with some scattered grains and clay and rock clasts. Similar sediments are also found infilling numerous burrows and biotraces. Extensive mottling and bioturbation are evident throughout. Clay clasts occur

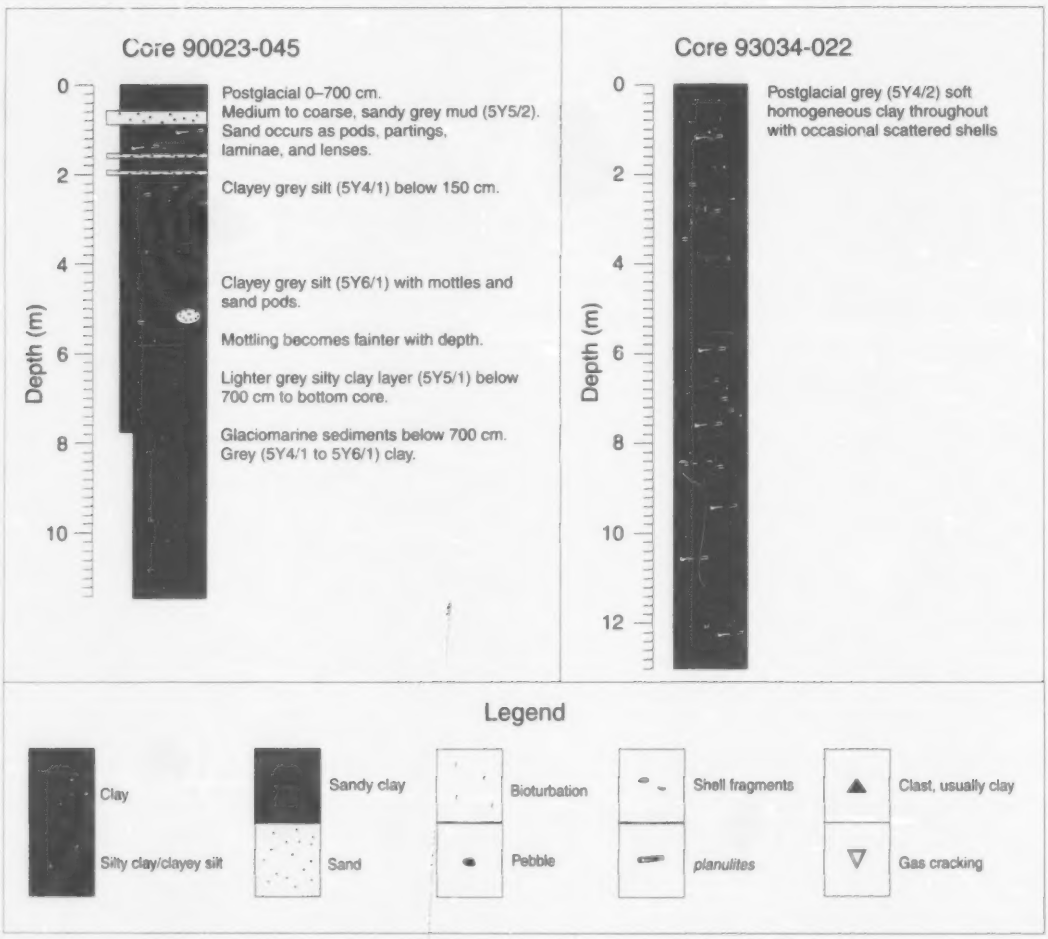

Figure 8. *Textural characteristics of postglacial sediments in cores 90023-045 and 93034-022 in Eastern and Western basins.*

primarily in the 412–512 cm and 104–105 cm intervals of core 90023-045. A thin zone of reddish-brown (5YR5/4) sediment occurs at 538 cm.

Core 93034-022 sampled thick postglacial sediments in Western basin (Fig. 8; MacLean, 2001, Fig. 5; MacLean et al., 2001, Fig. 26), where they typically occur as grey (5Y4/2), homogeneous, bioturbated clays containing little or no silt throughout the entire 1252 cm core length. Occasional, small, limestone clasts are present, mainly between 220 cm and 174 cm. Concentrated zones of shell fragments were located visually and by X-radiographic examination at 873–877 cm, 748–753 cm, 670–685 cm, 377–394 cm, and 215–222 cm. Associated biogenic traces such as *planulites* and occasional dwelling features are also scattered throughout this entire sequence. Gas cracking due to the high organic nature of the sediments was observed thoughout the core below 300 cm.

SUMMARY

Four main Quaternary sediment units have been recognized in Hudson Strait and Ungava Bay. These comprise ice-contact, ice-contact–debris flow (locally in Eastern basin), glaciomarine, and postglacial sediments. The ice-contact unit represents the basal Quaternary sequences that blanket bedrock, infill depressions, and form constructional topographic features. Sediments of this unit are matrix-supported, clast-rich diamicts that are barren of microfossils and macrofossils. Deposition has occurred subglacially or at margins of grounded ice sheets.

Glaciomarine sediments overlie ice-contact deposits in basinal areas of Hudson Strait and Ungava Bay. They typically are composed of laminated silts and clays and contain variable numbers of dropstones. Commonly, these sediments are rhythmically banded with thin silt and fine to very fine sand laminae (rhythmites), which resemble deposits termed cyclopsams and cyclopels (Powell and Molnia, 1989). Clay clasts are a variable, but not uncommon component of these sediments. This remobilized material is a potential source of, or contributor to, anomalous foraminiferal assemblages encountered in proximal glaciomarine sediments and of anomalous age dates derived from those fauna in many localities in this region.

Postglacial muddy sediments overlie glaciomarine sediments in the basins. For the most part, these are relatively thin deposits only a few metres in thickness, but thick deposits (up to 30 m) occur in several localities. Typically these are fine-grained, clayey sediments that are extensively mottled and burrowed with some silty and sandy burrow infillings. Thick deposits are rich in organic material and contain gas. Occasional ice-rafted dropstones are also present in these sediments.

A thin (10–15 cm) veneer of sandy and gravelly sediments mantles the seabed in many current-swept areas. These sediments have been derived through the winnowing action of bottom currents on exposed seabed sediments, plus probable input of some material rafted by the seasonal ice cover.

ACKNOWEDGMENTS

Grateful thanks are extended to D.A. Hodgson, J. Josenhans, and J. Shaw for helpful comments and review of this paper.

REFERENCES

Andrews, J.T., MacLean, B., Kerwin, M., Manley, W., Jennings, A.E., and Hall, F.
1995: Final stages in the collapse of the Laurentide Ice Sheet, Hudson Strait, Canada, NWT: ^{14}C AMS dates, seismic stratigraphy, and magnetic susceptibility logs; Quaternary Science Reviews, v. 14, p. 983–1004.

Hardy, I.A.
1991: Vanishing biogenic sedimentary structures; *in* Society for the Preservation of Natural History Collections, Sixth Annual Meeting, May 6–11, 1990, Abstract Proceedings, p. 16.

Jennings, A.E., Vilks, G., Deonarine, B., Silis, A., and Weiner, N.
2001: Foraminiferal biostratigraphy and paleoceanography; *in* Marine Geology of Hudson Strait and Ungava Bay, Eastern Arctic Canada: Late Quaternary Sediments, Depositional Environments, and Late Glacial–Deglacial History Derived from Marine and Terrestrial Studies, (ed.) B. MacLean; Geological Survey of Canada, Bulletin 566.

MacLean, B.
2001: Introduction: geographic setting and studies; *in* Marine Geology of Hudson Strait and Ungava Bay, Eastern Arctic Canada: Late Quaternary Sediments, Depositional Environments, and Late Glacial–Deglacial History Derived from Marine and Terrestrial Studies, (ed.) B. MacLean; Geological Survey of Canada, Bulletin 566.

MacLean, B., Hardy, I., Jennings, A.E., Manley, W.F., and Kerwin, M.W.
1994: Late glacial ice in eastern Hudson Strait: new offshore evidence; *in* 24th Arctic Workshop, Institute of Arctic and Alpine Research, University of Colorado, March 17–19, Program and Abstracts, p. 132–134.

MacLean, B., Vilks, G., Deonarine, B.
1992: Depositional environments and history of late Quaternary sediments in Hudson Strait and Ungava Bay: further evidence from seismic and biostratigraphic data; Géographie physique et Quaternaire, v. 46, p. 311–329.

MacLean, B., Vilks, G., Hardy, I., Deonarine, B., Jennings, A.E., and Manley, W.F.
2001: Quaternary sediments in Hudson Strait and Ungava Bay; *in* Marine Geology of Hudson Strait and Ungava Bay, Eastern Arctic Canada: Late Quaternary Sediments, Depositional Environments, and Late Glacial–Deglacial History Derived from Marine and Terrestrial Studies, (ed.) B. MacLean; Geological Survey of Canada, Bulletin 566.

Miller, G.H. and Kaufman, D.S.
1990: Rapid fluctuations of the Laurentide ice sheet at the mouth of Hudson Strait: new evidence for ocean/icesheet interactions as a control on the Younger Dryas; Paleoceanography, v. 5, no. 6, p. 907–919.

Powell, R.D. and Molnia, B.F.
1989: Glacimarine sedimentary processes, facies and morphology of the south-southeast Alaska Shelf and Fiords; Marine Geology, v. 85, p. 359–390.

Silis, A.B.
1993: Late Quaternary foraminiferal biostratigraphy of Hudson Strait; Geological Survey of Canada, Open File 3340, 127 p.

Vilks, G., MacLean, B., Deonarine, B., Currie, C.G., and Moran, K.
1989: Late Quaternary paleoceanography and sedimentary environments in Hudson Strait; Géographie physique et Quaternaire, v. 43, no. 2, p. 161–178.

Studies of sediment colour, whole-core magnetic susceptibility, and sediment magnetism of the Hudson Strait–Labrador Shelf region: *CSS Hudson* cruises 90023 and 93034

F.R. Hall[1], J.T. Andrews[2], M. Kerwin[2], and L.M. Smith[2]

Hall, F.R., Andrews, J.T., Kerwin, M., and Smith, L.M., 2001: Studies of sediment colour, whole-core magnetic susceptibility, and sediment magnetism of the Hudson Strait–Labrador Shelf region: CSS Hudson cruises 90023 and 93034; in Marine Geology of Hudson Strait and Ungava Bay, Eastern Arctic Canada: Late Quaternary Sediments, Depositional Environments, and Late Glacial–Deglacial History Derived from Marine and Terrestrial Studies, (ed.) B. MacLean; Geological Survey of Canada, Bulletin 566, p. 161–170.

Abstract: Two rapidly measured parameters, colour spectra and whole-core magnetic susceptibility, can provide important data regarding sediment provenance. These parameters can be measured prior to a sediment core being sampled and at closely spaced intervals. When combined with reliable age control, these data can be useful in making environmental interpretations. Within the region of Hudson Strait, the primary controls on these two parameters are particles derived from the Dubawnt Group "red stained" rhyolite from the western portion of the basin and the Paleozoic limestone rocks that underlie most of the basin.

Résumé : Le spectre chromatique et la susceptibilité magnétique de la carotte entière sont deux paramètres rapides à mesurer qui peuvent fournir des données importantes sur la provenance des sédiments. Ces mesures peuvent être effectuées à intervalles rapprochés avant l'échantillonnage d'une carotte. En combinaison avec un contrôle chronologique fiable, ces données peuvent s'avérer utiles à l'interprétation des milieux. Dans la région du détroit d'Hudson, des particules provenant de la rhyolite «de coloration rouge» du Groupe de Dubawnt dans la partie occidentale du bassin et celles tirant leur origine des calcaires paléozoïques dont se compose la majeure partie du bassin, constituent les principaux déterminants de ces deux paramètres.

[1] Department of Geology and Geophysics, University of New Orleans, New Orleans, Louisiana, U.S.A. 70148

[2] Geology Department, Institute for Arctic and Alpine Research, University of Colorado, Campus Box 450, Boulder, Colorado, U.S.A. 80309-0450

INTRODUCTION

During the Wisconsinan Ice Age, Hudson Strait served as a conduit for the flow of glaciers that originated from Ungava and Labrador peninsulas and Baffin Island, Hudson Bay, and adjacent areas. Moreover, within the region of the Baffin Island–Hudson Strait–Labrador Shelf, the majority of sediments that were retrieved with modern piston-coring technology comprise sequences deposited during and after the last ice age; however, determining the flow-path directions in this region, particularly within Hudson Strait, is somewhat controversial (e.g. Gray (2001) contrasting with Manley and Miller (2001)), making the linkages between terrestrial and marine sequences a critical component in recreating the environmental history of the region. Studying the composition of sediments provides an important indicator of the terrestrial sources of particles that can be linked to specific sedimentological processes.

To accomplish this feat, sedimentary provenance must be determined and placed within a reliable age-control scheme. In this paper, we present the results of two types of rapidly measured parameters that can be performed on whole-core sections during a research cruise: colour spectra and whole-core magnetic susceptibility. In addition, we include data from more detailed sediment-magnetic analyses (Thompson and Oldfield, 1984; King and Channel, 1991) extracted on discrete samples from most of these cores; these data are presented in the Appendix. These analyses were performed on sediment cores extracted from cruises 90023, 92028, and 93034 (Fig. 1) onboard the *CSS Hudson*.

As colour is a fundamental property of rocks and sediments, it can be used to track distinctive bedrock provenances. For example, sections of a core which are high in carbonate (mostly detrital in this region) will commonly be of lighter (whiter) colour than material contributed from redbeds or black shale. The development of relatively inexpensive and portable spectrophotometers coupled to laptop computers has made the acquisition of these data simple (Andrews and Freeman, 1996).

The magnetic parameters used in this study (King and Channel, 1991) are indicators of the variable physical properties of the magnetic minerals within the cores. These properties include variations in the concentration, grain size, and composition of the magnetic mineral suite. Note that magnetic mineral suites are commonly composed of complex mixtures of minerals. Therefore, the data collected here reflect the relative changes of these minerals within a core. More absolute indicators require examining magnetic mineral extractions (Hall and King, 1989; Bloemendal et al., 1991).

Magnetic susceptibility is a measure of the concentration of magnetic, mostly ferrimagnetic minerals (e.g. (titano)magnetite; Hall and King (1989)). The values collected reflect many processes including the susceptibility of the source rock (Hall and Reed, 1996), distance from the source area (Hall, 1998; Hall et al., 1999), dilution by biogenic tests (Robinson, 1990), and postdepositional chemical alteration, particularly during reduction diagenesis (e.g. Karlin and Levi, 1983; Bloemendal et al., 1991).

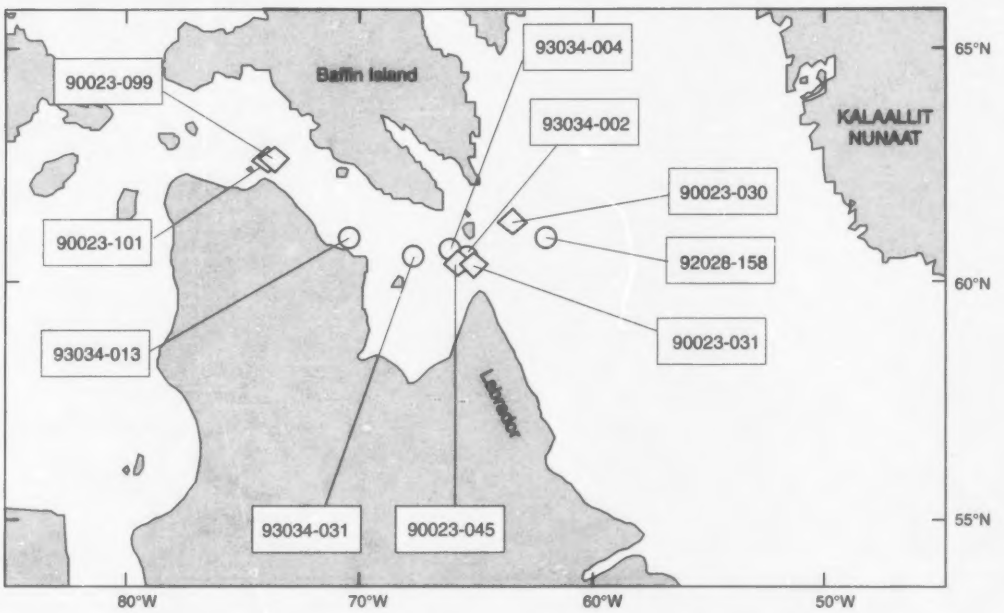

Figure 1. *Locations of the cores discussed in the text as well as the Appendix. The diamonds represent cores studied by Kerwin (1994, 1996) and the circles were cores studied by F. Hall.*

Within the region studied, postdepositional alteration does not appear to be a significant process affecting these sediments (Hall et al., 1999). In addition, total microfossil populations and organic carbon concentrations are low. The low organic carbon contents are also important for colour analyses as the organic compounds can mask the colour of the sedimentary particles. Therefore, the overall data collected should primarily reflect the source area.

In the eastern portion and various other sites in Hudson Strait, an important control on both colour and magnetic susceptibility (ms) is the input of red sedimentary particles that probably originated from the Dubawnt Group, which occurs west of Hudson Bay. Sediments derived from Dubawnt Group rocks form an extensive and distinct debris train to the east and southeast (Shilts et al., 1979). These sediments have been recognized on islands in northern Hudson Bay (Shilts, 1980) and on Nottingham Island at the western end of Hudson Strait (Laymon, 1992).

The red colouration of these rocks is probably the mineral hematite whereas the magnetic signature of the other local outcrops is dominated by the ferrimagnetic components such as magnetite. Hematite has a two order-of-magnitude weaker magnetic susceptibility signal than magnetite (Hunt et al., 1995). Furthermore, rhyolite samples without red staining have magnetic susceptibility values higher than red-stained samples (W. Freeman, pers. comm., 1995). Therefore, the input of the redbed material should yield redder colouration and lower magnetic susceptibility values within the core than the other granitic particles.

In the western portion of Hudson Strait, an important control on colour and magnetic susceptibility is input of detrital carbonate eroded from the Paleozoic bedrock within Hudson Strait, Hudson Bay, and Foxe Basin (*see* Wheeler et al., 1996; MacLean, 2001, Fig. 1). The bulk magnetic susceptibility values of this source rock are commonly diamagnetic (i.e. have negative magnetic susceptibility values: Hall et al., 1999). Therefore, increased detrital carbonate deposition will yield 'whiter' colour interval and lowered magnetic susceptibility values.

The results reported here are a part of ongoing research at the Institute of Arctic and Alpine Research, University of Colorado in collaboration with GSC (Atlantic), and the University of New Orleans. Much of the data was collected relatively recently and is thus unpublished within the peer-reviewed literature. Therefore, the emphasis of this text is the reporting of the data collected. Moreover, analyses of terrestrial samples for these parameters is still in its infancy.

Previous studies

Andrews et al. (1995b) used whole-core magnetic susceptibility (wcms) measurements to describe major regional variations in provenance and style of sedimentation and to correlate between the major depocentres of Hudson Strait. Kerwin (1994, 1996) performed detailed sedimentological and sediment-magnetic analyses on sediment cores within and proximal to Hudson Strait. His data correlated between Eastern and Western basins the presence of a 'redbed' deposit dated close to the final deglaciation of Hudson Bay. Although proximal to ironstone formations of Labrador, this facies was most likely associated with hematite-rich sediments eroded from the Proterozoic Dubawnt Group rhyolite (Shilts, 1980; Aylsworth and Shilts, 1991).

Hall et al. (1999) reported on the results of sediment-magnetic analyses from a core from the Saglek Bank–Karlsefni trough region of the Labrador Shelf. Their results demonstrated a direct link between these data and probable source rock which included the granitic material from Labrador and detrital carbonate from Hudson Strait. High detrital carbonate content was linked with the flushing of Hudson Strait. Curiously, however, Hall et al. (1999) did not find evidence for the Dubawnt Group red rhyolite at their site.

METHODS

Colour spectrophotometry

During the 1990 and 1993 cruises, the colour spectrums of split cores were determined quantitatively using a Colormet™ system; however, onboard tests indicated some variability with repeat measurements. As a follow-up study, sediment colour was measured on core photographs using the Colortron™ instrument which quantified colour over the equivalent of 1 x 1 cm of core face (Andrews and Freeman, 1996) and using the tripartite L a* b* colour scheme. The L parameter is a measure of black (0) to white (300) whereas the other two axes have limits of +300 and -300 and record the red to green, and blue to yellow, respectively. The data were smoothed using a five-point running mean so as to minimize anomalous data in the records.

Sediment magnetism

Measurements of sediment-magnetism included both whole-core and discrete-sample techniques. In addition to the cores collected during *CSS Hudson* cruises 90023 and 93034 reported here, whole-core magnetic susceptibility (wcms) measurements were undertaken on cores collected during *CSS Hudson* cruises 87033 and 92028 (Vilks et al., 1989; Andrews and Stravers, 1993; Manley et al., 1993; Kerwin, 1994, 1996; Hall et al., 1999). The sensor loop was 12.5 cm in diameter whereas the inner-core diameter was 10 cm.

Discrete samples were collected from the 90023, 93034, and 92028 cores (Fig. 1). Magnetic susceptibility (both discrete and whole-core) was measured using the Bartington Instruments™ system. Anhysterectic remanent magnetizations (ARM: peak AC field = 0.99 T, DC field = 0.1 T) were applied using DTECH PARM™ system at the United States Geological Survey (Denver, Colorado) on all reported cores except core 93034-002. Isothermal remanent magnetizations (IRM) were applied using a forward field of either 1.2 T (Kerwin, 1994) or 1.7 T using the ASC Scientific Impulse Magnetizer®. Reversed-field IRM was applied at -0.3 T. From these results, the compositional parameters HIRM and S were calculated using the equations:

$$HIRM = (IRM_{1.2 \text{ or } 1.7\,T} - IRM_{-0.3\,T})/2 \quad (1)$$

$$S = -(IRM_{-0.3\,T}/IRM_{1.2 \text{ or } 1.7\,T}) \quad (2)$$

All magnetic measurements performed on these cores were dry-mass corrected. Using dry-mass corrected data is critical for these studies as they allow for direct comparisons with data collected from potential source areas. Wet-mass or volume-corrected data must take into account the bulk density of the samples prior to comparison with source rock.

Age control

Age control was accomplished via AMS ^{14}C dates collected mostly on biogenic carbonate (Manley and Jennings, 1996). These dates are given as $\pm$ 1 σ values and were reservoir corrected using a value of 450 years.

RESULTS AND DISCUSSION

The sediment magnetism data for all the cores are given in the Appendix. Figure 2 shows a comparison between the two colour systems for core 92028-158, using the parameter L. The solid lines on the curves represent five-point running means. The downcore trends of the two data sets are similar with an offset of about nine units on average. This offset can result from many factors including internal differences in the electronics of the two instruments. Nonetheless, the fact that the trends of the data are so similar is encouraging.

The L and a* data from cores 90023-101, 90023-045, 90023-030, and 92028-158 are shown in Figure 3. The core from Western basin (90023-101) is lighter (i.e. higher L values) than cores from the Eastern basin whereas cores from the Eastern basin have more negative a* values (i.e. a redder hue). Furthermore, the core in Resolution basin (90023-030) has several sections that are distinctly lighter than Eastern basin core 90023-045.

The whiter toned sediments in core 90023-030 were deposited during the glacial readvance which resulted in deposition of Heinrich event H-0, in the North Atlantic Ocean at ca. 11 ka BP (Andrews et al., 1995a). This colouration is consistent with the deposition of detrital carbonate often associated with Heinrich event sedimentation (Piper and Skene, 1998).

Kerwin (1996) showed that the characteristic rock magnetic signal within the low whole-core magnetic susceptibility interval of core 90023-045 between about 6.0 m and 6.5 m, is compatible with sediment with an enhanced hematite content (Fig. 4). Furthermore, the hematite content from the Dubawnt Group was particularly seen in relatively low values of the $S_{-0.3\,T}$ parameter. The $S_{-0.3\,T}$ reflects the proportion of magnetite/hematite: lower values indicate increased hematite deposition (King and Channel, 1991). This interval of low $S_{-0.3\,T}$ values occurs in sediments deposited at ca. 8 ka BP and associated with the collapse of the last remnants of the Laurentide Ice Sheet.

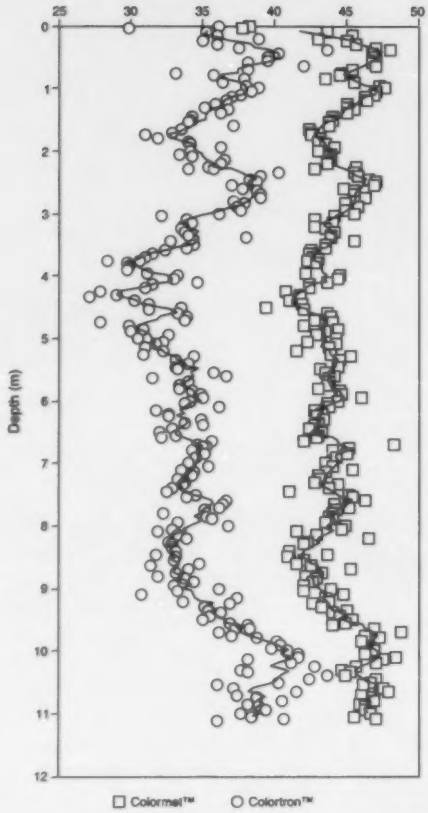

Figure 2. Comparison of the onboard measurement of L, using the Colormet™ (1993) and measurement of L from photographs. The L parameter is a measure of black (0) to white (300). The heavy, solid lines are five-point smoothed curves which show considerable parallelism.

The Dubawnt Group contains a significant proportion of rocks that are not red stained. It seems unlikely that the ice sheets would solely erode the red rocks. Hall and Reed (1996) mixed crushed redbed and granite samples in varying proportions from two Nova Scotia outcrops. They demonstrated that variability in HIRM could be minimal with regards to the redbed content whereas $S_{-0.3\,T}$ parameter best defines the redbed content. Moreover, they suggested that the redbed material must be at least 15% of the mixture to be deciphered by these methods. Therefore, this lack of distinction of red sediment in colour and HIRM in core 90023-045 may result from the mixing of rock types.

Regional variations in sediment magnetism properties from cores 90023-030, 90023-031, 90023-045, 90023-101, and 920028-158 were further examined by plots such as Figure 5 ($S_{-0.3\,T}$ vs. X). The cores extend along the axis of Hudson Strait onto the Labrador–Baffin shelf. In general, X shows there is a gradient in these measurements with values from core site 90023-045<90023-101<90023-030 <90023-031<92028-158; however, $S_{-0.3\,T}$ shows less variability other than low values (high hematite) associated

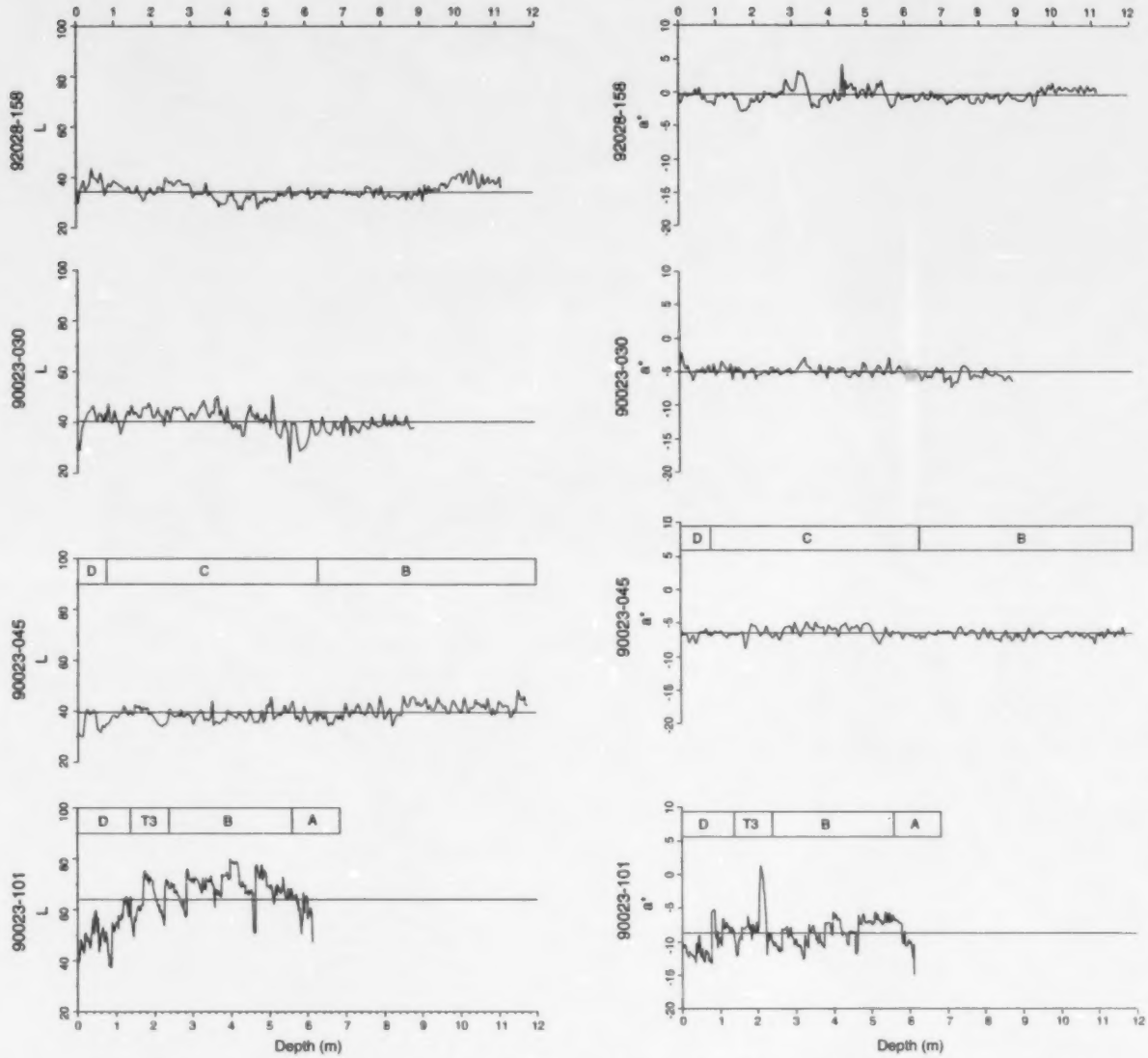

Figure 3. *Plot of colour of sediments in cores 90023-101, 90023-045, 90023-030, and 92028-158 in terms of two parameters, L and a*. A – glacial marine ice-proximal environment; B – glacial marine ice-distal environment, T – transitional environments, C – early postglacial environment, and D – postglacial environment.*

mostly with the cores from Eastern basin and Hatton basin. These results demonstrate the importance of provenance as a control on sediment magnetism properties.

CONCLUSIONS

The results of these analyses demonstrate that the rapidly measured parameters of colour spectra and sediment magnetism, especially magnetic susceptibility, are robust indicators of provenance. In particular, the presence of red material originating from the Dubawnt Group west of Hudson Bay and the Paleozoic limestone from the western portion of the region are clearly delineated with these data. When age control is included, these results can be used to decipher glacial and deglacial environmental changes. In particular, the deposition of Paleozoic limestone particles occurred during the formation of Heinrich event H-0 (ca. 11–10 ka BP) whereas the deposition of red sediment is associated with the flushing of Hudson Strait at the end of the last ice age.

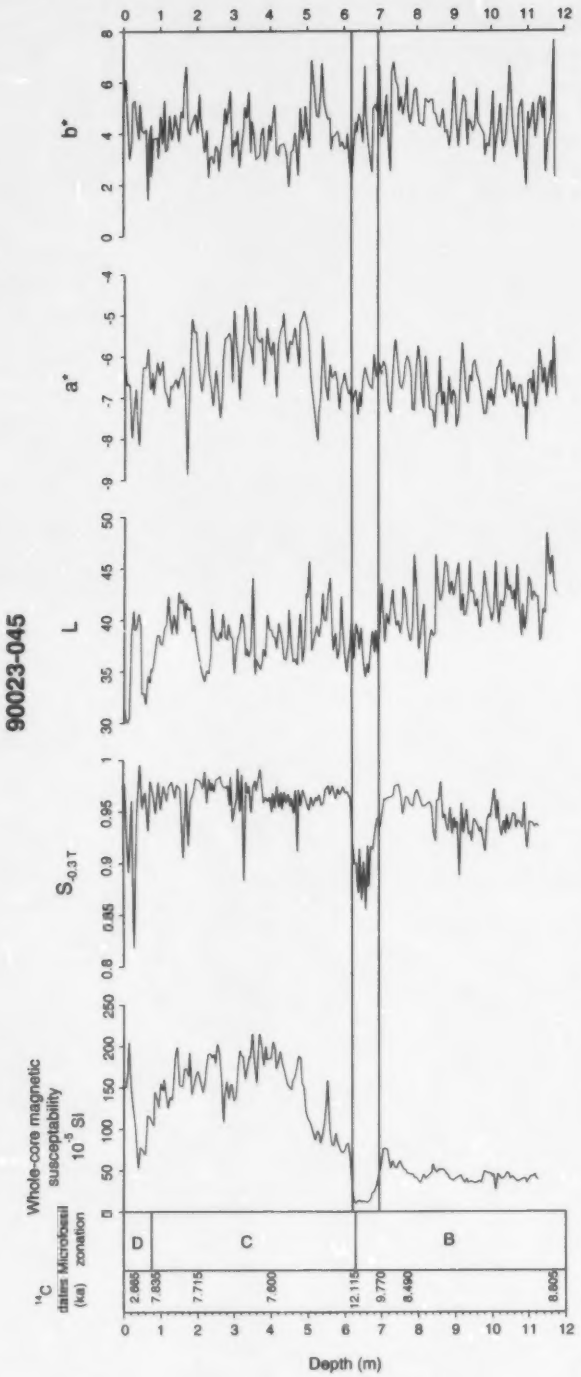

Figure 4. *Downcore variations of whole-core magnetic susceptibility, $S_{-0.3\ T}$, and the tripartite colour L, a*, b* measurement system for 90239-045 from measuring colour photographs of the archive half of the core. B – glacial marine ice-distal environment, C – early postglacial environment, D – postglacial environment*

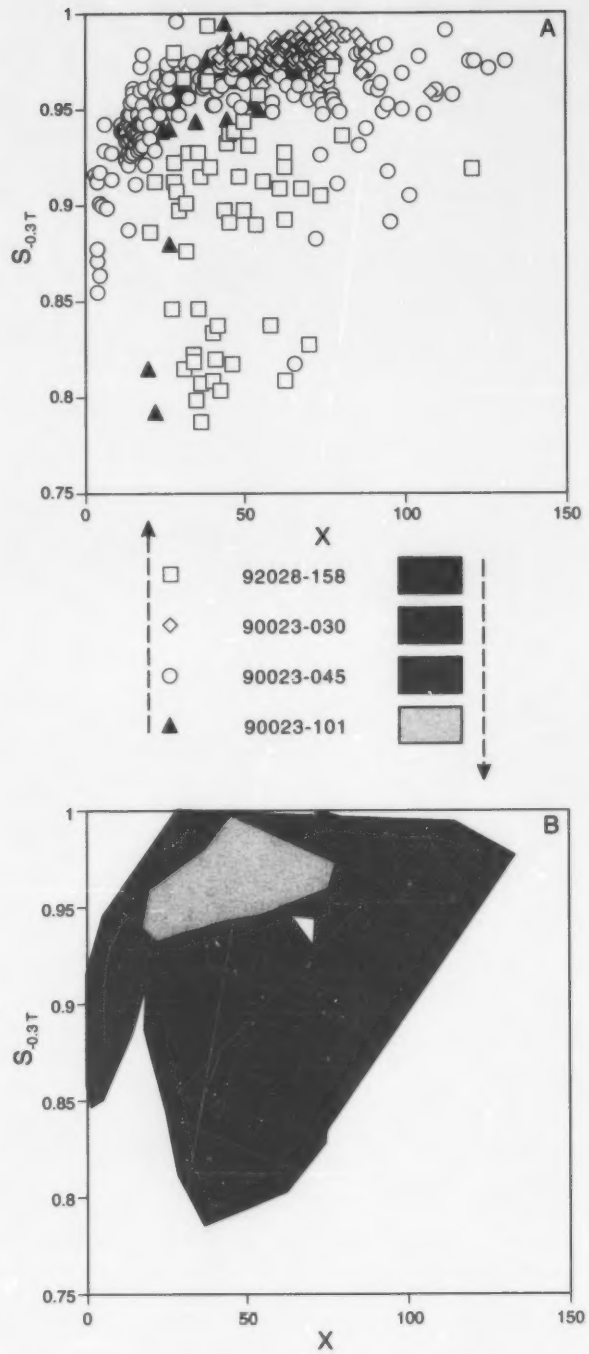

Figure 5. A) *$S_{-0.3T}$ versus X parameter for four cores along a transect from western Hudson Strait (90023-101) to Eastern basin (90023-045) to the Baffin shelf (90023-030; Hatton basin, 92028-158).* ***B)*** *Interpretation of data.*

ACKNOWLEDGMENTS

The authors wish to thank D.A. Hodgson, H. Josenhans, and J. Shaw for helpful comments and review of this paper.

REFERENCES

Andrews, J.T. and Freeman, W.
1996: The measurement of sediment color using the "ColortonTM" spectrophotometer; Arctic and Alpine Research, v. 28, p. 524–528.

Andrews, J.T. and Stravers, J.A.
1993: Magnetic susceptibility of late Quaternary marine sediments, Frobisher Bay, N.W.T.: an indicator of ice sheet/ocean interactions; Quaternary Science Reviews, v. 12, p. 157–167.

Andrews, J.T., Bond, G., Jennings, A.E., Kerwin, M., Kirby, M., MacLean, B., Manley, W., and Miller, G.H.
1995a: A Heinrich like-event, H-0 (DC-0): source(s) for detrital carbonate in the North Atlantic during the Younger Dryas chronozone; Paleoceanography, v. 10, p. 943–952.

Andrews, J.T., MacLean, B., Kerwin, M., Manley, W., Jennings, A.E., and Hall, F.
1995b: Final stages in the collapse of the Laurentide Ice Sheet, Hudson Strait, Canada, NWT: based on 14C AMS dates and magnetic susceptibility logs; Quaternary Science Reviews, v. 14, p. 983–1004.

Aylsworth, J.M. and Shilts, W.W.
1991: Surficial geology of Coats and Mansel Islands, Northwest Territories; Geological Survey of Canada, Paper 89-23, p. 26

Bloemendal, J., King, J.W., Hall, F.R., and Dol, S.-J.
1991: Rock-magnetism of late Neogene and Pleistocene deep-sea sediments: relationship to sediment source, diagenetic processes, and sediment lithology; Journal of Geophysical Research, v. 97, p. 4361–4375.

Gray, J.T.
2001: Patterns of ice flow and deglaciation chronology for southern coastal margins of Hudson Strait and Ungava Bay; *in* Marine Geology of Hudson Strait and Ungava Bay, Eastern Arctic Canada: Late Quaternary Sediments, Depositional Environments, and Late Glacial–Deglacial History Derived from Marine and Terrestrial Studies, (ed.) B. MacLean; Geological Survey of Canada, Bulletin 566.

Hall, F.R.
1998: "What is Magnetic Susceptibility"; Arctic Workshop, Institute for Arctic and Alpine Research, University of Colorado, Boulder, Colorado, Minicourse, 19 p.

Hall, F.R. and King, J.W.
1989: Rock-Magnetic Stratigraphy of Site 645 (Baffin Bay) from ODP Leg 105; *in* Proceedings ODP, Scientific Results, (ed.) S.P. Srivastiva, M. Arthur, and B. Clement, v. 105, p. 843–859.

Hall, F.R. and Reed, S.J.
1996: Rock (mineral)-magnetic properties of post-glacial (16 to 0.5 ka) sediments from the Emerald Basin (Scotian Shelf), Canada; *in* Late Quaternary Paleoceanography of the North Atlantic Margins, (ed.) J.T. Andrews, W.E.N. Austin, H. Bergsten, and A.E. Jennings; Geological Society Special Publication No. 111, p. 103–115.

Hall, F.R., Andrews, J.T., Jennings, A., Vilks, G., and Moran, K.
1999: Late Quaternary sediments and chronology of the NE Labrador Shelf (Karlsefni Trough, Saglek Bank): links to glacial history; Bulletin of the Geological Society of America, v. 111, p. 1700–1713.

Hunt, C.P., Moskowitz, B.M., and Banerjee, S.K.
1995: Magnetic properties of rocks and minerals; *in* Rock Physics and Phase Relations: a Handbook of Physical Constants, (ed.) T.J. Ahrens; American Geophysical Union, p. 189–204.

Jennings, A.E., Vilks, G., Deonarine, B., Silis, A., and Weiner, N.
2001: Foraminiferal biostratigraphy and paleoceanography; *in* Marine Geology of Hudson Strait and Ungava Bay, Eastern Arctic Canada: Late Quaternary Sediments, Depositional Environments, and Late Glacial–Deglacial History Derived from Marine and Terrestrial Studies, (ed.) B. MacLean; Geological Survey of Canada, Bulletin 566.

Karlin, R. and Levi, S.
1983: Diagenesis of magnetic minerals in Recent haemipelagic sediments; Nature, v. 303, p. 327–330.

Kerwin, M.W.
1994: Final stages in the collapse of the Laurentide Ice Sheet: a rock magnetic and sedimentological study from Hudson Strait, Canada; M.Sc. thesis, University of Colorado, Boulder, Colorado, 189 p.
1996: A regional stratigraphic isochron (ca. 8000 C-14 years B.P.) from final deglaciation of Hudson Strait; Quaternary Research, v. 46, p. 89–98.

King, J.W. and Channel, J.E.T.
1991: Sedimentary magnetism, environmental magnetism, and magnetostratigraphy; Reviews of Geophysics, Supplement, p. 358–370.

Lamon, C.A.
1992: Glacial geology of western Hudson Strait, Canada, with reference to Laurentide Ice Sheet diynamics; Geological Society of America, Bulletin, v. 104, p. 1169–1177.

MacLean, B.
2001: Bedrock geology of Hudson Strait and Ungava Bay; *in* Marine Geology of Hudson Strait and Ungava Bay, Eastern Arctic Canada: Late Quaternary Sediments, Depositional Environments, and Late Glacial–Deglacial History Derived from Marine and Terrestrial Studies, (ed.) B. MacLean; Geological Survey of Canada, Bulletin 566.

Manley, W.F. and Jennings, A.E.
1996: Radiocarbon Date List; Institute for Arctic and Alpine Research, Paper No. 12, University of Colorado, Boulder, Colorado, 163 p.

Manley, W.F. and Miller, G.H.
2001: Glacial–geological record on southern Baffin Island reflecting late glacial ice-sheet dynamics in the eastern Hudson Strait region; *in* Marine Geology of Hudson Strait and Ungava Bay, Eastern Arctic Canada: Late Quaternary Sediments, Depositional Environments, and Late Glacial–Deglacial History Derived from Marine and Terrestrial Studies, (ed.) B. MacLean; Geological Survey of Canada, Bulletin 566.

Manley, W.F., MacLean, B., Kerwin, M., and Andrews, J.T.
1993: Magnetic susceptibility as a Quaternary correlation tool: examples from Hudson Strait sediment cores; *in* Current Research, Part D; Geological Survey of Canada, Paper 93-1D, p. 137–145.

Piper, D.J.W. and Skene, K.I.
1998: Latest Pleistocene ice-rafting events on the Scotian margin (eastern Canada) and their relationship to Heinrich events; Paleoceanography, v. 13, p. 205–214.

Robinson, S.G.
1990: Applications for whole-core magnetic susceptibility measurements of deep-sea sediments: Leg 115 results; *in* Proceedings of the Ocean Drilling Program, Scientific Results, (ed.) R.A. Duncan, J. Backman, and L.C. Peterson, v. 115, p. 737–771.

Shilts, W.W.
1980: Flow patterns in the central North American ice sheet; Nature, v. 286, p. 213–218.

Shilts, W.W., Cunningham, C.M., and Kaszycki, C.A.
1979: Keewatin Ice Sheet – re-evaluation of the traditional concept of the Laurentide Ice Sheet; Geology, v. 7, p. 535–541.

Thompson, R. and Oldfield, F.
1984: Environmental Magnetism; Allen & Unwin, Winchester, Massachusetts, 227 p.

Vilks, G., MacLean, B., Deonarine, B., Currie, C.G., and Moran, K.
1989: Late Quaternary paleoceanography and sedimentary environments in Hudson Strait; Géographie physique et Quaternaire, v. 43, p. 161–176.

Wheeler, J.O., Hoffman, P.F., Card, K.D., and Davidson, A., Sanford, B.V., Okulitch, A.V., and Roest, W.R. (comp.)
1996: Geological Map of Canada; Geological Survey of Canada, Map 1860A, scale 1:5 000 000.

APPENDIX

The sediment magnetic results for all cores examined thus far are shown graphically in this appendix. All discrete sample data are dry-mass corrected. We consider it important that these data be given as mass-corrected values so as to compare these results with local outcrop samples. Using volume-corrected or wet-mass corrected values means that the core sample data must be corrected for bulk density prior to comparison with local outcrops. Although the sample cubes commonly used in these studies are consistent with regards to volume, still volume differences do occur between cubes. In addition, the amount of material used does include air pockets that inevitably occur when filling the cubes.

The results given are indicative of the concentration (whole-core magnetic susceptibility and discrete sample X: Fig. A-1 and A-2), grain-size (XARM/X (higher values = finer sizes): Fig. A-3), and composition (HIRM and $S_{-0.3\,T}$ (relative "hematite" concentration and "magnetite/hematite" ratio): Fig. A-4 and A-5).

Glacial, glacial marine, and postglacial interpretations were adapted from Jennings et al. (2001). On these figures, A represents glacial marine ice-proximal environment; B is glacial marine ice-distal environment, T is transitional environments, C is early postglacial environment, and D is postglacial environment. Age dates are in thousands of radiocarbon years. Stratigraphic inversions of some age dates reflect inclusion of reworked material in some of the dated samples (*see* Jennings et al., 2001).

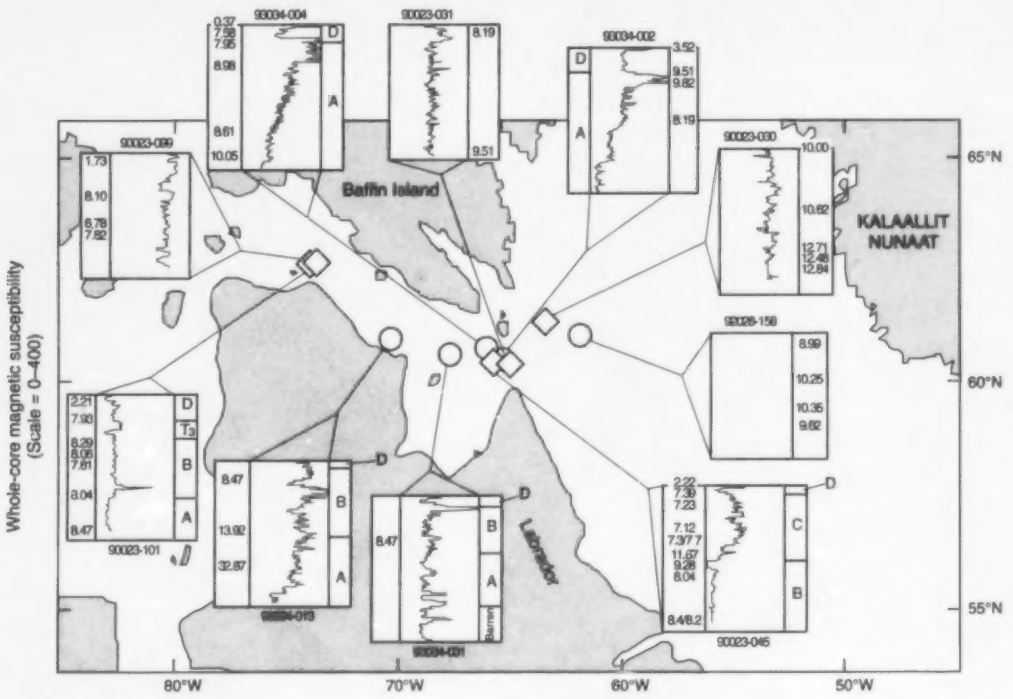

Figure A-1. *Whole-core magnetic susceptibility data for all cores examined in the study area.*

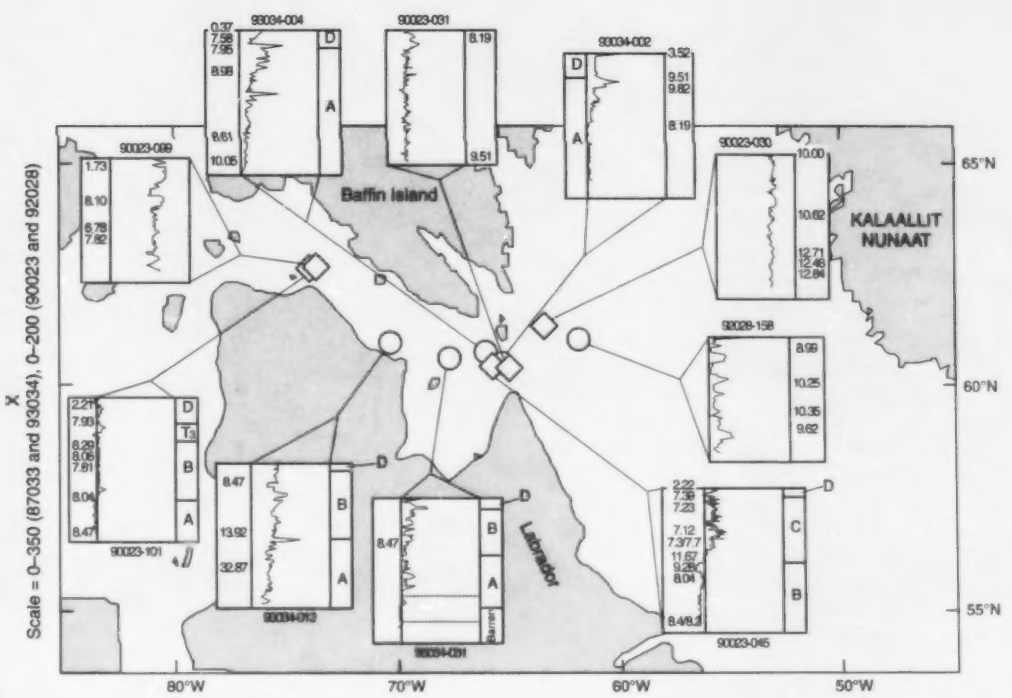

Figure A-2. *Discrete sample magnetic susceptibility for all cores examined in the study area.*

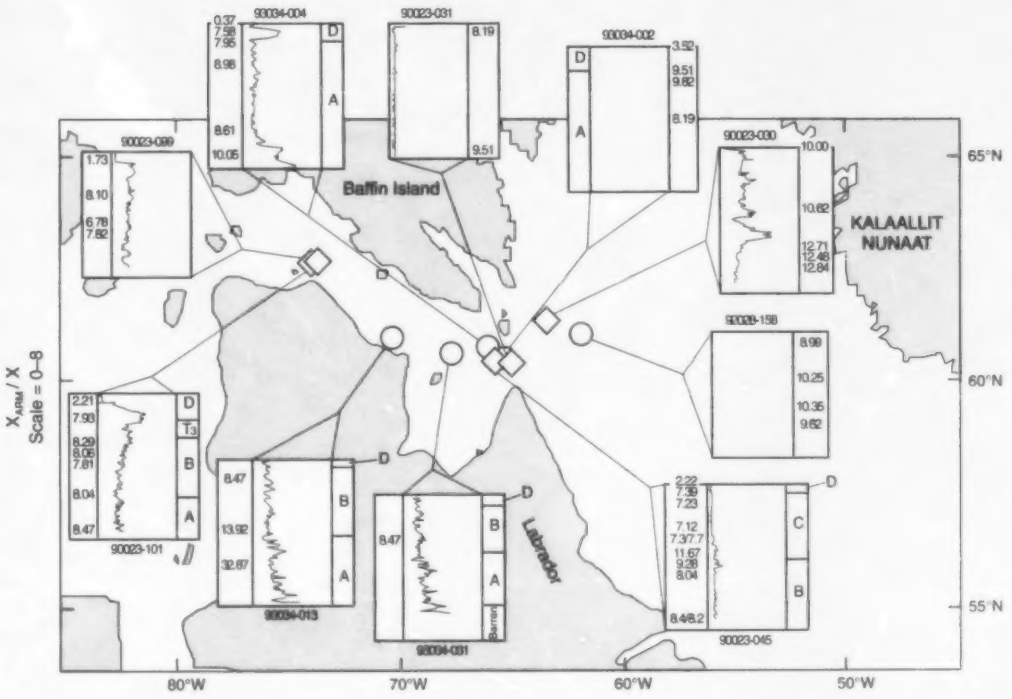

Figure A-3. *XARM/X data for all the cores examine in the study area.*

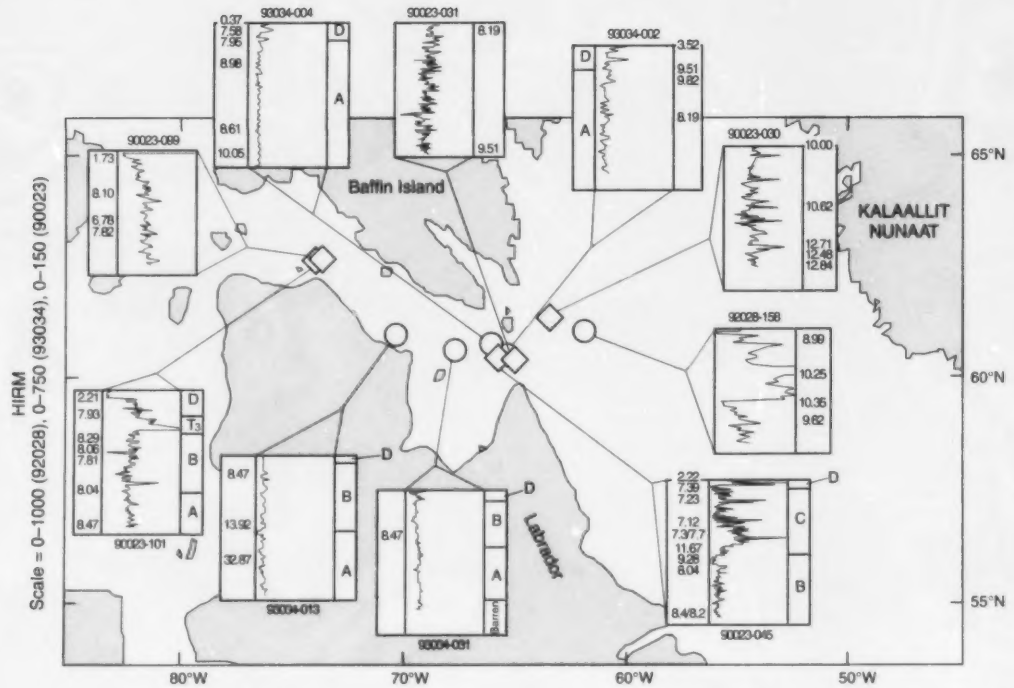

Figure A-4. HIRM data for all the cores examined in the study area.

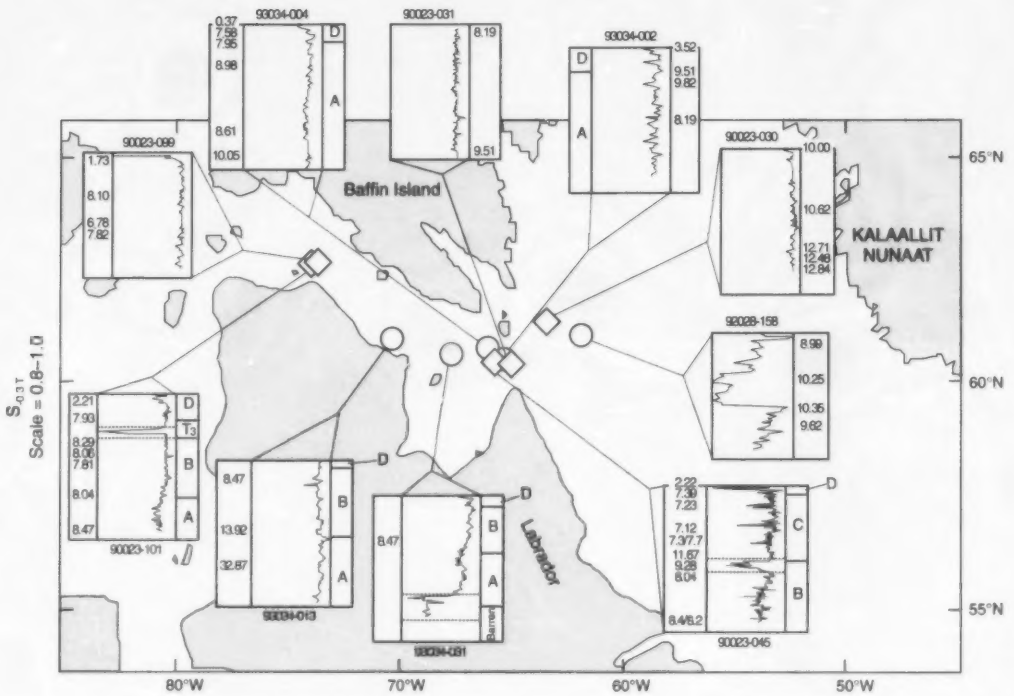

Figure A-5. $S_{-0.3\,T}$ data for all the cores examined in the study area.

Ice dynamics modelling of the Hudson Strait region at late glacial time

W.T. Pfeffer[1]

Pfeffer, W.T., 2001: Ice dynamics modelling of the Hudson Strait region at late glacial time; in *Marine Geology of Hudson Strait and Ungava Bay, Eastern Arctic Canada: Late Quaternary Sediments, Depositional Environments, and Late Glacial–Deglacial History Derived from Marine and Terrestrial Studies, (ed.) B. MacLean; Geological Survey of Canada, Bulletin 566, p. 171–179.*

Abstract: Ice dynamics modelling was undertaken to a) simulate in a physically realistic numerical model, glacial events between ca. 11 ka BP and ca. 9 ka BP (DC-0 and Gold Cove) and during the Noble Inlet event inferred from observations in the vicinity of Hudson Strait and on Baffin Island; and b) to examine the compatibility of terrestrial and marine observations and model results.

Modelling results indicate that successful advance of ice across eastern Hudson Strait from an initial position on Quebec–Labrador required an ice dome to have an initial maximum thickness of at least 2200 m. Highest discharge fluxes occurred as the ice crossed the deep Eastern basin in Hudson Strait and continued until a stable position was reached on the Meta Incognita Peninsula side of the strait. Results confirm the plausibility of successful advance of ice across Hudson Strait.

Radiocarbon dates from mollusc shells indicate the existence of at least partial open-water conditions in or adjacent to Eastern basin between Gold Cove and Noble Inlet advances.

Ice dynamics and the quantity of available ice do not seem to impose any significant limitations on the timing and character of the Noble Inlet advance as determined by the terrestrial and marine geological data.

Résumé : Un modèle numérique de dynamique glaciaire physiquement réaliste a été mis au point pour a) simuler les événements glaciaires qui se sont produits entre environ 11 ka BP et environ 9 ka BP (DC-0 et Gold Cove) et pendant l'événement de Noble Inlet et qui ont été déduits à partir d'observations faites dans la région du détroit d'Hudson et dans l'île de Baffin, et b) examiner la compatibilité des observations faites en milieux marins et terrestres avec les résultats de la modélisation.

Selon le modèle, une avancée glaciaire qui traverse le secteur oriental du détroit d'Hudson à partir de la région Québec–Labrador nécessite la présence d'un dôme glaciaire d'une épaisseur maximale initiale d'au moins 2200 m. Les taux d'écoulement les plus importants sont obtenus lorsque la glace traverse le bassin Est profond jusqu'à ce qu'elle atteigne une position stable sur la péninsule Meta Incognita. Les résultats confirment qu'il est plausible qu'une avancée glaciaire ait traversé le détroit d'Hudson.

La datation au radiocarbone de coquilles de mollusques indique qu'entre l'avancée de Gold Cove et celle de Noble Inlet, les eaux étaient au moins partiellement libres dans le bassin Est ou dans les zones adjacentes.

La dynamique glaciaire et la quantité de glace disponible ne semblent pas restreindre de façon importante la chronologie et la nature de l'avancée de Noble Inlet déterminées par les données géologiques recueillies en milieux marins et terrestres.

[1] Institute of Arctic and Alpine Research, University of Colorado, Boulder, Colorado U.S.A. 80309

INTRODUCTION

Outlet glaciers and ice streams in the Hudson Strait region of Eastern Canada appear to have played significant roles in the evacuation of ice from the interior of the Laurentide Ice Sheet at intervals in the past, and may also have influenced climate through the discharge of icebergs into the North Atlantic Ocean. The occurrence of ice and its climatological importance is determined on the basis of observations in the marine and terrestrial records, and also to a large degree on theoretical grounds. Both the theory and the observations are incomplete, however, and significant uncertainties remain to be resolved concerning the actual glacial events on land, in Hudson Strait, and on the continental shelf, and to what degree discharges of glacier ice and meltwater from Hudson Strait influenced North Atlantic Ocean circulation.

Two sources of uncertainty about how glaciers influenced events in the North Atlantic Ocean lie in difficulties reconciling the terrestrial and marine records and in confirming that the events inferred from those observations are compatible with our best present theoretical understanding of ice dynamics. This paper describes ice dynamics modelling undertaken with two objectives in mind. The first objective is to reconstruct in a physically realistic numerical model the glacial events inferred from observations in the vicinity of Ungava Bay, eastern Hudson Strait, and southeastern Baffin Island between ca. 11.0 ka BP and 9.0 ka BP. The second objective is to examine the compatibility of the terrestrial observations and model results together with the marine observations and model results. Because the glacial events in this region were complex in character and our understanding of the underlying processes is far from complete, the modelling is limited in scope. The reconstruction of glacial events is intended to test in a general sense whether an advancing margin originating from Ungava Bay could cross the deep Eastern basin of Hudson Strait under reasonable physical conditions, despite ice loss by calving. The numerical model produces other features in addition to this result, and these features may appear simplistic in comparison to details inferred from terrestrial and marine geology. The numerical model is designed to be driven to a large degree by geological constraints, and the constraints used have been applied mostly in the central and northeast portions of Quebec–Labrador and Hudson Strait; details of the results in other parts of the modelled region are unconstrained and are not intended to be interpreted in detail.

RELATED PREVIOUS WORK

Broecker (1994) hypothesized that the discharge of large quantities of glacier ice into the North Atlantic Ocean has the capacity to force the cessation of North Atlantic Ocean deep-water formation and consequently block the release of oceanic heat to the atmosphere in the North Atlantic Ocean. Oceanographic modelling by Rahmstorf (1995) indicated that the effect of fresh water and ice rafting on deep-water formation and climate can be profound and rapid. Marine sediment layers found across the North Atlantic Ocean (Heinrich, 1988) containing large clasts presumed to be transported by ice rafting provide evidence of episodic iceberg production and transport in the North Atlantic Ocean (termed Heinrich events); moreover, the timing of these events appears to coincide with major climate transitions shown in a variety of paleoclimate records (Broecker, 1994). Patterns of marine deposition in the northeast Atlantic Ocean and Labrador Sea strongly suggest that at least Heinrich events H-0, H-1, and H-2 originate from Hudson Strait (Andrews and Tedesco, 1992; Dowdeswell et al., 1995; Andrews et al., 1995). Additional observations in Hudson Strait (Andrews et al., 2001; MacLean et al., 2001a, b) support the presence of icebergs in the strait, but direct terrestrial evidence of glacier advance or retreat associated with calving events is lacking.

Terrestrial investigations in western Hudson Strait ranging from the early twentieth century (Bell, 1884, 1901) to recent work (Laymon, 1992; Bruneau and Gray, 1997; Gray, 2001) detail evidence of an ice stream flowing in Hudson Strait at undetermined times in the past. Drainage of the Laurentide Ice Sheet interior through Hudson Strait has been a principle feature of various maps and reconstructions of full and late glacial conditions, including studies by Shilts (1980), Denton and Hughes (1981), Fisher et al. (1985), and Dyke and Prest (1987). Fisher et al. (1985) interpreted an ice stream in Hudson Strait under certain specified basal conditions in a model of the entire Laurentide Ice Sheet, whereas MacAyeal (1993) assumed the presence of a high-flux ice stream in a model of internally controlled cyclic discharges of ice into the North Atlantic Ocean. MacAyeal's (1993) model addressed oceanographic questions, however, and invoked Hudson Strait as the logical single source for high fluxes of ice. The study did not consider geological evidence supporting specific characteristics of the proposed ice stream. Marshall et al. (1996) analyzed several aspects of geological constraints on fast flow in the Laurentide Ice Sheet, but did not investigate Hudson Strait specifically. Of the numerical models representing glacier flow in Hudson Strait, only those of Fisher et al. (1985) and Pfeffer et al. (1997) addressed ice-stream characteristics in the context of the constraints imposed by terrestrial and marine geology on ice-stream flux, geometry, and evolution and constraints imposed on mass balance by paleoclimatic evidence.

Whereas terrestrial and marine evidence indicates that an ice stream occupied Hudson Strait at times in the past, the times at which it may have been present are obscured by the most recent occupation of the strait by glacier ice following the last glacial maximum. At ca. 11 ± 0.1 ka BP, northeastward-flowing ice originating from a source in Quebec–Labrador crossed the eastern portion of Hudson Strait to Meta Incognita Peninsula (Miller et al., 1988; Miller and Kaufman, 1990; Kaufman et al., 1993). Marine evidence from the Baffin Island Shelf (Andrews et al., 1995) indicates that DC-0 and the equivalent H-0 was associated with this cross-strait flow.

Miller and Kaufman (1990) and Andrews et al. (1995) considered the possibility that glacier advance and retreat in the Hudson Strait region might have triggered the Younger Dryas, based on the spatial and temporal structure of advance of ice across Hudson Strait from northern Quebec and Labrador onto southern Baffin Island. Advance was initiated

as early as ca.11.0 ka BP (contemporaneous with the onset of DC-0 (H-0) (Andrews et al., 1995) and culminated in two maxima at ca. 9.9 ka ± 100 BP (Gold Cove advance) and ca. 8.7 ka ± 100 BP (Noble Inlet advance) (Kaufman et al., 1993; Manley, 1995; Manley and Miller, 2001).

The model results presented here are a simulation of local ice dynamics compatible with the ca. 11 000–9000 BP evidence in the vicinity of eastern Hudson Strait and southeastern Baffin Island. The model results are also used to infer characteristics of the subsequent Noble Inlet advance.

MODEL CONSTRUCTION AND IMPLEMENTATION

Model formulation and specification of boundary conditions for the Gold Cove advance summarized here are described in greater detail in Pfeffer et al. (1997) and Fastook and Chapman (1989). In brief, calculations are done with a two-dimensional ('map plane') finite-element model in which bedrock height, ice-surface height, ice-surface gradient, and column-integrated flux are given at each nodal point in a two-dimensional map space. Numerical solutions give the time-varying ice height on realistic bedrock terrain. Integrated column-averaged velocities provide the ice flux arising from local driving stress, determined as a function of ice thickness H, and surface elevation gradient $\vec{\nabla}h$, and local longitudinal velocity gradients. The fluxes are combined, and individual element flux $\vec{Q}$ is determined for each quadrilateral element based on the gradient of surface elevation:

$$\vec{Q}(x,y,t) = \vec{U}H = -k(x,y,t)\vec{\nabla}h(x,y,t) \qquad (1)$$

where $\vec{U}$ is the vertically averaged total ice velocity and $k(x,y,t)$ is a nonlinear coefficient derived from velocity gradients in the column. Co-ordinates x and y are orthogonal horizontal spatial axes, and t is time. A continuity equation is solved at each time step to determine the new ice-surface elevation created by processes of interelement flow and surface mass balance. The time-varying ice height is given by

$$\frac{\partial h}{\partial t} = \dot{a} - \nabla \cdot \vec{Q} \qquad (2)$$

where $\dot{a}$ and $\vec{Q}$ are the spatially and temporally variable mass balance and ice flux, respectively.

Model strategy

Simulations derived from numerical models are limited by the extent of knowledge of the physical processes represented in the model, information available to constrain boundary conditions, and by computational considerations which limit spatial and temporal resolution and numerical accuracy. Because of these limitations, models can be designed to yield certain classes of information only. The model presented here was designed specifically to test the hypothesized advance of ice across Hudson Strait from the Ungava platform to Meta Incognita Peninsula. The initial geometry and basal boundary conditions were chosen in the simplest form compatible with this objective. Simplifications have been made to this end that are not in concordance with the terrestrial geology or probable ice geometry elsewhere in the modelled region (most notably on the western portion of Ungava Peninsula and the Gulf of St. Lawrence region), and the model is not intended to portray conditions in these areas.

Initial conditions

The simulation region extends from the Gulf of St. Lawrence to the north shore of Cumberland Sound (Baffin Island) and from Hudson Bay to the Labrador Sea. Bedrock topography at 9216 nodes covering the model region is interpolated from the 5 min ETOPO5 digital terrain model (National Oceanic and Atmospheric Administration, 1988). The initial ice geometry chosen was the simplest that would allow investigation of advance in the Ungava Bay–eastern Hudson Strait region of the ice-sheet margin. The initial geometry was also chosen on the basis of Kleman et al.'s (1994) inference that a single dome occupied the Quebec–Labrador region. Subsequent reanalysis has re-established the currently accepted ridge-and-saddle topography (e.g. Gray, 2001, Fig. 11; MacLean et al., 2001a, Fig. 1), but with some important exceptions that will be discussed, the single-dome topography will suffice for the purpose of an initial investigation of cross-strait advance.

An initial ice-sheet configuration compatible with bedrock topography and inferred mass balance was developed in the model by specifying an arbitrary large positive mass balance over a circular region approximately 700 km in diameter, centred in Quebec–Labrador south of Ungava Bay. Ice was allowed to accumulate until approximately the desired initial geometry was obtained (ca. 1000 years model time); subsequently the mass balance was reduced to values compatible with the inferred climate (the first of three mass balance phases described below), and the ice dome allowed to stabilize over about another 300 years. The resulting quasi-steady-state ice dome had a maximum central thickness (2200 m) and location consistent with Peltier's (1994) calculations based on isostatic rebound and Kleman et al.'s (1994) analysis of landforms in Quebec–Labrador. The ice thickness was a maximum value compatible with Peltier (1994; Edwards (1995) suggested that Peltier's net ice volume may have been an underestimate) and was centred slightly to the northeast of Peltier's placement of the maximum ice thickness. Eastern Hudson Strait was initially ice-free. Whereas no definitive evidence exists which constrains ice conditions in eastern Hudson Strait immediately prior to DC-0, marine conditions at the nearby Resolution basin and southeast Baffin Island Shelf indicate relatively warm and possibly seasonally ice-free conditions (Andrews et al., 1995).

Mass balance

Mass balance plays a key role in the reproduction of the dynamics of advance and retreat at DC-0–Younger Dryas time, and must be allowed to vary over time to reproduce the

observations. This is not surprising in view of the rapidly varying climatic conditions at the Younger Dryas–Preboreal transition. Mass balance was simulated in three phases based on the central Greenland GISP2 ice-core paleoclimate record (Alley et al., 1993): a cold, dry Younger Dryas condition; a high-accumulation, low-equilibrium-line-altitude condition (transitional I) following the Younger Dryas corresponding in time to the Gold Cove advance; and a high-accumulation, high-equilibrium-line-altitude condition (transitional II) during recession from Gold Cove advance. Mass-balance parameters for the sequence of changes during and following the Younger Dryas are summarized in Table 1. Mass balance for the Younger Dryas was constructed by shifting the modern mass balance (constructed from observations for the modern Devon ice cap (Haeberli and Hoelzle, 1988, 1993) and central west Greenland (Ohmura, 1993)) to a cold, low-accumulation, low-equilibrium-line-altitude environment. The high-accumulation, low-equilibrium-line-altitude (transitional I) environment was constructed based on the timing and magnitude of shifts in precipitation and temperature from the GISP2 ice-core record (Alley et al., 1993) to drive the ice advance to Gold Cove by doubling accumulation at the Younger Dryas termination. Accumulation and temperature increased at all elevations, with accumulation dominating temperature at low elevations, resulting in a depressed equilibrium-line altitude at the time of the Gold Cove advance. Finally, recession from Gold Cove advance occurred as a consequence of increased ablation and elevated equilibrium-line altitude, following warming of +7°C (from -25°C to -18°C, Alley et al., 1993) over the Younger Dryas–Holocene transition (transitional II).

Calving

Calving is included in the model as an ablation term acting at elements along the perimeter of floating ice margins. Calving flux is calculated as a product of iceberg size, estimated by the probable position of fracture at a distance behind a floating ice cliff equal to one ice thickness (Reeh, 1968), and the time required for a single iceberg to calve, determined by integrating a theoretically derived depth-dependent crack-propagation rate based on calculations by Fastook and Schmidt (1982). The calving speed (specified individually for each element along the calving boundary) is

$$C = \frac{q_c}{e_w^2} \qquad (3)$$

where q_c is the calving flux and e_w is the element width. Calving speed C is treated as a mass-balance term in the calving element. Calving can eliminate perimeter elements altogether, allowing retreat of a floating margin. The calving flux calculation as described appears to be very conservative (low flux for given thickness), but no appropriate observational data exist for comparison.

Basal sliding

Kleman et al. (1994) interpreted a set of convergent flow indicators south of Ungava Bay to be a pre-Late Wisconsin relict landscape preserved by frozen, no-slip bed conditions in the Late Wisconsin. In accordance with this, sliding was not allowed anywhere above modern sea-level south of Hudson Strait. At the start of the simulation, sliding was allowed wherever ice was present in Ungava Bay, Hudson Strait, and all regions to the north of Hudson Strait; the initiation of sliding defined the onset of ice advance. Kleman et al.'s (1994) interpretation of superimposed landforms on Quebec–Labrador imposed a constraint on basal boundary conditions that was held fixed throughout these model experiments. The constraint of no basal sliding above modern sea-level in Quebec–Labrador was the most restrictive limitation on the modelled advance, and required that the mass-balance parameters be adjusted to the limits of what are plausible on the basis of paleoclimatic data in order to reproduce the Gold Cove advance. The use of initial basal conditions compatible with the Kleman et al. (1994) presentation excluded the formerly proposed and subsequently accepted (Shilts, 1980; MacLean et al., 2001a) flow divide trending north-northwest from central Quebec to the Ungava Peninsula. The division of flow into separate streams on the Ungava platform was also excluded, although with the notable exception of Gray's (2001) inferences about ice thickness at Akpatok Island, no evidence of stream flow exists on the platform.

MODEL RESULTS

Figures 1–3 show representative surface elevation maps and cross-sections of the ice dome originating from Quebec–Labrador at stages from the initial configuration to recession following the Gold Cove maximum. Model simulations were made in three phases: 1) advance across Hudson Strait to a stable position on Meta Incognita Peninsula and Resolution

Table 1. Mass-balance parameters used in model reconstruction of Gold Cove advance.

Glacial stages	Annual accumulation, (% change from present)	Difference in T_{ann} (present-reconstructed, °C)	Summer temperature (°C)	Annual ablation (m ice)	Annual mass balance (m ice)	Equilibrium line elevation (m above sea level)
Younger Dryas	50	10	4.8	0.15	0.5	300
Transition I	100	-8	4.0	0.25	0.7	120
Transition II	100	-2	0.5	4.20	0.0	1300

Island, coincident with the start of DC-0–Younger Dryas time; 2) advance from Meta Incognita Peninsula and Resolution Island to Hall Peninsula coincident with the Gold Cove advance; and 3) rapid retreat from Hall Peninsula to Meta Incognita Peninsula and Resolution Island. Model result times correspond to calendar year intervals, and where possible, equivalent times in the ^{14}C chronology are identified. The initiation of the first advance across Hudson Strait corresponds in time to the onset of the Younger Dryas, at ca. 11 ± 0.1 ka BP.

Advance across Hudson Strait

Given the fixed spatial pattern of sliding, successful advance of ice across eastern Hudson Strait from an initial position on Quebec–Labrador required an initial maximum ice thickness of at least 2000 m (Fig. 1). Initial ice heights less than this resulted in drawdown of the central portion of the dome and insufficient upstream ice flux to overcome calving in Eastern basin. Using a 2200 m initial ice height, advance to Meta Incognita Peninsula and Resolution Island occurred in approximately 300–400 years, with the highest discharge fluxes during this phase (0.0025 Sverdrup (Sv)) occurring as ice crossed the deep Eastern basin. After reaching Meta Incognita Peninsula and Resolution Island, the terminus stabilized in shallow water and maintained equilibrium at this position (with consequent stabilization in thickness and discharge) over a moderate range of reasonable mass-balance values. Figure 2 shows the ice configuration at the stable Meta Incognita Peninsula and Resolution Island position. Given the constraints of ice thickness and the location of sliding, the advance to Meta Incognita Peninsula and Resolution Island is a robust result and confirms in a general way the geologically inferred advance of ice across Hudson Strait. The constraints of ice thickness and location of sliding are important qualifications, however. As was described earlier, basal sliding was allowed in the model everywhere below modern sea level in Ungava Bay and Hudson Strait. Specifically, no channellized flow was defined in Ungava Bay, which, if specified, could have given variable ice thickness, and more particularly thickness more compatible with Gray's (2001) depiction of events at Akpatok Island.

Gold Cove advance

With the distribution of sliding held fixed in space and time, conditions of mass balance and calving were chosen which allowed for the following events: 1) rapid ice advance beyond Meta Incognita Peninsula and Resolution Island to Hall Peninsula (ca. 400 years or less), 2) ice thickness at Hall Peninsula consistent with observations of coverage of summits

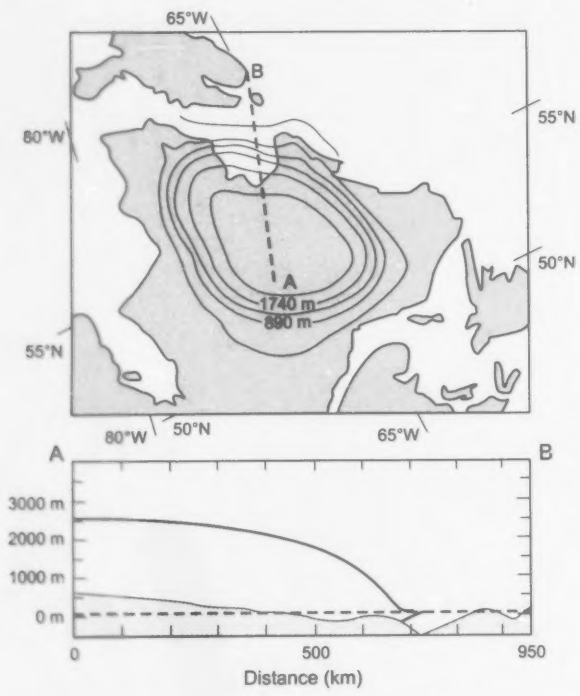

Figure 1. *Initial ice geometry on Quebec–Labrador. Map region includes northern Quebec, Ungava Bay, Hudson Strait, and southern Baffin Island. Lower panel shows elevation transect along line AB in upper panel* (modified from *Pfeffer et al., 1997, Fig. 3). Hatched area in lower panel denotes bedrock.*

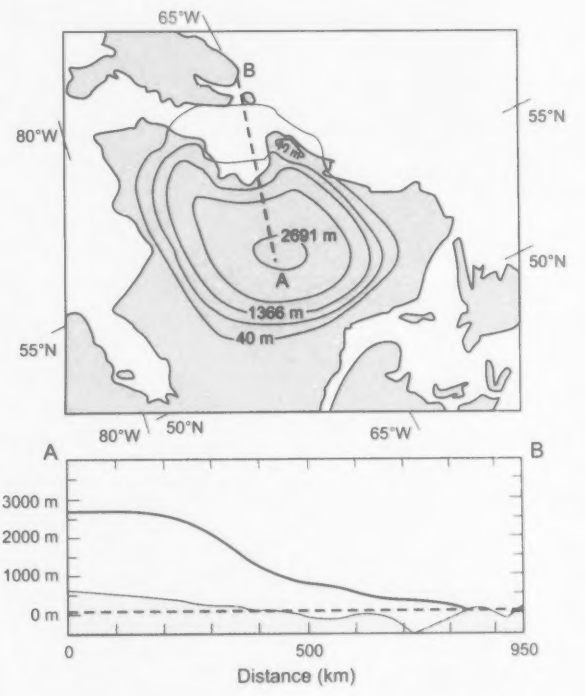

Figure 2. *Modelled stable position at Meta Incognita Peninsula and Resolution Island* (modified from *Pfeffer et al., 1997, Fig. 4). Hatched area in lower panel denotes bedrock.*

(more than 400 m a.s.l.; Kaufman et al., 1993), and 3) rapid retreat from Hall Peninsula to Meta Incognita Peninsula and Resolution Island (400 years or less). The northern margin of the advance, extended at the Meta Incognita Peninsula and Resolution Island position, was dynamically isolated from the main dome and changes in mass balance at the main dome were found to have no immediate or short-term effect on the Meta Incognita Peninsula and Resolution Island margin. An abrupt increase in precipitation (compatible with the GISP2 ice-core accumulation record) preceding a rise in equilibrium-line altitude at the termination of the Younger Dryas was used to drive the onset of the Gold Cove advance at ca. 10.2 ka BP. Rapid initial advance was driven by increased accumulation in the extended lobe over Hudson Strait. Mass balance provided sufficient accumulation to produce rapid advance of ice past the stable Meta Incognita Peninsula and Resolution Island position to Gold Cove but was at the upper limit of reasonable accumulation rates and delivered ice of only about 100 m thickness to Hall Peninsula. Actual ice thickness on Hall Peninsula during the Gold Cove advance is constrained by observations of bedrock striations at 370 m a.s.l. on Loks Land (easternmost Hall Peninsula) (Kaufman et al., 1993), so the model underestimates ice thickness at Hall Peninsula. The shape of the advanced lobe on Meta Incognita and Hall peninsulas (Fig. 3) matches remarkably well the spatial pattern inferred from the terrestrial geology (Kaufman et al., 1993). Further experiments with greater (and probably unrealistic) accumulation rates failed to produce substantially thicker ice at Hall Peninsula.

The timing of the changes to a higher accumulation rate controls the timing of advance to Gold Cove. The time at which the increase in accumulation is applied is determined here by the model response and acts as a tuning parameter. The mass-balance shift for Gold Cove is supported by GISP2 ice-core data only for a very brief period (about 5–25 years) in central Greenland but is maintained in the Hudson Strait region during the duration of the Gold Cove advance. This is an unrealistically long time in the context of the GISP2 ice-core record but is necessary in context of the model boundary conditions to force the advance. A recalibration of the relation between isotopic ratios and temperature (Cuffey et al., 1994) indicates that the temperature rise at the termination of the Younger Dryas was greater than previously inferred, so the increase in mass balance demanded by the model (arising from a warmer, wetter environment) may be more reasonable than would be expected on the basis of the earlier GISP2 ice-core results. Kaufman et al. (1993) showed ^{14}C dates which constrain the occupation of Frobisher Bay by ice to about 100–500 years. The model results shown here are consistent with this constraint.

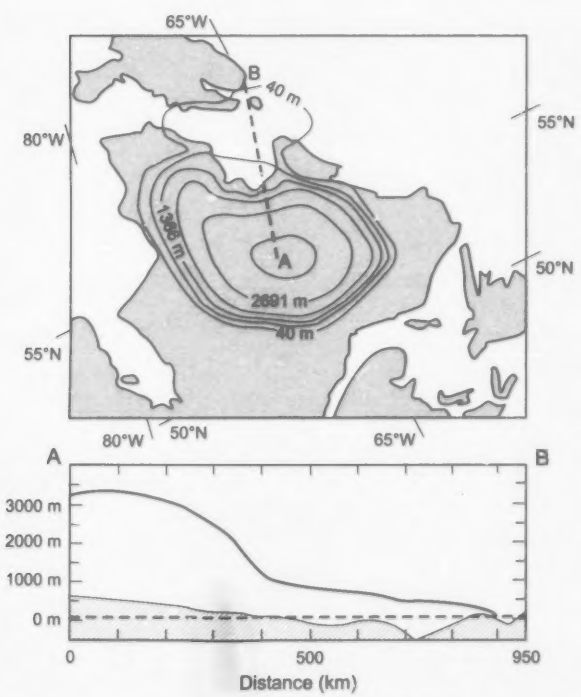

Figure 3. *Modelled Gold Cove maximum extent corresponding to geological interpretation at ca. 9.9 ka BP (from Pfeffer et al., 1997, Fig. 5). Hatched area in lower panel denotes bedrock.*

NOBLE INLET ADVANCE

Manley and Miller (2001) gave a description of the Noble Inlet advance, including the inferred approximate timing of onset (8.9 ka BP), maximum extent (8.77 ka BP), and final deglaciation (8.4 ka BP). The marine sedimentation record in Eastern basin and inferences relevant to ice conditions in Hudson Strait at Noble Inlet time are presented in Jennings et al. (1998) and in MacLean et al. (2001b). Gray (2001) discussed terrestrial evidence from Akpatok Island in Ungava Bay, that indicates either the absence of a Quebec–Labrador source south of Ungava Bay for Noble Inlet ice or a restriction of ice flow in Ungava Bay to the east of Akpatok Island at the time of the Noble Inlet advance.

The model simulation described above for the Gold Cove advance was carried out as far as recession from Gold Cove, but the Noble Inlet readvance was not modelled. Features of the Noble Inlet advance can be characterized, however, by drawing inferences from the ice volume, geometry, mass balance, and dynamic behavior in the strait during the Gold Cove results. The features of the Noble Inlet advance inferred by these means are general in character, and should not be extended too far in specific details. In particular, Gray's (2001) evidence for ice-free conditions on Akpatok Island during the Noble Inlet advance is not specifically accounted for in the discussion below, nor was it specifically excluded by model results.

At the time of the maximum extent of the Gold Cove advance, the model simulation indicates that approximately 8.14×10^{13} m^3 of ice (7.46×10^{13} m^3 water equivalent) was grounded below sea level beyond the north coast of Quebec–Labrador. On the basis of ice-marginal elevations at Pritzler

Harbour and modelled ice-surface slopes across Hudson Strait (derived from the Gold Cove advance), the ice volume grounded below sea level at the Noble Inlet maximum is estimated to be approximately 6.47×10^{13} m^3 (5.93×10^{13} m^3 water equivalent).

CONDITIONS IN HUDSON STRAIT BETWEEN GOLD COVE AND NOBLE INLET ADVANCES

Manley and Jennings (1996) reported reworked single molluscs in glaciomarine sediments at cores 93034-004 and 93034-052 on the north flank of Eastern basin which date to ca. 9.0 ka BP, shortly before the probable time of the onset of the Noble Inlet advance at ca. 8.9 ka BP. Whereas the reworked shells were deposited in their final position after Noble Inlet advance and recession, they evidently lived in a location adjacent and accessible to Eastern basin. This supports partially or completely ice-free conditions in some region adjacent to the Eastern basin at ca. 9.0 ka BP, between the culmination of Gold Cove and the Noble Inlet readvance. Open water in Hudson Strait prior to Noble Inlet could have developed during the retreat from Gold Cove as the south- or southwestward-retreating margin left the southern coast of Baffin Island and retreated into the deeper waters of the Eastern basin. Recession may have slowed temporarily as the margin reached the metastable Meta Incognita Peninsula and Resolution Island position, but would have accelerated, probably accompanied by the formation of a vigorous calving embayment, as the margin retreated into Eastern basin. Because of that vigorous calving, retreat is unlikely to have been reversed before the margin reached the far side of Eastern basin, where a more stable (but still receding) position could be established on the Ungava platform.

The flux and volume demands for the creation of partially open-water conditions before the Noble Inlet advance and for the Noble Inlet advance itself can be estimated from the strait bathymetry and geological constraints on the thickness and extent of ice, and from the volume demands compared to the ice volume available in the main dome on Quebec–Labrador. The bathymetric volume of the relevant portion of Hudson Strait, approximately from Héricart Bay to Resolution and Button islands and below modern sea level, is approximately 1.28×10^{13} m^3, and the volume of the minimum grounded ice thickness in the same area is 1.40×10^{13} m^3. The modelled metastable Meta Incognita Peninsula and Resolution Island position (Fig. 2) contains 4.0×10^{13} m^3 of ice grounded in Hudson Strait, whereas the maximum Gold Cove position (Fig. 3) contains 8.14×10^{13} m^3 of ice grounded in Hudson Strait and in Frobisher Bay to the north. The calving flux out of Hudson Strait between recession from Gold Cove and advance to Noble Inlet (approximately 600 years between 9.6 ka BP and 9.0 ka BP), can be estimated by bracketing the volume of ice to be evacuated between the minimum and maximum values given above. The ice volume grounded in Hudson Strait and on the Ungava platform at the onset of recession from Gold Cove is fairly tightly constrained by mapped terminus positions on Hall Peninsula (and to a lesser extent in northern Labrador) together with the model results; however, the minimum ice volume immediately prior to the Noble Inlet readvance is constrained only by the observation (MacLean et al., 2001a) that some amount of open water existed adjacent to the Eastern basin at some point during the retreat. The ice flux inferred from the above volumes and the 600 year time interval for removal is 2.33×10^{10} m^{3}a^{-1} = 0.0007 Sv for the minimum grounded volume, 6.67×10^{10} m^{3}a^{-1} = 0.002 Sv for the Meta Incognita Peninsula and Resolution Island volume, and 13.6×10^{10} m^{3}a^{-1} = 0.004 Sv for the Gold Cove maximum volume. On the basis of Rahmstorf's (1995) analysis, none of these discharge fluxes appear to be likely to have a significant effect on ocean circulation taken by themselves, nor do they constitute significant sea-level change inputs. Fairbanks (1989) showed sea-level input rates at this time (mwp-1B) to be about $6–7 \times 10^{12}$ m^{3}a^{-1} (~ 0.2 Sv); the estimated input from Hudson Strait constitutes approximately 0.3–2.0% of this amount.

ICE DYNAMICS DURING THE NOBLE INLET AND GOLD COVE ADVANCES

Refilling of part or all of the grounded ice in Hudson Strait during the Noble Inlet advance requires a discharge from the diminishing ice volume on Quebec–Labrador that can be estimated once again from the inferred volume of ice in the strait at the Noble Inlet maximum extent. The same bathymetric volume between Héricart Bay and Resolution and Button islands is used; the surface elevations were constrained by the presence of ice at about 350 m a.s.l. in the vicinity of Pritzler Harbor that allowed drainage through the York canyons. Estimating a surface slope of 0.2° across Hudson Strait (a typical value for fast ice-stream flow, and reproduced in the model simulation of the Gold Cove advance), the volume of ice in Hudson Strait at the maximum extent of the Noble Inlet advance is about 6.47×10^{13} m^3. Advance to the Noble Inlet maximum position occurred over about 130 years between 8.9 ka BP and 8.77 ka Bp. Given the volume and geometry of ice in the strait as estimated here, and assuming that Hudson Strait was initially entirely ice-free at the onset of advance, then the average ice velocity leaving the Ungava platform (across a line approximately from the Eider Islands to Killiniq Island) and entering Hudson Strait would have been approximately 1700 m/year. This velocity is well within observed velocities on modern ice streams. The volume of ice in Hudson Strait as estimated is also only 4% of the modelled volume grounded on Quebec–Labrador. Ice dynamics and the quantity of available ice do not therefore appear to impose any significant limitations on the timing and character of the Noble Inlet advance as determined by the terrestrial and marine geological observations (Stravers et al., 1992; Manley and Miller, 2001; MacLean et al., 2001b).

The ice elevation profile inferred here gives surface elevations of about 800 m over Akpatok Island at the Noble Inlet maximum, in contrast with Gray's (2001) inference that Akpatok Island was not overridden by northward-flowing ice during the Noble Inlet advance, with ice passing to the east of the island. The ice elevations presented here are the product of modelling which allows flow equally across all of Ungava

Bay, both west and east of Akpatok Island. Given observational evidence on which to base the constraint, flow could have been restricted to the east of Akpatok Island by designating sliding in that part of Ungava Bay only, but Gray's (2001) evidence from Akpatok Island (the only evidence at present which bears on this issue) was not available at the time of the modelling, and the simplest flow condition (uniform across Ungava Bay) was adopted.

Another question to be addressed is what mechanism forced the Noble Inlet advance. The Gold Cove advance is assumed here to have been forced by the onset of sliding following long-term warming during deglaciation but prior to the Younger Dryas. The Noble Inlet advance may have been forced by basal warming following the termination of the Younger Dryas. Freezing or thawing at the bed under the Quebec–Labrador dome would have been influenced by the combined effects of atmospheric temperature, ice thickness, and thermal advective and conductive time scales, with thinner ice presenting a shorter conductive and advective thermal pathway for heat exchange between the bed and the atmosphere. The ice dynamics response to a pattern of temperature and accumulation changes can be complex. Longitudinal extension and thinning caused by thawing of the bed following the delayed arrival of a warm pulse from the surface would allow a faster response (through a shorter thermal pathway) to a subsequent cold pulse. Note that forcing through changes in transmission of heat to and from the bed occurs at different time scales than forcing through changes in mass balance which cause changes in ice thickness and surface slope (Clarke et al., 1999). The advance to Gold Cove from the Meta Incognita Peninsula and Resolution Island position has been modelled as the consequence of additional ice thickness accumulated with no time lag following the end of the Younger Dryas. Changes in sliding arising from the advection of cold Younger Dryas ice to the bed are delayed by the conductive and advective time scales, however, and the effects of Younger Dryas cooling may in fact have occurred after the effects of the post-Younger Dryas increase in accumulation.

From the perspective of glacier dynamics, the most coherent way to interpret the Gold Cove and Noble Inlet advances may be to reconsider them as a single advance forced by long-term warming during the glacial–Holocene transition. This single advance was divided into two parts by a hiatus initiated when basal sliding was interrupted by refreezing due to the arrival of cold Younger Dryas ice at the bed, and ultimately terminated by thawing and resumption of sliding caused by post-Younger Dryas warming. The Gold Cove advance was initiated immediately (no time lag) following increased accumulation at the end of the Younger Dryas, whereas the thermal effects of the onset of cold Younger Dryas conditions and the resumption of warm conditions following the Younger Dryas are lagged by at least 1100 years for the interval from the onset of the Younger Dryas to Gold Cove maximum, and approximately 1300 years for the interval from the end of the Younger Dryas to the onset of the Noble Inlet advance.

The inferences made here about the Noble Inlet advance are based on order-of-magnitude arguments, and are to a degree qualitative. Future work with a thermomechanical model will help to quantify these arguments.

ACKNOWLEDGMENTS

This work was improved by discussions with John Andrews, Anne Jennings, Brian MacLean, and by careful reviews and comments by James Gray, Doug Hodgson, Heiner Josenhans, and John Shaw.

REFERENCES

Alley, R.B., Meese, D.A., Shuman, C.A., Gow, A.J., Taylor, K.C., Grootes, P.M., White, J.W.C., Ram, M., Waddington, E.D., Mayewski, P.A., and Zielinski, G.A.
1993: Abrupt increase in Greenland snow accumulation at the end of the Younger Dryas event; Nature, v. 362, p. 527–529.

Andrews, J.T. and Tedesco, K.
1992: Detrital carbonate-rich sediments, northwestern Labrador Sea: implications for ice-sheet dynamics and iceberg rafting (Heinrich) events in the North Atlantic; Geology, v. 20, p. 1087–1090.

Andrews, J.T., Jennings, A.E., Kerwin, M., Kirby, M., Manley, W., Miller, G.H., Bond, G., and MacLean, B.
1995: A Heinrich-like event, H-0 (DC-0): source(s) for detrital carbonate in the North Atlantic during the Younger Dryas chronozone; Paleoceanography, v. 10, p. 943–952.

Andrews, J.T., Jennings, A.E., and MacLean, B.
2001: Late Quaternary stratigraphy of Hatton and Resolution basins east of Hudson Strait; *in* Marine Geology of Hudson Strait and Ungava Bay, Eastern Arctic Canada: Late Quaternary Sediments, Depositional Environments, and Late Glacial–Deglacial History Derived from Marine and Terrestrial Studies, (ed.) B. MacLean; Geological Survey of Canada, Bulletin 566.

Bell, R.
1884: Observaions on the geology, minerology, zoology, and botany of the Labrador coast, Hudson's Strait and Bay; Geological Survey of Canada, Report of Progress 1882-83-84, v. 1, Part D, p. 5–62.
1901: Report of an exploration on the northern side of Hudson Strait; Geological Survey of Canada, Annual Report, Volume X, Part M, 38 p.

Broecker, W.S.
1994: Massiveiceberg discharges as triggers for global climate change; Nature, v. 372, p. 421–424.

Bruneau, D. and Gray, J.T.
1997: Ecoulements glaciers et deglaciation hative (ca 11 ka BP) du nord-est de la peninsule d'Ungava, Quebec, Canada; Canadian Journal of Earth Sciences, v. 34, p. 1089–1100.

Clarke, G.K.C., Marshall, S.J., Hillaire-Marcel, C., Bilodeau, G., and Veiga-Pires C.
1999: A glacidogical perspective on Heinrich events; *in* Mechanisms of Millenial-Scale Global Climate Change, (ed.) P.U. Clarke, R.S. Webb, and L.D. Keigwin; American Geophysical Union Monogrph, v. 112, p. 243–263.

Cuffey, K.M., Alley, R.B., Grootes, P.M., Bolzan, J.M., and Anandakrishnan, S.
1994: Calibraton of the delO18 isotopic paleothermometer for central Greenlad, using borehole temperatures; Journal of Glaciology, v. 40, n. 135, p. 341–349.

Denton, G.H. and Hughes, T.J.
1981: The Artic ice sheet: an outrageous hypothesis; *in* The Last Great Ice Sheets, (ed.) G.H. Denton and T.J. Hughes; John Wiley, New York, New York, 484 p.

Dowdeswell, J./., Maslin, M.A., Andrews, J.T., and McCave, I.N.
1995: Iceberg production, debris rafting, and extent and thickness of Heinrich layrs (H-1, H-2) in North Atlantic sediments; Geology, v. 23, p. 301–04.

Dyke, A.S. and Prest, V.K.
1987: Late Wisconsinan and Holocene history of the Laurentide Ice Sheet; Géographie physique et Quaternaire, v. 41, p. 237–263.
Edwards, R.L.
1995: Paleotopography of glacial-age ice sheets; Science, v. 267, p. 536.
Fairbanks, R.G.
1989: A 17,000-year glacio-eustatic sea level record: influence of glacial melting rates on the Younger Dryas event and deep-ocean circulation; Nature, v. 342, p. 637–642.
Fastook, J. and Chapman, J.E.
1989: A map-plane finite element model: three modeling experiments; Journal of Glaciology, v. 35, no. 119, p. 48–52.
Fastook, J. and Schmidt, W.
1982: Finite element analysis of calving from ice fronts; Annals of Glaciology, v. 3, p. 103–106.
Fisher, D.A., Reeh, N., and Langley, K.
1985: Objective reconstruction of the late Wisconsinan Laurentide Ice Sheet and the significance of deformable beds; Géographie physique et Quaternaire, v. 39, p. 229–238.
Gray, J.T.
2001: Patterns of ice flow and deglaciation chronology for southern coastal margins of Hudson Strait and Ungava Bay; *in* Marine Geology of Hudson Strait and Ungava Bay, Eastern Arctic Canada: Late Quaternary Sediments, Depositional Environments, and Late Glacial–Deglacial History Derived from Marine and Terrestrial Studies, (ed.) B. MacLean; Geological Survey of Canada, Bulletin 566.
Haeberli, W. and Muller, P. (ed.)
1988: Fluctuations of Glaciers, 1980-1985; International Association of Hydrological Sciences and United Nations Environmental Program World Glacier Monitoring Service, Zurich, Switzerland, 290 p.
1993: Fluctuations of Glaciers, 1985-1990; International Association of Hydrological Sciences and United Nations Environmental Program World Glacier Monitoring Service, Zurich, Switzerland, 322 p.
Heinrich, H.
1988: Origin and consequences of cyclic rafting in the northeast Atlantic Ocean during the past 130,000 years; Quaternary Research, v. 29, p. 142–152.
Jennings, A.E., Manley, W.F., MacLean, B., and Andrews, J.T.
1998: Marine evidence for the last glacial advance across eastern Hudson Strait, eastern Canadian Arctic; Journal of Quaternary Science, v. 13, no. 6, p. 501–505.
Kaufman, D.S., Miller, G.H., Stravers, J.A., and Andrews, J.T.
1993: An abrupt early Holocene (9.9-9.6 kyr BP) ice stream advance at the mouth of Hudson Strait, Arctic Canada; Geology, v. 21, p. 1063–1066.
Kleman, J., Borgstrom, I., and Hattestrand, C.
1994: Evidence for a relict glacial landscape in Quebec-Labrador; Palaeogeography, Palaeoclimatology, Palaeoecology, v. 111, p. 217–228.
Laymon, C.A.
1992: Glacial Geology of western Hudson Strait, Canada, with reference to Laurentide Ice Sheet dynamics; Geological Society of America, Bulletin, v. 104, p. 1169–1177.
MacAyeal, D.R.
1993: Binge/purge oscillations of the Laurentide Ice Sheet as a cause of the north Atlantic's Heinrich events; Paleoceanography, v. 8, p. 775–784.
MacLean, B., Andrews, J.T., Gray, J.T., Hall, F.R., Hardy, I., Jennings, A.E., Manley, W.F., Pfeffer, W.T., and Vilks, G.
2001a: Hudson Strait Quaternary sediments and late glacial and deglaciation history: a discussion and summary; *in* Marine Geology of Hudson Strait and Ungava Bay, Eastern Arctic Canada: Late Quaternary Sediments, Depositional Environments, and Late Glacial–Deglacial History Derived from Marine and Terrestrial Studies, (ed.) B. MacLean; Geological Survey of Canada, Bulletin 566.
MacLean, B., Vilks, G., Hardy, I., Deonarine, B., Jennings, A.E., and Manley, W.F.
2001b: Quaternary sediments in Hudson Strait and Ungava Bay; *in* Marine Geology of Hudson Strait and Ungava Bay, Eastern Arctic Canada: Late Quaternary Sediments, Depositional Environments, and Late Glacial–Deglacial History Derived from Marine and Terrestrial Studies, (ed.) B. MacLean; Geological Survey of Canada, Bulletin 566.
Manley, W.F.
1995: Late-glacial record of ice sheet/ocean interactions, Hudson Strait and southern Baffin Island, eastern Canadian Arctic; Ph.D. thesis, Department of Geology, University of Colorado, Boulder, Colorado, 252 p.
Manley, W. and Jennings, A.E. (comp.)
1996: Radiocarbon Date List VIII: Eastern Canadian Arctic, Labrador, northern Quebec, East Greenland Shelf, Iceland Shelf, and Antarctica; Institute of Arctic and Alpine Research, University of Colorado, Occasional Paper no. 50, 163 p.
Manley, W.F. and Miller, G.H.
2001: Glacial–geological record on southern Baffin Island reflecting late glacial ice-sheet dynamics in the eastern Hudson Strait region; *in* Marine Geology of Hudson Strait and Ungava Bay, Eastern Arctic Canada: Late Quaternary Sediments, Depositional Environments, and Late Glacial–Deglacial History Derived from Marine and Terrestrial Studies, (ed.) B. MacLean; Geological Survey of Canada, Bulletin 566.
Marshall, S.J., Clarke, G.K.C., Dyke, A.S., and Fisher, D.A.
1996: Geological and topographic controls on fast flow in the Laurentide and Cordilleran Ice Sheets; Journal of Geophysical Research, v. 101, no. B8, p. 17 827–17 839.
Miller, G.H. and Kaufman, D.S.
1990: Rapid fluctuations of the Laurentide Ice Sheet at the mouth of Hudson Strait: new evidence for ocean/ice-sheet interactions as a control on the Younger Dryas; Paleoceanography, v. 5, p. 907–919.
Miller, G.H., Hearty, P.J., and Stravers, J.A.
1988: Ice sheet dynamics and glacial history of southeasternmost Baffin Island and outermost Hudson Strait; Quaternary Research, v. 30, p. 116–136.
National Oceanic and Atmospheric Administration
1988: Digital relief of the surface of the earth; Data Announcement, 88-MGG-02, National Geophysical Data Centre, Boulder, Colorado.
Ohmura, A.
1993: ETH Greenland Ice Sheet Program: an overview, mass balance and related topics of the Greenland Ice Sheet; (ed.) N. Reeh and H. Oerter; Open File Series, 93/5, Swiss Federal Institute of Technology, Zurich, Switzerland, 108 p.
Peltier, W.R.
1994: Ice-age paleotopography; Science, v. 265, p. 195–201.
Pfeffer, W.T., Dyurgerov, M., Kaplan, M., Dwyer, J., Sassolas, C., Jennings, A., Raup, B., and Manley, W.
1997: Numerical modeling of late Glacial Laurentide advance of ice across Hudson Strait: insights into terrestrial and marine geology, mass balance, and calving flux; Paleoceanography, v. 12, p. 97–110.
Rahmstorf, S.
1995: Bifurcations of the Atlantic thermohaline circulation in response to changes in the hydrological cycle; Nature, v. 378, p. 145–149.
Reeh, N.
1968: On the calving of ice from floating glaciers and ice shelves; Journal of Glaciology, v. 7, no. 50, p. 215–232.
Shilts, W.W.
1980: Flow patterns in the central North American Ice Sheet; Nature, v. 286, p. 213–218.
Stravers, J.A., Miller, G.H., and Kaufman, D.S.
1992: Late glacial ice margins and deglacial chronology for southeastern Baffin Island and Hudson Strait, eastern Canadian Arctic; Canadian Journal of Earth Sciences, v. 29, p. 1000–1017.

Hudson Strait Quaternary sediments and late glacial and deglaciation history: a discussion and summary

B. MacLean[1], J.T. Andrews[2], J.T. Gray[3], F.R. Hall[4], I. Hardy[1], A.E. Jennings[2], W.F. Manley[2], W.T. Pfeffer[2], G. Vilks[5]

MacLean, B., Andrews, J.T., Gray, J.T., Hall, F.R., Hardy, I., Jennings, A.E., Manley, W.F., Pfeffer, W.T., and Vilks, G., 2001: Hudson Strait Quaternary sediments and late glacial and deglaciation history: a discussion and summary; in *Marine Geology of Hudson Strait and Ungava Bay, Eastern Arctic Canada: Late Quaternary Sediments, Depositional Environments, and Late Glacial–Deglacial History Derived from Marine and Terrestrial Studies, (ed.) B. MacLean; Geological Survey of Canada, Bulletin 566, p. 181–191.*

Abstract: Thick, multisequence deposits of ice-contact sediments in the deep floors of Eastern and Western basins and on the seaward side of the sill at the entrance to Hudson Strait attest to the magnitude of glacial ice streams in Hudson Strait. Some of these are thought to have extended to the shelf edge and to be a source of Heinrich events in the Labrador Sea and North Atlantic Ocean. Later south-to-north ice advances across Eastern basin onto southeastern Baffin Island were less far-reaching seaward. The sediment record in the floor of Eastern basin and on its northern and northwestern flanks show that the basin was occupied by a grounded and progressively thinning ice sheet during the time of the Noble Inlet advance recognized on southeastern Baffin Island. Chronological data and similarities in the marine-terrestrial ice-sheet behaviour patterns suggest that this was one and the same ice sheet. Three potential sources for this advance are examined: Baffin Island, a Hudson Strait ice stream, and Quebec–Labrador. The data suggest that the source of this event was a surge of Quebec–Labrador ice centred through Ungava Bay.

Résumé : D'épais dépôts à séquences multiples de sédiments de contact glaciaire trouvés dans les zones profondes des bassins Est et Ouest, ainsi qu'au large du seuil situé à l'entrée du détroit d'Hudson, témoignent de l'ampleur des courants glaciaires dans le détroit d'Hudson. On croit que certains de ces courants auraient atteint la bordure de la plate-forme continentale et occasionné des événements Heinrich dans la mer du Labrador et l'Atlantique Nord. Les avancées qui ont par la suite traversé le détroit d'Hudson du sud au nord pour atteindre la partie sud-est de l'île de Baffin ne se sont pas étendues aussi loin au large. Les données sédimentaires recueillies sur le fond du bassin Est ainsi que sur ses flancs nord et nord-ouest indiquent qu'une nappe glaciaire ancrée qui s'amincissait graduellement occupait le bassin au moment de l'avancée de Noble Inlet mise en évidence dans le sud-est de l'île de Baffin. Les données chronologiques et le comportement similaire des glaces en milieux marins et terrestres portent à croire qu'il ne s'agissait que d'une seule et même nappe glaciaire. L'article examine trois sources possibles de cette avancée glaciaire : l'île de Baffin, un courant glaciaire sur le détroit d'Hudson et la région Québec–Labrador. Les données indiquent que cet événement serait le résultat d'une avancée de la glace de la région Québec–Labrador centrée sur la baie d'Ungava.

[1] Geological Survey of Canada (Atlantic), Bedford Institute of Oceanography, Dartmouth, Nova Scotia B2Y 4A2
[2] Institute of Arctic and Alpine Research, University of Colorado, Boulder, Colorado, U.S.A. 80309
[3] Department of Geography, University of Montreal, P.O. Box 6128, Station A, Montreal, Quebec H3C 3J7
[4] Department of Geology and Geophysics, University of New Orleans, 2000 Lakeside Drive, New Orleans, Louisiana, U.S.A. 70148-2850
[5] Geological Survey of Canada (Atlantic), Bedford Institute of Oceanography, Dartmouth, Nova Scotia B2Y 4A2 (deceased)

INTRODUCTION

Published reconstructions of the Laurentide Ice Sheet virtually all indicate a large proportion of the ice sheet drained toward the Labrador Sea through Hudson Strait (Boulton et al., 1985; Fisher et al., 1985; Hughes, 1987; Dyke and Prest, 1987; Andrews, 1989) with ice and meltwater fluxes of 10^2–10^3 km^3/year (Oerlemans, 1993). Glacial ice-flow patterns indicate drawdown of ice along Hudson Strait from Hudson Bay and Foxe Basin together with ice that entered the strait from Ungava Peninsula and from southern Baffin Island (*see* e.g. Dyke and Prest, 1987; Laymon, 1988, 1991, 1992; Andrews, 1989; Vincent, 1989; Gray, 2001; Manley and Miller, 2001).

Thick, acoustically massive, multisequence deposits of what are considered to be ice-contact sediments lie on bedrock in the deep floors of Eastern and Western basins, and on the continental shelf in the lee of the sill at the eastern entrance to Hudson Strait, where they total 360 m in thickness. These attest to the magnitude of Hudson Strait glacial ice streams, some of which are thought to have extended to the outer edge of the continental shelf. Large quantities of sediment and meltwater derived from them are considered to be a source of Heinrich event deposits in the Labrador Sea and North Atlantic Ocean (Heinrich, 1988; Broecker et al., 1992; Bond et al., 1992; Andrews and Tedesco, 1992; Hillaire-Marcel et al., 1994; Andrews, 1998).

Ages of the sediment members that form the thick ice-contact deposits at the sill and deep in the basin successions in Hudson Strait and in Hatton basin on the shelf seaward of Hudson Strait have not been established, but as indicated above it seems probable that at least some of these are contemporaneous with Heinrich event sediments. Acoustically dense ice-contact deposits seen on seismic profiles to underlie more recent ice-contact or glaciomarine sediments in parts of central and western areas of the strait may be a product of some of the same ice streams that deposited sediments low in the basin sequences, at the sill, and on the continental shelf.

Mollusc fragments reworked into till on Meta Incognita Peninsula of Baffin Island yielded dates in the range of 41–23 ka BP (^{14}C dates) (Blake, 1966; Manley, 1995; Manley and Miller, 2001). A date of 25.2 ka BP from Maiden Island (Bruneau and Gray, 1991), and dates of 31 ka BP, 37 ka BP, and 38 ka BP from Wales Island (Gray and Lauriol, 1985; Gray *in* Manley and Jennings, 1996; Gray, 2001, Fig. 4) have been obtained for marine shell fragments in till. Dates of 32.8 ka BP on foraminifers that are presumed to comprise or include transported specimens in core 93034-013 in the south-central region of Hudson Strait, and of 27.2 ka BP from foraminifers and a mollusc fragment in core 93034-018 southwest of Big Island, also lie within the mid-Wisconsinan time frame. These signify the presence of marine conditions prior to the Late Wisconsinan. The deposits at the sill and in the deep basin successions may include sediments that are substantially older. The last deglaciation of Hudson Strait and the marine-based Laurentide Ice Sheet probably began about 14 ka BP following Heinrich event 1 and continued to ca. 8 ka BP (Andrews et al., 1995b). Shell fragments in a diamicton at a locality on the northwestern part of Akpatok Island dated at 11 970 ± 70 BP later reoccupied by Ungava Bay ice (Gray et al., 1993), and an "old" date of 11 665 ± 260 BP on foraminiferal assemblages (that comprised or included reworked material) may indicate that Hudson Strait was open in whole or in part ca. 12–11 ka BP. Thick glaciomarine sections e.g. offshore Wakeham Bay and shell dates in the 11–10 ka BP range from raised marine sediments at Deception Bay (though problematic) may be further indications of that opening. Marine (glaciomarine) conditions may have continued in parts of central and western Hudson Strait during the Gold Cove advance, and likely during the subsequent less extensive Noble Inlet advance (Fig. 1; Andrews et al., 1995b).

Multiple-sequence, ice-contact deposits 100 m in thickness southeast of Nottingham Island in the western part of the strait, and 150 m in thickness in eastern Ungava Bay, like those at the sill at the eastern entrance to Hudson Strait and in the basin floors, result from repeated advances and retreats of glacial ice. Each of those deposits contains up to five or more members. The geometry of the sediments southeast of Nottingham Island (MacLean et al., 2001, Fig. 2, 3, 8) indicates that successive events overlapped and appear to have erosionally planed preceding ice-contact sequences (MacLean et al., 2001, Fig. 8). As a result, it is difficult to determine the extent of many of the original deposits and the associated ice advances; however, the apparently more limited extent of the latest sequences suggests that they were the product of more localized, late advances of glacial ice pinned on the islands and shallow platform areas at the western end of the strait. Sediment deposits at the sill at the eastern entrance to Hudson Strait and from adjoining Hatton basin (Andrews et al., 2001, Fig. 4, 5) similarly indicate that the latest glacial ice advances to reach that area were significantly more limited in seaward extent than earlier advances. The morphology of the thick ice-contact deposit in eastern Ungava Bay (MacLean et al., 2001, Fig. 9) indicates the later advances either were not as extensive as preceding ones or the sediments they deposited were erosionally truncated, possibly by later ice flowing north-northeastward in the marginal channel.

Elsewhere in Hudson Strait and Ungava Bay ice-contact sediments mainly range from a few metres or less to a few tens of metres in thickness. Moraines occur in several localities. The largest of these features lie in two locations on opposite sides of the strait: one offshore Héricart Bay in the south-central part of the strait (MacLean et al., 2001, Fig. 12); and the other east of Big Island on the north side of the strait (MacLean et al., 2001, Fig. 13). These features differ significantly from one another in acoustic character and setting. The moraine north of Héricart Bay lies on acoustically stratified sediments that are interpreted to be glaciomarine. The relatively acoustically transparent character of the morainal sediments, preservation of underlying beds, and the regional ice-marginal setting suggest that deposition of this feature may have been by the thin, late ice readvance recorded at other offshore localities in the Héricart Bay area, that began before 8500 BP and lasted until 8000–7800 BP. The moraine east of Big Island comprises two or more ice-contact sequences

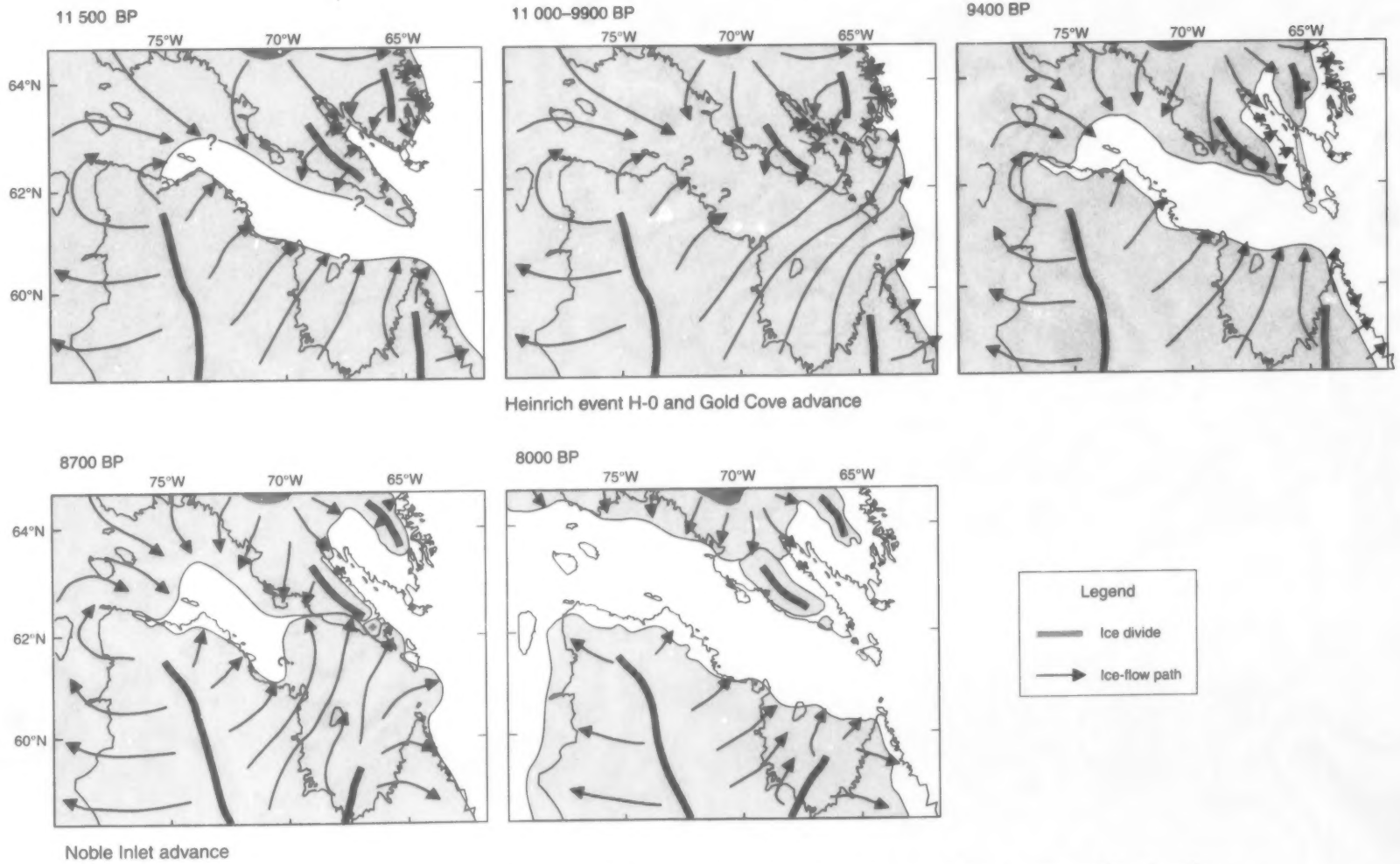

Figure 1. *Pattern and chronology of the final stages of deglaciation in and around Hudson Strait based on terrestrial and marine geological data and* ^{14}C *dates from shells in raised sediments and from shells and foraminifers in sediment cores* (modified from *Andrews et al., 1995b, Fig. 4, Quaternary Science Reviews, v. 14, p. 983–1004, © 1996. Reprinted with permission from Elsevier Science).*

of acoustically massive, dense-appearing sediments. That feature may mark the limit of southward-flowing Baffin Island ice (Manley, 1995), and possibly the boundary between Baffin Island ice and a Hudson Strait ice stream. Smaller morainal features that occur in several other localities indicate ice margin, stillstand, or ice-sheet grounding–lift-off positions. Small moraines on the central platform in Ungava Bay (MacLean et al., 2001, Fig. 14, 67) may mark stillstand positions of the retreating ice margin on the platform.

Glaciomarine sediments extensively overlie ice-contact sediments in Eastern, Western, and Southwestern basins, and in parts of central Hudson Strait and Ungava Bay. They laterally are transitional to ice-contact sediments in many basin margin settings. Glaciomarine ice-proximal and ice-distal deposits are key marine sources for information on depositional environments, the timing of associated late glacial events, and the deglaciation history in Hudson Strait and Ungava Bay.

Postglacial muddy sediments in most areas are thin (<1–2 m) to absent, which reflects a relatively starved sediment environment in most offshore areas since retreat of glacial conditions from the region; however, thick deposits (up to 30 m) occur locally in Western basin, Burgoyne Bay, southern Ungava Bay, and to a more limited extent in Eastern basin. These expanded sections represent venues for studies related to changes in climatic and oceanographic conditions during the last ca. 8000 years. Early postglacial offshore oceanographic influences in eastern Hudson Strait gave way at about 5500 BP to colder, less saline oceanographic conditions of the present day (Vilks et al., 1989); a change also found in the Frobisher Bay area by Osterman (1982) that she attributed to re-establishment of the "Baffin-Labrador Current". Winnowing of sediments by tidal currents has created a sandy and/or gravelly lag a few centimetres thick at the immediate seabed in most nonbasin areas and some probable local exposures of bedrock.

MARINE-TERRESTRIAL RELATIONSHIPS

The terrestrial records of the late glacial history of southern Baffin Island, and of Ungava Peninsula and relevant parts of Labrador peninsula have been discussed by Manley and Miller (2001) and by Gray (2001) respectively, and a brief regional summary is included in MacLean (2001). Three late glacial ice advances have been inferred from terrestrial (Baffin Island) and Southeast Baffin Island Shelf data to have crossed eastern Hudson Strait from Quebec–Labrador ice centres and to have variably overridden parts of southeastern Baffin Island and adjacent inner parts of the continental shelf between 11–10 ka BP (H-0 event), 9.9–9.6 ka BP (Gold Cove advance), and 8.9–8.4 ka BP (Noble Inlet advance). Glacial ice from Cumberland Sound or other northern sources was a component of the H-0 event (Andrews et al., 1995a, 1998; Jennings et al., 1996; Andrews, 1998). As indicated later in this paper and elsewhere in this bulletin there has been debate in the literature concerning the origin of the Gold Cove and Noble Inlet events. Some concerns and diverse views regarding the Noble Inlet event exist among the authors of this bulletin.

The correlations and setting proposed below were derived from the geological record in conjunction with glaciological modelling information concerning ice-sheet thickness and behaviour from studies by Pfeffer et al. (1997) and Pfeffer (2001). The marine record in Eastern basin of Hudson Strait provides evidence regarding environments, stratigraphic relations, facies changes, ice-sheet grounding line (lift-off)–water depth relationships, and chronologies that primarily relate to the period of time during and following the Noble Inlet event.

Glaciomarine sediments that overlie ice-contact sediments in the floor and on the lower northern and northwestern flanks of Eastern basin are laterally transitional to ice-contact sediments at former ice-sheet grounding (lift-off) positions upslope on the basin flanks. Presence of these transitions on six survey tracks that transect the northern and northwestern flanks of the basin over a distance of 110 km and recognized in similar depths on southern margin transects indicate they were basin-wide events. Glaciomarine sediments are absent above the upper grounding line on the flanks of Eastern basin except for a few small, local occurrences on the northern periphery of the basin and a slight upslope extension in the west and northwest (MacLean et al., 2001, Fig. 1).

Two main stages of successive upslope glaciomarine to ice-contact transition have been recognized on the northern flank of Eastern basin. The lower transition occurs at present-day water depths between about 442 m and 422 m, and the upper one between depths of approximately 404 m and 345 m. There are also indications locally of transitions at slightly greater depths. Thickening of the ice-contact deposits adjacent to the transition areas (e.g. MacLean et al., 2001, Fig. 34) suggests these mark brief stillstand–lift-off positions as the ice sheet, which originally was grounded in the bottom of the basin, thinned, and waned. On the more gently sloping northwest flank of the basin a succession of lift-off features between present depths of 454 m and 347 m similarly indicate progressive upslope migration of the ice-sheet grounding line. The 404–345 m depths associated with the upper grounding line closely approximate (or are just slightly shallower than) the 400–385 m depths at the sill at the eastern entrance to Hudson Strait. This, and the general absence of glaciomarine sediments above the upper grounding line on the northern flank of Eastern basin suggest that when the upper grounding line was reached, the ice sheet ceased to be grounded at the sill, at which time the ice became unstable and rapid evacuation of the ice sheet from most areas of Eastern basin soon followed. Glacial ice, however, did remain in Ungava Bay for some time after the ice emptied from Eastern basin.

Radiocarbon (AMS) dates of 8470 ± 60 BP, 8590 ± 85 BP, and 8625 ± 75 BP were obtained from three cores (cores 93034-031, 90023-042, and 90023-052, respectively) (MacLean et al., 2001, Table 2) collected in stratigraphically and acoustically relatively similar glaciomarine sequences on and adjoining the lower northern flank of Eastern basin. The

relative similarity of the dates, stratigraphic sections, and settings (e.g. MacLean et al., 2001, Fig. 31, 35, 36, 37, 38, 39) indicate that the information these dates provide regarding the age of these sediments is reliable. The dated sediments upslope are transitional to ice-contact sediments at the upper grounding line. A comparable AMS radiocarbon date of 8575 ± 90 BP (core 93034-006) (MacLean et al., 2001, Table 2) obtained on paired valves of *Portlandia arctica* from glaciomarine sediments that locally occur in a small valley between cuesta ridges 20 km south of Meta Incognita Peninsula (MacLean et al., 2001, Fig. 40) strongly supports the age information from the other cores. The dates and settings document the late stages of a progressively thinning ice sheet that occupied Eastern basin until ca. 8500–8400 BP, or shortly thereafter. That time closely coincides with the end of the Noble Inlet glacial event on Meta Incognita Peninsula at ca. 8400 BP. This is further supported by foraminiferal assemblages and a radiocarbon date on paired valves of a *Portlandia arctica* specimen in core 90023-045 (MacLean et al., 2001, Table 2) in the floor of Eastern basin, which indicate that glaciomarine ice-proximal conditions had given way to ice-distal conditions in that area by ca. 8350 BP (Jennings et al., 2001).

There is a similarity in the general pattern of ice-sheet behavior in Eastern basin to that interpreted for the Noble Inlet advance on southeastern Meta Incognita Peninsula by e.g. Stravers (1986), Miller et al. (1988), Miller and Kaufman (1990), Stravers et al. (1992), Manley (1995), and Manley and Miller (2001). Sediments of the large delta at York Sound on Frobisher Bay were derived from erosion of deep gorges (York gorges) across Meta Incognita Peninsula by drainage from ice-dammed lakes at 365 m elevation on the Hudson Strait side of the drainage divide (Mercer, 1956; Blake, 1966). Six radiocarbon dates between 8970 ± 190 BP and 8620 ± 175 BP indicate that sediment deposition at the York delta (*see* Muller, 1980; Manley, 1995; Manley and Miller, 2001) primarily occurred during the early part of the time period ascribed to the Noble Inlet advance. This suggests ice thicknesses required to hold up the glacial lakes south of the Meta Incognita Peninsula drainage divide were greatest during that period i.e. during the early part of the advance; but decreased below the 365 m threshold level of the York gorges after about 8620 BP, as a calving margin at the eastern end of the strait began to draw down the central mass of the ice (Manley, 1995). Residual ice on southeastern Meta Incognita Peninsula lasted until ca. 8400 BP.

The timing and manner of ice-sheet thinning displayed on eastern Meta Incognita Peninsula is in accord with the pattern and chronology of ice-sheet behavior recorded in Eastern basin. This, and the various factors cited earlier all strongly suggest that the glacial ice sheet that occupied Eastern basin between ca. 8900 BP and 8500–8400 BP was the same ice sheet that formed the Noble Inlet advance on Meta Incognita Peninsula. Dates from Eastern basin indicate that the evacuation of ice from Eastern basin approximately coincided with (slightly preceded) the demise of Noble Inlet ice on Meta Incognita Peninsula.

The source of the ice that dammed the glacial lakes feeding the York gorges and of the Noble Inlet event, i.e. an advance of ice from Quebec–Labrador, versus an advance of local Meta Incognita Peninsula ice, have been discussed (Stravers, 1986; Miller et al., 1988; Stravers et al., 1992; Manley, 1995; Manley and Miller, 2001) and debated (England and Smith, 1993; Kaufman et al., 1993b). At the time those debates took place an ice sheet of sufficient magnitude to be fully grounded throughout Eastern basin had not been recognized from the then existing marine data, and a floating ice shelf was visualized — a different situation from that proposed in this report, in ice-volume requirements, ice-sheet stability, and substantially greater thickness, which is especially relevant given the elevations required to dam the glacial lakes on Meta Incognita Peninsula.

Whether or not Gold Cove ice completely withdrew from Eastern basin prior to the Noble Inlet advance is not established, but as noted by Jennings et al. (1998) and Pfeffer (2001), dates of 9340 ± 395 BP and 9010 ± 95 BP from Pritzler Harbour (*see* Manley, 1995), ca. 9100 ± 480 BP on shells from core 77021-154 in the floor of Eastern basin (Fillon and Harmes, 1982), and ca. 9000 BP on reworked single molluscs in cores 93034-002 and 93034-004 on the northern flank of Eastern basin, suggest at least partial glacial ice withdrawal from eastern Hudson Strait in the time between Gold Cove and Noble Inlet events; however, it is likely that glacial ice continued to occupy at least the central platform area in Ungava Bay between these events, as it apparently did for a few hundred years following the departure of Noble Inlet ice from most other areas bordering Eastern basin.

Glacial ice of the Noble Inlet advance (and presumably similarly Gold Cove ice) overrode, eroded, and remolded some of the previously deposited sequences in Eastern basin (but sequences deep beneath the basin floor escaped reworking by the later, thinner ice sheets). Dates ranging between 9505 ± 75 BP and 10 620 ± 60 BP mainly on benthonic foraminifers, or foraminifers and shell fragments, from ice-proximal sediments, and one of 11 665 ± 260 BP in postglacial sediments, in five cores (90023-045, 93034-002, 93034-004, 93034-029, 93034-031) from Eastern basin (MacLean et al., 2001, Table 2) are interpreted to result from incorporation of material reworked from earlier deposits and are not chronologically or biostratigraphically correct; however, these and older dates from other offshore and terrestrial localities referred to earlier, which in many instances predate the late Wisconsinan, indicate the prior existence of marine conditions in Hudson Strait.

WHAT WAS THE SOURCE OF THE ICE THAT OCCUPIED EASTERN BASIN DURING THE NOBLE INLET EVENT?

There is good evidence that glacial ice was present in Eastern basin of Hudson Strait at the time of the Noble Inlet glacial ice advance recognized on Meta Incognita Peninsula. What was the source of this ice? The geographic setting suggests it must

have come from one of three sources, or some combination of these: Baffin Island, a Hudson Strait ice stream, or a pulse of Quebec–Labrador ice centred south of Ungava Bay.

With regard to a potential southern Baffin Island source, several factors appear to rule this out as a major source area for Eastern basin ice at the time of the Noble Inlet event. The terrestrial record and ice-flow patterns on eastern Meta Incognita Peninsula (*see* e.g. Blake, 1966; Stravers, 1986; Stravers et al., 1992; Manley, 1995; Manley and Miller, 2001) are not indicative of such a major ice flow from Baffin Island into Hudson Strait. Although there is evidence on Meta Incognita Peninsula of southerly ice flow towards Hudson Strait, that primarily occurred in the region west of Barrier Inlet (Manley, 1995). Ice-flow indicators from the easternmost part of the peninsula (*see* references above) and the geometry of morainal bank deposits in Savage basin (Stravers and Powell, 1997) show that ice flow in that region was to the northeast. It also does not seem probable that Meta Incognita Peninsula could have produced the large ice volumes required to completely fill Eastern basin with grounded ice during the Noble Inlet event, nor to overcome the large ice losses due to calving that would occur until the ice became stabilized at the sill and within the basin (*see* Pfeffer et al. (1997) and Pfeffer (2001) regarding ice losses in this manner associated with ice flow across Hudson Strait).

A Hudson Strait ice stream of sufficient thickness and magnitude to ground in the more than 900 m deep Eastern basin (and to reach elevations of 365 m on eastern Meta Incognita Peninsula) would have affected ice-free areas of Baffin Island and Ungava Peninsula bordering the strait, including its western reaches, to elevations of several hundred metres. What does the available evidence indicate? Hudson Bay, which was covered by glacial ice at 8400 BP, was deglaciated by ca. 8000 BP (Dyke and Prest, 1987; Josenhans and Zevenhuizen, 1990). Deglaciation of Nottingham, Salisbury, and Mill islands and the adjacent area of northern Ungava Peninsula at the western end of the strait did not occur before 8100 BP (Laymon, 1988), and residual ice remained on Nottingham Island until ca. 7200 BP (Laymon, 1991). This agrees with the marine data that suggest the presence of glacial ice in the offshore adjacent to Nottingham Island until ca. 7500 BP or later (MacLean et al. 2001). The southern coast of Foxe Peninsula was not deglaciated before 7700 BP (Laymon, 1988); however, to the east, deglaciation of the Deception Bay–Cape de Nouvelle-France region of Ungava Peninsula occurred earlier. Shell horizons at localities in Deception River valley yielded a wide range of dates from which Gray et al. (1993) concluded that marine conditions existed in that region by at least 9 ka BP and possibly as early as 10.7 ka BP, though uncertainties surround the earlier date. As noted by Gray (2001) early opening may have been followed by a period of closure until ca. 9.4 ka BP, i.e. during the time of the Gold Cove advance. The ice front withdrew to a position 15 km inland from the coast, and extended offshore to the west between Deception Bay and Salluit (Bruneau et al., 1990). Shells from near the top of glaciomarine sediment deposits onshore in the area between the former inland ice-front position and the coast yielded reservoir-corrected radiocarbon ages of 9.3 ka BP, 8.8 ka BP, and 8.7 ka BP (Gray et al., 1992). Evidence from a locality 11 km southwest of Cape de Nouvelle-France indicates that ice impinged on the coast shortly before 8.6 ka BP (site elevation 100 m) (Gray et al., 1992), and extrapolations based on emergence-curve data for Charles Island suggested the presence of an ice sheet in that area until 8 ka BP (Gray et al., 1993); however, the last ice flow recorded on northern Charles Island was to the north-northeast, which Gray (2001) suggested probably was a brief ice surge from the nearby Ungava Peninsula. Earlier ice flow was west-east. Ages ranging between 8.8 ka BP and 8.4 ka BP on shells from terrestrial localities in the Cape de Nouvelle-France to Wales Island region (Gray et al., 1993; Gray, 2001) indicate that that area of Hudson Strait was not occupied by glacial ice during the time of the Noble Inlet advance (Fig. 1).

Definitive chronological data from marine cores in glaciomarine sediments in Western and Southwestern basins are very limited due to meagre molluscan and foraminiferal populations and the presence of reworked material; however, the results suggest that glaciomarine conditions persisted in Western and Southwestern basin areas until at least ca. 7700 BP.

Farther east, in the isolated occurrence of glaciomarine sediments southwest of Big Island (MacLean et al., 2001, Fig. 1, 4, 49), two dates from core 93034-018 (MacLean et al., 2001, Table 2): 8540 ± 80 BP on foraminifers and ostracodes in glaciomarine ice-distal sediments; and 8675 ± 65 BP on shell fragments from near the base of postglacial sediments are not in correct stratigraphic order. The upper (8675 BP) date must include reworked material. That, and the presence of much older material deeper in the section suggest that the 8540 BP date should be regarded with some caution. Though similar to the dates from Eastern basin, it is important to note that the depositional environment in the 8540 BP interval here was ice distal. This locality is situated near the 8.5 ka BP ice-margin position for Baffin Island ice inferred by Stravers (1986). The locality would lie in the path of a Hudson Strait ice stream.

In the Héricart Bay and Wakeham Bay offshore regions on the south side of the strait, approximately opposite Big Island (MacLean, 2001, Fig. 1, 4, 5), thick sequences of acoustically stratified sediments occur at the various core localities (MacLean et al., 1992; MacLean et al., 2001, Fig. 4, 45, 46, 47, 48). Thicknesses beneath dated intervals considered to be reliable amount to 13.6 m below the 8350 BP interval in core 90023-107 (11 m below the 8950 BP interval); 15.5 m below the 8380 BP interval in core 90023-066; 13.5 m below the 8465 BP interval in core 93034-013; and 17 m below the 8480 BP interval in core 90023-071. If sedimentation rates in the underlying sequences were similar to those within the dated parts of cores 90023-066 and 93034-013, deposition of glaciomarine sediments possibly commenced at those localities by about 10 000–9800 BP (i.e. following the H-0 event). The dates and thickness of the sections suggest that glacial ice did not extend across the core 90023-066, 90023-107, and 93034-013 localities at the time of the Noble Inlet advance. The downcore extrapolations suggest that ice of the Gold Cove advance also may not have overridden these

localities in the Héricart Bay area. If it did so, it appears not to have extended as far west as the core 90023-071 locality off Wakeham Bay (MacLean, 2001, Fig. 5; MacLean et al., 2001, Fig. 48) where glaciomarine deposition possibly began as early as ca. 11 000–10 000 BP on the basis of the section thickness. It is highly unlikely that these areas could have remained ice-free if a major ice stream flowed down Hudson Strait at the time of the Noble Inlet event. There was a subsequent small glacial readvance in the Héricart Bay area that began before 8500 BP and lasted until 8000–7800 BP. This possibly was coincident with the brief late northeastward–north-northeastward ice surge of limited extent noted by Gray (2001) farther west on Ungava Peninsula and on Charles Island.

The inferences drawn from the data in western and central regions of Hudson Strait are that, while glacial ice existed in parts of Hudson Strait at the time of the Noble Inlet advance, no major down-the-strait flow of Hudson Strait ice occurred that was of sufficient thickness or magnitude to have generated the events associated with that time period in Eastern basin or on eastern Meta Incognita Peninsula.

Ungava Bay and the surrounding Quebec–Labrador region was considered by Stravers (1986), Miller et al. (1988), Stravers et al. (1992), Kaufman et al. (1993b), Manley (1995), and Manley and Miller (2001) to have been the source area for the Noble Inlet and Gold Cove advances on the basis of ice-flow directions, provenance of erratics, and sediment deposits on Meta Incognita Peninsula. It was also considered to be a source area for the H-0 advance (Miller and Kaufman, 1990; Andrews et al., 1994, 1995a, b).

The terrestrial record in the region surrounding Ungava Bay shows a pattern of convergent ice flow into Ungava Bay from the south and west, and impingement on the northern tip of Labrador by ice flowing to the northeast or east-northeast out of the bay (Gray and Lauriol, 1985; Lauriol and Gray, 1987; Allard et al., 1989; Gray et al., 1993, 1996; Gray, 2001).

Akpatok Island shows a complex glacial record comprising a local ice cap and impingement of continental ice from various sources (Gray et al., 1994; Giugni et al., 1996). Gray et al. (1994) inferred that ice caps developed during early and late Wisconsinan glaciations and that they existed prior to the invasion(s) by foreign ice. The local ice cap occupied the northeastern part of the island and possibly extended onto the adjacent part of the platform that occupies the central part of Ungava Bay. Ice from southwestern Ungava Bay flowed eastward across the southern part of the island and then swung northeastward along the east side of the island as part of the northward surge of ice out of Ungava Bay (Gray et al., 1994, Fig. 1; Gray, 2001, Fig. 6, 11). Ridges of ice-contact sediment and associated north-south trending ice-keel scours on the central platform east-southeast of Akpatok Island may relate to the northward ice surge. Ice flowing eastward from the western side of Ungava Bay impinged on the western and northwestern parts of Akpatok Island (Gray, 2001, Fig. 6), overtopped the local ice cap, and abutted the ice flowing northeastward along the east coast of the island (Gray et al., 1994). There is no evidence of overriding of central and western areas of the island by northward-moving late glacial ice (Gray et al., 1994; Giugni et al., 1996; Gray, 2001). Radial flow patterns relate to final retreat of the local ice cap.

The northern margins of Akpatok Island became free of glacial ice between 8200 BP and 7600 BP (Gray et al., 1994), and deglaciation of the southern coast of Ungava Bay occurred ca. 7300–7000 BP. Glacial ice remained nearby onshore until 6.5 ka BP and later (Gray and Lauriol, 1985; Lauriol and Gray, 1987; Allard et al., 1989).

These deglaciation dates are compatible with the change from ice-proximal to ice-distal conditions in Eastern basin following evacuation of Noble Inlet ice from the basin ca. 8500–8400 BP, and the subsequent change to postglacial marine conditions ca. 8000–7800 BP

Modelling studies by Pfeffer et al. (1997) and Pfeffer (2001) indicate the glaciological plausibility of glacial ice centred through Ungava Bay successfully advancing across eastern Hudson Strait from a Quebec–Labrador source area onto southeastern Baffin Island. Ice accumulation in the modelling simulation reached a maximum thickness of 2200 m centred south of Ungava Bay. The modelling studies indicate that the quantity of ice available from such a Quebec–Labrador dome and ice dynamics could accommodate an ice sheet of the thickness required for it to be fully grounded on the floor of Eastern basin, and with surface elevations of sufficient height to have dammed the glacial lakes draining into the York gorges at the time of the Noble Inlet advance. Sufficient upstream flux would be available to overcome drawdown due to calving as the ice initially crossed Eastern basin. Stability would be reached when the ice terminus reached shallower waters adjacent to Meta Incognita Peninsula, Resolution Island, at the western margin of Eastern basin, and at the sill at the entrance to the strait. Generally similar behavior and constraints would have pertained to all the late glacial ice advances across the strait despite variations in their northward and regional extent.

The origin of parallel-subparallel ice-keel scour marks that trend east-southeast, approximately parallel to the axis of Hudson Strait in several shallow-water localities (≥ 100 m) adjacent to eastern Meta Incognita Peninsula, where terrestrial ice-flow directions are to the northeast and north-northeast, is uncertain. Although the consistent and parallel alignment of these features is unlike the more random scours and pits often associated with individual iceberg groundings (some examples of which also occur in this area), their orientation parallels the principal current flow direction in that region. Though other origins cannot be ruled out, these features possibly originated from either large floating ice masses exiting the strait during evacuation of Noble Inlet ice from eastern Hudson Strait or the eastward passage of large floating ice masses during breakup of ice in western Hudson Strait and Hudson Bay as envisaged by Stravers et al. (1992) and Kaufman et al. (1993b), or a late (but relatively thin) Hudson Strait ice stream as suggested by England and Smith (1993).

As pointed out by Gray (2001) there are some concerns and potential difficulties with a source for the Noble Inlet advance centred through Ungava Bay. Among these is the

lack of evidence of northward ice flow on Akpatok Island except for erratics emplaced during earlier glacial events. From this, Gray (2001) inferred that if ice surges out of Ungava Bay occurred at the time of the Noble Inlet event they must have passed to the east of Akpatok Island. The spatial relationships with Akpatok Island situated as it is on the western edge of the platform towards the western side of the bay, together with the evidence of diversion of ice easterly across the southern part of the island, then flowing northward along the east side buttressed by ice on the island seem to be compatible with and provide support for that contention. This suggests that a large ice mass occupied most of Akpatok Island and that passage west of the island was blocked to northward-flowing ice; however, glaciological modelling studies (Pfeffer, 2001) indicate an ice thickness requirement of about 800 m at Akpatok Island for an ice advance across Hudson Strait from Ungava Bay conformable with the late glacial records relating to the Noble Inlet event interpreted from eastern Meta Incognita Peninsula and from Eastern basin. That is some 400 m in excess of the 400 m relief of the island above the adjacent platform. To have a compatible fit, either the ice cap and overlying western-sourced ice on the island would have had to be overridden during the peak of the advance by northward-flowing ice, leaving no footprint on the island, or the combined thickness of ice cap and western-sourced ice on the island was such that no overriding by northerly flowing ice occurred, and virtually all of the ice flow out of Ungava Bay would have passed to the east of Akpatok Island. There would also be some drawdown into the marginal channel east of the platform that would have funnelled ice to the north-northeast at least during early stages of the advance. The Ungava Bay morphology (MacLean, 2001, Fig. 1) suggests that ice from southern and southwestern Ungava Bay passing through the marginal channel south and east of the platform would be flowing in the general direction of Resolution Island. This may account for the presence of iron-formation erratics on Resolution and Edgell islands and on the northern tip of Labrador peninsula, and their absence on Meta Incognita Peninsula, noted by Gray (2001).

The possibility of reduced salinities in western Hudson Strait as a result of meltwater input while eastern Hudson Strait was blocked by the postulated across-the-strait late ice advances was noted by Stravers (1986). Our marine studies have not provided direct evidence as to whether or not this occurred. Dates within the 8.8–8.4 ka BP time period from *Portlandia arctica* valves from the Cape de Nouvelle-France and De Martigny Promontory regions (Gray et al., 1993; Gray, 2001) indicate the existence of molluscs in western Hudson Strait during the time of the Noble Inlet advance: a concern regarding the interpretation of a Quebec–Labrador source for that glacial event that has not been resolved (Lauriol and Gray, 1997; Gray, 2001). Possibly the continued presence of these fauna could be accounted for by a) the relatively short duration of Noble Inlet blockage; b) the lag time required for significant changes in salinity to develop in the large area in Hudson Strait west of the ice advance; and c) continued existence of marine waters beneath meltwater layers, which, if present, may have provided a favourable environment for the survival of marine benthonic fauna (A. Aitken, pers. comm., 1998). With regard to c), however, Gray (2001) noted that several of the mollusc samples obtained were from localities where water depths would have been relatively shallow (within 50 m of the marine limit), and he considered this to be indicative of continuing marine circulation.

The available regional marine and terrestrial data summarized in the foregoing discussion suggests readvance of glacial ice from Quebec–Labrador sources centred through Ungava Bay as the most probable of the three potential source areas for the late glacial events recorded in Eastern basin and on southeastern Baffin Island at the time of the Noble Inlet advance; however, as noted in the foregoing papers and discussion there are some unresolved problems and concerns, and some diverse opinions exist among the authors of this report concerning this interpretation.

DOWNSTREAM ICE AND SEDIMENT DISPERSAL

Effects of major Hudson Strait glacial ice and meltwater discharge events are considered to be widespread in the form of at least some of the Heinrich events and associated changes in paleoceanographic conditions recorded in Labrador Sea and North Atlantic Ocean sediments. Seaward extent of the ice exiting the strait was variable and changes in water current patterns also have played a role in the destination of ice-transported sediments.

Heinrich events H-0, H-1, H-2, and possibly H-3 are recorded in cores 75009IV-055 and 75009IV-056 in the Labrador Sea seaward of the entrance to Hudson Strait (Andrews and Tedesco, 1992; Andrews et al., 1994; Kirby, 1996), but the subsequent Gold Cove and Noble Inlet events are not (Andrews and Tedesco, 1992; Andrews et al., 1995a; Andrews et al., 2001). In examining potential sediment sources, Andrews et al. (1993, 1998), Jennings et al. (1996), and Andrews (1998) noted that no evidence of sediment derived from erosion of Tertiary strata underlying the shelf by ice crossing the shelf during H-1 and H-2 events is present in cores 75009IV-055 and 75009IV-056, and questioned the seaward extent of grounded ice streams on the shelf at the time of those events. Jennings et al. (1996) deduced that either those ice streams did not extend farther seaward than the sill at the entrance to Hudson Strait or inner part of the shelf, or that deposits of ice-contact sediments emplaced by earlier advances to the outer shelf protected the underlying bedrock from erosion during later advances. We favour the latter interpretation on the basis of sediment units and relationships in Hatton basin and on the outer part of the shelf (Andrews et al., 2001, Fig. 4, 5). Excavation of the bedrock depression in which Hatton basin lies probably was by early glacial erosion. We would expect that evidence of Tertiary material removed from the shelf by the initial Hudson Strait ice streams lies deeper in the Labrador Sea section.

Thick deposits of ice-contact sediments on the outer part of the shelf seaward from Hudson Strait and in the subsurface of Hatton and Eastern basins attest to the magnitude and

extent of some of the glacial ice streams that have come out of Hudson Strait. Evidence of sediment transport to the outer shelf and deep sea is provided by Seamark™ 1 sidescan imagery, which indicates a large dispersal channel on the continental slope seaward from Hudson Strait. Subparallel east-west-trending ice-keel scours on the outer shelf terminate abruptly at the head of the dispersal channel at the shelf break (B. MacLean, unpub. report, 1994).

Advances of glacial ice to the outer part of the shelf and shelf break are considered to have been associated with major streams of Laurentide ice transiting Hudson Strait, whereas late south-to-north advances across eastern Hudson Strait were less far-reaching in a seaward (eastward) direction, extending only to the sill at the entrance to the strait and innermost part of the shelf.

The uppermost sequences in the multiple sequence ice-contact deposits at the sill at the entrance to the strait are of limited extent compared to those that occur lower in the sections there and in Hatton basin. Glaciomarine sediments at the west side of Hatton basin adjoining the sill at the entrance to Hudson Strait in present depths shallower than 610 m were deformed by glacial ice that deposited till at the sill (Josenhans et al., 1986; Josenhans *in* Piper et al., 1990). Facies and stratigraphic relationships are not sharply defined on the Huntec™ high-resolution profile; however, the data suggest that the till may grade laterally into the sediments that form the upper part of the Hatton basin glaciomarine sequence (H.W. Josenhans, pers. comm., 1996) where dates in the 8990–8335 BP range in cores 92028-158 (900–905 cm interval) and 84035-014 (82 cm interval) (Manley and Jennings, 1996) conform relatively well with the time span of the Noble Inlet advance. The lowermost dated interval (9 m) (9620 ± 95 BP) in core 92028-158 (Jennings *in* Manley and Jennings, 1996) is underlain by 11 m of acoustically stratified glaciomarine sediments. This is further indication that grounded glacial ice of the Noble Inlet, Gold Cove, and probably H-0 events did not extend far seaward of Hudson Strait. Older dates of 13 000 ± 220 BP from core 77021-150 on the outer part of the shelf, and 11 275 ± 125 BP from Hatton basin (Evans, 1990; Kaufman and Williams, 1992) indicate deglaciation of the outer shelf and Hatton basin occurred by 13–12 ka BP (Andrews et al., 2001).

Hillaire-Marcel et al. (1994) proposed that distribution of glacially derived sediments in the Labrador Sea and North Atlantic Ocean was by two main mechanisms: ice rafting and turbidity currents. They postulated that the latter mechanism was responsible for long-distance, North Atlantic Ocean transport of sediments from the edge of the shelf and slope derived from surging of Hudson Strait ice. Hillaire-Marcel et al. (1994) also inferred from sedimentological and isotopic data that the circulation gyre as it now exists in the Labrador Sea, characterized by southward water flow along the southeast Baffin Island and Labrador margins was interrupted during glacial and interstadial intervals.

Carbonate-rich glaciomarine sediments that overlie predominantly Labrador-derived till on the Labrador shelf were considered by Josenhans et al. (1986) and Kaufman et al. (1993a) to have originated with late glacial, and Gold Cove ice from Hudson Strait–Ungava Bay. Andrews et al. (1995a) suggested similar southward transport by the Labrador Current of icebergs from the H-0 ice margin on the inner shelf off Hudson Strait. That event was multisourced from Hudson Strait and Cumberland Sound (Andrews et al., 1995a, 1998; Kirby, 1996; Andrews, 1998). The transport of iceberg flux from the Gold Cove and Noble Inlet events southward along the shelf by the Labrador Current rather than eastward into the deep sea appears to account for the absence of sediments associated with those events in Labrador Sea cores seaward from Hudson Strait, and similarly absence of H-0 sediments from some of those cores.

HUDSON STRAIT AND UNGAVA BAY: A NATURAL LABORATORY FOR FUTURE STUDIES

Hudson Strait and Ungava Bay constitute an extensive natural laboratory for further study of a wide variety of Quaternary sedimentary and environmental parameters and settings. These include: paleosedimentary and paleoceanographic conditions and interactions in numerous former ice-margin settings; further delineation of the glacial history of the region; relationships between Laurentide ice and Heinrich and paleoceanographic-climate events; the record of global change from expanded sediment sections postdating 8 ka BP that are present in several localities; parameters such as debris-flow mechanisms and their effects in Eastern basin; and development and testing of glaciological-geological models. As pointed out by Andrews and Tedesco (1992), ice surges that have occurred in this region may represent analogues for behaviour of Antarctic ice in the future in response to global warming and rising sea levels.

ACKNOWLEDGMENTS

The authors of this paper gratefully acknowledge helpful discussion with H. Josenhans, G.H. Miller, and others during the course of this study. Special thanks are also extended to D.A. Hodgson, H. Josenhans, and J. Shaw for review of this paper and for their helpful comments.

REFERENCES

Allard, M., Fournier, A., Gahe, E., and Seguin, M.K.
1989: Le Quaternaire de la côte sud-est de la Baie d'Ungava, Québec nordique; Géographie physique et Quateraire, vol. 43, p. 325–336.

Andrews, J.T.
1989: Quaternary geology of the northeastern Canadian Shield; *in* Chapter 3 of Quaternary Geology of Canada and Greenland, (ed.) R.J. Fulton; Geological Survey of Canada, Geology of Canada, no. 1, p. 276–317 (*also* Geological Society of America, The Geology of North America, v. K-1).
1998: Abrupt changes (Heinrich events) in late Quaternary North Atlantic marine environments: a history and review of data and concepts; Journal of Quaternary Science, v. 13, p. 3–16.

Andrews, J.T. and Tedesco, K.
1992: Detrital carbonate-rich sediments, northwestern Labrador Sea: implications for ice-sheet dynamics and iceberg rafting (Heinrich) events in the North Atlantic; Geology, v. 20, p. 1087–1090.

Andrews, J.T., Bond, G., Jennings, A.E., Kerwin, M., Kirby, M., MacLean, B., Manley, W., and Miller, G.H.
1995a: A Heinrich-like event, H-0 (DC-0): source(s) for detrital carbonate in the North Atlantic during the Younger Dryas chronozone; Paleoceanography, v. 10, no. 5, p. 943–952.

Andrews, J.T., Jennings, A.E., and MacLean, B.
2001: Late Quaternary stratigraphy of Hatton and Resolution basins east of Hudson Strait; *in* Marine Geology of Hudson Strait and Ungava Bay, Eastern Arctic Canada: Late Quaternary Sediments, Depositional Environments, and Late Glacial–Deglacial History Derived from Marine and Terrestrial Studies, (ed.) B. MacLean; Geological Survey of Canada, Bulletin 566.

Andrews, J.T., Kirby, M., Jennings, A.E., and Barber, D.C.
1998: Late Quaternary stratigraphy, chronology, and depositional processes on the slope of S.E. Baffin Island, detrital carbonate and Heinrich events: implications for onshore glacial history; Géographie physique et Quaternaire, v. 52, no. 1, p. 91–105.

Andrews, J.T., MacLean, B., Kerwin, M., Manley, W., Jennings, A.E., and Hall, F.
1995b: Final stages in the collapse of the Laurentide Ice Sheet, Hudson Strait, Canada, NWT: ^{14}C AMS dates, seismic stratigraphy, and magnetic susceptibility logs; Quaternary Science Reviews, v. 14, p. 983–1004.

Andrews, J.T., Tedesco, K., Briggs, W.M., and Evans, L.W.
1994: Sediments, sedimentation rates, and environments, southeast Baffin Shelf and northwest Labrador Sea, 8-26 ka; Canadian Journal of Earth Sciences, v. 31, p. 90–103.

Andrews, J.T., Tedesco, K., and Jennings, A.E.
1993: Heinrich events: chronology and processes, east-central Laurentide Ice Sheet and NW Labrador Sea; *in* Ice in the Climate System, (ed.) W.R. Peltier; Springer-Verlag, Berlin-Heidelberg, p. 167–186.

Blake, W., Jr.
1966: End moraines and deglaciation chronology in northern Canada with special reference to southern Baffin Island; Geological Survey of Canada, Paper 66-26, 31 p.

Bond, G., Heinrich, H., Broeker, W.S., Labeyrie, L., McManus, J., Andrews, J.T., Huon, S., Jantschit, R., Clasen, S., Simet, C., Tedesco, K., Klas, M., Bonani, G., and Ivy, S.
1992: Evidence for massive discharges of icebergs into the glacial Northern Atlantic; Nature, v. 360, Springer-Verlag, Berlin-Heidelberg, p. 245–249.

Boulton, G.S., Smith, G.D., Jones, A.S., and Newsome, J.
1985: Glacial geology and glaciology of the last mid-latitude ice sheets; Journal Geological Society of London, v. 142, p. 447–474.

Broecker, W.S., Bond, G., McManus, J., Klas, M., and Clark, E.
1992: Origin of the North Atlantic's Heinrich events; Climate Dynamics, v. 6, p. 265–273.

Bruneau, D. and Gray, J.T.
1991: Géologie des formations en surface, région de Salluit et du cap de Nouvelle-France, Québec; Commission géologique du Canada, carte 11-1990, échelle de 1/250 000.

Bruneau, D., Gray, J.T., and Lauriol, B.
1990: Glacial flow patterns and chronology of ice retreat in the Charles Island-Cap de Nouvelle-France sector of Hudson Strait; *in* 19th Arctic Workshop, Institute of Arctic and Alpine Research, University of Colorado, Boulder, Colorado, March 8–10, 1990, Program and Abstracts, p. 15–17.

Dyke, A.S. and Prest, V.K.
1987: Late Wisconsinan and Holocene history of the Laurentide Ice Sheet; Géographie physique et Quaternaire, v. XLI, no. 2, p. 237–263.

England, J. and Smith, I.R.
1993: Late glacial ice margins and deglacial chronology for southeastern Baffin Island and Hudson Strait, eastern Canadian Arctic: discussion; Canadian Journal of Earth Sciences, v. 30, p. 1749–1752.

Evans, L.W.
1990: Late Quaternary stratigraphy of the Hatton and Resolution Basins, Southeast Baffin Island Shelf, N.W.T., Canada; M.Sc. thesis, University of Colorado, Boulder, Colorado, 188 p.

Fillon, R.H. and Harmes, R.A.
1982: Northern Labrador Shelf glacial chronology and depositional environments; Canadian Journal of Earth Sciences, v. 19, p. 162–192.

Fisher, D.A., Reeh, N., and Langley, K.
1985: Objective reconstruction of the late Wisconsinan Laurentide Ice Sheet and the significance of deformable beds; Géographie Physique et Quaternaire, v. 39, p. 229–238.

Giugni, L., Thibault, E., and Gray, J.T.
1996: Erratic deposits as a tool for interpretation of ice flow patterns affecting Akpatok Island, Ungava Bay, N.W.T.; *in* 26th Arctic Workshop, Institute of Arctic and Alpine Research, University of Colorado, Boulder, Colorado, March 14–16, 1996, Program with Abstracts, p. 36–37.

Gray, J.T.
2001: Patterns of ice flow and deglaciation chronology for southern coastal margins of Hudson Strait and Ungava Bay; *in* Marine Geology of Hudson Strait and Ungava Bay, Eastern Arctic Canada: Late Quaternary Sediments, Depositional Environments, and Late Glacial–Deglacial History Derived from Marine and Terrestrial Studies, (ed.) B. MacLean; Geological Survey of Canada, Bulletin 566.

Gray, J.T. and Lauriol, B.
1985: Dynamics of the late Wisconsin ice sheet in the Ungava Peninsula, interpreted from geomorphical evidence; Arctic and Alpine Research, v. 17, p. 279–310.

Gray, J.T., Bruneau, D., MacLean, B., and Lauriol, B.
1992: Glacial flow patterns and chronology of ice retreat in western Hudson Strait: a terrestrial and marine record; *in* 22nd Arctic Workshop, Institute of Arctic and Alpine Research, University of Colorado, Boulder, Colorado, March 5–7, 1992, Abstracts, p. 56–60.

Gray, J.T., Brynczka, T., Giugni, L., Thibauld, E., and Lauriol, B.
1994: Multiple flow patterns of the Laurentide ice sheet on Akpatok Island, Ungava Bay, Arctic Canada; *in* 24th Arctic Workshop, Institute of Arctic and Alpine Research, University of Colorado, Boulder, Colorado, March 17–19, 1994, Program and Abstracts, p. 160–162.

Gray, J., Decker, V., Guindon, L., Guenette, C., and Clark, C.
1996: Late glacial ice flow patterns in the northwest Torngat Mountains: evidence for an important local dispersal centre, *in* 26th Arctic Workshop, Institute of Arctic and Alpine Research, University of Colorado, Boulder, Colorado, March 14–16, 1996, Program with Abstracts, p. 43–44b.

Gray, J.T., Lauriol, B., Bruneau, D., and Ricard, J.
1993: Postglacial emergence of Ungava Peninsula and its relationship to glacial history; Canadian Journal of Earth Sciences, v. 30, p. 1676–1696.

Heinrich, H.
1988: Origin and consequences of cyclic ice rafting in the Northeast Atlantic Ocean during the past 130,000 years; Quaternary Research, v. 29, p. 143–152.

Hillaire-Marcel, C., DeVernal, A., Bilodeau, G., and Wu, G.
1994: Isotope stratigraphy, sedimentation rates, deep circulation, and carbonate events in the Labrador Sea during the last - 200 ka; Canadian Journal of Earth Sciences, v. 31, p. 63–89.

Hughes, T.
1987: Ice dynamics and deglaciation models when ice sheets collapsed; *in* North America and Adjacent Oceans During the Last Glaciation; (ed.) W.F. Ruddiman and H.E.J. Wright; Geological Society of America, p. 183–220.

Jennings, A.E., Manley, W.F., MacLean, B., and Andrews, J.T.
1998: Marine evidence for the last glacial advance across Eastern Hudson Strait, Eastern Canadian Arctic; Journal of Quaternary Science, v. 13, p. 501–514.

Jennings, A.E., Tedesco, K.A., Andrews, J.T., and Kirby, M.E.
1996: Shelf erosion and glacial ice proximity in the Labrador Sea during and after Heinrich events (H-3 or 4 to H-0) as shown by foraminifera; *in* Late Quaternary Paleoceanography of the North Atlantic Margins, (ed.) J.T. Andrews, W.E.N. Austin, H. Bergsten, and A.E. Jennings; Geological Society of London, Special Publication 111, p. 29–49.

Jennings, A.E., Vilks, G., Deonarine, B., Silis, A., and Weiner, N.
2001: Foraminiferal biostratigraphy and paleoceanography; *in* Marine Geology of Hudson Strait and Ungava Bay, Eastern Arctic Canada: Late Quaternary Sediments, Depositional Environments, and Late Glacial–Deglacial History Derived from Marine and Terrestrial Studies, (ed.) B. MacLean; Geological Survey of Canada, Bulletin 566.

Josenhans, H.W. and Zevenhuizen, J.
1990: Dynamics of the Laurentide Ice Sheet in Hudson Bay, Canada; Marine Geology, v. 92, p. 1–26.

Josenhans, H.W., Zevenhuizen, J., and Klassen, R.A.
1986: The Quaternary geology of the Labrador Shelf; Canadian Journal of Earth Sciences, v. 23, p. 1190–1213.

Kaufman, D.S. and Williams, K.M.
1992: Radiocarbon Date List VII: Baffin Island, N.W.T., Canada; Institute of Arctic and Alpine Research, University of Colorado, Occasional Paper, no. 48, 82 p.

Kaufman, D.S., Miller, G.H., Stravers, J.A., and Andrews, J.T.
1993a: Abrupt early Holocene (9.9–9.6 ka) ice stream advance at the mouth of Hudson Strait, Arctic Canada; Geology, v. 21, p. 1063–1066.

Kaufman, D.S., Miller, G.H., Stravers, J.D., Manley, W.F., and Duvall, M.L.
1993b: Late glacial ice margins and deglaciation chronology for souteastern Baffin Island and Hudson Strait, Eastern Canadian Arctic: reply; Canadian Journal of Earth Sciences, v. 30, p. 1753–1758.

Kirby, M.E.
1996: Mid to Late Wisconsin ice sheet/ocean interactions in the Northwest Labrador Sea: sedimentology, provenance, process, and chronology; M.Sc. thesis, University of Colorado, Boulder, Colorado, 194 p.

Lauriol, B. and Gray, J.T.
1987: The decay and disappearance of the late Wisconsinan ice sheet in Ungava Bay, northern Québec, Canada; Arctic and Alpine Research, v. 19, p. 109–126.
1997: La composition isotopique des mollusques marins et sa relation à la déglaciation de la péninsule d'Ungava, Canada; Géographie physique et Quaternaire, vol. 51, p. 185–199.

Laymon, C.A.
1988: Glacial geology of western Hudson Strait, Canada, with reference to Laurentide Ice Sheet dynamics; Ph.D. thesis, University of Colorado, Boulder, Colorado, 345 p.
1991: Marine episodes in Hudson Strait and Hudson Bay, Canada, during the Wisconsin Glaciation; Quaternary Research, v. 35, p. 53–62.
1992: Glacial geology of western Hudson Strait, Canada, with reference to Laurentide Ice Sheet dynamics; Geological Society of America, Bulletin, v. 104, p. 1169–1177.

MacLean, B.
2001: Introduction: geographic setting and studies; *in* Marine Geology of Hudson Strait and Ungava Bay, Eastern Arctic Canada: Late Quaternary Sediments, Depositional Environments, and Late Glacial–Deglacial History Derived from Marine and Terrestrial Studies, (ed.) B. MacLean; Geological Survey of Canada, Bulletin 566.

MacLean, B., Vilks, G., and Deonarine, B.
1992: Depositional environments and history of late Quaternary sediments in Hudson Strait and Ungava Bay: further evidence from seismic and biostratigraphic data; Géographie physique et Quaternaire, v. 46, p. 311–329.

MacLean, B., Vilks, G., Hardy, I., Deonarine, B., Jennings, A.E., and Manley, W.F.
2001: Quaternary sediments in Hudson Strait and Ungava Bay; *in* Marine Geology of Hudson Strait and Ungava Bay, Eastern Arctic Canada: Late Quaternary Sediments, Depositional Environments, and Late Glacial–Deglacial History Derived from Marine and Terrestrial Studies, (ed.) B. MacLean; Geological Survey of Canada, Bulletin 566.

Manley, W.F.
1995: Late-glacial record of ice-sheet/ocean interactions, Hudson Strait and southern Baffin Island, Eastern Canadian Arctic; Ph.D. thesis, University of Colorado, Boulder, Colorado, 262 p.

Manley, W.F. and Jennings, A.E.
1996: Radiocarbon Date List VIII: Eastern Canadian Arctic, Labrador, Northern Quebec, East Greenland Shelf, Iceland Shelf, and Antarctica; Institute of Arctic and Alpine Research, University of Colorado, Occasional Paper, no. 50, 163 p.

Manley, W.F. and Miller, G.H.
2001: Glacial–geological record on southern Baffin Island reflecting late glacial ice-sheet dynamics in the eastern Hudson Strait region; *in* Marine Geology of Hudson Strait and Ungava Bay, Eastern Arctic Canada: Late Quaternary Sediments, Depositional Environments, and Late Glacial–Deglacial History Derived from Marine and Terrestrial Studies, (ed.) B. MacLean; Geological Survey of Canada, Bulletin 566.

Mercer, J.H.
1956: Geomorphology and glacial history of southernmost Baffin Island; Geological Society of America, Bulletin, v. 67, p. 553–570.

Miller, G.H. and Kaufman, D.S.
1990: Rapid fluctuations of the Laurentide ice sheet at the mouth of Hudson Strait: new evidence for ocean/icesheet interactions as a control on the Younger Dryas; Paleoceanography, v. 5, no. 6, p. 907–919.

Miller, G.H., Hearty, P.J., and Stravers, J.A.
1988: Ice-sheet dynamics and glacial history of southeasternmost Baffin Island and outermost Hudson Strait; Quaternary Research, v. 30, p. 116–136.

Muller, D.S.
1980: Glacial geology and Quaternary history of southeast Meta Incognita Peninsula, Baffin Island, Canada; M.Sc. thesis, University of Colorado, Boulder, Colorado, 211 p.

Oerlemans, J.
1993: Evaluating the role of climate cooling in iceberg production and Heinrich events; Nature, v. 364, p. 783–785.

Osterman, L.E.
1982: Late Quaternary history of southern Baffin Island, Canada; a study of foraminifera and sediments from Frobisher Bay; Ph.D. thesis, University of Colorado, Boulder, Colorado, 378 p.

Pfeffer, W.T.
2001: Ice dynamics modelling of the Hudson Strait region at late glacial time; *in* Marine Geology of Hudson Strait and Ungava Bay, Eastern Arctic Canada: Late Quaternary Sediments, Depositional Environments, and Late Glacial–Deglacial History Derived from Marine and Terrestrial Studies, (ed.) B. MacLean; Geological Survey of Canada, Bulletin 566.

Pfeffer, W.T., Dyurgerov, M., Kaplan, M., Dwyer, J., Sassolas, C., and Jennings, A.
1997: Numerical modelling of late glacial Laurentide advance of ice across Hudson Strait at Younger Dryas time: insights into terrestrial and marine geology, mass balance, and calving flux; Paleoceanography, v. 12, p. 97–110.

Piper, D.J.W., Mudie, P.J., Fader, G.B., Josenhans, H.W., MacLean, B., and Vilks, G.
1990: Quaternary Geology; Chapter 10 *in* Geology of the Continental Margin of Eastern Canada, (ed.) M.J. Keen and G.L. Williams; Geological Survey of Canada, Geology of Canada, no. 2, p. 475–607 (*also* Geological Society of America, The Geology of North America, v. I-1).

Stravers, J.A.
1986: Glacial geology of outer Meta Incognita Peninsula, southern Baffin Island, Arctic Canada; Ph.D. thesis, University of Colorado, Boulder, Colorado, 231 p.

Stravers, J.A. and Powell, R.D.
1997: Glacial debris flow deposits on the Baffin Island shelf: seismic facies architecture of till-tongue-like deposits; Marine Geology, v. 143, p. 151–168.

Stravers, J.A., Miller, G.H., and Kaufman, D.S.
1992: Late glacial ice margins and deglacial chronology for southeastern Baffin Island and Hudson Strait, eastern Canadian Arctic; Canadian Journal of Earth Sciences, v. 29, p. 1000–1017.

Vilks, G., MacLean, B., Deonarine, B., Currie, C.G., and Moran, K.
1989: Late Quaternary paleoceanography and sedimentary environments in Hudson Strait; Géographie physique et Quaternaire, v. 43, no. 2, p. 161–178.

Vincent, J-S.
1989: Quaternary geology of the southeastern Canadian Shield; *in* Chapter 3 of Quaternary Geology of Canada and Greenland, (ed.) R.J. Fulton; Geological Survey of Canada, Geology of Canada, no. 1, p. 249–275 (*also* Geological Society of America, The Geology of North America, v. K-1).

Author Index

Andrews, J.T. 57, 161, 181
(e-mail: john.t.andrews@colorado.edu)
B. Deonarine 71, 127
Gray, J. 31, 181
(e-mail : Grayj@geog.umontreal.ca)
Hall, F.R. 161, 181
(e-mail: frhall@uno.edu)
Hardy, I. 71, 147, 181
(e-mail: IHardy@nrcan.gc.ca)
Jennings, A.E. 57, 71, 127, 181
(e-mail: jenninga@spot.colorado.edu)
Kerwin, M. 161
(e-mail: Kerwin@colorado.edu)
MacLean, B. 5, 57, 65, 71, 181
(e-mail: brimacle@nrcan.gc.ca)
Manley, W.F. 19, 71, 181
(e-mail: william.manley@colorado.edu)
Miller, G.H. 19
(e-mail: gmiller@colorado.edu)
Pfeffer, W.T. 171, 181
(e-mail: pfeffer@tintin.colorado.edu)
Silis, A. 127
(e-mail: astride.silis@sympatico.ca)
Smith, L.M. 161
(e-mail: Laryn.Smith@colorado.edu)
Vilks, G. 71, 127, 181
(deceased)
Weiner, N. 127
(e-mail: Nancy.Weiner@colorado.edu)

MAPS NOT FILMED

CARTES NON REPRODUITES

micromedia
a division of IHS Canada

20 Victoria Street
Toronto, Ontario M5C 2N8
Tel.: (416) 362-5211
Toll Free: 1-800-387-2689
Fax: (416) 362-6161
Email: info@micromedia.on.ca